IAEA-TECDOC-1211

Charged particle cross-section database for medical radioisotope production: diagnostic radioisotopes and monitor reactions

Final report of a co-ordinated research project

INTERNATIONAL ATOMIC ENERGY AGENCY IAEA

May 2001

The originating Section of this publication in the IAEA was:

Nuclear Data Section
International Atomic Energy Agency
Wagramer Strasse 5
P.O. Box 100
A-1400 Vienna, Austria

CHARGED PARTICLE CROSS-SECTION DATABASE FOR
MEDICAL RADIOISOTOPE PRODUCTION:
DIAGNOSTIC RADIOISOTOPES AND MONITOR REACTIONS

IAEA, VIENNA, 2001
IAEA-TECDOC-1211
ISSN 1011–4289

Printed by the IAEA in Austria
May 2001

FOREWORD

Medical applications of nuclear radiation are of considerable interest to the IAEA. Cyclotrons and accelerators, available in recent years in an increasing number of countries, are being used for the production of radioisotopes for both diagnostic and therapeutic purposes. The physical basis of this production is described through interaction of charged particles, such as protons, deuterons and alphas, with matter. These processes have to be well understood in order to produce radioisotopes in an efficient and clean manner.

In addition to medical radioisotope production, reactions with low energy charged particles are of primary importance for two major applications. Techniques of ion beam analysis use many specific reactions to identify material properties, and in nuclear astrophysics there is interest in numerous reaction rates to understand nucleosynthesis in the Universe.

A large number of medically oriented cyclotrons have been running in North America, western Europe and Japan for more than two decades. In recent years, 30–40 MeV cyclotrons have been installed in several other countries (e.g. Australia, Argentina, Taiwan (China), China (Shanghai and Beijing), the Republic of Korea, the Islamic Republic of Iran, Indonesia) and smaller cyclotrons (E_p < 20 MeV) have been purchased or ordered by the Democratic People's Republic of Korea and Egypt. All those countries have either started or will soon start producing standard gamma emitting radioisotopes such as ^{67}Ga, ^{111}In, ^{201}Tl and ^{123}I, commonly employed in diagnostic investigations using gamma cameras and single photon emission computed tomographs (SPECT). Although the production methods are well established, there are no evaluated and recommended nuclear data sets available. The need for standardization was thus imminent. This was pointed out at three IAEA meetings:

- Consultants Meeting on Nuclear Data for Medical Radioisotope Production (IAEA, Vienna, April 1981) — Report INDC(NDS)-123,
- Consultants Meeting on Data Requirements for Medical Radioisotope Production, Tokyo, April 1987 (Ed. K. Okamoto, IAEA, Vienna, 1988) — Report INDC(NDS)-195,
- Advisory Group Meeting on Intermediate Energy Data for Applications, Working Group on Nuclear Data for Medical Applications (IAEA, Vienna, October 1990) — Report INDC(NDS)-245.

Based on the recommendations made at these meetings, a modest attempt was made to collect the available information on monitor reactions in the following report:

O. Schwerer and K. Okamoto: Status Report on Cross-Sections of Monitor Reactions for Radioisotope Production, Report INDC(NDS)-218 (IAEA, Vienna, 1989).

During the past twenty years, many laboratories have reported a large body of experimental data relevant to medical radioisotope production, and the charged particle data centres have compiled most of these data. However, no systematic effort had been devoted to their standardization. Such a task would be too ambitious for any single national laboratory, implying a need for well focused international effort. Under these circumstances, the IAEA decided to undertake and organize the Co-ordinated Research Project (CRP) on Development of Reference Charged Particle Cross-Section Database for Medical Radioisotope Production.

The project was initiated in 1995. It focused on radioisotopes for diagnostic purposes and on the related beam monitor reactions in order to meet current needs. It constituted the first

major international effort dedicated to standardization of nuclear data for radioisotope production. It covered the following areas:

- Compilation of data on the most important reactions for monitoring light ion charged particle beams (p, d, ^{3}He, α). Evaluation of the available data (both by fitting and theory).
- Compilation of production cross-section data on radioisotopes most commonly used in medicine. Evaluation of the data.
- Development of calculational tools for predicting unknown data.

The CRP involved 11 experts from nine institutes and national radioisotope production centres. The participants met at three Research Co-ordination Meetings held in Vienna in 1995 (Report INDC(NDS)-349), Faure (Cape Town), South Africa in 1997 (Report INDC(NDS)-371) and Brussels, Belgium in 1998 (Report INDC(NDS)-388).

Although the major emphasis in the CRP was on the energy region up to 30 MeV, higher energy data up to 60–80 MeV were also considered. It was realized that the evaluation methodology for charged particle data was not yet well developed and some teach-in effort was initially necessary. The CRP produced a much needed database and a handbook, covering reactions used for monitoring beam currents and for routine production of medically important radioisotopes. It is believed that the recommended cross-sections are accurate enough to meet the demands of all current applications, although further development of evaluation methodology and more experiments will be needed for exact determination of the errors and their correlations. In addition to the cross-sections, yields of the radioisotopes, calculated from the recommended data, are provided for the convenience of the user. A part of the results has been used in the Reference Neutron Activation Library, which was developed under another CRP.

The database is available cost-free on the following Web page: **http://www-nds.iaea.org/medical/**.

The IAEA wishes to thank all the participants of the project for their invaluable contributions to the preparation of the database. The leading role of S.M. Qaim (FZ Jülich) and T.F. Tárkányi (ATOMKI Debrecen) is acknowledged. The assistance of K. Gul, A. Hermanne, M.G. Mustafa, F.M. Nortier, B. Scholten, Yu. Shubin, S. Takács and Y. Zhuang in the preparation of this publication is gratefully acknowledged. The IAEA staff member responsible for this report was P. Obložinský of the Division of Physical and Chemical Sciences.

EDITORIAL NOTE

CONTENTS

Chapter 1

INTRODUCTION

(Prepared by S.M. Qaim)

1.1. DATA NEEDS

Charged particle induced nuclear reaction cross-sections are of interest for many applications. Of considerable significance are the excitation functions obtained via the activation technique. Those data find applications in several fields, for example,

- radioisotope production, primarily for medical applications (but also for industrial and agricultural use)
- monitoring of light charged particle beams (p, d, ^{3}He, α) available at cyclotrons and accelerators
- surface analysis in industrial applications
- astrophysics and cosmochemistry.

A comprehensive compilation of 86 charged particle induced reactions involving light nuclei ($1 \leq Z \leq 14$) was recently completed [1.1]. Those data are of particular interest for applications in astrophysics. Similarly detailed measurements and compilations of medium and high-energy data of relevance to cosmochemistry are also available [1.2, 1.3]. Furthermore, efforts are under way to compile and identify low energy data of interest to ion beam analysis [1.4], surface and thin layer activation analysis, primarily for industrial applications [1.5]. In this report we limit ourselves to a discussion of nuclear data relevant to the first two above mentioned fields.

Importance of nuclear data in radioisotope production programme

In the radioisotope production programme, nuclear data are needed mainly for optimisation of production routes. This involves a selection of the projectile energy range that will maximize the yield of the product and minimize that of the radioactive impurities (for early reviews on this topic see [1.6, 1.7]). Whereas the non-isotopic impurities produced can be removed by chemical separations, the level of isotopic impurities can be suppressed only using enriched isotopes as target materials and/or by a careful selection of the particle energy range effective in the target.

The radioisotope ^{123}I ($T_{½}$ = 13.2 h), a commonly used halogen nuclide for labelling biomolecules for diagnostic studies using single photon emission computed tomography (SPECT), for example, can be produced via various routes. Its production via the ^{124}Te(p,2n)^{123}I reaction furnishes a good example of the importance of nuclear data. In order to decrease the level of isotopic impurities in the ^{123}I produced, it is essential to use highly enriched ^{124}Te as target material. However, due to the competing ^{124}Te(p,n)^{124}I reaction it is not possible to eliminate the ^{124}I impurity completely, even if ^{124}Te is 100% enriched. Fig. 1.1, based on the excitation function measurements described in Refs [1.8, 1.9], shows that the ideal proton energy range for the production of ^{123}I is $E_p = 25.0 \rightarrow 18.0$ MeV, i.e. the energy of the incident protons should be selected as 25.0 MeV and the thickness of the tellurium target should degrade the incident energy only to 18.0 MeV.

Under these conditions the level of ^{124}I impurity in ^{123}I at the end of bombardment (EOB) amounts to about 1%. Evidently, it is necessary to know the excitation functions of the various competing reactions accurately.

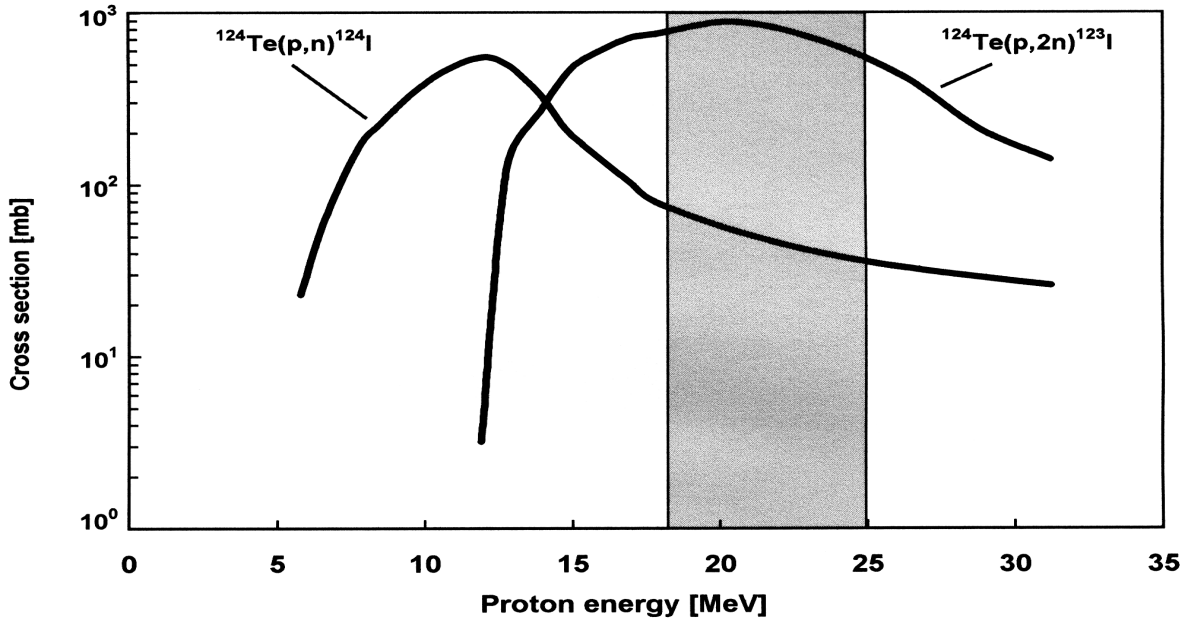

Fig. 1.1. Excitation functions of ^{124}Te(p,n)^{124}I and ^{124}Te(p,2n)^{123}I reactions. The optimum energy range for the production of ^{123}I is E_p = 25.0 → 18.0 MeV [1.9].

The radioactive impurities have a dual effect: firstly, they affect the line spread function in imaging adversely and secondly, cause enhanced radiation dose to the patient. If the amount of a longer-lived impurity is too high, it may jeopardise the whole advantage of the short-lived radioisotope used. It may then be necessary to look for an alternative route of production for the desired radioisotope. This was so in the case of ^{123}I. The ^{124}Xe(p,x)^{123}Xe $\xrightarrow[2.1\,h]{\beta^+,EC}$ ^{123}I route was developed, although the highly enriched target gas is very expensive. Today this process is used routinely and delivers ^{123}I of the highest purity.

Besides isotopic impurities discussed above, in recent years our awareness of isomeric impurities has also increased. Several medically interesting research type radioisotopes have isomeric states which are rather disturbing. A few examples are ^{94m}Tc (^{94g}Tc), ^{120g}I (^{120m}I), etc. The isomeric impurities cannot be controlled through a careful adjustment of the energy window (as mentioned above). Since the isomeric cross-section ratio is primarily dependent on the type of reaction involved (for a review see [1.10]), it is essential to investigate all the possible production routes and then to choose the reaction and the energy range giving the best results. Obviously, nuclear data play here a very important role.

Some users tend to hold the view that full information on the excitation function of the nuclear reaction used for the production of an isotope is not essential and that only experimental thick target yield data are sufficient. This approach may be more practical but it remains empirical since the experimental yield reflects only the specific conditions prevalent during the production process. It is strongly dependent on factors such as time of irradiation, beam current, physical form of the target material, etc. An accurate knowledge of the excitation function, and therefrom the theoretical thick target yield, however, helps in designing target systems capable of giving optimum yields.

Significance of nuclear data in monitoring charged particle beam

One of the major problem areas in work with charged particles is the characterization of the beam. The beam intensity can be measured by collecting the charge passing through the sample in a Faraday cup. However, if proper precautions are not taken to eliminate the effect of secondary electrons, the measurement may lead to rather erroneous results.

It is more convenient to determine the charged particle flux via a monitor reaction whose cross-section in the energy region of interest is well known. A schematic arrangement of the sample and monitor foils in a commonly used irradiation geometry is shown in Fig. 1.2. Since the target and monitor foils are in close contact, any small change in the beam profile does not affect the results. The beam flux obtained is thus quite reliable. However, as expected, the intrinsic error is dependent on the error in the excitation function of the monitor reaction (for an early review on this topic see [1.11]). Because of its simplicity and reliability, the use of monitor reactions in activation cross-section work is very common. Any charged particle data evaluation programme therefore ought to devote full attention to both the charged particle beam current monitor reactions (comparable to threshold standard reactions in neutron metrology) and the radionuclide production reactions.

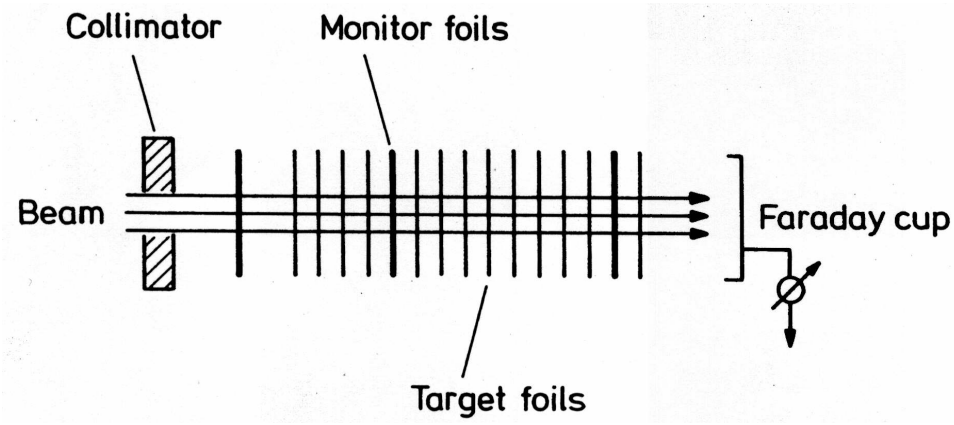

Fig. 1.2. Schematic arrangement of target and monitor foils for irradiation with a charged particle beam.

1.2. SCOPE OF EVALUATION WORK

A systematic treatment and evaluation of all charged particle data would involve an enormous effort. Due to limited resources, the Nuclear Data Section of the IAEA decided in 1995 to concentrate on one particular topic, namely, data relevant to the production of medically important radioisotopes. A recent IAEA survey on cyclotrons used for radionuclide production in member states revealed that 206 cyclotrons in 34 countries are used exclusively or partially for isotope production [1.12]. The endeavour undertaken to evaluate the data was therefore timely and worthwhile. Primarily, data in the low energy range up to 30 MeV are required. But for production of certain radioisotopes higher energy data, up to about 80 MeV, are gaining importance.

Monitor reactions

The most important and commonly employed nuclear reactions for monitoring light ion charged particle beams (p, d, ^{3}He, α) should be considered. Most of the cyclotrons used for medical radioisotope production are two particle machines, accelerating protons and deuterons. However, occasionally four particle machines are also used, especially in the production of research related radioisotopes. Some of the examples are: ^{48}Ti(^{3}He,3n)^{48}Cr, ^{75}As(^{3}He,3n)^{75}Br, ^{75}As(^{3}He,2n)^{76}Br, ^{nat}Mo(^{3}He,x)^{97}Ru, ^{35}Cl(α,n)^{38}K, ^{75}As(α,2n)^{77}Br, ^{209}Bi(α,2n)^{211}At, etc. Furthermore, in charged particle activation analysis and surface layer analysis, ^{3}He- and α-beams are often employed. It was therefore considered worthwhile to take into account ^{3}He- and α particle beam monitoring as well, although the emphasis should be on reactions used for p and d monitoring.

Reactions for production of medically relevant radioisotopes

The medically relevant radioisotopes can be divided into two groups, viz. diagnostic and therapeutic radioisotopes. The radionuclidic purity and minimum radiation dose requirements are more stringent in the case of diagnostic radioisotopes than for therapy related radionuclides. The field of endoradiotherapy, i.e. internal therapy with radioisotopes, has been pursued for a long time (for recent reviews see [1.13, 1.14]). The thyroid therapy with radioiodine is well established. In other areas, fast developments are occurring. Many of the therapeutic radioisotopes are reactor produced. A few cyclotron therapy related radioisotopes are finding increasing applications. However, the respective databases are rather weak. In the presently described first evaluation effort, therefore, attention was paid only to diagnostic radioisotopes.

The diagnostic radioisotopes are further classified into two groups, depending upon their decay characteristics and mode of detection. A widely and commonly used technique involves the detection of a dominant γ ray via SPECT (single photon emission computed tomography). A faster and more quantitative technique, however, consists of the detection of the two 511 keV γ rays in coincidence which are formed in the annihilation of a positron. This technique, known as positron emission tomography (PET), is a very fast developing field and holds great promise for biofunctional research and clinical diagnosis (^{18}FDG).

The major aim of the present endeavour was to evaluate the production data of all the cyclotron produced and commonly used γ- and β^{+}-emitters (SPECT and PET radioisotopes).

1.3. EVALUATION METHODOLOGY

During the past thirty years, several laboratories have reported a large body of experimental data, and the charged particle data centres have compiled many of those data in EXFOR form. However, till 1995 no international effort had been devoted to the evaluation of the data. The use of nuclear theory for reliable prediction of cross-section data was and is even today limited. In fact the whole evaluation methodology for charged particle data is still at an early stage of development. The steps and procedures adopted here are described below.

Compilation of data

For many reactions the available experimental data are extensive, but for others they are scanty. Some of the reactions have been studied by a large number of groups over a period of several decades. The experimental techniques have been constantly improved over the years, both in terms of beam current determination and radioactivity measurement. Extensive

literature surveys were performed and all the data were compiled. The reliability of those data was checked. In several cases renormalisation of the data was necessary. Some of the very discrepant data were rejected. Thereafter evaluations were performed.

Nuclear model calculations

For a better understanding of the experimental data it is instructive and advantageous to perform nuclear model calculations and compare the experimental and calculated data. The calculational methods used during the present project included both Hauser-Feshbach type statistical model (incorporating precompound effects) and exciton model. In the medium and heavy mass region (monitor reactions and γ emitters) the model calculations met with varying degrees of success. For light mass β^+ emitters no calculational method was successful.

Fitting of data

In many cases, especially the light mass β^+ emitters, some averaging and fitting methods were employed. In order to reproduce resonances, some energy adjustments and magnitude normalisations were also done.

In general it was found that the nuclear model calculations could reproduce the excitation functions reliably only for the simple reaction channels like (p,n), (p,2n), etc. on medium and heavy mass nuclei. In most of the other cases, therefore, heavy reliance was placed on the data fitting methods.

1.4. OVERVIEW OF THE PRESENT TECDOC

The co-ordinated research project (CRP) was initiated in 1995 and brought to completion at the end of 1999. This technical document summarizes the results of the CRP and presents the evaluated data for general use.

After this introductory chapter, consideration is given to the handling of experimental data in Chapter 2. A description of data compilation and analysis is followed by an account of the semi-empirical methods of fitting used. Chapter 3 deals with the nuclear model calculations and a brief discussion of their strengths and deficiencies.

The detailed results of evaluations are summarized in Chapters 4 and 5. These chapters constitute the main body of this report and attempt to fulfil the major aims of the CRP. Chapter 4 deals with beam monitor reactions. Chapter 5 contains two sections, Section 5.1 encompassing reactions used in the production of γ ray emitting radioisotopes, and Section 5.2 positron emitters. For each individual reaction, at first all the collected experimental data are given. After a careful analysis only the most reliable and concordant data are considered. Thereafter the results of various calculations and evaluations are described and compared with the selected experimental data. A recommended curve is then presented which agrees very closely with the experimental data. Finally, based on that curve, the recommended numerical values of reaction cross-sections are tabulated. This scheme is followed for all the major monitor and radioisotope production reactions.

It is believed that the recommended cross-sections should be accurate enough to meet the demands of most of the presently envisaged applications. An exact definition of the errors and their correlations is, however, as yet not possible. Further development in the evaluation methodology is needed.

For some nuclear processes only scanty information was available, although the production route is rather important and is already in practical use. In those cases the data are given with some comments. The existing values should be adopted till more experimental data are reported and a new evaluation becomes worthwhile.

Many practical users prefer, instead of reaction cross-sections, information on integral production yields. The expected yields of various products were therefore calculated from the recommended excitation functions and the result for each respective reaction is given in Chapter 5.

It is hoped that the recommended cross-section curves and tables would help the radionuclide producing community considerably in choosing the optimum conditions for the production of a particular radionuclide. Furthermore, a comparison of experimental and calculated integral yields would reveal the efficiency of the production process, in particular of targetry and chemical processing.

1.5. AVAILABILITY OF DATA

The database developed during this project and the evaluated data (both in graphical and numerical form) are given in the present report. For more practice oriented users the calculated yields of the radioisotopes are also given. The data can be obtained electronically from the Web server at http://www-nds.iaea.or.at/medical/.

REFERENCES TO CHAPTER 1

[1.1] ANGULO, C., ARNOULD, M., RAYET, M., et al., A compilation of charged-particle induced thermonuclear reaction rates, Nucl. Phys. **A656** (1999) 1–181.

[1.2] MICHEL, R., GLORIS, M., LANGE, H.-J., et al., Nuclide production by proton-induced reactions on elements ($6 \leq Z \leq 29$) in the energy range from 800 to 2600 MeV, Nucl. Instr. Methods in Phys. Res. **B103** (1995) 183–222.

[1.3] MICHEL, R., BODEMANN, R., BUSEMANN, H., Cross sections for the production of residual nuclides by low- and medium-energy protons from the target elements C, N, O, Mg, Al, Si, Ca, Ti, V, Mn, Fe, Co, Ni, Cu, Sr, Y, Zr, Nb, Ba and Au, Nucl. Inst. Methods in Phys. Res. **B129** (1997) 153–193.

[1.4] Handbook of Modern Ion Beam Materials Analysis, (Tesmer, J.R., Nastasi, M., Eds), Materials Research Society, Pittsburgh, PA (1995) 1–704.

[1.5] INTERNATIONAL ATOMIC ENERGY AGENCY, The Thin Layer Activation Method and its Applications in Industry, IAEA-TECDOC-924, Vienna (1997) 1–143.

[1.6] QAIM, S.M., Nuclear data relevant to cyclotron produced short-lived medical radioisotopes, Radiochimica Acta **30** (1982) 147–162.

[1.7] QAIM, S.M., "Medical radioisotopes and nuclear data", Proc. Consultants Meeting on Data Requirements for Medical Radioisotope Production, Tokyo, Japan, 1987 (Okamoto, K., Ed.), Rep. INDC(NDS)-195, IAEA, Vienna (1988) 25–32.

[1.8] KONDO, K., LAMBRECHT, R.M., WOLF, A.P., ^{123}I production for radiopharmaceuticals XX. Excitation functions of the ^{124}Te(p,2n)^{123}I and ^{124}Te(p,n)^{124}I reactions and the effect of target enrichment on radionuclidic purity, Int. J. Appl. Radiat. Isot. **28** (1977) 395–401.

[1.9] SCHOLTEN, B., KOVÁCS, Z., TÁRKÁNYI, F., QAIM, S.M., Excitation functions of ^{124}Te(p,xn)^{124,123}I reactions from 6 to 31 MeV with special reference to the production of ^{124}I at a small cyclotron, Appl. Radiat. Isot. **46** (1995) 255–259.

[1.10] QAIM, S.M., "Recent developments in the study of isomeric cross sections", Proc. Int. Conf. Nuclear Data for Science and Technology, Gatlinburg, 1994 (Dickens, J.K., Ed.), American Nuclear Society, La Grange Park, IL (1994) 186–192.

[1.11] HASHIZUME, A., "Monitor reactions for the production of radioisotopes for medical use", Proc. Consultants Mtg on Data Requirements for Medical Radioisotope Production, Tokyo, Japan, 1987 (Okamoto, K., Ed.), Rep. INDC(NDS)-195, IAEA, Vienna (1988) 44–53.

[1.12] INTERNATIONAL ATOMIC ENERGY AGENCY, Directory of Cyclotrons used for Radionuclide Production in Member States, IAEA-TECDOC-1007, Vienna (1998) 1–436.

[1.13] HOEFNAGEL, C.A., Radionuclide therapy revisited, Eur. J. Nucl. Med. **18** (1991) 408–431.

[1.14] STÖCKLIN, G., QAIM, S.M., RÖSCH, F., The impact of radioactivity on medicine, Radiochimica Acta **70/71** (1995) 249–272.

Chapter 2
EXPERIMENTAL EVALUATION

Experimental data play a key role in the evaluation of nuclear reaction cross-sections. This general statement is particularly valid for reactions with charged particles where the predictive capabilities of nuclear reaction model codes and the evaluation methodology are not yet fully established.

Though a large number of experimental investigations were performed during the last five decades, the experimental cross-section database for the production of nuclides with light charged particles is not reliable. The data scattered in the literature are often contradictory and, except for a few reactions, there are no evaluations.

In this situation, the experimental evaluation had to start with a thorough compilation of data. The next step was a careful analysis of those data and a selection of concordant data. The third step then consisted of fitting the selected data with appropriate analytical functions. These three steps are described below in more detail.

2.1. COMPILATION OF EXPERIMENTAL DATA

(Prepared by F. Tárkányi)

The list of reactions chosen is given in Table 2.1. The four participating experimental laboratories, viz. ATOMKI Debrecen (Hungary), VUB Brussels (Belgium), INC-FZ Jülich (Germany) and NAC Faure (South Africa), collected and evaluated the literature data; in case of necessity they did some additional experimental work, and finally performed a selection of the best sets of data for evaluation. The data were collected and selected over broad energy ranges to assure better reliability of the fitting process. The compilation and selection occurred as an iterative process.

A scheme was agreed upon regarding the sources of literature data and the method of selection, but it became clear that the set rules could not be applied universally to all reactions. Therefore, each group handled the data according to its experience. The compilation process was co-ordinated by the Debrecen group (Hungary).

In search of the original works, the following sources were used:

- Primary Journals,
- EXFOR data base of the Nuclear Data Section, International Atomic Energy Agency,
- Nuclear Data Sheets (recent references),
- INIS database of the International Atomic Energy Agency,
- Chemical Abstracts (1947–1992),
- Bibliographies of Brookhaven National Laboratory (Burrows and Dempsey [2.1], Holden [2.2], Karlstrom and Christman [2.3]),
- Reports of the International Atomic Energy Agency (Dmitriev [2.4], Gandrias-Cruz and Okamoto [2.5]),
- Compilations on specific reactions: (Vokulov [2.6], Tendow [2.7], Landolt Börnstein Series [2.8], Landolt Börnstein New Series [2.9–2.12], Tobailem [2.13, 2.14], Albert [2.15, 2.16], Münzel [2.17], and a few others [2.18, 2.19].

During compilations the cross-sections were taken from the original publications except when they were available through the EXFOR databases. In this case the updated EXFOR values were used; however, the original publications were in most cases also consulted in detail and they are referenced in this text. The EXFOR accession number is added to the reference of the original work.

For obtaining details on measurements five different groups of literature sources were used:

- *Simple numerical or graphical data in different compilations*. An example is the newest compilation in Landolt Börnstein Series [2.9]. An advantage of these compilations is the availability of broad range of data. However, these data are usually presented without errors. Furthermore, no information about the quality of results is available, and finally the compiled data in many cases do not correspond to the original publications. There are also large uncertainties in digitising the figures and occasionally correct interpretation of the published results (isotopic, natural, or cumulative cross-sections, many different yield definitions etc.) is missing. These compilations were usually not checked by independent experts and there is only a small possibility for correction *a posteriori*.

- *EXFOR computerized library*. This is a world-wide compilation of experimental data in computer format. Its extended format includes not only the numerical values but also some limited information on the measurements, data evaluation and error estimation. In principle these data files contain the latest corrected values. The reliability and accuracy of the data are ensured by a check through the original authors or independent experts.

- *Original publications*. There may be significant differences between EXFOR text and the content of the original publication. The EXFOR contains numerical results and some limited information on the experimental background, but not the details. Formulas, discussions and an explanation of how data were obtained, and why it is thought that the obtained results are correct, are usually missing. Therefore, in data evaluation, when the quality of the data is judged only by the EXFOR alone, the detailed information in the original publication may be missed.

- *PhD theses*. Often such theses provide a lot of details on experiments and evaluations. Usually they contain reliable information. In many cases a big advantage is that they contain rough data without “cosmetics”, and the reason of disagreement can be more easily identified. Such theses are, however, available only if submitted recently.

- *Specific evaluations*. These are evaluated files containing some explanations, where weak points and necessary corrections of the individual works are already discussed by a well qualified expert. The data sets are shown in comparison with results of other experiments, as well as with theoretical predictions on the magnitude, shape and threshold of the excitation function. They are very valuable for subsequent evaluations, both as data sources and for selection.

Unfortunately, some older works presented cross-sections/yield calculations only in graphical form. This was mainly because the journals did not accept the data both in tabular and graphical forms. Therefore, the use of those values is possible only with the introduction of an additional (systematic and non-systematic) uncertainty both in particle energy scale and cross-section value. Usually the investigators did not publish their energy error calculations. However, in some cases energy error assessment were presented, primarily for the first and

last foils of the stacks. Some groups published cross-section data not only without energy errors but without cross-section error estimation as well. The usefulness of those data in the evaluation process is questionable but they were added to our compilation.

During the compilation and evaluation processes the original publications were studied in detail by the participating groups. A table for each reaction was constructed containing the most important experimental parameters and the references of the used nuclear and stopping power data, the investigated energy range and the number of experimental data points. A correction for the outdated decay data was also performed and the data sets were reproduced in figures to see tendencies and discrepancies. On the bases of the emerging consistencies and trends, the contradictory and scattered data were rejected (deselected). In case of lack of data new measurements were proposed, taking into account the limited time period, available accelerators and other resources. Series of new measurements were done to clear the situation for a few reactions and energy ranges, collected in the Table 2.1.

In view of practical applications, for beam *monitor reactions* cumulative cross-sections for elements of natural isotopic composition (so called elemental cross-sections) were compiled. The independent cross-sections measured using enriched targets were transformed by the compiler to cumulative and elemental cross-sections, taking into account the composition of the natural element, thresholds of different reactions, and half-lives of the short-lived parents. For production of *diagnostic isotopes*, the cross-sections refer to 100% enrichment of the target nuclide (isotopic cross-sections). Cross-sections measured using natural targets (elemental cross-sections) were also employed in our compilation, but only up to the threshold of the next contributing reaction. In those cases we extrapolated the cross-section values measured on natural targets to 100% enrichment of the target nuclide. In a few cases production cross-sections for natural targets were also compiled, reflecting the effective production yields from target elements. In all cases independent (direct) cross-sections were collected not taking into account the decay of parents. For definition and calculation of the production yields, we refer to the comprehensive work of Bonardi [2.20].

2.2. ANALYSIS AND SELECTION OF EXPERIMENTAL DATA

(Prepared by F. Tárkányi)

The number of works on experimental cross-sections for each reaction included in the present project, found after a thorough search of the literature, is shown in Table 2.1.

Many of the older measurements were performed at electrostatic accelerators and at cyclotrons using stacked foil technique and activation assessment without chemical separation on natural targets. The most common procedure for measuring the beam intensities was the application of a Faraday cup. NaI or Ge detectors were used for detecting gamma rays from the decay of the product nuclei. In a few cases highly enriched targets were used. In some cases special experimental techniques, such as beam current measurements with calorimeters, chemical separation of the reaction products, direct counting of the produced secondary particles or determination of the activity by measuring positrons, were also used. Isotopic and/or elemental cross-sections were reported depending on the energy regions and the targets used. In the case of isotopic cross-sections we transformed the data to elemental cross-sections. Unfortunately, in several cases the definition of the presented cross-section values were so unclear that even after repeated trials we were not fully satisfied with our conversion results.

TABLE 2.1. SUMMARY OF WORK ON COMPILATION AND SELECTION OF EXPERIMENTAL DATA

Beam monitor reactions	Reaction	Energy range (MeV)	Compiling laboratory	New measurements*	Number of available data sets	Number of selected data sets
Protons	$^{27}Al(p,x)^{22}Na$	30–100	NAC Faure		14	9
	$^{27}Al(p,x)^{24}Na$	30–100	ATOMKI Debrecen		16	11
	$^{nat}Ti(p,x)^{48}V$	5–30	ATOMKI Debrecen	Szelecsényi (2000)	16	6
	$^{nat}Ni(p,x)^{57}Ni$	13–50	ATOMKI Debecen	Szelecsényi (1999)	21	15
	$^{nat}Cu(p,x)^{56}Co$	50–100	NAC Faure		7	4
	$^{nat}Cu(p,x)^{62}Zn$	14–60	INC-FZ Jülich	Hermanne (1999)	13	4
	$^{nat}Cu(p,x)^{63}Zn$	4.5–50	INC-FZ Jülich		24	9
	$^{nat}Cu(p,x)^{65}Zn$	2.5–100	INC-FZ Jülich		30	10
Deuterons	$^{27}Al(d,x)^{22}Na$	29.5–80	ATOMKI Debrecen	Takács (2000)	5	3
	$^{27}Al(d,x)^{24}Na$	15–80	ATOMKI Debrecen	Takács (2000)	16	13
	$^{nat}Ti(d,x)^{48}V$	9–50	ATOMKI Debrecen	Takács (1997), Takács (2000)	5	4
	$^{nat}Fe(d,x)^{56}Co$	8–50	ATOMKI Debrecen	Takács (1997), Takács (2000)	9	7
	$^{nat}Ni(d,x)^{61}Cu$	2.5–50	ATOMKI Debrecen	Takács (1997), Takács (2000)	6	4
^{3}He particles	$^{27}Al(^{3}He,x)^{22}Na$	10–100	ATOMKI Debrecen		7	6
	$^{27}Al(^{3}He,x)^{24}Na$	25–100	ATOMKI Debrecen		6	5
	$^{nat}Ti(^{3}He,x)^{48}V$	16–100	ATOMKI Debrecen	Ditrói (1997), Ditrói (1999)	4	4
α particles	$^{27}Al(\alpha,x)^{22}Na$	29–100	ATOMKI Debrecen		13	10
	$^{27}Al(\alpha,x)^{24}Na$	50–100	ATOMKI Debrecen		16	11
	$^{nat}Ti(\alpha,x)^{51}Cr$	5–40	ATOMKI Debrecen	Hermanne (1999)	11	6
	$^{nat}Cu(\alpha,x)^{66}Ga$	8–30	ATOMKI Debrecen	Tárkányi (1999)	17	9
	$^{nat}Cu(\alpha,x)^{67}Ga$	15–50	ATOMKI Debrecen	Tárkányi (1999)	14	8
	$^{nat}Cu(\alpha,x)^{65}Zn$	15–50	ATOMKI Debrecen	Tárkányi (1999)	15	8

Production of diagnostic radioisotopes	Reaction	Energy range (MeV)	Compiling laboratory	New measurements *	Number of available data sets	Number of selected data sets
Gamma ray emitters	$^{67}Zn(p,n)^{67}Ga$	2–25	ATOMKI Debrecen	Szelecsényi (1998), Hermanne (1999)	11	8
	$^{68}Zn(p,2n)^{67}Ga$	13–30	ATOMKI Debrecen	Hermanne (1999)	10	7
	$^{nat}Kr(p,xn)^{81}Rb$	14.5–80	NAC Faure		6	3
	$^{82}Kr(p,2n)^{81}Rb$	14.5–30	NAC Faure		4	4
	$^{111}Cd(p,n)^{111}In$	4–30	ATOMKI Debrecen		9	9
	$^{112}Cd(p,2n)^{111}In$	11.5–35	ATOMKI Debrecen		4	3
	$^{123}Te(p,n)^{123}I$	4–20	ATOMKI Debrecen		8	4
	$^{124}Te(p,2n)^{123}I$	12–30	ATOMKI Debrecen		5	3
	$^{124}Te(p,n)^{124}I$	5–30	ATOMKI Debrecen		8	2
	$^{127}I(p,5n)^{123}Xe$	37–100	NAC Faure		9	8
	$^{127}I(p,3n)^{125}Xe$	20–100	NAC Faure		9	9
	$^{124}Xe(p,2n)^{123}Cs$	16.5–40	INC-FZ Jülich		2	2
	$^{124}Xe(p,pn)^{123}Xe$	15.5–40	INC-FZ Jülich		2	2
	$^{203}Tl(p,3n)^{201}Pb$	18–36	VUB Brussels		8	4
	$^{203}Tl(p,4n)^{202m}Pb$	9–27	VUB Brussels		4	4
	$^{203}Tl(p,2n)^{200}Pb$	27.5–36	VUB Brussels		6	4
Positron emitters	$^{14}N(p,\alpha)^{11}C$	4–25	INC-FZ Jülich		13	9
	$^{16}O(p,\alpha)^{13}N$	6–20	INC-FZ Jülich		13	9
	$^{15}N(p,n)^{15}O$	4–20	INC-FZ Jülich		11	10
	$^{14}N(d,n)^{15}O$	1–15	INC-FZ Jülich		9	5
	$^{18}O(p,n)^{18}F$	2.5–20	INC-FZ Jülich		6	6
	$^{nat}Ne(d,\alpha)^{18}F$	1.5–21	INC-FZ Jülich	Fenyvesi (1997)	6	3
	$^{69}Ge(p,2n)^{68}Ge$	13–40	VUB Brussels		3	2
	$^{nat}Ga(p,x)^{68}Ge$	11.5–60	VUB Brussels		3	2
	$^{85}Rb(p,4n)^{82}Sr$	36.5–70	NAC Faure		1	1
	$^{nat}Rb(p,x)^{82}Sr$	33–100	NAC Faure		3	2

* The references to new measurements are given in Chapters 4 and 5.

At the evaluation stage we met all the problems well known to evaluators. On the basis of the information reported in the original publications and in the earlier compilations it is practically impossible, with a few exceptions, to assess the quality of the data and to find reasons for the disagreements with other publications. In accordance with the discussions in the literature and our own experience, the main possible sources of errors or reasons for discrepancies among the experimental data are the following:

Beam current determination. While relying on monitor reactions the main problem could originate from the use of outdated monitor cross-sections. Another source of error is improper use of monitors, especially a wrong estimation of real energy of the bombarding particle in an energy region where the excitation function curve has a steep slope (which leads to an under- or overestimation of the beam flux). Not accounting for the real target thickness is also a common source of error. In case of direct measurement of number of incoming particles through deposited electrical charge, there are strong requirements on residual gas pressure, isolation, suppression of secondary electrons etc., which in most of the cases are not fulfilled properly. A frequent error is the miscalculation of the number of particles from the total collected charge if one forgets to take into account the ionisation state of the bombarding particle (error by a factor of two for alphas and ^{3}He particles). These effects result in lower cross-sections. When working with collimators with diameters comparable to those of the target foils, not all particles coming into the Faraday cup can effectively bombard the target nuclei. This problem results in an underestimation of the cross-section.

Determination of number of target nuclei. It is difficult to determine the number of target nuclei with high precision, but an error in the number of target nuclei below five percent can be achieved easily. Main difficulties in the case of thin solid targets are the uncertainty on the chemical state (surface oxidation), non-uniformity in the thickness of the foil, improper estimation of the shape or dimensions influencing the thickness derived from weighing. In case of gas targets the well known density reduction along the beam due to the heat effects, not well defined geometry due to thin window and non-atmospheric pressure, and miscalculation of the number of atoms in case of two atom molecular gas are the main sources of errors. For the stacked target irradiation all the above factors result in cumulative effects while determining the energy along the stack.

Measurement of the radioactivity. In the determination of absolute activity the main sources of error are as follows: faulty estimation of the detector efficiency especially in the low energy region, self absorption in case of low energy gamma rays, deviation between point source calibration and the used extended targets, dead time and pile up corrections, and finally the use of incorrect decay data.

Calculation of the cross-section. Errors are introduced by the nuclear data used, improperly derived activation formula in complex decays, wrong estimation of contributing processes (possible parent decay), unclear definition of the calculated quantity, and by improper estimation of the effect of the final thickness of the target.

Determination of the energy scale. Large errors in the energy scale are introduced by improper estimation of the energy of the primary beam, large uncertainties in the effective thickness of the targets, the cumulative effect of the stacked foil technique and of the absorber used to vary the energy of the incoming beam. Accelerators used for data measurement for nuclear physics usually have tools to measure the energy of the used external beams. The electrostatic generators usually have excellent energy resolution and energy calibration while those used only for isotope production are not so well calibrated in energy.

Estimation of uncertainties of the cross-sections and the energy scale. There are not well accepted rules to estimate the uncertainty of the obtained cross-section values and their energy scale. As discussed above, many factors contribute to the assessment of the error of the obtained cross-section values. The most frequently used and easiest way to estimate the total uncertainty is to assess the contributing effects independently and then to combine them in quadrature. Usually not only the final result, but also the estimated uncertainties of the contributing processes are presented in original publications. It remains unresolved and unclear how estimations of the uncertainties of the contributing processes were done. There can be very large errors in estimation of the number of bombarding particles, in the efficiency of the used detector, in the homogeneity and the thickness of the target, etc.

Irradiation of a highly enriched target results in higher activities of the produced isotopes compared to natural composition, and thus smaller statistical errors and disturbing reactions occur. The results were, however, not always better, because the technology introduces some additional uncertainties. The real isotopic composition may not always correspond to the certification of the target manufacturer and the quality of the target is usually lower compared to the natural target. The situation is the same with the chemical separation of the final product. It has many advantages but in some cases it introduces significant errors into the final result. Often it is mandatory to apply new technologies, and to avoid the disturbing activities, but one should consider that each manipulation introduces new uncertainties.

Unfortunately often only a small part of the above mentioned error parameters are mentioned in the publications. We had therefore to rely on a limited number of documented factors and simultaneously to consider the results of all other reactions in the publication as well as to check the results of other published works from the same authors. Also some empirically developed systematics of the investigated reactions and the results of theoretical predictions can be used. The theoretical predictions play an important role in screening the large errors in the energy scale and the systematics of experimental cross-sections in defining the magnitude of the excitation function.

Another drawback was that in several publications instead of original data some deduced values were published after not well defined transformations based on different theoretical models or experimental systematics. This practice made practically all measurements uncheckable and unusable both as regards original and deduced data. The original data can be recovered only with the help of authors of the original publications, which, in case of older publications, is either impossible or very time consuming.

No strict rules were followed regarding the selection of the most reliable data. Except for a few publications having extra large uncertainties, for most of the data nearly similar (10–20%) data uncertainties were published. The observed disagreements are, however, large (factors). Therefore, it was concluded that, with the exception of a few works, most of the cited errors did not reflect the accuracy of the measurement.

In case of large sets of independent measurements, data having significant deviations from other results and from the predictions of systematics, were critically examined, searching for simple errors, miscalculations or some systematic errors. When no reason was found, the data set was usually rejected (deselected). A somewhat higher confidence was accorded to the most recent works, done with more modern irradiation and detection techniques and works done earlier at physics machines, using careful measurements of all possible contributing parameters. Larger weight was given to works done by groups having shown reliability in methods and measurements. In case of monitor reactions an important factor was the newly performed experiments on inter-comparison of different reactions. It

gave significant help to complete the experimental data set and to select the most reliable data. In the frame of the CRP many new measurements were done (see Table 2.1), but still not enough to solve contradictions in data of some very important reactions like $^{124}Xe(p,x)^{123}I$.

For some publications results of integral measurements were also used to choose between groups of data. Such integral measurements could be useful not only for selection of the best experimental data, but also for validation of recommended data.

In case of nuclear reactions used for production of positron emitters the excitation functions have a resonance character at low energies. For successful fitting it was necessary to consider those resonances (consistent data set). Therefore special corrections were made by the compilers in the energy scale of the activation data. Those corrections were based on data obtained with higher precision by direct particle counting.

The compilations and selections resulted in a great progress to define the status of the nuclear data of the investigated reactions and to complete the database. The compilations show that for several reactions there are numerous experiments, but the status of the data, with very few exceptions, is still not satisfactory. For other reactions only very few and in some cases not very consistent experimental results exist, which greatly affect the quality of the recommended data.

2.3. METHODS OF FITTING

(Prepared by P. Obložinský, Yu.N. Shubin and Y. Zhuang)

When the status of the experimental data set is appropriate, meaning that a reasonable amount of independent measurements have been published that do not show inexplicable discrepancies between them and that for all points reliable error estimations are available, a purely statistical fit over the selected data points can be performed. Often, such fits use analytical functions, the most prominent being polynomials. Thus, the well known spline fit approximates the data piece by piece by a set of polynomials. A more general class of analytical functions are rational functions defined as the ratio of two polynomials. These functions have a capability to approximate, in a natural way, nuclear reaction cross-sections in the resonance region, a behavior exhibited in the present project by several light nuclei.

In the following paragraphs two methods of fitting applied in the present project are shortly described. We start with the spline fit and proceed with the Padé fit based on rational functions. Our description essentially follows the work done by the groups in CNDC Beijing and IPPE Obninsk, respectively.

2.3.1. Spline fit

The spline fit method uses the technique of piece wise approximation of experimental data by specifying important points (termed knots of the spline), applying individual interpolation in each interval between two knots, and matching these interpolations so that the first and second derivatives are continuous at the knots. Interpolation functions are polynomials, usually of the 3rd order (cubic). By meeting the condition of continuous derivatives, one gets a continuous and smooth fit with minimum twisting (oscillating behavior) of the fitting curve. A particular feature of the spline method is that the fit in an interval is remarkably independent of data in other intervals.

Evaluation of cross-sections by the spline fit was first described some 30 years ago [2.21]. Since then, the description of the method become a part of many textbooks [2.22, 2.23], and it was applied widely in nuclear data evaluations. The present description is limited to basic ideas, followed by specific improvements worked out by the CNDC Beijing and used in their SPF code.

Consider a set of experimental data

$$x_i, F_i, \sigma_i, \text{ with } i = 1, \ldots, N, \tag{2.1}$$

where F_i is the measured cross-section with the uncertainty σ_i at the energy x_i. Knots, in general not identical with the experimental points, are placed along the x-axis as judged to be needed,

$$x = \xi_1, \ldots, \xi_n, \tag{2.2}$$

the spline s(x) is constructed piece wise, for each interval as a polynomial

$$s(x) = \sum_{k=0}^{3} a_{jk} x^k \quad \text{where} \quad \xi_j \le x \le \xi_{j+1} \tag{2.3}$$

with continuous derivatives at knots

$$s'(\xi_j), s''(\xi_j) \quad \text{where } j = 1, \ldots, n-1, \tag{2.4}$$

and minimized using the least squares functional

$$\chi^2 = \sum_{i=1}^{N} (s(x_i) - F_i)^2 / \sigma_i^2 \ . \tag{2.5}$$

Several methods have been previously adopted for the spline fitting [2.21–2.24], but some optimization problems remained to be solved:

- Knots have to be selected by a user, making the fit a time consuming procedure with somewhat arbitrary result.
- Cubic splines are not always adequate for complex shapes of curves.
- Calculated uncertainties of the fit value are not always representative.

The Beijing group [2.25] improved the spline fit method and developed the associated computer code SPF. Its basic advantage is generalization for multi-set data, use of any order spline as the base, automated knot optimization and statistically correct calculation of fit uncertainties. In particular, the code can handle discrepant sets of data, assuming that each set can be characterized by its overall weight. Input to the code, in addition to the experimental data (1), is a set of initial knots (2), along with the weight for each set of data. The code uses the iterative procedure, by first fitting the experimental data with the initial knots, then the knots are optimized and the data are fitted again. The reduced χ^2 value, differences between experimental data and fit values, and new knots are given as output at each iteration.

The code runs in an interactive mode. Selection of the base spline order, the number of iterations and fit results are controlled during the interactive process. In order to fit the curves with various shapes, splines with different order can be selected and used in the code (for

instance, the second order for straight lines, the third order for parabolas, the fourth or higher order for peak structures, etc.). In this way, SPF is a more sophisticated and a more advanced tool compared with the traditional cubic spline fit.

The SPF code is a part of the Nuclear Cross Section Evaluation System of the CNDC Beijing. It is interfaced with other related codes. SPF was developed for and used in evaluation of many data for neutron nuclear data files. Fits of charged particle cross-sections performed under the present project represent another application of the SPF code.

2.3.2. Padé fit

The Padé approximation, proposed by H.E. Padé almost hundred years ago [2.26], has become one of the most important interpolation techniques of statistical mathematics [2.26–2.29].

A Padé-I approximant of the order L for a function f(x) is a rational function which has the first L terms of the power series expansion identical with the corresponding terms of the Taylor series of f(x). The Padé-I approximant allows one to bypass convergency limit of the Taylor series. However, one has to calculate high order derivatives of the approximating function. Therefore, Padé-I is not suitable for functions given in a tabular form, particularly when there are significant uncertainties. For the purposes of the present project, where one aims to fit experimental cross-sections measured at various incident energies, one should use the Padé-II approximation.

A Padé-II approximant for a function f(x) is a rational function

$$p_L(x) = R(x)/Q(x), \tag{2.6}$$

where R and Q are polynomials described by altogether L coefficients, exactly matching the function f(x) in L points

$$p_L(x_j) = f(x_j),\ j=1,2,...,L. \tag{2.7}$$

It should be noted that we do not show degrees of polynomials R and Q explicitly since we limit our description on the recurrent solution where these degrees are defined internally.

Until recently, application of the Padé approximation in data fitting and, more generally, in data processing and analysis was hindered by two obstacles. First, there is a difficulty of realization since rational approximants unlike polynomials lead to complicated nonlinear systems of equations in the least squares method. Second, there is a special form of approximant instability — possible real pole-zero pairs (noise doublets). The method to circumvent these two difficulties is based on a recursive calculation of many approximants differing by a choice of interpolation knots along with their statistical optimization by discrete sorting.

Eqs (2.6 and 2.7) result in a system of linear equations for coefficients which may be solved using either determinants or recurrent expressions. The simplest recurrent expression is

$$p_L(x) = \frac{R_{L-1}(x) + \gamma_L (x - x_{L-1}) R_{L-2}(x)}{Q_{L-1}(x) + \gamma_L (x - x_{L-1}) Q_{L-2}(x)}, \tag{2.8a}$$

where the coefficient γ_L can be readily determined from the condition

$$p_L(x_L) = f(x_L)\,, \tag{2.8b}$$

and the initial polynomials are constant

$$R_0(x) = 0, \quad R_1(x) = f(x_1) \text{ and } Q_0(x) = 1, Q_1(x) = 1\,. \tag{2.8c}$$

It can be easily shown that Eqs (2.8) satisfy definition (2.6) and condition (2.7).

Assume the experimental data set (1) with N points. Then, essential stages of the Padé-II approximation of these data are the following:

- chose an initial set of L supporting points (interpolation knots) among the experimental data points ($L << N$),
- apply the recurrent algorithm (8) to these L points and interpolate them with a rational function $p_L(x)$,
- compute $p_L(x)$ for all experimental points and minimize the functional, usually of the type (4),

$$\chi^2 = \sum_{i=1}^{N} (p_L(x_i) - F_i)^2 / \sigma_i^2\,. \tag{2.9}$$

The minimization is done by an iteration using the concept of discrete optimization (sorting). This means that one goes over all possibilities of choosing L points from the available experimental points N, constructs corresponding approximants, computes (9) and looks for its minimum. Once this is completed, L is changed and iteration is repeated until an overall minimum is found from among all discrete possibilities available.

One of the advantages of the discrete optimization as compared to the continuous least squares method (LSM) is the possibility to use a variety of functionals. Theoretical estimates show that the mean quadratic deviation of the approximant, found by the discrete optimization, from the continuous LSM solution is about $(N/L)^{1/2}$ times smaller than the LSM deviation from the exact curve (valid for $L << N$). Thus, the approximant is statistically equivalent to the LSM solution.

The Padé approximant, as a rational function, can be expressed by a set of polynomial coefficients or by a set of the coefficients of the polar expansion. The polar expansion makes use of analytical properties of rational functions in the complex plane. To this end one uses complex vaiables $z = x + iy$ and replaces $p_L(x)$ by $p_L(z)$ that can be expanded as

$$p_L(z) = c + \sum_{\ell} \frac{a_\ell}{z - \eta_\ell} + \sum_{k} \frac{\alpha_k (z - \varepsilon_k) + \beta_k}{(z - \varepsilon_k)^2 + \gamma_k^{\,2}}\quad . \tag{2.10}$$

This may be also called the resonance expansion, with ε_k and γ_k being the energy and the total half-width of the k-th resonance level, and α_k and β_k being partial widths and interference parameters. The first sum corresponds to real poles, the second sum to complex poles.

A prominent disturbing feature of numerically generated rational approximants is the appearance of real poles (zero denominators) inside the approximation interval which is physically senseless and makes the approximant unusable. It appears that the poles are closely accompanied by real zeros of the numerator. These couples constitute so-called noise doublets that prevented wide use of Padé approximants in data fitting.

In the method described above, the noise doublets are not only neutralized but they become in a sense useful. The noise doublets correspond to the terms with $z \approx \eta_\ell$ inside the interval of approximation and with relatively small coefficients a_l in the first sum of Eq. (2.10). In the present method these terms are just cancelled, eliminated from the sum and the regularization gives satisfactory results. Normally, the noise doublets appear with increasing L at final stages of the approximation and indicate, together with statistical criteria, that analytical information is exhausted.

The situation may be different if some points in the input experimental data deviate abnormally from the general trend. In this case the noise doublets appear at relatively low L near those 'bad' points, describing them by local singularities rather than by smooth components. When the singularities are eliminated the resulting regularized curve practically ignores the marked bad points. This is a way to identify automatically points with aberrations.

From the point of view of statistical mathematics the method of discrete optimization is equivalent to the least squares, therefore the experimental data set must be statistically consistent. In the case when there are several sets of experimental data and discrepancies between different sets are significantly larger than their declared uncertainties, statistical processing (fitting) of the data by the described method is possible only after selection of data by an expert. This was found to be fairly frequent the case in the present project, therefore critical analysis and selection of experimental data was applied to all reactions (see Section 2.2 for more details).

The Padé code constructs the approximating rational function, giving the coefficients of the polar expansion (10) for each resonance. Thus, we have an analytical expression, which can be easily calculated at any energy point.

A simple version of the Padé-II code, applicable to cases with a limited number of experimental points, parameters and span of experimental data ($N \leq 500$, $L \leq 40$, $F_i^{\max} / F_i^{\min} \leq 10^6$), is already suitable for many practical situations. The method is also very convenient for calculations of error bands and covariance matrices. A detailed description of the method adopted in IPPE Obninsk and in the present project can be found in the book [2.30] with general outline in Refs [2.31, 2.32].

REFERENCES TO CHAPTER 2

[2.1] BURROWS, T.W., DEMPSEY, P., The Bibliography of the Integral Charged Particle Nuclear Data, 4th Ed. Suppl. 1–2, Rep. BNL-NCS-50640, Brookhaven (1980).

[2.2] HOLDEN, E., RAVAMATARAM, S., DUNFORD, C.L., Integral Charged Particle Nuclear Data Bibliography, 1st Ed. Suppl. 1–5, Rep. BNL-NCS-51771, Brookhaven (1985, 1986, 1987, 1988, 1989).

[2.3] KARLSTROM, I., CHRISTMAN, D.R., Accelerator Produced Nuclides for Use in Biology and Medicine, Rep. BNL-50448 Vol. 1–3, Brookhaven (1975, 1978, 1983).

[2.4] DMITRIEV, P.P., Radionuclide Yield in Reactions with Protons, Deuterons, Alpha Particles and Helium-3, Rep. INDC(CCP)-263, IAEA, Vienna (1986).

[2.5] GANDRIAS-CRUZ, D., OKAMOTO, K., Status on Compilation of Nuclear Data for Medical Radioisotopes Produced by Accelerators, Rep. INDC(NDS)-209, IAEA, Vienna (1998).
[2.6] VUKOLOV, V.A., CHUKREEV, F.E., Evaluated Cross-Sections used as Proton Beam Monitors, Rep. INDC(CCP)-330, IAEA, Vienna (1991).
[2.7] TENDOW, Y., HASHIZUME, A., OHKUBA, Y., KITAO, K., Excitation function for ^{67}Ga production, Riken Accel. Prog. Rep. 23 (1989) 105.
[2.8] KELLER, K.A., LANGE, J., MUNZEL, H., PFENNING, G., Excitation Functions for Charged-Particle Induced Nuclear Reactions, Landolt-Börnstein, Series, Group I, Vol. 5/b, Berlin (1973).
[2.9] ILJINOV, A.S., SEMENOV, V.G., SEMENOVA, M.P., SOBOLEVSKY, N.M., UDOVENKO, L.V., Production of Radionuclides at Intermediate Energies, Landolt-Börnstein, New Series, Group I, Vol. 13, Berlin-Heidelberg-New York, Springer:
– Subvol. A, 1991: Interactions of Protons with Targets from He to Br.
– Subvol. B, 1992: Interactions of Protons with Targets from Kr to Te.
– Subvol. C, 1993: Interactions of Protons with Targets from I to Am.
– Subvol. D, 1994: Interactions of Protons with Nuclei (Supplement to I/13A, B, C).
[2.10] SEMENOV, V.G., SEMENOVA, M.P., SOBOLEVSKY, N.M., Interaction of Deuterons, Tritons and ^{3}He-nuclei with Nuclei in Production of Radionuclides at Intermediate Energies, Landolt-Börnstein New series, Group I, Vol. 13F, Springer-Verlag, Berlin (1995).
[2.11] SEMENOV, V.G., SEMENOVA, M.P., SOBOLEVSKY, N.M., Interaction of α–Particles with Targets from He to Rb in Production of Radionuclides at Intermediate Energies, Landolt-Börnstein New series, Group I, Vol. 13G, Springer-Verlag, Berlin (1996).
[2.12] SEMENOV, V.G., SEMENOVA, M.P., SOBOLEVSKY, N.M., Interaction of α–Particles with Targets in Production of Radionuclides at Intermediate Energies, Landolt-Börnstein New series, Group I, Vol. 13H, Springer-Verlag, Berlin (1996).
[2.13] TOBAILEM, J., DE LASSUS, ST-GENIES, C.H., LEVEQUE, L., Sections Efficaces des Réactions Nucléaires induites par Protons, Deuterons, Particules Alpha, I. Réactions Nucléaires Moniteurs, Note CEA-N-1466 (1), CEA, France (1971).
[2.14] TOBAILEM, J., DE LASSUS ST-GENIES, C.H., Sections Efficaces des Réactions Nucléaires induites par Protons, Deuterons, Particules Alpha, III-Fer, Note CEA-N-1466 (1), CEA, France (1971).
[2.15] ALBERT, P., BLONDIAUX, G., DEBRUN, J.L., GIOVAGNOLI, A., VALLADON, M., "Activation cross-sections for elements from lithium to sulphur", Handbook on Nuclear Activation Data, Technical Reports Series No. 273, IAEA, Vienna (1987) 479.
[2.16] ALBERT, P., BLONDIAUX, G., DEBRUN, G.L., GIOVAGNOLI, A., VALLADON, M., "Thick target yields for the production of radioisotopes", Handbook on Nuclear Activation Data, Technical Reports Series No. 273, IAEA, Vienna (1987) 537.
[2.17] MUNZEL, H., et al., Karlsruhe Charged Particle Reaction Data Compilation, Physics Data, Karlsruhe (1982).
[2.18] SCHWERER, O., OKAMOTO, K., Status Report of Monitor Reactions for Radioisotope Production, Report INDC(NDS)-218, IAEA, Vienna (1989).
[2.19] HASHIZUME, A., "Monitor reactions for the production of radioisotopes for medical use", Proc. Consultants Meeting on Data Requirements for Medical Radioisotope Production, Tokyo, Japan, 1987 (Okamoto, K., Ed.), Rep. INDC(NDS)-195, IAEA, Vienna (1988) 44.

[2.20] BONARDI, M., "The contribution to nuclear data for biomedical radioisotope production from the Milan cyclotron facility", Proc. Consultants Meeting on Data Requirements for Medical Radioisotope Production, Tokyo, Japan, 1987 (Okamoto, K., Ed.), Rep. INDC(NDS)-195, IAEA, Vienna (1988) 98.
[2.21] HORSLEY, A., et al., Curve fitting and statistical techniques for use in the mechanised evaluation of neutron cross sections, Nucl. Instr. and Methods **62** (1968) 29.
[2.22] DE BOOR, C., A Practical Guide to Splines, Springer-Verlag, Berlin (1978) 129–143.
[2.23] SCHUMAKER, L.L., Spline Function: Basic Theory, J. Wiley, New York (1981) 108–118.
[2.24] RUIZHE, LIU, Atomic Energy Science and Technology **30** (1980) 316 (in Chinese).
[2.25] TINGJIN, LIU, et al., Rep. CNIC-00390 (1989).
[2.26] PADÉ, H.E., "Sur la représentation d'une fonction par des fractions rationnelles", Ann. L'Ecole Norm., 1892, No. **9** (3), 3–93.
[2.27] BAKER JR., G.A., GAMMEL, J.L., Ed., The Padé Approximants in Theoretical Physics, Academic Press, New York (1970).
[2.28] GRAVES-MORRIS, P.R., Ed., Padé Approximants and their Applications, Academic Press, New York (1973).
[2.29] BAKER Jr., G.A., Essential of Padé approximants, Acad. Press, New York (1975).
[2.30] VINOGRADOV, V.N., GAI, E.V., RABOTNOV, N.S., "Analytical approximation of data in nuclear and neutron physics", Energoatomizdat, Moscow (1987), in Russian.
[2.31] BADIKOV, S.A., GAI, E.V., GUSEINOV, M.A., RABOTNOV, N.S., "Padé - Approximants in curve fitting and resonance analysis", Proc. Third IMSL User Group Europe Conference, Bologna, Italy, 1990, B11.
[2.32] BADIKOV, S.A., GAI, E.V., GUSEINOV, M.A., RABOTNOV, N.S., "Nuclear data processing, evaluation, transformation and storage with Padé – approximants", Proc. Int. Conf. on Nuclear Data for Science and Technology, Jülich, Germany, 1991 (Qaim, S.M., Ed.), Springer-Verlag, Berlin (1992) 182.

Chapter 3

THEORETICAL EVALUATIONS

(Prepared by M.G. Mustafa, K. Gul, P. Obložinský, Yu.N. Shubin and Y. Zhuang)

Creation of a Reference Charged Particle Cross-Section Database for Medical Radioisotope Production requires the evaluation of both experimental and modeled cross-sections for beam monitor reactions and for radionuclide (positron and gamma emitters) production reactions. It was recognized at the first meeting of the present co-ordinated research project (CRP) in Vienna in 1995 that modeling will play an important role in predicting cross-sections where measurements are either not available or have large discrepancies. Because of the volume of work involving almost fifty reactions in the CRP, it was decided to use modeling as a guide rather than for full evaluation (although in some cases the CRP used the modeled cross-sections as the recommended values). Thus the modeling was done using global input parameters.

This chapter describes the modeling by four different groups: Livermore, Obninsk, Beijing and Islamabad. First, a general overview of nuclear reaction models that may be used in calculating cross-sections below 100 MeV is given. This is followed by a short description of the codes and calculations actually used by the four groups. (The codes have similar basic reaction physics, but they differ in details and in actual applications.) The final section presents a discussion of the modeling with its successes and failures in reproducing experimental data using global input parameters.

3.1. NUCLEAR REACTION MODELS

The specific reactions involved in this CRP are given in earlier sections. The energies for these reactions range from the threshold (several MeV) to about one hundred MeV with protons, deuterons, ^{3}He and alpha particles as projectiles, and targets ranging from light (nitrogen) to heavy (bismuth) masses. The nuclear reaction theories and models covering the target-projectile and energy ranges relevant to this CRP include various preequilibrium models (Blann [3.1], Gadioli and Hodgson [3.2]) coupled with the Hauser-Feshbach theory [3.3] or the Weisskopf-Ewing evaporation model [3.4]. Intranuclear cascade models [3.5-3.8] could be used in this energy regime, but have not been used for this CRP. The quantum mechanical, multistep direct reaction theories (Feshbach et al. [3.9], Udagawa et al. [3.10], Nishioka et al. [3.11]) have started to play a role in this energy range, but the modeling has not yet matured to the level of a routine application to data evaluations. Also R-matrix calculations (Lane and Thomas [3.12]), which are quite complex but more appropriate for lighter targets, such as, ^{14,15}N and ^{16,18}O, are not done here. The CRP relied on evaluation of the experimental cross-sections to obtain the recommended values for targets below $A < 30$. For other targets the cross-sections were modeled using preequilibrium-evaporation formalisms, as described below and in the following section.

The commonly used preequilibrium models are the exciton model and the hybrid model (Gadioli and Hodgson [3.2], Blann [3.1]). Both these semiclassical models originate from the pioneering paper by J.J. Griffin [3.13]. The nuclear state is characterized by the excitation energy of the composite nucleus and the exciton number, which is the total number of particles above and holes below the Fermi surface. It is assumed that all possible ways of sharing the excitation energy between different particle-hole configurations with the same exciton number have equal *a priori* probability. The exciton number changes during the reaction process as a result of intranuclear two-body collisions. At each stage of the reaction

there may be a non-zero probability that a particle is emitted. If this happens at an early stage, we speak of pre-equilibrium emission. If the emission does not occur at an early stage, the system eventually reaches the equilibrium or evaporation stage. This stage is described by the Weisskopf-Ewing formalism [3.4] (which does not treat angular momentum and parity explicitly) or more rigorously by the Hauser-Feshbach formalism [3.3] which explicitly treats vector coupling of spins and parities between compound and residual nuclei and ejectiles. Preequilibrium models have been widely used in modeling nuclear cross-sections below 200 MeV and have provided an adequate description of the high-energy tails (i. e., the region between the evaporation peak and the discrete states) of the outgoing particle spectra (Blann et al. [3.14], Michel and Nagel [3.15]). The details of the preequilibrium and evaporation models are given as appropriate in the next section on "codes and calculations". Here the essential ideas are provided with some simple expressions.

Several formulations of PE decay are in use; these are the hybrid, the geometry dependent hybrid (GDH) and the exciton model formulations. These approaches rely on a quantity called the partial state density, which is the number (per MeV) of energy partitions available for a Fermi gas where every partition of p particles and h holes is assumed to occur with equal *a priori* probability. The first expression for this partial state density was due to Ericson and Strutinsky [3.16],

$$\rho_n(E) = g(gE)^{n-1}/(p!h!(n-1)!)\,, \tag{3.1}$$

where *n*, the exciton number, equals the number of excited particles *p* plus holes *h*, *E* is the excitation energy in MeV, and *g* the single particle level density at the Fermi energy. PE decay models in use make the assumption that within each exciton hierarchy, all configurations are populated with equal *a priori* probability.

The second quantity in the Griffin (exciton) model is the exciton-exciton transition rate. This may be given by the "golden rule" of the first-order time-dependent perturbation theory,

$$\lambda_{nn'} = \frac{2\pi}{\hbar}\left|M\right|^2 \rho_{n'}(E)\,, \tag{3.2}$$

where $|M|^2$ is the square of the matrix element corresponding to a residual two-body interaction. For most applications an energy- and mass-dependent average value for $|M|^2$ is used.

The probability for the preequilibrium emission of a particle with energy ε is given by

$$W_p(\varepsilon)d\varepsilon = \sum_n \frac{\rho_{n-1}(U)\rho_c(\varepsilon)d\varepsilon}{\rho_n(E)}\,. \tag{3.3}$$

Here the sum is over all possible exciton states, which may be reached starting with a given initial exciton number. The residual nuclear excitation energy *U* is given by $U = E - (\varepsilon + B)$, where *B* is the binding energy of the emitted particle.

The Griffin model was extended by Blann [3.17] and others (Williams [3.18]; Obložinský et al. [3.19]), and gives more complete expressions for the exciton–exciton transition rates.

$$\lambda_{n,n-2} = \frac{2\pi}{\hbar}\left|M\right|^2 g\,\frac{ph(n-2)}{2} \tag{3.4a}$$

$$\lambda_{n,n} = \frac{2\pi}{\hbar}|M|^2 g^2 E \frac{p(p-1)+4ph+h(h-1)}{2n} \tag{3.4b}$$

$$\lambda_{n,n+2} = \frac{2\pi}{\hbar}|M|^2 \frac{g^3 E^2}{2(n+1)}. \tag{3.4c}$$

It is worth pointing out here that one significant difference between the exciton model and the hybrid model formulations is in the treatment of these transition rates. The hybrid and the geometry dependent hybrid models do not use the "matrix element" formulations (see next section).

After the preequilibrium emissions, the Hauser-Feshbach or Weisskopf-Ewing theories treat the remainder of the reaction process. A compact formula for the cross-section for a reaction A(a,b)B may be written as:

$$\sigma_{ab} = \sum_{J\pi} \frac{T_a T_b}{\sum_i \sum_c T_{ic}}, \tag{3.5}$$

where the index *i* stands for the different types of outgoing particles (n,p,d,..), and the T's are the transmission coefficients calculated from an optical potential for particles a and b. The index *c* stands for all possible final states which are either discrete excited levels of the residual nucleus or a continuum of levels described by a level density formula. A recent handbook by IAEA [3.67] is an excellent source of information on optical potentials, various level density formulations and other aspects of modeling reaction cross-sections.

Three groups and K. Gul (Islamabad, Pakistan) were involved in modeling cross-sections for this CRP. The group at Obninsk used the ALICE-IPPE code [3.20], the group from China used the Spec code [3.21] and the Livermore group used ALICE-HMS [3.22] for nucleon induced reactions and ALICE-91 [3.23] for deuteron, ^{3}He and alpha induced reactions. The ALICE family of codes are based on the hybrid, the geometry-dependent hybrid (GDH) or the HMS preequilibrium models and the Weisskopf-Ewing evaporation formalism. The Spec code is also constructed within the framework of the Weisskopf-Ewing evaporation formalism, but preequilibrium decay is calculated from the master equation exciton model [3.1]. The ALICE-HMS code uses a Monte Carlo precompound formulation with Weisskopf-Ewing evaporation. The lack of angular momentum and parity treatments in the Weisskopf-Ewing formalism used in these codes may be of some concern for certain aspects of reaction yields, (e.g. isomer yield calculations). But these codes are fast and convenient to use, i.e. when many natural isotopes are involved and many particles are emitted in the reaction process, and have generally been found to be adequate when cross-sections for isomeric states are not needed. Gul used codes, HFMOD [3.24] and PREMOD [3.25], in his calculations. The HFMOD code is based on the Hauser-Feshbach formalism and the PREMOD code is based on the concept of the geometry-dependent hybrid preequilibrium model generalized to include discrete levels, and to conserve angular momentum and parity. For complete formulations of the codes used in this CRP we refer to the appropriate references, but some of the highlights are given in the next section.

3.2. CODES AND CALCULATIONS

A variety of codes (such as GROGI, STAPRE, ALICE, GNASH, SPEC and their modifications) have been developed on the basis of equilibrium and preequilibrium reaction mechanisms. These codes have similar physics with different degrees of complexity in input preparation and require different computing times. Some of them are used when detailed

properties of nuclear reactions are needed, including population of discrete levels. For example, the STAPRE and GNASH codes are good choices if one needs to have information on each channel participating in the reaction process, and when the excitation energy (and the number of open channels) is not too large. On the other hand, when the number of open channels is large and it is impossible or very time consuming to provide all the required input data with sufficient accuracy, the advantages of these detailed codes may be reduced. In such a case, the faster codes with less effort in input preparation are often more practical choices. The ALICE family of codes developed by Blann and a recent modification by the Obninsk group fall in this class, and are used in the calculations of the reaction cross-sections for medical radioisotope production for the present CRP. We refer to recent international code comparisons for further details on many of the codes in current use (Pearlstein [3.26], Blann et al. [3.14], Michel and Nagel [3.15]).

3.2.1. ALICE-91 code

This is the latest released version of the standard ALICE code at Livermore (Blann [3.23]), which uses hybrid or geometry dependent hybrid precompound models and Weisskopf-Ewing evaporation for the equilibrium part of the reaction process. The basic physics has been widely described in the literature, but most physics can be found in (Blann [3.1]; Blann and Vonach [3.27]). Earlier versions of ALICE did not include gamma ray competition with nucleon, deuteron and alpha emissions. The gamma competition is included since 1990. The gamma emission rate is calculated by microscopic reversibility based on the giant dipole with Lorentzian line shape (Blann et al. [3.28]). The ALICE code uses the Fermi gas level density and has the option of using the shell-dependent level densities from Katatria and Ramamurthy [3.29]. The code includes multiple preequilibrium nucleon emission. Some of these features are described below.

Hybrid model formulation

The hybrid model (Blann [3.1]) for precompound decay may be written as

$$\frac{d\sigma}{d\varepsilon} = \sigma_R \sum_{n=n_0}^{\bar{n}} \frac{X_\nu^n \, \rho_{n-1}(U)}{\rho_n(E)} \, \frac{\lambda_c(\varepsilon)}{\lambda_c(\varepsilon) + \lambda_+(\varepsilon)} D_n d\varepsilon \,, \tag{3.6}$$

where the terms in the first set of brackets are the Ericson partial state densities, and X_ν^n is the number of excitons of type ν (ν = neutron or proton) which are available for emission in the energy range ε to $\varepsilon + d\varepsilon$, and $U = E - B_\nu - \varepsilon$, where B_ν is the binding energy of particle type ν, neutron or proton. The term $\lambda_c(\varepsilon)$ is the rate of nucleon emission into the continuum, and $\lambda_+(\varepsilon)$ is the competing rate of two body collisions for the nucleons at energy ε. The factor D_n is a depletion factor, which represents the fraction of the population surviving decay prior to reaching the *n* exciton configuration.

The factor X_ν^n represents the exciton numbers for neutrons and protons for a given total exciton state n. The default values in the ALICE code for neutron induced reactions are

$$X_n^3 = \frac{2(3Z + 2N)}{(3Z + 2N + 3Z)} \tag{3.7a}$$

and

$$X_p^3 = 2 - X_n^3 \,, \tag{3.7b}$$

and for proton induced reactions

$$X_p^3 = \frac{2(3N+2Z)}{(3N+2Z+3N)} \tag{3.7c}$$

and

$$X_n^3 = 2 - X_p^3 . \tag{3.7d}$$

These choices are guided by the fact that for nucleon induced reactions the initial exciton state is a 2p-1h and that the n-p scattering cross-section is three times that of n-n or p-p scattering.

The corresponding values for deuteron and alpha induced reactions are 1,1 and 2,2. These initial values are assumed to increase by 0.5 in successive values of n in Eq. (6), as the particle exciton number increases by 1.

The nucleon-nucleon scattering rate is based on either the imaginary optical potential, where the mean free path is given by (Blann [3.30])

$$L(\varepsilon) = \left[\frac{\hbar^2}{4m} \frac{1}{W^2} \left(\varepsilon + V + \sqrt{(\varepsilon+V)^2 + W^2} \right) \right]^{1/2} \tag{3.8a}$$

$$\cong \frac{\hbar^2}{2mW} \sqrt{2m/\hbar^2 (\varepsilon + V)} , \tag{3.8b}$$

or on Pauli-corrected nucleon-nucleon scattering cross-sections, where the mean free path is given by (Kikuchi and Kawai [3.62])

$$L(\varepsilon) = \frac{1}{\rho \overline{\sigma}_0} , \tag{3.9}$$

where ρ is the density of nuclear matter and $\overline{\sigma}_0$ is the Pauli-corrected nucleon-nucleon (N-N) scattering cross-section, appropriately weighted for target neutron and proton numbers. The intranuclear transition rate $\lambda_+(\varepsilon)$ is the quotient of nucleon velocity (in the potential well) divided by the mean free path. A closed form expression valid for nuclear matter of average density is given as (Blann [3.1])

$$\lambda_+(\varepsilon) = 1.4 \text{ x } 10^{21} (\varepsilon + B_\nu) - 6 \text{ x } 10^{18} (\varepsilon + B_\nu)^2 / \text{sec} , \tag{3.10}$$

where $\varepsilon + B_\upsilon$ is the energy of nucleon ν above the Fermi energy. The continuum emission rate, $\lambda_c(\varepsilon)$ is given by microscopic reversibility as

$$\lambda_c(\varepsilon) = (2s+1)\Omega \frac{4\pi p^2 dp}{h^3} \frac{\sigma \nu}{\Omega g} , \tag{3.11}$$

where s is the nucleon spin, Ω the laboratory volume, p the nucleon momentum in the continuum, g the single particle level density in the nucleus, v the nucleon velocity in the laboratory, and σ the inverse cross-section. With these last two equations and the Ericson partial state density expression, we can calculate absolute PE spectra with Eq. (3.6). When we calculate N-N collision rates in the code ALICE, we have two options. One is to use the imaginary optical potential given by Becchetti and Greenlees [3.53]; the other is to use

Eq. (3.9) calculating $\overline{\sigma}_0$ based on expressions due to Kikuchi and Kawai [3.62] weighted for composite nucleus N and Z (rather than using the approximation of Eq. (3.10).

All the discussions above apply to a single precompound nucleon emission. Multiple nucleon emission, such as, nn, np and pp emissions are also treated in the ALICE-91 code (Blann and Vonach [3.27]).

Multiple particle emission

Multiple precompound decay processes must be considered at higher excitations since they are important in determining the cross-section surviving to the (equilibrium) compound nucleus, and in determining yields of products which require multiple precompound emission for population, e.g. a (p, 2p) reaction on a heavy element target. There are two types of multiple precompound decay which might be considered. Type I results when a nucleus emits more than one exciton from a single exciton hierarchy. It may be seen that, e.g. in a two particle-one-hole configuration, up to two particles could be emitted; in a three particle-two-hole configuration up to three particles could be emitted, etc.

The second type of multiple precompound decay (type II) would be described by the sequence "particle emission, one or more two body intranuclear transitions in daughter nucleus, particle emission." If the intervening two-body transitions are omitted from this sequence, it becomes type I multiple emission. In the type II sequence for nucleon induced reactions, the leading term would be two particle-two-hole. Results confirm the speculation that type I multiple precompound decay is far more important than type II for most reactions at moderate excitations. Because the first particle emission leaves a range of residual excitations and exciton numbers, a calculation of type II emission becomes more complex and time consuming than for type I emission.

To extend Eq. (3.6) to higher energies and maintain its simplicity, we have made some arbitrary assumptions to estimate type I multiple particle emission branches. We define those assumptions which are based on simple probability arguments.

If P_n and P_p represents the total number of neutron and proton excitons emitted from a particular exciton number configuration, we assume that

$$P_{np} = P_n P_p \tag{3.12}$$

is the number of either type of particle emitted in coincidence with the other from the same nucleus and exciton hierarchy. This definition covers P_{pn} since in an emission from the same exciton number there is no distinction to be made.

We assume that the number of neutrons which are emitted in coincidence with another neutron from a particular exciton number configuration is given by

$$P_{nn} = 2\frac{P_n}{2}\frac{P_n}{2}, \tag{3.13}$$

with the fraction of the reaction cross-section decaying by the emission of two coincident neutrons being $P_{nn}/2$ The value of P_{nn} is restricted to be $\leq P_n - P_{np}$. Similar expressions are used for proton-proton coincident emissions.

The number of neutrons (protons) emitted from the n-exciton configuration, which is not in coincidence with another particle, is given by

$$P_n\,(\text{n only}) = P_n - P_{nn} - P_{np} \tag{3.14a}$$

$$P_p \text{ (p only)} = P_p - P_{pp} - P_{np} \tag{3.14b}$$

and the fraction of the population F_n which had survived decay of the exciton number in question is

$$F_n = 1. - P_n(\text{n only}) - P_p(\text{p only}) - P_{pp}/2 - P_{nn}/2 - P_{np} \tag{3.15}$$

This fraction would multiply the fractional population which had survived to the n exciton state, i.e. is the depletion factor multiplier.

From the calculated total precompound neutron emission spectrum $d\sigma_n(\varepsilon)/d\varepsilon$, the cross-section which could be involved in the emission of two neutrons is calculated as

$$\sigma_{2n} = \int_{U=0}^{E-B_{2n}} \frac{d\sigma_n(\varepsilon)}{d\varepsilon} d\varepsilon\,, \tag{3.16}$$

where B_{2n} represents the sum of first and second neutron binding energies.

Similarly the neutron cross-section which could be emitted in coincidence with protons is given by

$$\sigma_{np} = \int_{U=0}^{E-B_n-B_p} \frac{d\sigma_n(\varepsilon)}{d\varepsilon} d\varepsilon\,, \tag{3.17}$$

where B_n is the binding energy of the first emitted neutron and B_p is the proton binding energy of the daughter nucleus following neutron emission. Similar integrals are made for the proton emission cross-section which could consist of two coincident protons, σ_p, and of a proton in coincidence with neutron, σ_{pn}. The cross-section available for the emission of a single nucleon $\sigma_{p)}$ is, of course, the sum of all $d\sigma(\varepsilon)/d\varepsilon$ (the integrals are replaced by sums since the code computes spectra at fixed energy intervals). For the daughter nucleus following emission of one and only one precompound neutron, we calculate

$$\sigma^{A-1,Z}(U) = \frac{d\sigma(\varepsilon)}{d\varepsilon}\frac{C_n}{\sigma_n}\,, \tag{3.18}$$

where $U - E - B_n - \varepsilon$; for the daughter nucleus following the coincident emission of two neutrons, we calculate

$$\sigma^{A-2,Z}(U) = \frac{d\sigma_n(\varepsilon)}{d\varepsilon}\frac{C_{nn/2}}{\sigma_{nn}}\,, \tag{3.19}$$

where $U = E - B_n - B_p - \varepsilon - \bar{\varepsilon}_{p(n)}$, and where $\bar{\varepsilon}_n$ is the average kinetic energy of the second neutron for a given energy ε of the first neutron. For the case of the daughter nucleus produced by the coincident emission of a neutron and a proton,

$$\sigma^{A-2,Z-1}(U) = \frac{C_{np}}{2\sigma_{np}}\frac{d\sigma_n(\varepsilon)}{d\varepsilon} + \frac{C_{np}}{2\sigma_{pn}}\frac{d\sigma_p(\varepsilon)}{d\varepsilon}\,, \tag{3.20}$$

where $U = E = B_n - B_p - \varepsilon - \bar{\varepsilon}_{p(n)}$ as previously defined, and where $\bar{\varepsilon}_{p(n)}$ is the average kinetic energy of the proton (neutron) emitted in coincidence with a neutron (proton) of kinetic

energy . An expression analogous to Eq. (3.19) is used for the case of two-proton emission. The quantities C_n, C_p, C_{np} and C_{nn} (C_{pp}) are defined as follows: C_n is the cross-section for emitting one and only one neutron summed over all exciton numbers, C_p is the same as C_n but for protons, C_{np} is for a neutron and a proton, and similarly for C_{nn} and C_{pp}.

Level densities and pairing options in ALICE-91

The Fermi gas level density used in the ALICE codes is described first for completeness. The level density expression is

$$\rho(U) \propto (U-\delta)^{-5/4} \exp\left[2\sqrt{a(U-\delta)}\right], \tag{3.21}$$

where U is the excitation energy and δis the pairing gap. The level density parameter a is given by, a = A/9, as a default option. The pairing in ALICE has two options: the backshift or a 'normal' shift with δ given by

$$\delta = 11/A^{1/2}. \tag{3.22}$$

The backshifted option uses true thermodynamic excitations for doubly even nuclei, and increases it by δ for odd A nuclei and 2 δ for doubly odd nuclei. The normal shift option, on the other hand, uses true thermodynamic excitations for odd A nuclei, reduces the excitation by δ for doubly even nuclei, and increases it by δ for doubly odd nuclei. In addition, ALICE has the option of using the a and δ parameters from the Kataria and Ramamurthy formalism, which includes shell and pairing effects.

The ALICE code has been used extensively and its predictive power is shown to be quite satisfactory up to 200 MeV (Blann et al. [3.14], Michel and Nagel [3.15]). The Livermore group has done all their calculations for *d*, ^{3}He, and alpha induced reactions for this CRP using the hybrid PE formulation. They used the Monte Carlo approach, ALICE-HMS, for nucleon induced reactions.

Geometry dependent hybrid model (GDH)

The basic idea (Blann [3.30]) is that nucleus has a density distribution which can affect PE decay in two ways. First, the nucleon mean free path is expected to be longer (on average about a factor of two) in the diffuse nuclear surface. Secondly, in a local density approximation, there is a density dependent limit to the hole depth; this will be expected to additionally modify the Ericson state densities with respect to use of a single, averaged potential depth. These two changes were incorporated into the 'geometry dependent hybrid model'. We present next a description of these changes with specific reference to the code ALICE. The Obninsk group uses the GDH formulation option of ALICE in their ALICE-IPPE code with some modifications, which are described later.

In order to provide a first order correction for the influence of nuclear density, the hybrid model may be reformulated as a sum of contributions, one term for each entrance channel impact parameter with parameters evaluated for the average local density of each impact parameter. In this way, the diffuse surface properties sampled by the higher impact parameters are crudely incorporated into the precompound decay formalism in the GDH model. The differential emission spectrum is given in the GDH model as

$$\frac{d\sigma_\upsilon(\varepsilon)}{d\varepsilon} \pi \lambda^2 \sum_{\ell=0}^{\infty} (2\ell+1) T_\ell P_\upsilon(\ell,\varepsilon), \tag{3.23}$$

where l is the entrance channel orbital angular momentum, T_l the transmission coefficient and $P_\nu(l,\varepsilon)$ is the decay probability at exit channel energy ε, as given in Eq. (3.6) . When the approach is used for incident nucleons, T_l is provided by an optical model subroutine. Whereas the intranuclear transition rates entering in the hybrid model are evaluated for nuclear densities averaged over the entire nucleus, those appropriate for the GDH model are averaged over the densities corresponding to the entrance channel trajectories, at least for the contributions from the first projectile-target interaction. The multi-particle preequilibrium emission is treated in the GDH model as it is described in the hybrid model.

The effect of limited hole depth is less physically established than the influence of density on mean free path; nonetheless it seems to be important in reproducing experimental spectral shapes. The result of this local density approximation limitation is to effectively reduce the degrees of freedom, especially for the higher incident partial waves (for which a lower maximum hole depth is predicted), thereby hardening and enhancing the predicted emission spectra. In our use of ALICE, we use the option under which the restriction on hole depth in the GDH model applies only to the first collision, for which there is some knowledge of average density at the collision site, and then only for nucleon induced reactions.

The original GDH model employed a Fermi density distribution function,

$$d(R_\ell) = d_s\left[\exp(R_\ell - C)/0.55\,\text{fm} + 1\right]^{-1}, \tag{3.24}$$

with

$$C = 1.07A^{1/3}\text{fm}, \tag{3.25}$$

taken from electron scattering results (Hofstadter [3.31]). The radius for the lth partial wave was defined by

$$R_\ell = \lambda\!\!\!^{-}(\ell + 1/2). \tag{3.26}$$

The charge radius C of Eq. (3.25) has been replaced in the present parameterization by a value characteristic of the matter (rather than charge) radius based on the droplet model work of Myers [3.46], plus a projectile range parameter $\lambda\!\!\!^{-}$,

$$C = 1.18A^{1/3}\left[1 - 1/(1.18A^{1/3})^2\right] + \lambda\!\!\!^{-}. \tag{3.27}$$

In the hybrid model, the average nuclear density is calculated by integration and averaging of Eq. (27) between R = 0 and R = C +2.75 fm. The single particle level densities are defined in the precompound routine of ALICE by

$$g_n = \frac{N}{28}, \text{ and } g_p = \frac{Z}{28}. \tag{3.28}$$

3.2.2. ALICE-HMS code and Livermore calculations

The ALICE-HMS code is based on a new precompound model described in (Blann [3.22]). This hybrid Monte Carlo simulation (HMS) model does not rely upon exciton state densities beyond three excitons, permits unlimited multiple precompound emission for each interaction and may be used to calculate exclusive particle spectra and yields. The evaporation part of the calculation is done with the usual Weisskopf-Ewing formalism, as in the ALICE-91 code.

The HMS precompound decay model is formulated to reduce several inconsistencies and limitations of earlier formulations, such as in the hybrid, GDH and exciton models. These precompound formulations have relied upon contributions from the entire exciton populations based on a sequence of two-body collisions. It is further assumed that all possible ways of sharing the excitation energy between different particle-hole configurations with the same exciton number have equal a-priori probability. It was clearly shown that equal a-priori population assumption may be valid only for states with the first exciton number (three excitons for nucleon induced reactions) (Blann and Vonach [3.27]) and not for higher exciton states (Bisplinghoff [3.32]). Additionally, existing precompound formulations were not suited for multiple PE emissions beyond two, yet this becomes important at energies above ~50 MeV. To overcome these problems, Blann developed the HMS Monte Carlo precompound model, which uses only the kinematically justified two and three exciton densities with unlimited precompound particle emission. The formulation otherwise follows the philosophy of the hybrid model. The new approach is therefore referred to as the hybrid Monte Carlo simulation (HMS) model. It should be valid up to the pion threshold.

In the HMS approach, incident nucleons that make only 3-exciton states are considered. For each nucleon energy (selected at weighted random from the possible range of energies) the nucleon will either be emitted, or will rescatter. If it is emitted, the emission probability is calculated from equations (3.6), (3.9), and (3.11) of the hybrid model, using the $n=n_0$ term only in Eq. (3.6). (The remaining two quasiparticles will share the balance of the excitation energy and will initiate their own 3-quasiparticle states and then either decay or rescatter.) If the initial nucleon rescatters, it will make a new 3-exciton state and the process of decy or rescatter continues. The hole energy is similarly allowed to initiate a 2hole–1particle state, etc. In this fashion each cascade treats only the physically justified 2 and 3 exciton states, and can treat any number of precompound decays for each cascade.

The HMS model enjoys another advantage over closed form decay models (exciton, hybrid, GDH) for calculation of particle spectra and recoil distributions. Because it is preformed in an event mode, the velocity of the emitting nuclide may be modified according to the angle and energy of each nucleon previously emitted, giving proper laboratory/center of mass transformations. The two-body assumption necessary in closed form calculations may be seen to be quite poor when comparisons are made between the two models.

The Monte Carlo precompound formulation is available at present for neutron and proton induced reactions, but not for deuteron, ^{3}He or alpha particle induced reactions. The Livermore group therefore used ALICE-HMS for proton induced reactions in this CRP, but used the ALICE-91 code for all other reactions. Both codes used optical models for incident nucleons, and for all inverse reaction cross-sections. The parameter sets used are described in (Blann and Vonach [3.27]).

The calculations by the Livermore group for this CRP are based on global optical potentials included in the code, and two level density options: Fermi gas level density or shell dependent level densities given by the model of Kataria and Ramamurthy [3.29]. For deuteron induced reactions Livermore studied the effects of the deuteron breakup in the entrance channel (Mustafa [3.33]) using a microscopic theory developed by Udagawa and Tamura [3.34, 3.35] coupled with a modified ALICE-91 code. In this approach the Udagwa and Tamura model was used to deduce the spectra of neutrons and protons transferred into the target nucleus (stripping to bound states and breakup-capture in the continuum); these were then assumed to initiate three-quasiparticle cascades. The deuteron cross-section that does not undergo stripping and breakup-capture was assumed to initiate a separate preequilibrium cascade. Detailed calculations were done for deuteron induced reactions on ^{48}Ti in order to

empirically select the best initial exciton number to use for deuteron induced reactions. The results were used to choose the precompound initial exciton number parameters for the remaining deuteron induced reactions for this CRP. The total number of initial excitons thus chosen in the calculation is two, i. e. one proton and one neutron above the Fermi surface. The ^{3}He induced reactions are also known to have a sizeable breakup cross-section. This problem has not been addressed here. Therefore, the choice of the initial exciton number for ^{3}He induced reactions and also for alpha induced reactions is arbitrary. Four excitons, two protons and 1 neutron (and one hole) are used for ^{3}He induced reactions, and four excitons, two protons and two neutrons, for alpha induced reactions. Because of the global nature of these parameters, the calculated cross-sections for this CRP should be used as a guide rather than as a fit to the experimental data. Using a single global parameter choice allows an estimation of the predictive powers of the models; varying parameters to fit each data set precludes this.

3.2.3. ALICE-IPPE code and Obninsk calculations

The ALICE-IPPE code is the ALICE-91 code version modified by the Obninsk group [3.20] to include the generalized superfluid level density model of Ignatyuk and colleagues [3.35-3.39] and preequilibrium cluster emissions. For the preequilibrium nucleon emission the geometry dependent hybrid (GDH) model is used. Calculation of the alpha particle spectra is performed taking into account both the pickup (Iwamoto and Harada [3.40], Sato et al. [3.41]) and knockout processes (Milazzo-Colli and Braga-Marcazzan [3.43], Ferrero et al. [3.44], Obložinský and Ribansky [3.45]). A phenomenological approach is used to describe direct emission of the deuteron (Dityuk et al. [3.20]). The triton and ^{3}He spectra are calculated according to the coalescence pickup model of Sato, Iwamoto and Harada [3.40]. The level density formalism includes both collective and non-collective effects, and excitation-energy-dependent shell effects. These level density improvements over the Fermi gas model are described here. For details on the cluster emission models and calculations we refer to (Dityuk et al. [3.20]) and references therein.

Generalized superfluid model of level densities

The Fermi gas model, as used in the ALICE-91 and ALICE-HMS codes, has a simple and convenient form for global applications. However, the model is inadequate when nuclear shell and collective effects become important. (A simple approach due to Kataria and Ramamurthy to incorporate shell structure effects in the level densities has been mentioned earlier and offered as an option in the ALICE codes.) Detailed microscopic calculations are now possible, but they are time consuming and their success in reproducing experimental level densities are yet to be proven. Ignatyuk and his colleagues at Obninsk have developed a phenomenological approach to level density calculations which includes both shell effects and collective enhancements (rotational and vibrational) to level densities. This is referred to as the generalized superfluid model and has been incorporated in the ALICE-IPPE code.

The level density expression has now three components:

$$\rho(U) = \rho_{qp}(U')K_{vib}(U')K_{rot}(U'), \tag{3.29}$$

where ρ_{qp} (U') is the level density due to quasiparticle (non-collective) nuclear excitations only, and K_{vib}(U') and K_{rot}(U') are the level density enhancements due to vibrational and rotational states, respectively, at the effective excitation energy U'.

The energy dependence of the quasiparticle level density is calculated on the basis of the superfluid nuclear model (Ignatyuk et al., 1979). The correlation function for the ground states of nuclei is defined as $\Delta_0 = 12.0/A^{1/2}$ MeV. This choice of Δ_0 is consistent with the systematics of nuclear masses (Myers [3.46]) and with analysis of the experimental data on neutron resonances (Ignatyuk *et al.* [3.39]). The critical temperature of the phase transition from superfluid to normal state, the condensation energy, the critical energy of the phase transition and the effective excitation energy are connected with the correlation function Δ_0 by the following equations:

$$t_{cr} = 0.567\ \Delta_0 \tag{3.30a}$$

$$U_{cr} = 0.472\, a_{cr}\, \Delta_0{}^2 - n\,\Delta_0 \tag{3.30b}$$

$$E_{con} = 0.152 \cdot a_{cr}\, \Delta_0{}^2 - n\,\Delta_0 \tag{3.30c}$$

$$U' = U + n\Delta_0 + \delta_{shift}\ , \tag{3.30d}$$

where n = 0,1 and 2 for even-even, odd and odd-odd nuclei, respectively, and the value of the excitation energy shift δ_{shift} is chosen on the basis of a consistent description of the level density of low lying collective levels and the data on neutron resonances.

The shell effects are included into consideration using the energy dependence of nuclear level density parameter a(U,A), determined phenomenologically:

$$a(U,Z,A) = \tilde{a}(A)\left(1 + \delta W(Z,A)\frac{\varphi(U'-E_{cond})}{U'-E_{cond}}\right) \quad \text{for} \quad U' > U_{cr} \tag{3.31a}$$

$$a(U,Z,A) = a(U_{cr},Z,A) \quad \text{for} \quad U' < U_{cr}\ , \tag{3.31b}$$

where the asymptotic value of level density parameter at high excitation energy is equal to

$$\tilde{a}(A) = 0.073A + 0.115A^{2/3}\ , \tag{3.32}$$

and where δW(Z,A) is the shell correction to the nuclear binding energy taken from the experimental values of nuclear masses or from the Myers-Swiatecki mass formula [3.42] when experimental masses are unknown. The function φ (U) = [1–exp(–γU)] is dimensionless and defines the energy dependence of the level density parameter at low excitation energies within the value of $\gamma = 0.4/A^{1/3}$ chosen from the neutron resonances.

The vibration enhancement of nuclear level density is presented in the following form

$$K_{vib} = \exp[\delta S - (\delta U / t)], \tag{3.33}$$

where δS and δU are the changes in the entropy and excitation energy, respectively, resulting from the vibrational modes. These changes are described by the relations of the Bose gas:

$$\delta S = \sum_{i=1}^{\infty}(2\lambda_i + 1)[(1+n_i)\ell n(1+n_i) - n_i \ell n(n_i)] \tag{3.34a}$$

$$\delta U = \sum_{i=1}^{\infty}(2\lambda_i + 1)\omega_i n_i\ , \tag{3.34b}$$

where ω_i and λ_i are the energies and the multipolarities of collective excited state, and n_i is its population at a given temperature. The attenuation of vibrational enhancement of level density at high temperatures is taken into account with the following occupation number dependence:

$$n_i = \frac{\exp[-\gamma_i/(2\omega_i)]}{\exp[\omega_i/t]-1}, \tag{3.35}$$

where Υ_i is the spreading width of the vibrational excitation and is given by

$$\gamma_i = 0.0075A^{1/3}\left(w_i^2 + 4\pi^2 t^2\right). \tag{3.36}$$

The quadrupole and octupole states are considered in the calculations only. The position of the lowest state for the all nuclei, with exception of ^{208}Pb, was defined by phenomenological equations which reproduced the experimental data well enough for middle weight nuclei:

$$\omega_2 = 30A^{-1/3}, \quad \omega_3 = 50A^{-1/3}. \tag{3.37}$$

For all spherical nuclei the coefficient of vibrational enhancement of the level $K_{vibr}(U')$ was taken into account according to Eq. (3.33). For deformed nuclei the enhancement of level density connected with the rotational mode of collective excitation $K_{rot}(U')$ was taken into account according to Bohr and Mottelson [3.47]:

$$K_{rot}(U) = \sigma_\perp^2\, g(U) = \sigma^2(1+\beta/3)g(U), \tag{3.38}$$

where σ^2 is the spin cut-off factor, and g(U) is the empirical function taking into account the attenuation of rotation modes at high energies as proposed by Hansen and Jensen [3.48]:

$$g(U) = \left[1+\exp(U-U_r)/d_r\right]^{-1}, \tag{3.39}$$

where the parameters of the attenuation function are connected with the quadrupole nuclear deformation β by the relations:

$$U_r = 120A^{-1/3}\beta^2;\ d_r = 1400A^{-2/3}\beta^2. \tag{3.40}$$

The parameter β is taken from Myers [3.46].

We have described above the important features of the level density calculations using the generalized superfluid model of Ignatyuk and colleagues, as included in the ALICE-IPPE code. These improvements over the Fermi gas model description of the level density are based on components of the nuclear structure theory, i.e. pairing, shell and collective effects.

3.2.4. SPEC code and Beijing calculations

SPEC (Shen and Zhang [3.21]) is a code for calculating the neutron or charged particle (p, d, t, ^{3}He, α) induced reactions on medium-heavy nuclei in the incident energy range up to 60 MeV including up to 6 successive emission processes per nucleus. For those reaction channels contributed only by 1~5 emission processes the incident energy can go up to 100 MeV. This program is written in FORTRAN-77.

SPEC is constructed within the framework of the optical model, the master equation exciton model (Blann [3.1]), and the Weisskopf-Ewing evaporation model [3.4]. For the first and second particle emission processes, the preequilibrium emission and evaporation are considered, but for 3-6 particle emission processes, only evaporation is considered. The

preequilibrium and direct reaction mechanisms of γ emission (Akkermans et al. [3.49]) are also included. The effect of the recoil nucleus is considered for calculating spectra.

The master equation exciton model is given by

$$\begin{aligned} -\delta_{n,n_0} &= \lambda\_(n+2,E)\tau(n+2,E)+\lambda_+(n-2,E)\tau(n-2,E) \\ &-[\lambda_+(n,E)+\lambda\_(n,E)+W_\ell(n,E)]\tau(n,E), \end{aligned} \tag{3.41}$$

where E is the excitation energy. The quantities γ_+ and $\gamma\_$ are the intranuclear transition rates. For composite particle emission, the pick-up mechanism of cluster formation (Iwamoto et al. [3.40], Sato et al. [3.41], Zhang et al. [3.50], Zhang et al. [3.51]) is used in the first and second particle emission processes. The cluster b is defined by the distribution of particles above and below the Fermi surface ℓ, m. By means of the detailed balance principle the emission rate of ℓ particles above Fermi surface can be expressed as

$$W_b^\ell(p,h,E,\varepsilon_b)=\frac{2I_b+1}{\pi^2\hbar^3}\mu_b\varepsilon_b\sigma_b(\varepsilon_b)F_{\ell,m}(\varepsilon_b) \tag{3.42a}$$

$$Q_{\ell,m}^b(p,h)\frac{\rho(p-\ell,h,E-\varepsilon_b-B_b)}{\rho(p,h,E)}, \tag{3.42b}$$

where I_b is the spin of the emitted particle *b,* ρ is the exciton state density, $\sigma_b(\varepsilon_b)$ is the inverse cross-section of the emitted particle b with outgoing energy ε_b, B_b is the binding energy of particle b in the system, $Q_{\ell,m}^b(p,h)$ is a combination factor and F_{lm} (ε_b) is the pick-up factor of the emitted particle.

The emission rate for a photon with energy *n* from a nucleus in the exciton state n is taken as (Akkermans et al. [3.49]):

$$W\gamma(n,\varepsilon_b)=\frac{\varepsilon_\gamma^2\sigma_a^\gamma(\varepsilon_\gamma)}{\pi^2\hbar^3C^2\rho_n(E)}\left\{\frac{g^2\varepsilon_\gamma\rho_{n-2}(E-\varepsilon_\gamma)}{g(n-2)+g^2\varepsilon_\gamma}+\frac{gn\rho_n(E-\varepsilon_\gamma)}{gn+g^2\varepsilon_\gamma}\right\}, \tag{3.43}$$

where g is the single particle level density. σ_i^γ is the giant resonance cross-section:

$$\sigma_a^\gamma(\varepsilon_\gamma)=\sum_{i=1}^{2}\frac{(\varepsilon_\gamma\Gamma_i)^2\sigma_i^\gamma}{(\varepsilon_\gamma\Gamma_i)^2+(\varepsilon_\gamma^2-E_i^2)^2}, \tag{3.44}$$

where Γ_i, E_i and σ_i^γ are two peak giant resonance parameters.

For the first emission of particle b, the spectrum is given by

$$\frac{d\sigma_b}{d\varepsilon_b}=\sigma_a\sum_{pn}\tau(p,h,E)\sum_\ell W_b^\ell(p,h,E,\varepsilon_b), \tag{3.45}$$

where σ_a is the absorption cross-section of the incident particle. The direct γ emission cross-section is

$$\sigma_\gamma^d=\sigma_a\frac{Y}{Y+\lambda_+(1)}, \tag{3.46}$$

where

$$\lambda_{+}(l) = \frac{\pi K}{2}\left(\frac{g}{A}\right)^{3} E \tag{3.47}$$

$$Y = \frac{1}{\pi^{2} h^{3} C^{2}} \int_{0}^{E} \varepsilon_{\gamma}^{2} \sigma_{a}^{\gamma}(\varepsilon_{\gamma}) \frac{1}{1+g\varepsilon_{\gamma}} d\varepsilon_{\gamma} , \tag{3.48}$$

where K is the exciton model constant and A is the mass number of the composite system.

The Gilbert-Cameron level density formula [3.52] was used in the program SPEC. The inverse cross-sections of the emitted particles used in statistical theory are calculated from the optical model. The partial widths for γ ray emission are calculated based on the giant dipole resonance model with two resonance peaks in both the evaporation model and the exciton model.

In the optical model calculation, the Becchetti and Greenlees [3.53] phenomenological optical potentials are used. The Neumanove methods are used to solve the radial equation of the optical model. Coulomb wave functions are calculated by the continued fraction method (Barnett et al. [3.54]).

The following nuclear data can be calculated by using the program SPEC: total emission cross-sections and spectra of all emitted particles; the partial emission cross-sections and spectra of all emitted particles from the first to sixth particle emission processes and different pick-up configurations (ℓ, m); the various yield cross-sections; total and elastic scattering cross-sections (only for neutron as projectile); total reaction cross-section; nonelastic scattering cross-sections; radiative capture cross-section; (x,np), (x,nα), (x,2n), (x,3n), (x,4n), (x,5n), (x,6n) cross-sections and so on. SPEC can not be used to calculate the direct inelastic scattering and compound elastic scattering cross-sections. The applications so far show that the SPEC is a useful and convenient code for users.

3.2.5. HFMOD, PREMOD codes and Islamabad calculations

Gul used the HFMOD code [3.24] for statistical model and PREMOD code [3.25] for preequilibrium model nuclear reaction calculations. The calculations from the two codes were combined after correcting the Hauser-Feshbach calculation for flux reduction in the preequilibrium mode.

HFMOD code

The HFMOD code is based on the Hauser-Feshbach formalism [3.3]. The angle-integrated cross-section from channel n to channel m is given by

$$\sigma_{nm} = \frac{\pi \lambda\!\!\!^{-2}}{(2i_n+1)(2I_n+1)} \sum_{JP} \frac{(2J+1)\sum_{\ell\ell' j j'} T_{\ell}^{n} T_{\ell}^{m}}{\sum_{\ell'' j'' q''} T_{\ell''}^{q''}} \tag{3.49}$$

where $\lambda\!\!\!^{-}$ is the rationalized wavelength of the particle of spin i_n incident on the target nucleus of spin I_n; ℓ, and j are the orbital angular momentum of the incoming particle and incident channel spin, and l' and j' are the orbital angular momentum of the outgoing particle and exit channel spin. J and P specify summation over all possible spin and parity values of the compound nucleus; q" specifies summation over all possible competing channels which

include particle and gamma emission, implying integration over the continuum states of the residual nuclei weighted by appropriate values of level densities. T_{ℓ}^{n} and $T_{\ell'}^{m}$ are the transmission coefficients of the incident and outgoing particles which are calculated using appropriate optical model parameters. The code has options for the calculation of level densities on the basis of the Gilbert-Cameron composite formula [3.52] or the formalism of Dilg et al. [3.55]. In the present calculations the energy level densities were computed using the formalism of Dilg et al. The competition from photon emission has also been included in the second stage while considering emission of a particle from the residual nuclei. Angular momentum and parity are conserved in both stages of the calculation. Transmission coefficients for photon emission are calculated on the basis of the single particle model of Aslam Lone [3.56] and Wilkinson [3.57]. (An option to use the Brink-Axel formalism for E1 emission is also available in the code.) The single particle energy level spacing is used as an adjustable parameter in all the calculations. Perey potentials [3.58] are used for protons and Wilmore-Hodgson potentials [3.59] are used for neutrons. Avrigeanu et al. potentials [3.60] are used for alpha particles and Vernotte et al. potentials [3.61] are used for helions.

PREMOD Code

The pre-equilibrium contribution to nuclear reactions is calculated using the PREMOD Code (Gul [3.25]). This code is based on the concept of the geometry-dependent hybrid model generalized to include discrete levels, and to conserve angular momentum and parity. The cross-section per level is given by

$$\sigma_{\upsilon}(E,U)=\frac{\pi\lambda\!\!\!^{-2}}{(2S+1)(2I+1)}\sum_{JP}(2J+1)\sum_{n}\sum_{\ell}T_{\ell}^{J}\sum_{\ell'}X_{\upsilon}^{n}\frac{\rho(p-1,U,J')}{\rho(p,h,E,J)}\quad\times$$

$$\frac{\frac{1}{2\pi\hbar g}(2S_{\upsilon}+1)(2\ell'+1)T_{\ell'}^{J}}{\sum_{q}\sum_{\ell'}\frac{1}{2\pi\hbar g}(2S_{\upsilon}+1)(2\ell'+1)T_{\ell'}^{J}+\lambda^{+}}D_{n}^{JP}\,, \tag{3.50}$$

where $\lambda\!\!\!^{-}$ is the rationalized wave length of the incident particle of spin S incident on the target of spin I. J and P are spin and parity of the composite state; n is the exciton number, which is equal to the sum of particle number p and hole number h. T_{ℓ}^{J} and $T_{\ell'}^{J}$ are the transmission coefficients of the incident and outgoing particles corresponding to partial waves l and l'; X_{υ}^{n} is the number of excitons of type ν (protons or neutrons) in the n-exciton state. p(p,h,E) is the state density of n-exciton configurations of the composite state characterized by excitation energy E, particle number p and hole number h (n=p+h). p(p-1, h, U) is the state density of the residual nucleus. D_{n}^{JP} is a depletion factor that takes into account the depletion of the flux due to the reaction taking place from exciton states characterized by exciton number less than n. S_{ν} is the spin of the outgoing particle of type ν. q specifies the sum over available channels for the emission of particle ν from the composite state to the discrete states, as well as states of constant density g in the continuum of the residual nucleus. The spin-dependent level density is calculated as recommended by Feshbach et al. [3.9].

$$\rho(n,E,J)=\rho(n,E)\quad R(E,n,J)\,, \tag{3.51a}$$

where

$$\rho(n,E)=\frac{g^n E^{n-1}}{p!n!(n-1)!}. \tag{3.51b}$$

The excitation energy E is corrected for the Pauli effect by replacing it with E', where

$$E'=E-P(h,p), \tag{3.52a}$$

and

$$P(h,p)=\frac{p^2+h^2+p-3h}{4g}. \tag{3.52b}$$

The spin-dependent factor R(E,n,J) is taken as

$$R(E,n,J)=\frac{2J+1}{\pi^{1/2}n^{3/2}\sigma^3}\exp\left[-\frac{(J+0.5)^2}{n\sigma^2}\right], \tag{3.53}$$

where the spin-cutoff parameter σ is given by

$$\sigma=\left(\frac{2c\tau}{\bar{n}}\right)^{1/2}, \tag{3.54a}$$

where τ is nuclear temperature given by

$$E=a\tau^2-\tau \quad \text{with} \quad a=\frac{\pi^2}{6}g. \tag{3.54b}$$

The following values as suggested by Feshbach et al. [3.9] are used.

$$a=\frac{A}{8}\text{MeV}^{-1} \qquad g=\frac{6}{\pi^2}\frac{A}{8}\text{MeV}^{-1} \qquad c=\frac{A^{5/3}}{90}\text{MeV}^{-1}. \tag{3.54c}$$

$\bar{n}$ is the average exciton number equal to $1/2(2gE)^{1/2}$. Particle emission is considered in competition with internal cascade transitions leading only to higher exciton number. The transition probability λ^+ from the state of exciton number n to n + 2 is equal to $2W/\hbar$ (Kikuchi and Kawai [3.62]), where W is the imaginary component of the optical model potential. The probability of existence X_υ^n of particle ν in n-exciton state can be calculated for neutron and proton induced reactions in which a nucleon is emitted, as described earlier for the ALICE code.

For nucleon induced reactions in which an alpha particle is emitted, the concept of the preformed alpha particle is assumed and the values of X_υ^n are calculated as described by Gadioli *et al.* [3.63] and Milazzo-Colli and Braga-Marcazzan [3.43].

$$X_a^n=\frac{\phi K_a^{p-1,h}}{\phi K_a^{p,h}+(1-\phi)K_n^{p,h}}, \tag{3.55}$$

where $K_a^{p,h}$ is a coefficient which represents the percentage of states containing an excited α particle and α-hole in the state level density corresponding to p+h excitons. $K_a^{p,h}$ is the coefficient representing the percentage of states of nucleons and nucleon-holes in the state level density corresponding to p + h excitons. The coefficient ϕ represents the probability that a neutron or proton interacts with a preformed alpha particle. In fact it is a normalization parameter and its values lie in the 0.5–1 range. The optical model parameters used for Hauser-Feshbach calculation are also used for pre-equilibrium calculations. The initial exciton number for nucleon, alpha and helion is taken as 3, 4, and 5, respectively.

3.3. DISCUSSION OF THE MODELING RESULTS

The codes used by the four different modeling groups for this CRP are described in the previous section. These codes are ALICE–91 and ALICE-HMS (Livermore), ALICE-IPPE (Obninsk), SPEC (Beijing), and HFMOD and PREMOD (Islamabad). In this section, we report modeling results for selected reactions to highlight the successes and failures of the modeling efforts by the four groups in reproducing the experimental data. (Comparison of the modeled cross-sections with experimental data for all the reactions in the CRP is shown in Chapters 4 and 5.) The calculations are based on global input parameters for optical potentials and level densities. The calculations start with the preequilibrium emissions followed by the evaporation. The preequilibrium models used are hybrid or geometry dependent hybrid (GDH) by all the codes, except for the SPEC and the ALICE-HMS, which use the master equation exciton model and Monte Carlo nucleon emissions, respectively. The evaporation is calculated according to the Weisskopf-Ewing model, except for the HFMOD code where the Hauser-Feshbach formalism is used. In terms of the level density descriptions, the Livermore group used the Fermi gas model level densities and the level densities from Kataria and Ramamurthy [3.29] with shell effects. The Obninsk group used level densities from the generalized superfluid model, which includes shell effects and collective enhancements. The Beijing group used the Gilbert–Cameron level densities and Gul (Islamabad) used backshifted Fermi gas model parameters of Dilg et al. [3.55]. Cluster preequilibrium emissions are included in the ALICE-IPPE calculations.

Because of the global nature of the input parameters, the calculated cross-sections are used mostly as a guide rather than a fit to the experimental data, although in some cases modeled cross-sections were chosen as the recommended values by this CRP. In general the calculated cross-sections show a better fit to the data for A >30, and also show a better fit for proton induced reactions over deuteron, ^{3}He and alpha. The poor fit to the lower mass targets may be attributed to the reaction mechanism used in the codes. It is known that nuclear structure plays a critical role in the lighter masses and that the R-matrix theory is more appropriate in modeling cross-sections for such targets. Because of the complexity in modeling such cross-sections, it was decided by the CRP not to pursue the modeling for light targets but to use only the experimental data for the evaluation. Another important modeling feature that was not explicitly included is the breakup of light projectiles, such as, the deuteron and ^{3}He, in the entrance channel of the reaction process. However, the Livermore group made their choice of the preequilibrium model parameters, namely the initial exciton numbers, from an investigation of the deuteron breakup (i.e. the stripping to the bound states and breakup-capture in the continuum) for d + ^{48}Ti reaction. The Obninsk group reduced their calculated cross-sections by a factor of 1.5 for deuteron induced reactions to account for such breakup processes.

In Fig. 3.1 we show the effects of the deuteron breakup in ^{48}Ti(d,2n)^{48}V cross-sections calculated by the Livermore group using the Udagawa and Tamura [3.10, 3.35] microscopic theory. In their approach the Udagwa and Tamura theory was used to deduce the spectra of neutrons and protons transferred into the target nucleus (stripping to bound states and breakup-capture in the continuum); these were then assumed to initiate three-quasiparticle preequilibrium cascade and evaporation. The deuteron cross-section that does not undergo stripping or breakup-capture was assumed to initiate a separate preequilibrium cascade and evaporation. In the figure the "breakup" refers to the sum of cross-sections from these two processes, i.e. the breakup and also the remaining cross-sections coming from the optical model reaction cross-section that did not undergo breakup. The three other curves, identified by 6-2-2, 3-1-1 and 2-1-1, are ALICE-91 calculations with no breakup. The numbers, e.g. 6-2-2, etc. are the initial exciton numbers (total, neutron and proton excitons). These calculations were done in order to empirically select the best initial exciton numbers to use for the deuteron induced reactions, when breakup can not be included explicitly. The best fit to the data near the peak cross-section is found when the breakup is included. The calculation with 2-1-1 is closer to the breakup model calculation and the data. However, note that even with these choices of the initial exciton numbers the calculated cross-sections are about a factor of two too high near the peak cross-section. Nevertheless, the Livermore group used 2-1-1 as the initial exciton numbers for the remaining calculations of the deuteron induced reactions for the CRP.

Another important feature in modeling cross-sections is the nuclear structures or structure effects that are included in the level density calculations. We show in Fig. 3.2 the cross-sections for ^{nat}Fe(d,x)^{56}Co reaction, where we compare the cross-sections calculated with level densities from the Fermi gas (FG) model and those from the Kataria and Ramamurthy (KR) formalism which includes shell and pairing effects. These are the two level density options that are available in the ALICE-91 code. The data in the figure are from Takacs *et al.* [3.65] and Clark *et al.* [3.66]. We conclude from the results in Fig. 3.2 that the calculated cross-sections may differ by a factor of two depending on the level density options used. We showed here one of the extreme cases for the reactions in this CRP. (The comparison of the modeled cross-sections with the experimental data for other reactions is given in Chapters 4 and 5.) It is worth to note that the calculations by the Obninsk group and those by Gul of Islamabad include shell effects but in a different way. Obninsk group also includes the collective effects in their level density calculations.

We show in Fig. 3.3 an example of the poor quality of fit for a lighter target. There are several reasons why we would expect a relatively poor fit to the data with present modeling. First, the lack of nuclear structure input in the calculation is a primary deficiency for such targets. Second, the Weisskopf-Ewing or Hauser-Feshbach formalisms are inappropriate for lighter targets. Third, ^{3}He is expected to breakup in the entrance channel, the effect may be smaller than that of the deuteron but it may still be sizable, and was not included here. Finally, the reaction process leading to ^{22}Na is quite complicated. Another example of (^{3}He,x) reaction is shown in Fig. 3.4. This is followed by a case of (p,x) reaction on very light target, Fig. 3.5, where again a poor fit is observed.

In two subsequent figures we show examples of good agreement between theoretical calculations and experimental data. In Fig. 3.6 we show a case of (p,n) reaction and in Fig. 3.7 a case of (p,3n) reaction. Gul's calculation was based on Hauser-Feshbach formalism with preequilibrium emissions. He used backshifted level densities from Dilg *et al*. and discrete levels for lower energies. He also made some adjustment to the spin cut-off parameters. This serves as an example of the quality of fit we may expect from a full Hauser-Feshbach

calculation for the middle to heavier mass targets. However, in this CRP most of the calculations were done using global parameters and the results were intended to be an aid to the evaluation, not a fit to the data.

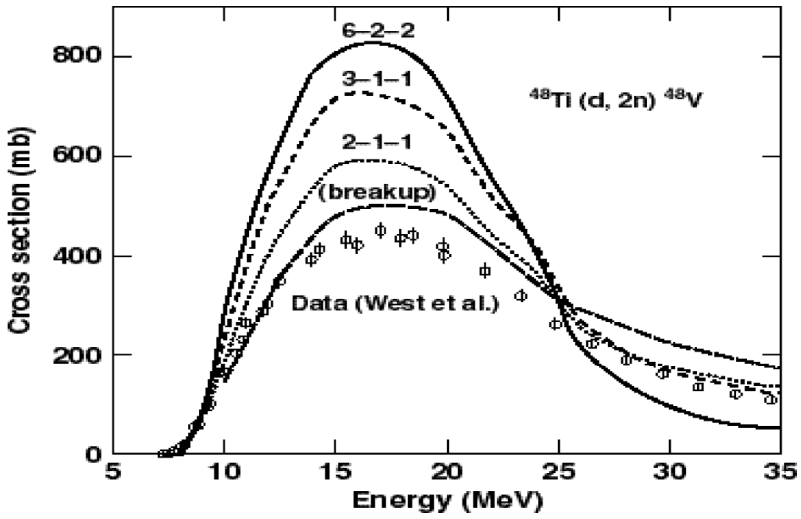

Fig. 3.1. $^{48}Ti(d,2n)^{48}V$ cross-sections including the deuteron breakup are compared with ALICE-91 calculations with several choices of the initial exciton numbers (6-2-2, 3-1-1, 2-1-1) and the data of West et al. [3.64].

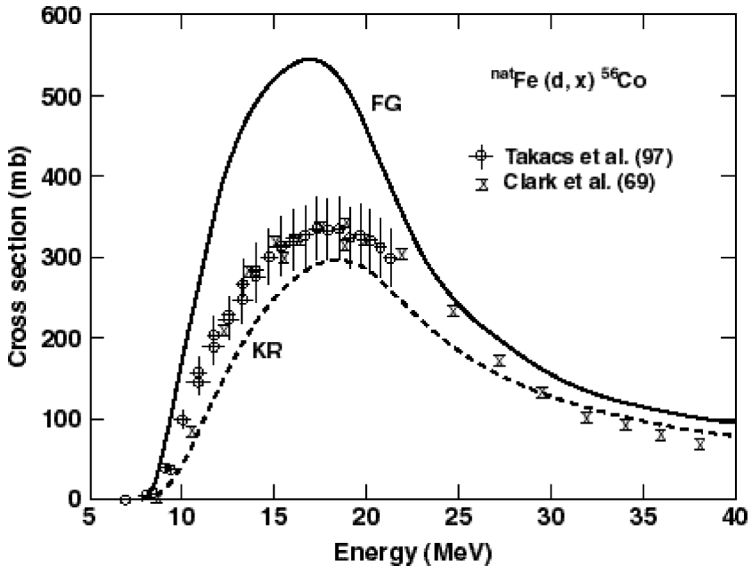

Fig. 3.2 $^{nat}Fe(d,x)^{56}Co$ reaction. The FG stands for the Fermi gas model level densities and KR for the Kataria and Ramamurthy [3.29] level densities with shell effects. The calculations were done by the ALICE-91 code, optical potentials used are described in Blann and Vonach [3.27].

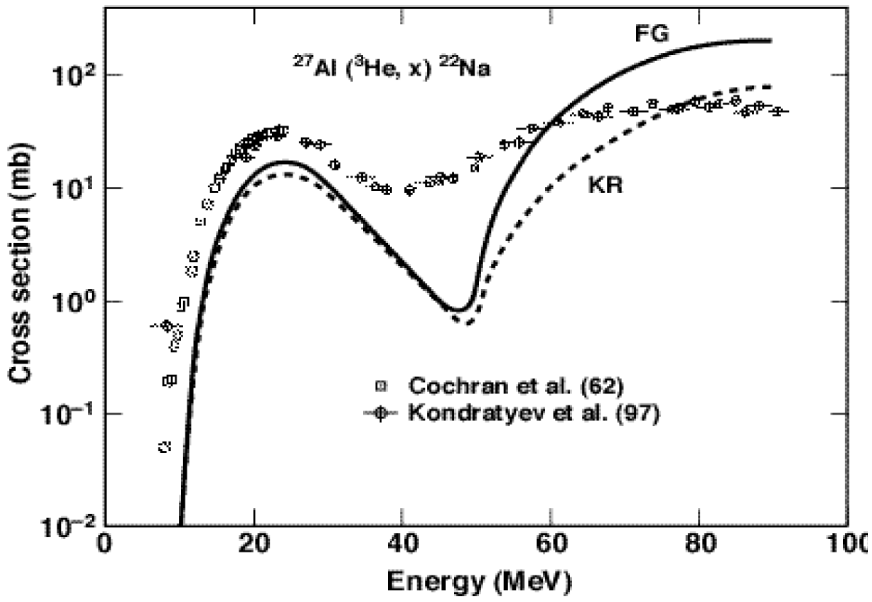

Fig. 3.3 $^{27}Al(^{3}He,x)^{22}Na$ reaction, an example of poor fit. ALICE-91 calculation with two level density options: Fermi gas (FG) model and Kataria-Ramamurthy (KR) formalism. See section 4.3.1. for references to experimental data.

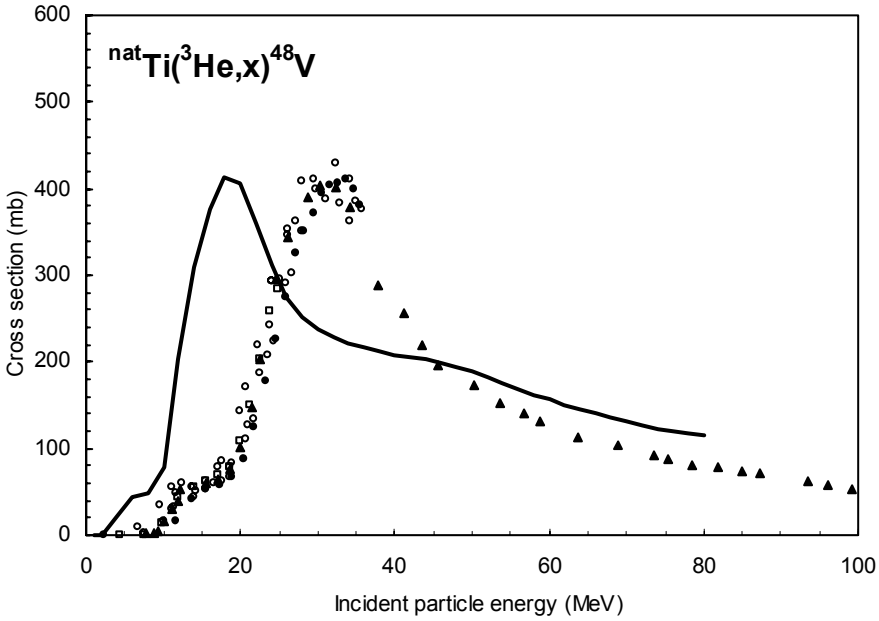

Fig. 3.4 ^{nat}Ti $(^{3}He,x)^{48}V$ reaction. Theoretical calculations using the code SPEC (Beijing) are compared with experimental data.

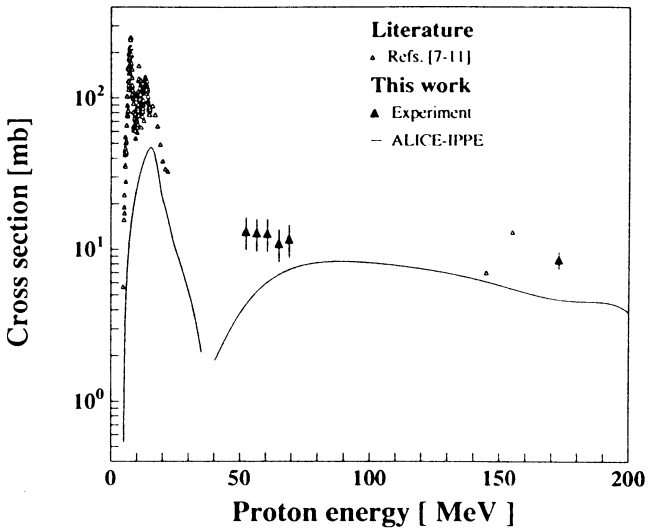

Fig 3.5 $^{nat}N(p,x)^{11}C$ reaction. Theoretical calculations by the code ALICE-IPPE (Obninsk) are compared with experimental data. Taken from Fassbender et al., Proc. Int. Conf. on Nuclear Data, Trieste 1997, p. 1646.

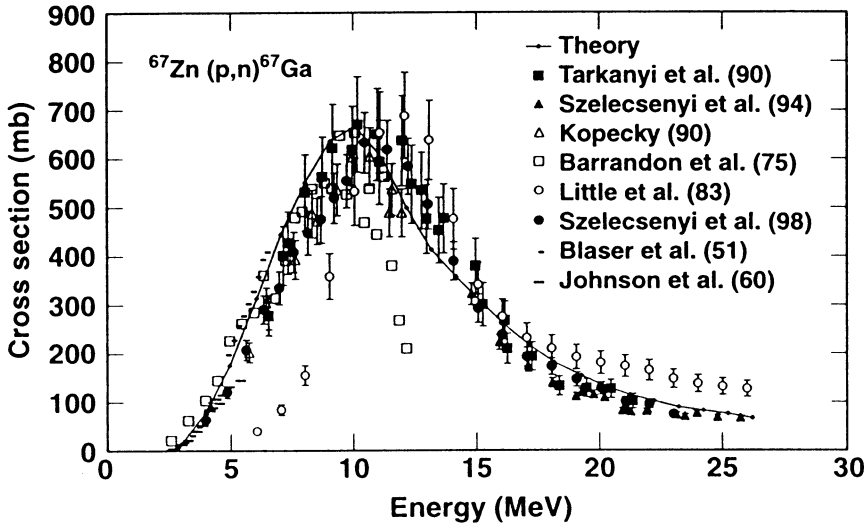

Fig. 3.6 $^{67}Zn(p,n)^{67}Ga$ reaction, an example of a good theoretical fit. The calculation was done by Gul (IAEA report INDC(NDS)-388, November 1998). See section 5.1.1. for references to the experimental data.

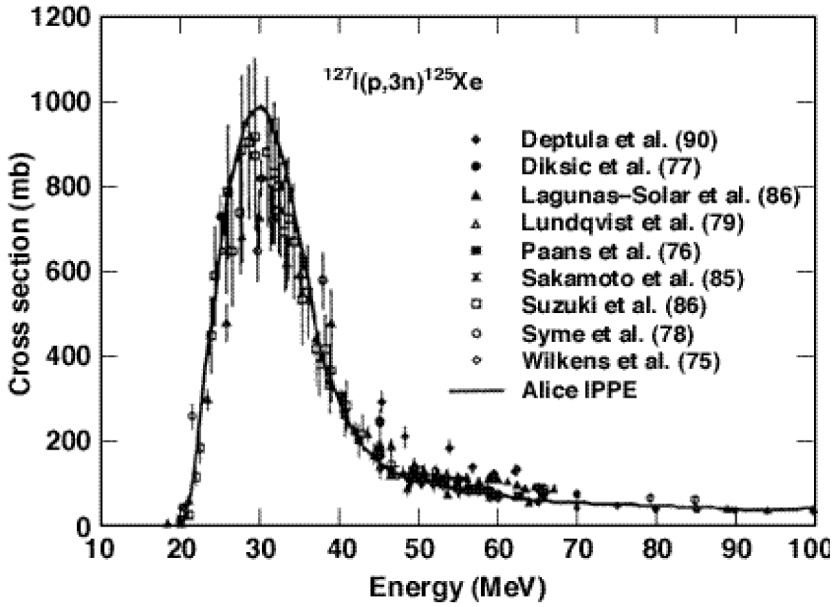

Fig. 3.7. $^{127}I(p,3n)^{125}Xe$ reaction, an example of a good fit. ALICE-IPPE calculation from Obninsk is shown as a fit to selected data. See section 5.1.11. for references to the experimental data.

In this section we discussed the general features of the modeled cross-sections and the quality of fit to the data. We described calculations by four different groups using mostly global parameters. We identified several deficiencies in reaction formalisms used in the calculations. We showed poor fit to the data for the lighter targets and provided an example of how to incorporate breakup effects in the ALICE-91 calculations for the deuteron-induced reactions. We show two examples of excellent fit to the data, one in which full Hauser-Feshbach calculation was done by Gul and the other from the Obninsk group where better level density data were used. Although in some cases modeled cross-sections were chosen as the recommended values by the CRP, the calculations were done using global input parameters and thus used as a guide to the evaluators rather than a fit to the experimental data. We did not expect these calculations to show a fit to the data better than a factor of two. The fit to the peak cross-section is expected to be somewhat better, but the discrepancy near the reaction threshold may be higher.

REFERENCES TO CHAPTER 3

[3.1] BLANN, M., Preequilibrium decay, Annu. Rev. Nucl. Sci. **25** (1975) 123–166.

[3.2] GADIOLI, E., HODGSON, P.E., Pre-equilibrium Nuclear Reactions, Clarendon Press, Oxford (1992).

[3.3] HAUSER, W., FESHBACH, H., The inelastic scattering of neutrons, Phys. Rev. **87** (1952) 366–373.

[3.4] WEISSKOPF, V.F., EWING, D.H., On the yield of nuclear reactions with heavy elements, Phys. Rev. **57** (1940) 472–485.

[3.5] BERTINI, H.W., Low-energy intranuclear cascade calculation, Phys. Rev. **131** (1963) 1801–1821.

[3.6] CHEN, K., FRAENKEL, Z., FRIEDLANDER, G., GROVER, J.R., MILLER, J.M., SHIMAMOTO, Y., VEGAS: A Monte Carlo simulation of intranuclear cascades, Phys. Rev. **166** (1968) 949–967.
[3.7] GUDIMA, K.K., MASHNIK, S.G., TONEEV, V.D., Cascade-exciton model of nuclear reactions, Nucl. Phys. **A401** (1983) 329–360.
[3.8] CUGNON, J., VOLANT, C., VUILLIER, S., Improved intranuclear cascade model for nucleon-nucleus interactions, Nucl. Phys. **A620** (1997) 475–509.
[3.9] FESHBACH, H., KERMAN, A., KOONIN, S., The statistical theory of multi-step compound and direct reactions, Ann. Phys. (NY) **125** 4 (1980) 29–476.
[3.10] UDAGAWA, T., TAMURA, T., Derivation of breakup-fusion cross sections from the optical theorem, Phys. Rev. C **24** (1981) 1348–1349.
[3.11] NISHIOKA, H., WEIDENMULLER, H.A., YOSHIDA, S., Statistical theory of prcompound reactions: The multistep direct process, Ann. Phys. (NY) **183** (1988) 166–187.
[3.12] LANE, A.M., THOMAS, R.G., R-matrix theory of nuclear reactions, Rev. Mod. Phys. **30** (1958) 257–353.
[3.13] GRIFFIN, J.J., Statistical model of intermidate structure, Phys. Rev. Lett. **17** (1966) 478–481.
[3.14] BLANN, M., GRUPPELAAR, H., NAGEL, P., RODENS, J., International code and model intercomparison for intermediate energy nuclear data, NEA Data Bank, OECD, Paris (1994).
[3.15] MICHEL, R., NAGEL, P., NSC/DOC(97)-1, NEA Data Bank, OECD, Paris (1997).
[3.16] ERICSON, T., The statistical model and nuclear level densities, Adv. Phys. **9** (1960) 423–511; STRUTINSKY, V.M., On the level density in the case of an energy gap, Proc. Congr. Int. Phys. Nucl. Paris (1958) 617.
[3.17] BLANN, M., Extensions of Griffin's statistical model for medium-energy nuclear reactions, Phys. Rev. Lett. **21** (1968) 1357–1360.
[3.18] WILLIAMS, F.C., Jr., Particle-hole state density in the uniform spacing model, Nucl. Phys. **A166** (1971) 231–240.
[3.19] OBLOZINSKY, P., RIBANSKY, I., BETAK, E., Intermediate-state transition rates in the exciton model, Nucl. Phys. **A226** (1974) 347–364.
[3.20] DITYUK, I., KONOBEYEV, A.YU., LUNEV, V.P., SHUBIN, YU.N., New version of the advanced computer code ALICE-IPPE, Rep. INDC(CCP)-410, IAEA, Vienna (1998).
[3.21] SHEN, Q., ZHANG, J., The SPEC Code, Commun. Nucl. Data Prog. **10** (1993) 53.
[3.22] BLANN, M., New precompound decay model, Phys. Rev. C **54** (1996) 1341–1349.
[3.23] BLANN, M., Recent progress and current status of preequilibrium reaction theories and computer code ALICE, Lawrence Livermore National Laboratory Rep., UCRL-JC-109052 (1991) (unpublished).
[3.24] GUL, K., A computer code based on Hauser-Feshbach and Moldauer theory for nuclear cross section calculations, Rep. INDC(PAK)-011, IAEA, Vienna (1995).
[3.25] GUL, K., Theoretical formulation of PREMOD code based on geometry-dependent hybrid model of nuclear pre-equilibrium reactions, Scientific Information Division Rep. SID-7, PINSTECH, Islamabad (1996).
[3.26] PEARLSTEIN, S., Nuclear Data for Science and Technology, Mito, Japan (1988) 115.
[3.27] BLANN, M., VONACH, H.K., Global test of modified precompound decay models, Phys. Rev. **C 28** (1983) 1475–1492.
[3.28] BLANN, M., REFFO, G., FABBRI, F., Calculation of γ-ray cascades in code ALICE, Nucl. Instrum. Methods in Phys. Research **A265** (1988) 490–494.

[3.29] KATARIA, S.K., RAMAMURTHY, V.S., Macrospic systematics of nuclear level densities, Nucl. Phys. **A349** (1980) 10–28.
[3.30] BLANN, M., A-priori preequilibrium decay models, Nucl. Phys. **A213** (1973) 570–588.
[3.31] HOFSTADTER, R., Nuclear and nucleon scattering of high-energy electrons, Annu. Rev. Nucl. Sci. **7** (1957) 231–316.
[3.32] BISPLINGHOFF, J., Configuration mixing in preequilibrium reactions: A new look at the hybrid-exciton controversy, Phys. Rev. C **33** (1986) 1569–1580.
[3.33] MUSTAFA, M.G., "Projectile breakup and Hauser-Feshbach modeling", Proc. Int. Conf. on Nuclear Data for Science and Technology, Trieste (G. Reffo, A. Ventura, C. Grandi, Eds) (1997) 274–276.
[3.34] TAMURA, T., UDAGAWA, T., LENSKE, H., Multistep direct reaction analysis of continuum spectra in reactions induced by light ions, Phys. Rev. C **26** (1982) 379–404.
[3.35] UDAGAWA, T., TAMURA, T., Formulation of elastic and inelastic breakup-fusion reactions, Phys. Rev. C **33** (1986) 494–503.
[3.36] IGNATYUK, A.V., Statistical Properties of Excited Atomic Nuclei (in Russian), Energoatomizdat, Moscow (1983), Translated into English by the International Atomic Energy Agency, Rep. INDC(CCP)-233, IAEA, Vienna (1985).
[3.37] IGNATYUK, A.V., ISTEKOV, K.K., SMIRENKIN, G.N., The role of collective effects in the systematics of nuclear level densities, Sov. J. Nucl. Phys. **29** 4 (1979) 450–454.
[3.38] BLOKHIN, A.I., IGNATYUK, A.V., SHUBIN, YU.N., Vibrational enhancement of the level density of nuclei in the iron region, Sov. J. Nucl. Phys. **48** 2 (1988) 232–236.
[3.39] IGNATYUK, A.V., WEIL, J.L., RAMAN, S., KAHANE, S., Density of discrete levels in ^{116}Sn, Phys. Rev. C **47** (1993) 1504–1513.
[3.40] IWAMOTO, A., HARADA, K., Mechanism of cluster emission in nucleon-induced preequilibrium reactions, Phys. Rev. C **26** (1982) 1821–1834.
[3.41] SATO, N., IWAMOTO, A., HARADA, K., Preequilibrium emission of light composite particles in the framework of the exciton model, Phys. Rev. C **28** (1983) 1527–1537.
[3.42] MYERS, W.D., SWIATECKI, W.J., Anomalies in nuclear masses, Arkiv Fysik **36** (1967) 343–352.
[3.43] MILAZZO-COLLI, L., BRAGA-MARCAZZAN, G.M., α-emission by preequilibrium processes in (n,α) reactions, Nucl. Phys. **A210** (1973) 297–306.
[3.44] FERRERO, A., GADIOLI ERBA, E., IORI, I., MOLHO, N., ZETTA, L., α-emission in proton induced reaction, Z. Phys. **A293** (1979) 123–134.
[3.45] OBLOZINSKY, P., RIBANSKY, I., Emission rate of preformed α-particles in preequilibrium decay, Phys. Lett. **B74** (1978) 6–12.
[3.46] MYERS, W.D., Droplet Model of Atomic Nuclei, IFI/Plenum, New York (1977).
[3.47] BOHR, A., MOTTELSON, B., Nuclear Structure, vol. 2, Benjamin Inc., New York and Amsterdam (1974).
[3.48] HANSEN, G., JENSEN, A., Energy dependence of the rotational enhancement factor in the level density, Nucl. Phys. **A406** (1983) 236–256.
[3.49] AKKERMANS, J.M., GRUPPELAAR, H., Analysis of continuum gamma-ray emission in precompound-decay reactions, Phys. Lett. **157B** (1985) 95–100.
[3.50] ZHANG, J., WEN, Y., WANG, S., SHI, X., Formation and emission of light particles in fast neutron induced reactions — a unified compound pre-equilibrium model, Commun. Theor. Phys. (Beijing, China) **10** (1988) 33–44.

[3.51] ZHANG J., YAN, S., WANG, C., The pick-up mechanism in composite particle emission processes, Z. Phys. **A344** (1992) 251–258.
[3.52] GILBERT, A., CAMERON, A.G.W., A composite nuclear-level density formula with shell corrections, Can. J. Phys. **43** (1965) 1446–1496.
[3.53] BECCHETTI, JR., F.D., GREENLESS, G.W., Nucleon-nucleus optical model parameters, A > 40, E < 50 MeV, Phys. Rev. **182** (1969) 1190–1209.
[3.54] BARNETT, A.R., FENG, D.H., STEED, J.W., GOLDFARB, L.J.B., Computer Phys. Commun. **8** (1974) 377–395.
[3.55] DILG, W., SCHANTL, W., VONACH, H., UHL, M., Level density parameters for the back-shifted Fermi gas model in the mass range 40 < A < 250, Nucl. Phys. **A217** (1973) 269–298.
[3.56] ASLAM LONE, M., in Proc. Third Int. Symp. on neutron capture gamma-ray spectroscopy and related topics (Eds. Chrien, R.E., Kane, W.R.), Plennum Press, New York (1978) 161.
[3.57] WILKINSON, D.H., Nuclear Spectroscopy (Part B) (Ed. Fay Azjenberg-Selov), Academic Press, New York (1960) 644.
[3.58] PEREY, F.G., Optical model analysis of proton elastic scattering in the range of 9 to 22 MeV, Phys. Rev. **131** (1963) 745–763.
[3.59] WILMORE, D., HODGSON, P.E., The calculation of neutron cross-sections from optical potentials, Nucl. Phys. **55** (1974) 673–694.
[3.60] AVRIGEANU, A., HODGSON, P.E., AVRIGEANU, M., Global optical potentials for emitted alpha particles, Phys. Rev. C **49** (1994) 2136–2141.
[3.61] VERNOTTE, J., BERRIER-RONSIN, G., KALIFA, J., TAMISIER, R., Optical model analysis of ^{3}He elastic scattering from s-d shell nuclei at 25 MeV, Nucl. Phys. **A390** (1982) 285–313.
[3.62] KIKUCHI, K., KAWAI, M., Nuclear Matter and Nuclear Reactions, North Holland, Amsterdam (1968).
[3.63] GADIOLI, E., GADIOLI ERBA, E., HOGAN, J.J., Preequilibrium decay of nuclei with A ~ 90 at excitation energies to 100 MeV, Phys. Rev. C **16** (1977) 1404–1424.
[3.64] WEST, JR., H.I., LANIER, R.G., MUSTAFA, M.G., NUCKOLLS, R.M., NAGLE, R.J., O'BRIEN, H., FREHAUT, J., ADAM, A., PHILIS, C., Some light-ion excitation-function measurements on titanium, yttrium, and europium, and associated results, Lawrence Livermore National Laboratory Rep. UCRL-ID-115738 (1993) (unpublished).
[3.65] TAKÁCS, S., TÁRKÁNYI, F., SONCK, M., HERMANNE, A., SUDAR, S., Study of deuteron induced reactions on natural iron and copper and their use for monitoring beam parameters and for thin layer activation technique, Proc. 14th Int. Conf. on Applications of Accelerators in Research and Industry, Denton, Texas, November 1996 (Eds. Dugan, J.L., Morgan, I.L.) AIP Conference Proceeding 392, AIP, Woodbury, New York (1997) 659.
[3.66] CLARK, J.W., FULMER, C.B., WILLIAMS, I.R., Excitation functions for radioactive nuclides produced by deuteron-induced reactions in iron, Phys. Rev. **179** (1969) 1104–1108.
[3.67] Handbook for Calculations of Nuclear Reaction Data: Reference Input Parameter Library, Rep. IAEA-TECDOC-1034, IAEA, Vienna (1998).

Chapter 4
BEAM MONITOR REACTIONS

(Prepared by F. Tárkányi, S. Takács, K. Gul, A. Hermanne, M.G. Mustafa, M. Nortier, P. Obložinský, S.M. Qaim, B. Scholten, Yu.N. Shubin, Zhuang Youxiang)

The list of beam monitor reactions evaluated in the present project includes altogether 22 reactions. Among them are 8 reactions for protons, 5 for deuterons, 3 for ^{3}He and 6 for α particles. Energies of incident particles cover the range from a few MeV up to 100 MeV.

The adopted evaluation procedure consisted of three steps, explained in more detail in Chapters 2 and 3. First, experimental data were collected and subjected to critical analysis, resulting in creation of a reduced set of selected experimental data to be used for further evaluation. The second step consisted of performing theoretical calculations with nuclear reaction model codes using global input parameters without any adjustment for individual reactions and comparison with the selected experimental data as well as of fitting those selected data. The third step represented final judgement as regards the agreement between selected experimental data, theoretical calculations and fits. Based on the consensus of all participants and evaluators involved in the present project, recommended cross-sections were chosen, most often the preferred choice being the fit.

In the following-sections, beam monitor reactions are grouped according to incident particles. For each reaction, the above 3 evaluation steps are described, each step being accompanied by a figure. Then, recommended cross-sections are presented in a tabular form.

The following notations for identification of fits and theoretical calculations are used in the figures:

fit Spline:	Spline fitting method described in Section 2.3.1.
fit Pade:	Padé fitting method described in Section 2.3.2.
Alice-HMS:	Calculations with the ALICE-91 code including the precompound Hybrid Monte Carlo simulation described in Section 3.2.2. Different options for level density descriptions are possible for this code: Fermi Gas model (FG), Back Shifted Fermi Gas model (BS) and Kataria and Ramamurthy formalism (KR), see 3.2.2.
Alice-91:	Calculations with the latest version of the standard ALICE code described in Section 3.2.1. Different options for the level density descriptions are possible for this code: Fermi Gas model (FG), Back Shifted Fermi Gas model (BS) and Kataria and Ramamurthy formalism (KR), see 3.2.2.
Alice-IPPE:	Calculations with the ALICE-91 code modified to include generalized superfluid level density and preequilibrium cluster emission as described in Section 3.2.3.
HF:	Calculations with the combined HFMOD-PREMOD codes described in Section 3.2.5.
Spec:	Calculations with the SPEC code described in Section 3.2.4.

4.1. PROTONS

Evaluated were 8 proton beam monitor reactions. Table 4.1 lists these contributing reactions, including the basic decay characteristics of product nuclei (half-lives, main γ-lines along with their intensities), and energy range of protons for which evaluations were performed.

TABLE 4.1. PROTON BEAM MONITOR REACTIONS

Reaction	$T_{1/2}$ of product nucleus	Main γ-lines		Proton energy range (MeV)
		Eγ (keV)	Iγ (%)	
$^{27}Al(p,x)^{22}Na$	2.60 a	1274.5	99.94	30–100
$^{27}Al(p,x)^{24}Na$	14.96 h	1368.6	100.0	30–100
		2754.0	99.94	
$^{nat}Ti(p,x)^{48}V$	15.98 d	983.5	99.99	5–30
		1312.0	97.49	
$^{nat}Ni(p,x)^{57}Ni$	1.50 d	1377.6	77.9	15–50
$^{nat}Cu(p,x)^{56}Co$	77.70 d	846.8	99.9	50–100
		1238.3	67.0	
$^{nat}Cu(p,x)^{62}Zn$	9.26 h	596.7	25.7	14–60
$^{nat}Cu(p,x)^{63}Zn$	38.1 min	669.8	8.4	4.5–50
		962.2	6.6	
$^{nat}Cu(p,x)^{65}Zn$	244.10 d	1115.5	50.75	2.5–100

4.1.1. $^{27}Al(p,x)^{22}Na$

There were 19 experimental papers published. Five works presented cross-sections only above 100 MeV or no numerical values were available and hence were not further considered. Additionally 5 works showed discrepant results and were not selected. The remaining 9 papers were selected for further evaluation. The list of related references below is accompanied with additional information. We mention availability of data in the computerized database EXFOR (if available, unique EXFOR reference number is given). Furthermore, we indicate a reason why a data set was excluded (reference denoted by an asterisk *).

*** Aleksandrov, V.N., Semenova, M.P., Semenov, V.G.:**
Cross-section of radionuclide production in the (p,x) reactions of Al and Si.
Atomnaya Energiya **64** (1988) 445
— Exfor: A0340
— Data excluded: found to be systematically too low.

*** Batzel, R.E., Coleman, G.H.:**
Cross-sections for the formation of ^{22}Na from aluminium and magnesium bombarded with protons.
Physical Review **93** (1954) 280
— Exfor: none
— Data excluded: no numerical values are available.

Bodemann, R., Busemann, H., Gloris, M., Leya, I., Michel, R., Schiekel, T., Herpers, U., Holmqvist, B., Condé, H., Malmborg, P., Dittrich-Hannen, B., Suter, M.:
New measurements of the monitor reactions $^{27}Al(p,x)^{7}Be$, $^{27}Al(p,3p3n)^{22}Na$, $^{27}Al(p,3pn)^{24}Na$ and $^{65}Cu(p,n)^{65}Zn$.
In Progress report on Nuclear Data Research in the Federal Republic of Germany, ed. Qaim, S.M., see Report NEA/NSC/DOC(95)10 and INDC (GER)-040 (1995) p. 29
— Exfor: none

*** Brun, C., Lefort, M., Tarrgo, X.:**
Détermination des intensités de faisceaux de protons de 40 a 150 MeV.
J. de Physique et le Radium **23** (1962) 371
— Exfor: none
— Data excluded, no numerical values are available.

Cumming, J.B.:
Absolute cross-section for the $^{12}C(p,pn)^{11}C$ reaction at 50 MeV.
Nuclear Physics **49** (1963) 417
— Exfor: B0095

Furukawa, M., Kume, S., Ogawa, S.K.:
Excitation functions for the formation of ^{7}Be and ^{22}Na in proton induced reactions on ^{27}Al.
Nuclear Physics **69** (1965) 362
— Exfor: P0016

*** Gauvin, H., Lefort, M., Torongo, X.:**
Emmission d' helions dans les reactions de spallation.
Nuclear Physics **39** (1962) 447
— Exfor: none
— Data excluded: found to be systematically shifted towards higher energies.

*** Grütter, A.:**
Excitation functions for radioactive isotopes produced by proton bombardment of Cu and Al in the energy range of 16 to 70 MeV.
Nuclear Physics **A383** (1982) 98
— Exfor: A0178
— Data excluded: found to be systematically too low.

Heydegger, H.R., Turkevich, A.L., Van Ginneken, A., Walpole, P.H.:
Production of ^{7}Be, ^{22}Na and ^{28}Mg from Mg, Al and SiO_2 by protons between 82 and 800 MeV.
Physical Review **C 14** (1976) 1506
— Exfor: none

*** Hintz, N.M., Ramsey, N.F.:**
Excitation functions to 100 MeV.
Physical Review **88** (1952) 19
— Exfor: B0076
— Data excluded, found to be systematically too high.

Korteling, R.G., Caretto, A.A.:
Energy dependence of ^{22}Na and ^{24}Na production cross-sections with 100-400 MeV protons.
Physical Review **C 1** (1970) 1960
— Exfor: C0253

Lagunas-Solar, M.C., Carvacho, O.F., Cima, R.R.:
Cyclotron production of PET radionuclides: ^{18}F (109.77min; β^+ 96.9%; EC 3.1%) from high-energy protons on metallic aluminium targets.
Applied Radiation Isotopes **39** (1988) 41
— Exfor: A0445

*** Michel, R., Bodemann, R., Busemann, H., Daunke, R., Gloris, M., Lange, J.H., Klug, B., Krins, A., Leya, I., Lüpke, M., Neumann, S., Reinhardt, H., Schnatz-Büttgen, M., Herpers, U., Schiekel Th., Sudbrock, F., Holmqvist, B., Condé, H., Malmborg, P., Suter, M., Dittrich-Hannen, B., Kubik, P.W., Synal, H.A., Filges, D.:**
Cross-sections for the production of residual nuclides by low- and medium-energy protons from the target elements C, N, O, Mg, Al, Si, Ca, Ti, V, Mn, Fe, Co, Ni, Cu, Sr, Y, Zr, Nb, Ba, and Au.
Nuclear Instruments Methods **B129** (1997) 153
— Exfor: O0276
— Data not considered. Inclusion of this data would not influence the recommended values.

Michel, R., Brinkman, G., Herr, W.:
Integral excitation functions for p-induced reactions.
In Progress Report on Nuclear Data Research in the Federal Republic of Germany, ed. Qaim, S.M., see Report NEANDC (E) -202 U vol. V, also Report INDC (GER)-21/L (1979) 68
— Exfor: A0151

*** Miyano, K.:**
The ^{7}Be, ^{22}Na and ^{24}Na production cross-sections with 22-52 MeV protons on ^{27}Al.
J. Physical Society Japan **34** (1973) 853
— Exfor: none
— Data excluded, no numerical values available.

Pulfer, P.:
Determination of absolute production cross-sections for proton induced reactions in the energy range 15 to 72 MeV and at 1820 MeV.
Thesis (1979), Universität Bern, unpublished
— Exfor: D0053

Steyn, G.F., Mills, S.J., Nortier, F.M., Simpson, B.R.S., Meyer, B.R.:
Production of ^{52}Fe via proton-induced reactions on manganese and nickel.
Applied Radiation Isotopes **41** (1990) 315
— Exfor: A0497

*** Williams, I.R., Fulmer, C.B.:**
Excitation functions for radioactive isotopes produced by protons below 60 MeV on Al, Fe and Cu.
Physical Review **162** (1967) 1055
— Exfor: B0073
— Data excluded, found to be systematically too low.

*** Walton, J.R., Yaniv, A., Heymann, D.:**
He and Ne cross-sections in natural Mg, Al and Si targets and radionuclide cross-sections in natural Si, Ca, Ti and Fe targets bombarded with 14–45 MeV protons.
J. Geophysical Research **78** (1973) 6428
— Exfor: none
— Data excluded, no numerical values available.

The data from all experimental papers where numerical values are available (14 papers), are collected in Fig. 4.1.1a. The scatter of data is large, illustrating the reasons why only nine papers were selected.

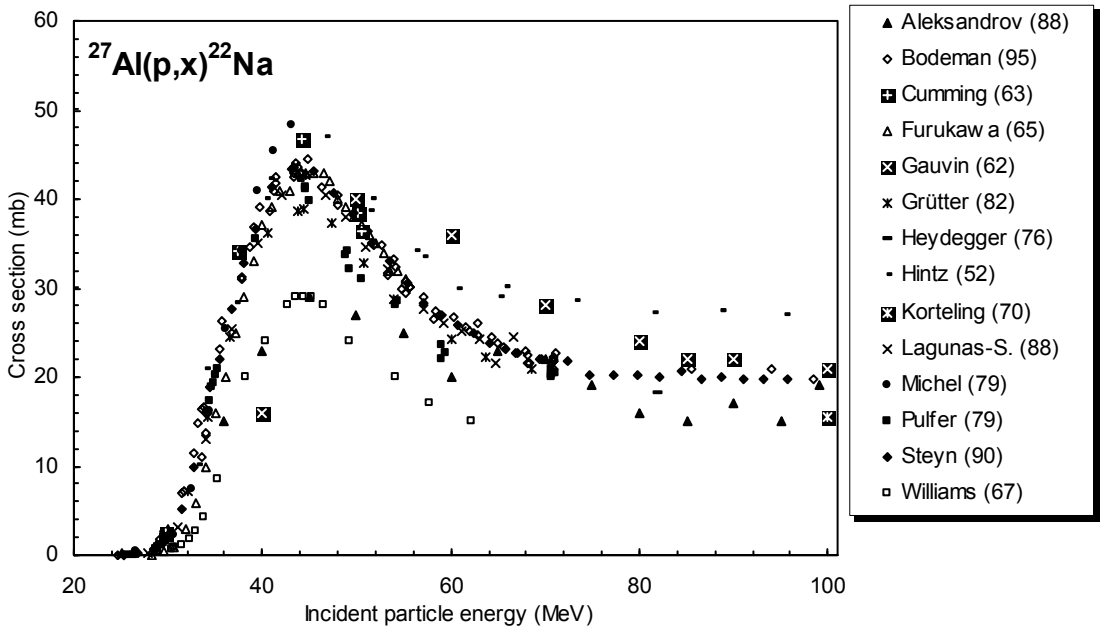

Figure 4.1.1a. All experimental data.

Cross-sections were calculated by two different versions of the nuclear reaction model code ALICE (denoted as HMS and as IPPE) and by two fitting procedures (Padé with 15 parameters and Spline). These results are compared to selected experimental data in Fig. 4.1.1b. It is seen that HMS model calculations systematically over-predict the data at energies above 35 MeV. ALICE-IPPE calculations describe experimental data reasonably well up to 55 MeV, but however overestimate the data at higher energy. Fits do much better, the best was judged to be the spline fit. Recommended cross-sections are compared with selected experimental data, including their error bars, in Fig. 4.1.1c. The corresponding numerical values are tabulated in Table 4.1.1.

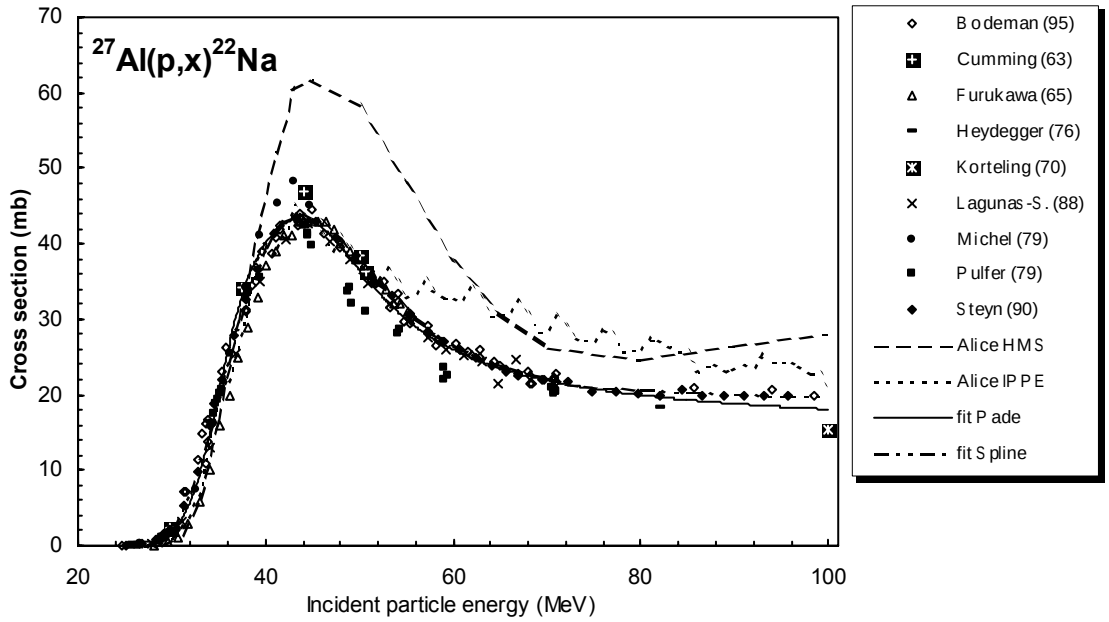

Figure 4.1.1b. *Selected experimental data in comparison with theoretical calculations and fits.*

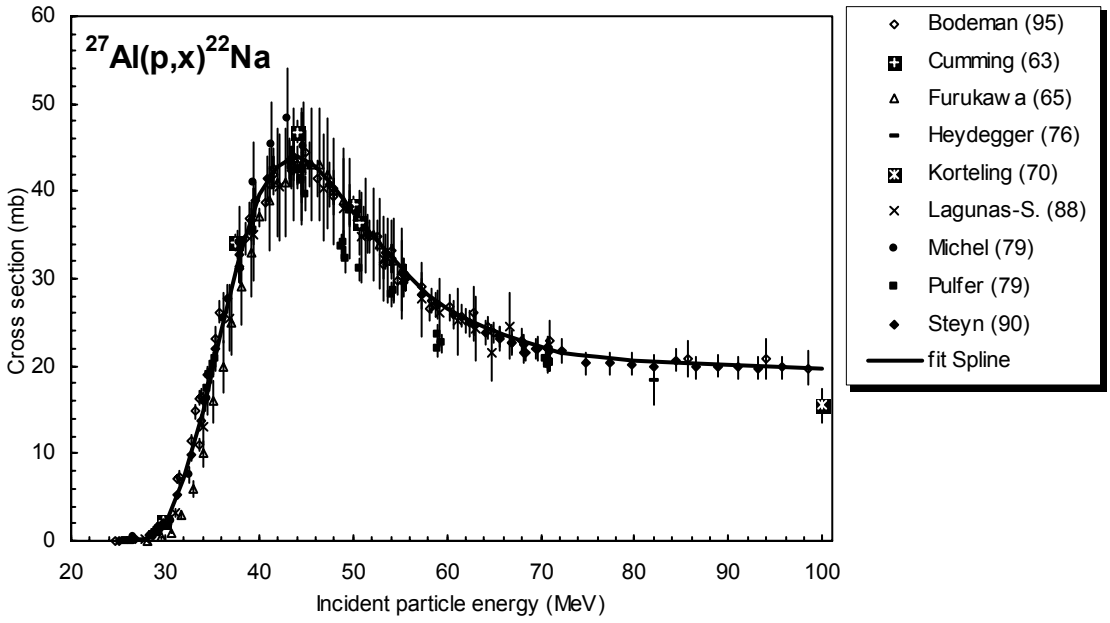

Figure 4.1.1c. *Selected experimental data and recommended cross-section curve.*

TABLE 4.1.1. RECOMMENDED CROSS SECTIONS FOR THE $^{27}Al(p,x)^{22}Na$ REACTION

Energy MeV	Cross-section mb	Energy MeV	Cross-section mb	Energy MeV	Cross-section mb	Energy MeV	Cross-section mb
30.0	1.9	48.0	40.7	66.0	23.6	84.0	20.5
30.5	2.8	48.5	40.0	66.5	23.4	84.5	20.4
31.0	4.0	49.0	39.3	67.0	23.2	85.0	20.4
31.5	5.4	49.5	38.6	67.5	23.0	85.5	20.4
32.0	7.0	50.0	37.9	68.0	22.8	86.0	20.4
32.5	8.8	50.5	37.2	68.5	22.6	86.5	20.3
33.0	10.7	51.0	36.5	69.0	22.5	87.0	20.3
33.5	12.8	51.5	35.8	69.5	22.3	87.5	20.3
34.0	14.9	52.0	35.1	70.0	22.2	88.0	20.3
34.5	17.2	52.5	34.4	70.5	22.0	88.5	20.3
35.0	19.4	53.0	33.8	71.0	21.9	89.0	20.2
35.5	21.7	53.5	33.1	71.5	21.8	89.5	20.2
36.0	23.9	54.0	32.5	72.0	21.6	90.0	20.2
36.5	26.1	54.5	31.9	72.5	21.5	90.5	20.2
37.0	28.3	55.0	31.3	73.0	21.4	91.0	20.2
37.5	30.3	55.5	30.8	73.5	21.4	91.5	20.1
38.0	32.3	56.0	30.2	74.0	21.3	92.0	20.1
38.5	34.1	56.5	29.7	74.5	21.2	92.5	20.1
39.0	35.9	57.0	29.2	75.0	21.1	93.0	20.1
39.5	37.4	57.5	28.7	75.5	21.1	93.5	20.1
40.0	38.8	58.0	28.2	76.0	21.0	94.0	20.0
40.5	40.0	58.5	27.8	76.5	21.0	94.5	20.0
41.0	41.1	59.0	27.4	77.0	20.9	95.0	20.0
41.5	42.0	59.5	27.0	77.5	20.9	95.5	20.0
42.0	42.6	60.0	26.6	78.0	20.9	96.0	20.0
42.5	43.2	60.5	26.3	78.5	20.8	96.5	19.9
43.0	43.5	61.0	26.0	79.0	20.8	97.0	19.9
43.5	43.7	61.5	25.7	79.5	20.7	97.5	19.9
44.0	43.8	62.0	25.4	80.0	20.7	98.0	19.9
44.5	43.7	62.5	25.2	80.5	20.7	98.5	19.9
45.0	43.6	63.0	24.9	81.0	20.6	99.0	19.8
45.5	43.3	63.5	24.7	81.5	20.6	99.5	19.8
46.0	42.9	64.0	24.4	82.0	20.6	100.0	19.8
46.5	42.4	64.5	24.2	82.5	20.5		
47.0	41.9	65.0	24.0	83.0	20.5		
47.5	41.3	65.5	23.8	83.5	20.5		

4.1.2. $^{27}Al(p,x)^{24}Na$

There were 27 experimental papers published. Five works presented cross-sections only above 100 MeV and six additional data sets showed discrepant results and were hence excluded from the selection process. The remaining 11 papers were considered for further selection. The list of related references given below is accompanied with additional information. We mention availability of data in the computerized database EXFOR (if available, unique EXFOR reference number is given). Furthermore, we indicate a reason why a data set was excluded (reference denoted by an asterisk *).

*** Brun, C., Lefort, M., Tarrago, X.:**
Détermination des intensités de faisceaux de protons de 40 a 150 MeV.
Journal de Physique et le Radium 23 (1962) 371
Data from: Tobailem, J., de Lassus St-Genies, C.-H., Leveque, L.: Sections efficaces des reactions nucleaires induites par protons, deutons, particules alpha. I reactions nucleaires moniteurs. Note CEA-N-1-1466(1), CEA, France, 1971.
— Exfor: none
— Data excluded: the maximum cross-sections are in good agreement with the values of the selected group, but the scale seems to be shifted to higher energies.

*** Chackett, G.A., Chackett, K.F., Reasbeck, P., Symonds, J.L., Waren, J.:**
Excitation functions up to 980 MeV for proton-induced reactions in ^{27}Al, relative to $^{12}C(p,pn)^{11}C$.
Proceedings of Physical Society (London), A69 (1956) 43.
Data from: Tobailem, J., de Lassus St-Genies, C.-H., and Leveque, L.: Sections efficaces des reactions nucleaires induites par protons, deutons, particules alpha. I reactions nucleaires moniteurs. Note CEA-N-1-1466(1), CEA, France, 1971.
— Exfor: none

*** Crandall, W.E, Millburn, G.P., Pyle, R.V., Birnbaum, W.:**
$C^{12}(x,xn)C^{11}$ and $Al^{27}(x,x2pn)Na^{24}$ reactions at high energies.
Physical Review **101** (1956) 329.
— Exfor: B0101

Cumming, J.B.:
Monitor reactions for high energy proton beams.
Annual Review of Nuclear and Particle Science **13** (1963) 261
— Exfor: B0022

*** Friendlander, G., Hudis, J., Wolfgang, R.L.:**
Disintegration of aluminum by protons in the energy range 0.4 to 3 MeV.
Physical Review **99** (1955) 263
— Exfor: C0264

Gauvin, H., Lefort, M., Terrago, X.:
Emmission d' hélions dans les réactions de spallation.
Nuclear Physics **39** (1962) 447
— Exfor: none

Gilbert, R.S.:
Private communications in Hicks, H.G., Stevenson, P.C., Nervik, W.E.:
Reaction $Al^{27}(p,3pn)Na^{24}$, Physical Review 102 (1956) 1390.
Data from: J. Tobailem, C.-H. de Lassus St-Genies and L. Leveque: Sections efficaces des reactions nucleaires induites par protons, deutons, particules alpha. I reactions nucleaires moniteurs. Note CEA-N-1-1466(1), CEA, France, 1971.
— Exfor: none

***Goebel, K., Harting, D., Kluyver, J.C., Kusumegi, A., Schultes, H.:**
The $^{12}C(p,n)^{11}C$ and $^{27}Al(p,3n)^{24}Na$ cross-sections at 591 MeV.
Nuclear Physics **24** (1961) 28
— Exfor: B0094
— Data excluded: only data points above 100 MeV.

Grütter, A.:
Excitation functions for radioactive isotopes produced by proton bombardment of Cu and Al in the energy range of 16 to 70 MeV.
Nuclear Physics **A383** (1982) 98
— Exfor: A0178

***Hicks, H.G., Stevenson, P.C., Nervik, W.E.:**
Reaction ^{27}Al (p,3pn) ^{24}Na.
Physical Review **102** (1956) 1390
— Exfor: C0257
— Data excluded: the maximum cross-sections are in good agreement with the values of the selected group but the scale seems to be shifted to higher energies.

***Hintz, N.M., Ramsey, N.E.:**
Excitation functions to 100 MeV.
Physical Review **102** (1952) 19
— Exfor: B0076
— Data excluded: significantly higher values, very old measurement using internal targets.

Hogan, J.J., Gadioli, E.:
Production of ^{24}Na from ^{27}Al by (35-100) MeV protons.
Nuovo Cimento **A3** (1978) 341
— Exfor: B0131

***Holub, R., Fowler, M., Yaffe, L., Zeller, A.:**
Formation of ^{24}Na in 'fission-like' reactions.
Nuclear Physics **A288** (1977) 291
— Exfor: B0082
— Data excluded: significantly higher values, shape near the maximum is strange

Lagunas-Solar, M.C., Carvacho, O.F., Cima, R.R.:
Cyclotron production of PET radionuclides: ^{18}F (109.77 min, β^+ 96.9%, EC 3.1%) from high-energy protons on metallic aluminium targets.
Applied Radiation Isotopes **39** (1988) 41
— Exfor: A0445

***Marquez, L.:**
The yield of ^{18}F from medium and heavy elements with 420 MeV protons.
Physical Review **86** (1952) 405
— Exfor: C0250
— Data excluded: only data points above 100 MeV.

***Meghir, S.:**
Excitation functions of some monitor reactions.
Thesis, McGill University, Canada (1962) reported in Devies, J.H., and Yaffe, L.: Canadian Journal Physics **41** (1963) 762
— Exfor: B0016
— Data excluded: significantly higher values, shape near the maximum is strange.

*** Michel, R., Pfeiffer, F., Stück, R.:**
Measurement and hybrid model analysis of integral excitation functions for the proton-induced reactions on vanadium, manganese and cobalt up to 200 MeV.
Nuclear Physics A441 (1985) 617, also in: Progress Report on Nuclear Data Research in the Federal Republic of Germany, ed. Cierjacks, S., Behrens, H., NEANDC(E)-242/U Vol. V, INDC(GER)-025/L (1983) 41
— Exfor: none

Michel, R., Dragovitsch, P., Englert, P., Pfeiffer, F., Stück, R., Theis, S., Begemann, F., Weber, H., Signer, P., Wieler, R., Filges, D., Cloth, P.:
On depth dependence of spallation reactions in a spherical thick diorite target homogeniously irradiated by 600 MeV protons. Simulation of production of cosmogenic nuclides in small meteorites.
Nuclear Instruments Methods **B16** (1986) 61
— Exfor: A0344

***Morrison, D.L., Caretto Jr., A.A.:**
Excitation functions of (p,xp) reactions.
Physical Review **127** (1962) 1731
— Exfor: P0040
— Data excluded: only data points above 100 MeV.

Miyano, K.:
The ^{7}Be, ^{22}Na and ^{24}Na production cross-sections with 22- to 55-MeV proton on ^{27}Al.
J. Physical Society Japan **34** (1973) 853
— Exfor: none

*** Parikh, V.:**
The activities induced in beryllium, oxygen and fluorine by protons of 220 MeV to 362 MeV. (Part I)
Nuclear Physics **18** (1960) 638
— Exfor: C0207

*** Parikh, V.:**
The activities induced in beryllium, oxygen and fluorine by protons of 220 MeV to 362 MeV (Part II).
Nuclear Physics **18** (1960) 646
— Exfor: C0208

***Prokoshkin Yu.D., Tyapkin, A.A.:**
Investigation of the excitation functions for the reactions $C^{12}(p,pn)C^{11}$, $Al^{27}(p,3pn)Na^{24}$ and $Al^{27}(p,3p,3n)Na^{22}$ in the 150-660 MeV energy range.
J. Experimental Theoretical Physics **32** (1957) 177
— Exfor: none
— Data excluded: only data points above 100 MeV.

Pulfer, P.:
Determination of absolute production cross-sections for proton induced reactions in the energy range 15 to 72 MeV and at 1820 MeV.
Thesis (1979), Universität Bern, unpublished
Data taken from EXFOR
— Exfor: D0053

***Stevenson, P.C., Folger, R.L.:**
Unpublished data.
Referred in: Hicks, H.G., Stevenson, P.C.,and Nervik, W.E.:
Reaction $Al^{27}(p,3pn)Na^{24}$., Physical Review 102 (1956) 1390.
Data from: J. Tobailem, C.-H. de Lassus St-Genies and, L. Leveque: Sections efficaces des reactions nucleaires induites par protons, deutons, particules alpha. I reactions nucleaires moniteurs. Note CEA-N-1-1466(1), CEA, France, 1971.
— Exfor: none
— Data excluded: only data points above 100 MeV

Williams, I.R., Fulmer, C.B.:
Excitation functions for radioactive isotopes produced by protons below 60 MeV in Al, Fe, and Cu.
Physical Review **162** (1967) 1055
— Exfor: B0073

Yule, H., Turkevich, A.:
Radiochemical studies of the (p,pn) reaction in complex nuclei in the 80-450 MeV range.
Physical Review **118** (1960) 1591
— Exfor: P0049

The data from all experimental papers where numerical values are available below 100 MeV (16 papers), are presented in Fig. 4.1.2a. The scatter of data is large, illustrating the reasons why only 11 papers were selected for evaluation.

Cross-sections were calculated by the nuclear reaction model codes ALICE-HMS and SPEC and by two fitting procedures (Padé with 15 parameters and Spline). These results are compared with the selected experimental data in Fig. 4.1.2b. It is seen that the model calculations do not reproduce the data satisfactorily except for SPEC in the energy range 60-80 MeV. Fits do much better, the best was judged to be the spline fit. Recommended cross-sections are compared with selected experimental data, including their error bars, in Fig. 4.1.2c. The corresponding numerical values are tabulated in Table 4.1.2.

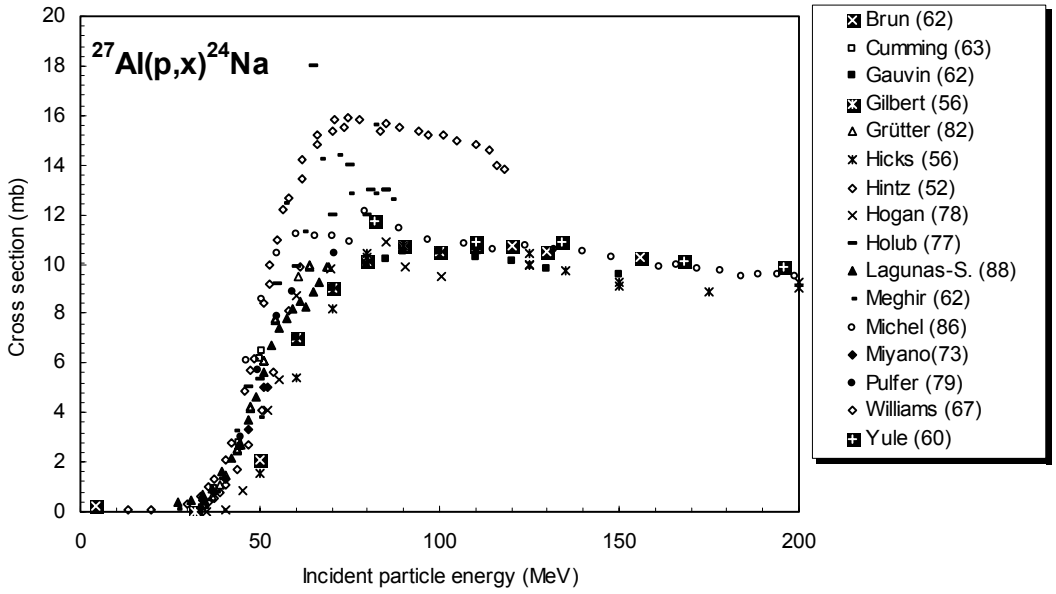

Figure 4.1.2a. All experimental data.

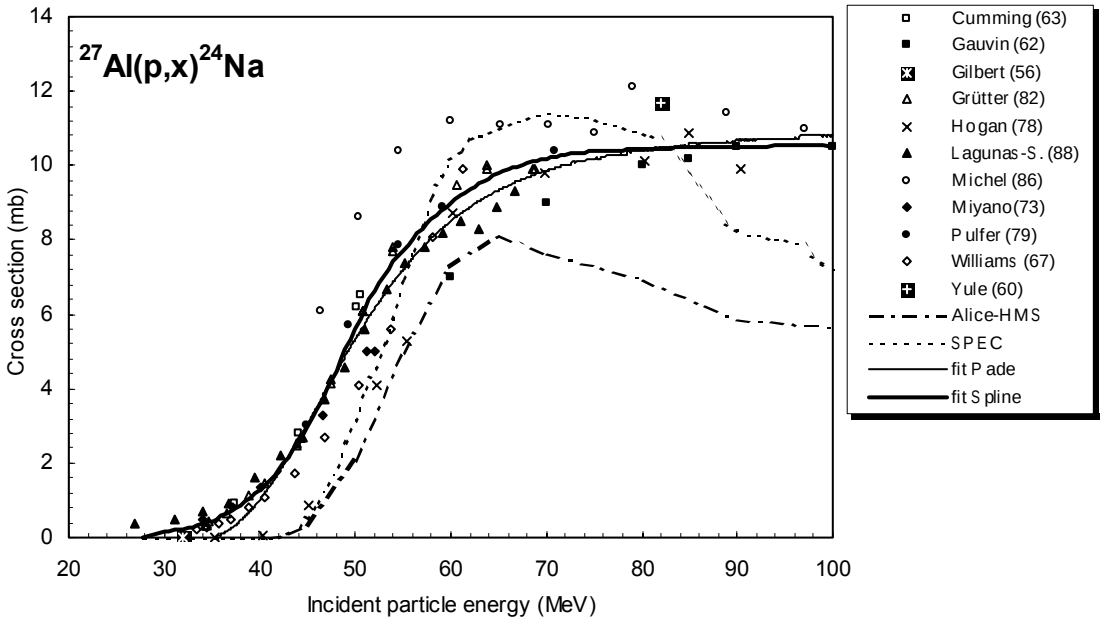

Figure 4.1.2b. Selected experimental data in comparison with theoretical calculations and fits.

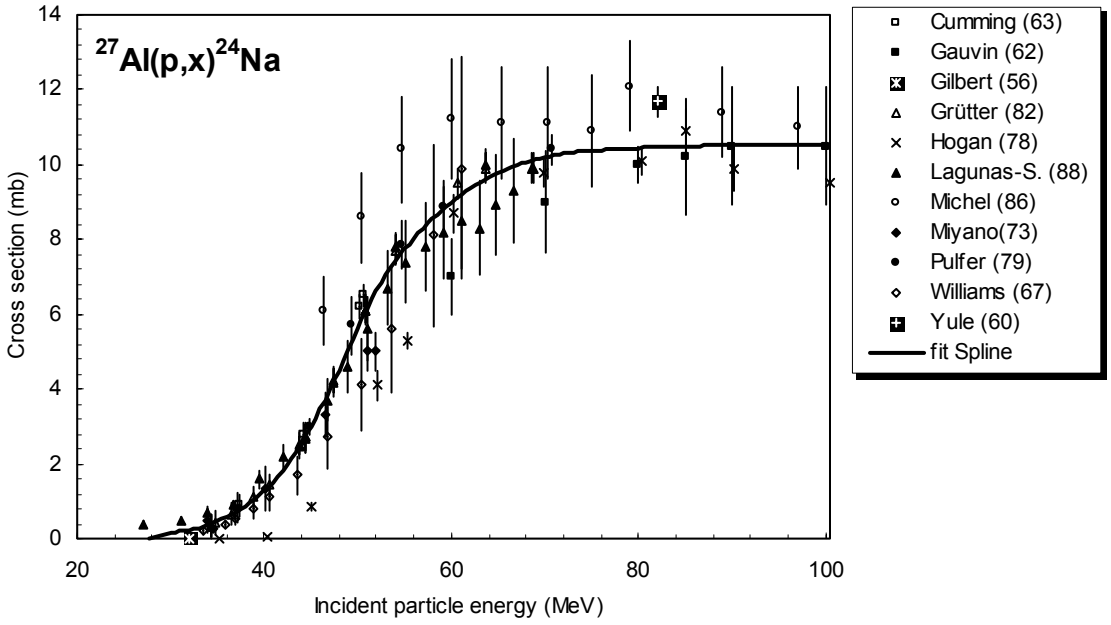

Figure 4.1.2c. Selected experimental data and recommended cross-section curve.

TABLE 4.1.2. RECOMMENDED CROSS SECTIONS FOR THE $^{27}Al(p,x)^{24}Na$ REACTION

Energy MeV	Cross-section mb	Energy MeV	Cross-section mb	Energy MeV	Cross-section mb	Energy MeV	Cross-section mb
30.0	0.16	47.0	3.97	64.0	9.66	81.0	10.45
30.5	0.17	47.5	4.23	64.5	9.72	81.5	10.46
31.0	0.19	48.0	4.49	65.0	9.78	82.0	10.46
31.5	0.21	48.5	4.77	65.5	9.84	82.5	10.47
32.0	0.23	49.0	5.05	66.0	9.89	83.0	10.47
32.5	0.26	49.5	5.34	66.5	9.94	83.5	10.48
33.0	0.29	50.0	5.62	67.0	9.98	84.0	10.48
33.5	0.33	50.5	5.89	67.5	10.02	84.5	10.48
34.0	0.36	51.0	6.15	68.0	10.06	85.0	10.49
34.5	0.41	51.5	6.39	68.5	10.10	85.5	10.49
35.0	0.46	52.0	6.62	69.0	10.13	86.0	10.50
35.5	0.51	52.5	6.84	69.5	10.17	86.5	10.50
36.0	0.57	53.0	7.04	70.0	10.20	87.0	10.50
36.5	0.63	53.5	7.23	70.5	10.23	87.5	10.51
37.0	0.70	54.0	7.40	71.0	10.25	88.0	10.51
37.5	0.78	54.5	7.57	71.5	10.28	88.5	10.51
38.0	0.87	55.0	7.73	72.0	10.30	89.0	10.51
38.5	0.96	55.5	7.88	72.5	10.32	89.5	10.52
39.0	1.06	56.0	8.02	73.0	10.33	90.0	10.52
39.5	1.16	56.5	8.16	73.5	10.35	90.5	10.52
40.0	1.27	57.0	8.30	74.0	10.36	91.0	10.52
40.5	1.39	57.5	8.43	74.5	10.37	91.5	10.52
41.0	1.52	58.0	8.55	75.0	10.38	92.5	10.53
41.5	1.66	58.5	8.67	75.5	10.39	93.0	10.53
42.0	1.81	59.0	8.79	76.0	10.39	94.0	10.53
42.5	1.98	59.5	8.89	76.5	10.40	94.5	10.53
43.0	2.15	60.0	9.00	77.0	10.41	95.5	10.53
43.5	2.34	60.5	9.09	77.5	10.41	96.0	10.53
44.0	2.55	61.0	9.19	78.0	10.42	97.0	10.53
44.5	2.76	61.5	9.28	78.5	10.43	97.5	10.53
45.0	2.99	62.0	9.36	79.0	10.43	98.5	10.53
45.5	3.22	62.5	9.44	79.5	10.44	99.0	10.53
46.0	3.46	63.0	9.52	80.0	10.44	100.0	10.52
46.5	3.71	63.5	9.59	80.5	10.45		

4.1.3. $^{nat}Ti(p,x)^{48}V$

A total of 16 published cross-section data sets, in the energy region considered, were found in the literature from which 10 data sets were not selected for evaluation. The remaining 6 papers were selected for further evaluation. For detailed description of the evaluation and selection see Szelecsényi et al. (1999). The list of related references given below is accompanied with additional information. We mention availability of data in the computerized database EXFOR (if available, unique EXFOR reference number is given). Furthermore, we indicate a reason why a data set was excluded (reference denoted by an asterisk *).

*** Barrandon, J.N., Debrun, J., L., Kohn, A., Spear, R.H.:**
Etude du dosage de Ti, V, Cr, Fe, Ni, Cu et Zn par activation avec des protons d'energie limitee a 20 MeV.
Nuclear Instruments Methods **127** (1975) 269
— Exfor: O0086
— Data excluded: systematically lower than those of the majority of other works.

*** Birattari, C., Bonardi, M., Resmini, F., Salomone, A.:**
Status report on radioisotope production for biomedical purposes at Milan AVF Cyclotron. Proceedings of Ninth International Conference on Cyclotrons (France) 1981, (ed. Gendreau, G.) p. 693.
Experimental details are published in Sabbioni, E., Marafante, E., Goetz, L., Birattari, C.: Cyclotron production of carrier free ^{48}V and preparation of different ^{48}V compounds for metabolic studies in rats. Radiochemical Radioanalytical Letters **31** (1977) 39
— Exfor: none
— Data excluded: energy scale shows a large shift.

Bodemann, R., Michel, R., Rosel, R., Herpers, U., Holmqvist, B., Conde, H., Malmborg, P.:
Production of radionuclides from target elements (22<Z<29) by proton-induced reactions up to 100 MeV.
Progress Report on Nuclear Data Research in the Federal Republic of Germany for the Period April 1, 1994 to March 31, 1995 (ed. Qaim, S.M.), INDC (GER)-040, Jül-3086, 1995, p. 27
— Exfor: none

*** Brodzinski, R.L., Rancitelli, L.A., Cooper, J.A., Wogman, N.A.:**
High-energy proton spallation of titanium.
Physical Review **4** (1971) 1250
— Exfor: C0271
— Data excluded: target irradiated with high energy protons, the cross-section values in the energy region of our interest have very high energy uncertainty.

*** Dittrich, B.:**
Radiochemische Untersuchung Protonen— und α-induzierter Spallations— und Fragmentationsreaktionen mit Hilfe der Gamma— und Beschleunigermassen-Spektrometrie.
Dissertation, Universität zu Köln, Köln 1990.
— Exfor: none
— Data excluded: data points available only above the 50 MeV upper limit.

*** Gadioli, E., Gadioli Erba, E., Hogan, J.J., Burns, K.I.:**
Emission of alpha particles in the interaction of 10-85 MeV protons with ^{48}Ti and ^{50}Ti.
Zeitschrift für Physik **A301** (1981) 289
— Exfor: D4060
— Data excluded: only the first 3 points could be converted by the compiler.

Kopecky, P., Szelecsényi, Molnár, T., Mikecz, P., Tárkányi, F.:
Excitation functions of (p,xn) reactions on ^{nat}Ti: monitoring of bombarding proton beams.
Applied Radiation Isotopes **44** (1993) 687
— Exfor: D4001

*** Levkovski, V.N.:**
Middle mass nuclides (A=40-100) activation cross-sections by medium energy (E=10-50 MeV) protons and α particles (experiments and systematics).
Inter-Vesi, Moscow, 1991
— Exfor: A0510
— Data excluded: cross-section data are systematically higher than those of the majority of other works and the cross-sections of the monitor reaction used by Levkovski for current measurement are not well measured.

*** Michel, R., Brinkmann, G., Weigel, H., Herr, W.:**
Proton-induced reactions on titanium with energies between 13 and 45 MeV.
J. Inorganic Nuclear Chemistry **40** (1978) 1845
— Exfor: B0100
— Data excluded: systematically higher than those of the majority of other works.

Michel, R., Brinkmann, G.:
On the depth-dependent production of radionuclides (44<A<59) by solar protons in extraterrestrial matter.
J. Radioanalytical Chemistry **59** (1980) 467
— Exfor: A0145

*** Stück, R.:**
Protonen-induzirte Reaktionen an Ti, V, Mn, Fe, Co und Ni. Messung und Hybrid Modell Analyse integraler Anregungsfunktionen und ihre Anwendung in Modellrechnungen zur Produktion kosmogener Nuklide.
Dissertation, Universität zu Köln, Köln, Germany 1983
— Exfor: A0100
— Data excluded: cross-sections available only above the 50 MeV upper limit.

Szelecsényi, F., Hermanne, A., Sonck, M., Takács, S., Scholten, B., Tárkányi, F.:
New cross-section data on ^{nat}Ti(p,x)^{48}V nuclear process for proton beam monitoring in radioisotope production.
Nuclear Instruments Methods B (submitted) 2000
— Exfor: none

Tanaka, S., Furukawa, M.:
Excitation functions for (p,n) reactions with titanium, vanadium, chromium, iron and nickel up to E_p=14 MeV.
J. Physical Society Japan **14** (1959) 1269
— Exfor: B0043

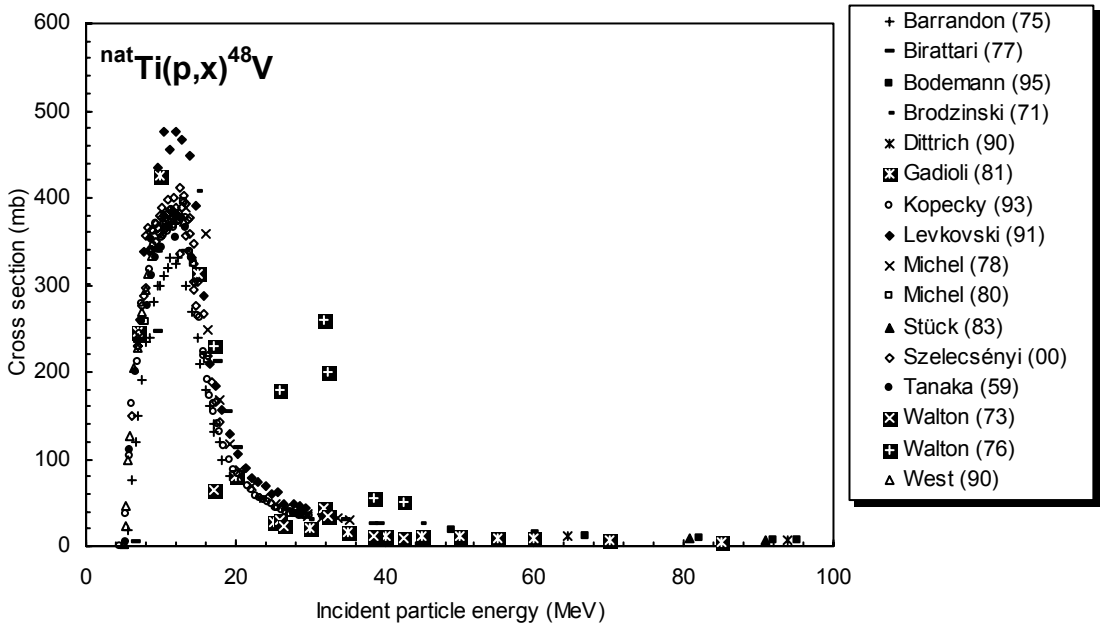

Figure 4.1.3a. All experimental data.

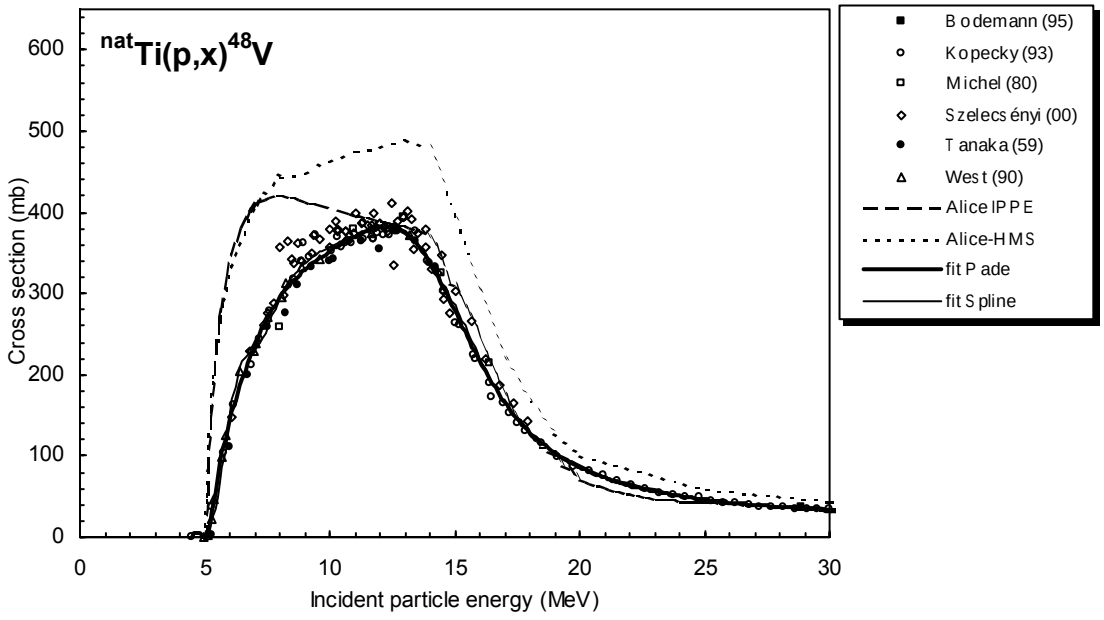

Figure 4.1.3b. Selected experimental data in comparison with theoretical calculations and fits.

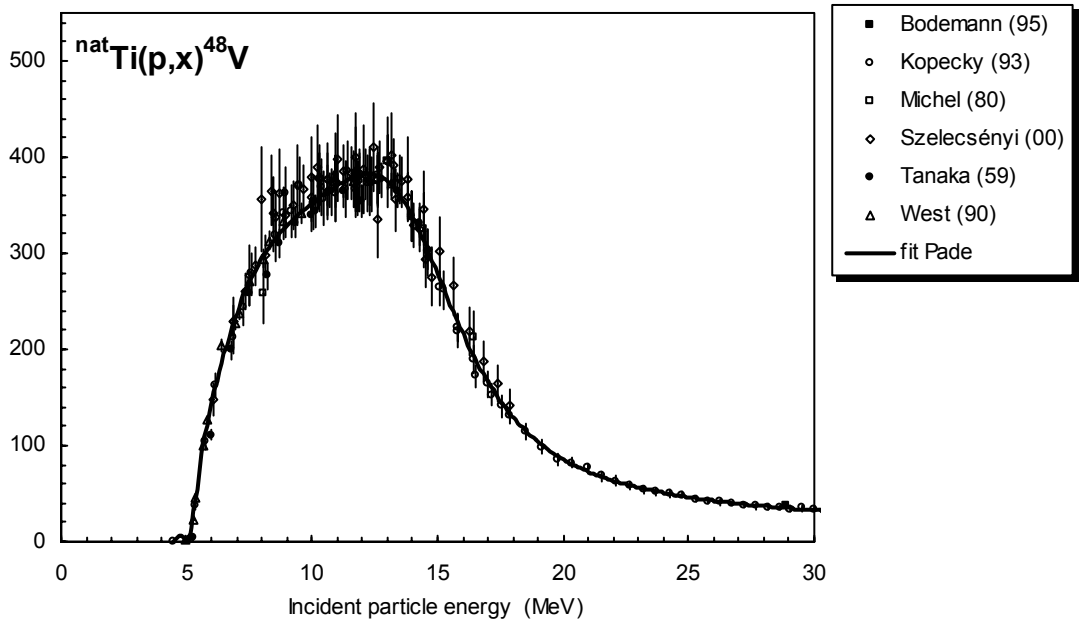

Figure 4.1.3c. Selected experimental data and recommended cross-section curve.

TABLE 4.1.3. RECOMMENDED CROSS-SECTIONS FOR THE $^{nat}Ti(p,x)^{48}V$ REACTION

Energy MeV	Cross-section mb	Energy MeV	Cross-section mb	Energy MeV	Cross-section mb	Energy MeV	Cross-section mb
5.0	0.5	11.5	378	18.0	129	24.5	48.4
5.5	73.9	12.0	382	18.5	115	25.0	46.3
6.0	145	12.5	382	19.0	104	25.5	44.3
6.5	196	13.0	375	19.5	93.9	26.0	42.6
7.0	237	13.5	361	20.0	85.7	26.5	41.0
7.5	270	14.0	338	20.5	78.8	27.0	39.6
8.0	295	14.5	310	21.0	72.9	27.5	38.2
8.5	314	15.0	279	21.5	67.8	28.0	37.0
9.0	329	15.5	247	22.0	63.4	28.5	35.8
9.5	341	16.0	216	22.5	59.6	29.0	34.8
10.0	352	16.5	189	23.0	56.3	29.5	33.7
10.5	362	17.0	166	23.5	53.3	30.0	32.8
11.0	370	17.5	146	24.0	50.7		

*** Walton, J.R., Yaniv, A., Heymann, D.:**
He and Ne cross-sections in natural Mg, Al and Si targets and radionuclide cross-sections in natural Si, Ca, Ti and Fe targets bombarded with 14 to 45 MeV protons.
J. Geophysical Research **78** (1973) 6428
— Exfor: none
— Data excluded: unreliable beam current determination.

*** Walton, J.R., Heymann, D., Yaniv, A.:**
Cross-sections for He and Ne isotopes in natural Mg, Al, and Si, He isotopes in CaF_2, Ar isotopes in natural Al, Si, Ti, Cr and stainless steel induced by 12 to 45 MeV protons.
J. Geophysical Research **81** (1976) 5689
— Exfor: none
— Data excluded: unreliable beam current determination.

West, Jr., H.I., Lanier, R.G., Mustafa, M.G.:
Excitation functions for the nuclear reactions on titanium leading to the production of ^{48}V, ^{44}Sc and ^{47} Sc, by proton, deuteron and triton irradiations at 0-35 MeV.
UCLR-ID-115738, November 1993
Physical Review C42 (1990) 683
— Exfor: none

The data from all experimental papers (16 papers) are presented in Fig. 4.1.3a. Only 6 papers were selected for evaluation.

Cross-sections were calculated by two different versions of the nuclear reaction model code ALICE (denoted as HMS and as IPPE) and by two fitting procedures (Padé with 17 parameters and Spline). These results are compared with the selected experimental data in Fig. 4.1.3b. It is seen that model calculations systematically over predict the data, particularly in the 5-12 MeV region. Fits do much better, the best was judged to be the Padé fit. Recommended cross-sections are compared with selected experimental data, including their error bars, in Fig. 4.1.3c. The corresponding numerical values are tabulated in Tab. 4.1.3.

4.1.4. $^{nat}Ni(p,x)^{57}Ni$

A total of 21 cross-section data sets were found in the literature in the energy range considered. From these 6 works were excluded while the remaining 15 papers were selected for further evaluation. The list of related references given below is accompanied with additional information. We mention availability of data in the computerized database EXFOR (if available, unique EXFOR reference number is given). Furthermore, we indicate a reason why a data set was excluded (reference denoted by an asterisk *).

It is well known that the ^{57}Ni isotope may also be produced via $^{58}Ni(n,2n)$ and $^{60}Ni(n,4n)$ reactions when Ni targets are irradiated with protons. The recent results of a Belgian-Hungarian collaboration, however, showed that the contribution of the neutron induced reactions to the production of ^{57}Ni is small even in case of full stopping at 40 MeV.

*** Aleksandrov, V.N., Semenova, M.P., Semenov, V.G.:**
Production cross-section of radionuclides in (p,x) reactions on copper and nickel nuclei.
Atomnaya Energiya **62** (1987) 411
— Exfor: A0351 and D4074
— Data excluded: fluctuating values and values seem to be systematically wrong.

*** Barrandon, J.N., Debrun, J.L., Kohn, A., Spear, R.H.:**
Etude du dosage de Ti, V, Cr, Fe, Ni, Cu et Zn par activation avec des protons d' energie limitée a 20 MeV.
Nuclear Instruments Methods **127** (1975) 269
— Exfor: O0086
— Data excluded: systematically low cross-section values.

Bodemann, R., Michel, R., Roesel, R., Herpers, U., Holmqvist, B., Conde, H., Malmborg, P.:
Production of radionuclides from target elements (22<Z<29) by proton-induced reactions up to 100 MeV.
Progress Report on Nuclear Data Research in the Federal Republic of Germany for the Period April 1, 1994 to March 31, 1995 (ed. Qaim, S.M.), INDC(GER)-040, Jül-3086, 1995, p. 27
— Exfor: none

Brinkman, G.A., Helmer, J., Lindner, L.:
Nickel and copper foils as monitors for cyclotron beam intensities.
Radiochemical Radioanalytical Letters **28** (1977) 9
— Exfor: none
Remarks: The compiler excluded the cross-section values which were below the threshold energy of the $^{nat}Ni(p,x)^{57}Ni$ process.

Brinkmann, G.:
Integrale Anregungsfunktionen für Protonen— und Alpha-induzierte Reaktionen an Targetelementen 22<Z<28.
Dissertation, Universität zu Köln, Cologne, Germany, 1979
— Exfor: none

Cohen, B.L., Newman, E., Handley, T.H.:
(p,pn) + (p,2n) and (p,2p) cross-sections in medium weight elements.
Physical Review **99** (1955) 723
— Exfor: B0049

*** Ewart, H.A., Blann, M.:**
Nuclear cross-sections for charged particle induced reactions.
Preprints ORNL CPX-1, CPX-2, Oak Ridge 1964
Numerical data are taken from Iljinov, A.S., Semenov, V.G., Semenova, Sobolevsky, N., M., Udovenko, L.V.: Production of Radionuclides at Intermediate Energies, Landolt-Börnstein New Series 13a (ed. Schopper, H.)
— Exfor: none
— Data excluded: major shift in the energy scale at low energies.

*** Furukawa, M., Shinohara, A., Narita, M., Kojima, S.:**
Production of ^{59,63}Ni from natural Ni irradiated with protons up to E_p= 40 MeV and decay of ^{56}Ni.
Annual Report 1990, Institute for Nuclear Study, University Tokyo, Japan, p. 35
Numerical data are taken from Iljinov, A.S., Semenov, V.G., Semenova, Sobolevsky, N.M., Udovenko, L.V. Production of Radionuclides at Intermediate Energies, Landolt-Börnstein New Series 13d (ed. Schopper, H.)
— Exfor: none
— Data excluded due to fluctuations. Unfortunately the original data and details on the method used were not available to the compiler.

*** Haasbroek, F.J., Steyn, J., Neirinckx, R.D., Burdzik, G.F., Cogneau, M., Wanet, P.:**
Excitation functions and thick target yields for radioisotopes induced in natural Mg, Co, Ni and Ta by medium energy protons.
Report CSIR-FIS-89 (1976), Applied Radiation Isotopes **28** (1977) 533
— Exfor: B0098
— Data excluded; large shift towards higher energy.

Kaufman, S.:
Reactions of protons with ^{58}Ni and ^{60}Ni.
Physical Review **117** (1960) 1532
— Exfor: B0055

Levkovski, V.N.:
Cross-section of medium mass nuclide activation (A=40-100) by medium energy protons and alpha particles (E=10-50 MeV).
Inter-Vesi, Moscow, 1991, USSR
— Exfor: A0510

Michel, R., Brinkmann, G.:
On the depth-dependent production of radionuclides (44<A<59) by solar protons in extraterrestrial matter.
J. Radioanalytical Chemistry **59** (1980) 467
— Exfor: A0145

Michel, R., Weigel, H., Herr, W.:
Proton-induced reactions on nickel with energies between 12 and 45 MeV.
Zeitschrift für Physik **A286** (1978) 393
— Exfor: B0083

Piel, H.:
Bestimmung der Anregungsfunktionen von (p,xn)-Reaktionen an Ni-Isotopen.
Diplomarbeit, Universität zu Köln, Cologne, Germany, 1991
— Exfor: none

Sonck, M., Hermanne, A., Szelecsényi, F., Takács, S., Tárkányi, F.:
Study of the $^{nat}Ni(p,x)^{57}Ni$ process up to 44 MeV for monitor purposes.
Applied Radiation Isotopes **49** (1998) 1533
— Exfor: D4062

Steyn, G.F., Mills, S.J., Nortier, F.M.:
Private communication (1996)
— Exfor: none

Stück, R.:
Protonen-induzierte Reaktionen an Ti, V, Mn, Fe, Co und Ni. Messung und Hybrid Modell Analyse integraler Anregungsfunktionen und ihre Anwendung in Modellrechnungen zur Produktion kosmogener Nuklide.
Dissertation, Universität zu Köln, Cologne, Germany, 1983
— Exfor: A0100

Szelecsényi, F., Hermanne, A., Sonck, M., Takács, S., Scholten, B., Tárkányi, F.:
New cross-section data on $^{nat}Ti(p,x)^{48}V$ nuclear process for proton beam monitoring in radioisotope production.
Nuclear Instruments Methods B (submitted)
— Exfor: none

Tanaka, S., Furukawa, M., Chiba, M.:
Nuclear reactions of nickel with protons up to 56 MeV.
J. Inorganic Nuclear Chemistry **34** (1972) 2419
— Exfor: B0020

Tárkányi, F., Szelecsényi, F., Kopecky, P.:
Excitation functions of proton induced nuclear reactions on natural nickel for monitoring beam energy and intensity.
Applied Radiation Isotopes **42** (1991) 513
— Exfor: D4002

*** Zhuravlev, B.V., Grusha, O.V. Ivanova, S.P., Trykova, V.I., Shubin Yu.N.:**
Analysis of neutron spectra in 22 MeV proton interactions with nuclei.
Yadarnaya Fizika **39** (1984) 264
— Exfor: A0271
— Data excluded: neutron spectrum measured with large possible error.

The data from all experimental papers where numerical values are available (21 papers), are collected in Fig. 4.1.4a. The scatter of 6 data sets is large, illustrating the reasons why only 15 papers were selected.

Cross-sections were calculated by two different versions of the nuclear reaction model code ALICE (denoted as HMS(FG) and as IPPE) and by two fitting procedures (Padé with 20 parameters and Spline). These results are compared with the selected experimental data in Fig. 4.1.4b. It is seen that HMS(FG) calculations do not reproduce the data over the whole energy region. The ALICE-IPPE calculation represents the data better. Fits are equally good, the best was judged to be the spline fit. Recommended cross-sections are compared with selected experimental data, including their error bars, in Fig. 4.1.4c. The corresponding numerical values are tabulated in Tab. 4.1.4.

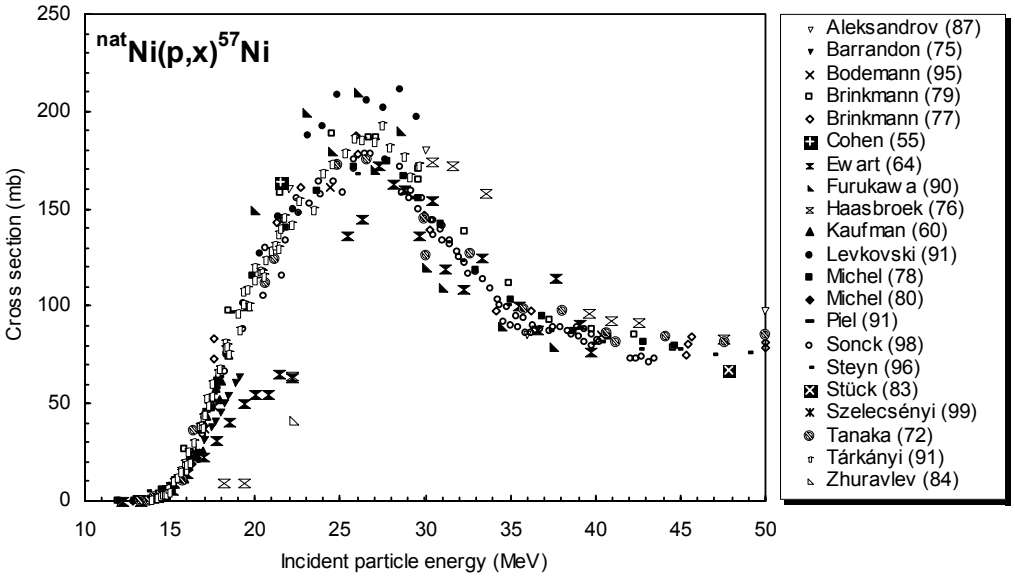

Figure 4.1.4a. All experimental data.

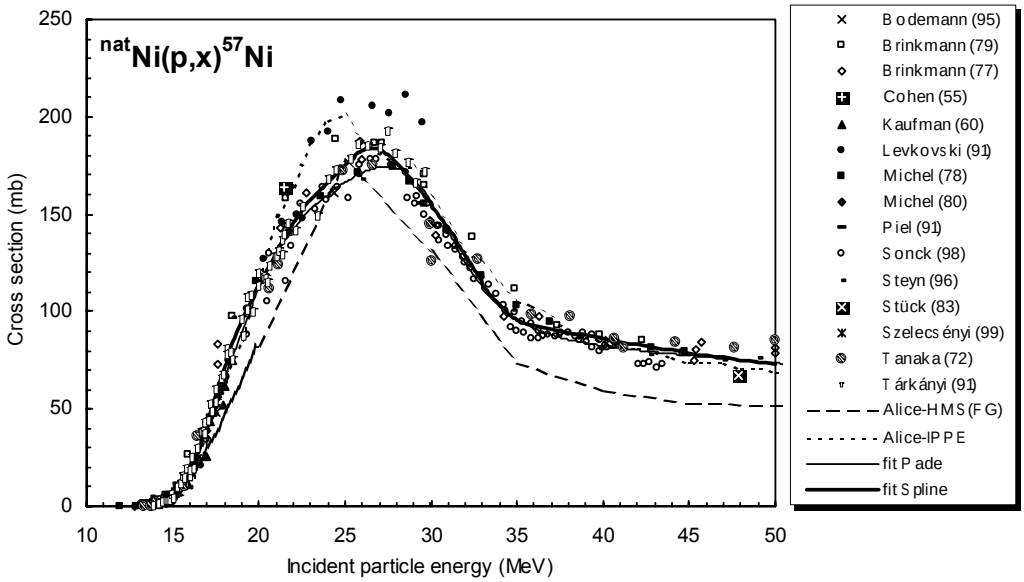

Figure 4.1.4b. Selected experimental data in comparison with theoretical calculations and fits.

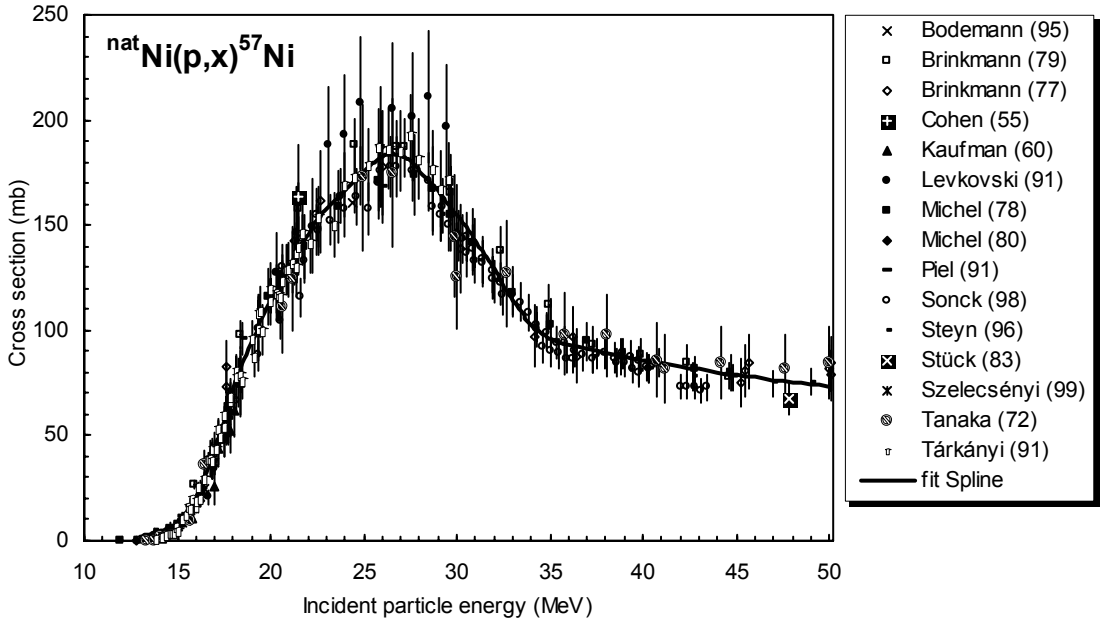

Figure 4.1.4c. Selected experimental data and recommended cross-section curve.

TABLE 4.1.4. RECOMMENDED CROSS-SECTION DATA FOR THE $^{nat}Ni(p,x)^{57}Ni$ REACTION

Energy MeV	Cross-section mb	Energy MeV	Cross-section mb	Energy MeV	Cross-section mb	Energy MeV	Cross-section mb
13.0	2.3	22.5	152	32.0	129	41.5	83.6
13.5	3.0	23.0	158	32.5	122	42.0	82.9
14.0	4.1	23.5	162	33.0	114	42.5	82.1
14.5	5.6	24.0	166	33.5	108	43.0	81.4
15.0	8.5	24.5	171	34.0	103	43.5	80.7
15.5	13.6	25.0	175	34.5	98.9	44.0	80.0
16.0	20.8	25.5	179	35.0	96.0	44.5	79.4
16.5	30.4	26.0	183	35.5	94.1	45.0	78.7
17.0	42.5	26.5	184	36.0	93.1	45.5	78.1
17.5	57.2	27.0	183	36.5	92.1	46.0	77.5
18.0	71.6	27.5	180	37.0	91.2	46.5	76.9
18.5	84.2	28.0	176	37.5	90.3	47.0	76.3
19.0	95.2	28.5	171	38.0	89.4	47.5	75.7
19.5	105	29.0	166	38.5	88.5	48.0	75.2
20.0	114	29.5	161	39.0	87.7	48.5	74.7
20.5	122	30.0	155	39.5	86.8	49.0	74.2
21.0	130	30.5	149	40.0	86.0	49.5	73.7
21.5	138	31.0	143	40.5	85.2	50.0	73.2
22.0	146	31.5	136	41.0	84.4		

4.1.5. $^{nat}Cu(p,x)^{56}Co$

A total of 7 published cross-section data sets, in the energy region considered, were found in the literature of which 3 were not considered for evaluation. The remaining 4 papers were selected for further evaluation. The list of related references given below is accompanied with additional information. We mention availability of data in the computerized database EXFOR (if available, unique EXFOR reference number is given). Furthermore, we indicate a reason why a data set was excluded (reference denoted by an asterisk *).

***Aleksandrov, V.N., Semenova, M.P., Semenov, V.G.:**
Production cross-section of radionuclide production in (p,x) at copper and nickel nuclei.
Atomnaya Energiya **62** (1987) 441
— Exfor: D4074
— Data excluded: cross-sections have large uncertainties and are at odds with the more recent measurements.

Bodemann, R., Michel, R., Rösel, R., Herpers, U., Holmqvist, B., Condé, H., Malmborg, P.:
Production of radionuclides from target elements (22 < Z < 29) by proton-induced reactions up to 100 MeV.
In Progress Report on Nuclear Data Research in the Federal Republic of Germany, ed. Qaim, S.M., NEA/NSC/DOC(95)10, INDC (GER)-040 (1995) 27.
— Exfor: none

Grütter, A.:
Excitation functions for radioactive isotopes produced by proton bombardment of Cu and Al in the energy range of 16 to 70 MeV.
Nuclear Physics **A383** (1982) 98
— Exfor: A0178

*** Heydegger, H.R., Garret, C.K., Van Ginneken, A.:**
Thin-target cross-sections for some Cr, Mn, Fe, Co, Ni, and Zn nuclides produced in copper by 82-416 MeV protons.
Physical Review **C6** (1972) 1235
— Exfor: none
— Data excluded: cross-sections have large uncertainties and are at odds with the more recent measurements.

Michel, R., Bodemann, R., Busemann, H., Daunke, R., Gloris, M., Lange, J.H., Klug, B., Krins, A., Leya, I., Lüpke, M., Neumann, S., Reinhardt, H., Schnatz-Büttgen, M., Herpers, U., Schiekel Th., Sudbrock, F., Holmqvist, B., Condé, H., Malmborg, P., Suter, M., Dittrich-Hannen, B., Kubik, P.W., Synal, H.A., Filges, D.:
Cross-sections for the production of residual nuclides by low— and medium-energy protons from the target elements C, N, O, Mg, Al, Si, Ca, Ti, V, Mn, Fe, Co, Ni, Cu, Sr, Y, Zr, Nb, Ba and Au.
Nuclear Instruments Methods **B129** (1997) 153
— Exfor: O0276

Mills, S.J., Steyn, G.F., Nortier, F.M.:
Experimental and theoretical excitation functions of radionuclides produced in the proton bombardment of copper up to 200 MeV.
Applied Radiation Isotopes **43** (1992) 1019
— Exfor: A0507

*** Williams, I.R., Fulmer, C.B.:**
Excitation functions for radioactive isotopes produced by protons below 60 MeV on Al, Fe and Cu.
Physical Review **162** (1967) 1055
— Exfor: B0073
— Data excluded: cross-sections have large uncertainties and are at odds with the more recent measurements.

The data from all experimental papers where numerical values are available (7 papers), are collected in Fig. 4.1.5a. The scatter of 3 data sets is large, therefore only 4 papers were selected.

Cross-sections were calculated with ALICE code (denoted as Alice-HMS(FG)) and by two fitting procedures (Padé with 8 parameters and Spline). These results are compared with the selected experimental data in Fig. 4.1.5b. It is seen that the calculation significantly overpredicts the data at energies above about 55 MeV. Fits do much better, the best was judged to be the spline fit. Recommended cross-sections are compared with selected experimental data, including their error bars, in Fig. 4.1.5c. The corresponding numerical values are tabulated in Tab. 4.1.5.

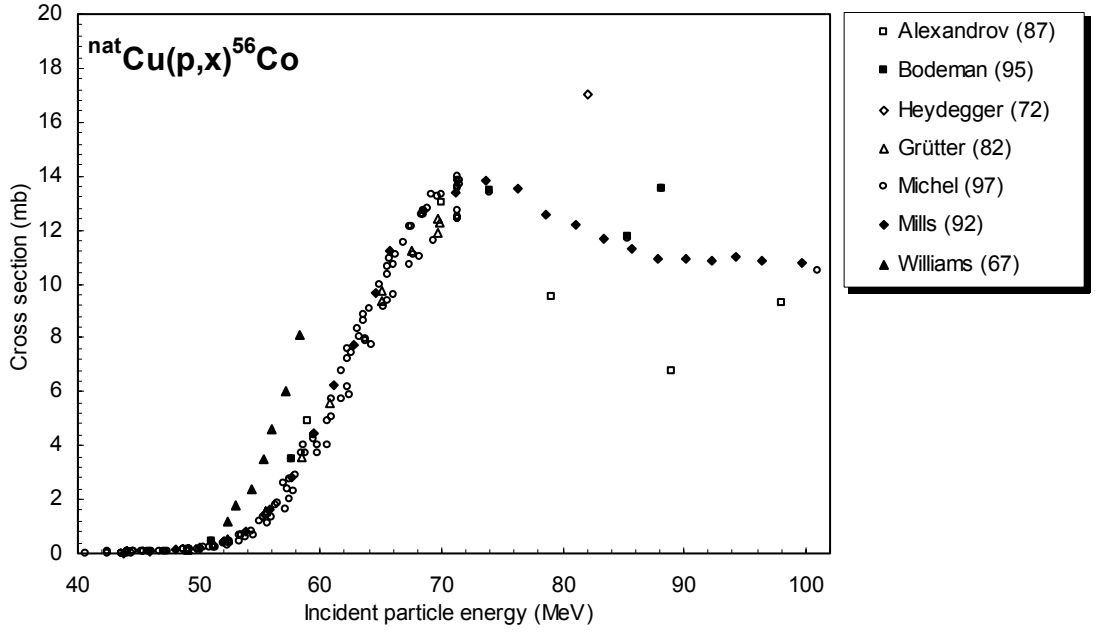

Figure 4.1.5a. All experimental data.

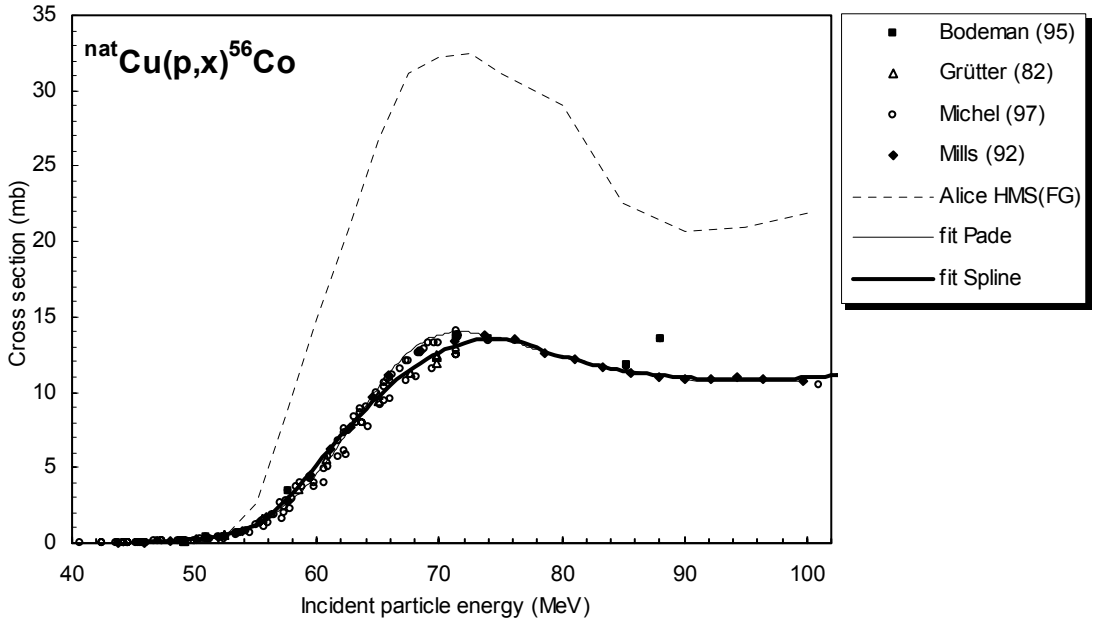

Figure 4.1.5b. Selected experimental data in comparison with theoretical calculations and fits.

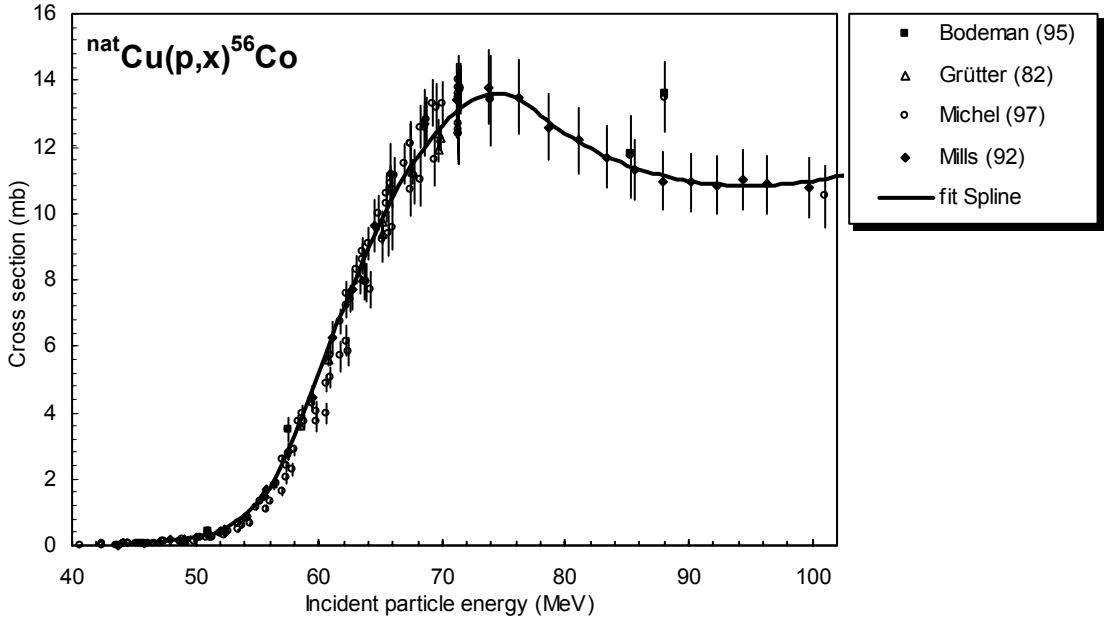

Figure 4.1.5c. Selected experimental data and recommended cross-section curve.

TABLE 4.1.5. RECOMMENDED CROSS-SECTION DATA FOR THE $^{nat}Cu(p,x)^{56}Co$ REACTION

Energy MeV	Cross-section mb	Energy MeV	Cross-section mb	Energy MeV	Cross-section mb	Energy MeV	Cross-section mb
50.0	0.2	63.0	8.1	76.0	13.5	89.0	11.0
50.5	0.3	63.5	8.5	76.5	13.4	89.5	11.0
51.0	0.3	64.0	8.9	77.0	13.2	90.0	11.0
51.5	0.4	64.5	9.3	77.5	13.1	90.5	10.9
52.0	0.5	65.0	9.7	78.0	12.9	91.0	10.9
52.5	0.6	65.5	10.1	78.5	12.8	91.5	10.9
53.0	0.7	66.0	10.5	79.0	12.6	92.0	10.9
53.5	0.8	66.5	10.8	79.5	12.5	92.5	10.9
54.0	0.9	67.0	11.1	80.0	12.4	93.0	10.9
54.5	1.1	67.5	11.4	80.5	12.3	93.5	10.8
55.0	1.3	68.0	11.7	81.0	12.1	94.0	10.8
55.5	1.5	68.5	12.0	81.5	12.0	94.5	10.8
56.0	1.8	69.0	12.2	82.0	11.9	95.0	10.8
56.5	2.1	69.5	12.5	82.5	11.8	95.5	10.8
57.0	2.5	70.0	12.7	83.0	11.8	96.0	10.8
57.5	2.9	70.5	12.8	83.5	11.7	96.5	10.8
58.0	3.3	71.0	13.0	84.0	11.6	97.0	10.9
58.5	3.8	71.5	13.2	84.5	11.5	97.5	10.9
59.0	4.2	72.0	13.3	85.0	11.5	98.0	10.9
59.5	4.7	72.5	13.4	85.5	11.4	98.5	10.9
60.0	5.2	73.0	13.5	86.0	11.3	99.0	10.9
60.5	5.7	73.5	13.5	86.5	11.3	99.5	10.9
61.0	6.2	74.0	13.6	87.0	11.2	100.0	11.0
61.5	6.7	74.5	13.6	87.5	11.2		
62.0	7.1	75.0	13.6	88.0	11.1		
62.5	7.6	75.5	13.5	88.5	11.1		

4.1.6. $^{nat}Cu(p,x)^{62}Zn$

A total of 13 experimental works have been reported up to 1999. The compiler did the corrections for gamma ray abundance of the product where it was necessary. However, even after the corrections, 9 papers were rejected and only 4 were selected for evaluation. The list of related references given below is accompanied with additional information. We mention availability of data in the computerized database EXFOR (if available, unique EXFOR reference number is given). Furthermore, we indicate a reason why a data set was excluded (reference denoted by an asterisk *).

*** Aleksandrov, V.N., Semenova, M.P., Semenov, V.G.:**
Production cross-sections of radionuclides in (p,x) reactions at copper and nickel nuclei.
Atomnaya Energiya **62** (1987) 411
— Exfor: D4074
— Data excluded: measurements done at 20 MeV intervals and errors are too large.

*** Coleman, G.H., Tewes, H.A.:**
Nuclear reactions of copper with various high-energy particles.
Physical Review **99** (1955) 288
— Exfor: C0238
— Data excluded: only one data point available.

*** Cohen, B.L., Newman,, E.:**
(p,pn) and (p,2n) cross-sections in medium weight elements.
Physical Review **99** (1955) 718
— Exfor: B0050
— Data excluded: only one data point available.

*** Dittrich, B.:**
Radiochemische Untersuchung Protonen— und α-induzierter Spallations— und Fragmentationsreaktionen mit Hilfe der Gamma— und Beschleunigermassen-Spektroskopie.
Dissertation, Universität zu Köln, Cologne, Germany, 1990
— Exfor: none
— Data excluded: only two data points available.

*** Ghoshal, S.N.:**
An experimental verification of the theory of compound nucleus.
Physical Review **80** (1950) 939
— Exfor: B0017
— Data excluded: cross-sections too high and a small energy shift is also observed.

*** Green, M.W., Lebowitz,, E.:**
Proton reactions with copper for auxiliary cyclotron beam monitoring.
Applied Radiation Isotopes **23** (1972) 342
— Exfor: B0074
— Data excluded: cross-sections are too small, also large scattering and energy shift are observed.

*** Greenwood, L.R., Smither, R.K.:**
Measurement of Cu spallation cross-sections at IPNS.
DOE/ER-0046/18 (1984) 11
— Exfor: none
— Data excluded: cross-sections of the $^{63}Cu(p,2n)^{62}Zn$ reaction were given above the threshold of the $^{65}Cu(p,4n)$ reaction.

Grütter, A.:
Excitation functions for radioactive isotopes produced by proton bombardment of Cu and Al in the energy range of 16 to 70 MeV.
Nuclear Physics **A383** (1982) 98
— Exfor: A0178

Hermanne, A., Szelecsényi, F., Sonck, M., Takács, S., Tárkányi, F., Van den Winkel, P.:
New cross-section data on $^{68}Zn(p,2n)^{67}Ga$ and $^{nat}Zn(p,xn)^{67}Ga$ nuclear reactions for the development of a reference data base.
J. Radioanalytical and Nuclear Chemistry **240** (1999) 623
— Exfor: none

Kopecky, P.:
Proton beam monitoring via the $Cu(p,x)^{58}Co$, $^{63}Cu(p,2n)^{62}Zn$ and $^{65}Cu(p,n)^{65}Zn$ reactions in copper.
Int. J. Applied Radiation Isotopes **36** (1985) 657
— Exfor: A0333

*** Levkovski, V.N.:**
Activation cross-sections for the nuclides of medium mass region (A = 40 — 100) with protons and α particles at medium (E = 10 — 50 MeV) energies. (Experiment and systematics).
Inter-Vesi, Moscow (1991)
— Exfor: A0510
— Data excluded: cross-sections of the $^{63}Cu(p,2n)^{62}Zn$ reaction were given above the threshold of the $^{65}Cu(p,4n)$ reaction.

*** Meadows, J.W.:**
Excitation functions for proton-induced reactions with copper.
Physical Review **91** (1953) 885
— Exfor: B0054
— Data excluded: cross-sections of the $^{63}Cu(p,2n)^{62}Zn$ reaction were given above the threshold of the $^{65}Cu(p,4n)$ reaction.

Mills, S.J., Steyn, G.F., Nortier, F.M.:
Experimental and theoretical excitation functions of radionuclides produced in proton bombardment of copper up to 200 MeV.
Applied Radiation Isotopes **43** (1992) 1019
— Exfor: A0507

The data from all experimental papers where numerical values are available (13 papers), are collected in Fig. 4.1.6a. The scatter of 9 data sets is large, therefore only 4 papers were selected.

Cross-sections were calculated by two different versions of the nuclear reaction model code ALICE (denoted as HMS(FG) and IPPE), by the nuclear reaction model code PREMOD-HFMOD (denoted as HF) and by two fitting procedures (Padé with 12 parameters and Spline). These results are compared with the selected experimental data in Fig. 4.1.6b. It is seen that model calculations give relatively good predictions, but fits do better. The best approximation was judged to be the spline fit. Recommended cross-sections are compared with selected experimental data, including their error bars, in Fig. 4.1.6c. The corresponding numerical values are tabulated in Tab. 4.1.6.

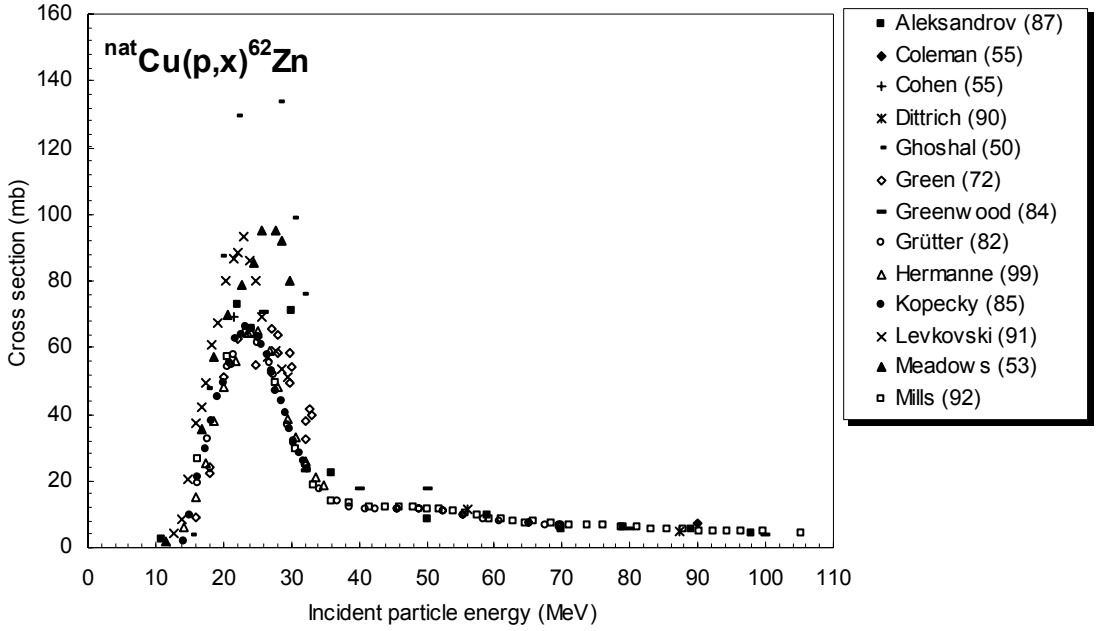

Figure 4.1.6a. All experimental data.

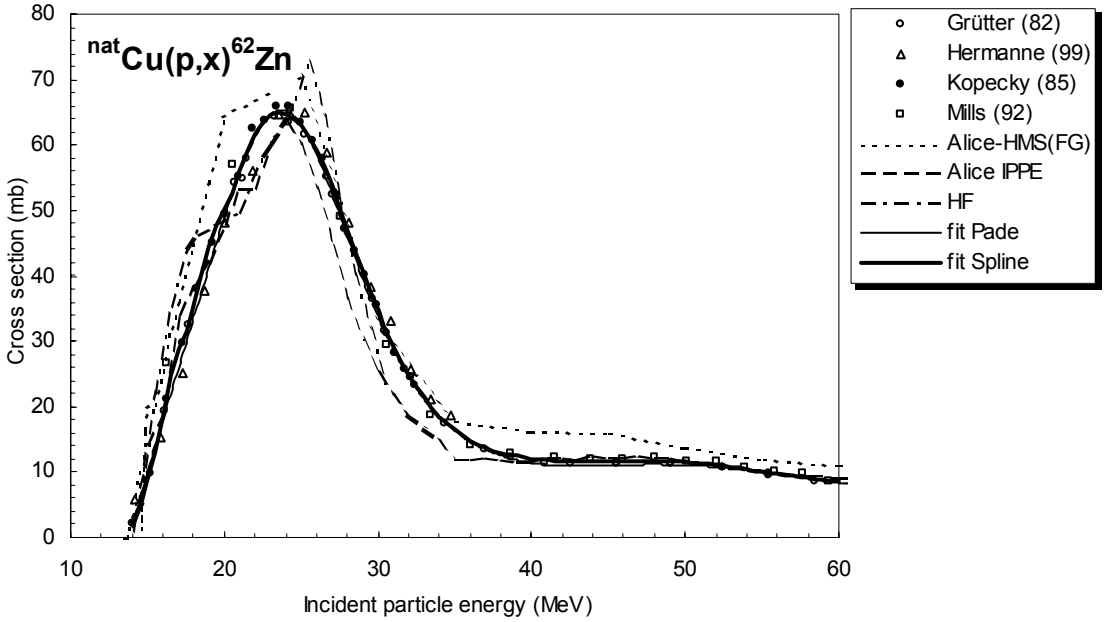

Figure 4.1.6b. Selected experimental data in comparison with theoretical calculations and fits.

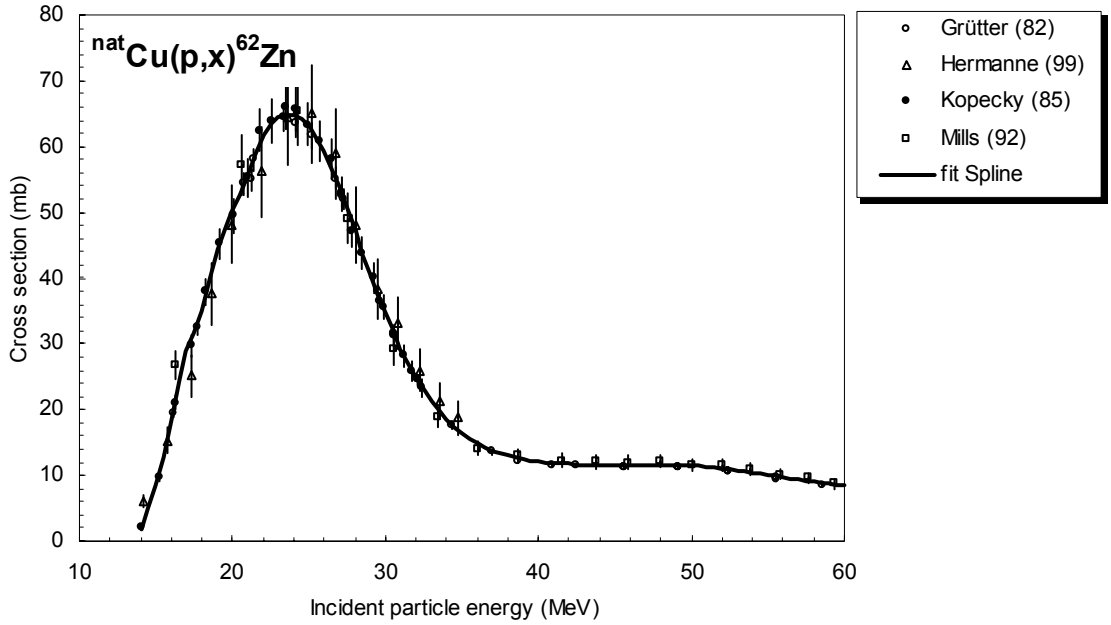

Figure 4.1.6c. Selected experimental data and recommended cross-section curve.

TABLE 4.1.6. RECOMMENDED CROSS-SECTION DATA FOR THE $^{nat}Cu(p,x)^{62}Zn$ REACTION

Energy MeV	Cross-section mb	Energy MeV	Cross-section mb	Energy MeV	Cross-section mb	Energy MeV	Cross-section mb
14.0	1.9	26.0	59.3	38.0	13.0	50.0	11.5
14.5	4.9	26.5	56.7	38.5	12.7	50.5	11.4
15.0	8.5	27.0	53.7	39.0	12.4	51.0	11.3
15.5	12.8	27.5	50.5	39.5	12.2	51.5	11.2
16.0	18.5	28.0	47.3	40.0	12.1	52.0	11.1
16.5	24.7	28.5	43.9	40.5	11.9	52.5	10.9
17.0	28.9	29.0	40.6	41.0	11.9	53.0	10.8
17.5	31.5	29.5	37.5	41.5	11.8	53.5	10.6
18.0	35.0	30.0	34.6	42.0	11.8	54.0	10.4
18.5	39.8	30.5	31.9	42.5	11.7	54.5	10.3
19.0	44.4	31.0	29.3	43.0	11.7	55.0	10.1
19.5	47.8	31.5	27.0	43.5	11.7	55.5	9.9
20.0	50.1	32.0	24.9	44.0	11.6	56.0	9.7
20.5	52.7	32.5	23.0	44.5	11.6	56.5	9.6
21.0	55.6	33.0	21.3	45.0	11.6	57.0	9.4
21.5	59.0	33.5	19.8	45.5	11.6	57.5	9.2
22.0	61.6	34.0	18.5	46.0	11.7	58.0	9.1
22.5	63.5	34.5	17.4	46.5	11.7	58.5	8.9
23.0	64.5	35.0	16.4	47.0	11.7	59.0	8.8
23.5	64.9	35.5	15.6	47.5	11.7	59.5	8.6
24.0	64.8	36.0	14.8	48.0	11.7	60.0	8.5
24.5	64.1	36.5	14.2	48.5	11.7		
25.0	63.0	37.0	13.7	49.0	11.6		
25.5	61.4	37.5	13.3	49.5	11.6		

4.1.7. $^{nat}Cu(p,x)^{63}Zn$

A total of 24 experimental works were found in the energy region considered. The compiler did the corrections for gamma ray abundance of the product where it was necessary. After these corrections 15 papers had to be rejected and the remaining 9 papers were selected for further evaluation. The list of related references given below is accompanied with additional information. We mention availability of data in the computerized database EXFOR (if available, unique EXFOR reference number is given). Furthermore, we indicate a reason why a data set was excluded (reference denoted by an asterisk *).

*** Albert, R.D., Hansen, L.F.:**
10 MeV proton reaction cross-sections for ^{63}Cu and ^{65}Cu.
Physical Review Letters **6** (1961) 13
— Exfor: none
— Data excluded: only one cross-section value.

*** Aleksandrov, V.N., Semenova, M.P., Semenov, V.G.:**
Production cross-sections of radionuclides in (p,x) reactions at copper and nickel nuclei.
Atomnaya Energiya **62** (1987) 411
— Exfor: A0351
— Data excluded: measurements at 20 MeV intervals; errors too large.

*** Antropov, A.E., Gusev, V.P., Zarubin, P.P., Ioannu, P.D., Padalko, V.Yu.:**
Measurements of total cross-sections for the (p,n) reaction on medium weight nuclei at the proton energy 6 MeV.
30th Annual Conference on Nuclear Spectroscopy and Nuclear Structure, Leningrad 18-21 March 1980, p. 316, Nauke, Leningrad (1980)
— Exfor: A0072
— Data excluded: only one cross-section value.

Barrandon, J.N., Debrun, J.L., Kohn, A., Spear, R.H.:
Étude du dosage de Ti, V, Cr, Fe, Ni, Cu et Zn par activation avec des protons d´énergie limitée a 20 MeV.
Nuclear Instruments Methods **127** (1975) 269
— Exfor: O0086

*** Blaser, J.-P., Boehm, F., Marmier, P., Peaslee, D.C.:**
Fonctions d´excitation de la réaction (p,n). (I)
Helvetia Physica Acta **24** (1951) 3
— Exfor: B0048
— Data excluded: large energy shift.

*** Chackett, K.F., Chackett, G.A., Ismail, L.:**
The (p,n) reaction cross-section of copper for 9.3 MeV protons.
Proceedings Physical Society (London) **80** (1962) 738
— Exfor: B0070
— Data excluded: only one cross-section value.

*** Coleman, G.H., Tewes, H.A.:**
Nuclear reactions of copper with various high-energy particles.
Physical Review **99** (1955) 288
— Exfor: C0283
— Data excluded: only one cross-section value.

Collé, R., Kishore, R., Cumming, J.B.:
Excitation functions for (p,n) reactions to 25 MeV on ^{63}Cu, ^{65}Cu and ^{107}Ag.
Physical Review **C9** (1974) 1819
— Exfor: B0057

*** Dell, G.F., Ploughe, W.D., Hausman, H.J.:**
Total reaction cross-sections in the mass range 45 to 65.
Nuclear Physics **64** (1965) 513
— Exfor: B0064
— Data excluded: only one cross-section value.

*** Ghoshal, S.N.:**
An experimental verification of the theory of compound nucleus.
Physical Review **80** (1950) 939
— Exfor: B0017
— Data excluded: large energy shift.

Grütter, A.:
Excitation functions for radioactive isotopes produced by proton bombardment of Cu and Al in the energy range of 16 to 70 MeV.
Nuclear Physics **A383** (1982) 98
— Exfor: A0178

Hansen, L.F., Albert, R.D.:
Statistical theory predictions for 5 — 11 MeV (p,n) and (p,p') nuclear reactions in ^{51}V, ^{59}Co, ^{63}Cu, ^{65}Cu, and ^{103}Rh.
Physical Review **128** (1962) 291
— Exfor: B0066

*** Hille, M., Hille, P., Uhl, M., Weisz, W.:**
Excitation functions of (p,n) and (α,n) reactions on Ni, Cu and Zn.
Nuclear Physics **A198** (1972) 625
— Exfor: B0058
— Data excluded: too high values compared with the results of others.

Howe, H.A.:
(p,n) cross-sections of copper and zinc.
Physical Review **109** (1958) 2085
— Exfor: B0060

*** Humes, R.M., Dell, G.F. Jr, Ploughe, W.D., Hausman, H.J.:**
(p,n) cross-sections at 6.75 MeV.
Physical Review **130** (1963) 1522
— Exfor: B0061
— Data excluded: only one cross-section value.

Johnson, C.H., Galonsky, A., Inskeep, C.N.:
Cross-sections for (p,n) reactions in intermediate-weight nuclei.
Progress Report ORNL-2910 (1960) 25
— Exfor: B0068

*** Jones, G.A., Schiffer, J.P., Huizenga, J.R., Wing, J.W.:**
Measurement of (p,n) cross-sections on Cu at 9.85 MeV.
Report TID-12696 (1961)
— Exfor: B0063
— Data excluded: only one cross-section value.

Levkovski, V.N.:
Activation cross-sections for the nuclides of medium mass region (A = 40-100) with protons and α particles at medium (E = 10-50 MeV) energies. (Experiment and systematics)
Inter-Vesi, Moscow (1991)
— Exfor: A0510
— Data excluded above 22 MeV: the ^{63}Cu(p,n)^{63}Zn reaction was measured above the threshold of the ^{65}Cu(p,3n)^{63}Zn reaction. Below 22 MeV, however, the cross-section data agree within the errors with the other selected data.

*** Meadows, J.W.:**
Excitation functions for proton-induced reactions with copper.
Physical Review **91** (1953) 885
— Exfor: B0054
— Data excluded: the ^{63}Cu(p,n)^{63}Zn reaction was measured above the threshold of the ^{65}Cu(p,3n)^{63}Zn reaction and the target consists of natural copper.

*** Meyer, V., Hintz, N.M.:**
Charged particle and total reaction cross-sections for protons at 9.85 MeV.
Physical Review Letters **5** (1960) 207
— Exfor: none
— Data excluded: only one cross-section value.

Mills, S.J., Steyn, G.F., Nortier, F.M.:
Experimental and theoretical excitation functions of radionuclides produced in proton bombardment of copper up to 200 MeV.
Applied Radiation Isotopes **43** (1992) 1019
— Exfor: A0507

*** Taketani, H., Alsford, W.P.:**
(p,n) cross-sections on ^{47}Ti, ^{51}V, ^{52}Cr, ^{59}Co, and ^{63}Cu from 4 to 6.5 MeV.
Physical Review **125** (1962) 291
— Exfor: B0051
— Data excluded: the error in proton energy was large.

Wing, J., Huizenga, J.R.:
(p,n) cross-sections of ^{51}V, ^{52}Cr, ^{63}Cu, ^{65}Cu, ^{107}Ag, ^{109}Ag, ^{111}Cd, ^{114}Cd and ^{139}La from 5 to 10.5 MeV.
Physical Review **128** (1962) 280
— Exfor: B0065

*** Yoshizawa, Y., Noma, H., Horiguchi, T., Katoh, T., Amemiya, A., Itoh, M., Hisatake, K., Sekikawa, M., Chida, K.:**
Isotope separator on-line at INS FM cyclotron.
Nuclear Instruments Methods **134** (1976) 93
— Exfor: none
— Data excluded: energy is shifted and the errors are too large.

The data from all experimental papers where numerical values are available (24 papers), are collected in Fig. 4.1.7a. The scatter of 15 data sets is large, therefore only 9 papers were selected.

Cross-sections were calculated by two different versions of the nuclear reaction model code ALICE (denoted as HMS(FG) and IPPE) and by two fitting procedures (Padé with 17 parameters and Spline). These results are compared with the selected experimental data in Fig. 4.1.7b. It is seen that model calculations give relatively good predictions, but fits do better. The best approximation was judged to be the Padé fit. Recommended cross-sections are compared with selected experimental data, including their error bars, in Fig. 4.1.7c. The corresponding numerical values are tabulated in Tab. 4.1.7.

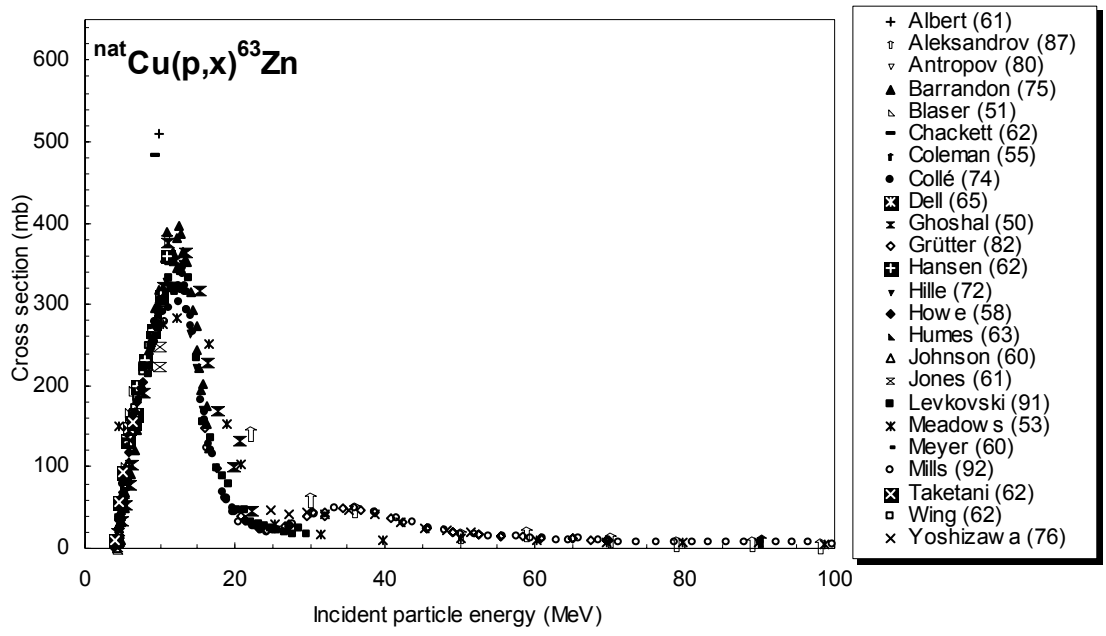

Figure 4.1.7a. All experimental data.

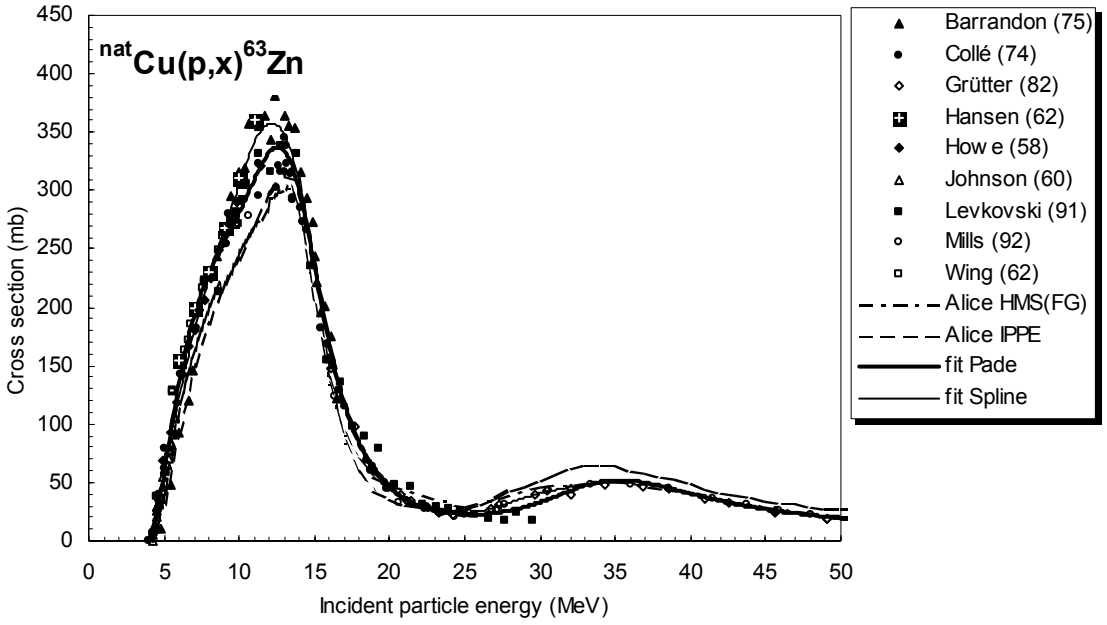

Figure 4.1.7b. Selected experimental data in comparison with theoretical calculations and fits.

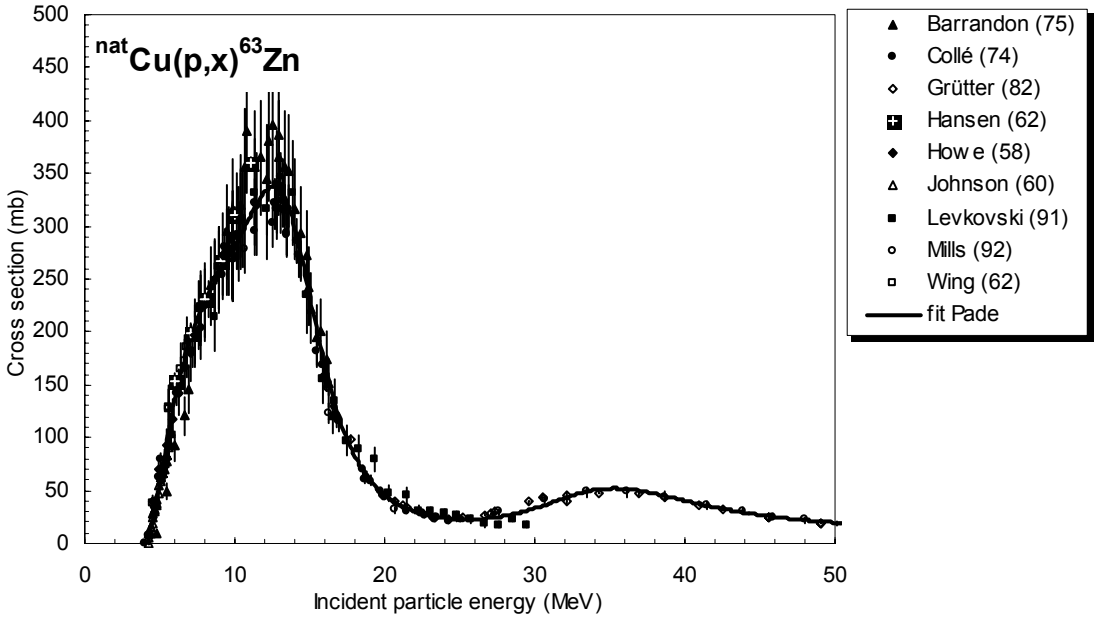

Figure 4.1.7c. Selected experimental data and recommended cross-section curve.

TABLE 4.1.7. RECOMMENDED CROSS-SECTION DATA FOR THE $^{nat}Cu(p,x)^{63}Zn$ REACTION

Energy MeV	Cross-section mb	Energy MeV	Cross-section mb	Energy MeV	Cross-section mb	Energy MeV	Cross-section mb
4.5	20.7	16.0	167	27.5	25.0	39.0	43.7
5.0	58.3	16.5	140	28.0	26.1	39.5	42.0
5.5	98.2	17.0	117	28.5	27.6	40.0	40.3
6.0	136	17.5	97.8	29.0	29.2	40.5	38.7
6.5	168	18.0	82.4	29.5	31.1	41.0	37.1
7.0	193	18.5	70.0	30.0	33.2	41.5	35.6
7.5	213	19.0	60.0	30.5	35.5	42.0	34.1
8.0	229	19.5	52.0	31.0	37.9	42.5	32.7
8.5	243	20.0	45.5	31.5	40.4	43.0	31.4
9.0	255	20.5	40.3	32.0	42.8	43.5	30.2
9.5	268	21.0	36.1	32.5	45.2	44.0	29.1
10.0	281	21.5	32.7	33.0	47.3	44.5	28.0
10.5	295	22.0	30.0	33.5	49.1	45.0	27.0
11.0	309	22.5	27.8	34.0	50.5	45.5	26.0
11.5	322	23.0	26.1	34.5	51.5	46.0	25.1
12.0	333	23.5	24.8	35.0	52.0	46.5	24.3
12.5	337	24.0	23.9	35.5	52.1	47.0	23.5
13.0	334	24.5	23.2	36.0	51.7	47.5	22.8
13.5	321	25.0	22.9	36.5	50.9	48.0	22.1
14.0	298	25.5	22.8	37.0	49.8	48.5	21.4
14.5	267	26.0	23.0	37.5	48.5	49.0	20.8
15.0	233	26.5	23.4	38.0	47.0	49.5	20.2
15.5	199	27.0	24.1	38.5	45.4	50.0	19.7

4.1.8. $^{nat}Cu(p,x)^{65}Zn$

A total of 30 published cross-section data sets were found in the literature in the energy range considered. While 21 papers were rejected, 9 were selected for further evaluation. The compiler did the corrections for gamma ray abundance where it was necessary.

The list of related references given below is accompanied with additional information. We mention availability of data in the computerized database EXFOR (if available, unique EXFOR reference number is given). Furthermore, we indicate a reason why a data set was excluded (reference denoted by an asterisk*).

*** Albert, R.D., Hansen, L.F.:**
10 MeV proton reaction cross-sections for ^{63}Cu and ^{65}Cu.
Physical Review Letters **6** (1961) 13
— Exfor: none
— Data excluded: only one or two cross-section values presented.

*** Albouy, G., Gusakow, M., Poffé, N., Sergolle, H., Valentin, L.:**
Réaction (p,n) a moyenne énergie.
Journal de Physique **23** (1962) 1000
— Exfor: B0106
— Data excluded: cross-section data not only too high but the energy error was also large.

*** Antropov, A.E., Gusev, V.P., Zarubin, P.P., Ioannu, P.D., Padalko, V.Yu.:**
Measurements of total cross-sections for the (p,n) reaction on medium weight nuclei at the proton energy 6 MeV.
30th Annual Conference on Nuclear Spectroscopy and Nuclear Structure, Leningrad, 18 — 21 March 1980, p. 316
— Exfor: A0072
— Data excluded: only one or two cross-section values presented.

Barrandon, J.N., Debrun, J.L., Kohn, A., Spear, R.H.:
Étude du dosage de Ti, V, Cr, Fe, Ni, Cu et Zn par activation avec des protons d´énergie limitée a 20 MeV.
Nuclear Instruments Methods **127** (1975) 269
— Exfor: O0086

*** Blaser, J.-P., Boehm, F., Marmier, P., Peaslee, D.C.:**
Fonctions d´excitation de la réaction (p,n). (I)
Helvetia Physica Acta **24** (1951) 3
— Exfor: B0048
— Data excluded: large energy shift.

*** Chackett, K.F., Chackett, G.A., Ismail, L.:**
The (p,n) reaction cross-section of copper for 9.3 MeV protons.
Proceedings Physical Society (London) **80** (1962) 738
— Exfor: B0070
— Data excluded: only one or two cross-section values presented.

Collé, R., Kishore, R., and Cumming, J.B.:
Excitation functions for (p,n) reactions to 25 MeV on ^{63}Cu, ^{65}Cu and ^{107}Ag.
Physical Review **C9** (1974) 1819
— Exfor: B0057

*** Dell, G.F., Ploughe, W.D., and Hausman, H.J.:**
Total reaction cross-sections in the mass range 45 to 65.
Nuclear Physics **64** (1965) 513
— Exfor: B0064
— Data excluded: only one or two cross-section values presented.

*** Dittrich, B.:**
Radiochemische Untersuchung Protonen- und α-induzierter Spallations— und Fragmentationsreaktionen mit Hilfe der Gamma- und Beschleunigermassen-Spektroskopie.
Dissertation, Universität zu Köln, Cologne, Germany, 1990
— Exfor: none
— Data excluded: only one or two cross-section values presented.

Dmitriev, P.P., Konstantinov, I.S., Krasnov, N.N.:
Excitation function for the ^{65}Cu (p,n)^{65}Zn reaction.
Atomnaya Energiya **24** (1968) 279
— Exfor: none

*** Gadioli, E., Grassi Strini, A.M., Lo Bianco, G., Strini, G., Tagliaferri, G.:**
Excitation functions of ^{51}V, ^{56}Fe, ^{65}Cu(p,n) reactions between 10 and 45 MeV.
Nuovo Cimento **A22** (1974) 547
— Exfor: B0027
— Data excluded: large energy shift.

*** Green, M.W., Lebowitz, E.:**
Proton reactions with copper for auxiliary cyclotron beam monitoring.
Applied Radiation Isotopes **23** (1972) 342
— Exfor: B0074
— Data excluded: too high cross-sections.

*** Greenwood, L.R., Smither, R.K.:**
Measurement of Cu spallation cross-sections at IPNS.
DOE/ER-0046/18 (1984) 11
— Exfor: none
— Data excluded: too high cross-sections.

Grütter, A.:
Excitation functions for radioactive isotopes produced by proton bombardment of Cu and Al in the energy range of 16 to 70 MeV.
Nuclear Physics **A383** (1982) 98
— Exfor: A0178

Hansen, L.F., Albert, R.D.:
Statistical theory predictions for 5 to 11 MeV (p,n) and (p,p′) nuclear reactions in ^{51}V, ^{59}Co, ^{63}Cu, ^{65}Cu, and ^{103}Rh.
Physical Review **128** (1962) 291
— Exfor: B0066

*** Heydegger, H.R., Garrett, C.K., Van Ginneken, A.:**
Thin-target cross-sections for some Cr, Mn, Fe, Co, Ni, and Zn nuclides produced in copper by 82 to 416 MeV protons.
Physical Review **C6** (1972) 1235
— Exfor: none
— Data excluded: only one or two cross-section values presented.

*** Howe, H.A.:**
(p,n) cross-sections of copper and zinc.
Physical Review **109** (1958) 2085
— Exfor: B0060
— Data excluded: too high cross-sections.

*** Humes, R.M., Dell, G.F.Jr, Ploughe, W.D., Hausman, H.J.:**
(p,n) cross-sections at 6.75 MeV.
Physical Review **130** (1963) 1522
— Exfor: B0061
— Data excluded: only one or two cross-section values presented.

Johnson, C.H., Galonsky, A., Ulrich, J.P.:
Proton strength functions from (p,n) cross-sections.
Physical Review **109** (1958) 1243
— Exfor: B0046

*** Johnson, C.H., Galonsky, A., Inskeep, C.N.:**
Cross-sections for (p,n) reactions in intermediate-weight nuclei.
Progress Report ORNL-2910 (1960) 25
— Exfor: B0068
— Data excluded: large energy shift.

*** Jones, G.A., Schiffer, J.P., Huizenga, J.R., Wing, J.W.:**
Measurement of (p,n) cross-sections on Cu at 9.85 MeV.
Report TID-12696 (1961)
— Exfor: B0063
— Data excluded: only one or two cross-section values presented.

*** Jung, P.:**
Helium production and long-term activation by protons and deuterons in metals for fusion reactor application.
J. Nuclear Materials **144** (1987) 43
— Exfor: none
— Data excluded: the three data points seemed too high.

*** Kormali, S.M., Swindle, D.L., Schweikert, E.A.:**
Charged particle activation of medium Z elements. II. Proton excitation functions.
J. Radioanalytical and Nuclear Chemistry **31** (1976) 437
— Exfor: D4073
— Data excluded: large energy shift.

Kopecky, P.:
Proton beam monitoring via the Cu(p,x)^{58}Co, ^{63}Cu(p,2n)^{62}Zn and ^{65}Cu(p,n)^{65}Zn reactions in copper.
Int. J. Applied Radiation Isotopes **36** (1985) 657
— Exfor: A0333

*** Levkovski, V.N.:**
Activation cross-sections for the nuclides of medium mass region (A = 40–100) with protons and α particles at medium (E = 10–50 MeV) energies. (Experiment and systematics)
Inter-Vesi, Moscow (1991)
— Exfor: A0150
— Data excluded: too high cross-sections.

*** Meyer, V., Hintz, N.M.:**
Charged particle and total reaction cross-sections for protons at 9.85 MeV.
Physical Review Letters **5** (1960) 207
— Exfor: none
— Data excluded: only one or two cross-section values presented.

Mills, S.J., Steyn, G.F., Nortier, F.M.:
Experimental and theoretical excitation functions of radionuclides produced in proton bombardment of copper up to 200 MeV.
Applied Radiation Isotopes **43** (1992) 1019
— Exfor: A0507
— Data excluded below 22 MeV, because they are energy shifted. Above 22 MeV the cross-section data agree within the errors with the other selected data and were included in the selection.

*** Shore, B.W., Wall, N.S., Irvine, J.W.Jr.:**
Interactions of 7.5 MeV protons with copper and vanadium.
Physical Review **123** (1961) 276
— Exfor: B0067
— Data excluded: only one or two cross-section values presented.

*** Switkowski, Z.E., Heggie, J.C.P., Mann, F.M.:**
Threshold effects in proton-induced reactions on copper.
Australian J. Physics **31** (1978) 253
— Exfor: none
— Data excluded: only neutron emission measured; cross-section data too low.

Wing, J., Huizenga, J.R.:
(p,n) cross-sections of ^{51}V, ^{52}Cr, ^{63}Cu, ^{65}Cu, ^{107}Ag, ^{109}Ag, ^{111}Cd, ^{114}Cd and ^{139}La from 5 to 10.5 MeV.
Physical Review **128** (1962) 280
— Exfor: B0065

The data from all experimental papers where numerical values are available (30 papers), are collected in Fig. 4.1.8a. The scatter of 21 data sets is large, therefore only 9 papers were selected.

Cross-sections were calculated by two different versions of the nuclear reaction model code ALICE (denoted as HMS(FG) and IPPE) and by two fitting procedures (Padé with 20 parameters and Spline). These results are compared with the selected experimental data in Fig. 4.1.8b. It is seen that model calculations give good predictions, but fits do better. The best approximation was judged to be the Padé fit. Recommended cross-sections are compared with selected experimental data, including their error bars, in Fig. 4.1.8c. The corresponding numerical values are tabulated in Tab. 4.1.8.

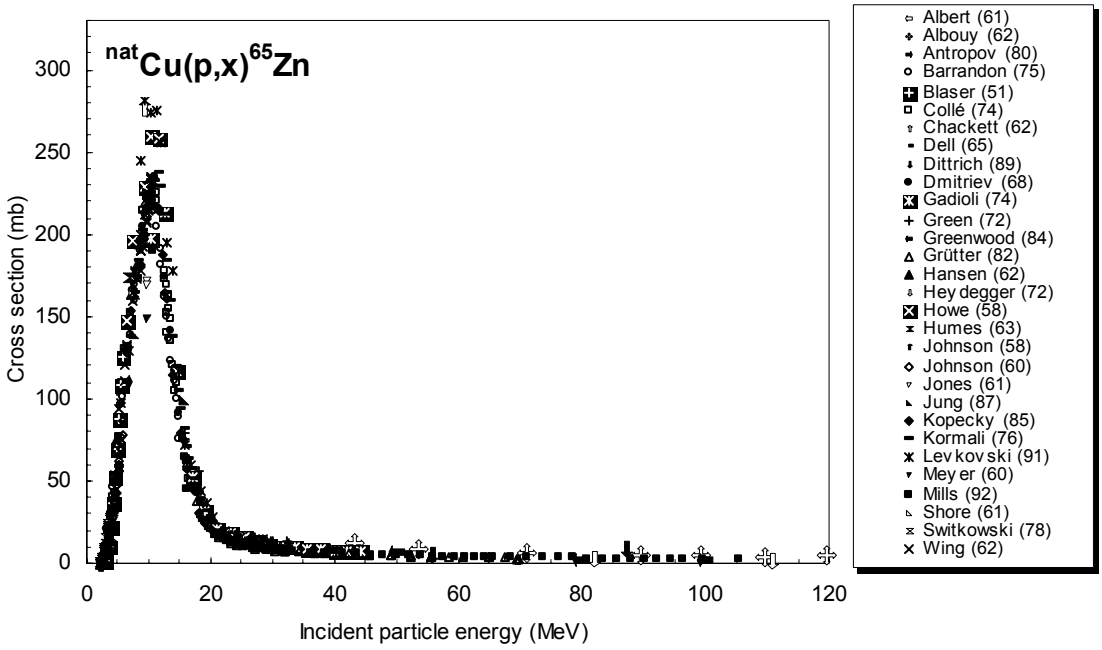

Figure 4.1.8a. All experimental data.

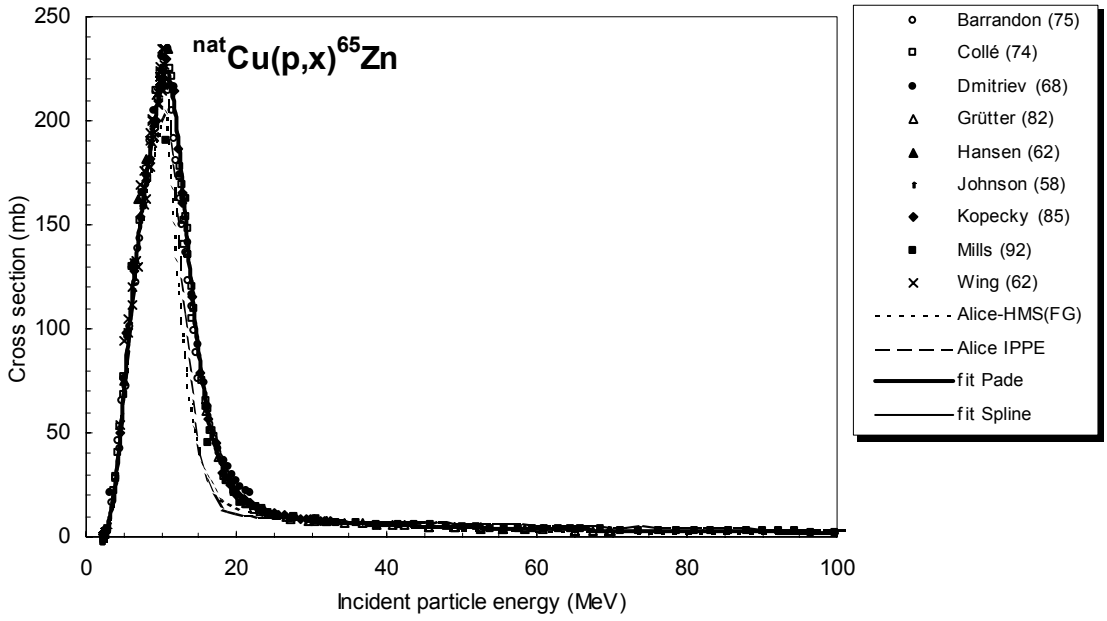

Figure 4.1.8b. Selected experimental data in comparison with theoretical calculations and fits.

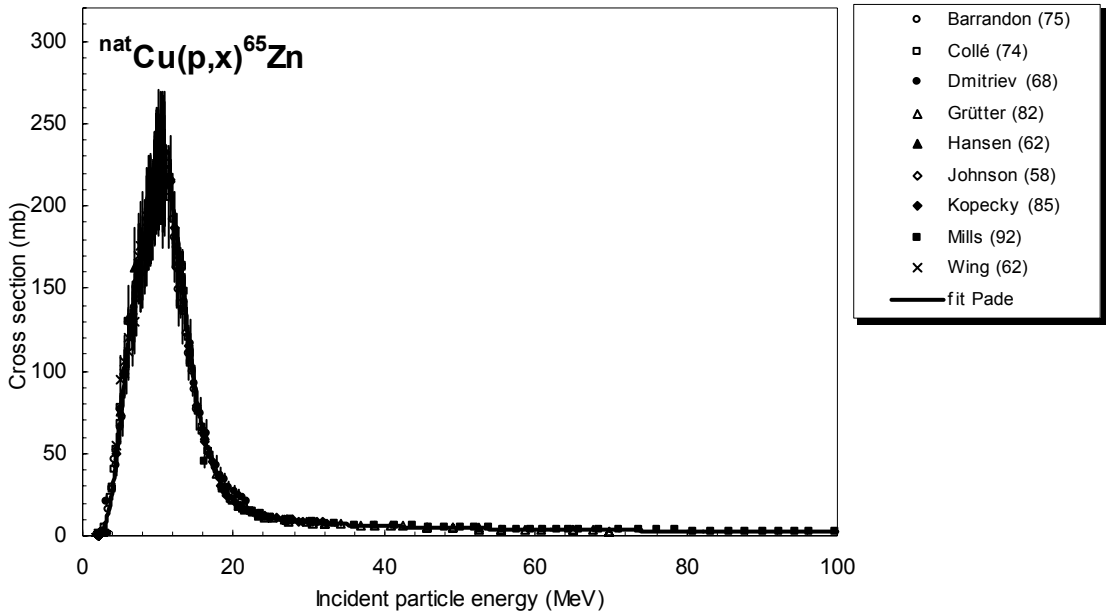

Figure 4.1.8c. Selected experimental data and recommended cross-section curve.

TABLE 4.1.8. RECOMMENDED CROSS-SECTION DATA FOR THE $^{nat}Cu(p,x)^{65}Zn$ REACTION

Energy MeV	Cross-section mb	Energy MeV	Cross-section mb	Energy MeV	Cross-section mb	Energy MeV	Cross-section mb
2.5	2.5	27.0	9.4	51.5	4.5	76.0	2.9
3.0	7.3	27.5	9.1	52.0	4.4	76.5	2.9
3.5	15.5	28.0	8.9	52.5	4.4	77.0	2.9
4.0	28.6	28.5	8.6	53.0	4.3	77.5	2.9
4.5	47.0	29.0	8.4	53.5	4.3	78.0	2.9
5.0	69.2	29.5	8.2	54.0	4.2	78.5	2.8
5.5	92.0	30.0	8.0	54.5	4.2	79.0	2.8
6.0	113	30.5	7.9	55.0	4.2	79.5	2.8
6.5	130	31.0	7.7	55.5	4.1	80.0	2.8
7.0	146	31.5	7.6	56.0	4.1	80.5	2.8
7.5	160	32.0	7.4	56.5	4.0	81.0	2.8
8.0	173	32.5	7.3	57.0	4.0	81.5	2.7
8.5	186	33.0	7.2	57.5	4.0	82.0	2.7
9.0	198	33.5	7.0	58.0	3.9	82.5	2.7
9.5	209	34.0	6.9	58.5	3.9	83.0	2.7
10.0	216	34.5	6.8	59.0	3.9	83.5	2.7
10.5	220	35.0	6.7	59.5	3.8	84.0	2.6
11.0	219	35.5	6.6	60.0	3.8	84.5	2.6
11.5	212	36.0	6.5	60.5	3.8	85.0	2.6
12.0	199	36.5	6.4	61.0	3.7	85.5	2.6
12.5	181	37.0	6.3	61.5	3.7	86.0	2.6
13.0	161	37.5	6.2	62.0	3.7	86.5	2.6
13.5	141	38.0	6.1	62.5	3.6	87.0	2.6
14.0	121	38.5	6.0	63.0	3.6	87.5	2.5
14.5	103	39.0	6.0	63.5	3.6	88.0	2.5
15.0	87.4	39.5	5.9	64.0	3.5	88.5	2.5

TABLE 4.1.8. (cont.)

Energy MeV	Cross-section mb	Energy MeV	Cross-section mb	Energy MeV	Cross-section mb	Energy MeV	Cross-section mb
15.5	73.9	40.0	5.8	64.5	3.5	89.0	2.5
16.0	62.7	40.5	5.7	65.0	3.5	89.5	2.5
16.5	53.3	41.0	5.6	65.5	3.5	90.0	2.5
17.0	45.7	41.5	5.6	66.0	3.4	90.5	2.4
17.5	39.4	42.0	5.5	66.5	3.4	91.0	2.4
18.0	34.2	42.5	5.4	67.0	3.4	91.5	2.4
18.5	30.0	43.0	5.4	67.5	3.3	92.0	2.4
19.0	26.5	43.5	5.3	68.0	3.3	92.5	2.4
19.5	23.7	44.0	5.2	68.5	3.3	93.0	2.4
20.0	21.3	44.5	5.2	69.0	3.3	93.5	2.4
20.5	19.3	45.0	5.1	69.5	3.2	94.0	2.3
21.0	17.7	45.5	5.1	70.0	3.2	94.5	2.3
21.5	16.3	46.0	5.0	70.5	3.2	95.0	2.3
22.0	15.1	46.5	5.0	71.0	3.2	95.5	2.3
22.5	14.1	47.0	4.9	71.5	3.1	96.0	2.3
23.0	13.3	47.5	4.8	72.0	3.1	96.5	2.3
23.5	12.5	48.0	4.8	72.5	3.1	97.0	2.3
24.0	11.9	48.5	4.7	73.0	3.1	97.5	2.3
24.5	11.3	49.0	4.7	73.5	3.1	98.0	2.2
25.0	10.9	49.5	4.6	74.0	3.0	98.5	2.2
25.5	10.4	50.0	4.6	74.5	3.0	99.0	2.2
26.0	10.1	50.5	4.5	75.0	3.0	99.5	2.2
26.5	9.7	51.0	4.5	75.5	3.0	100.0	2.2

4.2. DEUTERONS

Five deuteron beam monitor reactions were evaluated. Table 4.2 lists these reactions, including the basic decay characteristics of the product nuclei (half-lives, main γ-lines along with their intensities) and energy range of deuterons for which evaluations were performed.

TABLE 4.2. DEUTERON BEAM MONITOR REACTIONS

Reaction	$T_{1/2}$ of product nucleus	Main γ-lines		Deuteron energy range (MeV)
		E_γ (keV)	I_γ (%)	
$^{27}Al(d,x)^{22}Na$	2.60 a	1274.5	99.94	29.5–80
$^{27}Al(d,x)^{24}Na$	14.96 h	1368.6	100.0	15–80
		2754.0	99.94	
$^{nat}Ti(d,x)^{48}V$	15.97 d	983.5	99.99	9–50
		1312.0	97.49	
$^{nat}Fe(d,x)^{56}Co$	77.70 d	846.8	99.9	8–50
		1238.3	67.0	
$^{nat}Ni(p,x)^{61}Cu$	3.40 h	283.0	12.5	2.5–50
		656.0	10.66	

4.2.1. $^{27}Al(d,x)^{22}Na$

A total of 5 cross-section data sets were found in the literature in the energy range considered. From these, 2 works were excluded while the remaining 3 were selected for further evaluation. For a detailed description of the analysis and selection see Takács et al. (2000). The list of related references given below is accompanied with additional information. We mention availability of data in the computerized database EXFOR (if available, unique EXFOR reference number is given). Furthermore, we indicate a reason why a data set was excluded (reference denoted by an asterisk *).

*** Karpeles, A.:**
Anregungsfunktionen für die Bildung von ^{68}Ge, ^{65}Zn und ^{22}Na bei der Deuteronenbestrahlung von Gallium and Aluminium.
Radiochimica Acta **12** (1969) 212
Numerical values taken from:, J. Tobailem, C.-H. de Lassus St-Genies and, L. Leveque: Sections efficaces des reactions nucleaires induites par protons, deuterons, particules alpha, I. Reactions Nucleaires Moniteurs.
CEA-N-1466(1), France, 1971
— Exfor: none
— Data excluded: systematically higher values over the comparable energy region.

Martens, U., Schweimer, G.W.:
Production of ^{7}Be, ^{22}Na, ^{24}Na and ^{28}Mg by irradiation of ^{27}Al with 52 MeV deuterons and 104 MeV alpha particles.
Zeitschrift für Physik **233** (1970) 170
— Exfor: B0142

Michel, R., Brinkmann, G., Galas, R., Stück, R.:
Production of ^{24}Na and ^{22}Na by ^{2}H induced reactions on aluminum. Production of ^{24}Na and ^{22}Na by ^{3}He induced reactions on aluminum.
Data provided by Michel, R. in 1982 to the EXFOR database.
— Exfor: A0158

*** Ring, S.O., Litz, L.M.:**
Excitation functions for ^{22}Na from deuterons on aluminum.
Physical Review **97** (1955) 427
Numerical values taken from: Landolt-Börnstein New Series Group I, Volume 13, Subvolume, F.
Production of Radionuclides at Intermediate Energies in Interactions of Deuterons, Tritons and ^{3}He-nuclei with Nuclei
Editor: Shopper, H., Contributors: Semenov, V.G., Semenova, M.P., Sobolevsky, N.M.
— Exfor: none
— Data excluded: unusual shape of excitation function.

Takács, S., Tárkányi, F., Sonck, M., Hermanne, A., Mustafa, M.G., Shubin Yu., Zhuang Youxiang:
New cross-sections and intercomparison of deuteron monitor reactions on Al, Ti, Fe, Ni and Cu.
Nucl. Instr. Meth. B (2000) submitted
See also: Takács, S., Tárkányi, F., Sonck, M., Hermanne, A.
Excitation functions for monitoring deuteron beams up to 50 MeV. Abstracts of Int. Conf. on Ion Beam Applications and European Conf. on Accelerator in Applied Research and Technology, 26-30 July 1999, Dresden, Germany, p. 72.
— Exfor: none

The data from all experimental papers where numerical values are available (5 papers), are collected in Fig. 4.2.1a. The scatter of 2 data sets is large, therefore only 3 papers were selected.

Cross-sections were calculated by two different versions of the nuclear reaction model code ALICE (denoted as 91(KR) and IPPE), by nuclear reaction model code SPEC and by two fitting procedures (Padé with 12 parameters and Spline). These results are compared with the selected experimental data in Fig. 4.2.1b. Obviously the results of model calculations do not represent well the experimental data. Fits do better. The best approximation was judged to be the Padé fit. Recommended cross-sections are compared with selected experimental data, including their error bars, in Fig. 4.2.1c. The corresponding numerical values are tabulated in Table 4.2.1.

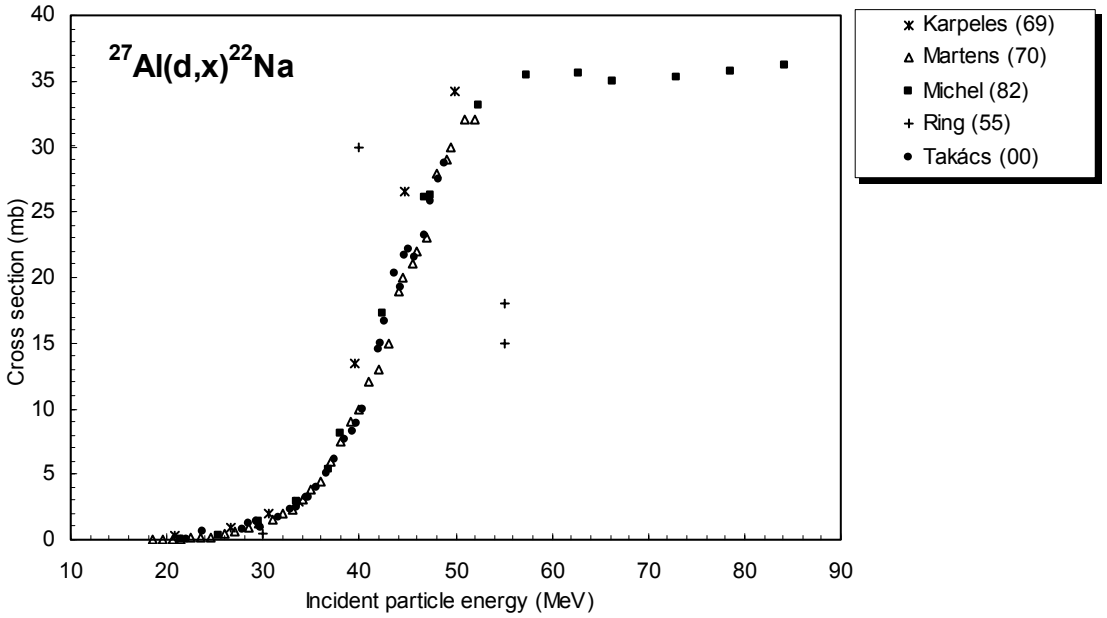

Figure 4.2.1a. All experimental data.

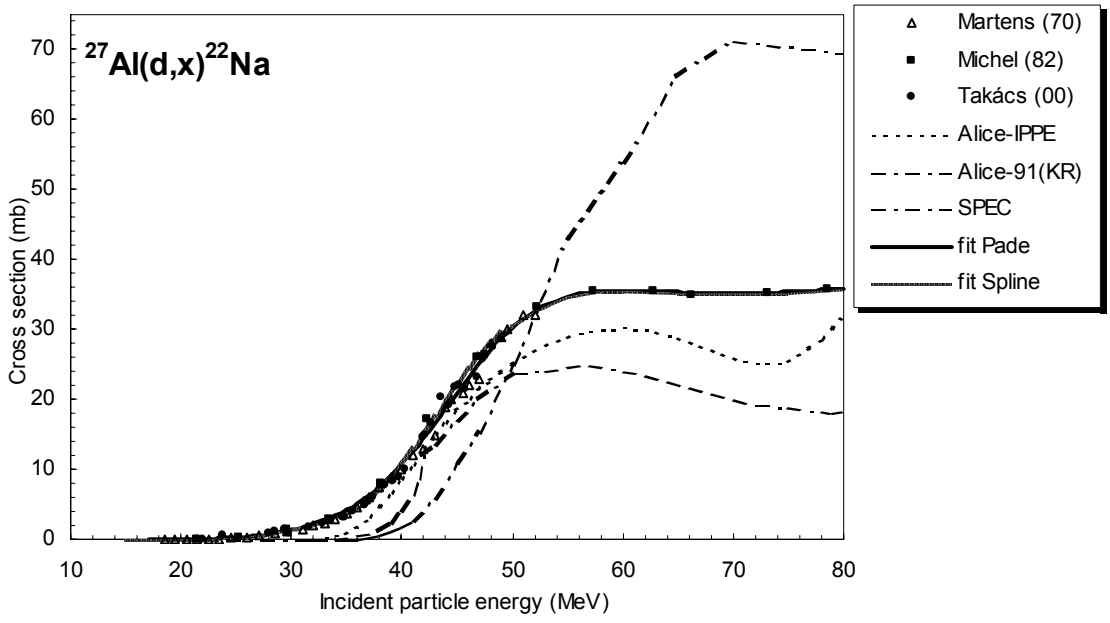

Figure 4.2.1b. Selected experimental data in comparison with theoretical calculations and fits.

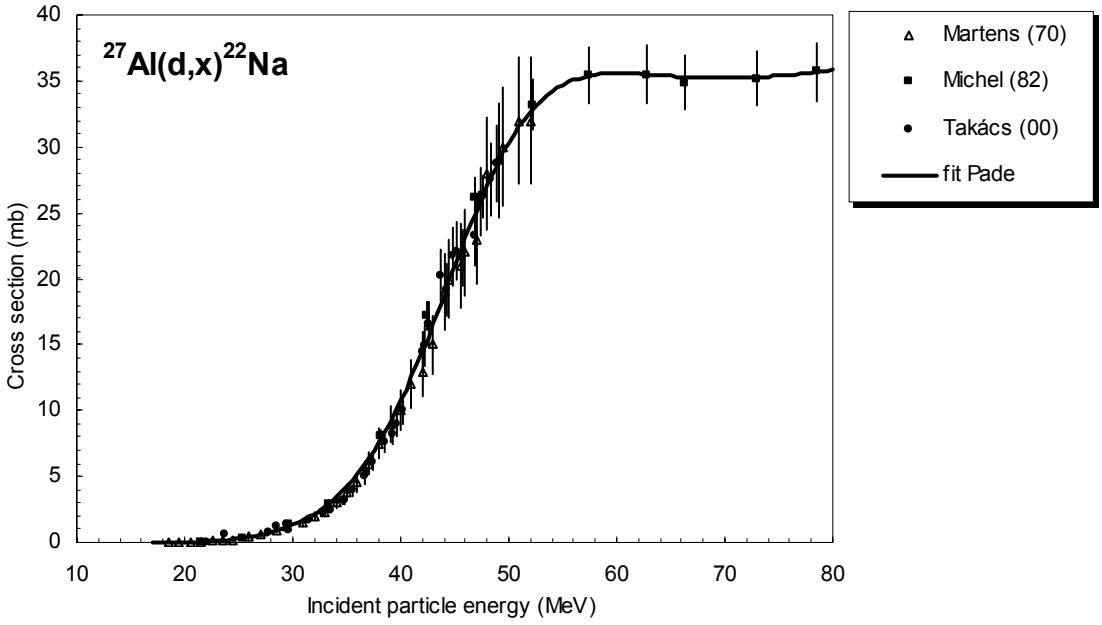

Figure 4.2.1c. Selected experimental data and recommended cross-section curve.

TABLE 4.2.1. RECOMMENDED CROSS-SECTIONS FOR THE $^{27}Al(d,x)^{22}Na$ REACTION

Energy MeV	Cross-section mb	Energy MeV	Cross-section mb	Energy MeV	Cross-section mb	Energy MeV	Cross-section mb
29.5	1.18	42.5	15.56	55.5	34.91	68.5	35.23
30.0	1.34	43.0	16.62	56.0	35.07	69.0	35.22
30.5	1.52	43.5	17.69	56.5	35.21	69.5	35.21
31.0	1.73	44.0	18.78	57.0	35.32	70.0	35.21
31.5	1.95	44.5	19.87	57.5	35.40	70.5	35.22
32.0	2.19	45.0	20.96	58.0	35.47	71.0	35.22
32.5	2.47	45.5	22.05	58.5	35.52	71.5	35.23
33.0	2.76	46.0	23.11	59.0	35.55	72.0	35.25
33.5	3.09	46.5	24.15	59.5	35.57	72.5	35.26
34.0	3.44	47.0	25.16	60.0	35.58	73.0	35.28
34.5	3.83	47.5	26.14	60.5	35.57	73.5	35.31
35.0	4.26	48.0	27.07	61.0	35.56	74.0	35.34
35.5	4.72	48.5	27.96	61.5	35.55	74.5	35.37
36.0	5.21	49.0	28.80	62.0	35.53	75.0	35.40
36.5	5.75	49.5	29.58	62.5	35.50	75.5	35.44
37.0	6.33	50.0	30.31	63.0	35.48	76.0	35.47
37.5	6.95	50.5	30.99	63.5	35.45	76.5	35.51
38.0	7.62	51.0	31.60	64.0	35.42	77.0	35.56
38.5	8.33	51.5	32.17	64.5	35.39	77.5	35.60
39.0	9.09	52.0	32.67	65.0	35.36	78.0	35.64
39.5	9.89	52.5	33.13	65.5	35.34	78.5	35.69
40.0	10.74	53.0	33.54	66.0	35.31	79.0	35.74
40.5	11.63	53.5	33.89	66.5	35.29	79.5	35.79
41.0	12.56	54.0	34.21	67.0	35.27	80.0	35.84
41.5	13.53	54.5	34.48	67.5	35.25		
42.0	14.53	55.0	34.71	68.0	35.24		

4.2.2. $^{27}Al(d,x)^{24}Na$

A total of 16 cross-section data sets (in 15 works) were found in the literature in the energy range considered. From these, 3 sets were excluded while the remaining 13 were selected for further evaluation. For a detailed description of the analysis and selection see Takács et al. (2000). The list of related references given below is accompanied with additional information. We mention availability of data in the computerized database EXFOR (if available, unique EXFOR reference number is given). Furthermore, we indicate a reason why a data set was excluded (reference denoted by an asterisk *).

Batzel, R., Crane, W.W.T., O'Kelley, G.D.:
The excitation function for the Al^{27} (d,αp)Na^{24} reaction.
Physical Review **91** (1953) 939
— Exfor: P0067
Remark: the results were controversial in different series (a and b). The shape of the excitation function near the maximum for series-a was strange, therefore this series of data was deselected. After a critical analysis, series-b, obtained with a 60 inch cyclotron was accepted for evaluation.

*** Crandall, W.E., Milburn, G.P., Pyle, R.V., Birnbaum, W.:**
C^{12}(x,xn)C^{11} and Al^{27} (x,x2pn)Na^{24} cross-sections at high energies.
Physical Review **101** (1956) 329
— Exfor: B0101
— Data excluded: only one high energy data point which was considerably higher than the bulk of the data.

Christaller, G.:
Europium Colloquium on, A.V., F. Cyclotrons. Eindhoven (1965)
Data from: Tobailem, J., de Lassus St-Genies, C.-H., Leveque, L.:
Sections efficaces des reactions nucleaires induites par protons, deutons, particules alpha. I reactions nucleaires moniteurs.
Note CEA-N-1-1466(1), CEA, France, 1971.
— Exfor: no

*** Hubbard, H.W.:**
Al^{27}(d,αp)Na^{24} cross-section.
Physical Review **75** (1949) 1470
— Exfor: no
— Data excluded: only one high energy data point, considerably higher than the bulk of the data.

Lenk, P.A., Slobodrian, R.J.:
Excitation function for the Al^{27}(d,αp)Na^{24} reaction between 0 and 28.1 MeV.
Physical Review **116** (1959) 1229
— Exfor: P0124
Remark: The data were reportedly normalised to absolute cross-sections of Batzel et al. (1953) series-b. That normalisation seems to be systematically too low, therefore these data were renormalised by the compiler by a factor of 1.18.

Martens, U., Schweimer, G.W.:
Production of ^{7}Be, ^{22}Na, ^{24}Na and ^{28}Mg by irradiation of ^{27}Al with 52 MeV deuterons and 104 MeV alpha particles.
Zeitschrift für Physik **233** (1970) 170
— Exfor: B0142

Michel, R., Brinkmann, G., Galas, M., Stück, R.:
Production of ^{24}Na and ^{22}Na by ^{2}H-induced reactions on aluminium. Production of ^{24}Na and ^{22}Na by ^{3}He-induced reactions on aluminium.
Private communication by Michel, R. (1982) to the EXFOR database.
— Exfor: A0158

Roehm, H.F., Verwey, C.J., Steyn, J., Rautenbach, W.L.:
Excitation functions for the ^{24}Mg(d,α)^{22}Na, ^{26}Mg(d,α)^{24}Na and ^{27}Al(d,αp)^{24}Na reactions.
J. Inorganic Nuclear Chemistry **31** (1969) 3345
— Exfor: B0099

Takács, S., Tárkányi, F., Sonck, M., Hermanne, A., Mustafa, M.G., Shubin Yu., Zhuang Youxiang:
New cross-sections and intercomparison of deuteron monitor reactions on Al, Ti, Fe, Ni and Cu.
Nucl. Instr. Meth. B (2000) submitted
See also: Takács, S., Tárkányi, F., Sonck, M., Hermanne, A.
Excitation functions for monitoring deuteron beams up to 50 MeV. Abstracts of Int. Conf. on Ion Beam Applications and European Conf. on Accelerator in Applied Research and Technology, 26-30 July 1999, Dresden, Germany, 72.
— Exfor: none

Tao Zhenlan, Zhu Fuying and Wang Gongqing:
Measurements of excitation function for Al-27(d,p+α)
Chinese J. Nuclear Techniques **2** (1987) 45
— Exfor: S0011

Watson, I.A., Waters, S.L., Bewley, D.K., Silvester, D.J.:
A method for the measurement of the cross-sections for the production of radioisotopes by charged particles from a cyclotron.
Nuclear Instruments Methods **106** (1973) 231
— Exfor: none

Weinreich, R., Probst, H.J., Qaim, S.M.:
Production of chromium-48 for applications in life sciences.
Int. J. Applied Radiation Isotopes **31** (1980) 223
— Exfor: A0169

Wilson, R.L., Frantsvog, D.J., Kunselman, A.R., Detraz, C., Zaidins, C.S.:
Excitation functions of reactions induced by ^{1}H and ^{2}H ions on natural Mg, Al and Si.
Physical Review **C13** (1976) 976
— Exfor: none

Zarubin, P.P.:
Excitation function of $^{27}Al(d,p\alpha)^{24}Na$ nuclear reaction.
XXIXth Annual Conference on Nuclear Spectroscopy and Nuclear Structures, Riga, 1979, p. 314. Numerical values taken from:, O. Schwerer and K Okamoto, INDC(NDS)-218/GZ+ (1989) IAEA, Vienna, Austria
— Exfor: none

Zhao Wen-rong, Lu Han-lin, Yu Wei-xiang and Cheng Jiang-tao:
Excitation function of $^{27}Al(d,p\alpha)^{24}Na$
Chinese J. Nuclear Physics **17** (1995) 160
— Exfor: none

The data from all experimental papers where numerical values are available (16 data sets in 15 papers), are collected in Fig. 4.2.2a. The scatter of 3 data sets is large, therefore only 13 data sets were selected for evaluation.

Cross-sections were calculated by two fitting procedures (Padé with 13 parameters and Spline). These results are compared with the selected experimental data in Fig. 4.2.2b. The best approximation was judged to be the Padé fit. Recommended cross-sections are compared with selected experimental data, including their error bars, in Fig. 4.2.2c. The corresponding numerical values are tabulated in Table 4.2.2.

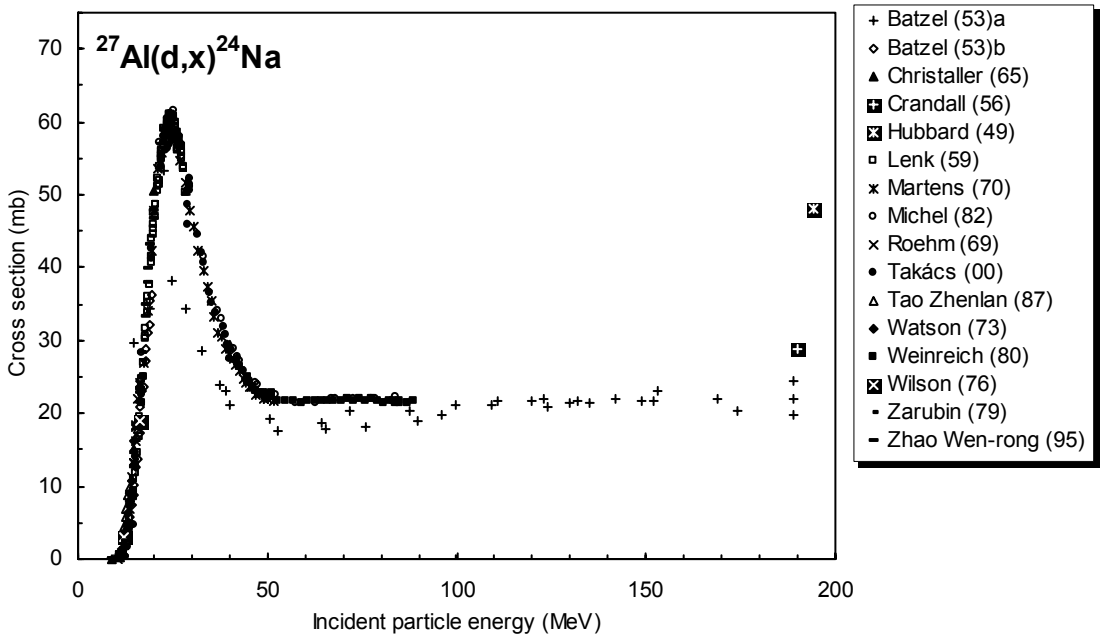

Figure 4.2.2a. All experimental data.

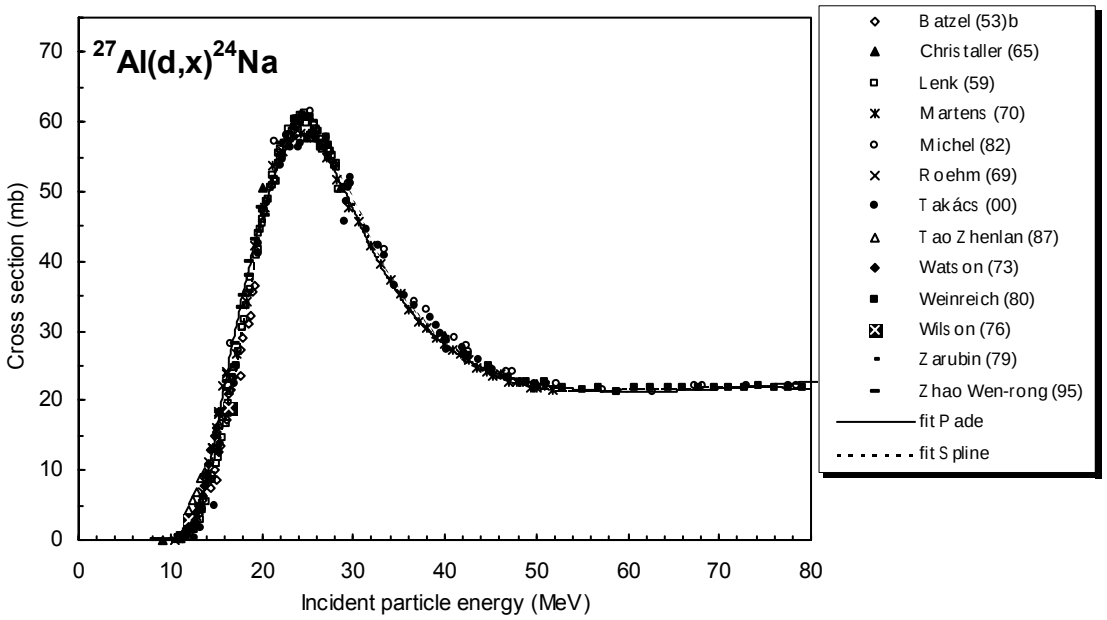

Figure 4.2.2b. Selected experimental data in comparison with fits.

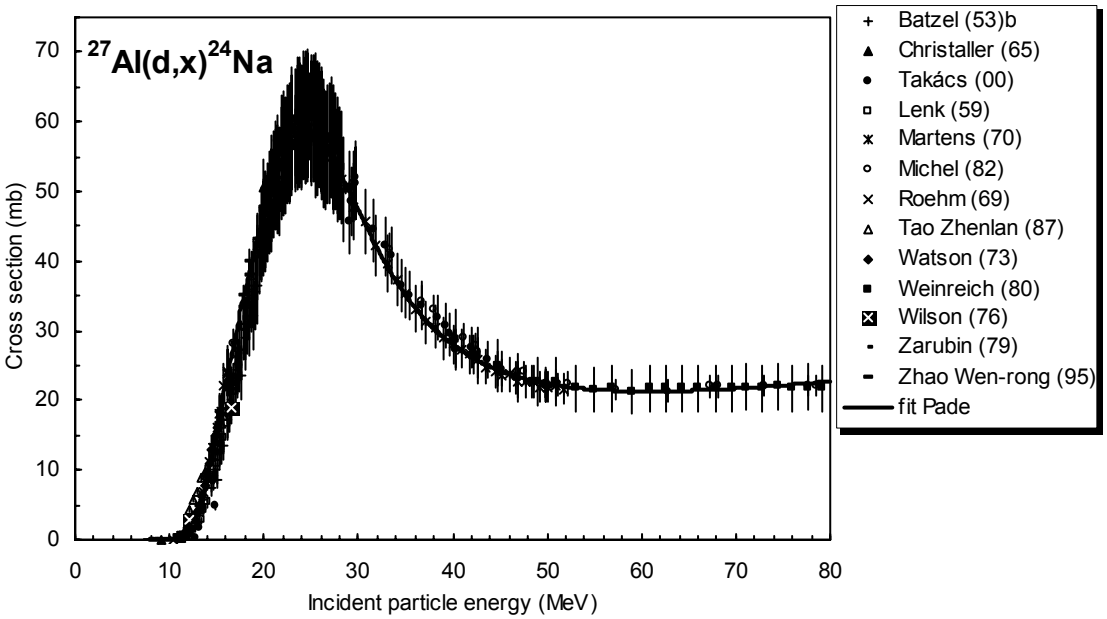

Figure 4.2.2c. Selected experimental data and recommended cross-section curve.

TABLE 4.2.2. RECOMMENDED CROSS-SECTIONS FOR THE $^{27}Al(d,x)^{24}Na$ REACTION

Energy MeV	Cross-section mb	Energy MeV	Cross-section mb	Energy MeV	Cross-section mb	Energy MeV	Cross-section mb
15.0	15.4	31.5	43.1	48.0	23.0	64.5	21.4
15.5	19.0	32.0	41.8	48.5	22.8	65.0	21.4
16.0	22.6	32.5	40.6	49.0	22.7	65.5	21.4
16.5	26.1	33.0	39.4	49.5	22.6	66.0	21.4
17.0	29.4	33.5	38.2	50.0	22.4	66.5	21.5
17.5	32.6	34.0	37.1	50.5	22.3	67.0	21.5
18.0	35.7	34.5	36.1	51.0	22.2	67.5	21.5
18.5	38.6	35.0	35.1	51.5	22.1	68.0	21.6
19.0	41.3	35.5	34.2	52.0	22.0	68.5	21.6
19.5	43.9	36.0	33.3	52.5	21.9	69.0	21.6
20.0	46.4	36.5	32.5	53.0	21.8	69.5	21.7
20.5	48.7	37.0	31.7	53.5	21.8	70.0	21.7
21.0	50.8	37.5	31.0	54.0	21.7	70.5	21.7
21.5	52.7	38.0	30.3	54.5	21.6	71.0	21.8
22.0	54.3	38.5	29.7	55.0	21.6	71.5	21.8
22.5	55.7	39.0	29.1	55.5	21.5	72.0	21.9
23.0	56.8	39.5	28.5	56.0	21.5	72.5	21.9
23.5	57.6	40.0	28.0	56.5	21.4	73.0	22.0
24.0	58.0	40.5	27.5	57.0	21.4	73.5	22.0
24.5	58.2	41.0	27.0	57.5	21.4	74.0	22.1
25.0	58.1	41.5	26.6	58.0	21.4	74.5	22.1
25.5	57.7	42.0	26.2	58.5	21.3	75.0	22.2
26.0	57.1	42.5	25.8	59.0	21.3	75.5	22.2
26.5	56.3	43.0	25.5	59.5	21.3	76.0	22.3
27.0	55.3	43.5	25.2	60.0	21.3	76.5	22.3
27.5	54.1	44.0	24.8	60.5	21.3	77.0	22.4
28.0	52.9	44.5	24.6	61.0	21.3	77.5	22.4
28.5	51.5	45.0	24.3	61.5	21.3	78.0	22.5
29.0	50.1	45.5	24.0	62.0	21.3	78.5	22.5
29.5	48.7	46.0	23.8	62.5	21.3	79.0	22.6
30.0	47.3	46.5	23.6	63.0	21.3	79.5	22.7
30.5	45.9	47.0	23.4	63.5	21.3	80.0	22.7
31.0	44.5	47.5	23.2	64.0	21.4		

4.2.3. ^{nat}Ti(d,x)^{48}V

A total of 5 cross-section data sets were found in the literature in the energy range considered. From these only 1 work was excluded while the remaining 4 works were selected for further evaluation. For a detailed description of the analysis and selection see Takács et al. (2000). The list of related references given below is accompanied with additional information. We mention availability of data in the computerized database EXFOR (if available, unique EXFOR reference number is given). Furthermore, we indicate a reason why a data set was excluded (reference denoted by an asterisk *).

Burgus, H.W., Cowan, G.A., Hadley, J.W., Hess, W., Shull, T., Stevenson, M.L., York, H.F.:
Cross-sections for the reactions $Ti^{48}(d,2n)V^{48}$, $Cr^{52}(d,2n)Mn^{52}$ and $Fe^{56}(d,2n)Co^{56}$.
Physical Review **95** (1954) 750
— Exfor: none
Remark: The shoulder at the low energy end of the excitation function of the ^{48}Ti(d,2n)^{48}V reaction was supposed to be due to a contribution from the ^{47}Ti(d,n) reaction. In the normalization to natural isotopic composition the compiler used the natural abundance of the ^{48}Ti for the whole energy range. The EC/β^+ value was also corrected.

*** Chen, K.L., Miller, J.M.:**
Comparison between reactions of alpha particles with scandium-45 and deuterons with titanium-47.
Physical Review **134** (1964) B1269
— Exfor: none
Remark: Cross-sections of the ^{47}Ti(d,n)^{48}V and ^{48}Ti(d,2n)^{48}V reactions were reported separately. The two reactions were summed by the compiler using the isotopic composition of ^{nat}Ti.
— Data excluded: too large estimated errors.

Takács, S., Sonck, M., Scholten, B., Hermanne, A., Tárkányi, F.:
Excitation functions of deuteron induced reactions on ^{nat}Ti for monitoring deuteron beams
Applied Radiation and Isotopes **48** (1997) 657
— Exfor: D4046
Remark: The elemental cross-section values were corrected according to the new results obtained by the authors, concerning more precise beam current measurement. The data were renormalised by 18% (see Takács et al., 2000).

Takács, S., Tárkányi, F., Sonck, M., Hermanne, A., Mustafa, M.G., Shubin Yu., Zhuang Youxiang:
New cross-sections and intercomparison of deuteron monitor reactions on Al, Ti, Fe, Ni and Cu.
Nuclear Instruments Methods B (submitted, 2000)
See also: Takács, S., Tárkányi, F., Sonck, M., Hermanne, A.
Excitation functions for monitoring deuteron beams up to 50 MeV. Abstracts of Int. Conf. on Ion Beam Applications and European Conf. on Accelerator in Applied Research and Technology, 26-30 July 1999, Dresden, Germany, p. 72.
— Exfor: none

West Jr., H.I., Lanier, R., G., and Mustafa, M.G.:
Excitation functions for the nuclear reactions on titanium leading to the production of ^{48}V, ^{44}Sc, and ^{47}Sc by proton, deuteron and triton irradiations at 0-35 MeV.
UCRL-ID-115738, 1993
— Exfor: none
Remark: The two reactions reported were summed by the compiler taking into account the isotopic composition of the natural Ti. At higher energies the (d,3n), and (d,4n) reactions on ^{49}Ti(5.4%) and ^{50}Ti(5.2%) also contribute to the production of the ^{48}V. These contributions were not measured by the authors. Their contributions were neglected.

The data from all experimental papers where numerical values are available (5 papers), are collected in Fig. 4.2.3a. From these 1 work was excluded while the remaining 4 works were selected for further evaluation.

Cross-sections were calculated by two different versions of the nuclear reaction model code ALICE (denoted as 91(KR) and IPPE) and by two fitting procedures (Padé with 16 parameters and Spline). These results are compared with the selected experimental data in Fig. 4.2.3b. It is seen that model calculations give higher maximum cross-section values than the experimental data. Fits do better. The best approximation was judged to be the Padé fit. Recommended cross-sections are compared with selected experimental data, including their error bars, in Fig. 4.2.3c. The data are recommended above 9 MeV deuteron energy only. The corresponding numerical values are tabulated in Table 4.2.3.

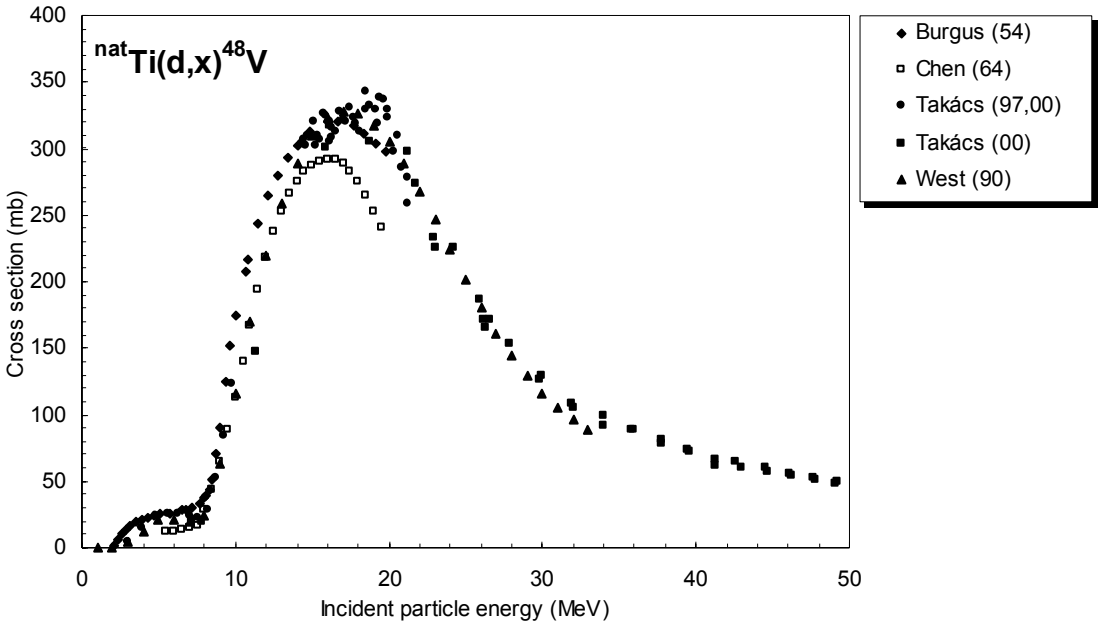

Figure 4.2.3a. All experimental data.

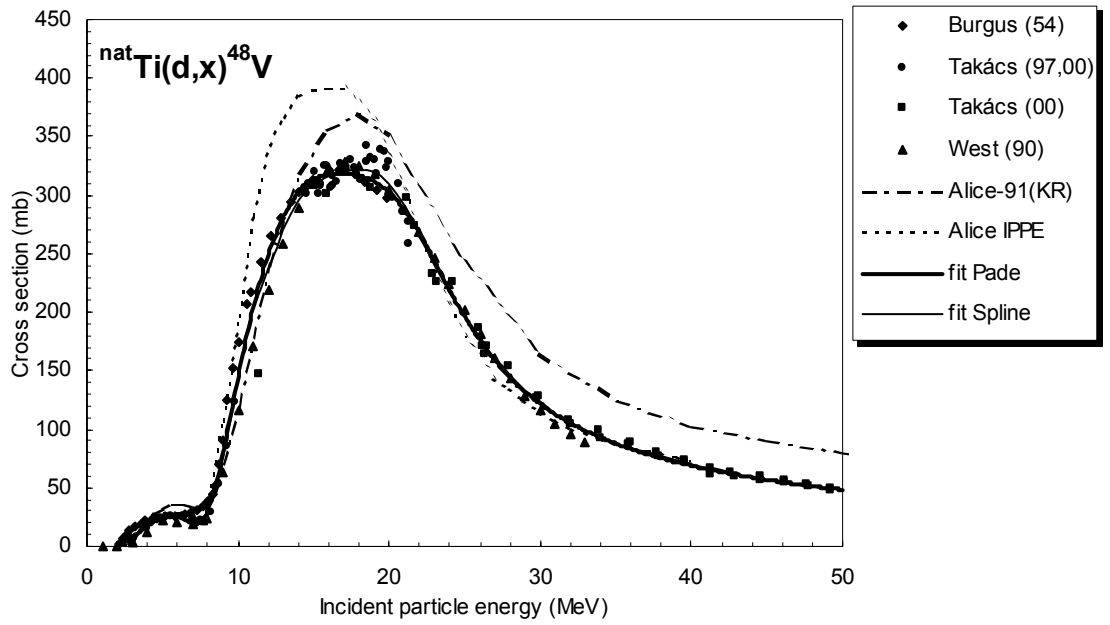

Figure 4.2.3b. Selected experimental data in comparison with theoretical calculations and fits.

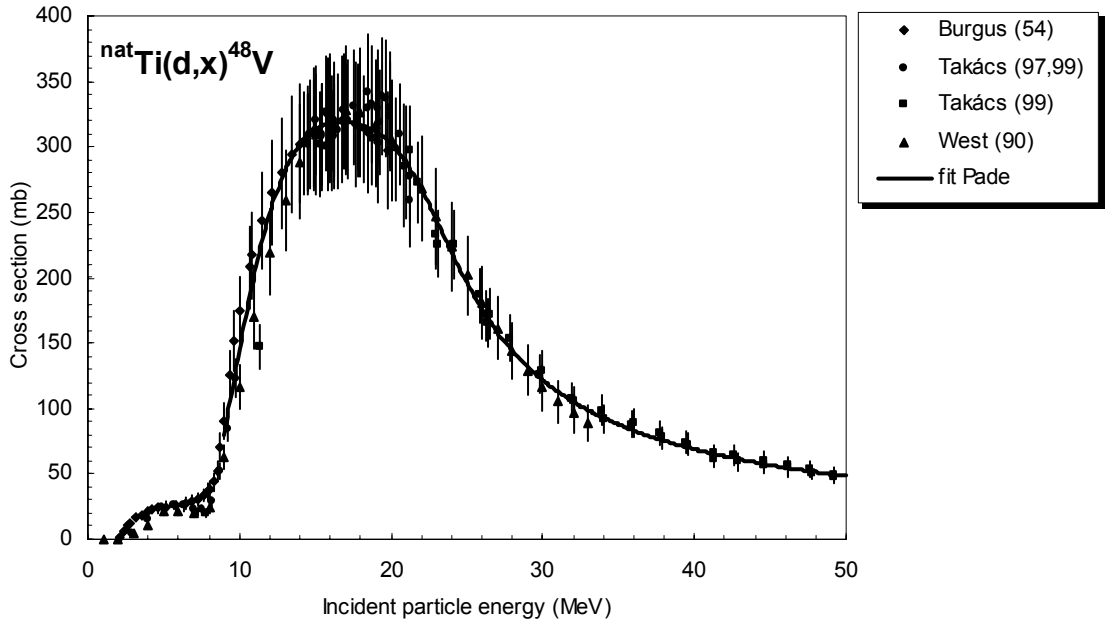

Figure 4.2.3c. Selected experimental data and recommended cross-section curve.

TABLE 4.2.3. RECOMMENDED CROSS-SECTIONS FOR THE ^{nat}Ti (d,x)^{48}V REACTION

Energy MeV	Cross-section mb	Energy MeV	Cross-section mb	Energy MeV	Cross-section mb	Energy MeV	Cross-section mb
9.0	80.1	19.5	308	30.0	122	40.5	67.5
9.5	112.4	20.0	303	30.5	117	41.0	66.1
10.0	144.9	20.5	296	31.0	113	41.5	64.8
10.5	175.7	21.0	288	31.5	109	42.0	63.5
11.0	203.6	21.5	278	32.0	105	42.5	62.3
11.5	228.2	22.0	268	32.5	102	43.0	61.1
12.0	249.4	22.5	256	33.0	99	43.5	60.0
12.5	267.3	23.0	244	33.5	96	44.0	58.9
13.0	281.8	23.5	231	34.0	93	44.5	57.9
13.5	293.4	24.0	219	34.5	90	45.0	56.8
14.0	302.3	24.5	207	35.0	87.8	45.5	55.9
14.5	308.9	25.0	196	35.5	85.4	46.0	54.9
15.0	313.5	25.5	186	36.0	83.2	46.5	54.0
15.5	316.4	26.0	176	36.5	81.1	47.0	53.1
16.0	318.2	26.5	167	37.0	79.1	47.5	52.2
16.5	319	27.0	159	37.5	77.2	48.0	51.4
17.0	319	27.5	151	38.0	75.4	48.5	50.6
17.5	318	28.0	144	38.5	73.7	49.0	49.8
18.0	317	28.5	138	39.0	72.0	49.5	49.1
18.5	315	29.0	132	39.5	70.5	50.0	48.3
19.0	312	29.5	127	40.0	69.0		

4.2.4. $^{nat}Fe(d,x)^{56}Co$

A total of 9 cross-section data sets were found in the literature in the energy range considered. From these, 2 works were excluded while the remaining 7 were selected for further evaluation. For a detailed description of the analysis and selection see Takács et al. (2000). The list of related references given below is accompanied with additional information. We mention availability of data in the computerized database EXFOR (if available, unique EXFOR reference number is given). Furthermore, we indicate a reason why a data set was excluded (reference denoted by an asterisk *).

*** Burgus, W.H., Cowan, G.A., Hadley, J.W., Hess, W., Shull, T., Stevenson, M.L., York, H.F.:**
Cross-sections for the reactions $Ti^{48}(d,2n)V^{48}$, $Cr^{52}(d,2n)Mn^{52}$ and $Fe^{56}(d,2n)Co^{56}$.
Physical Review **95** (1954) 750
— Exfor: none
Remark: The data given as isotopic cross-sections were renormalised for natural target composition and multiplied by 0.25/0.38 by the compiler taking into account the new values for β^+ branching ratio.
— Data excluded: significantly lower than the values of other authors.

Clark, J.W., Fulmer, C.B., Williams, I.R.:
Excitation functions for radioactive nuclides produced by deuteron-induced reactions in iron.
Physical Review **179** (1969) 1104
— Exfor: none
Remark: The compiler has performed a new normalisation to get the absolute values. For this normalisation the corrected and new results of Takács et al. (1997) and Takács et al. (1999), respectively, were employed.

Irwine, J.W.:
The Science and Engineering of Nuclear Power, (Ed. Goodman, C.)
Vol II.223., Addison-Wesley Press Inc., Cambridge (Mass) 1949
The data were taken from: Tobailem, J., de Lassus St-Genies, C.-H.:
Sections efficaces des reactions nucleaires induites par protons, deutons, particules alpha. III. Fer
CEA-N-1466(3), 1975, CEA, France
— Exfor: none

*** Jung, P.:**
Helium production and long-term activation by protons and deuterons in metals for fusion reactor application.
J. Nuclear Materials **144** (1987) 43
— Exfor: none
— Data excluded: significantly lower than the values of other authors.

Sudár, S., Qaim, S.M.:
Excitation functions of proton and deuteron induced reactions on iron and alpha-particle induced reactions on manganese in the energy region up to 25 MeV.
Physical Review **C50** (1994) 2408
— Exfor: D4018

Takács, S., Tárkányi, F., Sonck, M., Hermanne, A., Sudár, S.:
Study of deuteron induced reactions on natural iron and copper and their use for monitoring beam parameters and for thin layer activation technique.
Application of Accelerators in Research and Industry. Proceedings of the 14th International Conference, Denton, Texas, November 1996. Eds: J.L. Dugan, I.L. Morgan, AIP Conference Proceedings 392, Woodbury, New York, AIP (1997) 659.
— Exfor: D4044
Remark: The elemental cross-section values were corrected according to the new results obtained by these authors concerning a more precise beam current measurement. The data were renormalized by 18% (see Takács et al., 2000).

Takács, S., Tárkányi, F., Sonck, M., Hermanne, A., Mustafa, M.G., Shubin Yu, Zhuang Youxiang:
New cross-sections and intercomparison of deuteron monitor reactions on Al, Ti, Fe, Ni and Cu.
Nuclear Instruments Methods B (submitted, 2000)
See also: Takács, S., Tárkányi, F., Sonck, M., Hermanne, A.
Excitation functions for monitoring deuteron beams up to 50 MeV. Abstracts of Int. Conf. on Ion Beam Applications and European Conf. on Accelerator in Applied Research and Technology, 26-30 July 1999, Dresden, Germany, p. 72.
— Exfor: none

Tao Zhenlan, Zhu Fuying, Qui Huiyuan, Wang Gonging:
Excitation functions of deuteron induced reactions on natural iron.
Atomic Energy Sciences and Technology **5** (1993) 506
— Exfor: S0015

Zhao Wen-rong, Lu Han-lin, Yu Wei-xiang, Cheng Jian-tao:
Excitation functions for reactions induced by deuteron in iron.
Chinese J. Nuclear Physics **17** (1995) 163
— Exfor: none

The data from all experimental papers where numerical values are available (9 papers), are collected in Fig. 4.2.4a. From these, 2 works were excluded while the remaining 7 were selected for further evaluation.

Cross-sections were calculated by two different versions of the nuclear reaction model code ALICE (denoted as 91(FG) and IPPE), by nuclear reaction model code SPEC and by two fitting procedures (Padé with 10 parameters and Spline). These results are compared with the selected experimental data in Fig. 4.2.4b. It is seen that the model calculations, particularly ALICE 91(FG), give higher maximum value than the experimental data. Fits do better. The best approximation was judged to be the spline fit. Recommended cross-sections are compared with selected experimental data, including their error bars, in Fig. 4.2.4c. The corresponding numerical values are tabulated in Table 4.2.4.

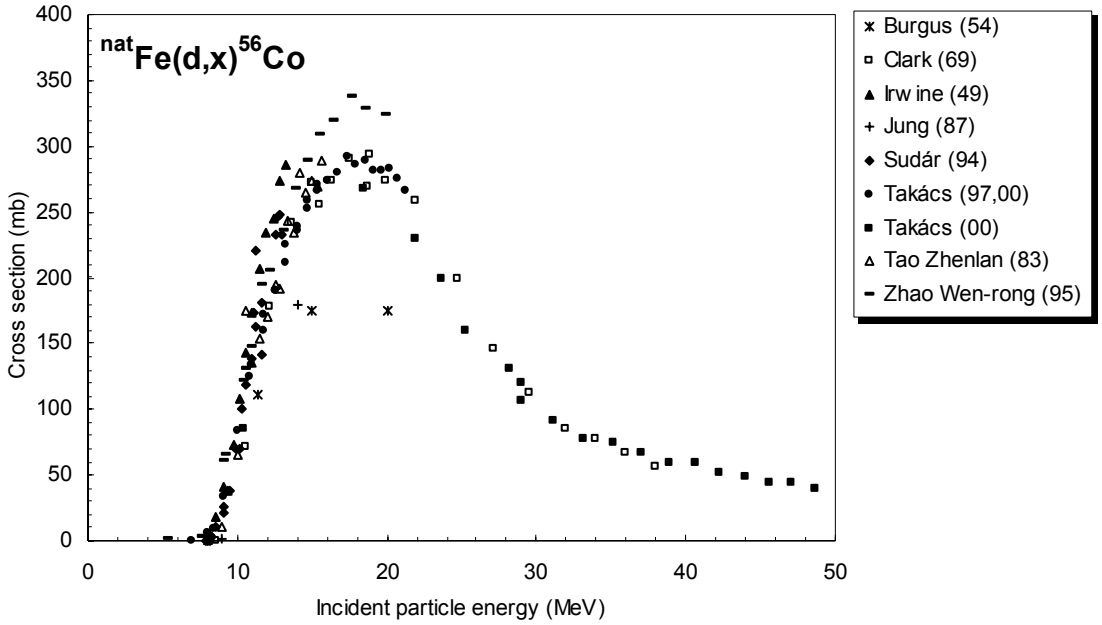

Figure 4.2.4a. All experimental data.

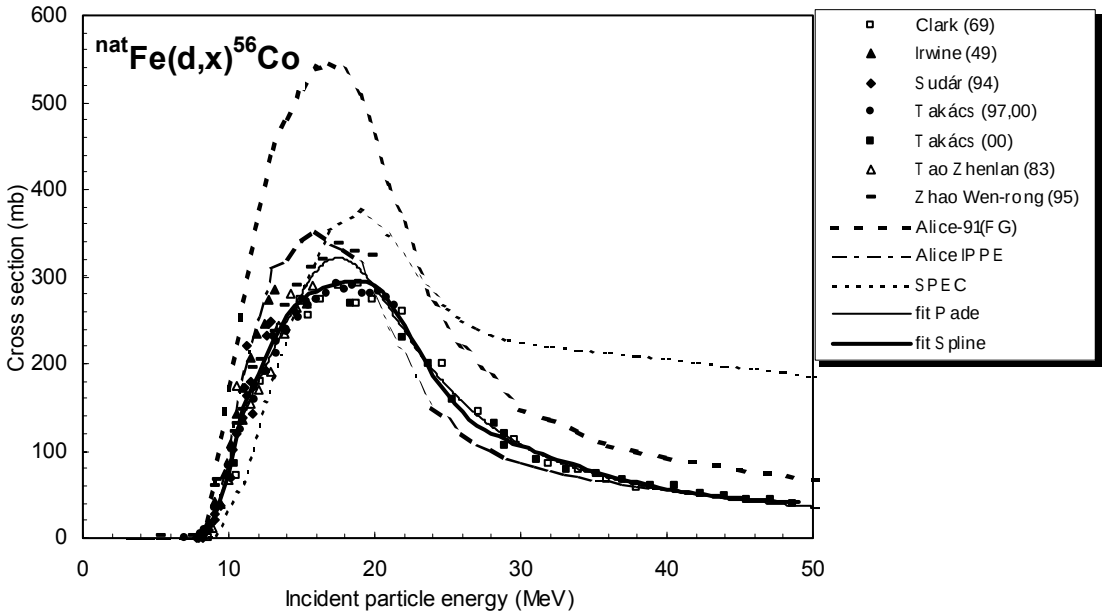

Figure 4.2.4b. Selected experimental data in comparison with theoretical calculations and fits.

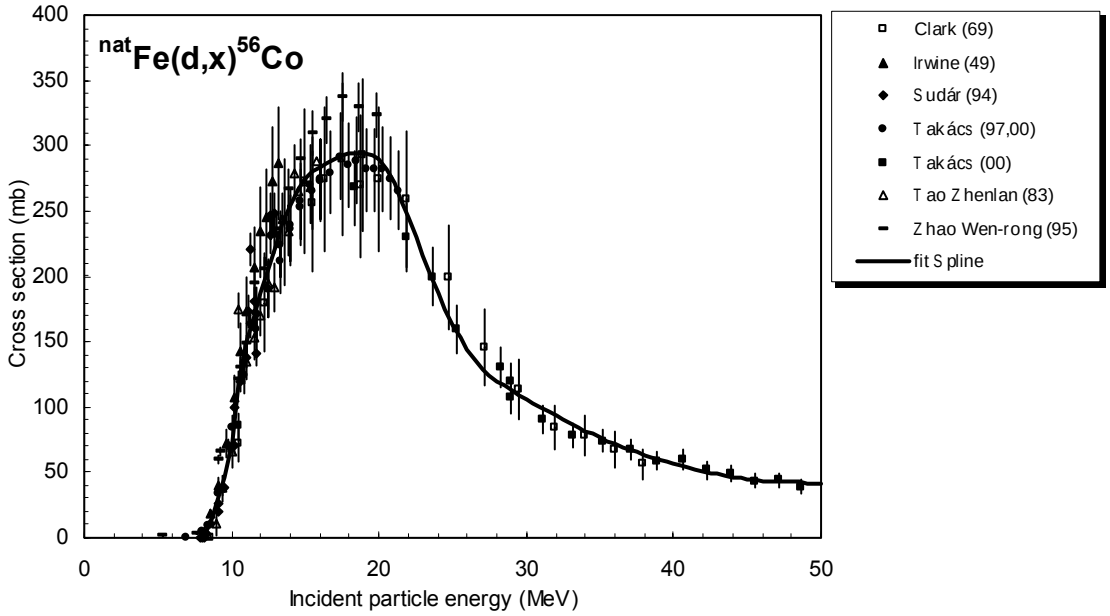

Figure 4.2.4c. Selected experimental data and recommended cross-section curve.

TABLE 4.2.4. RECOMMENDED CROSS-SECTIONS FOR THE $^{nat}Fe(d,x)^{56}Co$ REACTION

Energy MeV	Cross-section mb	Energy MeV	Cross-section mb	Energy MeV	Cross-section mb	Energy MeV	Cross-section mb
8.0	0.4	18.5	294.6	29.0	112.7	39.5	57.9
8.5	10.2	19.0	294.4	29.5	109.2	40.0	56.3
9.0	26.0	19.5	293.2	30.0	105.8	40.5	54.8
9.5	46.0	20.0	289.4	30.5	102.5	41.0	53.3
10.0	73.1	20.5	282.2	31.0	99.2	41.5	51.9
10.5	117.7	21.0	271.5	31.5	96.1	42.0	50.7
11.0	150.3	21.5	258.3	32.0	93.0	42.5	49.5
11.5	170.3	22.0	244.6	32.5	90.1	43.0	48.4
12.0	187.4	22.5	230.5	33.0	87.2	43.5	47.4
12.5	205.7	23.0	215.9	33.5	84.4	44.0	46.5
13.0	224.6	23.5	201.0	34.0	81.7	44.5	45.6
13.5	241.3	24.0	187.2	34.5	79.1	45.0	44.9
14.0	255.1	24.5	174.6	35.0	76.6	45.5	44.2
14.5	266.2	25.0	163.1	35.5	74.2	46.0	43.7
15.0	274.5	25.5	152.9	36.0	71.8	46.5	43.2
15.5	280.0	26.0	143.9	36.5	69.6	47.0	42.8
16.0	283.8	26.5	136.1	37.0	67.4	47.5	42.5
16.5	287.1	27.0	129.5	37.5	65.3	48.0	42.3
17.0	289.9	27.5	124.1	38.0	63.4	48.5	42.2
17.5	292.2	28.0	119.9	38.5	61.5	49.0	42.1
18.0	293.9	28.5	116.3	39.0	59.7	50.0	42.0

4.2.5. $^{nat}Ni(d,x)^{61}Cu$

A total of 6 cross-section data sets were found in the literature in the energy range considered. From these, 2 works were excluded while the remaining 4 were selected for further evaluation. For a detailed description of the analysis and selection see Takács et al. (2000). The list of related references given below is accompanied with additional information. We mention availability of data in the computerized database EXFOR (if available, unique EXFOR reference number is given). Furthermore, we indicate a reason why a data set was excluded (reference denoted by an asterisk *).

Budzanowski, A., Grotowski, K.:
Elastic scattering angular distributions and total cross-sections for the interactions of 12.8 MeV deuterons with Ni^{58} and Ni^{60} nuclei.
Physics Letters **2** (1962) 280
— Exfor: D4053

Coetzee, P.P., Peisach, M.:
Activation cross-sections for deuteron-induced reactions on some elements of the first transition series, up to 5.5 MeV.
Radiochimica Acta **17** (1972) 1
— Exfor: D4054

***Cogneau, M., Gilly, L.J., Cara, J.:**
Absolute cross-sections and excitation functions for deuteron-induced reactions on nickel isotopes between 2 and 12 MeV.
Nuclear Physics **A99** (1967) 689
— Exfor: no
— Data excluded: values seem too high and have energy shift.

Takács, S., Sonck, M., Azzam, A., Hermanne, A., Tárkányi, F.:
Activation cross-section measurements of deuteron induced reactions on ^{nat}Ni with special reference to beam monitoring and production of ^{61}Cu for medical purpose.
Radiochimica Acta **76** (1997) 15
— Exfor: D4045
Remark: The elemental cross-sections reported in this work were corrected according to the new results obtained by the authors, concerning a more precise beam current measurement. Their data above 10 MeV were renormalized by 18% by the compiler (see Takács et al., 2000).

Takács, S., Tárkányi, F., Sonck, M., Hermanne, A., Mustafa, M.G., Shubin Yu., Zhuang Youxiang:
New cross-sections and intercomparison of deuteron monitor reactions on Al, Ti, Fe, Ni and Cu.
Nuclear Instruments Methods B (2000) submitted
See also: Takács, S., Tárkányi, F., Sonck, M., Hermanne, A.
Excitation functions for monitoring deuteron beams up to 50 MeV. Abstracts of Int. Conf. on Ion Beam Applications and European Conf. on Accelerator in Applied Research and Technology, 26-30 July 1999, Dresden, Germany, p. 72.
— Exfor: none

*** Zweit, J., Smith, A.M., Downey, S., Sharma, H.L.:**
Excitation functions for deuteron induced reactions in natural nickel: production of no-carrier-added ^{64}Cu from enriched ^{64}Ni targets for positron emission tomography.
Applied Radiation Isotopes **42** (1991) 193
— Exfor: D4056
— Data excluded: too few data near the maximum, maximum is too high.

The data from all experimental papers where numerical values are available (6 papers), are collected in Fig. 4.2.5a. From these, 2 works were excluded while the remaining 4 were selected for further evaluation.

Cross-sections were calculated by two different versions of the nuclear reaction model code ALICE (denoted as 91(FG) and IPPE), by the model code SPEC and by two fitting procedures (Padé with 10 parameters and Spline). These results are compared with the selected experimental data in Fig. 4.2.5b. The results of model calculations give higher maximum cross-section value than the experimental data and generally overestimate them. Fits do better. The best approximation was judged to be the Padé fit. Recommended cross-sections are compared with selected experimental data, including their error bars, in Fig. 4.2.5c. The corresponding numerical values are tabulated in Table 4.2.5.

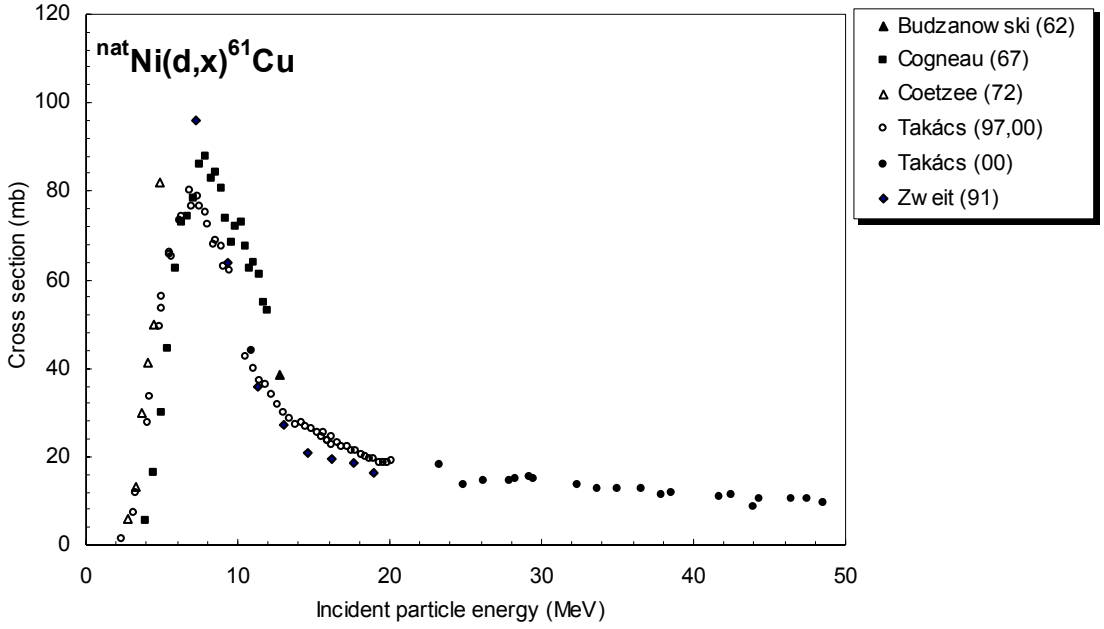

Figure 4.2.5a. All experimental data.

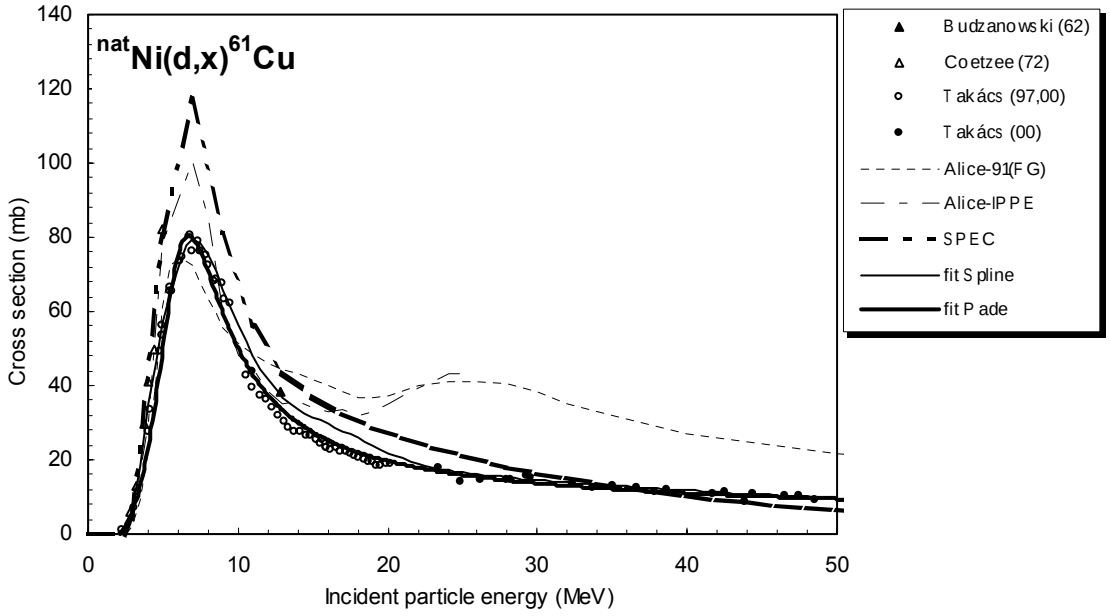

Figure 4.2.5b. Selected experimental data in comparison with theoretical calculations and fits.

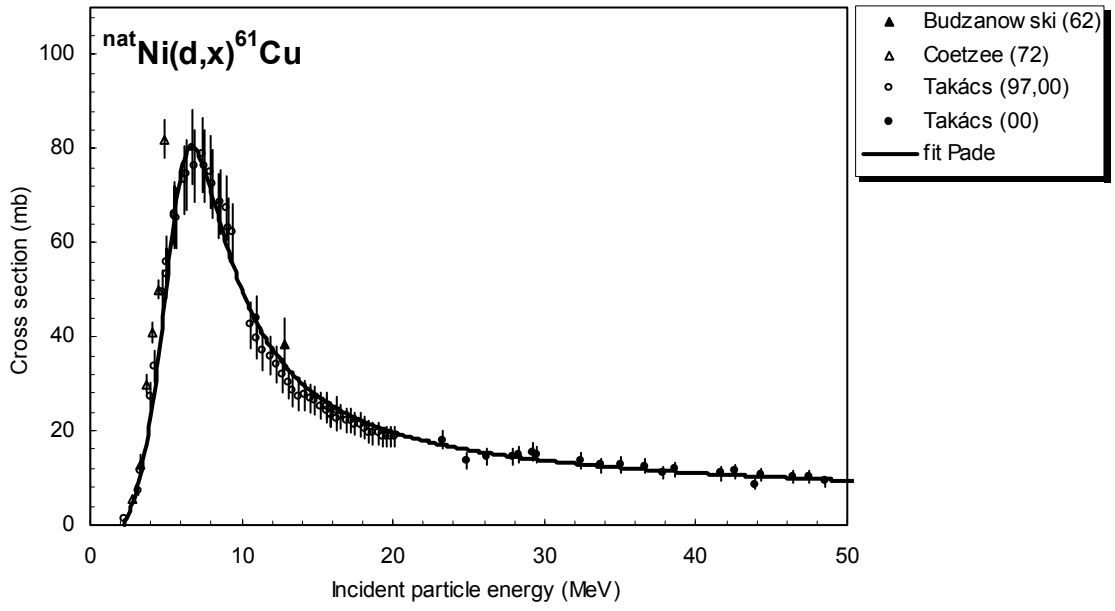

Figure 4.2.5c. Selected experimental data and recommended cross-section curve.

TABLE 4.2.5. RECOMMENDED CROSS-SECTIONS FOR THE $^{nat}Ni(d,x)^{61}Cu$ REACTION

Energy MeV	Cross-section mb	Energy MeV	Cross-section mb	Energy MeV	Cross-section mb	Energy MeV	Cross-section mb
2.5	2.1	14.5	28.7	26.5	15.2	38.5	11.3
3.0	6.7	15.0	27.4	27.0	14.9	39.0	11.2
3.5	13.6	15.5	26.3	27.5	14.7	39.5	11.1
4.0	23.2	16.0	25.3	28.0	14.5	40.0	11.0
4.5	35.9	16.5	24.4	28.5	14.3	40.5	10.9
5.0	50.5	17.0	23.5	29.0	14.1	41.0	10.8
5.5	64.6	17.5	22.8	29.5	13.9	41.5	10.7
6.0	75.1	18.0	22.1	30.0	13.7	42.0	10.7
6.5	80.0	18.5	21.4	30.5	13.5	42.5	10.6
7.0	79.7	19.0	20.8	31.0	13.3	43.0	10.5
7.5	76.0	19.5	20.2	31.5	13.2	43.5	10.4
8.0	70.7	20.0	19.7	32.0	13.0	44.0	10.3
8.5	65.0	20.5	19.2	32.5	12.9	44.5	10.2
9.0	59.5	21.0	18.8	33.0	12.7	45.0	10.2
9.5	54.5	21.5	18.3	33.5	12.6	45.5	10.1
10.0	50.1	22.0	17.9	34.0	12.4	46.0	10.0
10.5	46.2	22.5	17.6	34.5	12.3	46.5	9.9
11.0	42.9	23.0	17.2	35.0	12.2	47.0	9.9
11.5	40.0	23.5	16.9	35.5	12.0	47.5	9.8
12.0	37.5	24.0	16.5	36.0	11.9	48.0	9.7
12.5	35.3	24.5	16.2	36.5	11.8	48.5	9.7
13.0	33.3	25.0	15.9	37.0	11.7	49.0	9.6
13.5	31.6	25.5	15.7	37.5	11.6	49.5	9.5
14.0	30.0	26.0	15.4	38.0	11.4	50.0	9.5

.

4.3. HELIUM-3

Three ^{3}He beam monitor reactions were evaluated. Table 4.3 lists these reactions, including the basic decay characteristics of the product nuclei (half-lives, main γ lines along with their intensities) and energy range of helium-3 for which evaluations were performed.

TABLE 4.3. ^{3}He BEAM MONITOR REACTIONS

Reaction	$T_{1/2}$ of product nucleus	Main γ lines		^{3}He energy range (MeV)
		E_γ (keV)	I_γ (%)	
^{27}Al(^{3}He,x)^{22}Na	2.60 a	1274.5	99.94	10–100
^{27}Al(^{3}He,x)^{24}Na	14.96 h	1368.6	100.0	25–100
		2754.0	99.94	
^{nat}Ti(^{3}He,x)^{48}V	15.98 d	983.5	99.99	16–100
		1312.0	97.49	

4.3.1. ^{27}Al(^{3}He,x)^{22}Na

A total of 7 cross-section data sets (in 5 publications) were found in the literature in the energy range considered. From these, 1 out of three data sets given in one work was excluded while all other sets were selected for further evaluation. The list of related references given below is accompanied with additional information. We mention availability of data in the computerized database EXFOR (if available, unique EXFOR reference number is given). Furthermore, we indicate a reason why a data set was excluded (reference denoted by an asterisk *).

Brill, O.D.:
Cross-sections of ^{3}He reactions with light nuclei.
Yadernaya Fizika 1 (1965) 55.
Numerical values taken from: Semenov, V.G., Semenova, M.P., Sobolevsky, N.M.: Production of Radionuclides at Intermediate Energies. Interactions of Deuterons, Tritons and ^{3}He-nuclei with Nuclei. Landolt-Börnstein, New Series, Group I, Volume 13, Subvolume, F., (ed. Schopper, H.), Springer, Berlin, 1995
— Exfor: none

Cochran, D.R.F., Knight, J.D.:
Excitation functions of some reactions of 6 to 24 MeV ^{3}He ions with carbon and aluminium.
Physical Review **128** (1962) 1281
— Exfor: P0081

Kondrat'ev, S.N., Lobach, I.Yu., Lobach Yu.N., Sklyarenko, V.D.:
Production of residual nuclei by ^{3}He-induced reactions on ^{27}Al and ^{nat}Cu.
Applied Radiation and Isotopes **48** (1997) 601
— Exfor: none

Lamb, J.F.:
Lawrence Berkeley Laboratory, University of California, Berkeley, Rep. UCRL-18981 (1969)
Numerical values taken from: Albert, P., Blondiaux, G., Debrun, J.L., Giovagnoli, A., Valladon, M.: Activation Cross-Sections for Elements from Lithium to Sulphur.
Handbook of Nuclear Activation Data, Technical Report Series No. 273, 1987, IAEA Vienna, p. 479
— Exfor: none
Remark: One data set from the three available ones was excluded from the evaluation because of too low values.

Michel, R., Brinkmann, G., Galas, R., Stück, R.:
Production of ^{24}Na and ^{22}Na by ^{2}H induced reactions on aluminium.
Production of ^{24}Na and ^{22}Na by ^{3}He induced reactions on aluminium.
Data provided by Michel, R., in 1982 to the EXFOR database
— Exfor: A0158

The data from all experimental papers where numerical values are available (7 data sets from 5 papers), are collected in Fig. 4.3.1a. One data set was removed from further evaluation.

Cross-sections were calculated by two different versions of the nuclear reaction model code ALICE (denoted as 91(KR) and IPPE), by the model code SPEC and by two fitting procedures (Padé with 12 parameters and Spline). These results are compared with the selected experimental data in Fig. 4.3.1b. The results of the model calculations do not represent well the experimental data, particularly above 40 MeV. Fits do better. The best approximation was judged to be the spline fit. Recommended cross-sections are compared with selected experimental data, including their error bars, in Fig. 4.3.1c. The corresponding numerical values are tabulated in Table 4.3.1.

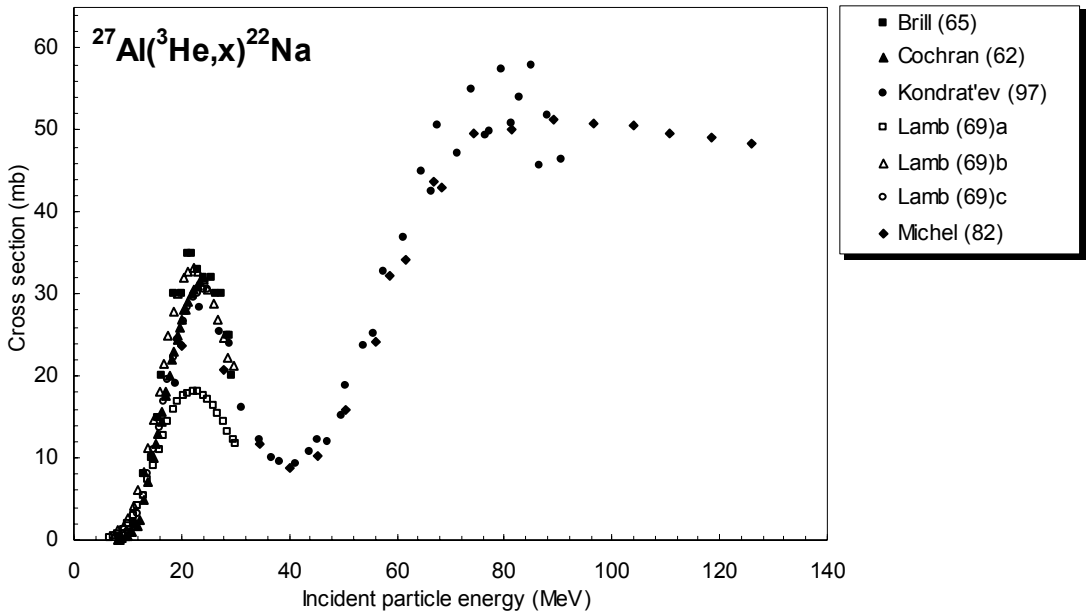

Figure 4.3.1a. All experimental data.

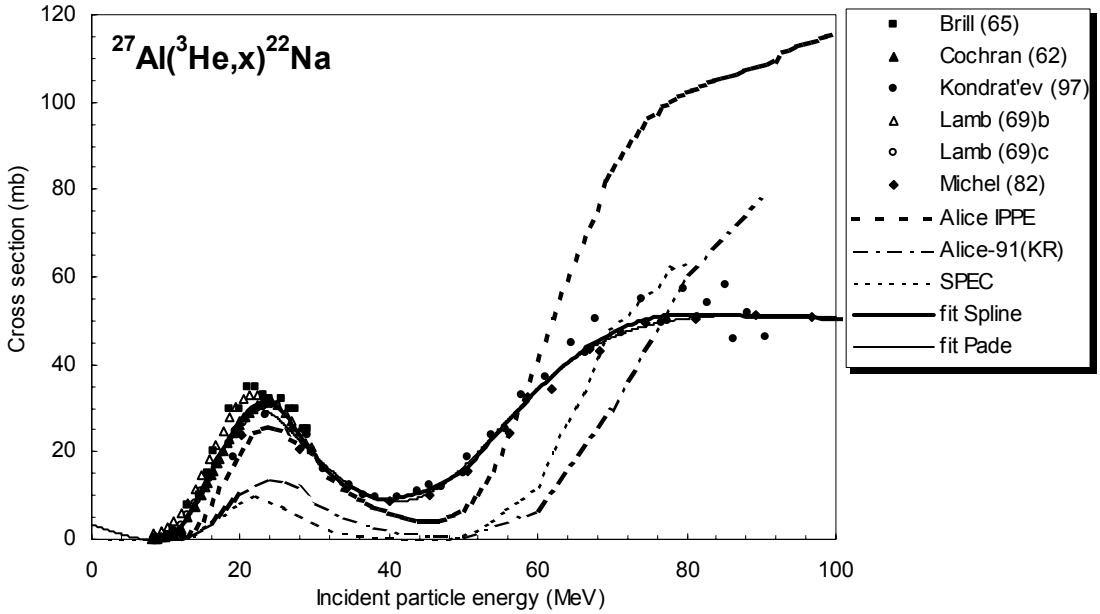

Figure 4.3.1b. Selected experimental data in comparison with theoretical calculations and fits.

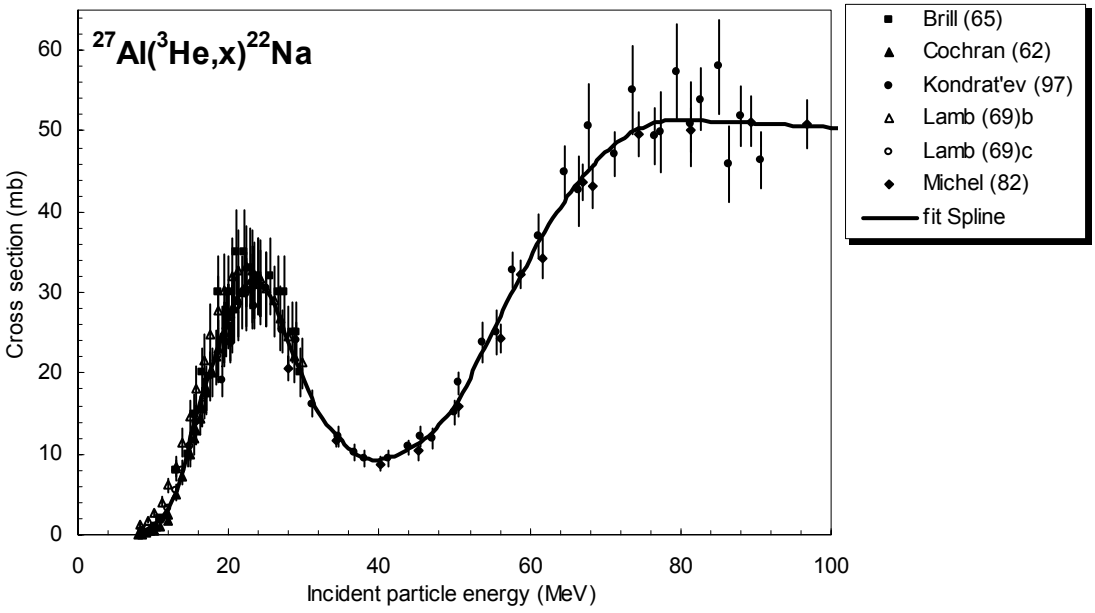

Figure 4.3.1c. Selected experimental data and recommended cross-section curve.

TABLE 4.3.1. RECOMMENDED CROSS-SECTIONS FOR THE $^{27}Al(^{3}He,x)^{22}Na$ REACTION

Energy MeV	Cross-section mb	Energy MeV	Cross-section mb	Energy MeV	Cross-section mb	Energy MeV	Cross-section mb
10.0	1.0	30.5	17.9	51.0	17.5	71.5	48.5
10.5	1.4	31.0	16.9	51.5	18.4	72.0	48.9
11.0	1.8	31.5	15.9	52.0	19.3	72.5	49.2
11.5	2.4	32.0	15.1	52.5	20.3	73.0	49.5
12.0	3.2	32.5	14.3	53.0	21.3	73.5	49.8
12.5	4.1	33.0	13.6	53.5	22.2	74.0	50.0
13.0	5.3	33.5	13.1	54.0	23.2	74.5	50.3
13.5	6.8	34.0	12.6	54.5	24.1	75.0	50.5
14.0	8.6	34.5	12.1	55.0	25.1	75.5	50.7
14.5	10.4	35.0	11.7	55.5	26.0	76.0	50.8
15.0	12.2	35.5	11.2	56.0	27.0	76.5	51.0
15.5	14.0	36.0	10.8	56.5	27.9	77.0	51.1
16.0	15.7	36.5	10.3	57.0	28.8	77.5	51.2
16.5	17.4	37.0	10.0	57.5	29.7	78.0	51.3
17.0	18.9	37.5	9.7	58.0	30.6	78.5	51.4
17.5	20.3	38.0	9.5	58.5	31.5	79.0	51.4
18.0	21.5	38.5	9.4	59.0	32.4	79.5	51.4
18.5	22.7	39.0	9.3	59.5	33.3	80.0	51.4
19.0	24.0	39.5	9.3	60.0	34.2	81.0	51.4
19.5	25.4	40.0	9.3	60.5	35.1	82.0	51.3
20.0	26.8	40.5	9.4	61.0	35.9	83.0	51.3
20.5	28.1	41.0	9.5	61.5	36.7	84.0	51.2
21.0	29.3	41.5	9.6	62.0	37.6	85.0	51.2
21.5	30.2	42.0	9.7	62.5	38.3	86.0	51.1
22.0	30.9	42.5	9.9	63.0	39.1	87.0	51.1
22.5	31.3	43.0	10.1	63.5	39.8	88.0	51.0
23.0	31.5	43.5	10.3	64.0	40.5	89.0	51.0
23.5	31.6	44.0	10.6	64.5	41.2	90.0	51.0
24.0	31.4	44.5	10.9	65.0	41.9	91.0	50.9
24.5	30.9	45.0	11.2	65.5	42.5	92.0	50.9
25.0	30.3	45.5	11.5	66.0	43.2	93.0	50.8
25.5	29.5	46.0	11.9	66.5	43.8	94.0	50.8
26.0	28.4	46.5	12.2	67.0	44.3	95.0	50.7
26.5	27.3	47.0	12.6	67.5	44.9	96.0	50.7
27.0	26.1	47.5	13.1	68.0	45.4	97.0	50.6
27.5	25.0	48.0	13.5	68.5	45.9	98.0	50.6
28.0	23.8	48.5	14.0	69.0	46.4	99.0	50.5
28.5	22.6	49.0	14.6	69.5	46.9	100.0	50.5
29.0	21.5	49.5	15.2	70.0	47.3		
29.5	20.3	50.0	15.9	70.5	47.7		
30.0	19.1	50.5	16.7	71.0	48.1		

4.3.2. $^{27}Al(^{3}He,x)^{24}Na$

A total of 6 cross-section data sets were found in the literature in the energy range considered. From these, 1 work was excluded while the remaining 5 papers were selected for further evaluation. The list of related references given below is accompanied with additional information. We mention availability of data in the computerized database EXFOR (if available, unique EXFOR reference number is given). Furthermore, we indicate a reason why a data set was excluded (reference denoted by an asterisk *).

Brill, O.D.:
Cross-sections of the reactions ^{3}He with light nuclei.
Yadernaya Fizika **1** (1965) 55
— Exfor: none

Cochran, D.R.F., Knight, J.D.:
Excitation functions of some reactions of 6 to 24 MeV ^{3}He ions with carbon and aluminium.
Physical Review **128** (1962) 1281
— Exfor: none

Frantsvog, D.J., Kunselman, A.R., Wilson, R.L., Zaidins, C.S., Detraz, C.:
Reactions induced by ^{3}He and ^{4}He ions on natural Mg, Al and Si.
Physical Review **C25** (1982) 770
— Exfor: none

Kondrat'ev, S.N., Lobach Yu.N., Skalyarenko, V.D., Tokarevsky, V.V.:
The absolute measurement of excitation functions for $^{27}Al(^{3}He,x)^{22,24}Na$, ^{7}Be reactions at E_{He}< 91 MeV.
Atomnaya Energiya **79** (1995) 307
— Exfor: A0553

*** Lamb, J.F.:**
Lawrence Berkeley Laboratory, University of California, Berkeley, Report UCLR-18981 (1969)
Data from: Albert, P., Blondiaux, G., Debrun, J.L., Giavagnoli, A., Vallandon, M., Activation cross-sections for elements from lithium to sulphur.
Handbook on Nuclear Activation Data, Technical Report Series No. 273, IAEA, Vienna, 1987, p. 479
— Exfor: none
— Data excluded: original publication not available to the compiler, values available only in graphical form in the compilation of Albert et al. (1987).

Michel, R., Brinkmann, G., Galas, M., Stück, R.:
Production of ^{24}Na and ^{22}Na by ^{2}H induced reactions on aluminium.
Production of ^{24}Na and ^{22}Na by ^{3}He induced reactions on aluminium.
Data provided by Michel, R. in 1982 to the EXFOR database.
— Exfor: A0158

The data from all experimental papers where numerical values are available (5 papers), are collected in Fig. 4.3.2a. One data set was excluded from further evaluation.

Cross-sections were calculated by two fitting procedures (Padé with 16 parameters and Spline). These results are compared with the selected experimental data in Fig. 4.3.2b. Both fits

represent the experimental data well. The best approximation was judged to be the spline fit. Recommended cross-sections are compared with selected experimental data, including their error bars, in Fig. 4.3.2c. The corresponding numerical values are tabulated in Table 4.3.2.

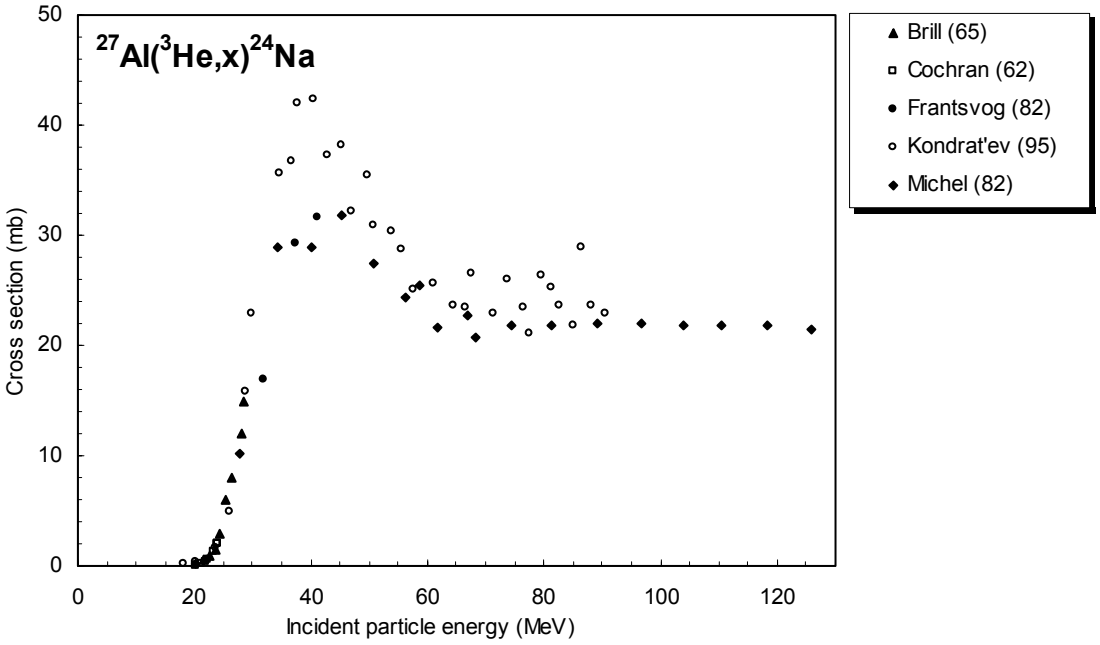

Figure 4.3.2a. All experimental data.

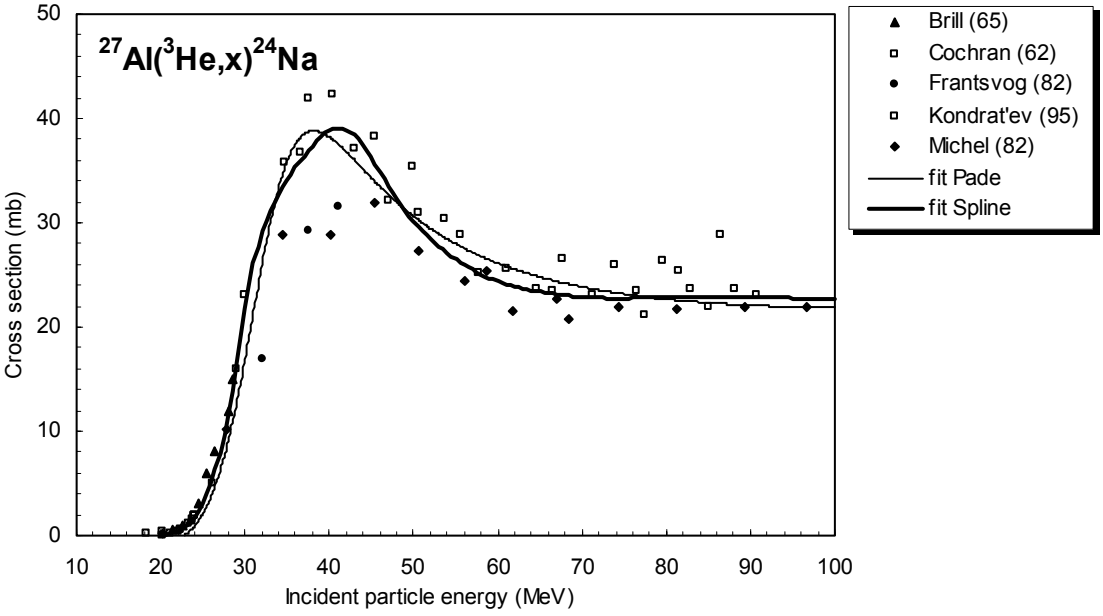

Figure 4.3.2b. Selected experimental data in comparison with fits.

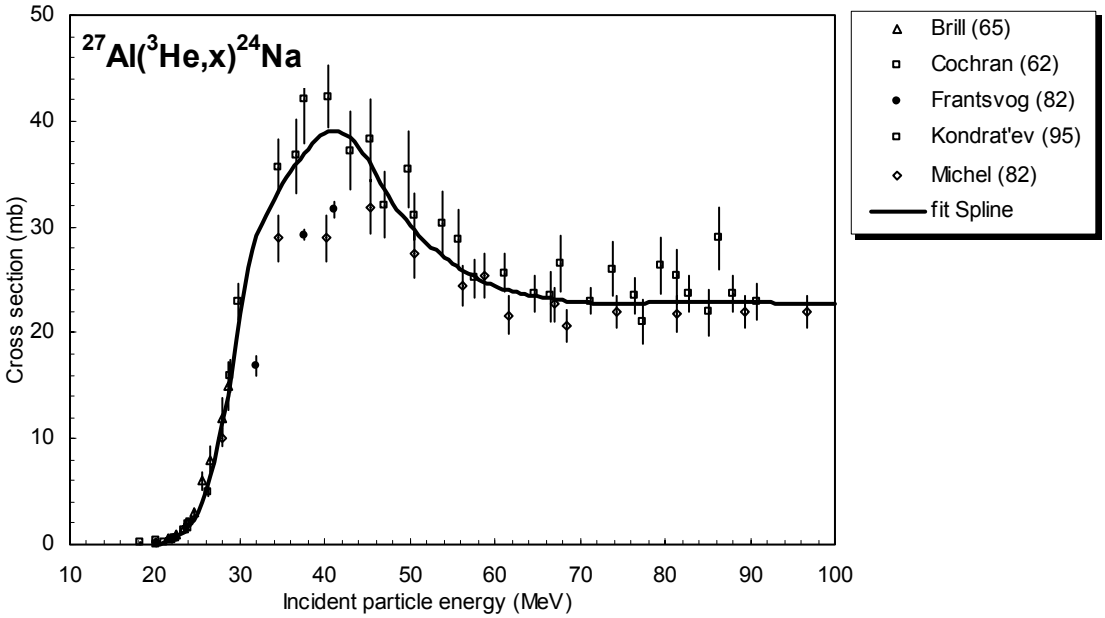

Figure 4.3.2c. Selected experimental data and recommended cross-section curve.

TABLE 4.3.2. RECOMMENDED CROSS-SECTIONS FOR THE $^{27}Al(^{3}He,x)^{24}Na$ REACTION

Energy MeV	Cross-section mb	Energy MeV	Cross-section mb	Energy MeV	Cross-section mb	Energy MeV	Cross-section mb
25.0	2.1	44.0	35.1	63.0	25.3	82.0	22.5
25.5	2.9	44.5	34.7	63.5	25.1	82.5	22.5
26.0	3.8	45.0	34.3	64.0	25.0	83.0	22.4
26.5	4.9	45.5	33.9	64.5	24.9	83.5	22.4
27.0	6.1	46.0	33.5	65.0	24.8	84.0	22.4
27.5	7.5	46.5	33.1	65.5	24.7	84.5	22.4
28.0	9.1	47.0	32.7	66.0	24.6	85.0	22.3
28.5	10.8	47.5	32.3	66.5	24.5	85.5	22.3
29.0	12.8	48.0	32.0	67.0	24.4	86.0	22.3
29.5	14.8	48.5	31.6	67.5	24.3	86.5	22.2
30.0	17.0	49.0	31.3	68.0	24.2	87.0	22.2
30.5	19.2	49.5	31.0	68.5	24.1	87.5	22.2
31.0	21.5	50.0	30.6	69.0	24.0	88.0	22.2
31.5	23.7	50.5	30.3	69.5	23.9	88.5	22.2
32.0	25.9	51.0	30.0	70.0	23.8	89.0	22.1
32.5	28.0	51.5	29.7	70.5	23.8	89.5	22.1
33.0	30.0	52.0	29.5	71.0	23.7	90.0	22.1
33.5	31.8	52.5	29.2	71.5	23.6	90.5	22.1
34.0	33.4	53.0	28.9	72.0	23.5	91.0	22.1
34.5	34.8	53.5	28.7	72.5	23.5	91.5	22.0
35.0	35.9	54.0	28.4	73.0	23.4	92.0	22.0
35.5	36.9	54.5	28.2	73.5	23.3	92.5	22.0
36.0	37.6	55.0	28.0	74.0	23.3	93.0	22.0
36.5	38.1	55.5	27.8	74.5	23.2	93.5	22.0
37.0	38.5	56.0	27.6	75.0	23.2	94.0	22.0
37.5	38.7	56.5	27.4	75.5	23.1	94.5	22.0
38.0	38.8	57.0	27.2	76.0	23.1	95.0	21.9
38.5	38.8	57.5	27.0	76.5	23.0	95.5	21.9
39.0	38.7	58.0	26.8	77.0	22.9	96.0	21.9
39.5	38.5	58.5	26.6	77.5	22.9	96.5	21.9
40.0	38.2	59.0	26.4	78.0	22.9	97.0	21.9
40.5	37.9	59.5	26.3	78.5	22.8	97.5	21.9
41.0	37.6	60.0	26.1	79.0	22.8	98.0	21.9
41.5	37.2	60.5	26.0	79.5	22.7	98.5	21.9
42.0	36.8	61.0	25.8	80.0	22.7	99.0	21.9
42.5	36.4	61.5	25.7	80.5	22.6	99.5	21.9
43.0	36.0	62.0	25.5	81.0	22.6	100.0	21.9
43.5	35.6	62.5	25.4	81.5	22.6		

4.3.3. $^{nat}Ti(^{3}He,x)^{48}V$

A total of 4 cross-section data sets were found in the literature in the energy range considered. All experimental data were in good agreement and were selected for further evaluation. The list of related references given below is accompanied with additional information. We mention availability of data in the computerized database EXFOR (if available, unique EXFOR reference number is given).

Ditrói, F., Ali, M.A., Tárkányi, F., Mahunka, I.:
Investigation of the ^{3}He induced reactions on natural Ti for the purpose of activation analysis and nuclear implantation.
Nuclear Data for Science and Technology, Trieste, 19-24 May 1997 (ed. Reffo, G., Ventura, A., Grandi, C.) Conference Proceedings Vol. 59, SIF, Bologna, 1997, p. 1746
— Exfor: none

Ditrói, F., Tárkányi, F., Ali, M.A., Andó, L., Heselius, S.-J., Shubin Yu., Zhuang Youxiang, Mustafa, M.G.:
Investigation of ^{3}He induced reactions on natural Ti for Thin Layer Activation (TLA), monitoring, activation analysis and production purposes.
Nuclear Instruments Methods B (1999) in press
— Exfor: none

Tárkányi, F., Szelecsényi, F., Kopecky, P.:
Cross-section data for proton, ^{3}He and α–particle induced reactions on ^{nat}Ni, ^{nat}Cu and ^{nat}Ti for monitoring beam performance.
Proceedings of International Conference on Nuclear Data for Science and Technology, Jülich, Germany, 13–17 May 1991, (ed. Qaim, S.M.), Springer-Verlag, Berlin, 1992, p. 529
— Exfor: D4080

Weinreich, R., Probst, H.J., Qaim, S.M.:
Production of Cr-48 for applications in life sciences.
Int. J. Applied Radiation Isotopes **31** (1980) 223
— Exfor: A0169

The data from all experimental papers where numerical values are available (4 papers) are collected in Fig. 4.3.3a. All experimental data are in good agreement and are selected for further evaluation.

Cross-sections were calculated by two different versions of the nuclear reaction model code ALICE (denoted as 91(FG) and IPPE), by the model code SPEC and by two fitting procedures (Padé with 12 parameters and Spline). These results are compared with the selected experimental data in Fig. 4.3.3b. The results of model calculations do not represent the experimental data well. Result of ALICE IPPE after normalization (ALICE IPPE norm) agrees relatively well with the experimental data, but fits do much better. The best approximation was judged to be the spline fit. Recommended cross-sections (above 16 MeV) are compared with selected experimental data, including their error bars, in Fig. 4.3.3c. The corresponding numerical values are tabulated in Table 4.3.3.

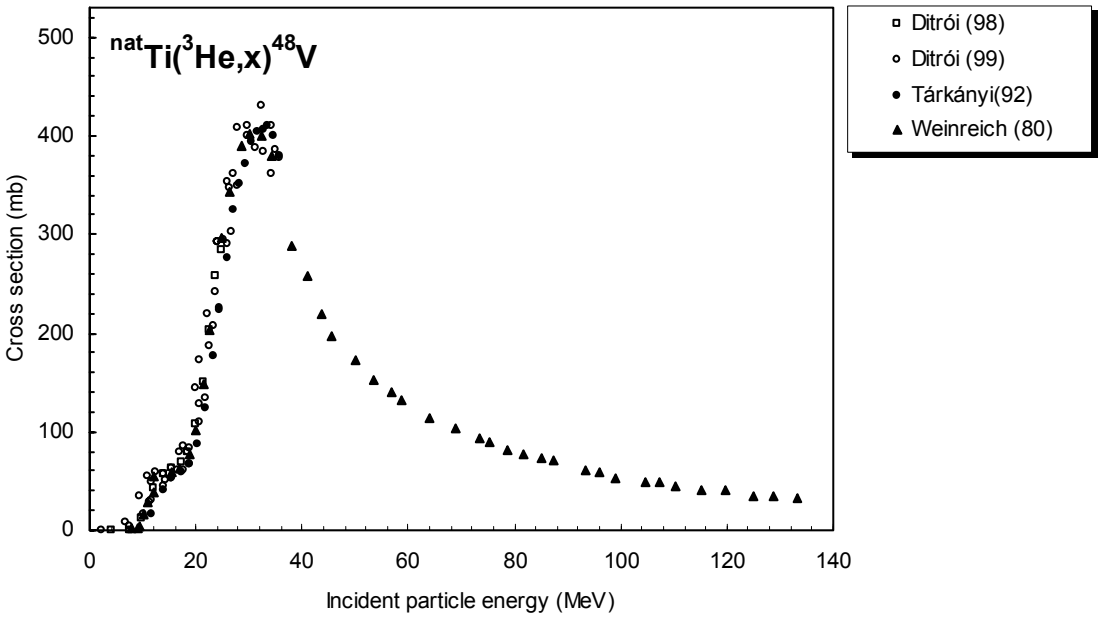

Figure 4.3.3a. All experimental data.

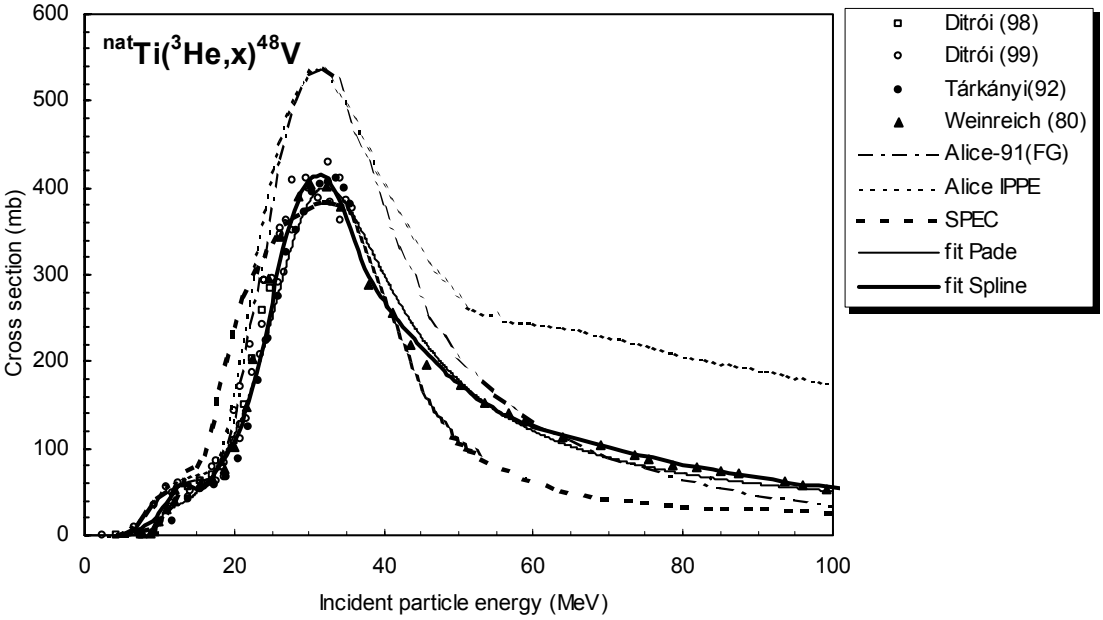

Figure 4.3.3b. Selected experimental data in comparison with theoretical calculations and fits.

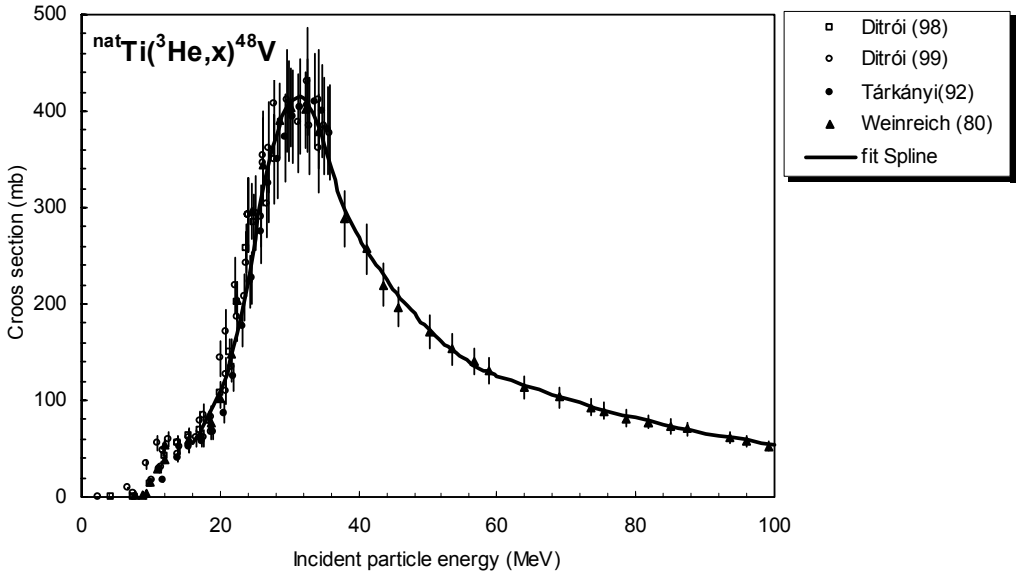

Figure 4.3.3c. Selected experimental data and recommended cross-section curve.

TABLE 4.3.3. RECOMMENDED CROSS-SECTIONS FOR THE $^{NAT}Ti(^{3}He,x)^{48}V$ REACTION

Energy MeV	Cross-section mb	Energy MeV	Cross-section mb	Energy MeV	Cross-section mb	Energy MeV	Cross-section mb
16.0	56.1	30.0	408	44.0	226	58.0	132
16.5	60.6	30.5	412	44.5	221	58.5	130
17.0	65.0	31.0	414	45.0	216	59.0	128
17.5	71.6	31.5	415	45.5	211	59.5	127
18.0	78.5	32.0	413	46.0	207	60.0	126
18.5	85.7	32.5	410	46.5	202	62.0	120
19.0	93.3	33.0	404	47.0	198	64.0	115
19.5	101.2	33.5	397	47.5	194	66.0	111
20.0	109.4	34.0	389	48.0	190	68.0	106
20.5	118.5	34.5	378	48.5	186	70.0	102
21.0	129.2	35.0	365	49.0	182	72.0	97
21.5	141.3	35.5	352	49.5	178	74.0	93
22.0	154.8	36.0	340	50.0	174	76.0	89
22.5	169.9	36.5	328	50.5	171	78.0	85
23.0	186.4	37.0	318	51.0	167	80.0	82
23.5	204.5	37.5	308	51.5	164	82.0	78
24.0	224.0	38.0	298	52.0	161	84.0	75
24.5	245.0	38.5	290	52.5	158	86.0	72
25.0	267.5	39.0	282	53.0	155	88.0	69.0
25.5	289.8	39.5	275	53.5	152	90.0	66.2
26.0	310.3	40.0	269	54.0	149	92.0	63.6
26.5	328.9	40.5	263	54.5	147	94.0	61.1
27.0	345.7	41.0	257	55.0	144	96.0	58.8
27.5	360.7	41.5	252	55.5	142	98.0	56.7
28.0	373.9	42.0	246	56.0	140	100.0	54.7
28.5	385.2	42.5	241	56.5	137		
29.0	394.7	43.0	236	57.0	135		
29.5	402.3	43.5	231	57.5	133		

4.4. ALPHA PARTICLES

Six α-particle beam monitor reactions were evaluated. Table 4.4 lists these reactions, including the basic decay characteristics of the product nuclei (half-lives, main γ lines along with their intensities) and energy range of α particles for which evaluations were performed.

TABLE 4.4. A-PARTICLE BEAM MONITOR REACTIONS

Reaction	$T_{1/2}$ of product nucleus	Main γ lines		α-particle energy range (MeV)
		E_γ (keV)	I_γ (%)	
$^{27}Al(\alpha,x)^{22}Na$	2.60 a	1274.5	99.94	29–100
$^{27}Al(\alpha,x)^{24}Na$	14.96 h	1368.6	100.0	50–100
		2754.0	99.94	
$^{nat}Ti(\alpha,x)^{51}Cr$	27.70 d	320.1	9.83	5–40
$^{nat}Cu(\alpha,x)^{66}Ga$	9.49 h	1039.3	37.9	8–30
$^{nat}Cu(\alpha,x)^{67}Ga$	3.26 d	93.3	37.0	15–50
		184.6	20.4	
$^{nat}Cu(\alpha,x)^{65}Zn$	244.10 d	1115.5	50.75	15–50

4.4.1. $^{27}Al(\alpha,x)^{22}Na$

A total of 13 cross-section data sets were found in the literature in the energy range considered. From these, 3 works were excluded while the remaining 10 were selected for further evaluation. The list of related references given below is accompanied with additional information. We mention availability of data in the computerized database EXFOR (if available, unique EXFOR reference number is given). Furthermore, we indicate a reason why a data set was excluded (reference denoted by an asterisk *).

Bouchard, G.H., Fairhall, A.W.:
Production of ^{7}Be in 30–42 MeV He-ion bombardment of oxygen, aluminium and copper.
Physical Review **116** (1959) 160
— Exfor: none

***Bowman, W.W., Blann, M.:**
Reactions of ^{51}V and ^{27}Al with 7–120 MeV α particles. (Equilibrium and non-equilibrium analysis).
Nuclear Physics **A131** (1969) 513
— Exfor: B0009
— Data excluded: large energy shift in comparison to the results of other works and data systematically lower than those of the other authors.

Ismail, M.:
Measurement and analysis of the excitation function for alpha-induced reactions on Ga and Sb isotopes.
Physical Review **C41** (1990) 87
— Exfor: none

Karpeles, A.:
Anregungsfunctionen für die Bildung von ^{68}Ge, ^{65}Zn und ^{22}Na bei der Bestrahlung von Zink und Aluminium mit α-Teilchen.
Radiochimica Acta **12** (1969) 115
— Exfor: none

***Lange, H.-J., Hahn, T., Michel, R., Schiekel, T., Roesel, R., Herpers, U., Hofmann, H.-J; Dittrich-Hannen, B., Suter, M., Woelfli, W., Kubik, P.W:**
Production of residual nuclei by alpha-induced reactions on C, N, Mg, Al, Si up to 170 MeV.
Applied Radiation and Isotopes **46** (1995) 93
— Exfor: A0517
— Data excluded: at high energies lower cross-section values. The trend of the excitation curve is also opposite to the other works.

Lindsay, R.H., Carr, R.J.:
He-ion induced reactions of aluminium and magnesium.
Physical Review **118** (1960) 1293
— Exfor: none

Martens, U., Schweimer, G.W.:
Production of ^{7}Be, ^{22}Na, ^{24}Na and ^{28}Mg by irradiation of ^{27}Al with 52 MeV deuterons and 104 MeV alpha particles.
Zeitschrift für Physik **233** (1970) 170
— Exfor: B0142

Michel, R., Brinkmann, G., Herr, W.:
Alpha-induced production of ^{24}Na and ^{22}Na from Al.
Progress Report on Nuclear Data Research in the Federal Republic of Germany, ed. Qaim, S.M., Report INDC(GER)-22/L (1980) 45
— Exfor: A0153

Porile, N.T.:
Study of the $Al^{27}(\alpha,Be^{7})Na^{24}$ reaction from threshold to 41 MeV.
Physical Review **127** (1962) 224
— Exfor: none

Probst, H.J., Qaim, S.M., Weinreich, R.:
Excitation functions of high-energy α-particle induced reactions on aluminium and magnesium: production of ^{28}Mg.
Int. J. Applied Radiation Isotopes **27** (1976) 431
— Exfor: B0174

Rattan, S.S., Singh, R.J.:
Alpha particle induced fission of ^{209}Bi.
Radiochimica Acta **38** (1985) 69
— Exfor: none

Rattan, S.S., Singh, R.J., Sahakundu, S.M., Prakash, S., Ramaniah, M.V.:
Alpha particle induced reactions of ^{209}Bi and ^{63,63}Cu.
Radiochimica Acta **39** (1986) 61
— Exfor: A0353

***Vysotskiy, O.N., Gaydaenko, S.A., Gonchar, A.V., Gorpinic, O.K., Kadkin, E.P., Kondrat'ev, S.N., Prokopenko, V.S., Rakitin, S.B., Saltykov, L.S., Sklyarenko, V.D., Strizh Yu.S., Tokaryevskiy, V.V.:**
The absolute cross-sections of long-lived radionuclides in reactions of alpha particles on aluminium-nuclei.
Abstract of Nuclear Spectroscopy Conference, Tashkent, USSR, 1989, p.365
— Exfor: A0424
— Data excluded: large energy shift compared with the results of other works.

The data from all experimental papers where numerical values are available (13 papers) are collected in Fig. 4.4.1a. The scatter of 3 data sets is large, therefore only 10 papers were selected for further evaluation.

Cross-sections were calculated by two different versions of the nuclear reaction model code ALICE (denoted as 91(BS) and IPPE) and by two fitting procedures (Padé with 12 parameters and Spline). These results are compared with the selected experimental data in Fig. 4.4.1b. The model calculations do not represent the experimental data well. Result of ALICE IPPE after normalisation (ALICE IPPE norm) reproduces better the experimental data, but fits do much better. The best approximation was judged to be the spline fit. Recommended cross-sections are compared with selected experimental data, including their error bars, in Fig. 4.4.1c. The corresponding numerical values are tabulated in Table 4.4.1.

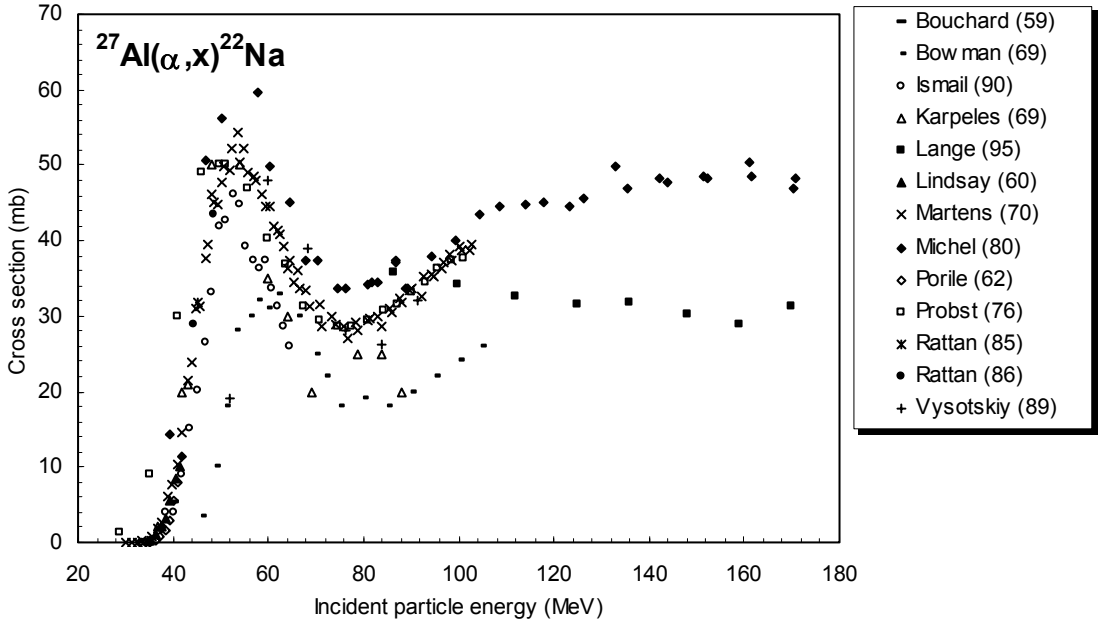

Figure 4.4.1a. All experimental data

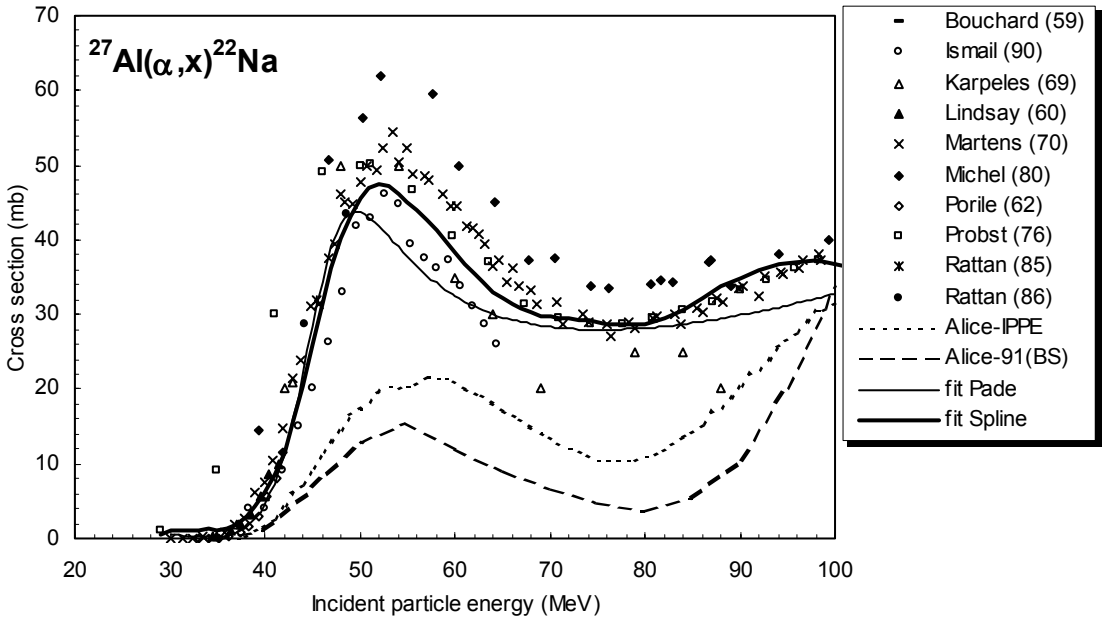

Figure 4.4.1b. Selected experimental data in comparison with theoretical calculations and fits.

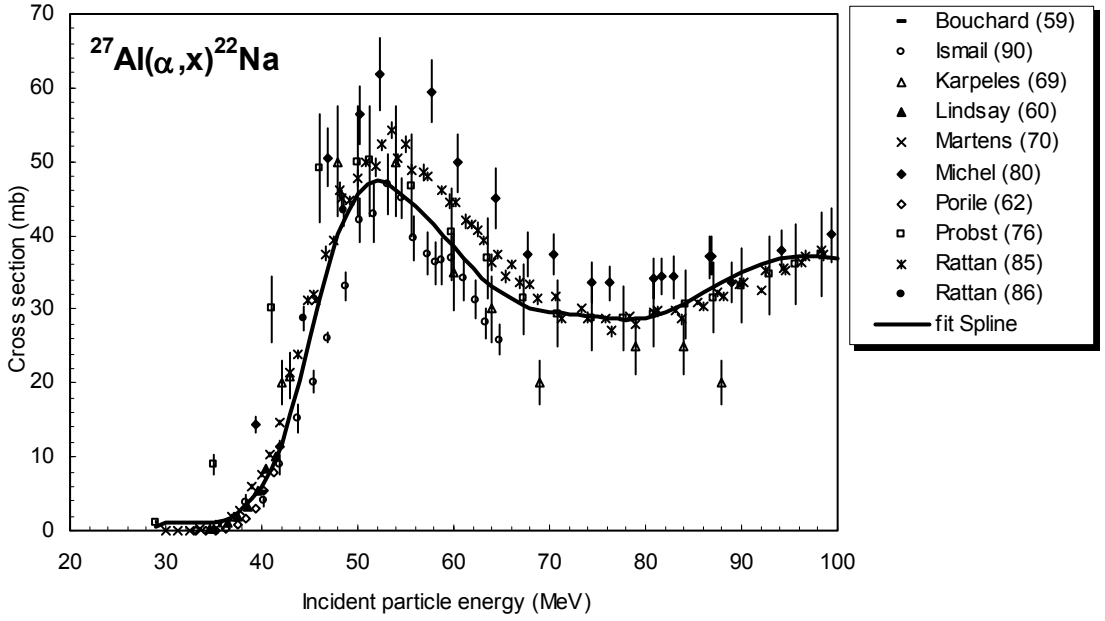

Figure 4.4.1c. Selected experimental data and recommended cross-section curve.

TABLE 4.4.1. RECOMMENDED CROSS-SECTIONS FOR THE $^{27}Al(\alpha,x)^{22}Na$ REACTION

Energy MeV	Cross-section mb	Energy MeV	Cross-section mb	Energy MeV	Cross-section mb	Energy MeV	Cross-section mb
29	0.5	45	26.0	61	36.9	77	28.6
30	1.0	46	31.6	62	35.5	78	28.6
31	1.1	47	36.3	63	34.2	79	28.7
32	1.2	48	40.2	64	33.1	80	28.8
33	1.2	49	43.3	65	32.2	82	29.5
34	1.2	50	45.5	66	31.4	84	30.7
35	1.2	51	46.8	67	30.7	86	32.2
36	1.4	52	47.4	68	30.2	88	33.7
37	2.0	53	47.2	69	29.9	90	35.0
38	3.0	54	46.3	70	29.7	92	36.1
39	4.3	55	45.0	71	29.5	94	36.8
40	6.1	56	43.9	72	29.4	96	37.1
41	8.5	57	42.7	73	29.3	98	37.1
42	11.7	58	41.4	74	29.1	100	36.8
43	15.6	59	40.0	75	29.0		
44	20.4	60	38.4	76	28.8		

4.4.2. $^{27}Al(\alpha,x)^{24}Na$

A total of 16 cross-section data sets were found in the literature in the energy range considered. From these, 5 works were excluded while the remaining 11 were selected for further evaluation. The list of related references given below is accompanied with additional information. We mention availability of data in the computerized database EXFOR (if available, unique EXFOR reference number is given). Furthermore, we indicate a reason why a data set was excluded (reference denoted by an asterisk *).

Bouchard, G.H., Fairhall, A.W.:
Production of ^{7}Be in 30-42 MeV He-ion bombardment of oxygen, aluminum and copper.
Physical Review **116** (1959) 160
— Exfor: none

***Bowman, W.W., Blann, M.:**
Reactions of ^{51}V and ^{27}Al with 7-120 MeV α particles (equilibrium and non-equilibrium analyses).
Nuclear Physics **A131** (1969) 513
— Exfor: B0009
— Data excluded: relatively low values and a systematic energy shift to higher energies.

*** Benzakin, J.R., Gauvin, H.:**
Private communication (1970)
Data from: Tobailem, J., de Lassus St-genies, C.-H., Leveque, L.: Sections efficaces des reactions nucleaires induites par protons, deutons, particules alpha. I reactions nucleaires moniteurs.
Note CEA-N-1-1466(1), CEA, France, 1971.
— Exfor: none
— Data excluded: systematically higher than the majority of others above the peak region.

***Crandall, W.E., Millburn, G.P., Pyle, R.V., BirnbaumW.:**
^{12}C (x,xn) ^{11}C and ^{l27}A(x,x2pn) ^{24}Na reactions at high energies.
Physical Review **101** (1956) 329
— Exfor: B0101
— Data excluded: only one data point in the high energy region that was not further considered.

Gordon, B.:
Nuclear and radiochemical research on special isotopes. Excitation functions of alpha particles on Aluminum-27.
Report: BNL-50082(S-70) (1967) 82
— Exfor: none

Hower, C.O.:
Thesis, Washington (1962)
Data from: Tobailem, J., de Lassus St-genies, C.-H., and Leveque, L.: Sections efficaces des reactions nucleaires induites par protons, deutons, particules alpha. I reactions nucleaires moniteurs.
Note CEA-N-1-1466(1), CEA, France, 1971.
— Exfor: none

Ismail, M.:
Measurement and analysis of alpha-induced reactions on Ga and Sb isotopes.
Physical Review **C41** (1990) 87
— Exfor: none

Ismail, M., Divatia, A.S.:
Measurements and analysis of alpha-induced reactions on Ta, Ag and Co.
Pramana — J. Physics **30** (1988) 193
— Exfor: none

*** Lindner, M., Osborne, R.N.:**
The cross-section for the reaction $^{27}Al(\alpha,\alpha 2pn)^{24}Na$ from threshold to 380 MeV.
Physical Review **91** (1953) 342
— Exfor: C0381
— Data excluded: energy scale has large uncertainties in the low energy region due to the very high primary alpha beam energy. It is also worth mentioning that the neutron background was high during the measurement and an old fashioned detection technique was employed.

*** Lindsay, R.H., Carr, R.J.:**
($^{4}He,^{7}Be$) reaction in magnesium, aluminium, titanium, cobalt and copper from threshold to 42 MeV.
Physical Review **120** (1960) 2168
— Exfor: P0063
— Data excluded: significantly higher than the results of other investigations and values were presented only in graphical form without error estimation.

Martens, U., Schweimer, G.W.:
Production of ^{7}Be, ^{22}Na, ^{24}Na and ^{28}Mg by irradiation of ^{27}Al with 52 MeV deuterons and 104 MeV alpha particles.
Zeitschrift für Physik **233** (1970) 170
— Exfor: B0142

Michel, R., Brinkmann, G., Herr, W.:
Alpha-induced production of ^{24}Na and ^{22}Na from Al.
Progress Report on Nuclear Data Research in the Federal Republic of Germany, ed. Qaim, S.M., Report INDC(GER)-22/L (1980) 45
— Exfor: A0153

Porile, N.T.:
Study of the $^{27}Al(\alpha,^{7}Be)^{24}Na$ reaction from threshold to 41 MeV.
Physical Review **127** (1962) 224
— Exfor: none

Probst, H.J., Qaim, S.M., Weinreich, R.:
Excitation functions of high-energy α-particle induced reactions on aluminium and magnesium: production of ^{28}Mg.
Int. J. Applied Radiation Isotopes **27** (1976) 431
— Exfor: B0174

Rattan, S.S., Singh, R.J., Sahakundu, S.M, Prakash, S., Ramaniah, M.V.:
Alpha particle induced reactions of ^{209}Bi and ^{63,65}Cu.
Radiochimica Acta **39** (1986) 61
— Exfor: A0353

Rattan, S.S., Singh, R.J.:
Alpha particle induced fission of ^{209}Bi.
Radiochimica Acta **38** (1985) 69
— Exfor: none

The data from all experimental papers where numerical values are available (16 papers) are collected in Fig. 4.4.2a. The scatter of 5 data sets is large, therefore only 11 papers were selected for further evaluation.

Cross-sections were calculated by two different fitting procedures (Padé with 18 parameters and Spline). These results are compared with the selected experimental data in Fig. 4.4.2b. It is seen that both fits reproduce the experimental data well. The best approximation was judged to be the Padé fit. Recommended cross-sections are compared with selected experimental data, including their error bars, in Fig. 4.4.2c. The corresponding numerical values are tabulated in Table 4.4.2.

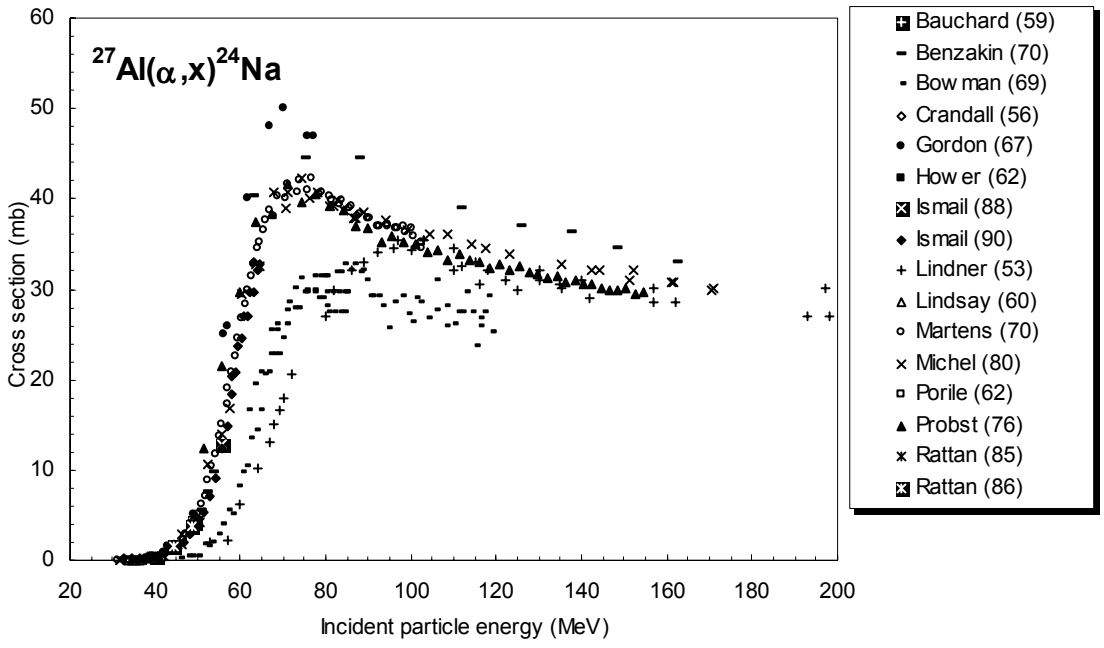

Figure 4.4.2a. All experimental data.

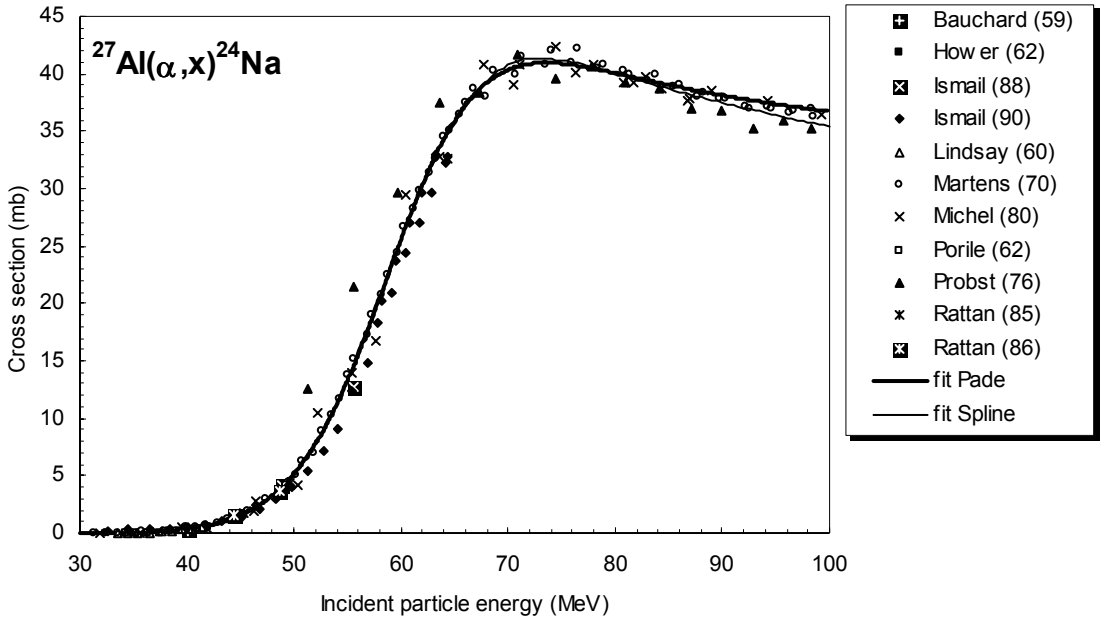

Figure 4.4.2b. Selected experimental data in comparison with fits.

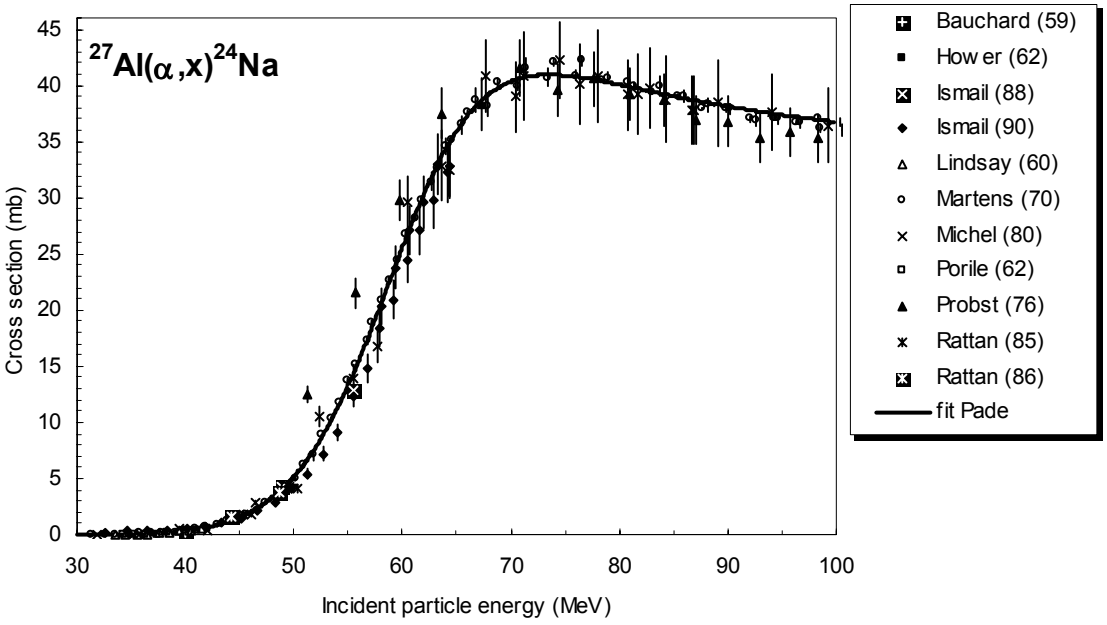

Figure 4.4.2c. Selected experimental data and recommended cross-section curve.

TABLE 4.4.2. RECOMMENDED CROSS-SECTIONS FOR THE $^{27}Al(\alpha,x)^{24}Na$ REACTION

Energy MeV	Cross-section mb	Energy MeV	Cross-section mb	Energy MeV	Cross-section mb	Energy MeV	Cross-section mb
50.0	5.2	63.0	32.5	76.0	40.8	89.0	38.3
50.5	5.8	63.5	33.4	76.5	40.7	89.5	38.2
51.0	6.4	64.0	34.3	77.0	40.6	90.0	38.1
51.5	7.1	64.5	35.2	77.5	40.6	90.5	38.1
52.0	7.8	65.0	36.0	78.0	40.5	91.0	38.0
52.5	8.6	65.5	36.7	78.5	40.4	91.5	37.9
53.0	9.4	66.0	37.3	79.0	40.3	92.0	37.8
53.5	10.3	66.5	37.9	79.5	40.2	92.5	37.7
54.0	11.3	67.0	38.4	80.0	40.1	93.0	37.7
54.5	12.3	67.5	38.8	80.5	40.0	93.5	37.6
55.0	13.3	68.0	39.2	81.0	39.9	94.0	37.5
55.5	14.4	68.5	39.6	81.5	39.8	94.5	37.4
56.0	15.6	69.0	39.9	82.0	39.7	95.0	37.4
56.5	16.8	69.5	40.2	82.5	39.6	95.5	37.3
57.0	18.0	70.0	40.4	83.0	39.4	96.0	37.2
57.5	19.2	70.5	40.5	83.5	39.3	96.5	37.2
58.0	20.5	71.0	40.7	84.0	39.2	97.0	37.1
58.5	21.8	71.5	40.8	84.5	39.1	97.5	37.0
59.0	23.1	72.0	40.9	85.0	39.0	98.0	37.0
59.5	24.3	72.5	40.9	85.5	38.9	98.5	36.9
60.0	25.6	73.0	41.0	86.0	38.8	99.0	36.8
60.5	26.9	73.5	41.0	86.5	38.8	99.5	36.8
61.0	28.1	74.0	41.0	87.0	38.7	100.0	36.7
61.5	29.2	74.5	40.9	87.5	38.6		
62.0	30.4	75.0	40.9	88.0	38.5		
62.5	31.5	75.5	40.8	88.5	38.4		

4.4.3. ^{nat}Ti(α,x)^{51}Cr

A total of 10 papers were found in the literature in the energy range considered. From these, 5 works were excluded while the remaining 6 were selected for further evaluation. For a detailed description of the selection and analysis of data see Hermanne et al. (1999). The list of related references given below is accompanied with additional information. We mention availability of data in the computerized database EXFOR (if available, unique EXFOR reference number is given). Furthermore, we indicate a reason why a data set was excluded (reference denoted by an asterisk *).

Chang, C.N., Kent, J.J., Morgan, J.F., Blatt, S.L.:
Total cross-section measurements by X ray detection of electron-capture of residual activity.
Nuclear Instruments Methods **109** (1973) 327
— Exfor: none

Hermanne, A., Sonck, M., Takács, S., Szelecsényi, F., Tárkányi, F.:
Excitation functions of alpha particle induced reactions on ^{nat}Ti with reference to monitoring and TLA.
Nuclear Instruments Methods **B152** (1999) 187
— Exfor: none
Data of Hermanne et al. (1999) are grouped into 7 series in the original publication; the compiler has reproduced them on the appropriate figure in two different data sets (labelled 'a' and 'b'). The series b was excluded because of systematically too low values.

*** Iguchi, A., Amano, H., Tanaka, S.:**
(α,n) cross-sections for ^{48}Ti and ^{51}V.
J. Atomic Energy Society Japan **2** (1960) 682
— Exfor: none
— Data excluded: seem to be shifted to lower energies since they have reported cross-section values below the threshold energy of the reaction.

*** Levkovski, V.N.:**
Middle Mass Nuclides (A = 40–100) Activation Cross-sections by Medium Energy (E = 10–50 MeV) Protons and Alpha particles. (Experiment and Systematics).
Inter-Vesi, Moscow (1991)
— Exfor: A0510
— Data excluded: values are too low.

*** Michel, R., Brinkmann, G., Stück, R.:**
Integral excitation functions of α-induced reactions on titanium, iron and nickel.
Radiochimica Acta **32** (1983) 173
— Exfor: A0148
— Data excluded: shifted to higher energy in the low energy region.

Morton, A.J., Tims, S.G., Scott, A.F.:
The ^{48}Ti(α,n)^{51}Cr and ^{48}Ti(α,p)^{51}V cross-sections.
Nuclear Physics **A128** (1992) 167
— Exfor: none

Tárkányi, F., Szelecsényi, F., Kopecky, P.:
Cross-section data for proton, ^{3}He and α-particle induced reactions on ^{nat}Ni, ^{nat}Cu and ^{nat}Ti for monitoring beam performance.
Proceedings of International Conference on Nuclear Data for Science and Technology, 13–17 May, 1991 Jülich, Germany (ed. Qaim, S.M.), Springer Verlag, Berlin, 1992, p. 529
— Exfor: D4080

Vonach, H., Haight, R.C., Winkler, G.:
(α,n) and total α-reaction cross-sections for ^{48}Ti and ^{51}V.
Physical Review **C28** (1983) 2278
— Exfor: C0318

Weinreich, R., Probst, H.J., Qaim, S.M.:
Production of chromium-48 for applications in life sciences.
Int. J. Applied Radiation Isotopes **31** (1980) 223
— Exfor: A0169

*** Xiufeng Peng, Fuqing He and Xianguan Long:**
Excitation functions for the reactions induced by alpha-particle impact of natural titanium
Nuclear Instruments Methods **B140** (1998) 9
— Exfor: none
— Data excluded: seem to be shifted to lower energies since they have reported cross-section values below the threshold energy of the reaction.

The data from all experimental papers where numerical values are available (10 papers, 11 data sets) are collected in Fig. 4.4.3a. The deviation or scatter of 5 data sets is large, therefore only 6 data sets were selected for further evaluation.

Cross-sections were calculated by two different versions of the nuclear reaction model code ALICE (denoted as 91(NP) and IPPE), by the model code SPEC and by two fitting procedures (Padé with 12 parameters and Spline). These results are compared with the selected experimental data in Fig. 4.4.3b. The curves of model calculations show energy shift towards lower energies and overestimation in the peak region. The best approximation was judged to be the Padé fit. Recommended cross-sections are compared with selected experimental data, including their error bars, in Fig. 4.4.3c. The corresponding numerical values are tabulated in Table 4.4.3.

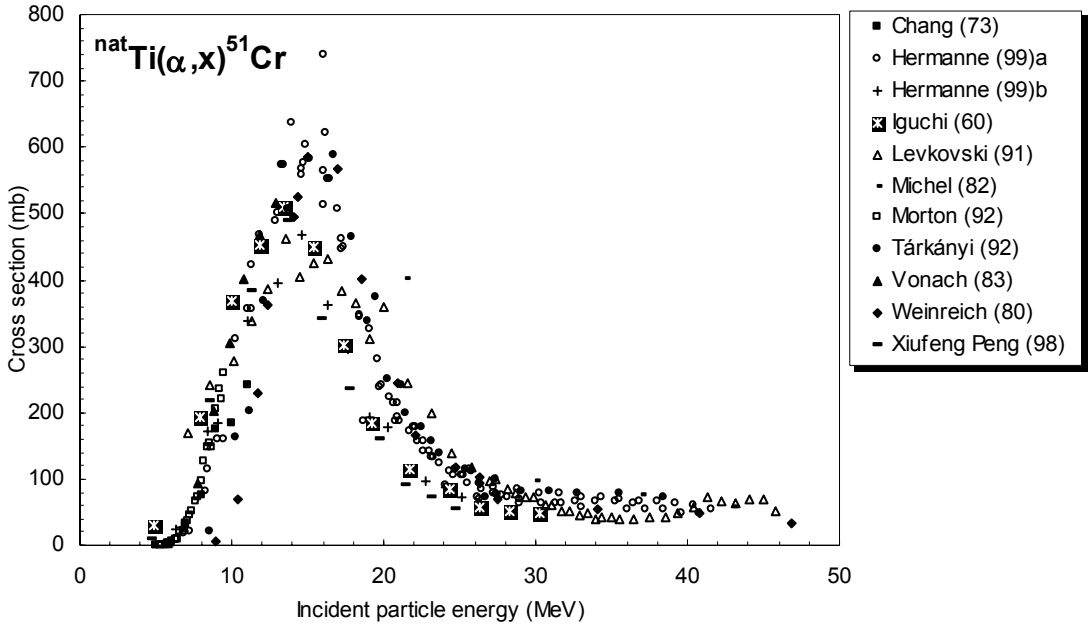

Figure 4.4.3a. All experimental data.

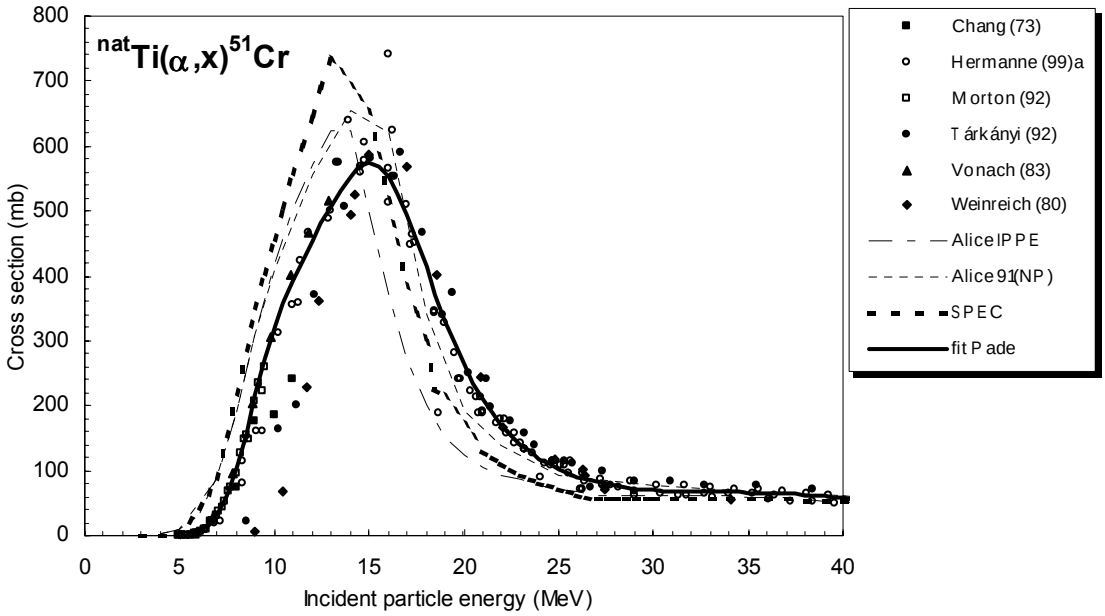

Figure 4.4.3b. Selected experimental data in comparison with theoretical calculations and fits.

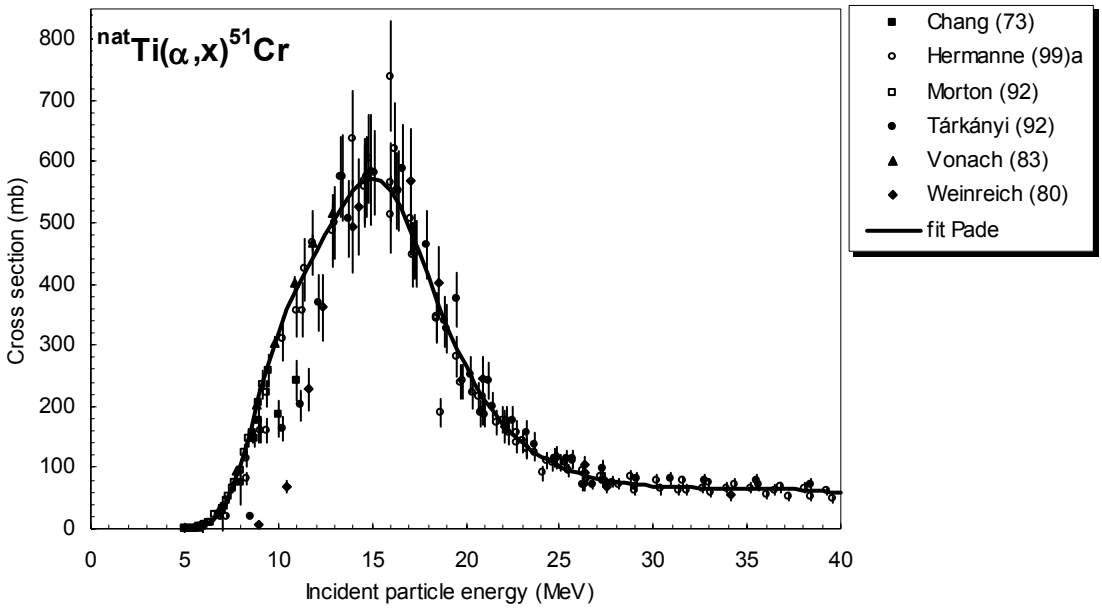

Figure 4.4.3c. Selected experimental data and recommended cross-section curve.

TABLE 4.4.3. RECOMMENDED CROSS-SECTIONS FOR THE $^{NAT}Ti(\alpha,x)^{51}Cr$ REACTION

Energy MeV	Cross-section mb	Energy MeV	Cross-section mb	Energy MeV	Cross-section mb	Energy MeV	Cross-section mb
5.0	0.2	14.0	553	23.0	140	32.0	67.2
5.5	1.4	14.5	568	23.5	129	32.5	66.9
6.0	5.4	15.0	574	24.0	119	33.0	66.8
6.5	14.6	15.5	569	24.5	110	33.5	66.7
7.0	32.2	16.0	554	25.0	103	34.0	66.6
7.5	61.7	16.5	528	25.5	96.3	34.5	66.5
8.0	105	17.0	493	26.0	90.9	35.0	66.3
8.5	159	17.5	454	26.5	86.4	35.5	66.1
9.0	218	18.0	412	27.0	82.5	36.0	65.7
9.5	273	18.5	371	27.5	79.2	36.5	65.2
10.0	320	19.0	332	28.0	76.5	37.0	64.6
10.5	360	19.5	296	28.5	74.2	37.5	63.8
11.0	394	20.0	263	29.0	72.4	38.0	62.9
11.5	424	20.5	235	29.5	70.8	38.5	61.8
12.0	453	21.0	210	30.0	69.7	39.0	60.5
12.5	481	21.5	189	30.5	68.7	39.5	59.2
13.0	508	22.0	170	31.0	68.0	40.0	57.6
13.5	532	22.5	154	31.5	67.5		

4.4.4. $^{nat}Cu(\alpha,x)^{66}Ga$

A total of 17 cross-section data sets were found in the literature in the energy range considered. From these, 8 works were excluded while the remaining 9 were selected for further evaluation. For detailed description of the analysis and selection see Tárkányi et al. (1999). Comparing the available results with each other, it can be seen that the data sets split into two groups. The list of related references given below is accompanied with additional information. We mention availability of data in the computerized database EXFOR (if available, unique EXFOR reference number is given). Furthermore, we indicate a reason why a data set was excluded (reference denoted by an asterisk *).

Bhardwaj, H.D., Gautam, A.K., Prasad, R.:
Measurement and analysis of excitation functions for alpha-induced reactions on copper.
Pramana — J. Physics **31** (1988) 109
— Exfor: A0465

*** Bonesso, O., Ozafran, M.J., Mosca, H.O., Vazquez, M.E., Capurr, O.AQ., Nassiff, S.J.:**
Study of pre-equilibrium effects on α−induced reactions on copper.
J. Radioanalytical and Nuclear Chemistry, Articles, **152** (1991) 189
— Exfor: none
— Data excluded: too low cross-section values.

Bryant, E.A., Cochran, D.R.F., Knight, J.D.:
Excitation functions of reactions of 7 to 24 MeV ^{3}He ions with ^{63}Cu and ^{65}Cu.
Physical Review **130** (1963) 1512
— Exfor: B0079

Hille, M., Hille, P., Uhl, M., Weisz, W.:
Excitation functions of (p,n) and (α,n) reactions on Ni, Cu and Zn.
Nuclear Physics **A198** (1972) 625
— Exfor: B0058

Levkovski, N.N.:
Middle Mass Nuclides (A=40-100) Activation Cross-sections by Medium Energy (E = 10–50 MeV) Protons and Alpha particles. (Experiment and Systematics).
Inter-Vesi, Moscow (1991)
— Exfor: A0510

*** Nassiff, S.J., Nassiff, W.:**
Cross-sections and thick target yields of alpha particle induced reactions.
IAEA Contract 2499/R1/RB
— Exfor: D0046
— Data excluded: unusual shape and cross-sections are too low.

*** Porges, K.G.:**
Alpha excitation functions of silver and copper.
Physical Review **101** (1956) 225
— Exfor: R0039
— Data excluded: too low cross-section values.

*** Porile, N.T., Morrison, D.L.:**
Reactions of ^{63}Cu and ^{65}Cu with alpha particles.
Physical Review **116** (1959) 1193
— Exfor: B0156
— Data excluded: unusual shape and cross-section values too low.

*** Rattan, S.S., Singh, R.J., Sahakundu, S.M., Prakash, S., Ramaniah, V.:**
Alpha particle induced reactions of ^{209}Bi and ^{63,65}Cu.
Radiochimica Acta **39** (1986) 61
— Exfor: A0353
— Data excluded: only one data point at high energy; cross-section is too low.

*** Rizvi, I.A., Ansari, M.A., Gautam, R.P., Singh, R.K.Y., Chaubey, A.K.:**
Excitation functions studies of (α,xpyn) reactions for ^{63,65}Cu and pre-equilibrium effect.
J. Physical Society Japan **56** (1987) 3135
— Exfor: none
— Data excluded: energy shifted or too low cross-sections.

*** Singh.N.L., Agarwal, S., Rama Rao, J.:**
Excitation functions for α–particle-induced reactions on light-mass nuclei.
Pramana — J. Physics **42** (1994) 349
— Exfor: none
— Data excluded: cross-section values are too low.

Sonck, M., Van Hoyweghen Y., Hermanne, A.:
Determination of the external beam energy of a variable energy multiparticle cyclotron.
Applied Radiation and Isotopes **47** (1996) 445
— Exfor: none

Stelson, P.H., McGowan, F.K.:
Cross-sections for (α,n) reactions for medium weight nuclei.
Physical Review **133** (1964) B911
— Exfor: P0070/C0185

Tárkányi, F., Szelecsényi, F., Kopecky, P.:
Cross-section data for proton, ^{3}He and α-particle induced reactions on ^{nat}Ni, ^{nat}Cu and ^{nat}Ti for monitoring beam performance.
Proceedings of International Conference on Nuclear Data for Science and Technology, 13–17 May 1991, Jülich, Germany (ed. Qaim, S.M.), Springer Verlag, Berlin, 1992, p. 529
— Exfor: D4080

Tárkányi, F., Szelecsényi, F., Takács, S., Hermanne, A., Sonck, M., Thielemans, A., Mustafa, M.G., Shubin Yu., Zhuang Youxiang:
New experimental data, compilation and evaluation for the ^{nat}Cu(α,x)^{66}Ga, ^{nat}Cu(α,x)^{67}Ga and ^{nat}Cu(α,x)^{65}Zn monitor reactions.
Nuclear Instruments Methods B (1999), in press
— Exfor: none

*** Zhukova, O.A., Kanasevich, V.I., Laptev, S.V., Chursin, G.P.:**
Excitation functions of α-particle induced reactions on copper isotopes at energies up to 38 MeV.
Izv. Akad. Nauk. Kaz. SSR. Ser. Fiz.-Mat., No. 4 (1970) 1
— Exfor: none
— Data excluded: too low cross-section values.

Zweit, J., Sharma, H., Downey, S.:
Production of gallium-66, a short-lived positron emitting radionuclide.
Int. J. Applied Radiation Isotopes **38** (1987) 499
— Exfor: none

The data from all experimental papers where numerical values are available (17 papers) are collected in Fig. 4.4.4a. The scatter of 8 data sets is large, therefore only 9 papers were selected for evaluation.

Cross-sections were calculated by two different versions of the nuclear reaction model code ALICE (denoted as 91(KR) and IPPE), by the model code PREMOD-HFMOD (denoted as HF) and by two fitting procedures (Padé with 12 parameters and Spline). These results are compared with the selected experimental data in Fig. 4.4.4b. It is seen that model calculations do not reproduce the data well, but that fits perform satisfactorily. The best approximation was judged to be the Padé fit. Recommended cross-sections are compared with selected experimental data, including their error bars, in Fig. 4.4.4c. The corresponding numerical values are tabulated in Table 4.4.4.

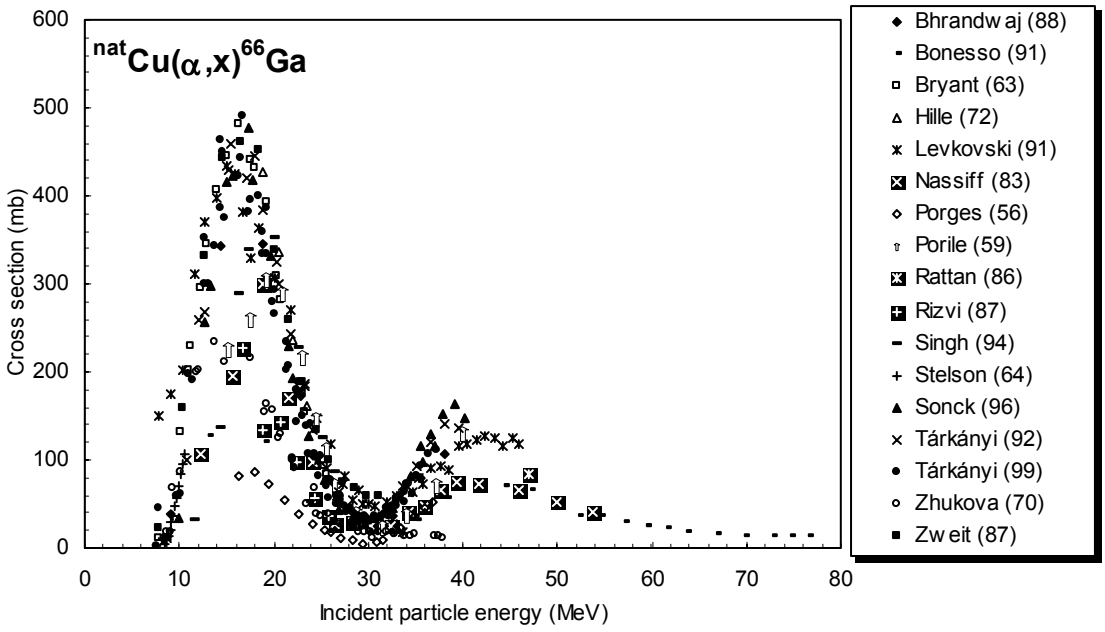

Figure 4.4.4a. All experimental data.

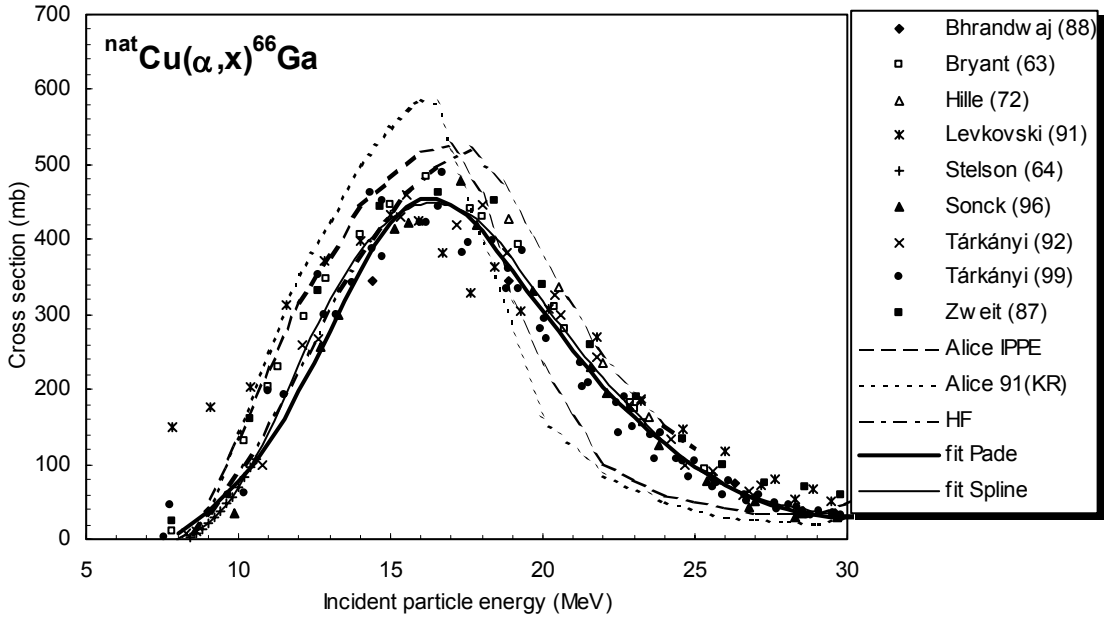

Figure 4.4.4b. Selected experimental data in comparison with theoretical calculations and fits.

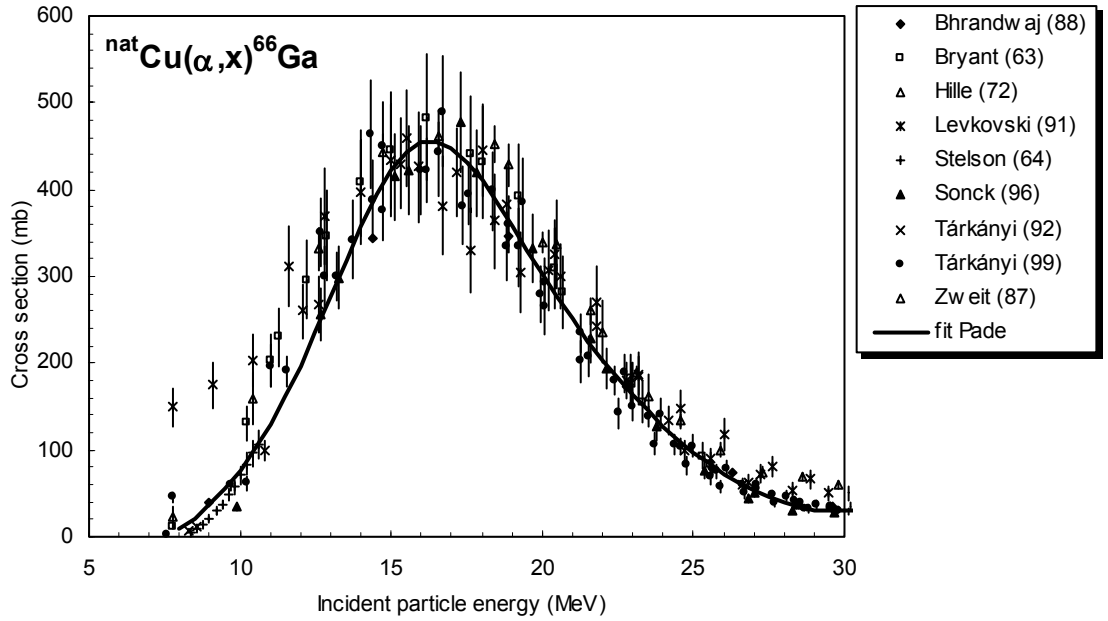

Figure 4.4.4c. Selected experimental data and recommended cross-section curve.

TABLE 4.4.4. RECOMMENDED CROSS-SECTIONS FOR THE $^{nat}Cu(\alpha,x)^{66}Ga$ REACTION

Energy MeV	Cross-section mb	Energy MeV	Cross-section mb	Energy MeV	Cross-section mb	Energy MeV	Cross-section mb
8.0	8.6	14.0	358	20.0	303	26.0	73
8.5	22	14.5	394	20.5	277	26.5	62
9.0	37	15.0	423	21.0	251	27.0	53
9.5	55	15.5	444	21.5	227	27.5	45
10.0	76	16.0	455	22.0	204	28.0	39
10.5	101	16.5	455	22.5	183	28.5	34
11.0	129	17.0	447	23.0	163	29.0	31
11.5	161	17.5	432	23.5	144	29.5	29
12.0	197	18.0	410	24.0	127	30.0	29
12.5	236	18.5	386	24.5	112		
13.0	277	19.0	359	25.0	97		
13.5	318	19.5	331	25.5	84		

4.4.5. $^{nat}Cu(\alpha,x)^{67}Ga$

A total of 14 cross-section data sets were found in the literature in the energy range considered. From these, 6 works were excluded while the remaining 8 were selected for further evaluation. For detailed description of the analysis and selection see Tárkányi et al. (1999). Comparing the available results with each other, it can be seen that the data sets split into two groups. The list of related references given below is accompanied with additional information. We mention availability of data in the computerized database EXFOR (if available, unique EXFOR reference number is given). Furthermore, we indicate a reason why a data set was excluded (reference denoted by an asterisk *).

Bhardwaj, H.D., Gautam, A.K., Prasad, R.:
Measurement and analysis of excitation functions for alpha-induced reactions on copper.
Pramana — J. Physics **31** (1988) 109
— Exfor: A0465

*** Bonesso, O., Ozafran, M.J., Mosca, H.O., Vazquez, M.E., Capurro, O.AQ., Nassiff, S.J.:**
Study of pre-equilibrium effects on α–induced reactions on copper.
J. Radioanalytical and Nuclear Chemistry, Articles **152** (1991) 189
— Exfor: none
— Data excluded: too low cross-section values.

Bryant, E.A., Cochran, D.R.F., Knight, J.D.:
Excitation functions of reactions of 7 to 24 MeV ^{3}He ions with ^{63}Cu and ^{65}Cu.
Physical Review **130** (1963) 1512
— Exfor: B0079

Graf, H.P., Münzel, H.:
Excitation functions for alpha particle reactions with molybdenum isotopes.
J. Inorganic Nuclear Chemistry **36** (1974) 3647
— Exfor: B0040

Levkovski, N.N.:
Middle Mass Nuclides (A=40-100) Activation Cross-sections by Medium Energy (E = 10–50 MeV) Protons and Alpha particles. (Experiment and Systematics).
Inter-Vesi, Moscow (1991)
— Exfor: A0510

Mohan Rao, A.V., Mukherjee, S., Rama Rao, J.:
Alpha particle induced reactions on copper and tantalum.
Pramana — J. Physics **36** (1991) 167
— Exfor: none

*** Porges, K.G.:**
Alpha excitation functions of silver and copper.
Physical Review **101** (1956) 225
— Exfor: R0039
— Data excluded: too low cross-section values.

*** Porile, N.T., Morrison, D.L.:**
Reactions of ^{63}Cu and ^{65}Cu with alpha particles.
Physical Review **116** (1959) 1193
— Exfor: B0156
— Data excluded: too low cross-section values.

*** Rizvi, I.A., Ansari, M.A., Gautam, R.P., Singh, R.K.Y., Chaubey, A.K.:**
Excitation functions studies of (α,xpyn) reactions for ^{63,65}Cu and pre-equilibrium effect.
J. Physical Society Japan **56** (1987) 3135
— Exfor: none
— Data excluded: too low cross-section values.

Singh, N.L. Agarwal, S., Rama Rao, J.:
Excitation functions for α-particle-induced reactions on light-mass nuclei.
Pramana — J. Physics **42** (1994) 349
— Exfor: none

Tárkányi, F., Szelecsényi, F., Takács, S., Hermanne, A., Sonck, M., Thielemans, A., Mustafa, M.G., Shubin Yu., Zhuang Youxiang:
New experimental data compilation and evaluation for the ^{nat}Cu(α,x)^{66}Ga, ^{nat}Cu(α,x)^{67}Ga and ^{nat}Cu(α,x)^{65}Zn monitor reactions.
Nuclear Instruments Methods B (1999), in press
— Exfor: none

Watson, I.A., Waters, S.L., Bewley, D.K., Silvester, D.J.:
A method for the measurement of the cross-sections for the production of radioisotopes by charged particles from a cyclotron.
Nuclear Instruments Methods **106** (1973) 231
— Exfor: none

*** Zhukova, O.A., Kanasevich, V.I., Laptev, S.V., Chursin, G.P.:**
Excitation functions of α particle induced reactions on copper isotopes at energies up to 38 MeV.
Izv. Akad. Nauk. Kaz. SSR. Ser. Fiz.-Mat., No. 4 (1970) 1
— Exfor: none
— Data excluded: too low cross-section values.

*** Zweit, J., Sharma, H., Downey, S.:**
Production of gallium-66, a short-lived positron emitting radionuclide.
Int. J. Applied Radiation Isotopes **38** (1987) 499
— Exfor: none
— Data excluded: too low cross-section values.

The data from all experimental papers where numerical values are available (14 papers) are collected in Fig. 4.4.5a. Out of them, 8 papers were selected for evaluation.

Cross-sections were calculated by two different versions of the nuclear reaction model code ALICE (denoted as 91(KR) and IPPE), by the model codes SPEC and PREMOD-HFMOD, and by two fitting procedures (Padé with 12 parameters and Spline). These results are compared with the selected experimental data in Fig. 4.4.5b. It is seen that model calculations do not reproduce the data well: energy shift is present for the ALICE

codes while the two other codes underestimate the cross-section values. Fits perform better. The best approximation was judged to be the spline fit. Recommended cross-sections are compared with selected experimental data, including their error bars, in Fig. 4.4.5c. The corresponding numerical values are tabulated in Table 4.4.5.

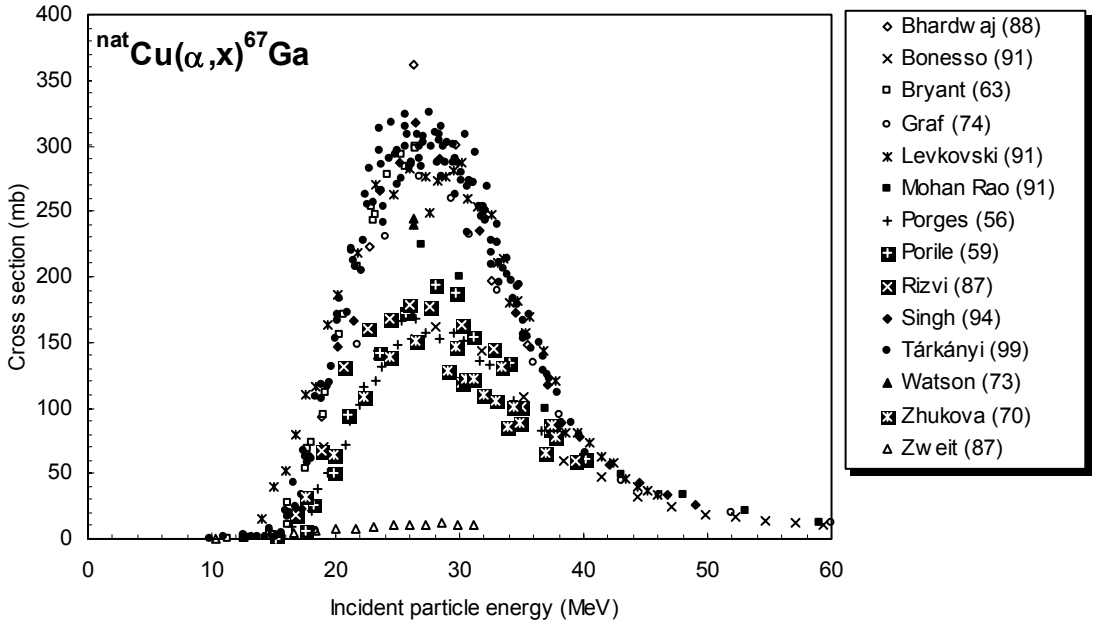

Figure 4.4.5a. All experimental data.

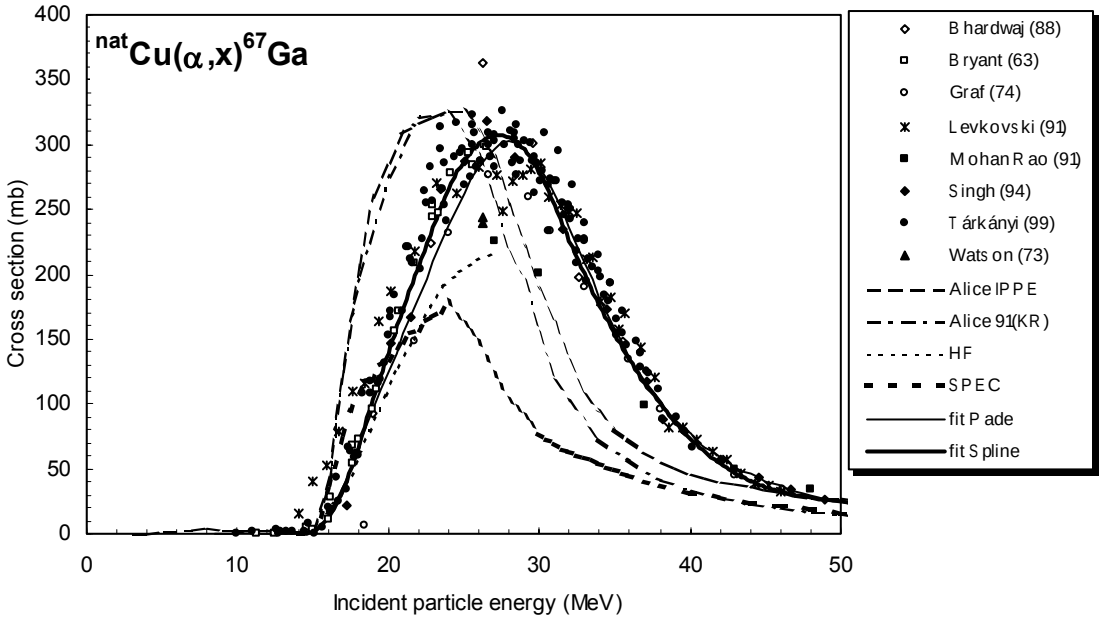

Figure 4.4.5b. Selected experimental data in comparison with theoretical calculations and fits.

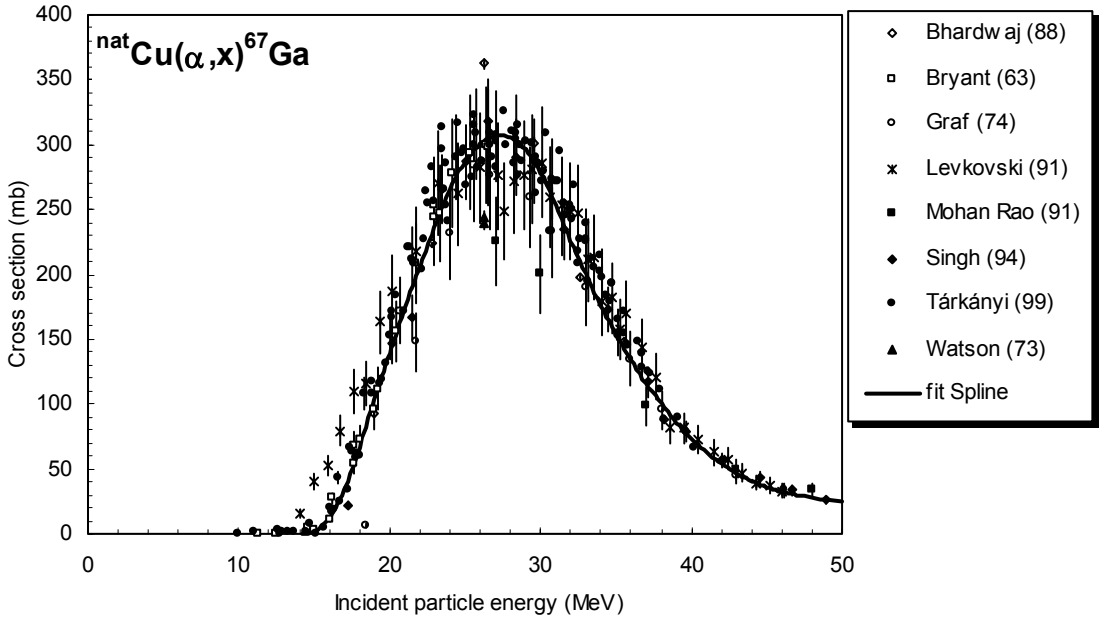

Figure 4.4.5c. Selected experimental data and recommended cross-section curve.

TABLE 4.4.5. RECOMMENDED CROSS-SECTIONS FOR THE $^{nat}Cu(\alpha,x)^{67}Ga$ REACTION

Energy MeV	Cross-section mb	Energy MeV	Cross-section mb	Energy MeV	Cross-section mb	Energy MeV	Cross-section mb
15.0	1.9	24.0	265	33.0	201	42.0	54
15.5	5.9	24.5	276	33.5	188	42.5	50
16.0	13	25.0	286	34.0	176	43.0	46
16.5	22	25.5	294	34.5	165	43.5	43
17.0	34	26.0	301	35.0	154	44.0	41
17.5	49	26.5	305	35.5	144	44.5	38
18.0	67	27.0	307	36.0	134	45.0	36
18.5	85	27.5	307	36.5	125	45.5	34
19.0	104	28.0	305	37.0	116	46.0	32
19.5	122	28.5	301	37.5	108	46.5	31
20.0	139	29.0	295	38.0	100	47.0	30
20.5	157	29.5	287	38.5	93	47.5	29
21.0	174	30.0	278	39.0	86	48.0	28
21.5	190	30.5	266	39.5	79	48.5	27
22.0	206	31.0	254	40.0	73	49.0	26
22.5	222	31.5	240	40.5	68	49.5	25
23.0	237	32.0	227	41.0	63	50.0	24
23.5	252	32.5	214	41.5	58		

4.4.6. $^{nat}Cu(\alpha,x)^{65}Zn$

A total of 15 cross-section data sets were found in the literature in the energy range considered, reporting individual or cumulative cross-sections. The compiler has calculated cumulative cross-sections in all cases where the two processes were measured separately. From these, 7 works were excluded while the remaining 8 were selected for further evaluation. For detailed description of the analysis and selection see Tárkányi et al. (1999). Comparing the available results with each other, it can be seen that the data sets split into two groups. The list of related references given below is accompanied with additional information. We mention availability of data in the computerized database EXFOR (if available, unique EXFOR reference number is given). Furthermore, we indicate a reason why a data set was excluded (reference denoted by an asterisk *).

Bhardwaj, H.D., Gautam, A.K., Prasad, R.:
Measurement and analysis of excitation functions for alpha-induced reactions on copper.
Pramana — J. Physics **31** (1988) 109
— Exfor: A0465

*** Bonesso, O., Ozafran, M.J., Mosca, H.O., Vazquez, M.E., Capurro, O.AQ., Nassiff, S.J.:**
Study of pre-equilibrium effects on α-induced reactions on copper.
J. Radioanalytical and Nuclear Chemistry, Articles **152** (1991) 189
— Exfor: none
— Data excluded: too low cross-section values.

Houck, F.S., Miller, J.M.:
Reactions of alpha particles with iron-54 and nickel-58.
Physical Review **123** (1961) 231
— Exfor: P0058

*** Lebowitz, E., Greene, M.W.:**
An auxiliary cyclotron beam monitor.
Int. J. Applied Radiation Isotopes **21** (1970) 625
— Exfor: B0154
— Data excluded: too low cross-section values.

Levkovski, N.N.:
Middle Mass Nuclides (A=40-100) Activation Cross-sections by Medium Energy (E = 10–50 MeV) Protons and Alpha particles. (Experiment and Systematics)
Inter-Vesi, Moscow (1991)
— Exfor: A0510

Lin, S.Y., Alexander, J.M.:
Reactions of ^{237}Np with ^{4}He near the interaction barrier.
Physical Review **C16** (1977) 688
— Exfor: B0088

*** Porges, K.G.:**
Alpha excitation functions of silver and copper.
Physical Review **101** (1956) 225
— Exfor: R0039
— Data excluded: too low cross-section values.

*** Porile, N.T., Morrison, D.L.:**
Reactions of ^{63}Cu and ^{65}Cu with alpha particles.
Physical Review **116** (1959) 1193
— Exfor: B0156
— Data excluded: large energy shift.

*** Rattan, S.S., Singh, R., J., Sahakundu, S.M., Prakash, S., Ramaniah, V.:**
Alpha particle induced reactions of ^{209}Bi and ^{63,65}Cu.
Radiochimica Acta **39** (1986) 61
— Exfor: A0353
— Data excluded: very low cross-section value.

*** Rizvi, I.A., Ansari, M.A., Gautam, R.P., Singh, R.K.Y., Chaubey, A.K.:**
Excitation functions studies of (α,xpyn) reactions for ^{63,65}Cu and pre-equilibrium effect.
J. Physical Society Japan **56** (1987) 3135
— Exfor: none
— Data excluded: large energy shift.

Ruddy, F.H.:
The formation and decay of the compound nucleus ^{68}Ge.
Dissertation, Simon Fraser University, Canada, 1963
— Exfor: none

Singh, N.L., Agarwal, S., Rama Rao, J.:
Excitation functions for a-particle-induced reactions on light-mass nuclei.
Pramana — J. Physics **42** (1994) 349
— Exfor: none

Tárkányi, F., Takács, S., Szelecsényi, F., Hermanne, A., Sonck, M., Thielemans, A., Mustafa, M.G., Shubin Yu., Zhuang Youxiang:
New experimental data, compilation and critical evaluation for the ^{nat}Cu(α,x)^{66}Ga, ^{nat}Cu(α,x)^{67}Ga, and ^{nat}Cu(α,x)^{65}Zn monitor reactions.
Nuclear Instruments Methods (1999), in press
— Exfor: none

Zhukova, O.A., Kanasevich, V.I., Laptev, S.V., Chursin, G.P.:
Excitation functions of α-particle induced reactions on copper isotopes at energies up to 38 MeV.
Izv. Akad. Nauk Kaz. SSR. Ser. Fiz.-Mat., No. 4 (1970) 1
— Exfor: none

*** Zweit, J., Sharma, H., Downey, S.:**
Production of gallium-66, a short-lived positron emitting radionuclide.
Int. J. Applied Radiation Isotopes **38** (1987) 499
— Exfor: none
— Data excluded: too low cross-section values.

The data from all experimental papers where numerical values are available (15 papers) are collected in Fig. 4.4.6a. The scatter of 7 data sets is large, therefore only 8 papers were selected for evaluation.

Cross-sections were calculated by two different versions of the nuclear reaction model code ALICE (denoted as 91(KR) and IPPE), by the model codes PREMOD-HFMOD (denoted as HF) and SPEC, and by two fitting procedures (Padé with 13 parameters and Spline). These results are compared with the selected experimental data in Fig. 4.4.6b. It is seen that the model calculations reproduce the data poorly, but fits are better. The best approximation was judged to be the Padé fit. Recommended cross-sections are compared with selected experimental data, including their error bars, in Fig. 4.4.6c. The corresponding numerical values are tabulated in Table 4.4.6.

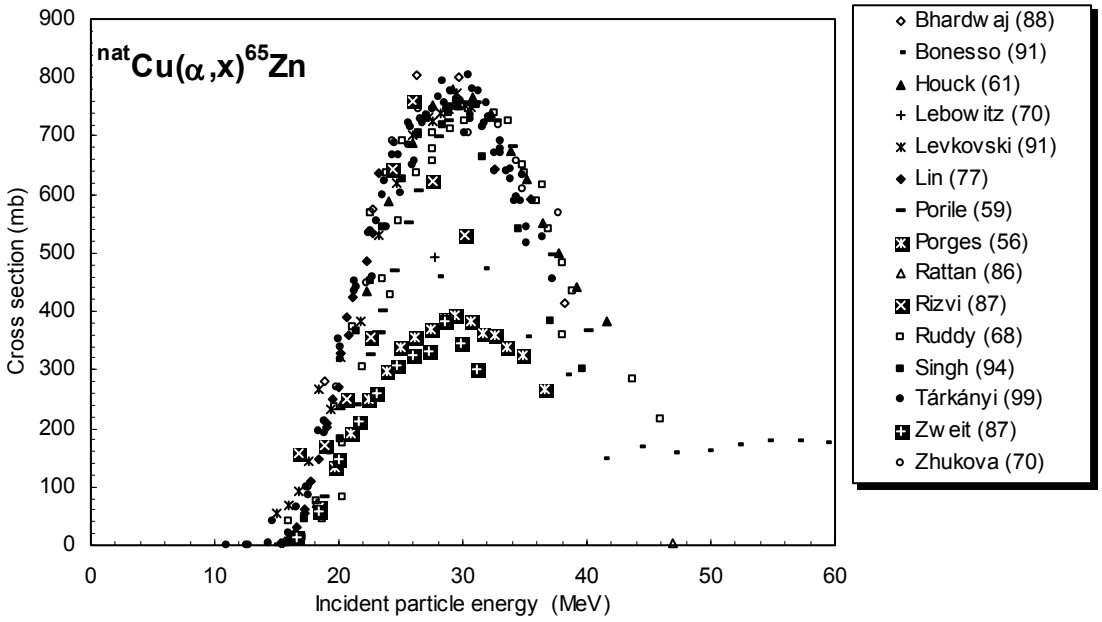

Figure 4.4.6a. All experimental data.

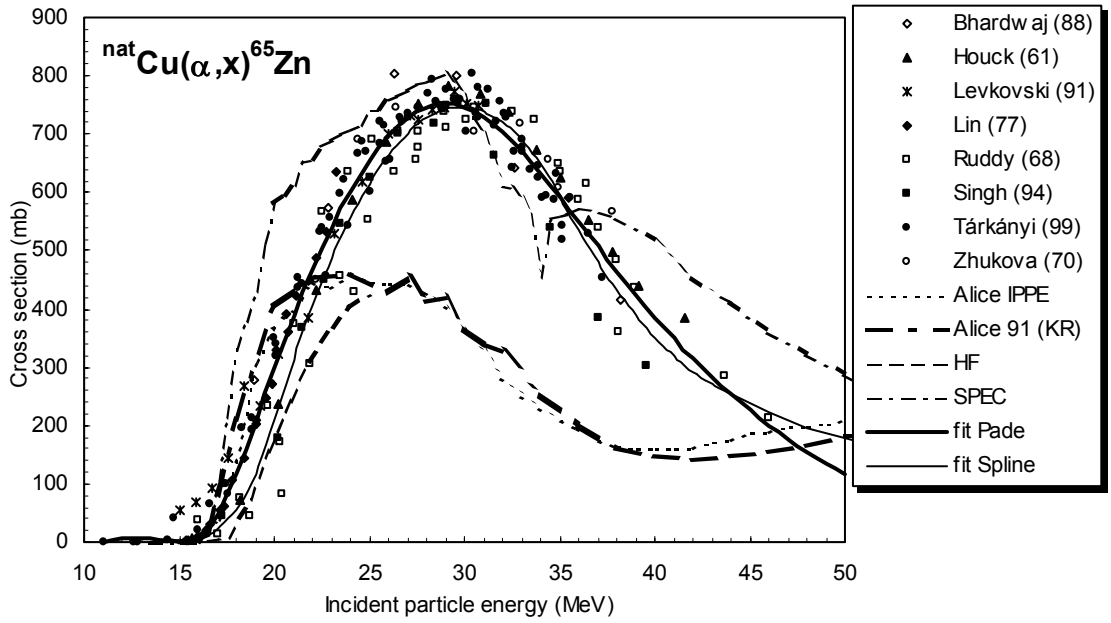

Figure 4.4.6b. Selected experimental data in comparison with theoretical calculations and fits.

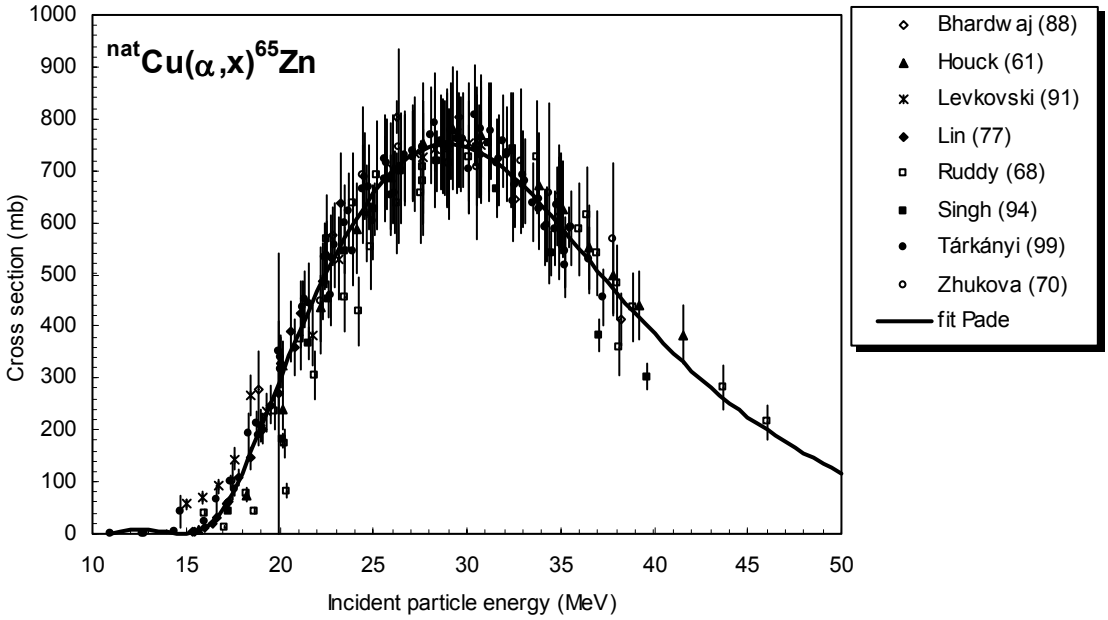

Figure 4.4.6c. Selected experimental data and recommended cross-section curve.

TABLE 4.4.6. RECOMMENDED CROSS-SECTIONS FOR THE $^{nat}Cu(\alpha,x)^{65}Zn$ REACTION

Energy MeV	Cross-section mb	Energy MeV	Cross-section mb	Energy MeV	Cross-section mb	Energy MeV	Cross-section mb
15.0	1.0	24.0	602.3	33.0	671.1	42.0	314.5
15.5	3.1	24.5	630.1	33.5	652.7	42.5	298.2
16.0	10.2	25.0	655.4	34.0	633.3	43.0	282.5
16.5	24.5	25.5	678.0	34.5	613.1	43.5	267.4
17.0	47.0	26.0	697.8	35.0	592.3	44.0	252.8
17.5	78.1	26.5	714.6	35.5	571.2	44.5	238.9
18.0	116.3	27.0	728.4	36.0	549.8	45.0	225.4
18.5	159.6	27.5	739.1	36.5	528.3	45.5	212.5
19.0	205.7	28.0	746.7	37.0	507.0	46.0	200.1
19.5	252.7	28.5	751.2	37.5	485.8	46.5	188.1
20.0	299.2	29.0	752.5	38.0	464.9	47.0	176.7
20.5	344.3	29.5	750.9	38.5	444.3	47.5	165.7
21.0	387.5	30.0	746.4	39.0	424.2	48.0	155.1
21.5	428.8	30.5	739.3	39.5	404.5	48.5	145.0
22.0	467.8	31.0	729.7	40.0	385.4	49.0	135.2
22.5	504.8	31.5	717.8	40.5	366.8	49.5	125.9
23.0	539.5	32.0	703.9	41.0	348.8	50.0	116.9
23.5	572.1	32.5	688.3	41.5	331.3		

Chapter 5
PRODUCTION CROSS-SECTIONS FOR DIAGNOSTIC RADIOISOTOPES

This chapter is devoted to the evaluation of reaction cross-sections for the most important accelerator produced radioisotopes used in medical diagnostic applications.

The chapter is divided into two parts. In section 5.1 we describe production reactions for gamma emitters. This is followed by section 5.2 where production reactions for positron emitters, are considered.

5.1. GAMMA EMITTERS

(Prepared by A. Hermanne, K. Gul, M.G. Mustafa, M. Nortier, P. Obložinský, S.M. Qaim, B. Scholten, Yu.N. Shubin, F. Tárkányi, S. Takács, Zhuang Youxiang)

The list of commonly used production reactions for gamma emitters evaluated in the present project includes 16 reactions, see Table 5.1. Among them are 12 reactions for isotope production and 4 reactions deal with disturbing radionuclidic impurities. Only reactions occurring on the same target isotope as the one used for the production are considered. Energies of incident particles cover the range from a few MeV up to 100 MeV.

The adopted evaluation procedure consisted of three steps, explained in more detail in Sections 2 and 3. First, experimental data were collected and subjected to critical analysis, resulting in the creation of a reduced set of selected experimental data to be used for further evaluation. The second step consisted of performing theoretical calculations with nuclear reaction model codes and comparison with the selected experimental data as well as of fitting those selected data. It has to be stressed that the calculations used global parameters for each code and that no adjustment for individual reactions was done. The third step entailed the final judgement regarding the agreement between the selected experimental data, theoretical calculations and fits. Based on the consensus of all participants and evaluators involved in the present project, recommended cross-sections were deduced, often the preferred choice being a fit. Finally, as a fourth step, yields in various representations were calculated on the basis of the recommended cross-sections.

In the following sections, production reactions for gamma emitters are presented. For each reaction, the above 4 steps are described, each step being accompanied by a figure. Finally, the recommended cross-sections and calculated yields are presented in tabular forms.

The following notations for identification of fits and theoretical calculations are used in the figures.

fit Spline:	Spline fitting method described in paragraph 2.3.1.
fit Pade:	Padé fitting method described in paragraph 2.3.2.
Alice-HMS:	Calculations with the ALICE-91 code including the precompound Hybrid Monte Carlo simulation described in paragraph 3.2.2. Different options for level density descriptions are possible for this code: Fermi Gas model (FG), Back Shifted Fermi Gas model (BS) and Kataria and Ramamurthy formalism (KR), see 3.2.2.

Alice-91: Calculations with the latest version of the standard ALICE code described in paragraph 3.2.1.
Different options for the level density descriptions are possible for this code and are noted as:
Fermi Gas model (FG), Back Shifted Fermi Gas model (BS) and Kataria and Ramamurthy formalism (KR), see 3.2.2.

Alice-IPPE: Calculations with the ALICE-91 code modified to include generalized superfluid level density and preequilibrium cluster emission as described in paragraph 3.2.3.

HF: Calculations with the combined HFMOD-PREMOD codes described in paragraph 3.2.5.

Spec: Calculations with the SPEC code described in paragraph 3.2.4.

TABLE 5.1. COMMONLY USED PRODUCTION REACTIONS FOR GAMMA EMITTERS. DENOTED BY ASTERISK * ARE REACTIONS YIELDING RADIONUCLIDIC IMPURITIES

Reaction	$T_{1/2}$ of product nucleus	Main γ lines		Proton energy
		E_γ (keV)	I_γ (%)	(MeV)
$^{67}Zn(p,n)^{67}Ga$	3.26 d	93.3	37.0	2–25
		184.6	20.4	
$^{68}Zn(p,2n)^{67}Ga$	3.26 d	93.3	37.0	13–30
		184.6	20.4	
$^{nat}Kr(p,x)^{81}Rb$	4.58 h	190.4	64.3	14.5–80
$^{82}Kr(p,2n)^{81}Rb$	4.58 h	190.4	64.3	14.5–30
$^{111}Cd(p,n)^{111}In$	2.8d	171.3	90.24	4–30
		245.4	94.0	
$^{112}Cd(p,2n)^{111}In$	2.8 d	171.3	90.24	11.5–35
		245.4	94.0	
$^{123}Te(p,n)^{123}I$	13.2 h	159.0	83.3	4–20
$^{124}Te(p,2n)^{123}I$	13.2 h	159.0	83.3	12–30
* $^{124}Te(p,n)^{124}I$	4.18 d	602.7	61.0	5–30
$^{127}I(p,5n)^{123}Xe$	2.08 h	148.9	49.0	37–100
* $^{127}I(p,3n)^{125}Xe$	16.9 h	188.4	54.9	20–100
$^{124}Xe(p,2n)^{123}Cs$	5.87 min	97.4	14.5	15.5–40
$^{124}Xe(p,pn)^{123}Xe$	2.08 h	148.9	49.0	16.5–40
$^{203}Tl(p,3n)^{201}Pb$	9.33 h	331.2	79.0	18–36
*	3.62 h	422.2	86.0	9–27
$^{203}Tl(p,2n)^{202m}Pb$		787.0	50.0	
* $^{203}Tl(p,4n)^{200}Pb$	21.5 h	147.6	37.7	27.5–36

Remarks: ^{123}Xe decays into ^{123}I, ^{123}Cs decays into ^{123}Xe, ^{125}Xe decays into ^{125}I, ^{201}Pb decays into ^{201}Tl, ^{202m}Pb decays into ^{202}Tl, ^{200}Pb decays into ^{200}Tl.

5.1.1. ^{67}Zn(p,n)^{67}Ga

A total of 11 cross-section data sets were found in the literature. From these, 3 data sets were excluded while the other 8 were selected for further evaluation. For detailed description of the analysis and selection see Szelecsényi et al. (1998). The list of related references given below is accompanied with additional information. We mention availability of data in the computerized database EXFOR (if available, unique EXFOR reference number is given). Furthermore, we indicate a reason why a data set was excluded (reference denoted by an asterisk *).

*** Barandon, J.N., Debrun, J.L., Kohn, A., Spear, R.H.:**
Etude du dosage de Ti, V, Cr, Fe, Ni, Cu et Zn par activation avec des protons d'energie limitee a 20 MeV.
Nuclear Instruments Methods **127** (1975) 269
— Exfor: O0086
— Data excluded: although very good agreement exists with the results of other groups up to 10 MeV, it is noted that the rapid decrease of the excitation function in the tail is unusual for a (p,n) reaction in this energy region.

Blaser, J.-P., Boehm, F., Marmier, P., Peaslee, D.C.:
Fonctions d'excitation de la reaction (p,n), I.
Helvetia Physica Acta **24** (1951) 3
— Exfor: B0048

Bonardi, M., Birattati, C.:
Optimization of irradiation parameters for Ga-67 production from Zn(p,xn) nuclear reactions.
J. Radioanalytical Chemistry **76** (1983) 311
— Exfor: none

Hermanne, A.:
Private communication (1994)
See: Szelecsényi et al. (1998) and Hermanne, A., Walravens, N., Cicchelli, O.:
Optimization of isotope production by cross-section determination. Proceedings of International Conference on Nuclear data for Science and Technology, May 1991 Jülich, Germany, (ed. Qaim, S.M.), Springer Verlag, Berlin (1992), p. 616
— Exfor: A0494
Remark: Since the values are "estimated" values above 12 MeV based on a ‘tail-fitting’procedure, the results are used only up to this energy.

Johnson, C.H., Galonsky, A., Inskeep, C.N.:
Cross-sections for (p,n) reactions in intermediate-weight nuclei.
ORNL-2910 (1960) 25
— Exfor: B0068

Kopecky, P.:
Cross-sections and production yields of ^{66}Ga and ^{67}Ga for proton reactions on natural zinc.
Applied Radiation Isotopes **41** (1990) 606
— Exfor: none

*** Levkovski, V.N.:**
Cross-sections of Medium Mass Nuclide Activation (A=40-100) by Medium Energy Protons and Alpha Particles (E = 10-50 MeV).
Inter-Vesi, 1991, Moscow, USSR
— Exfor: A0510
— Data excluded: although the energy position of the cross-section maximum is in good agreement with the majority of the other works, the cross-section values were unexpectedly high over the whole energy range.

*** Little, F.E., Lagunas-Solar, M.C.:**
Cyclotron production of ^{67}Ga. Cross-sections and thick-target yields for the ^{67}Zn(p,n) and ^{68}Zn(p,2n) reactions.
Int. J. Applied Radiation Isotopes **34** (1983) 631
— Exfor: A0321
— Data excluded: energy shift towards higher energy.

Nortier, F.M., Mills, S., Steyn, G.F.:
Excitation functions and yields of relevance to the production of ^{67}Ga by proton bombardment of ^{nat}Zn and ^{nat}Ge up to 100 MeV.
Applied Radiation Isotopes **42** (1991) 353
— Exfor: A0498

Szelecsényi, F., Boothe, T.E., Takács, S., Tárkányi, F., Tavano, E.:
Evaluated cross-section and thick target yield data bases of Zn + p processes for practical applications.
Applied Radiation Isotopes **49** (1998) 1005
— Exfor: C0506

Tárkányi, F., Szelecsényi, F. Kovács, Z., Sudár, S.:
Excitation functions of proton induced nuclear reactions on enriched ^{66}Zn, ^{67}Zn and ^{68}Zn: production of ^{67}Ga and ^{66}Ga.
Radiochimica Acta **50** (1990) 19
— Exfor: D4004

The data from papers where experimental numerical values were available (11 papers) are collected in Fig. 5.1.1a. From these, 3 works were excluded while the remaining 8 were selected for further evaluation.

Cross-sections were calculated by two different versions of the nuclear reaction model code ALICE (denoted as HMS and IPPE), by the model codes PREMOD-HFMOD (denoted as HF) and SPEC, and by two fitting procedures (Padé with 8 parameters and Spline). These results are compared with the selected experimental data in Fig. 5.1.1b. Obviously the model calculations overpredict the data in the rising part of the curve while beyond the maximum they underestimate the cross-sections. The best approximation was judged to be the Padé fit. Recommended cross-sections are compared with selected experimental data, including their error bars, in Fig. 5.1.1c. Yields calculated from the recommended cross-sections are presented in Fig. 5.1.1d. The corresponding numerical values for recommended cross-sections and yields are tabulated in Table 5.1.1a and Table 5.1.1b, respectively.

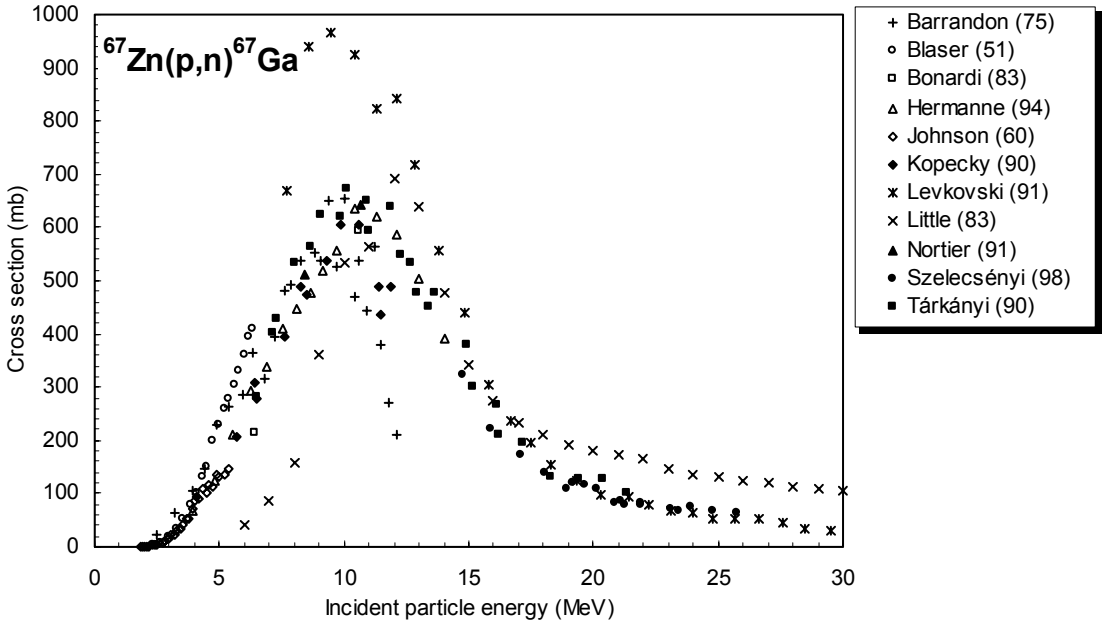

Figure 5.1.1a. All experimental data.

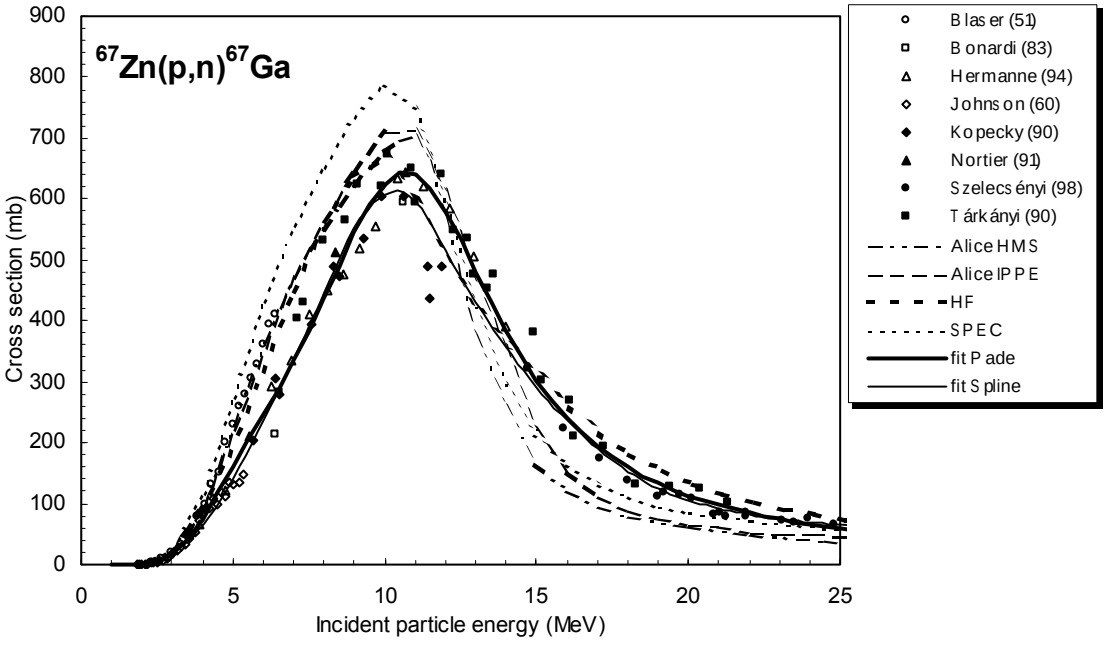

Figure 5.1.1b. Selected experimental data in comparison with theoretical calculations and fits.

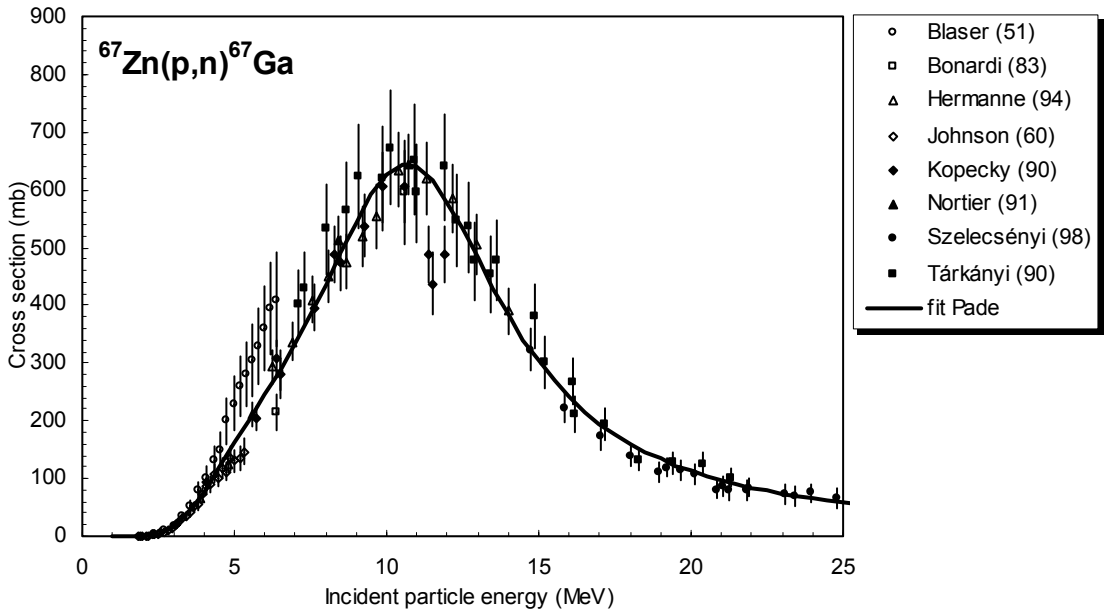

Figure 5.1.1c. Selected experimental data and recommended cross-section curve.

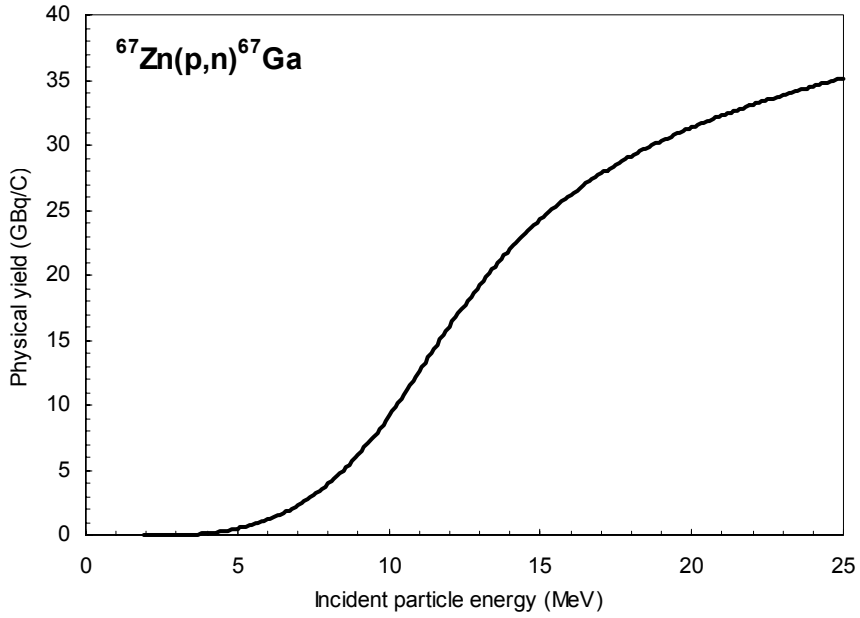

Figure 5.1.1d. Yield of ^{67}Ga calculated from the recommended cross-sections.

TABLE 5.1.1a. RECOMMENDED CROSS-SECTIONS FOR THE $^{67}Zn(p,n)^{67}Ga$ REACTION

Energy MeV	Cross-section mb	Energy MeV	Cross-section mb	Energy MeV	Cross-section mb	Energy MeV	Cross-section mb
2.0	0.4	8.0	436	14.0	384	20.0	113.2
2.5	4.6	8.5	490	14.5	341	20.5	104.8
3.0	16.6	9.0	544	15.0	303	21.0	97.3
3.5	40.2	9.5	591	15.5	270	21.5	90.6
4.0	75.5	10.0	626	16.0	241	22.0	84.6
4.5	118	10.5	643	16.5	216	22.5	79.2
5.0	161	11.0	640	17.0	195	23.0	74.3
5.5	204	11.5	617	17.5	176	23.5	69.9
6.0	245	12.0	579	18.0	160.0	24.0	66.0
6.5	288	12.5	532	18.5	145.9	24.5	62.3
7.0	334	13.0	481	19.0	133.6	25.0	59.0
7.5	383	13.5	431	19.5	122.7		

TABLE 5.1.1b. YIELDS CALCULATED FROM THE RECOMMENDED CROSS-SECTION DATA FOR THE $^{67}Zn(p,n)^{67}Ga$ REACTION. Y: PHYSICAL YIELD, A_1: ACTIVITY AFTER 1 HOUR AND 1 μA IRRADIATION, A_2: SATURATION ACTIVITY FOR 1 μA IRRADIATION

Energy	Physical yield	Activity		Energy	Physical yield	Activity	
MeV	GBq/C	GBq	GBq	MeV	GBq/C	GBq	GBq
	Y	A_1	A_2		Y	A_1	A_2
2.0	0.0001	0.0000003	0.00004	14.0	22.0	0.08	8.9
2.5	0.002	0.00001	0.001	14.5	23.2	0.08	9.4
3.0	0.01	0.0001	0.01	15.0	24.3	0.09	9.9
3.5	0.05	0.0002	0.02	15.5	25.3	0.09	10.3
4.0	0.1	0.0005	0.1	16.0	26.2	0.09	10.6
4.5	0.3	0.001	0.1	16.5	27.0	0.10	11.0
5.0	0.5	0.002	0.2	17.0	27.8	0.10	11.3
5.5	0.8	0.003	0.3	17.5	28.5	0.10	11.6
6.0	1.2	0.004	0.5	18.0	29.1	0.10	11.9
6.5	1.7	0.01	0.7	18.5	29.8	0.11	12.1
7.0	2.3	0.01	0.9	19.0	30.3	0.11	12.3
7.5	3.0	0.01	1.2	19.5	30.9	0.11	12.5
8.0	3.9	0.01	1.6	20.0	31.4	0.11	12.7
8.5	5.0	0.02	2.0	20.5	31.8	0.11	12.9
9.0	6.2	0.02	2.5	21.0	32.3	0.12	13.1
9.5	7.6	0.03	3.1	21.5	32.7	0.12	13.3
10.0	9.2	0.03	3.7	22.0	33.1	0.12	13.5
10.5	10.8	0.04	4.4	22.5	33.5	0.12	13.6
11.0	12.6	0.05	5.1	23.0	33.8	0.12	13.8
11.5	14.3	0.05	5.8	23.5	34.2	0.12	13.9
12.0	16.1	0.06	6.5	24.0	34.5	0.12	14.0
12.5	17.7	0.06	7.2	24.5	34.8	0.12	14.2
13.0	19.3	0.07	7.8	25.0	35.1	0.13	14.3
13.5	20.7	0.07	8.4				

5.1.2. ^{68}Zn(p,2n)^{67}Ga

A total of 10 cross-section data sets were found in the literature. Five works used highly enriched ^{68}Zn targets for cross-section measurements. There are five "production cross-section" measurements for the ^{nat}Zn(p,xn)^{67}Ga process; those results can also be used for evaluation between 17 and 30 MeV. In this energy range the contribution of the ^{67}Zn(p,n)^{67}Ga reaction can be neglected due to its low cross-section and due to the low isotopic abundance of ^{67}Zn in a natural zinc matrix. The influence of the ^{70}Zn(p,4n)^{67}Ga process to the production cross-section is also negligible because of the very low isotopic abundance of ^{70}Zn in natural zinc (0.62%). From these 10 data sets, 3 were excluded while the 7 others were selected for further evaluation. The list of related references given below is accompanied with additional information. We mention availability of data in the computerized database EXFOR (if available, unique EXFOR reference number is given). Furthermore, we indicate a reason why a data set was excluded (reference denoted by an asterisk *).

Barandon, J.N., Debrun, J.L., Kohn, A., Spear, R.H.:
Etude du dosage de Ti, V, Cr, Fe, Ni, Cu et Zn par activation avec des protons d'energie limitee a 20 MeV.
Nuclear Instruments Methods **127** (1975) 269
— Exfor: O0086

Bonardi, M., Birattati, C.:
Optimization of irradiation parameters for Ga-67 production from Zn(p,xn) nuclear reactions.
J. Radioanalytical Chemistry **76** (1983) 311
— Exfor: none

Hermanne, A.:
Private communication (1994)
See: Szelecsényi et al. (1998) and Hermanne, A., Walravens, N., Cicchelli, O.:
Optimization of isotope production by cross-section determination. Proceedings of International Conference on Nuclear data for Science and Technology, May 1991, Jülich, Germany, (ed. Qaim, S.M.), Springer Verlag, Berlin (1992), p. 616
— Exfor: A0494

Hermanne, A., Szelecsényi, F., Sonck, M., Takács, S., Tárkányi, F., Van den Winkel, P.:
New cross-section data on ^{68}Zn(p,2n)^{67}Ga and ^{nat}Zn(p,xn)^{67}Ga nuclear reactions for the development of a reference data base.
J. Radioanalytical Nuclear Chemistry **240** (1999) 623
— Exfor: none

*** Kopecky, P.:**
Cross-sections and production yields of ^{66}Ga and ^{67}Ga for proton reactions on natural zinc.
Applied Radiation Isotopes **41** (1990) 606
— Exfor: none
— Data excluded: cross-section values too low.

Levkovski, V.N.:
Cross-sections of Medium Mass Nuclide Activation (A=40-100) by Medium Energy Protons and Alpha Particles (E=10-50 MeV).
Inter-Vesi, 1991, Moscow, USSR
— Exfor: A0510

*** Little, F.E., Lagunas-Solar, M.C.:**
Cyclotron production of ^{67}Ga. Cross-sections and thick-target yields for the ^{67}Zn(p,n) and ^{68}Zn(p,2n) reactions.
Int. J. Applied Radiation Isotopes **34** (1983) 631
— Exfor: A0321
— Data excluded: energy shift towards higher energy.

*** McGee, T., Rao, C.L., Saha, G.B., Yaffe, L.:**
Nuclear interactions of ^{45}Sc and ^{68}Zn with protons of medium energy.
Nuclear Physics **A150** (1970) 11
— Exfor: B0053
— Data excluded: cross-section values too low (even after normalisation by the compiler).

Nortier, F.M., Mills, S., Steyn, G.F.:
Excitation functions and yields of relevance to the production of ^{67}Ga by proton bombardment of ^{nat}Zn and ^{nat}Ge up to 100 MeV.
Applied Radiation Isotopes **42** (1991) 353
— Exfor: A0498

Tárkányi, F., Szelecsényi, F., Kovács, Z., Sudár, S.:
Excitation functions of proton induced nuclear reactions on enriched ^{66}Zn, ^{67}Zn and ^{68}Zn. Production of ^{67}Ga and ^{66}Ga.
Radiochimica Acta **50** (1990) 19
— Exfor: D4004

The data from papers where experimental numerical values were available (10 papers), are collected in Fig. 5.1.2a. From these, 2 works were excluded while the remaining 8 were selected for further evaluation.

Cross-sections were calculated by two different versions of the nuclear reaction model code ALICE (denoted as HMS and IPPE), by the model codes PREMOD-HFMOD (denoted as HF) and SPEC, and by Padé fitting with 9 parameters). These results are compared with the selected experimental data in Fig. 5.1.2b. Obviously the model calculations generally overpredict the data in the rising part of the curve while beyond the maximum they underestimate the cross-sections. The best approximation was judged to be the Padé fit. Recommended cross-sections are compared with selected experimental data, including their error bars, in Fig. 5.1.2c. Yields calculated from the recommended cross-sections are presented in Fig. 5.1.2d. The corresponding numerical values for recommended cross-sections and yields are tabulated in Table 5.1.2a and Table 5.1.2b, respectively.

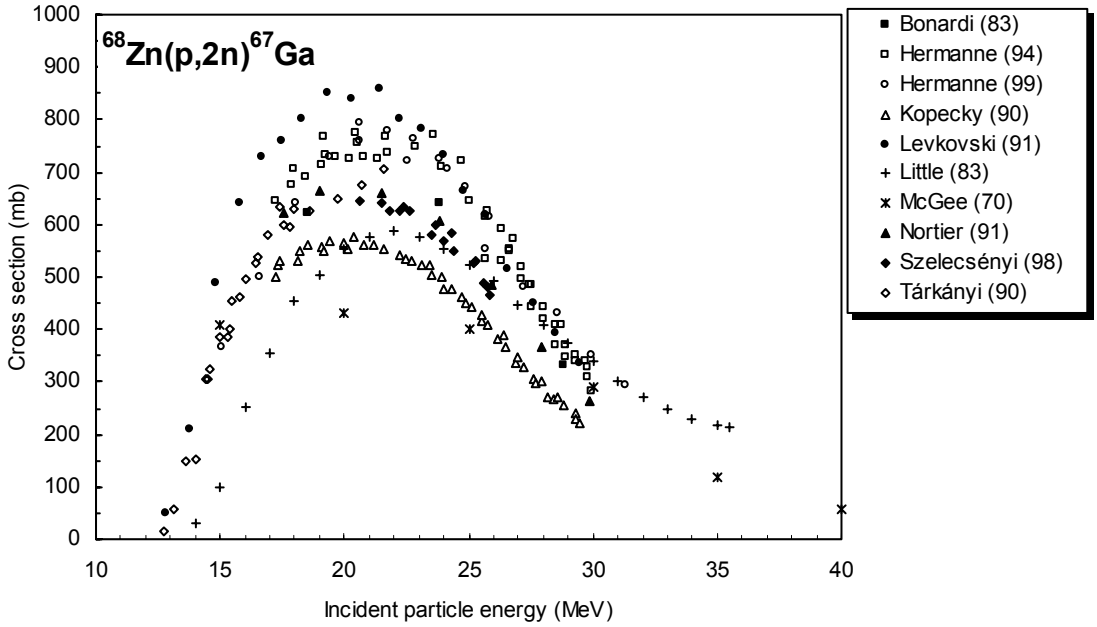

Figure 5.1.2a. All experimental data.

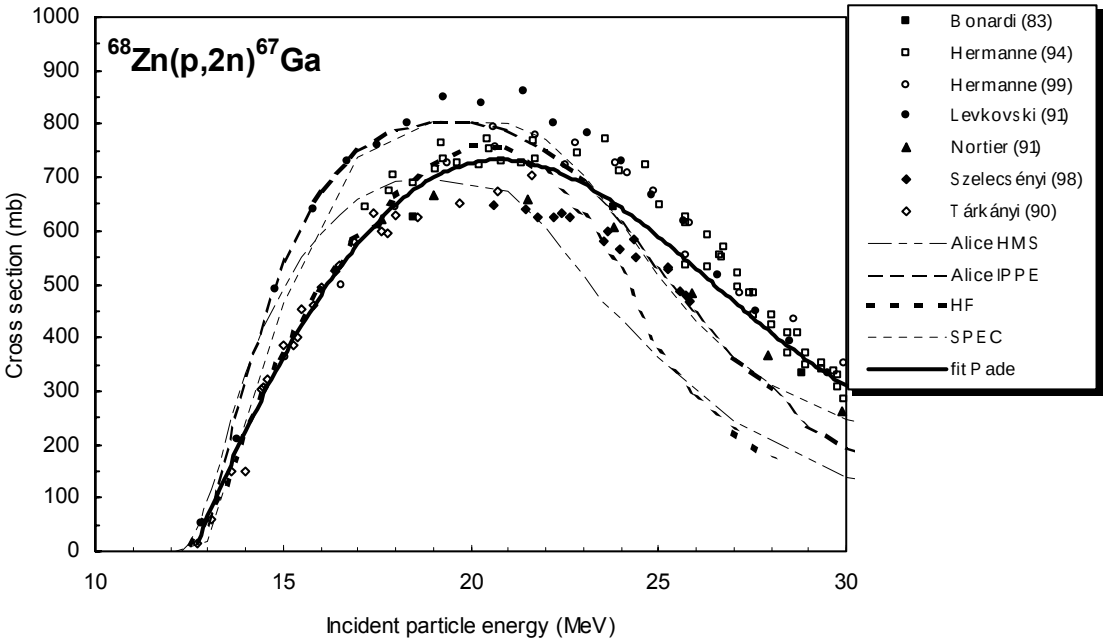

Figure 5.1.2b. Selected experimental data in comparison with theoretical calculations and fits

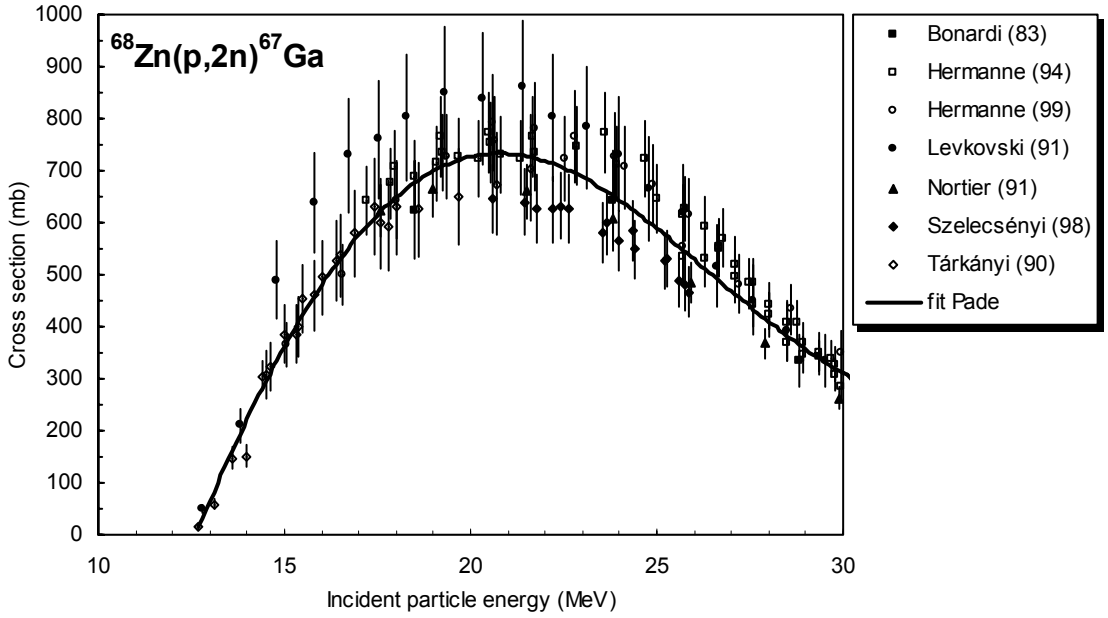

Figure 5.1.2c. Selected experimental data and recommended cross-section curve.

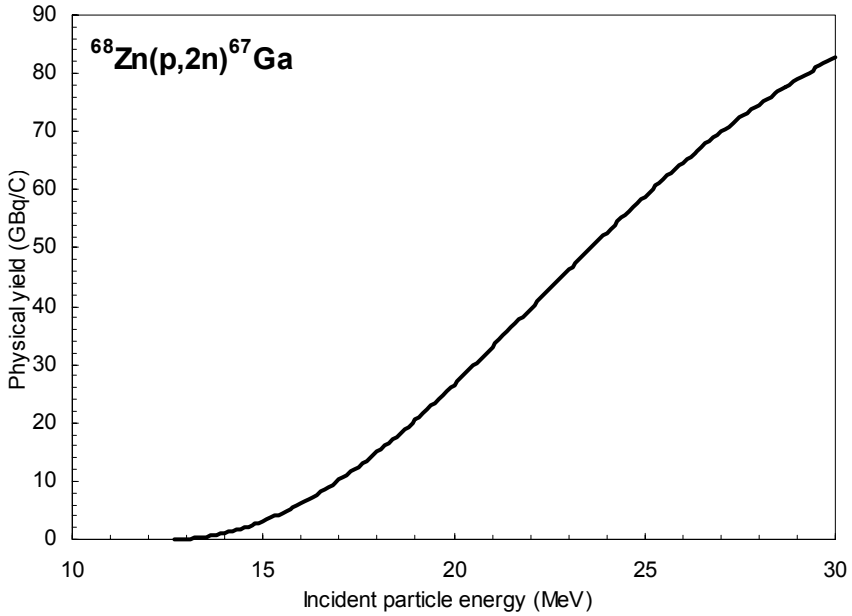

Figure 5.1.2d. Yield of ^{67}Ga calculated from the recommended cross-sections.

TABLE 5.1.2a. RECOMMENDED CROSS-SECTIONS FOR THE $^{68}Zn(p,2n)^{67}Ga$ REACTION

Energy MeV	Cross-section mb	Energy MeV	Cross-section mb	Energy MeV	Cross-section mb	Energy MeV	Cross-section mb
13.0	65.6	17.5	615	22.0	719	26.5	499
13.5	147.1	18.0	649	22.5	705	27.0	468
14.0	224	18.5	677	23.0	688	27.5	438
14.5	296	19.0	699	23.5	667	28.0	409
15.0	362	19.5	716	24.0	643	28.5	382
15.5	424	20.0	727	24.5	617	29.0	356
16.0	480	20.5	732	25.0	589	29.5	332
16.5	531	21.0	733	25.5	559	30.0	310
17.0	576	21.5	728	26.0	529		

TABLE 5.1.2b. YIELDS CALCULATED FROM THE RECOMMENDED CROSS-SECTION DATA FOR THE $^{68}Zn(p,2n)^{67}Ga$ REACTION. Y: PHYSICAL YIELD, A_1: ACTIVITY AFTER 1 HOUR AND 1 μA IRRADIATION, A_2: SATURATION ACTIVITY FOR 1 μA IRRADIATION

Energy	Physical yield	Activity		Energy	Physical yield	Activity	
MeV	GBq/C	GBq	GBq	MeV	GBq/C	GBq	GBq
	Y	A_1	A_2		Y	A_1	A_2
13.0	0.1	0.0004	0.0	22.0	39.6	0.14	16.1
13.5	0.5	0.002	0.2	22.5	43.0	0.15	17.5
14.0	1.1	0.004	0.4	23.0	46.2	0.17	18.8
14.5	2.0	0.01	0.8	23.5	49.5	0.18	20.1
15.0	3.1	0.01	1.3	24.0	52.7	0.19	21.4
15.5	4.5	0.02	1.8	24.5	55.8	0.20	22.7
16.0	6.2	0.02	2.5	25.0	58.8	0.21	23.9
16.5	8.1	0.03	3.3	25.5	61.8	0.22	25.1
17.0	10.2	0.04	4.1	26.0	64.6	0.23	26.3
17.5	12.5	0.04	5.1	26.5	67.3	0.24	27.4
18.0	15.0	0.05	6.1	27.0	69.9	0.25	28.4
18.5	17.7	0.06	7.2	27.5	72.4	0.26	29.4
19.0	20.5	0.07	8.3	28.0	74.7	0.27	30.4
19.5	23.5	0.08	9.6	28.5	76.9	0.28	31.3
20.0	26.6	0.10	10.8	29.0	79.0	0.28	32.1
20.5	29.8	0.11	12.1	29.5	80.9	0.29	32.9
21.0	33.0	0.12	13.4	30.0	82.8	0.30	33.7
21.5	36.3	0.13	14.8				

5.1.3. ^{nat}Kr(p,x)^{81}Rb

A total of 6 data sets (in 5 papers) were found in the literature in the energy range considered. From these, 2 works were excluded while the 3 others were selected for further evaluation. The list of related references given below is accompanied with additional information. We mention availability of data in the computerized database EXFOR (if available, unique EXFOR reference number is given). Furthermore, we indicate a reason why a data set was excluded (reference denoted by an asterisk *).

Acerbi, E., Birattari, C., Bonardi, M., De Martinis, C., Salomone, A.:
Kr(p,xn) excitation functions and ^{81}Rb-^{81m}Kr generator studies.
Int. J. Applied Radiation Isotopes **32** (1981) 465
— Exfor: none

Kovács, F., Tárkányi, F., Qaim, S.M., Stöcklin, G.:
Excitation functions for the formation of some radioisotopes of rubidium in proton induced nuclear reactions on ^{nat}Kr, ^{82}Kr and ^{83}Kr with special reference to the production of ^{81}Rb(^{81m}Kr) generator radionuclide.
Applied Radiation Isotopes **42** (1991) 329
— Exfor: A0489
Remark: Data on natural Kr (Kovács b) excluded; too low cross-sections values.
The data measured on enriched target (Kovács a) were normalised and included in the evaluation up to 20 MeV as Kovács, B.

*** Lamb, J.F., Baker, G.A., Goris, M.L., Khetigan, A., Moore, H.A., Neesan, W.C., Winchell, H.S.:**
Production and clinical evaluation of a commercial krypton-81m gas generator and its delivery system.
British, J. Radiology Special Report 15: Clinical and Experimental Applications of Krypton-81m. (ed. Lavender, J.P.) (British Institute of Radiology, London, 1978), p. 23.
— Exfor: none
— Data excluded: cross-section values extremely high.

*** Mulders, J.J.L.:**
Yield curves and beam current dependent production rates of Rb radioisotopes produced by protons on a krypton gas target.
Int. J. Applied Radiation Isotopes **35** (1984) 475
— Exfor: none
— Data excluded: too low cross-section values.

Steyn, G.F., Mills, S.J., Nortier, F.M., Haasbroek, F.J.:
Integral excitation functions for ^{nat}Kr+p up to 116 MeV and optimization of the production of ^{81}Rb for ^{81m}Kr generators.
Applied Radiation Isotopes **42** (1991) 361
— Exfor: A0499

The data from papers where experimental numerical values were available (6 data sets in 5 papers) are collected in Fig. 5.1.3a. From these, 3 data sets were selected for further evaluation. All the data denote cumulative cross-sections, I.e. the summed values for the formation of ^{81}Rb (directly as well as via the decay of the 30.3 min ^{81m}Rb).

Cross-sections were calculated by the nuclear reaction model codes ALICE (denoted as IPPE), and SPEC, and by two fitting procedures (Padé with 13 parameters and Spline). These results are compared with the selected experimental data in Fig. 5.1.3b. It is seen that ALICE-IPPE gives a reasonable description of the shape of the excitation function but is shifted to lower energy. Calculations with SPEC show less energy shift but underestimate the cross-sections. The best approximation was judged to be the spline fit. Recommended cross-sections are compared with the experimental data, including their error bars, in Fig. 5.1.3c. Yields calculated from the recommended cross-sections are presented in Fig. 5.1.3d. The corresponding numerical values for recommended cross-sections and yields are tabulated in Table 5.1.3a and Table 5.1.3b, respectively. It needs to be pointed out that ^{81}Rb is formed both directly and via the decay of 30.3 min ^{81m}Rb. The physical yield and the yield/μAh are thus unrealistic. We therefore give only the saturation yield.

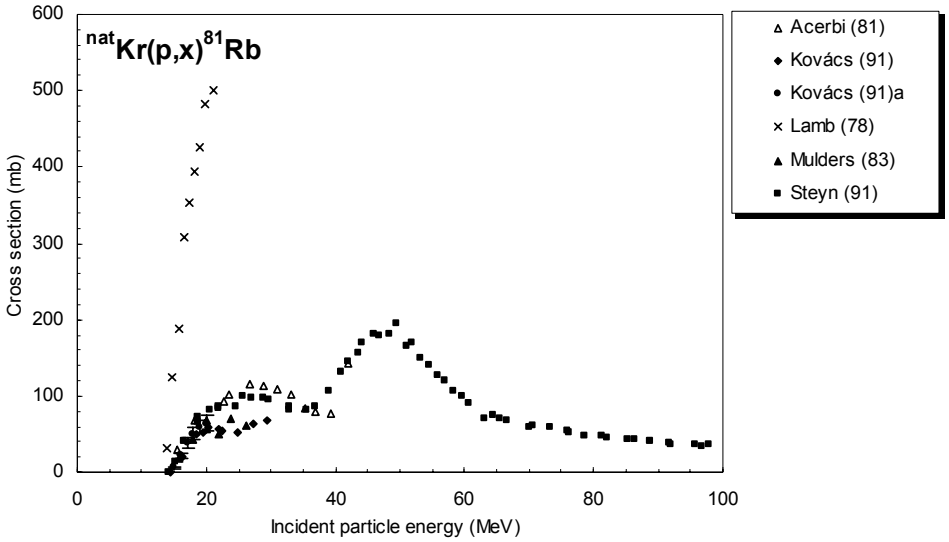

Figure 5.1.3a. All experimental data.

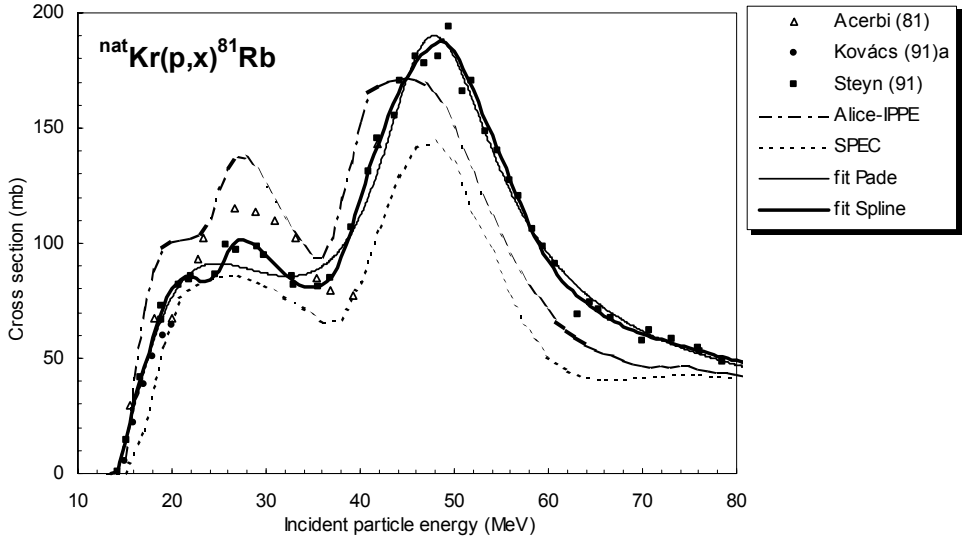

Figure 5.1.3b. Selected experimental data in comparison with theoretical calculations and fits.

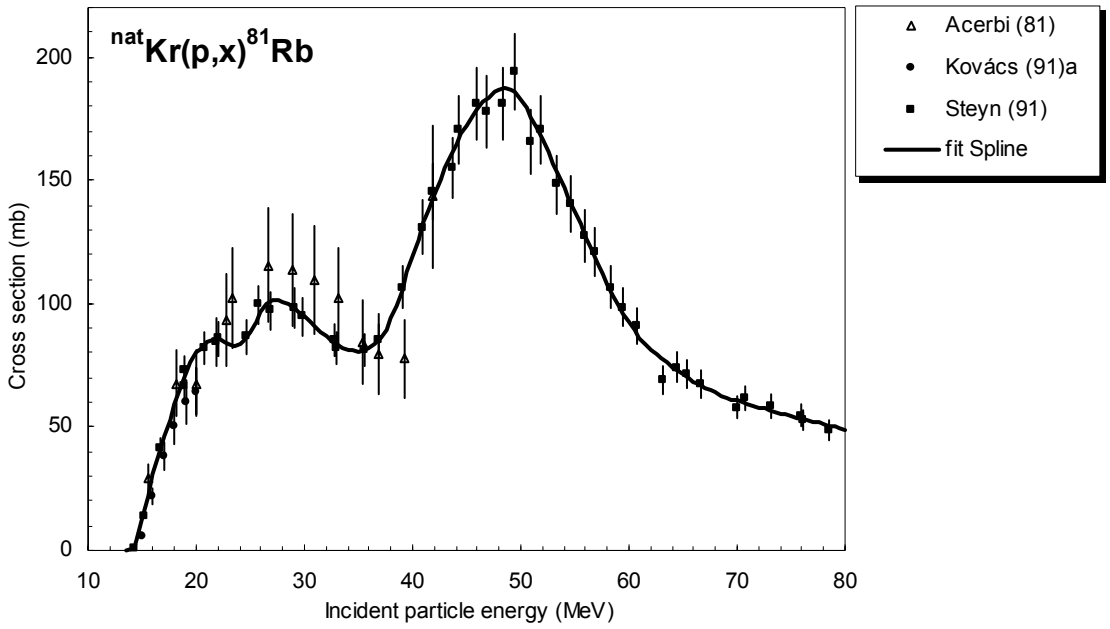

Figure 5.1.3c. Selected experimental data and recommended cross-section curve.

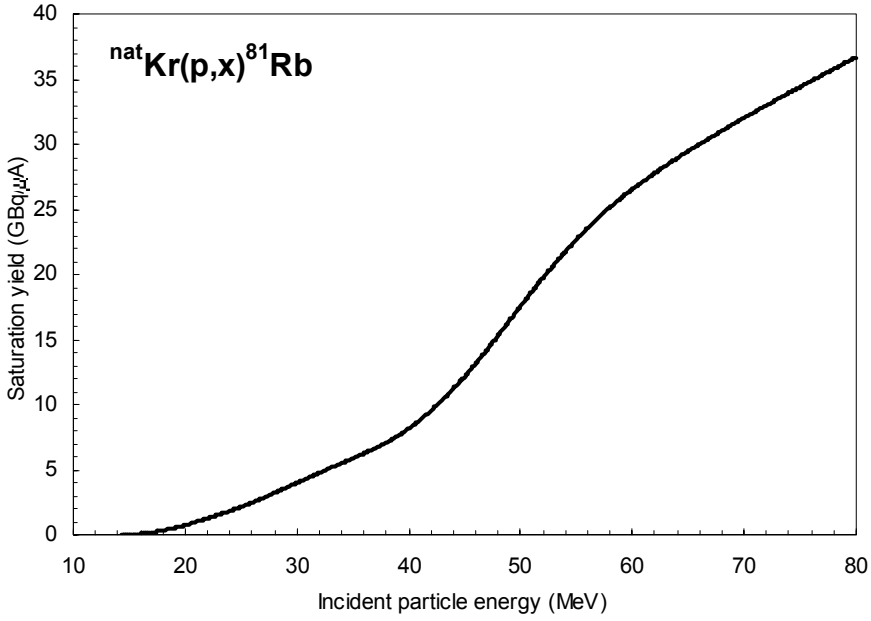

Figure 5.1.3d. Yield of ^{81}Rb calculated from the recommended cross-sections.

TABLE 5.1.3a. RECOMMENDED CROSS-SECTIONS FOR THE $^{NAT}Kr(p,x)^{81}Rb$ REACTION

Energy MeV	Cross-section mb	Energy MeV	Cross-section mb	Energy MeV	Cross-section mb	Energy MeV	Cross-section mb
14.5	4.2	31.0	90.6	47.5	185.5	64.0	74.3
15.0	13.0	31.5	88.7	48.0	186.8	64.5	72.7
15.5	21.9	32.0	86.7	48.5	187.4	65.0	71.2
16.0	30.8	32.5	84.8	49.0	187.0	65.5	69.8
16.5	38.6	33.0	83.3	49.5	185.5	66.0	68.4
17.0	46.0	33.5	82.1	50.0	182.9	66.5	67.2
17.5	52.7	34.0	81.3	50.5	179.5	67.0	66.0
18.0	59.1	34.5	80.8	51.0	175.6	67.5	64.9
18.5	65.7	35.0	80.7	51.5	171.2	68.0	63.9
19.0	71.8	35.5	81.0	52.0	166.6	68.5	62.9
19.5	76.4	36.0	81.8	52.5	161.6	69.0	62.0
20.0	79.9	36.5	83.4	53.0	156.6	69.5	61.2
20.5	82.4	37.0	86.0	53.5	151.7	70.0	60.5
21.0	84.1	37.5	89.5	54.0	146.9	70.5	59.9
21.5	85.3	38.0	93.9	54.5	142.1	71.0	59.2
22.0	85.6	38.5	99.3	55.0	137.3	71.5	58.6
22.5	84.7	39.0	105.6	55.5	132.3	72.0	58.0
23.0	83.5	39.5	112.4	56.0	127.3	72.5	57.4
23.5	83.1	40.0	119.3	56.5	122.3	73.0	56.8
24.0	83.8	40.5	125.9	57.0	117.2	73.5	56.2
24.5	85.5	41.0	132.2	57.5	112.3	74.0	55.6
25.0	88.3	41.5	138.3	58.0	107.7	74.5	55.0
25.5	92.3	42.0	144.2	58.5	103.4	75.0	54.4
26.0	96.4	42.5	149.9	59.0	99.3	75.5	53.8
26.5	99.6	43.0	155.3	59.5	95.6	76.0	53.3
27.0	101.3	43.5	160.2	60.0	92.2	76.5	52.7
27.5	101.7	44.0	164.7	60.5	89.0	77.0	52.1
28.0	101.0	44.5	168.8	61.0	86.2	77.5	51.6
28.5	99.8	45.0	172.4	61.5	83.7	78.0	51.0
29.0	98.3	45.5	175.9	62.0	81.4	78.5	50.5
29.5	96.6	46.0	179.0	62.5	79.4	79.0	49.9
30.0	94.6	46.5	181.6	63.0	77.6	79.5	49.4
30.5	92.6	47.0	183.8	63.5	75.9	80.0	48.9

TABLE 5.1.3b. YIELDS CALCULATED FROM THE RECOMMENDED CROSS-SECTION DATA FOR THE $^{NAT}Kr(p,x)^{81}Rb$ REACTION. A_2: SATURATION ACTIVITY FOR 1 μA IRRADIATION (*)

Energy MeV	Activity GBq A_2	Energy MeV	Activity GBq A_2	Energy MeV	Activity GBq A_2	Energy MeV	Activity GBq A_2
14.5	0.0018	31.0	4.38	47.5	14.8	64.0	28.9
15.0	0.013	31.5	4.57	48.0	15.3	64.5	29.2
15.5	0.04	32.0	4.76	48.5	15.9	65.0	29.5
16.0	0.07	32.5	4.94	49.0	16.4	65.5	29.8
16.5	0.12	33.0	5.12	49.5	17.0	66.0	30.0
17.0	0.17	33.5	5.31	50.0	17.6	66.5	30.3
17.5	0.24	34.0	5.49	50.5	18.1	67.0	30.5
18.0	0.32	34.5	5.67	51.0	18.7	67.5	30.8
18.5	0.41	35.0	5.86	51.5	19.2	68.0	31.0
19.0	0.51	35.5	6.05	52.0	19.7	68.5	31.3
19.5	0.62	36.0	6.24	52.5	20.3	69.0	31.5
20.0	0.74	36.5	6.43	53.0	20.8	69.5	31.8
20.5	0.86	37.0	6.64	53.5	21.3	70.0	32.0
21.0	0.99	37.5	6.85	54.0	21.8	70.5	32.3
21.5	1.12	38.0	7.07	54.5	22.2	71.0	32.5
22.0	1.26	38.5	7.31	55.0	22.7	71.5	32.8
22.5	1.40	39.0	7.57	55.5	23.1	72.0	33.0
23.0	1.54	39.5	7.85	56.0	23.6	72.5	33.2
23.5	1.68	40.0	8.15	56.5	24.0	73.0	33.5
24.0	1.82	40.5	8.46	57.0	24.4	73.5	33.7
24.5	1.97	41.0	8.80	57.5	24.8	74.0	33.9
25.0	2.12	41.5	9.16	58.0	25.2	74.5	34.2
25.5	2.29	42.0	9.53	58.5	25.5	75.0	34.4
26.0	2.46	42.5	9.93	59.0	25.9	75.5	34.6
26.5	2.64	43.0	10.34	59.5	26.2	76.0	34.9
27.0	2.83	43.5	10.78	60.0	26.5	76.5	35.1
27.5	3.02	44.0	11.22	60.5	26.9	77.0	35.3
28.0	3.22	44.5	11.69	61.0	27.2	77.5	35.6
28.5	3.41	45.0	12.17	61.5	27.5	78.0	35.8
29.0	3.61	45.5	12.66	62.0	27.8	78.5	36.0
29.5	3.80	46.0	13.17	62.5	28.1	79.0	36.2
30.0	4.00	46.5	13.69	63.0	28.4	79.5	36.5
30.5	4.19	47.0	14.22	63.5	28.7	80.0	36.7

* Regarding the yield values see ‘Remark’ in the appendix.

5.1.4. ^{82}Kr(p,2n)^{81}Rb

Only one publication was found in the literature that used enriched gas targets for cross-section measurement [Kovács et al. (1991)]. The three "production cross-section" measurements for the ^{nat}Kr(p,xn)^{81}Rb process by Acerbi et al. (1981), Steyn et al. (1991) and Kovács et al. (1991), can, however, also be used for evaluation up to 22 MeV after normalisation. They were therefore added to the database. The list of related references given below is accompanied with additional information. We mention availability of data in the computerized database EXFOR (if available, unique EXFOR reference number is given). Furthermore, we indicate a reason why a data set was excluded (reference denoted by an asterisk *).

Acerbi, E., Birattari, C., Bonardi, M., De Martinis, C., Salomone, A.:
Kr(p,xn) excitation functions and ^{81}Rb-^{81m}Kr generator studies.
Int. J. Applied Radiation Isotopes **32** (1981) 465
— Exfor: no

Kovács, F., Tárkányi, F., Qaim, S.M., Stöcklin, G.:
Excitation functions for the formation of some radioisotopes of rubidium in proton induced nuclear reactions on ^{nat}Kr, ^{82}Kr and ^{83}Kr with special reference to the production of ^{81}Rb(^{81m}Kr) generator radionuclide.
Remark: Kovács a are data on enriched targets; Kovács b are normalised data from natural targets.
Applied Radiation Isotopes **42** (1991) 329
— Exfor: A0489

Steyn, G.F., Mills, S.J., Nortier, F.M., Haasbroek, F.J.:
Integral excitation functions for ^{nat}Kr+p up to 116 MeV and optimization of the production of ^{81}Rb for ^{81m}Kr generators.
Applied Radiation Isotopes **42** (1991) 361
— Exfor: A0499

The data from papers where experimental numerical values were available (4 data sets) are collected in Fig. 5.1.4a. From these, 3 works used natural Kr target and their results were normalised to represent data on ^{82}Kr. All the 4 works were selected for further evaluation. All the data denote cumulative cross-sections, I.e. the summed values for the formation of ^{81}Rb (directly as well as via the decay of the 30.3 min ^{81m}Rb).

Cross-sections were calculated by the nuclear reaction model codes ALICE-IPPE and SPEC, and by two fitting procedures (Padé with 6 parameters and Spline). These results are compared with the selected experimental data in Fig. 5.1.4b. It can be seen that model calculations generally do not reproduce the cross-sections well. The best approximation was judged to be the spline fit. Recommended cross-sections are compared with the experimental data, including their error bars, in Fig. 5.1.4c. Yields calculated from the recommended cross-sections are presented in Fig. 5.1.4d. The corresponding numerical values for recommended cross-sections and yields are tabulated in Table 5.1.4a and Table 5.1.4b, respectively. As discussed in section 5.1.3, only the saturation yields are given.

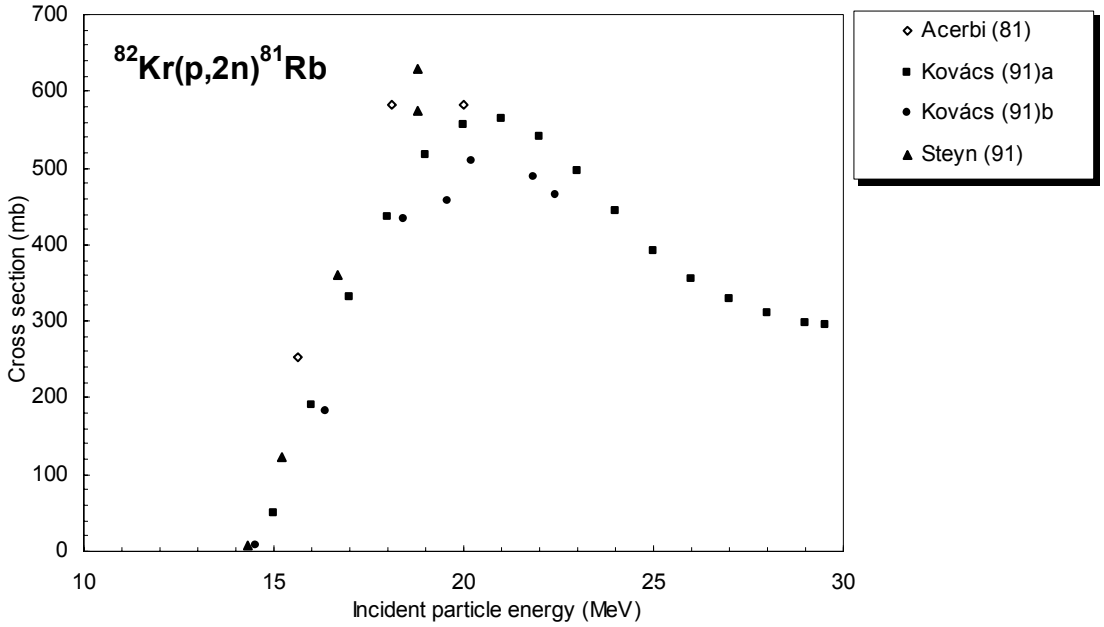

Figure 5.1.4a. All experimental data.

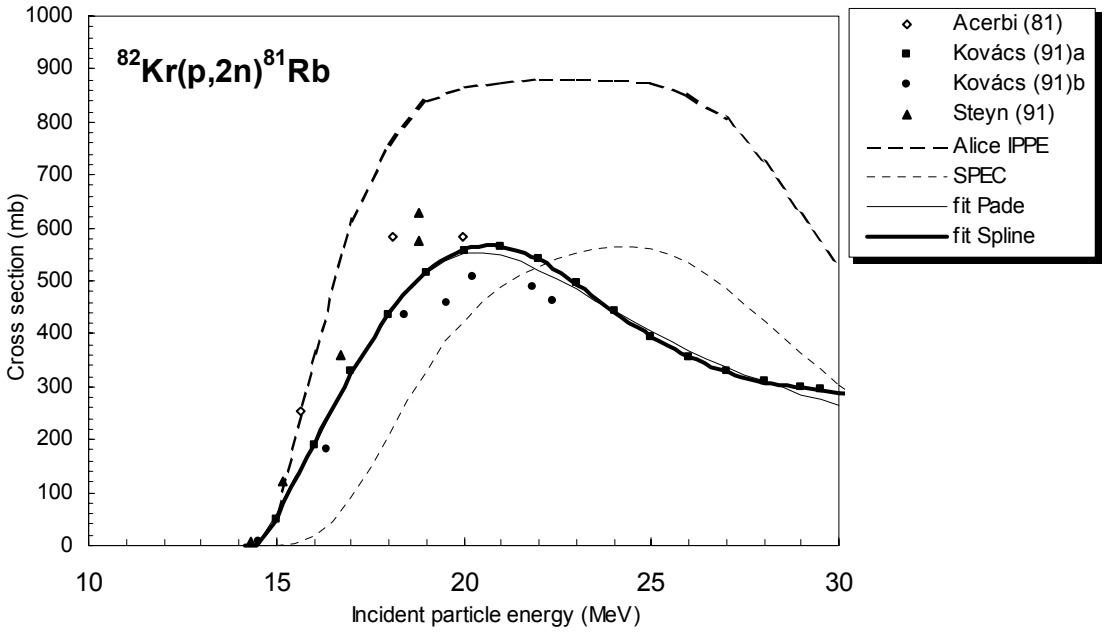

Figure 5.1.4b. Selected experimental data in comparison with theoretical calculations and fits

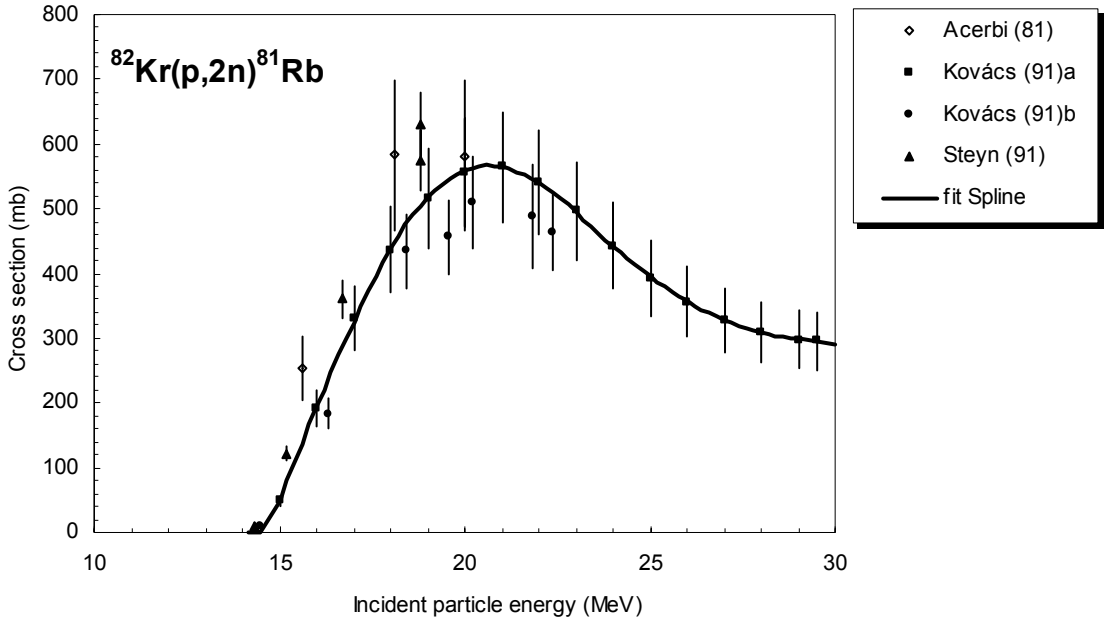

Figure 5.1.4c. Selected experimental data and recommended cross-section curve.

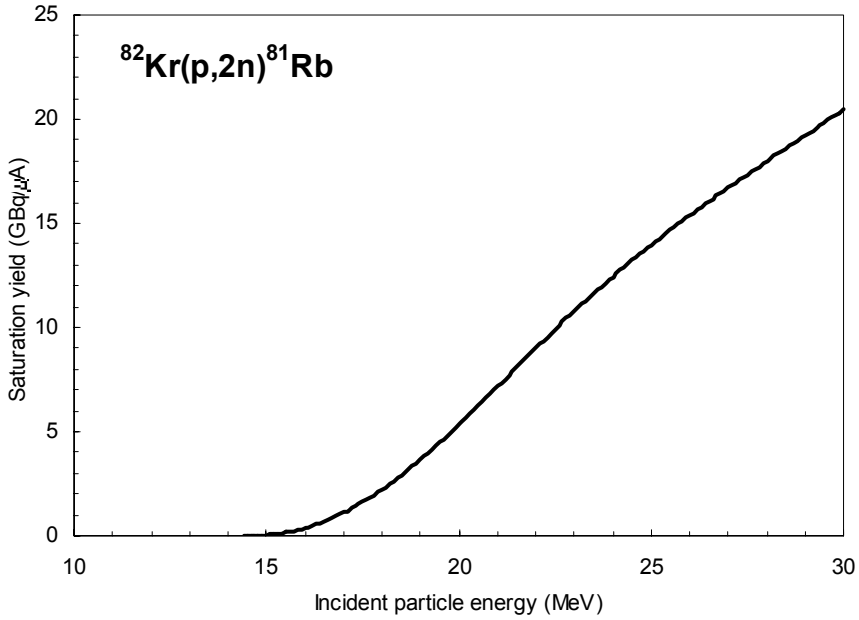

Figure 5.1.4d. Yield of ^{81}Rb calculated from the recommended cross-sections.

TABLE 5.1.4a. RECOMMENDED CROSS-SECTIONS FOR THE $^{82}Kr(p,2n)^{81}Rb$ REACTION

Energy MeV	Cross-section mb	Energy MeV	Cross-section mb	Energy MeV	Cross-section mb	Energy MeV	Cross-section mb
14.5	5.1	18.5	482	22.5	519	26.5	341
15.0	48.6	19.0	517	23.0	494	27.0	328
15.5	121.0	19.5	543	23.5	468	27.5	317
16.0	193.3	20.0	559	24.0	442	28.0	309
16.5	261.1	20.5	566	24.5	417	28.5	302
17.0	325	21.0	564	25.0	395	29.0	297
17.5	384	21.5	555	25.5	375	29.5	293
18.0	437	22.0	540	26.0	357	30.0	289

TABLE 5.1.4b. YIELDS CALCULATED FROM THE RECOMMENDED CROSS-SECTION DATA FOR THE $^{82}Kr(p,2n)^{81}Rb$ REACTION. A_2: SATURATION ACTIVITY FOR 1 μA IRRADIATION (*)

Energy MeV	Activity GBq A_2	Energy MeV	Activity GBq A_2	Energy MeV	Activity GBq A_2	Energy MeV	Activity GBq A_2
14.5	0.0015	18.5	2.91	22.5	9.91	26.5	16.1
15.0	0.036	19.0	3.66	23.0	10.8	27.0	16.7
15.5	0.15	19.5	4.48	23.5	11.6	27.5	17.4
16.0	0.37	20.0	5.35	24.0	12.4	28.0	18.0
16.5	0.69	20.5	6.25	24.5	13.2	28.5	18.6
17.0	1.11	21.0	7.16	25.0	14.0	29.0	19.2
17.5	1.62	21.5	8.09	25.5	14.7	29.5	19.8
18.0	2.22	22.0	9.01	26.0	15.4	30.0	20.5

* Regarding the yield values see ‘Remark’ in the appendix.

5.1.5. ^{111}Cd(p,n)^{111}In

A total of 9 cross-section data sets were found in the literature. All publications were selected for further evaluation. The list of related references given below is accompanied with additional information. We mention availability of data in the computerized database EXFOR (if available, unique EXFOR reference number is given). Furthermore, we indicate a reason why a data set was excluded (reference denoted by an asterisk *).

Blaser, J.-P., Boehm, F., Marmier, P., Peaslee, D.C.:
Fonctions d' excitation de la reaction (p,n) (I).
Helvetia Physica Acta **24** (1951) 3
— Exfor: B0048

Blosser, H.G.:
Survey of (p,n) reactions at 12 MeV.
Physical Review **100** (1955) 1340
— Exfor: B0052

Marten, M., Schüring, A., Scobel, W.:
Preequilibrium neutron emission in ^{109}Ag(^{3}He,xn) and ^{111}Cd(p,xn) reactions.
Zeitschrift für Physik **A322** (1985) 103
— Exfor: A0335

Nortier, F.M., Mills, S.J., Steyn, G.F.:
Excitation functions and production rates of relevance to production of ^{111}In by proton bombardment of ^{nat}Cd and ^{nat}In up to 100 MeV.
Applied Radiation Isotopes **41** (1990) 1201
— Exfor: A0500

Otozai, K., Kume, S., Mito, A., Okamura, H., Tsujoni, R., Kanchiku, Y., Katoh, T., Gotoh, H.:
Excitation functions for the reactions induced by protons on Cd up to 37 MeV.
Nuclear Physics **80** (1966) 335
— Exfor: P0019

Skakun, E.A., Iordakesku, A., Lutsik, V.A., Rakivnenko Yu.N., Romany, I., A.:
Excitation functions and isomeric ratios for ^{111}Cd(p,n)^{111m,g}In and ^{113}Cd(p,n)^{113m,g}In.
Abstracts of XXIXth Symposium on Nuclear Spectroscopy and Nuclear Stucture, Riga, 1979, Nauka, Leningrad, p. 209
— Exfor: A0135

Skakun, E., Kljucherev, A.P., Rakivnenko Yu.N., Romany, I.A.:
Excitation functions of (p,n)— and (p,2n) reactions on cadmium isotopes.
Izvestiya Academy Nauk. SSSR, Ser. Fiz. **39** (1975) 24
— Exfor: A0001

Tárkányi, F., Szelecsényi, F., Kopecky, P., Molnár, T., Andó, L., Mikecz, P., Tóth, Gy., Rydl, A.:
Cross-sections of proton induced reactions on enriched ^{111}Cd and ^{112}Cd for the production of ^{111}In for use in nuclear medicine.
Applied Radiation Isotopes **45** (1994) 239
— Exfor: D4027

Wing, J., Huizenga, J.R.:
(p,n) cross-sections of ^{51}V, ^{52}Cr, ^{63}Cu, ^{65}Cu, ^{107}Ag, ^{109}Ag , ^{111}Cd, ^{139}La from 5 to 10.5 MeV.
Physical Review **128** (1962) 280
— Exfor: B0065

The data from papers where experimental numerical values were available (9 papers) are collected in Fig. 5.1.5a. All works were selected for further evaluation. All the data denote cumulative cross-sections, I.e. the summed values for the formation of ^{111}In (directly as well as via the decay of the 7.6 min ^{111m}In).

Cross-sections were calculated by two different versions of the nuclear reaction model code ALICE (denoted as HMS and IPPE) and by a spline fitting procedure. These results are compared with the selected experimental data in Fig. 5.1.5b. Whereas ALICE-HMS does not represent the data well, agreement of ALICE-IPPE is very good, even without any normalisation, and it was chosen to be the best approximation. Recommended cross-sections are compared with selected experimental data, including their error bars, in Fig. 5.1.5c. Yields calculated from the recommended cross-sections are presented in Fig. 5.1.5d. The corresponding numerical values for recommended cross-sections and yields are tabulated in Table 5.1.5a and Table 5.1.5b respectively. As ^{111}In is formed both directly and via the decay of 7.6 min ^{111}In, we give only the saturation yield.

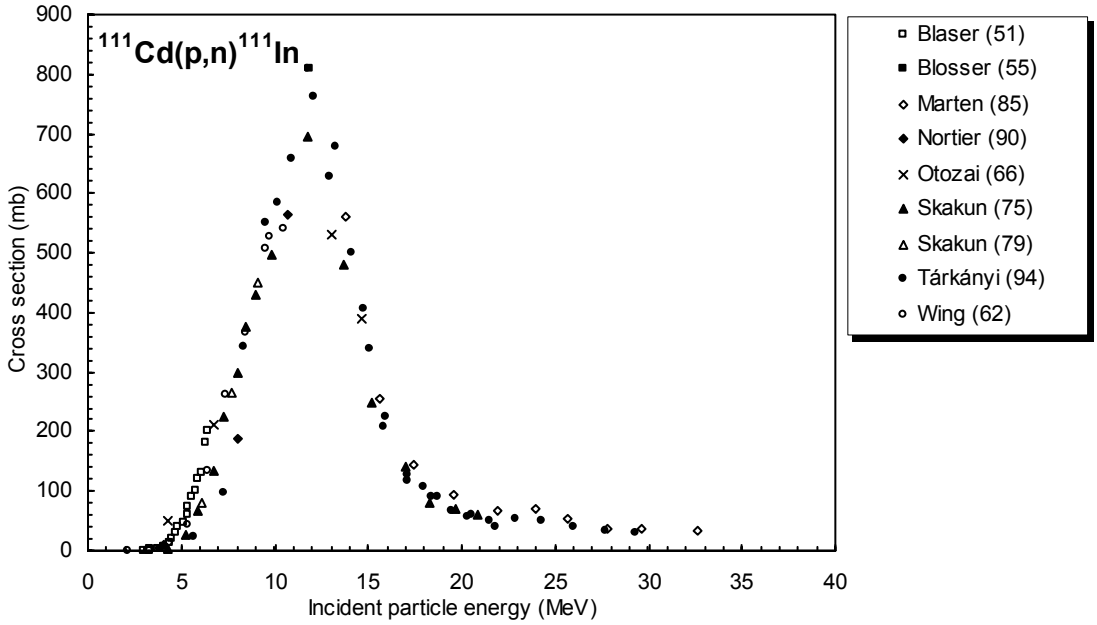

Figure 5.1.5a. All experimental data.

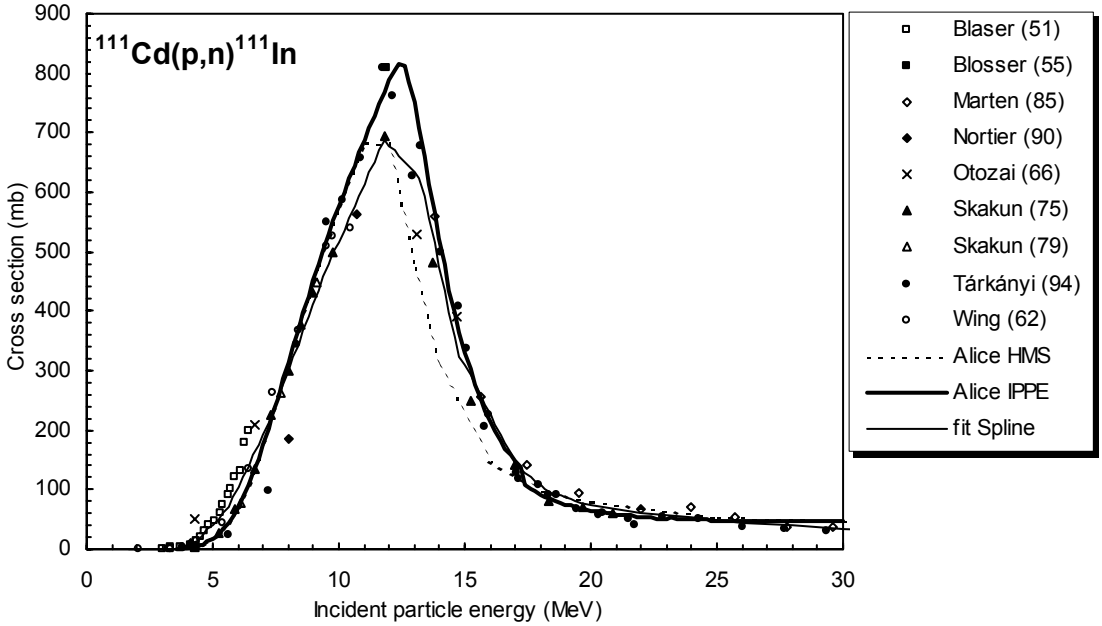

Figure 5.1.5b. Selected experimental data in comparison with theoretical calculations and fits.

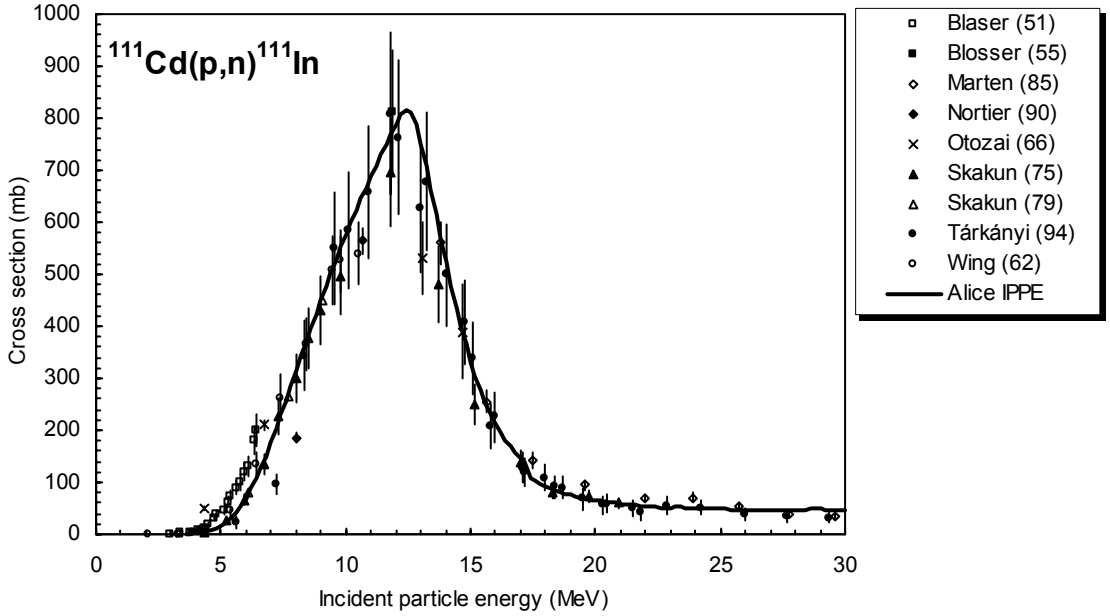

Figure 5.1.5c. Selected experimental data and recommended cross-section curve.

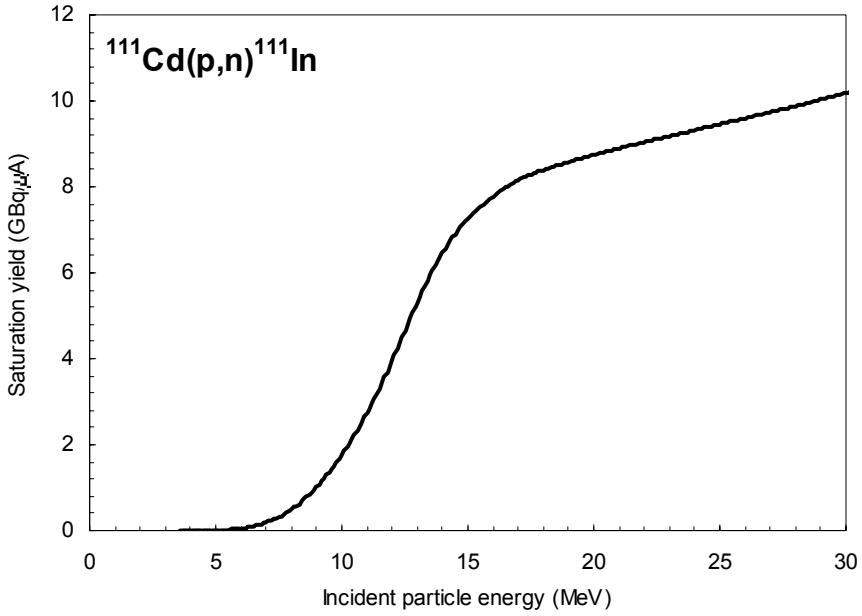

Figure 5.1.5d. Yield of ^{111}In calculated from the recommended cross-sections.

TABLE 5.1.5a. RECOMMENDED CROSS-SECTIONS FOR THE $^{111}Cd(p,n)^{111}In$ REACTION

Energy MeV	Cross-section mb	Energy MeV	Cross-section mb	Energy MeV	Cross-section mb	Energy MeV	Cross-section mb
4.0	2.2	11.0	688	18.0	92.2	25.0	48.5
4.5	6.8	11.5	742	18.5	82.7	25.5	47.8
5.0	17.3	12.0	791	19.0	75.5	26.0	47.3
5.5	37.0	12.5	805	19.5	69.9	26.5	47.0
6.0	69.9	13.0	749	20.0	65.5	27.0	46.9
6.5	117	13.5	641	20.5	61.9	27.5	46.7
7.0	176	14.0	522	21.0	58.9	28.0	46.7
7.5	243	14.5	417	21.5	56.4	28.5	47.4
8.0	314	15.0	332	22.0	54.1	29.0	48.1
8.5	383	15.5	265	22.5	52.2	29.5	47.9
9.0	451	16.0	214	23.0	50.8	30.0	47.6
9.5	515	16.5	176	23.5	51.8		
10.0	576	17.0	147	24.0	50.4		
10.5	633	17.5	106	24.5	49.3		

TABLE 5.1.5b. YIELDS CALCULATED FROM THE RECOMMENDED CROSS-SECTION DATA FOR THE $^{111}Cd(p,n)^{111}In$ REACTION. A_2: SATURATION ACTIVITY FOR 1 μA IRRADIATION (*)

Energy MeV	Activity GBq A_2	Energy MeV	Activity GBq A_2	Energy MeV	Activity GBq A_2	Energy MeV	Activity GBq A_2
4.0	0.0005	11.0	2.74	18.0	8.39	25.0	9.46
4.5	0.0025	11.5	3.32	18.5	8.49	25.5	9.53
5.0	0.008	12.0	3.96	19.0	8.58	26.0	9.60
5.5	0.022	12.5	4.64	19.5	8.67	26.5	9.67
6.0	0.050	13.0	5.32	20.0	8.75	27.0	9.74
6.5	0.103	13.5	5.94	20.5	8.82	27.5	9.81
7.0	0.19	14.0	6.47	21.0	8.90	28.0	9.88
7.5	0.32	14.5	6.90	21.5	8.97	28.5	9.95
8.0	0.49	15.0	7.26	22.0	9.04	29.0	10.03
8.5	0.73	15.5	7.55	22.5	9.11	29.5	10.10
9.0	1.01	16.0	7.78	23.0	9.18	30.0	10.18
9.5	1.36	16.5	7.98	23.5	9.25		
10.0	1.76	17.0	8.15	24.0	9.32		
10.5	2.22	17.5	8.28	24.5	9.39		

* Regarding the yield values see ‘Remark’ in the appendix.

5.1.6. ^{112}Cd(p,2n)^{111}In

A total of 4 cross-section data sets were found in the literature. From these only 1 work was excluded while the 3 others were selected for further evaluation. The list of related references given below is accompanied with additional information. We mention availability of data in the computerized database EXFOR (if available, unique EXFOR reference number is given). Furthermore, we indicate a reason why a data set was excluded (reference denoted by an asterisk *).

*** Nieckarz, W.J. Jr., Caretto, A.A. Jr.:**
Production of ^{111}In and ^{114m}In from separated isotopes of cadmium using 70 to 400 MeV protons.
Physical Review **178** (1969) 1887
— Exfor: C0345
— Data excluded: values reported only above the investigated energy range.

Otozai, K., Kume, S., Mito, A., Okamura, H., Tsujoni, R., Kanchiku, Y., Katoh, T., Gotoh, H.:
Excitation functions for the reactions induced by protons on Cd up to 37 MeV.
Nuclear Physics **80** (1966) 335
— Exfor: P0019

Skakun, E., Kljucherev, A.P., Rakivnenko Yu.N., Romany, I.A.:
Excitation functions of (p,n)— and (p,2n) reactions on cadmium isotopes.
Izvestiya Academy Nauk SSSR, Ser. Fiz. **39** (1975) 24
— Exfor: A0001

Tárkányi, F., Szelecsényi, F., Kopecky, P., Molnár, T., Andó, L., Mikecz, P., Tóth Gy., Rydl, A.:
Cross-sections of proton induced reactions on enriched ^{111}Cd and ^{112}Cd for the production of ^{111}In for use in nuclear medicine.
Applied Radiation Isotopes **45** (1994) 239
— Exfor: D4027

The data from papers where experimental numerical values were available (4 papers) are collected in Fig. 5.1.6a. From these 1 work was excluded while the remaining 3 works were selected for further evaluation. All the data denote cumulative cross-sections, I.e. the summed values for the formation of ^{111}In (directly as well as via the decay of the 7.6 min ^{111m}In).

Cross-sections were calculated by two different versions of the nuclear reaction model code ALICE (denoted as HMS and IPPE) and by a spline fitting procedure. These results are compared with the selected experimental data in Fig. 5.1.6b. The model calculations represent the experimental data well. The best approximation was, however, judged to be the spline fit. Recommended cross-sections are compared with selected experimental data, including their error bars, in Fig. 5.1.6c. Yields calculated from the recommended cross-sections are presented in Fig. 5.1.6d. The corresponding numerical values for recommended cross-sections and yields are tabulated in Table 5.1.6a and Table 5.1.6b respectively. As ^{111}In is formed both directly and via the decay of 7.6 min ^{111m}In, we give only the saturation yield.

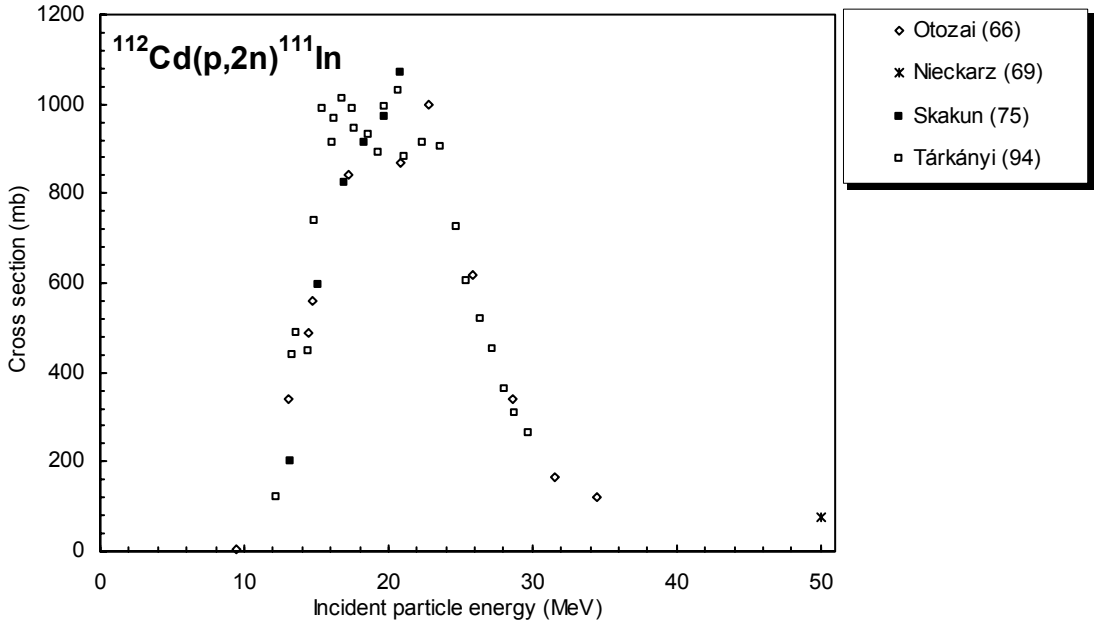

Figure 5.1.6a. All experimental data.

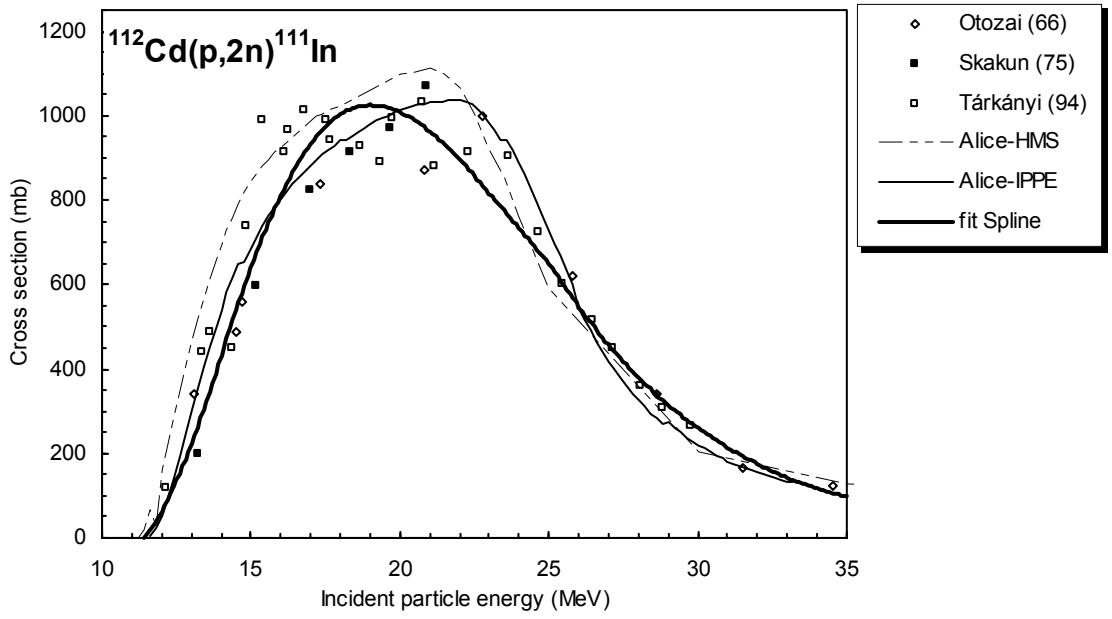

Figure 5.1.6b. Selected experimental data in comparison with theoretical calculations and fits

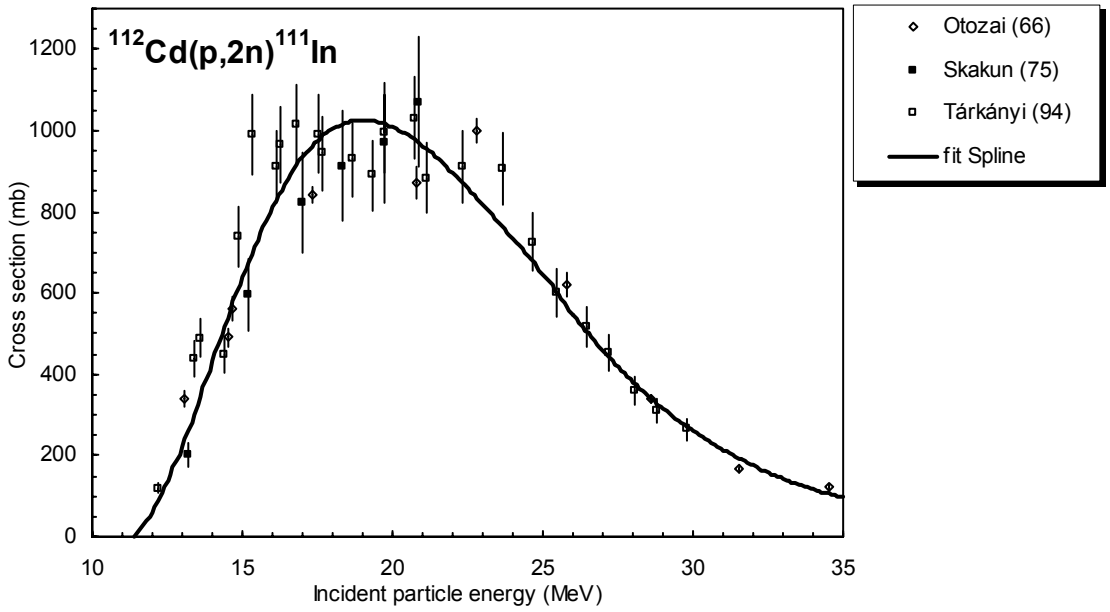

Figure 5.1.6c. Selected experimental data and recommended cross-section curve.

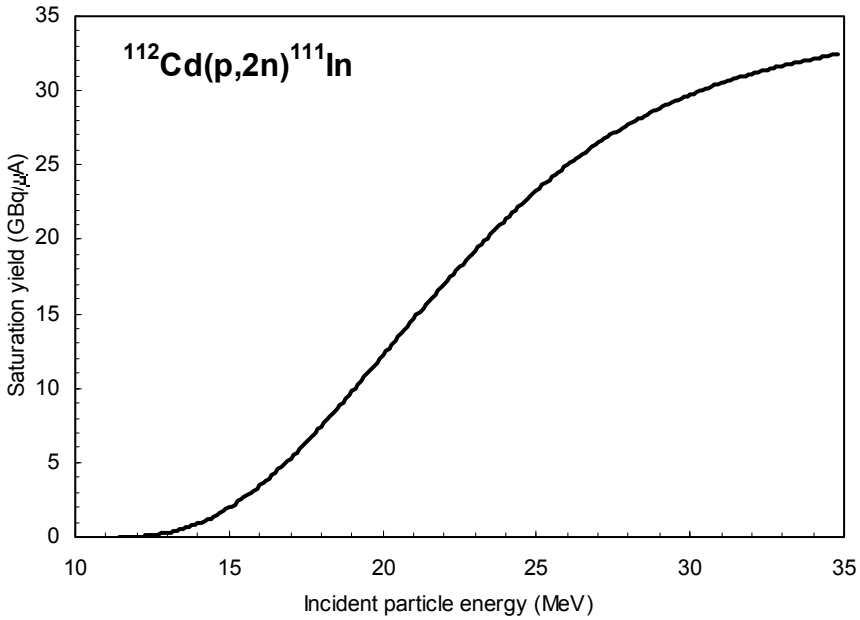

Figure 5.1.6d. Yield of ^{111}In calculated from the recommended cross-sections.

TABLE 5.1.6a. RECOMMENDED CROSS-SECTIONS FOR THE $^{112}Cd(p,2n)^{111}In$ REACTION

Energy MeV	Cross-section mb	Energy MeV	Cross-section mb	Energy MeV	Cross-section mb	Energy MeV	Cross-section mb
11.5	8.8	17.5	975	23.5	775	29.5	286
12.0	61.1	18.0	1004	24.0	733	30.0	260
12.5	137	18.5	1020	24.5	691	30.5	236
13.0	222	19.0	1025	25.0	647	31.0	214
13.5	324	19.5	1021	25.5	598	31.5	194
14.0	431	20.0	1008	26.0	547	32.0	175
14.5	538	20.5	988	26.5	500	32.5	158
15.0	638	21.0	962	27.0	458	33.0	142
15.5	730	21.5	930	27.5	418	33.5	129
16.0	811	22.0	895	28.0	381	34.0	116
16.5	879	22.5	857	28.5	346	34.5	106
17.0	934	23.0	817	29.0	315	35.0	97.7

TABLE 5.1.6b. YIELDS CALCULATED FROM THE RECOMMENDED CROSS-SECTION DATA FOR THE $^{112}Cd(p,2n)^{111}In$ REACTION. A_2: SATURATION ACTIVITY FOR 1 μA IRRADIATION (*)

Energy MeV	Activity GBq A_2	Energy MeV	Activity GBq A_2	Energy MeV	Activity GBq A_2	Energy MeV	Activity GBq A_2
11.5	0.0014	17.5	6.35	23.5	20.3	29.5	29.3
12.0	0.033	18.0	7.45	24.0	21.4	30.0	29.7
12.5	0.12	18.5	8.60	24.5	22.3	30.5	30.1
13.0	0.29	19.0	9.79	25.0	23.3	31.0	30.5
13.5	0.54	19.5	11.0	25.5	24.2	31.5	30.8
14.0	0.90	20.0	12.2	26.0	25.0	32.0	31.1
14.5	1.37	20.5	13.4	26.5	25.8	32.5	31.4
15.0	1.96	21.0	14.6	27.0	26.5	33.0	31.7
15.5	2.65	21.5	15.8	27.5	27.1	33.5	31.9
16.0	3.44	22.0	17.0	28.0	27.7	34.0	32.1
16.5	4.33	22.5	18.2	28.5	28.3	34.5	32.3
17.0	5.31	23.0	19.3	29.0	28.8	35.0	32.5

* Regarding the yield values see ‘Remark’ in the appendix.

5.1.7. ^{123}Te(p,n)^{123}I

A total of 8 cross-section data sets (in 7 papers) were found in the literature. Four sets were rejected and the remaining 4 sets were selected for further evaluation. The list of related references given below is accompanied with additional information. We mention availability of data in the computerized database EXFOR (if available, unique EXFOR reference number is given). Furthermore, we indicate a reason why a data set was excluded (reference denoted by an asterisk *).

*** Acerbi, E., Birattari, C., Castiglioni, M., Resmini, F.:**
Production of ^{123}I for medical purposes at the Milan AVF cyclotron.
Int. J. Applied Radiation Isotopes **26** (1975) 741
— Exfor: A0266
Remark: the compiler calculated the cross-sections for the above reaction up to the threshold energy of the ^{124}Te(p,2n) reaction using the results measured on natural tellurium targets.
— Data excluded: shifted to higher energies.

*** Barrall, R.C., Beaver, J.E., Hupf, H.B., Rubio, F.F.:**
Production of Curie quantities of high purity I-123 with 15 MeV protons.
Eur. J. Nuclear Medicine **6** (1981) 411
— Exfor: none
— Data excluded: only one low energy point reported, too low cross-section value.

Hupf, H.B., Eldridge, J.S., Beaver, J.S.:
Production of iodine-123 for medical applications.
Int. J. Applied Radiation Isototopes **19** (1968) 345
— Exfor: none

Mahunka, I., Andó, L., Mikecz, P., Tcheltsov, A.N., Suvorov, I.A.:
Iodine-123 production at a small cyclotron for medical use.
J. Radioanalytical Nuclear Chemistry, Letters **213** (1996) 135
— Exfor: none

Scholten, B., Qaim, S.M., Stöcklin, G.:
Excitation functions of proton induced nuclear reactions on natural tellurium and enriched ^{123}Te: production of ^{123}I via the ^{123}Te(p,n)^{123}I process at a low energy cyclotron.
Applied Radiation Isotopes **40** (1989) 127
— Exfor: A0473
Remark: The compiler also calculated the cross-sections for the above reaction up to the threshold energy of the ^{124}Te(p,2n) reaction using the results measured on natural tellurium targets.

*** Van den Bosch, R., De Goeij, J.J.M., Van der Heide, J.A., Tertoolen, W., Theelen, H.M.J., Zegers, C.:**
A new approach to target chemistry for the iodine-123 production via the ^{124}Te(p,2n) reaction.
Int. J. Applied Radiation Isotopes **28** (1977) 255
— Exfor: B0167
— Data excluded: shifted to higher energies, too high cross-section values.

*** Zweit, J., Bakir, M., A., Ott, R.T., Sharma, H.L., Cox, M., Goodall, R.**
Excitation functions of proton induced reactions in natural tellurium: Production of no-carrier added iodine-124 for PET applications.
Proc. 4th International Workshop on Targetry and Target Chemistry, PSI Villigen, Switzerland, 9-12 Sept. 1992, ed. Weinreich, R., p. 76.
— Exfor: none
Remark: The compiler calculated the cross-sections for the above reaction up to the threshold energy of the ^{124}Te(p,2n) reaction using the results measured on natural tellurium targets.
— Data excluded: systematically too low cross-section values.

The data from papers where experimental numerical values were available (8 data sets from 7 papers) are collected in Fig. 5.1.7a. From these, 4 sets were excluded while the remaining 4 were selected for further evaluation.

Cross-sections were calculated by the nuclear reaction model code ALICE-IPPE. The results are compared with the selected experimental data in Fig. 5.1.7b. The result of model calculation, after normalization, excellently reproduces the experimental data. The IPPE calculation normalized to the data of Scholten (1989) and Mahunka (1996) was hence chosen as the recommended data. Recommended cross-sections are compared with selected experimental data, including their error bars, in Fig. 5.1.7c. Yields calculated from the recommended cross-sections are presented in Fig. 5.1.7d. The corresponding numerical values for recommended cross-sections and yields are tabulated in Table 5.1.7a and Table 5.1.7b, respectively.

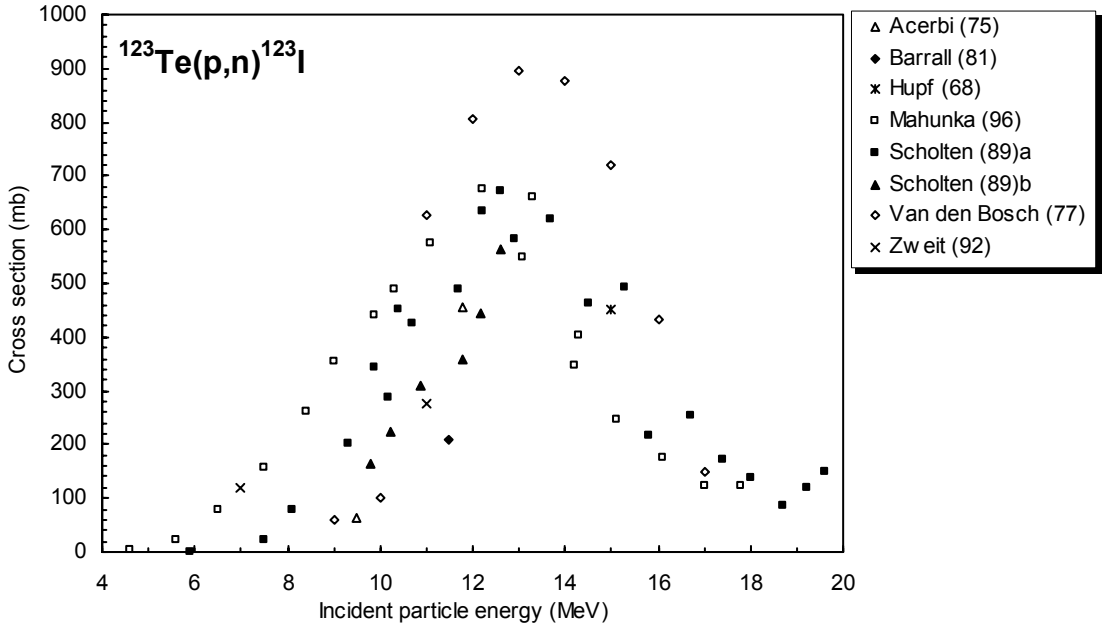

Figure 5.1.7a. All experimental data.

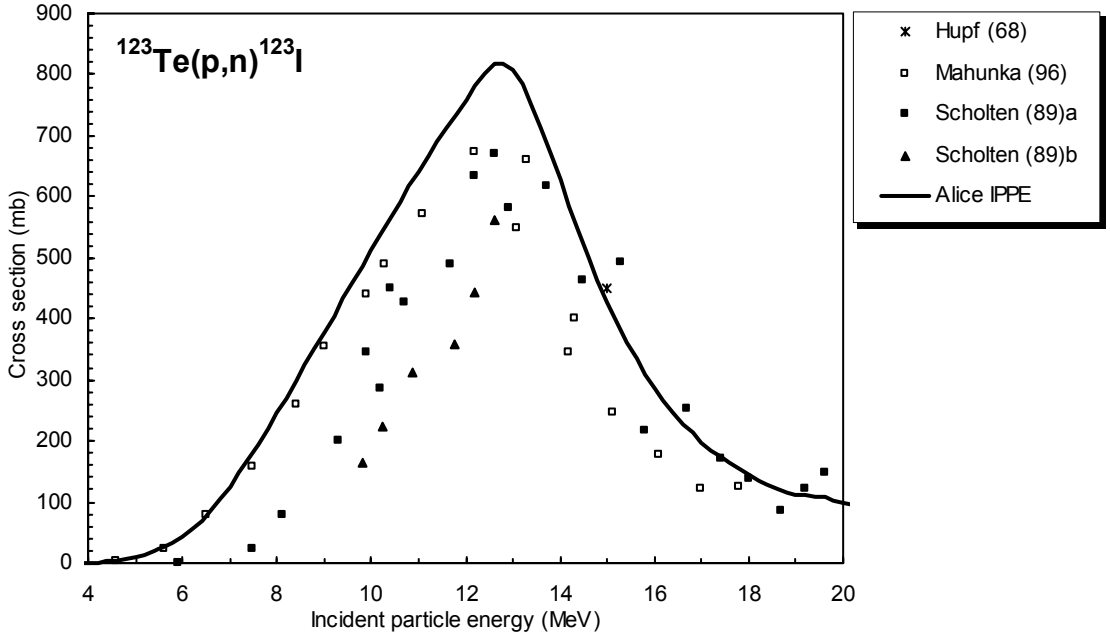

Figure 5.1.7b. Selected experimental data in comparison with theoretical calculations and fits.

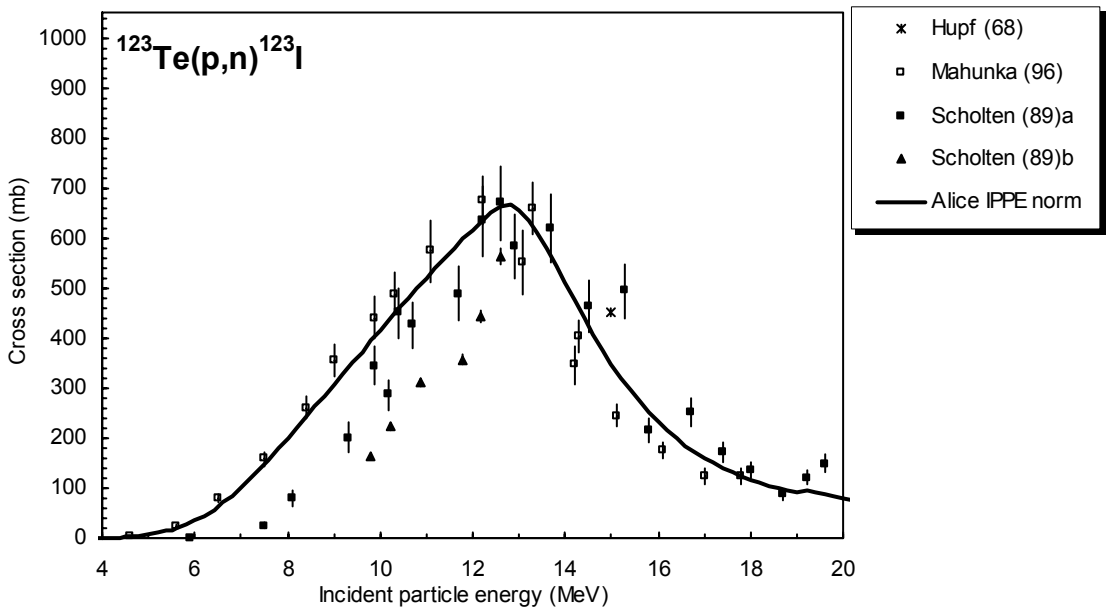

Figure 5.1.7c. Selected experimental data and recommended cross-section curve.

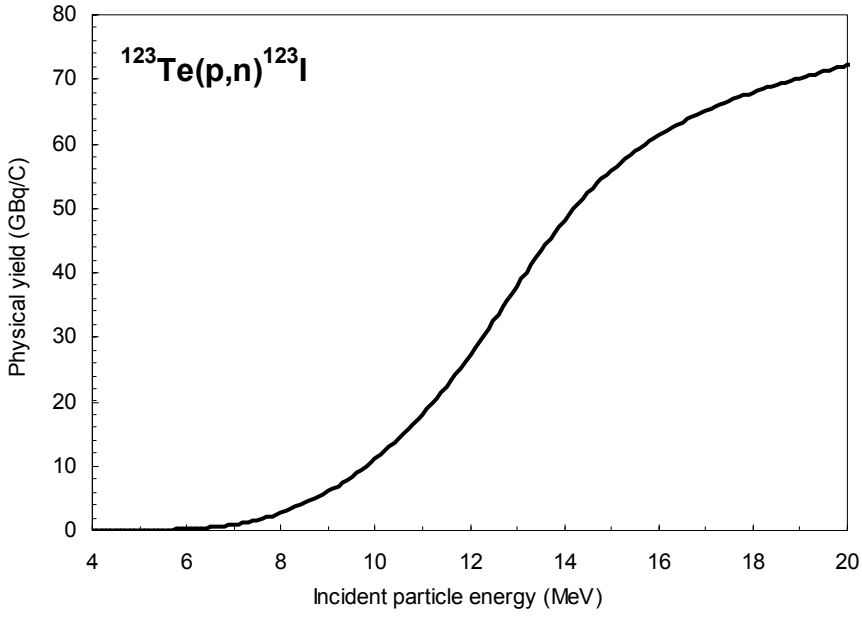

Figure 5.1.7d. Yield of ^{123}I calculated from the recommended cross-sections.

TABLE 5.1.7a. RECOMMENDED CROSS-SECTIONS FOR THE $^{123}Te(p,n)^{123}I$ REACTION

Energy MeV	Cross-section mb	Energy MeV	Cross-section mb	Energy MeV	Cross-section mb	Energy MeV	Cross-section mb
4.0	0.7	8.5	252	13.0	646	17.5	136
4.5	2.5	9.0	307	13.5	593	18.0	117
5.0	7	9.5	362	14.0	511	18.5	102
5.5	17	10.0	416	14.5	424	19.0	92
6.0	35	10.5	469	15.0	347	19.5	89
6.5	64	11.0	521	15.5	284	20.0	80
7.0	102	11.5	572	16.0	232		
7.5	148	12.0	621	16.5	192		
8.0	199	12.5	652	17.0	161		

TABLE 5.1.7b. YIELDS CALCULATED FROM THE RECOMMENDED CROSS-SECTION DATA FOR THE $^{123}Te(p,n)^{123}I$ REACTION. Y: PHYSICAL YIELD, A_1: ACTIVITY AFTER 1 HOUR AND 1 μA IRRADIATION, A_2: SATURATION ACTIVITY FOR 1 μA IRRADIATION

Energy MeV	Physical yield GBq/C Y	Activity MBq A_1	Activity GBq A_2	Energy MeV	Physical yield GBq/C Y	Activity MBq A_1	Activity GBq A_2
4.0	0.0012	0.004	0.0001	12.5	32.4	114	2.22
4.5	0.0077	0.03	0.001	13.0	37.9	133	2.60
5.0	0.03	0.10	0.00	13.5	43.3	152	2.97
5.5	0.1	0.3	0.01	14.0	48.1	169	3.30
6.0	0.2	0.8	0.02	14.5	52.3	184	3.59
6.5	0.5	1.7	0.03	15.0	55.9	196	3.83
7.0	1.0	3.4	0.07	15.5	58.8	206	4.03
7.5	1.7	6.0	0.12	16.0	61.3	215	4.20
8.0	2.8	9.7	0.19	16.5	63.4	222	4.34
8.5	4.2	14.7	0.29	17.0	65.1	228	4.46
9.0	6.1	21.3	0.42	17.5	66.6	234	4.57
9.5	8.4	29.3	0.57	18.0	68.0	238	4.66
10.0	11.1	39.0	0.76	18.5	69.1	243	4.74
10.5	14.4	50.4	0.98	19.0	70.2	246	4.81
11.0	18.1	63.5	1.24	19.5	71.2	250	4.88
11.5	22.4	78.5	1.53	20.0	72.2	253	4.95
12.0	27.2	95.3	1.86				

5.1.8. ^{124}Te(p,2n)^{123}I

A total of 5 cross-section data sets were found in the literature (in 4 works) in the energy region considered. From these, 2 sets were excluded while the 3 others were selected for further evaluation. The list of related references given below is accompanied with additional information. We mention availability of data in the computerized database EXFOR (if available, unique EXFOR reference number is given). Furthermore, we indicate a reason why a data set was excluded (reference denoted by an asterisk *).

*** Acerbi, E., Birattari, C., Castiglioni, M., Resmini, F.:**
Production of ^{123}I for medical purposes at the Milan AVF cyclotron.
Int. J. Applied Radiation Isotopes **26** (1975) 741
— Exfor: A0266
— Data excluded: significantly higher than those of the other authors.

Kondo, K., Lambrecht, R.M., Wolf, A.P.:
^{123}I production for radiopharmaceuticals-XX. Excitation functions of the ^{124}Te(p,2n)^{123}I and ^{124}Te(p,n)^{124}I reactions and effect of target enrichment on radionuclidic purity.
Int. J. Applied Radiation Isotopes **28** (1977) 395
— Exfor: B0090
Remark: 2 sets of data are available on targets of different enrichment, indicated Kondo a and Kondo b.

Scholten, B., Kovács, Z., Tárkányi, F., Qaim, S.M.:
Excitation functions of ^{124}Te(p,xn)^{124,123}I reactions from 6 to 31 MeV with special reference to the production of ^{124}I at a small cyclotron.
Applied Radiation Isotopes **46** (1995) 255
— Exfor: D4019

*** Van den Bosch, R., De Goeij, J.J.M., Van der Heide, J.A., Tertoolen, W., Theelen, H.M.J., Zegers, C.:**
A new approach to target chemistry for the iodine-123 production via the ^{124}Te(p,2n) reaction.
Int. J. Applied Radiation Isotopes **28** (1977) 255
— Exfor: B0167
— Data excluded: values are significantly higher than those of the other authors.

The data from papers where experimental numerical values were available (5 sets) are collected in Fig. 5.1.8a. From these, 2 works were excluded while the remaining 3 were selected for further evaluation.

Cross-sections were calculated by two different versions of the nuclear reaction model code ALICE (denoted as HMS and IPPE). The results are compared with the selected experimental data in Fig. 5.1.8b. The model calculations somewhat overestimate the cross-section in the rising part of the curve but in general reproduce the shape of the excitation function well. After normalization to the maximum value of Kondo et al. (1977) and Scholten et al. (1995) the IPPE calculation was chosen as the best approximation. Recommended cross-sections are compared with selected experimental data, including their error bars, in Fig. 5.1.8c. Yields calculated from the recommended cross-sections are presented in Fig. 5.1.8d. The corresponding numerical values for recommended cross-sections and yields are tabulated in Table 5.1.8a and Table 5.1.8b, respectively.

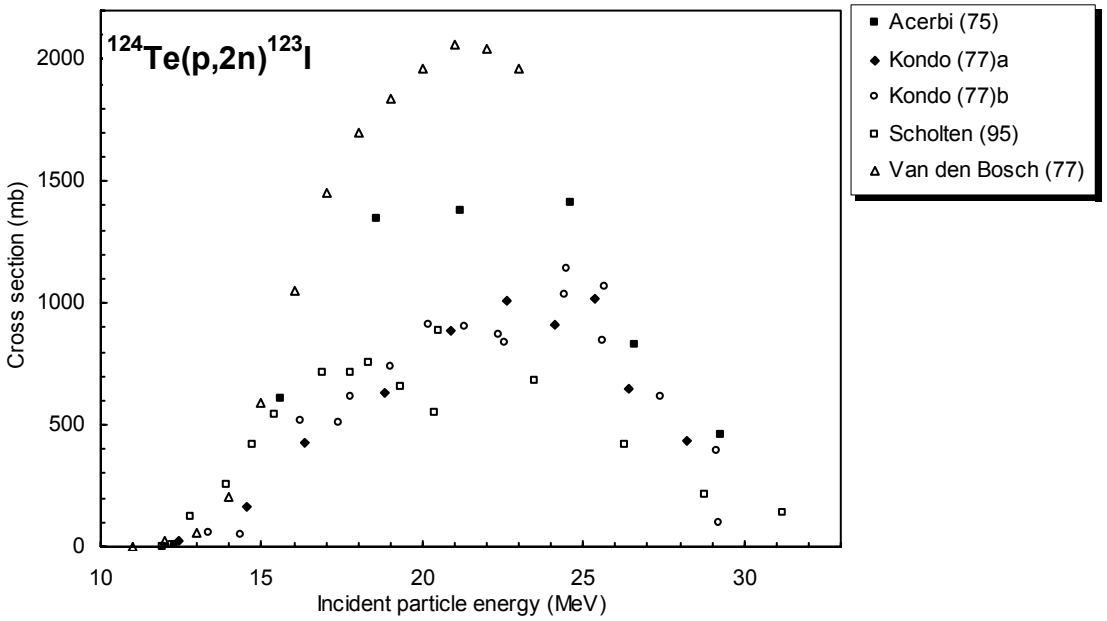

Figure 5.1.8a. All experimental data.

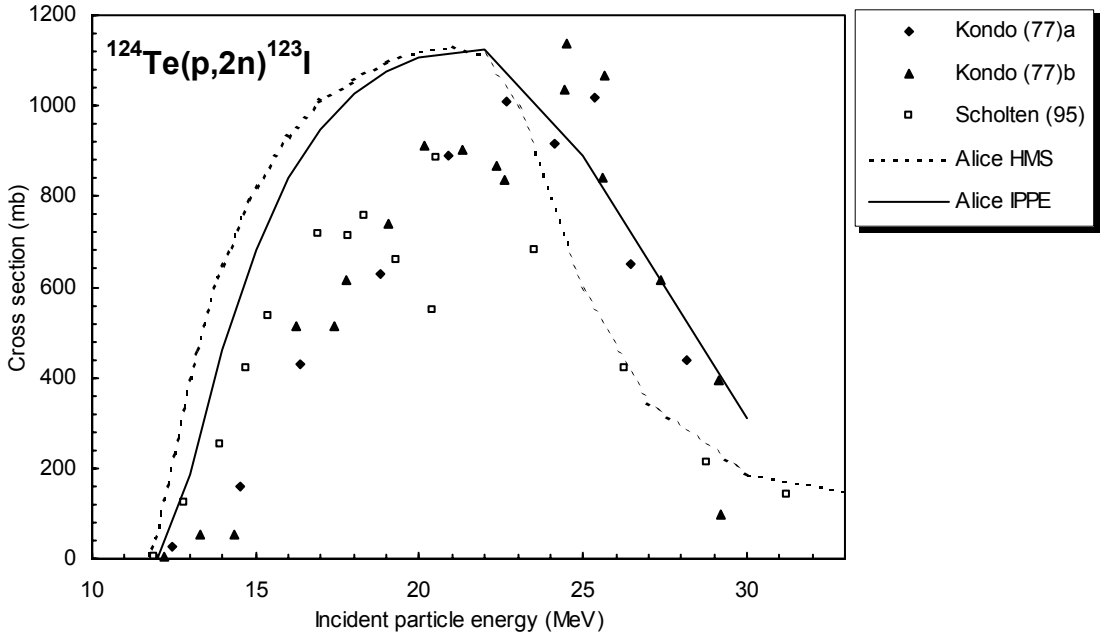

Figure 5.1.8b. Selected experimental data in comparison with theoretical calculations and fits.

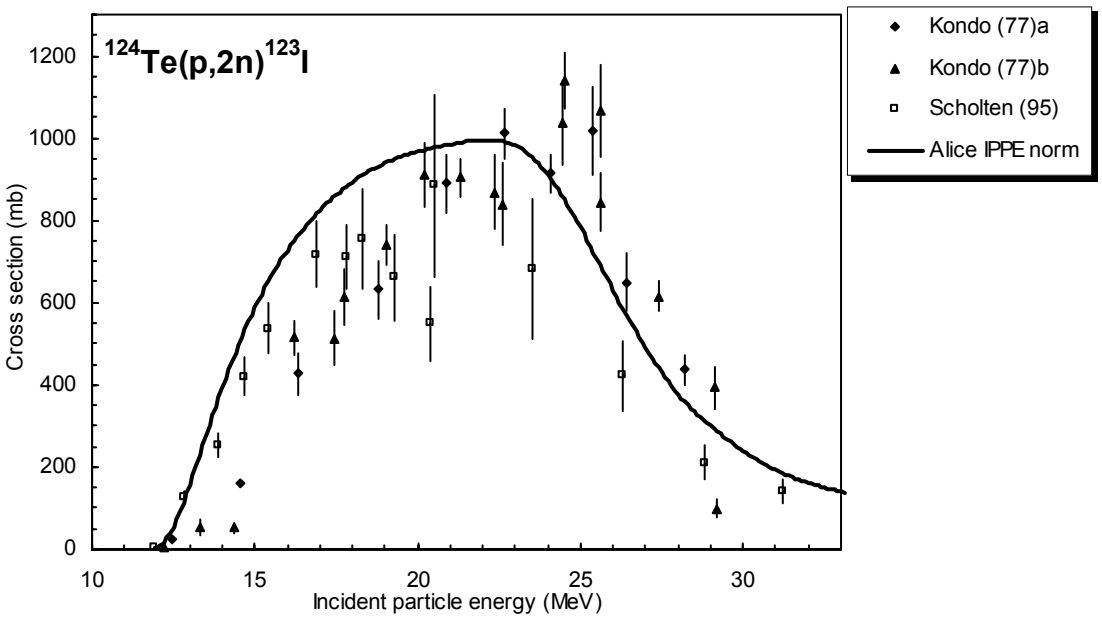

Figure 5.1.8c. Selected experimental data and recommended cross-section curve.

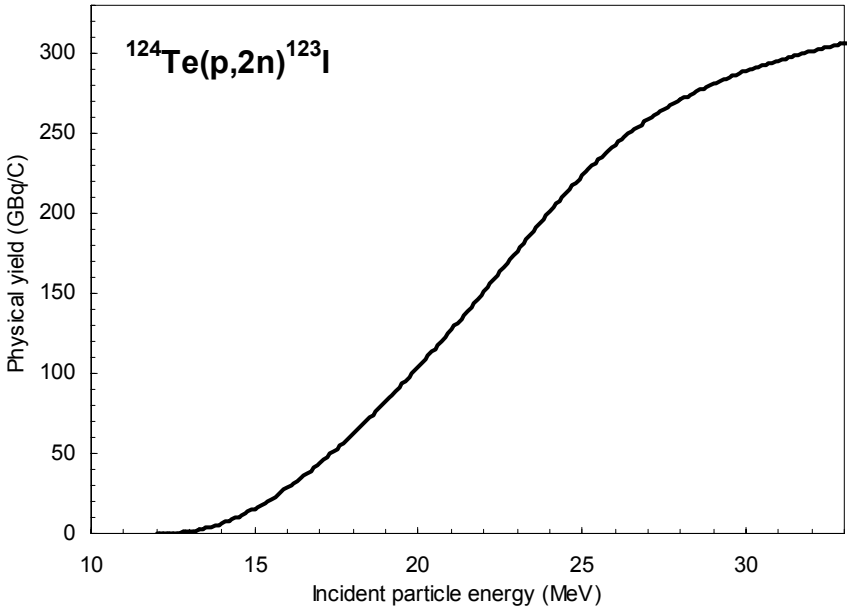

Figure 5.1.8d. Yield of ^{123}I calculated from the recommended cross-sections.

TABLE 5.1.8a. RECOMMENDED CROSS-SECTIONS FOR THE $^{124}Te(p,2n)^{123}I$ REACTION.

Energy MeV	Cross-section mb	Energy MeV	Cross-section mb	Energy MeV	Cross-section mb	Energy MeV	Cross-section mb
12.0	3.7	17.0	825	22.0	995	27.0	490
12.5	55.4	17.5	862	22.5	994	27.5	429
13.0	157	18.0	893	23.0	981	28.0	377
13.5	277	18.5	919	23.5	954	28.5	334
14.0	394	19.0	939	24.0	910	29.0	301
14.5	499	19.5	955	24.5	851	29.5	269
15.0	589	20.0	967	25.0	782	30.0	239
15.5	664	20.5	976	25.5	706		
16.0	728	21.0	984	26.0	630		
16.5	780	21.5	991	26.5	558		

TABLE 5.1.8b. YIELDS CALCULATED FROM THE RECOMMENDED CROSS-SECTION DATA FOR THE $^{124}Te(p,2n)^{123}I$ REACTION. Y: PHYSICAL YIELD, A_1: ACTIVITY AFTER 1 HOUR AND 1 μA IRRADIATION, A_2: SATURATION ACTIVITY FOR 1 μA IRRADIATION.

Energy MeV	Physical yield GBq/C Y	Activity MBq A_1	Activity GBq A_2	Energy MeV	Physical yield GBq/C Y	Activity MBq A_1	Activity GBq A_2
12.0	0.0059	0.021	0.0004	21.5	139	487	9.53
12.5	0.2480	0.87	0.017	22.0	151	530	10.4
13.0	1.21	4.23	0.08	22.5	164	574	11.2
13.5	3.2	11.2	0.22	23.0	176	618	12.1
14.0	6.3	22.0	0.43	23.5	189	662	12.9
14.5	10.4	36.6	0.72	24.0	201	705	13.8
15.0	15.6	54.7	1.07	24.5	213	746	14.6
15.5	21.6	75.9	1.48	25.0	224	784	15.3
16.0	28.5	99.9	1.95	25.5	234	820	16.0
16.5	36.0	126	2.47	26.0	243	852	16.6
17.0	44.2	155	3.03	26.5	251	881	17.2
17.5	53.0	186	3.64	27.0	258	906	17.7
18.0	62.4	219	4.28	27.5	265	929	18.2
18.5	72.2	253	4.95	28.0	271	950	18.6
19.0	82.5	289	5.65	28.5	276	968	18.9
19.5	93.1	327	6.39	29.0	281	985	19.2
20.0	104	365	7.14	29.5	285	1000	19.5
20.5	116	405	7.92	30.0	289	1013	19.8
21.0	127	446	8.71				

5.1.9. ^{124}Te(p,n)^{124}I

Although in recent years ^{124}I has been gaining importance as a therapeutic isotope, especially with regard to quantitative dosimetry, in the context of ^{123}I production via the (p,2n) reaction on ^{124}Te it represents a disturbing radionuclidic impurity.

A total of 8 cross-section data sets (in 6 papers) were found in the literature in the energy region considered. From these, 6 sets were excluded while the remaining 2 were selected for further evaluation. The list of related references given below is accompanied with additional information. We mention availability of data in the computerized database EXFOR (if available, unique EXFOR reference number is given). Furthermore, we indicate a reason why a data set was excluded (reference denoted by an asterisk *).

Acerbi, E., Birattari, C., Castiglioni, M., Resmini, F.:
Production of ^{123}I for medical purposes at the Milan AVF cyclotron.
Int. J. Applied Radiation Isotopes **26** (1975) 741
— Exfor: A0266
Remark: Values obtained on natural targets (Acerbi a, see Fig. 5.1.9a) were excluded because of energy shift towards higher energies.

*** Kondo, K., Lambrecht, R.M., Wolf, A.P.:**
^{123}I production for radiopharmaceuticals-XX. Excitation functions of the ^{124}Te(p,2n)^{123}I and ^{124}Te(p,n)^{124}I reactions and effect of target enrichment on radionuclidic purity.
Int. J. Applied Radiation Isotopes **28** (1977) 395
— Exfor: B0090
— Data excluded: energy shift towards higher energies.
Remark: 2 sets of data are available on targets of different enrichments and are included (Kondo a and Kondo b, see Fig. 5.1.9a).

Scholten, B., Kovács, Z., Tárkányi, F., Qaim, S.M.:
Excitation functions of ^{124}Te(p,xn)^{124,123}I reactions from 6 to 31 MeV with special reference to the production of ^{124}I at a small cyclotron.
Applied Radiation Isotopes **46** (1995) 255
— Exfor: D4019

*** Scholten, B., Qaim, S.M., Stöcklin, G.:**
Excitation functions of proton induced nuclear reactions on natural tellurium and enriched ^{123}Te: Production of ^{123}I via the ^{123}Te(p,n)^{123}I process at a low energy cyclotron.
Applied Radiation Isotopes **40** (1989) 127
— Exfor: A0473
— Data excluded: energy shift towards higher energies.

*** Van den Bosch, R., De Goeij, J.J.M., Van der Heide, J.A., Tertoolen, W., Theelen, H.M.J., Zegers, C.:**
A new approach to target chemistry for the iodine-123 production via the ^{124}Te(p,2n) reaction.
Int. J. Applied Radiation Isotopes **28** (1977) 255
— Exfor: B0167
— Data excluded: energy shift towards higher energies.

*** Zweit, J., Bakir, M., A., Ott, R.T., Sharma, H.L., Cox, M., Goodall, R.:**
Excitation functions of proton induced reactions in natural tellurium: production of no-carrier added iodine-124 for PET applications.
Proc. 4th International Workshop on Targetry and Target Chemistry, PSI Villigen, Switzerland, Sept. 9-12 (1992), ed. Weinreich, R., p. 76.
— Exfor: none
— Data excluded: energy shift towards higher energies.

The data from papers where experimental numerical values were available (8 data sets from 7 papers) are collected in Fig. 5.1.9a. From these 6 works were excluded while the remaining 2 were selected for further evaluation.

Cross-sections were calculated by the nuclear reaction model code ALICE IPPE. The results are compared with the selected experimental data in Fig. 5.1.9b. The result of the model calculation, after normalization, excellently reproduces the experimental data. The IPPE calculation (normalized to Scholten et al. (95) and Acerbi et al. (75b) maximum cross-section values) was chosen as the recommended data. Recommended cross-sections are compared with selected experimental data, including their error bars, in Fig. 5.1.9c. Yields calculated from the recommended cross-sections are presented in Fig. 5.1.9d. The corresponding numerical values for recommended cross-sections and yields are tabulated in Table 5.1.9a and Table 5.1.9b, respectively.

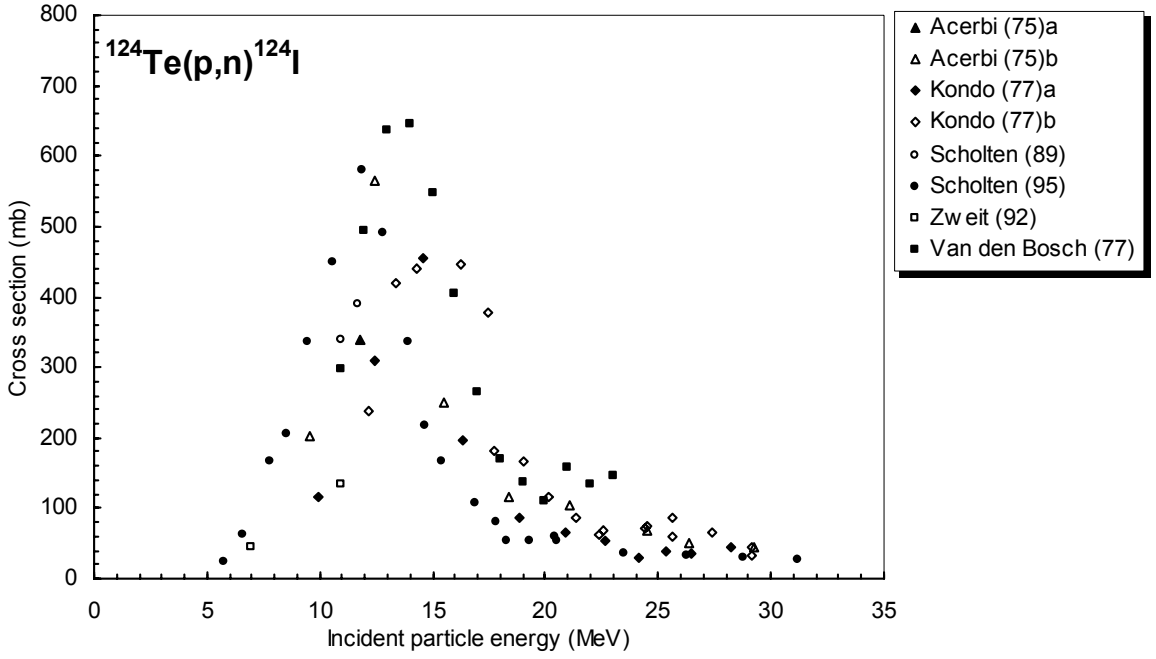

Figure 5.1.9a. All experimental data.

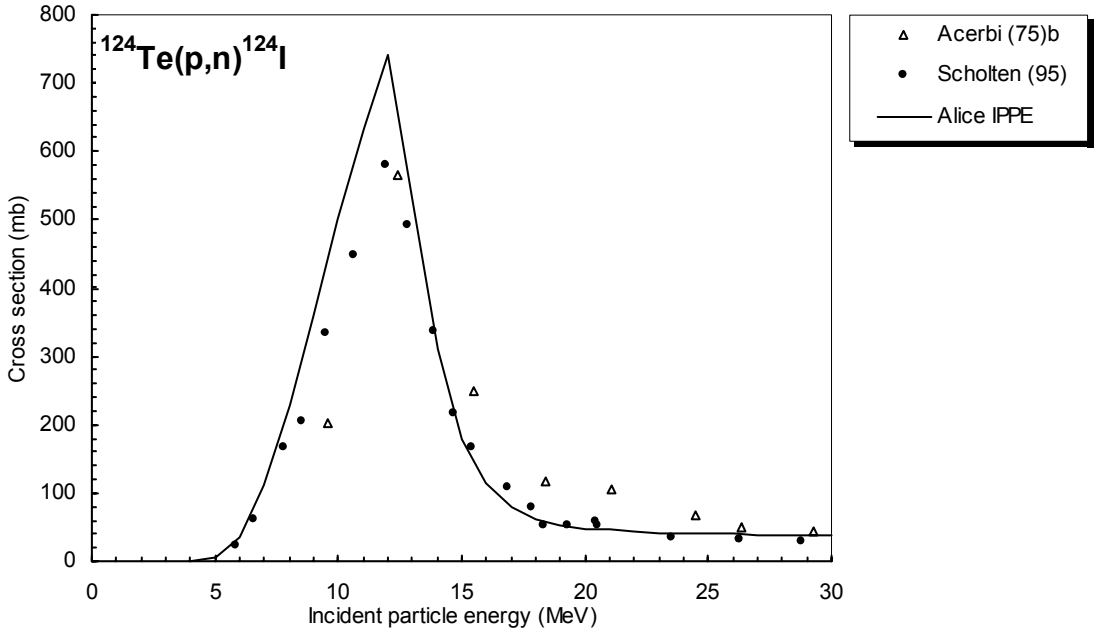

Figure 5.1.9b. Selected experimental data in comparison with theoretical calculations.

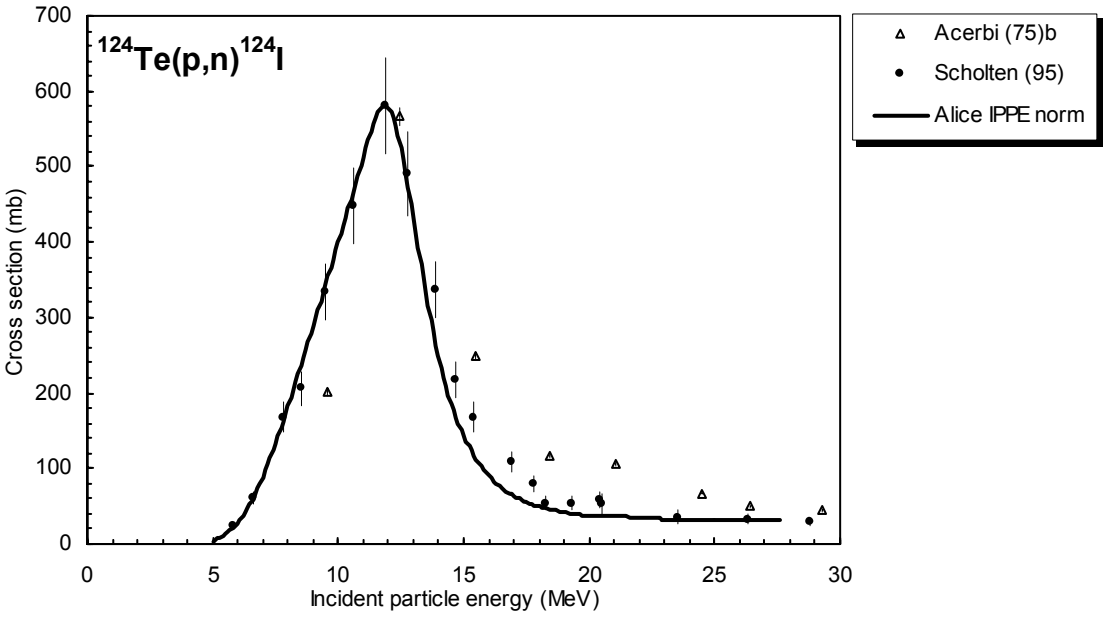

Figure 5.1.9c. Selected experimental data and recommended cross-section curve.

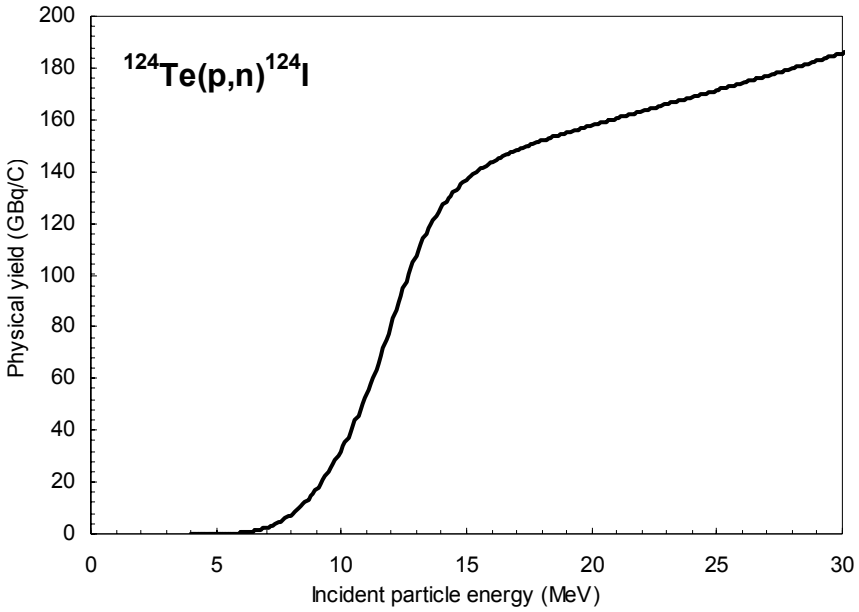

Figure 5.1.9d. Yield of ^{124}I calculated from the recommended cross-sections.

TABLE 5.1.9a. RECOMMENDED CROSS-SECTIONS FOR THE ^{124}Te(p,n)^{124}I REACTION.

Energy MeV	Cross-section mb	Energy MeV	Cross-section mb	Energy MeV	Cross-section mb	Energy MeV	Cross-section mb
5.0	3.6	11.5	565	18.0	49.6	24.5	32.0
5.5	12.50	12.0	579	18.5	45.3	25.0	31.8
6.0	27.36	12.5	525	19.0	41.9	25.5	31.7
6.5	52.9	13.0	431	19.5	39.0	26.0	31.7
7.0	88.8	13.5	333	20.0	37.3	26.5	31.6
7.5	133.3	14.0	249	20.5	37.0	27.0	31.5
8.0	183.1	14.5	186	21.0	37.0	27.5	31.4
8.5	235	15.0	143	21.5	36.0	28.0	31.3
9.0	289	15.5	112	22.0	34.6	28.5	31.1
9.5	344	16.0	90	22.5	33.6	29.0	30.9
10.0	400	16.5	74.7	23.0	33.0	29.5	30.6
10.5	455	17.0	63.4	23.5	32.6	30.0	30.4
11.0	512	17.5	55.4	24.0	32.2		

TABLE 5.1.9b. YIELDS CALCULATED FROM THE RECOMMENDED CROSS-SECTION DATA FOR THE $^{124}Te(p,n)^{124}I$ REACTION. Y: PHYSICAL YIELD, A_1: ACTIVITY AFTER 1 HOUR AND 1 μA IRRADIATION, A_2: SATURATION ACTIVITY FOR 1 μA IRRADIATION.

Energy	Physical yield	Activity		Energy	Physical yield	Activity	
MeV	GBq/C	MBq	GBq	MeV	GBq/C	MBq	GBq
	Y	A_1	A_2		Y	A_1	A_2
5.0	0.0279	0.0924	0.0006	18.0	152	504	3.30
5.5	0.1353	0.449	0.00294	18.5	153	509	3.33
6.0	0.434	1.439	0.0094	19.0	155	514	3.36
6.5	1.092	3.62	0.0237	19.5	156	519	3.39
7.0	2.32	7.68	0.0503	20.0	158	523	3.42
7.5	4.33	14.37	0.094	20.5	159	528	3.45
8.0	7.33	24.32	0.16	21.0	160	532	3.48
8.5	11.46	38.0	0.25	21.5	162	537	3.51
9.0	16.84	55.9	0.37	22.0	163	542	3.54
9.5	23.6	78.2	0.51	22.5	165	546	3.57
10.0	31.8	105.5	0.69	23.0	166	550	3.60
10.5	41.5	137.7	0.90	23.5	167	555	3.63
11.0	52.8	175	1.15	24.0	169	559	3.66
11.5	66.0	219	1.43	24.5	170	564	3.69
12.0	80.6	267	1.75	25.0	171	568	3.72
12.5	95.0	315	2.06	25.5	173	573	3.75
13.0	107.6	357	2.34	26.0	174	577	3.78
13.5	117.8	391	2.56	26.5	175	582	3.81
14.0	126	417	2.73	27.0	177	587	3.84
14.5	132	437	2.86	27.5	178	592	3.87
15.0	137	453	2.96	28.0	180	596	3.90
15.5	140	465	3.05	28.5	181	601	3.93
16.0	143	476	3.11	29.0	183	606	3.97
16.5	146	484	3.17	29.5	184	611	4.00
17.0	148	491	3.22	30.0	186	616	4.03
17.5	150	498	3.26				

5.1.10. $^{127}I(p,5n)^{123}Xe \rightarrow ^{123}I$

A total of 9 cross-section data sets were found in the literature in the energy region considered. From these, 1 set was excluded while the other 8 were selected for further evaluation. The list of related references given below is accompanied with additional information. We mention availability of data in the computerized database EXFOR (if available, unique EXFOR reference number is given). Furthermore, we indicate a reason why a data set was excluded (reference denoted by an asterisk *).

Deptula, C., Khalkin, V.A., Han, K.S., Knotek, O., Konov, V.A., Mikecz, P., Popenkova, L.M., Rurarz, E., Zaitseva, N.G.:
Excitation function and yields for medically important generators $^{82}Sr \rightarrow ^{82}Rb$, $^{123}Xe \rightarrow ^{123}I$ and $^{201}Bi \rightarrow ^{201}Pb \rightarrow ^{201}TI$ obtained with 100 MeV protons.
Nucleonika **35** (1990) 3
— Exfor: O0306

Diksic, M., Yaffe, L.:
A study of I-127(p,xn) and I-127(p, pxn) reactions with special emphasis on production of Xe-123.
J. Inorganic Nuclear Chemistry **39** (1977) 1299
— Exfor: B0081
Remark: Data were adjusted upwards by 30% because the authors used a very old gamma abundance value which is higher than the more recent values.

Lagunas-Solar, M.C., Carvacho, O.F., Liu, B., Jin, Y., Sun, Z.X.:
Cyclotron production of high-purity I-123. A Revision of excitation functions, thin target and cumulative yields for I-127(p,xn) reactions.
Applied Radiation Isotopes **37** (1986) 823
— Exfor: A0363-A0362

*** Lundqvist, H., Malmborg, P., Langstrom, B., and Chiengmai, S.N.:**
Simple production of ^{77}Br and ^{123}I and their use in the labelling of [^{77}Br]BrUdR and [^{123}I]IUdR.
Int. J. Applied Radiation Isotopes **30** (1979) 39
— Exfor: none
— Data excluded: cross-section values too low.

Paans, A.M.J., Vaalburg, W., van Herk, G., Woldring, M.G.:
Excitation function for the production of I-123 via the I-127(p,5n)Xe-123 reaction.
Int. J. Applied Radiation Isotopes **27** (1976) 465
— Exfor: A0161

Sakamoto, K., Dohniwa, M., Okada, K.:
Excitation functions for (p,xn) and (p,pxn) reactions on natural, $^{79+81}Br$, $^{85+87}Rb$, ^{127}I and ^{133}Cs up to E_p = 52 MeV
Applied Radiation Isotopes **36** (1985) 481
— Exfor: None

Syme, D.B., Wood, E., Blair, I.M., Kew, I., Perry, M., Cooper, P.:
Yield curves for cyclotron production of I-123 and I-125 and I-121 by I-127(p,xn)-reactions.
Int. J. Applied Radiation Isotopes **29** (1978) 29
— Exfor: R0007

Suzuki, K.:
Production of pure ^{123}I by the ^{127}I(p,5n)^{123}Xe → ^{123}I-reaction.
Radioisotopes **35** (1986) 235
— Exfor: none

Wilkens, S.R., Shimose, S.T., Hines, H.H., Jungerman, J.A., Hegedus, F., DeNardo, G.L.:
Excitation functions and yields for I-123 production using the I-123(p,5n) Xe-123 reaction.
Int. J. Applied Radiation Isotopes **26** (1975) 279
— Exfor: R0024

The data from papers where experimental numerical values were available (9 papers), are collected in Fig. 5.1.10a. From these, 1 work was excluded while the remaining 8 works were selected for further evaluation.

Cross-sections were calculated by two different versions of the nuclear reaction model code ALICE (denoted as HMS and IPPE) and a spline fit. The results are compared with the selected experimental data in Fig. 5.1.10b. The model calculations overpredict the data. The result of ALICE IPPE describes the data well. The spline fit was judged as giving the best agreement with experimental data. Recommended cross-sections are compared with selected experimental data, including their error bars, in Fig. 5.1.10c. Yields calculated from the recommended cross-sections are presented in Fig. 5.1.10d. The corresponding numerical values for recommended cross-sections and yields are tabulated in Table 5.1.10 and Table 5.1.10b, respectively.

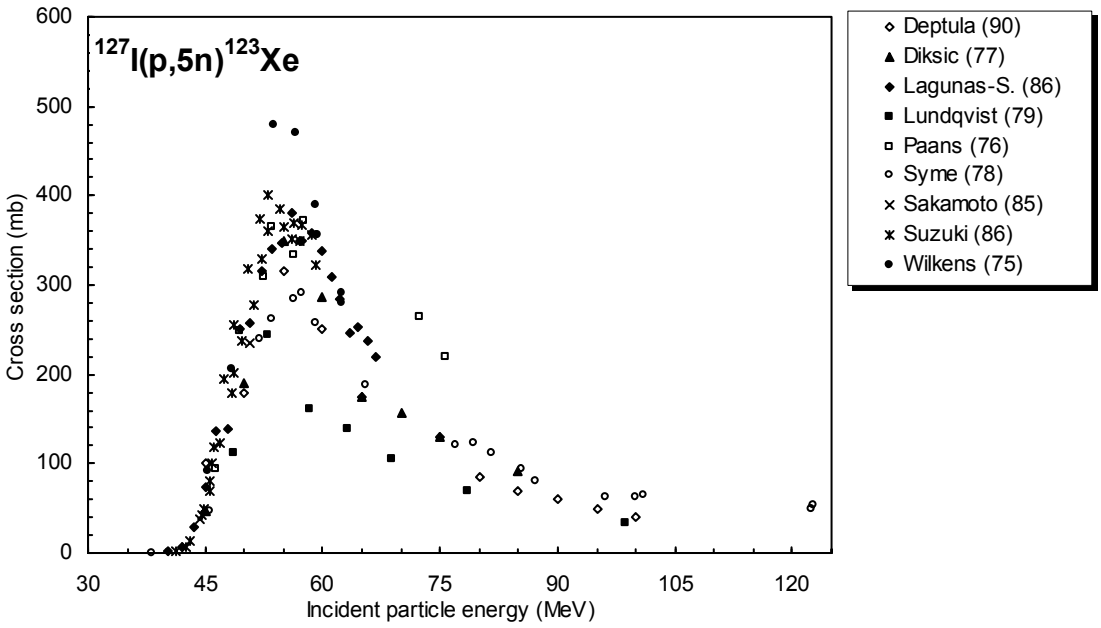

Figure 5.1.10a. All experimental data.

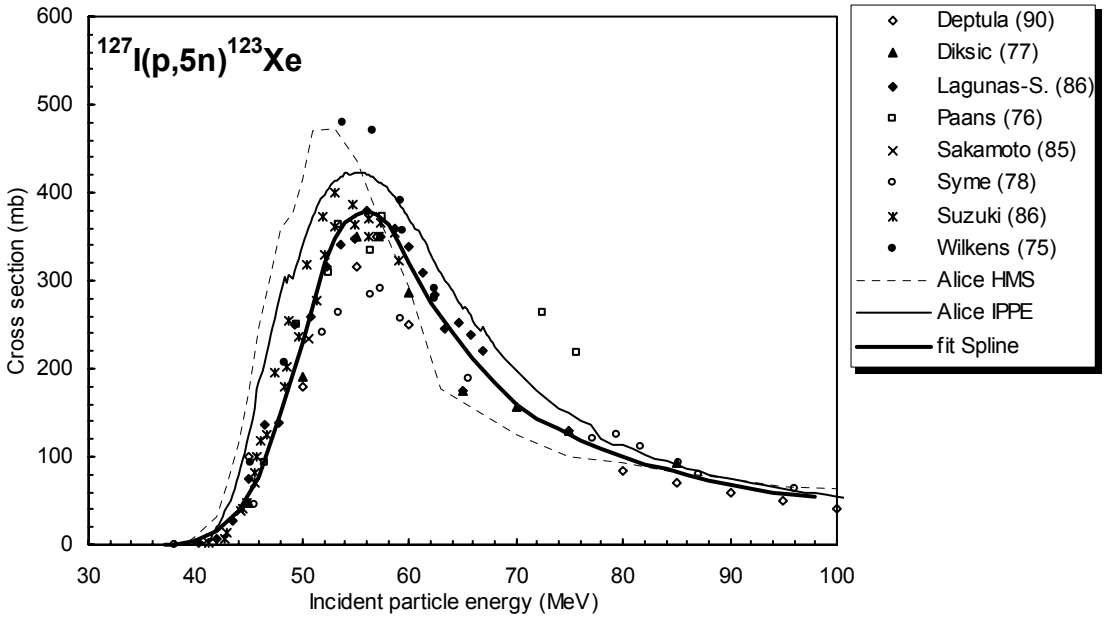

Figure 5.1.10b. Selected experimental data in comparison with theoretical calculations and fits

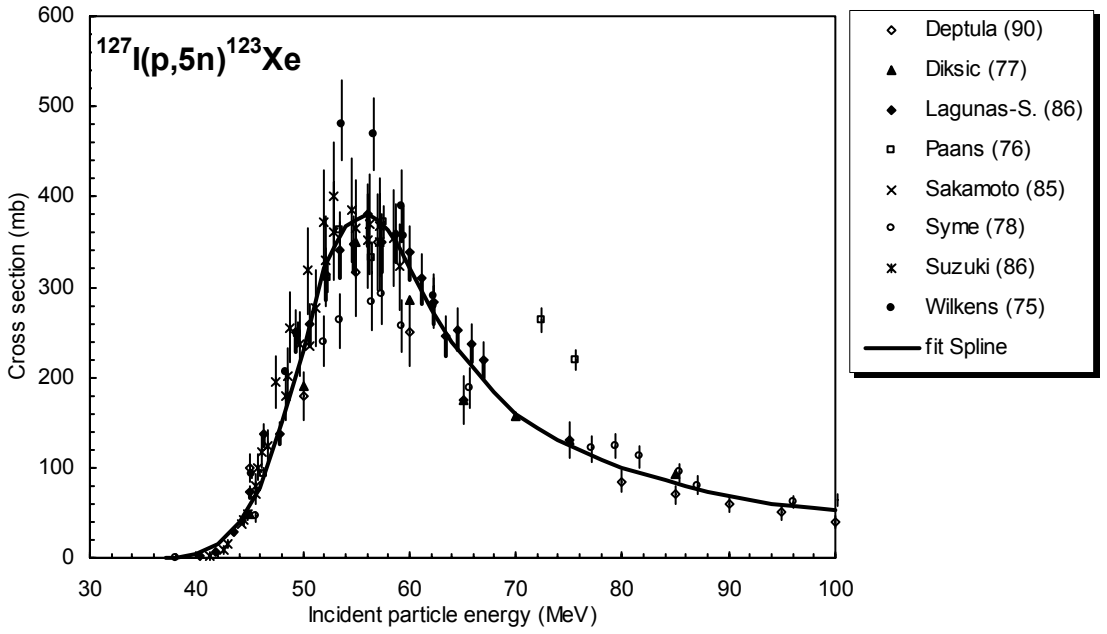

Figure 5.1.10c. Selected experimental data and recommended cross-section curve.

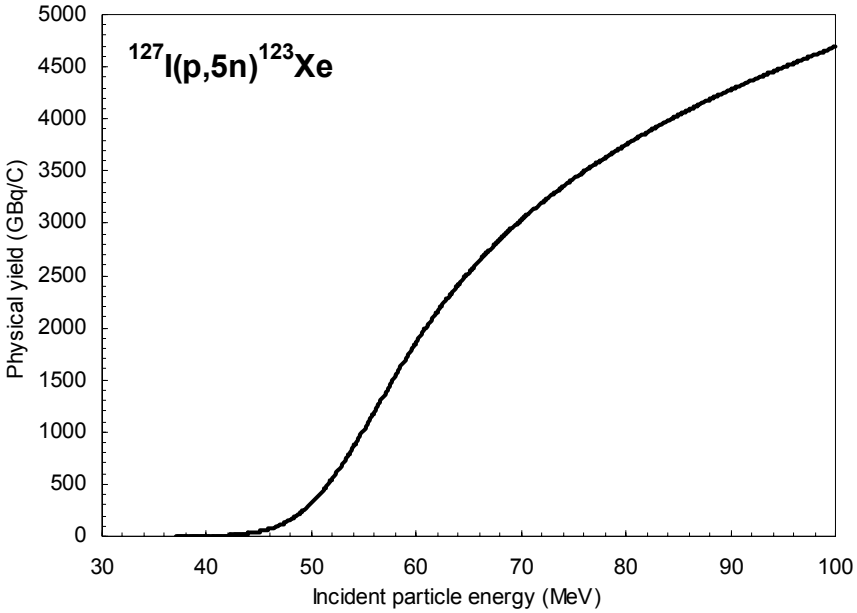

Figure 5.1.10d. Yield of ^{123}Xe calculated from the recommended cross-sections.

TABLE 5.1.10a. RECOMMENDED CROSS-SECTIONS FOR THE $^{127}I(p,5n)^{123}Xe$ REACTION.

Energy MeV	Cross-section mb	Energy MeV	Cross-section mb	Energy MeV	Cross-section mb	Energy MeV	Cross-section mb
37.0	0.0	53.0	345	69.0	171	85.0	83.1
37.5	0.06	53.5	357	69.5	166	85.5	81.6
38.0	0.32	54.0	366	70.0	160	86.0	79.9
38.5	0.94	54.5	372	70.5	156	86.5	78.2
39.0	1.96	55.0	377	71.0	151	87.0	76.4
39.5	3.33	55.5	379	71.5	148	87.5	74.7
40.0	5.00	56.0	379	72.0	144	88.0	73.1
40.5	6.96	56.5	378	72.5	140	88.5	71.6
41.0	9.34	57.0	374	73.0	137	89.0	70.3
41.5	12.3	57.5	369	73.5	134	89.5	69.1
42.0	16.0	58.0	361	74.0	131	90.0	68.0
42.5	20.6	58.5	353	74.5	128	90.5	67.0
43.0	26.0	59.0	343	75.0	125	91.0	66.0
43.5	32.1	59.5	332	75.5	122	91.5	65.0
44.0	38.9	60.0	321	76.0	119	92.0	64.0
44.5	46.4	60.5	310	76.5	116	92.5	63.0
45.0	55.0	61.0	299	77.0	113	93.0	61.9
45.5	65.2	61.5	288	77.5	111	93.5	61.0
46.0	77.7	62.0	277	78.0	108	94.0	60.0
46.5	92.8	62.5	267	78.5	106	94.5	59.1
47.0	110	63.0	258	79.0	103	95.0	58.4
47.5	129	63.5	249	79.5	101	95.5	57.6
48.0	149	64.0	240	80.0	99.0	96.0	57.0
48.5	169	64.5	232	80.5	97.1	96.5	56.4
49.0	190	65.0	225	81.0	95.3	97.0	55.9
49.5	212	65.5	218	81.5	93.6	97.5	55.4
50.0	233	66.0	211	82.0	92.0	98.0	55.0
50.5	255	66.5	204	82.5	90.4	98.5	54.6
51.0	276	67.0	197	83.0	88.9	99.0	54.2
51.5	296	67.5	190	83.5	87.5	99.5	53.9
52.0	315	68.0	184	84.0	86.0	100.0	53.5
52.5	331	68.5	177	84.5	84.6		

TABLE 5.1.10b. YIELDS CALCULATED FROM THE RECOMMENDED CROSS-SECTION DATA FOR THE $^{127}I(p,5n)^{123}Xe$ REACTION. Y: PHYSICAL YIELD, A_1: ACTIVITY AFTER 1 HOUR AND 1 μA IRRADIATION, A_2: SATURATION ACTIVITY FOR 1 μA IRRADIATION.

Energy	Physical yield	Activity		Energy	Physical yield	Activity	
MeV	GBq/C	MBq	GBq	MeV	GBq/C	GBq	GBq
	Y	A_1	A_2		Y	A_1	A_2
37.0	0.000	0.000	0	69.0	2943	9.01	31.8
37.5	0.005	0.015	0.00	69.5	2988	9.15	32.3
38.0	0.04	0.11	0.00	70.0	3032	9.28	32.8
38.5	0.15	0.46	0.00	70.5	3075	9.42	33.2
39.0	0.41	1.25	0.00	71.0	3117	9.54	33.7
39.5	0.88	2.71	0.01	71.5	3159	9.67	34.1
40.0	1.63	5.00	0.02	72.0	3199	9.79	34.6
40.5	2.72	8.31	0.03	72.5	3239	9.92	35.0
41.0	4.20	12.8	0.05	73.0	3278	10.03	35.4
41.5	6.18	18.9	0.07	73.5	3316	10.15	35.8
42.0	8.79	26.9	0.09	74.0	3353	10.27	36.2
42.5	12.2	37.4	0.13	74.5	3390	10.38	36.6
43.0	16.6	50.8	0.18	75.0	3426	10.49	37.0
43.5	22.1	67.6	0.24	75.5	3462	10.60	37.4
44.0	28.9	88.4	0.31	76.0	3497	10.71	37.8
44.5	37.1	113	0.40	76.5	3531	10.81	38.1
45.0	46.9	144	0.51	77.0	3565	10.91	38.5
45.5	58.6	179	0.63	77.5	3598	11.01	38.9
46.0	72.7	223	0.79	78.0	3630	11.11	39.2
46.5	89.7	274	0.97	78.5	3662	11.21	39.6
47.0	110	337	1.19	79.0	3693	11.31	39.9
47.5	134	411	1.45	79.5	3724	11.40	40.2
48.0	162	497	1.76	80.0	3754	11.49	40.6
48.5	195	597	2.11	80.5	3784	11.58	40.9
49.0	232	711	2.51	81.0	3813	11.67	41.2
49.5	274	839	2.96	81.5	3842	11.76	41.5
50.0	321	982	3.46	82.0	3871	11.85	41.8
50.5	372	1139	4.02	82.5	3899	11.94	42.1
51.0	429	1312	4.63	83.0	3927	12.02	42.4
51.5	490	1499	5.29	83.5	3954	12.11	42.7
52.0	556	1701	6.00	84.0	3982	12.19	43.0
52.5	626	1916	6.76	84.5	4009	12.27	43.3
53.0	700	2142	7.56	85.0	4035	12.35	43.6
53.5	777	2378	8.39	85.5	4062	12.43	43.9
54.0	857	2623	9.25	86.0	4087	12.51	44.2
54.5	939	2875	10.14	86.5	4113	12.59	44.4
55.0	1023	3132	11.05	87.0	4138	12.67	44.7
55.5	1108	3393	11.97	87.5	4162	12.74	45.0
56.0	1194	3657	12.90	88.0	4186	12.82	45.2
56.5	1281	3922	13.84	88.5	4210	12.89	45.5
57.0	1368	4187	14.77	89.0	4234	12.96	45.7
57.5	1454	4450	15.70	89.5	4257	13.03	46.0
58.0	1539	4711	16.62	90.0	4279	13.10	46.2
58.5	1623	4968	17.53	90.5	4302	13.17	46.5

TABLE 5.1.10b. (cont.)

Energy	Physical yield	Activity		Energy	Physical yield	Activity	
MeV	GBq/C	MBq	GBq	MeV	GBq/C	GBq	GBq
	Y	A_1	A_2		Y	A_1	A_2
59.0	1705	5219	18.42	91.0	4324	13.24	46.7
59.5	1785	5465	19.28	91.5	4346	13.31	47.0
60.0	1863	5705	20.13	92.0	4368	13.37	47.2
60.5	1939	5937	20.95	92.5	4390	13.44	47.4
61.0	2013	6163	21.75	93.0	4411	13.51	47.7
61.5	2085	6382	22.52	93.5	4432	13.57	47.9
62.0	2154	6594	23.27	94.0	4453	13.63	48.1
62.5	2221	6800	23.99	94.5	4474	13.70	48.3
63.0	2286	6999	24.70	95.0	4494	13.76	48.5
63.5	2350	7193	25.38	95.5	4514	13.82	48.8
64.0	2411	7382	26.05	96.0	4534	13.88	49.0
64.5	2471	7565	26.69	96.5	4554	13.94	49.2
65.0	2529	7744	27.32	97.0	4574	14.00	49.4
65.5	2586	7918	27.94	97.5	4594	14.07	49.6
66.0	2641	8087	28.54	98.0	4614	14.13	49.8
66.5	2695	8252	29.12	98.5	4633	14.19	50.1
67.0	2748	8412	29.68	99.0	4653	14.25	50.3
67.5	2798	8568	30.23	99.5	4673	14.31	50.5
68.0	2848	8719	30.77	100.0	4692	14.37	50.7
68.5	2896	8866	31.28				

5.1.11. $^{127}I(p,3n)^{125}Xe \rightarrow ^{125}I$

This reaction is the major contributor to radionuclidic impurities in the ^{123}I produced via the reaction described in section 5.1.10.

A total of 9 cross-section data sets were found in the literature. All were selected for further evaluation. The list of related references given below is accompanied with additional information. We mention availability of data in the computerized database EXFOR (if available, unique EXFOR reference number is given). Furthermore, we indicate a reason why a data set was excluded (reference denoted by an asterisk *).

Deptula, C., Khalkin, V.A., Han, K.S., Knotek, O., Konov, V.A., Mikecz, P., Popenkova, L.M., Rurarz, E., Zaitseva, N.G.:
Excitation function and yields for medically important generators $^{82}Sr \rightarrow ^{82}Rb$, $^{123}Xe \rightarrow ^{123}I$ and $^{201}Bi \rightarrow ^{201}Pb \rightarrow ^{201}TI$ obtained with 100 MeV protons.
Nucleonika **35** (1990) 3
— Exfor: O0306

Diksic, M., Yaffe, L.:
A study of I-127(p,xn) and I-127(p, pxn) reactions with special emphasis on production of Xe-123.
J. Inorganic Nuclear Chemistry **39** (1977) 1299
— Exfor: B0081
Remark: Data were corrected upwards by 30% because the authors used a very old γ-abundance value.

Lagunas-Solar, M.C., Carvacho, O.F., Liu, B., Jin, Y., Sun, Z.X.:
Cyclotron production of high-purity I-123. A Revision of excitation functions, thin target and cumulative yields for I-127(p,xn) reactions.
Applied Radiation Isotopes **37** (1986) 823
— Exfor: A0363-A0362

Lundqvist, H., Malmborg, P., Langstrom, B., Chiengmai, S.N.:
Simple production of ^{77}Br and ^{123}I and their use in the labelling of [^{77}Br]BrUdR and [^{123}I]IUdR.
Int. J. Applied Radiation Isotopes **30** (1979) 39
— Exfor: none

Paans, A.M.J., Vaalburg, W., van Herk, G., Woldring, M.G.:
Excitation function for the production of I-123 via the I-127(p,5n)Xe-123 reaction.
Int. J. Applied Radiation Isotopes **27** (1976) 465
— Exfor: A0161

Sakamoto, K., Dohniwa, M., Okada, K.:
Excitation functions for (p,xn) and (p,pxn) reactions on natural, $^{79+81}Br$, $^{85+87}Rb$, ^{127}I and ^{133}Cs up to $E_p = 52$ MeV.
Applied Radiation Isotopes **36** (1985) 481
— Exfor: None

Syme, D.B., Wood, E., Blair, I.M., Kew, I., Perry, M., Cooper, P.:
Yield curves for cyclotron production of I-123 and I-125 and I-121 by I-127(p, xn)-reactions.
Int. J. Applied Radiation Isotopes **29** (1978) 29
— Exfor: R0007

Suzuki, K.:
Production of pure ^{123}I by the ^{127}I(p,5n)^{123}Xe → ^{123}I-reaction.
Radioisotopes **35** (1986) 235
— Exfor: none

Wilkens, S.R., Shimose, S.T., Hines, H.H., Jungerman, J.A., Hegedus, F., DeNardo, G.L.:
Excitation functions and yields for I-123 production using the I-123(p,5n) Xe-123 reaction.
Int. J. Applied Radiation Isotopes **26** (1975) 279
— Exfor: R0024

The data from papers where experimental numerical values were available (9 papers) are collected in Fig. 5.1.11a. All were selected for further evaluation.

Cross-sections were calculated by the nuclear reaction model code ALICE IPPE. The results are compared with the selected experimental data in Fig. 5.1.11b. The result of the model calculations reproduces well the experimental data, without any normalisation. Therefore it was chosen as recommended cross-sections. Recommended cross-sections are compared with selected experimental data, including their error bars, in Fig. 5.1.11c. Yields calculated from the recommended cross-sections are presented in Fig. 5.1.11d. The corresponding numerical values for recommended cross-sections and yields are tabulated in Table 5.1.11a and Table 5.1.11b, respectively.

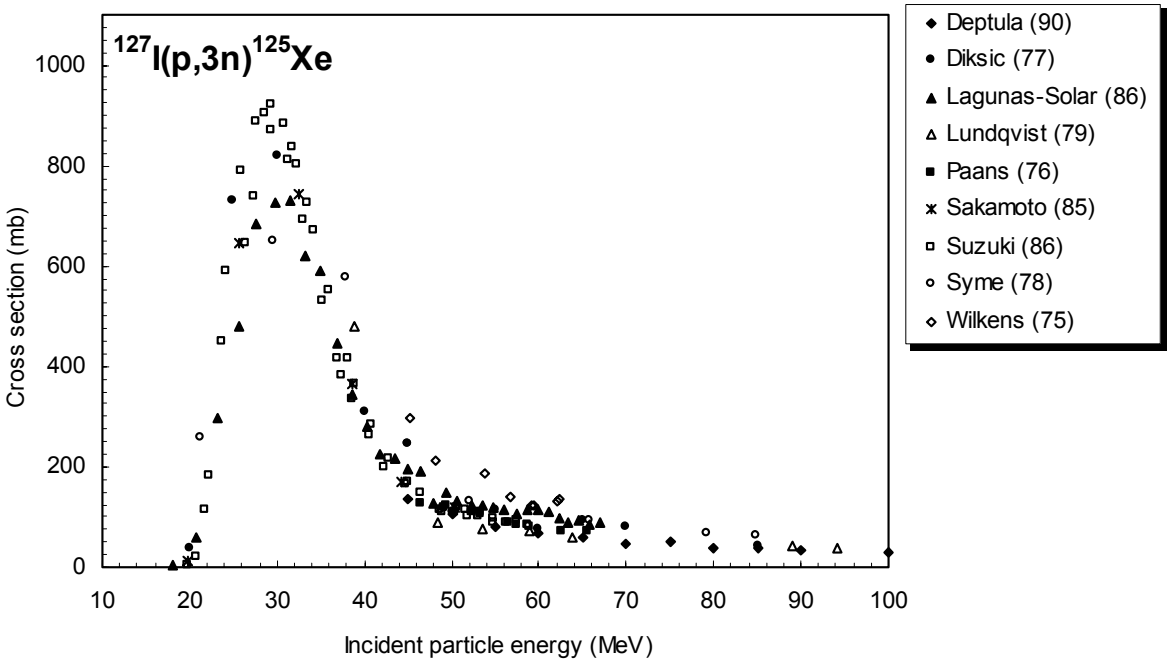

Figure 5.1.11a. All experimental data.

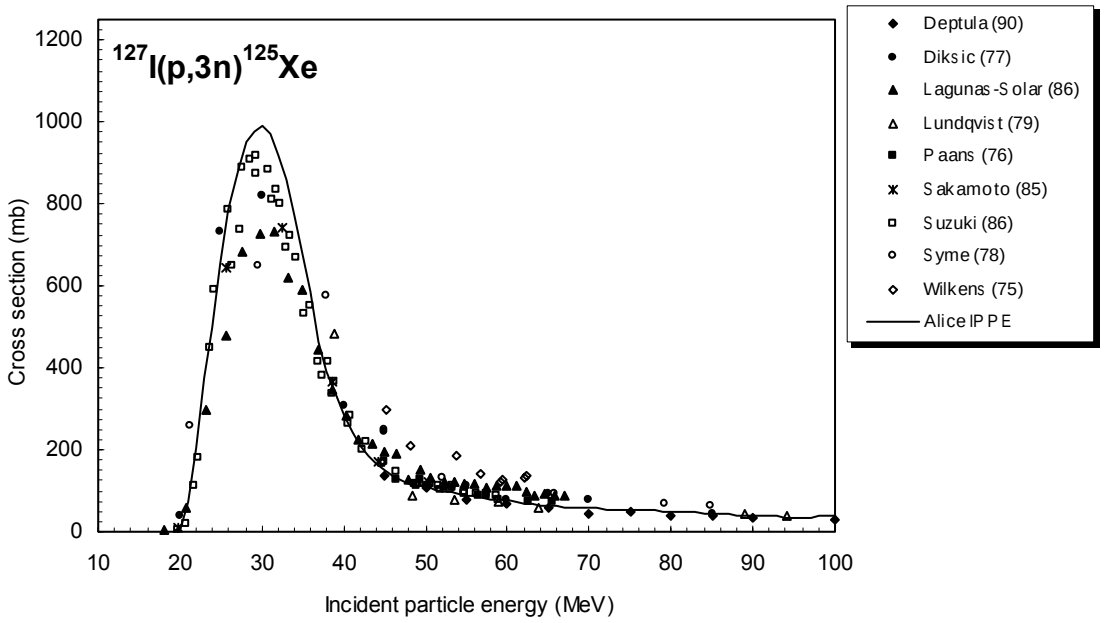

Figure 5.1.11b. Selected experimental data in comparison with theoretical calculation.

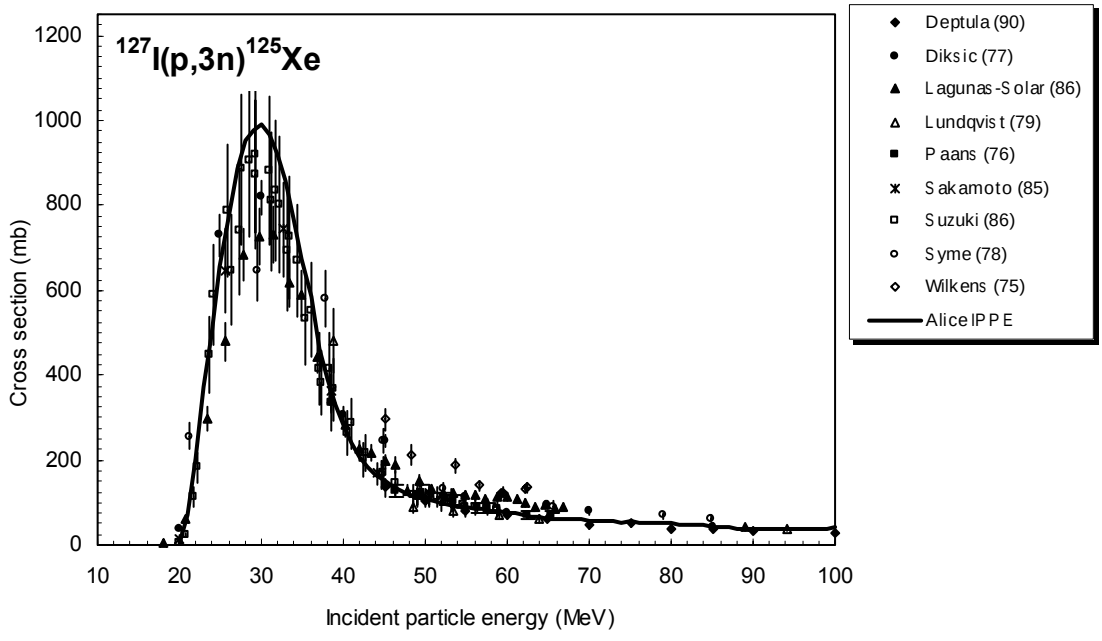

Figure 5.1.11c. Selected experimental data and recommended cross-section curve.

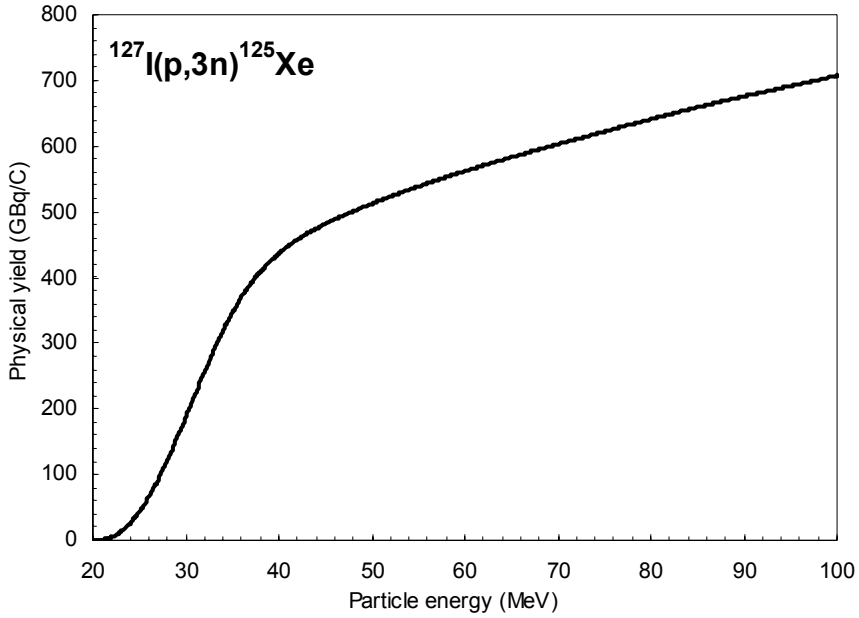

Figure 5.1.11d. Yield of ^{125}Xe calculated from the recommended cross-sections.

TABLE 5.1.11a. RECOMMENDED CROSS-SECTIONS FOR THE $^{127}I(p,3n)^{125}Xe$ REACTION

Energy MeV	Cross-section mb	Energy MeV	Cross-section mb	Energy MeV	Cross-section mb	Energy MeV	Cross-section mb
20.0	3.9	40.5	261	61.0	73.9	81.5	48.1
20.5	32.0	41.0	242	61.5	71.9	82.0	47.6
21.0	71.4	41.5	224	62.0	69.6	82.5	47.1
21.5	130	42.0	209	62.5	67.8	83.0	46.6
22.0	204	42.5	195	63.0	66.5	83.5	46.1
22.5	285	43.0	184	63.5	65.7	84.0	45.7
23.0	365	43.5	174	64.0	64.9	84.5	45.2
23.5	438	44.0	165	64.5	64.2	85.0	44.8
24.0	509	44.5	158	65.0	63.5	85.5	44.3
24.5	580	45.0	150	65.5	62.8	86.0	43.9
25.0	652	45.5	143	66.0	62.1	86.5	43.7
25.5	719	46.0	136	66.5	61.3	87.0	43.0
26.0	781	46.5	130	67.0	60.8	87.5	41.6
26.5	835	47.0	126	67.5	60.7	88.0	40.1
27.0	882	47.5	121	68.0	60.7	88.5	39.5
27.5	919	48.0	118	68.5	60.2	89.0	39.3
28.0	948	48.5	116	69.0	59.5	89.5	38.9
28.5	969	49.0	114	69.5	58.9	90.0	38.5
29.0	982	49.5	113	70.0	58.3	90.5	38.1
29.5	988	50.0	110	70.5	57.8	91.0	37.7
30.0	988	50.5	108	71.0	57.2	91.5	37.3
30.5	981	51.0	105	71.5	56.5	92.0	37.0
31.0	967	51.5	102	72.0	56.0	92.5	37.1
31.5	947	52.0	100	72.5	55.5	93.0	37.2
32.0	921	52.5	97.7	73.0	54.9	93.5	36.9
32.5	890	53.0	95.6	73.5	54.1	94.0	36.4
33.0	855	53.5	93.7	74.0	53.9	94.5	36.0
33.5	815	54.0	91.9	74.5	55.0	95.0	35.7
34.0	772	54.5	90.5	75.0	55.8	95.5	35.5
34.5	726	55.0	89.1	75.5	54.9	96.0	35.5
35.0	678	55.5	87.6	76.0	53.5	96.5	35.8
35.5	628	56.0	86.0	76.5	52.8	97.0	36.3
36.0	575	56.5	84.5	77.0	52.5	97.5	36.8
36.5	522	57.0	83.1	77.5	52.0	98.0	37.4
37.0	472	57.5	81.7	78.0	51.5	98.5	38.0
37.5	428	58.0	80.5	78.5	51.0	99.0	38.7
38.0	391	58.5	79.4	79.0	50.5	99.5	39.5
38.5	359	59.0	78.4	79.5	50.1	100.0	40.2
39.0	331	59.5	77.2	80.0	49.6		
39.5	305	60.0	76.1	80.5	49.1		
40.0	282	60.5	75.2	81.0	48.6		

TABLE 5.1.11b. YIELDS CALCULATED FROM THE RECOMMENDED CROSS-SECTION DATA FOR THE $^{127}I(p,3n)^{125}Xe$ REACTION. Y: PHYSICAL YIELD, A_1: ACTIVITY AFTER 1 HOUR AND 1 μA IRRADIATION, A_2: SATURATION ACTIVITY FOR 1 μA IRRADIATION.

Energy	Physical yield	Activity		Energy	Physical yield	Activity	
MeV	GBq/C	MBq	GBq	MeV	GBq/C	GBq	GBq
	Y	A_1	A_2		Y	A_1	A_2
20.0	0.010	0.035	0.00088	60.5	564	1.99	49.5
20.5	0.27	0.97	0.024	61.0	566	2.00	49.7
21.0	1.0	3.5	0.09	61.5	569	2.01	49.9
21.5	2.4	8.5	0.21	62.0	571	2.01	50.1
22.0	5	17	0.42	62.5	573	2.02	50.3
22.5	8	29	0.73	63.0	575	2.03	50.5
23.0	13	46	1.14	63.5	577	2.03	50.6
23.5	19	67	1.66	64.0	579	2.04	50.8
24.0	26	91	2.27	64.5	581	2.05	51.0
24.5	34	120	2.99	65.0	583	2.06	51.2
25.0	43	153	3.81	65.5	585	2.06	51.3
25.5	54	190	4.73	66.0	587	2.07	51.5
26.0	66	231	5.76	66.5	589	2.08	51.7
26.5	78	276	6.87	67.0	591	2.08	51.9
27.0	92	325	8.08	67.5	593	2.09	52.0
27.5	107	376	9.36	68.0	595	2.10	52.2
28.0	122	430	10.7	68.5	597	2.11	52.4
28.5	138	486	12.1	69.0	599	2.11	52.6
29.0	154	543	13.5	69.5	601	2.12	52.7
29.5	171	602	15.0	70.0	603	2.13	52.9
30.0	188	662	16.5	70.5	605	2.13	53.1
30.5	205	722	18.0	71.0	607	2.14	53.2
31.0	222	783	19.5	71.5	609	2.15	53.4
31.5	239	843	21.0	72.0	610	2.15	53.6
32.0	256	902	22.4	72.5	612	2.16	53.8
32.5	272	960	23.9	73.0	614	2.17	53.9
33.0	288	1016	25.3	73.5	616	2.17	54.1
33.5	304	1071	26.7	74.0	618	2.18	54.3
34.0	319	1123	28.0	74.5	620	2.19	54.4
34.5	333	1174	29.2	75.0	622	2.19	54.6
35.0	346	1221	30.4	75.5	624	2.20	54.8
35.5	359	1266	31.5	76.0	626	2.21	54.9
36.0	371	1307	32.5	76.5	628	2.21	55.1
36.5	381	1345	33.5	77.0	630	2.22	55.3
37.0	391	1380	34.3	77.5	632	2.23	55.4
37.5	400	1412	35.1	78.0	633	2.23	55.6
38.0	409	1442	35.9	78.5	635	2.24	55.8
38.5	416	1469	36.6	79.0	637	2.25	55.9
39.0	424	1494	37.2	79.5	639	2.25	56.1
39.5	430	1518	37.8	80.0	641	2.26	56.3
40.0	437	1540	38.3	80.5	643	2.27	56.4
40.5	442	1560	38.8	81.0	645	2.27	56.6
41.0	448	1579	39.3	81.5	646	2.28	56.7
41.5	453	1597	39.8	82.0	648	2.29	56.9
42.0	458	1614	40.2	82.5	650	2.29	57.1

TABLE 5.1.11b. (cont.)

Energy	Physical yield	Activity	Energy	Physical yield	Activity		
MeV	GBq/C Y	MBq A_1	GBq A_2	MeV	GBq/C Y	GBq A_1	GBq A_2
42.5	462	1630	40.6	83.0	652	2.30	57.2
43.0	466	1645	40.9	83.5	654	2.31	57.4
43.5	471	1660	41.3	84.0	655	2.31	57.5
44.0	474	1673	41.6	84.5	657	2.32	57.7
44.5	478	1687	42.0	85.0	659	2.32	57.8
45.0	482	1699	42.3	85.5	661	2.33	58.0
45.5	485	1711	42.6	86.0	662	2.34	58.1
46.0	489	1723	42.9	86.5	664	2.34	58.3
46.5	492	1734	43.2	87.0	666	2.35	58.4
47.0	495	1745	43.4	87.5	668	2.35	58.6
47.5	498	1756	43.7	88.0	669	2.36	58.7
48.0	501	1766	44.0	88.5	671	2.37	58.9
48.5	504	1777	44.2	89.0	672	2.37	59.0
49.0	507	1787	44.5	89.5	674	2.38	59.2
49.5	509	1797	44.7	90.0	676	2.38	59.3
50.0	512	1807	45.0	90.5	677	2.39	59.4
50.5	515	1817	45.2	91.0	679	2.39	59.6
51.0	518	1827	45.5	91.5	680	2.40	59.7
51.5	521	1836	45.7	92.0	682	2.41	59.8
52.0	523	1845	45.9	92.5	683	2.41	60.0
52.5	526	1855	46.2	93.0	685	2.42	60.1
53.0	528	1864	46.4	93.5	687	2.42	60.3
53.5	531	1873	46.6	94.0	688	2.43	60.4
54.0	533	1882	46.8	94.5	690	2.43	60.5
54.5	536	1890	47.0	95.0	691	2.44	60.7
55.0	538	1899	47.3	95.5	693	2.44	60.8
55.5	541	1908	47.5	96.0	694	2.45	60.9
56.0	543	1916	47.7	96.5	696	2.45	61.1
56.5	546	1925	47.9	97.0	697	2.46	61.2
57.0	548	1933	48.1	97.5	699	2.47	61.4
57.5	550	1941	48.3	98.0	701	2.47	61.5
58.0	553	1950	48.5	98.5	702	2.48	61.6
58.5	555	1958	48.7	99.0	704	2.48	61.8
59.0	557	1966	48.9	99.5	706	2.49	61.9
59.5	560	1974	49.1	100.0	708	2.50	62.1
60.0	562	1982	49.3				

5.1.12. $^{124}Xe(p,2n)^{123}Cs \rightarrow ^{123}Xe \rightarrow ^{123}I$

A total of 2 cross-section data sets were found in the literature and both could be used for evaluation.

The list of related references given below is accompanied with additional information. We mention availability of data in the computerized database EXFOR (if available, unique EXFOR reference number is given). Furthermore, we indicate a reason why a data set was excluded (reference denoted by an asterisk *).

Kurenkov, N.V., Malinin, A.B., Sebyakin, A.A., Venikov, N.I.:
Excitation functions of proton induced nuclear reactions on Xe-124: production of I-123.
J. Radioanalytical Nuclear Chemistry Letters **135** (1989) 39
— Exfor: A0436

Tárkányi, F., Qaim, S.M., Stöcklin, G., Sajjad, M., Lambrecht, R.M., Schweickert, H.:
Excitation functions of (p,2n) and (p,pn) reactions and differential and integral yields of I-123 in proton induced nuclear reactions on highly enriched Xe-124.
Applied Radiation Isotopes **42** (1991) 221
— Exfor: D4029

The data from papers where experimental numerical values were available (2 papers) are collected in Fig. 5.1.12a. Both were selected for further evaluation.

Cross-sections were calculated by two different versions of the nuclear reaction model code ALICE (denoted as HMS and IPPE), by the model code PREMOD-HFMODE-MOD (denoted as HF) and by two fitting procedures (Padé with 10 parameters and Spline). The results are compared with the selected experimental data in Fig. 5.1.12b. It is seen that the ALICE code overpredicts the experimental cross-sections while the code HF and fits perform better. The best approximation was judged to be the Padé fit. Recommended cross-sections are compared with selected experimental data, including their error bars, in Fig. .1.12c. Yields calculated from the recommended cross-sections are presented in Fig. 5.1.12d. The corresponding numerical values for recommended cross-sections and yields are tabulated in Table 5.1.12a, Table 5.1.12b. respectively.

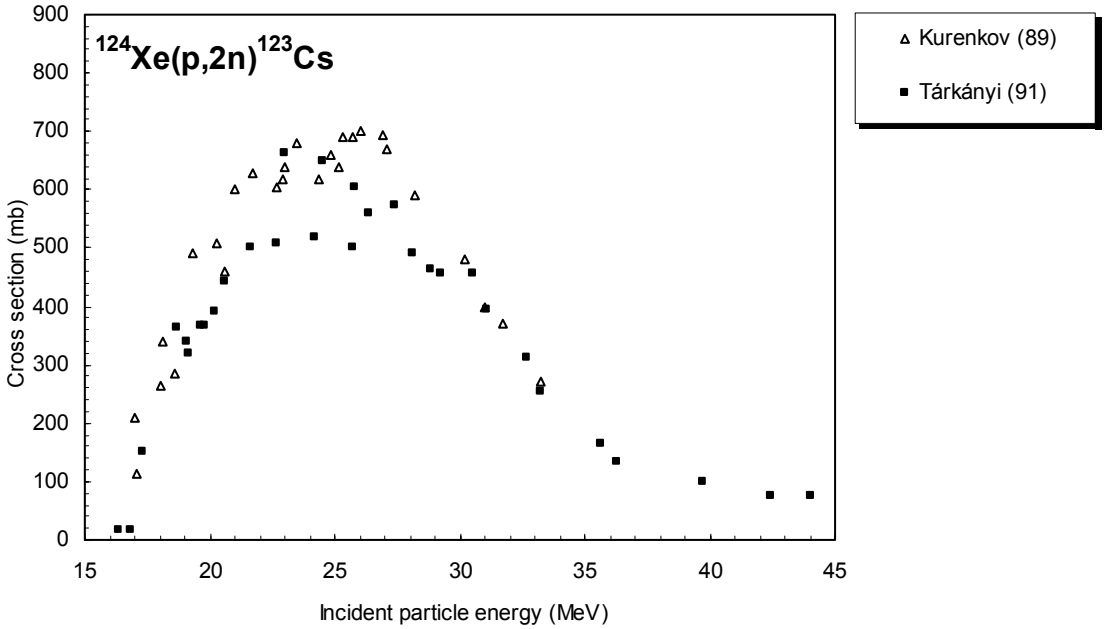

Figure 5.1.12a. All experimental data.

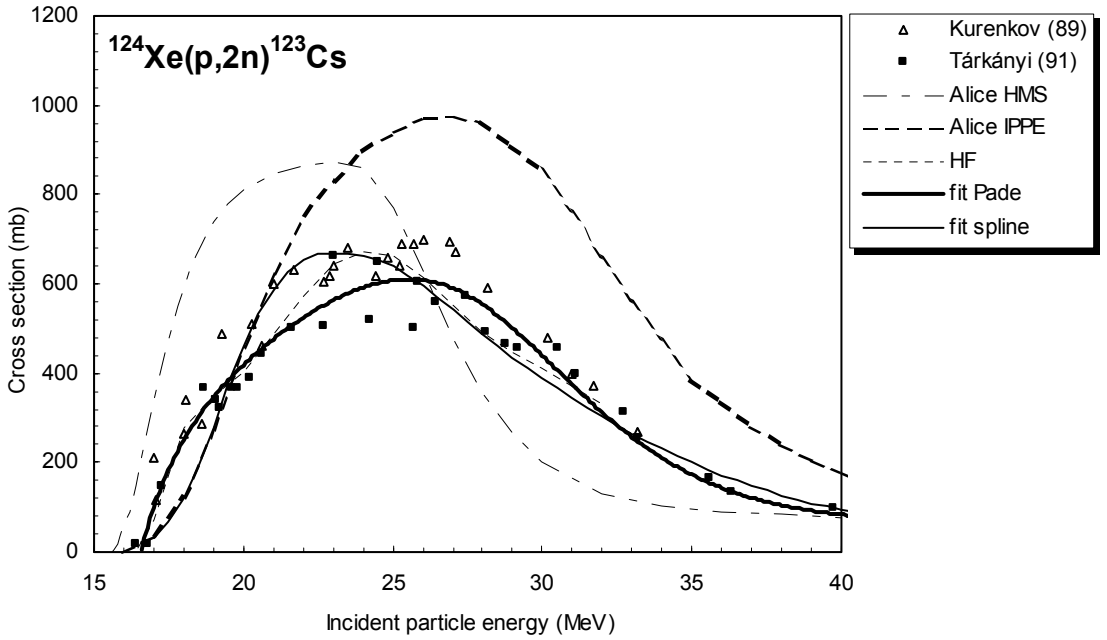

Figure 5.1.12b. Selected experimental data in comparison with theoretical calculations and fits

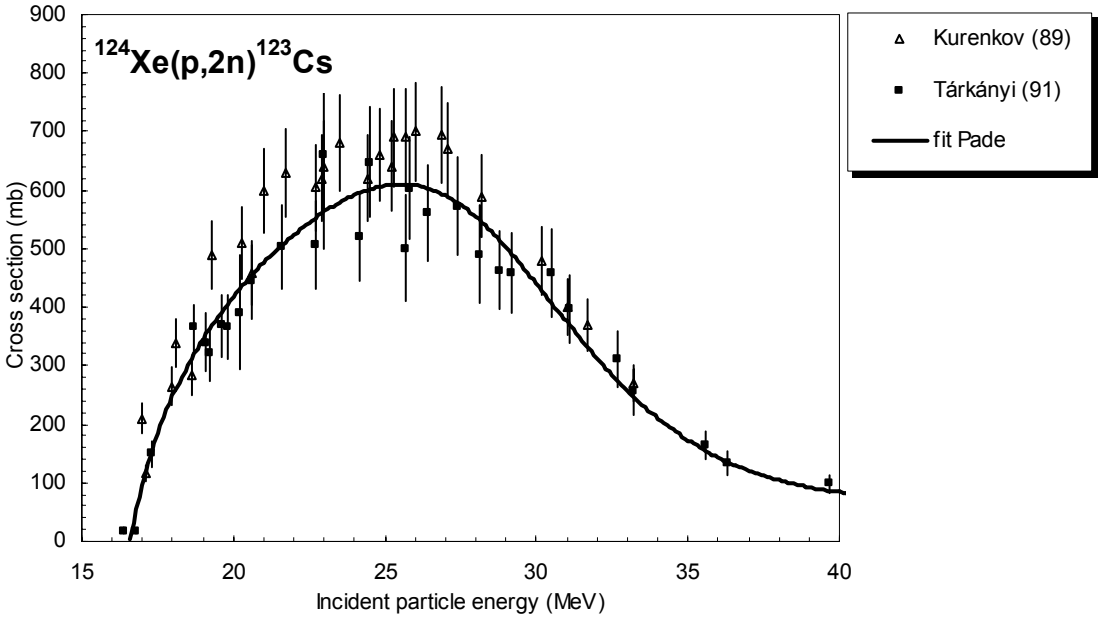

Figure 5.1.12c. Selected experimental data and recommended cross-section curve.

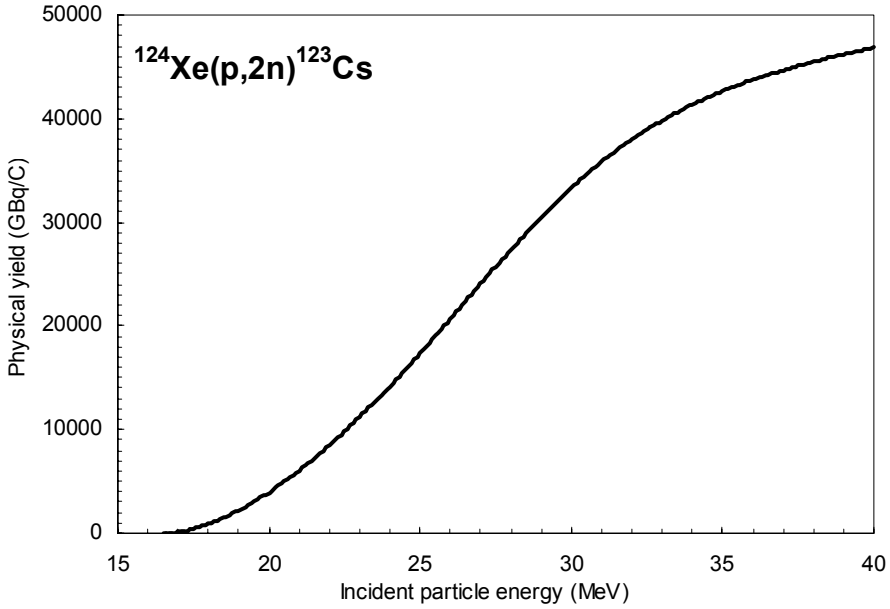

Figure 5.1.12d. Yield of ^{123}Cs calculated from the recommended cross-sections.

TABLE 5.1.12a. RECOMMENDED CROSS-SECTIONS FOR THE $^{124}Xe(p,2n)^{123}Cs$ REACTION

Energy MeV	Cross-section mb	Energy MeV	Cross-section mb	Energy MeV	Cross-section mb	Energy MeV	Cross-section mb
16.5	0.10	22.5	545	28.5	530	34.5	190
17.0	97.1	23.0	563	29.0	502	35.0	173
17.5	183	23.5	579	29.5	472	35.5	157
18.0	249	24.0	592	30.0	440	36.0	143
18.5	302	24.5	602	30.5	408	36.5	131
19.0	346	25.0	608	31.0	375	37.0	121
19.5	385	25.5	611	31.5	343	37.5	112
20.0	418	26.0	608	32.0	313	38.0	104
20.5	449	26.5	602	32.5	284	38.5	98.0
21.0	476	27.0	590	33.0	257	39.0	92.5
21.5	501	27.5	574	33.5	233	39.5	87.9
22.0	524	28.0	554	34.0	210	40.0	84.1

TABLE 5.1.12b. YIELDS CALCULATED FROM THE RECOMMENDED CROSS-SECTION DATA FOR THE $^{124}Xe(p,2n)^{123}Cs$ REACTION. Y: PHYSICAL YIELD, A_1: ACTIVITY AFTER 1 HOUR AND 1 μA IRRADIATION, A_2: SATURATION ACTIVITY FOR 1 μA IRRADIATION (*)

Energy MeV	Physical yield GBq/C Y	Activity GBq A_1	Activity GBq A_2	Energy MeV	Physical yield GBq/C Y	Activity GBq A_1	Activity GBq A_2
16.5	0.143	0.00002	0.00002	28.5	28947	14.7	14.7
17.0	105	0.053	0.054	29.0	30475	15.5	15.5
17.5	417	0.212	0.21	29.5	31933	16.2	16.2
18.0	888	0.45	0.45	30.0	33314	16.9	16.9
18.5	1491	0.76	0.76	30.5	34613	17.6	17.6
19.0	2210	1.12	1.12	31.0	35826	18.2	18.2
19.5	3033	1.54	1.54	31.5	36951	18.8	18.8
20.0	3952	2.01	2.01	32.0	37991	19.3	19.3
20.5	4960	2.52	2.52	32.5	38948	19.8	19.8
21.0	6053	3.07	3.08	33.0	39825	20.2	20.2
21.5	7227	3.67	3.67	33.5	40629	20.6	20.6
22.0	8479	4.30	4.31	34.0	41364	21.0	21.0
22.5	9805	4.98	4.98	34.5	42037	21.3	21.4
23.0	11201	5.69	5.69	35.0	42654	21.7	21.7
23.5	12664	6.43	6.43	35.5	43220	21.9	22.0
24.0	14185	7.20	7.21	36.0	43742	22.2	22.2
24.5	15759	8.00	8.01	36.5	44225	22.5	22.5
25.0	17377	8.82	8.83	37.0	44673	22.7	22.7
25.5	19027	9.66	9.67	37.5	45092	22.9	22.9
26.0	20701	10.5	10.5	38.0	45485	23.1	23.1
26.5	22385	11.4	11.4	38.5	45857	23.3	23.3
27.0	24065	12.2	12.2	39.0	46210	23.5	23.5
27.5	25729	13.1	13.1	39.5	46548	23.6	23.7
28.0	27360	13.9	13.9	40.0	46874	23.8	23.8

* Regarding the yield values see ‘Remark’ in the appendix.

5.1.13 ^{124}Xe(p,pn)^{123}Xe→^{123}I

A total of 2 cross-section data sets were found in the literature and could be used for evaluation. The list of related references given below is accompanied with additional information. We mention availability of data in the computerized database EXFOR (if available, unique EXFOR reference number is given). Furthermore, we indicate a reason why a data set was excluded (reference denoted by an asterisk *).

Kurenkov, N.V., Malinin, A.B., Sebyakin, A.A., Venikov, N.I.:
Excitation functions of proton induced nuclear reactions on Xe-124: Production of I-123.
J. Radioanalytical Nuclear Chemistry Letters **135** (1989) 39
— Exfor: A0436

Tárkányi, F., Qaim, S.M., Stöcklin, G., Sajjad, M., Lambrecht, R.M., Schweickert, H.:
Excitation functions of (p,2n) and (p,pn) reactions and differential and integral yields of I-123 in proton induced nuclear reactions on highly enriched Xe-124.
Applied Radiation Isotopes **42** (1991) 221
— Exfor: D4029

The data from papers where experimental numerical values were available (2 papers), are collected in Fig. 5.1.13a. Both of them give independent formation cross-sections of ^{123}Xe, I.e. without the contribution of the ^{123}Cs→^{123}Xe decay process. Both were selected for further evaluation.

Cross-sections were calculated by two different versions of the nuclear reaction model code ALICE (denoted as HMS and IPPE), by the model code PREMOD-HFMOD (denoted as HF) and by two fitting procedures (Padé with 10 parameters and Spline). Separate Padé fittings were done for the two data sets (denoted by K and T for data set of Kurenkov et al., Tárkányi et al. respectively). The results are compared with the selected experimental data in Fig. 5.1.13b. It is seen that the ALICE HMS and the HF overpredict the cross-sections while the code ALICE IPPE results in too high values above 30 MeV. The separate Padé calculations fit well to the corresponding experimental data. The best approximation was judged to be the Padé fits, but no decision was made; therefore both the results are given here. Fitted cross-sections are compared with selected experimental data, including their error bars, in Fig. 5.1.13c. Yields calculated from the fitted cross-sections are presented in Fig. 5.1.13d. The corresponding numerical values for cross-sections and yields are tabulated in Table 5.1.13a and Table 5.1.13b, respectively.

The large differences in experimental data and calculated cross-sections for this reaction reflect the following comments:
(1) difficulty in experimental measurement and data evaluation for gas targets;
(2) difficulty in determining the independent formation cross-section of a radionuclide when it is also formed via the decay of a strong short-lived precursor (difference of two large numbers);
(3) theoretical calculations for the (p, pn) process are not as reliable as for (p,xn) reactions;
(4) internal contradictions in yields and cross-sections were observed in Kurenkov et al. (89);
(5) the reaction contributes only to a small extent to the total ^{123}I production on ^{124}Xe targets.

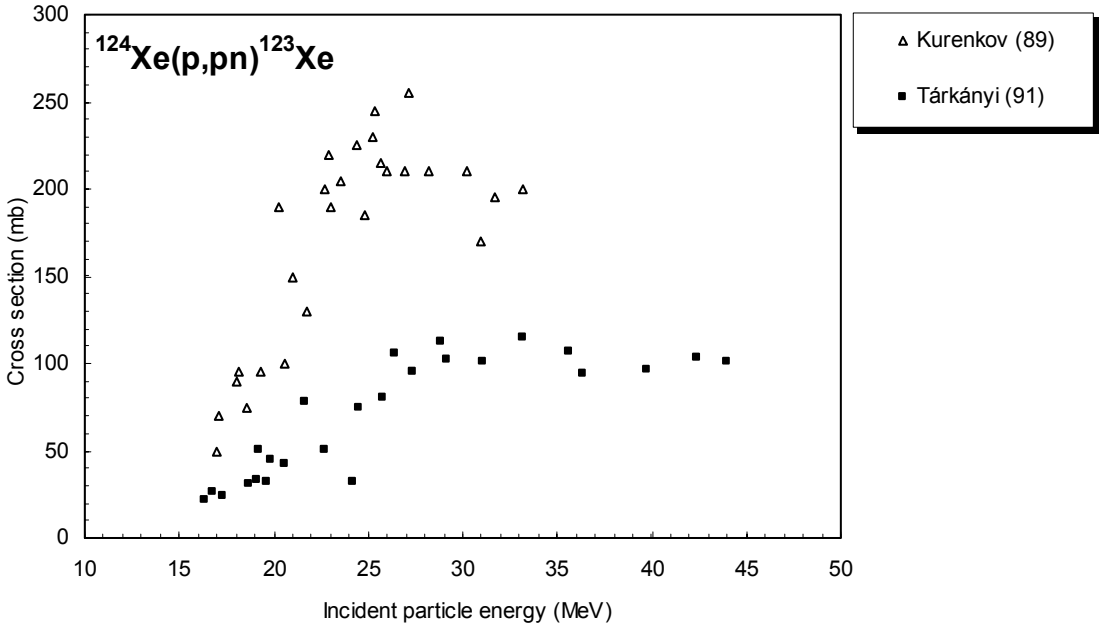

Figure 5.1.13a. All experimental data.

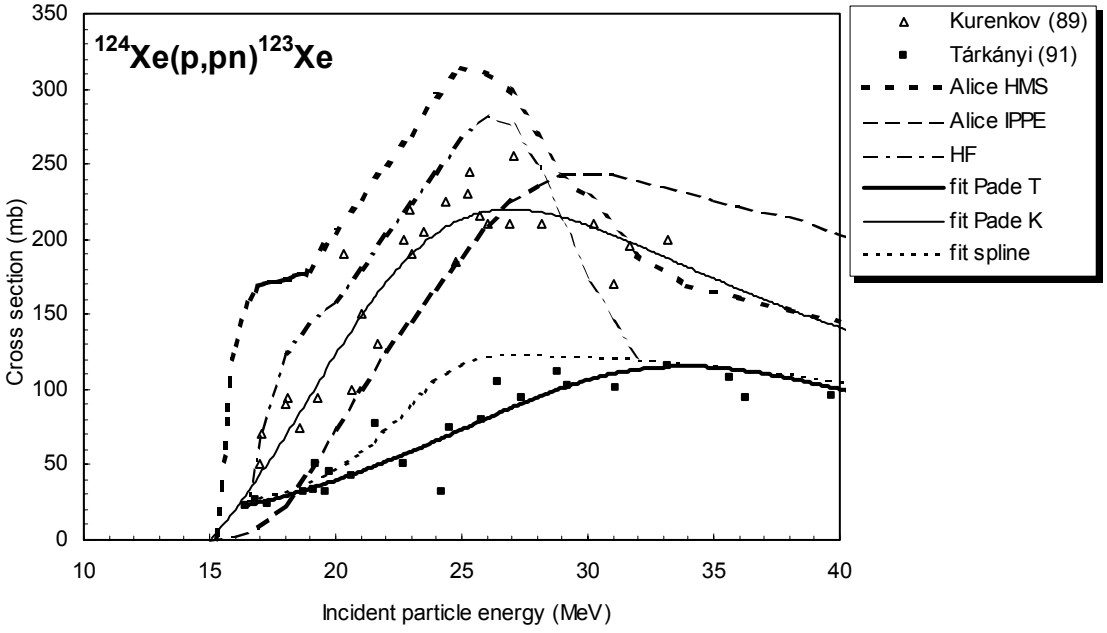

Figure 5.1.13b. Experimental data in comparison with theoretical calculations and fits.

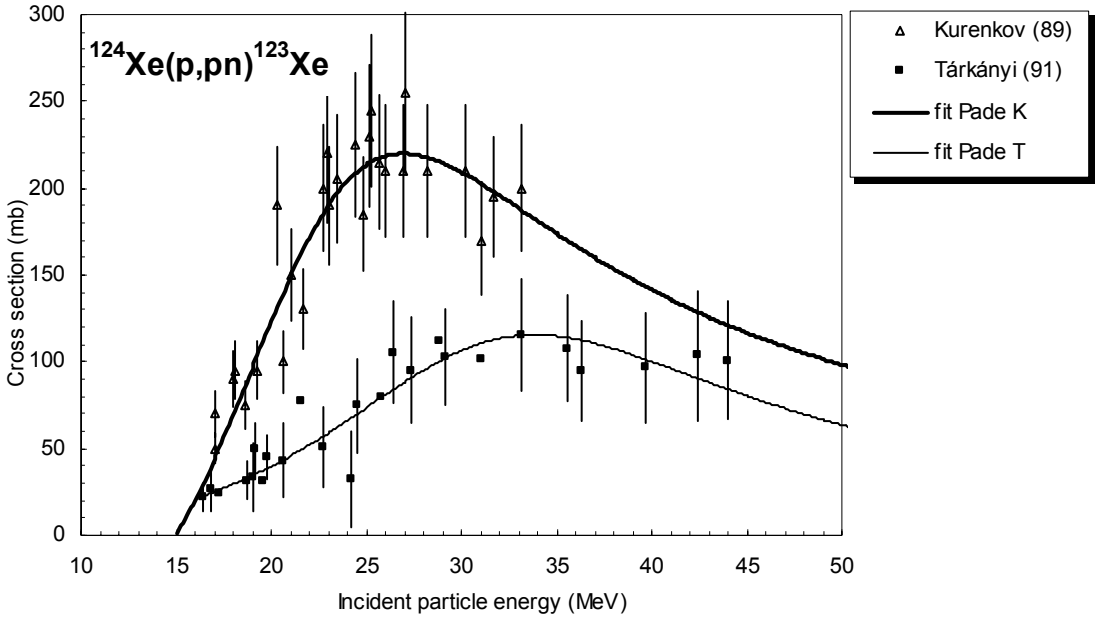

Figure 5.1.13c. Experimental data and fitted cross-section curves.

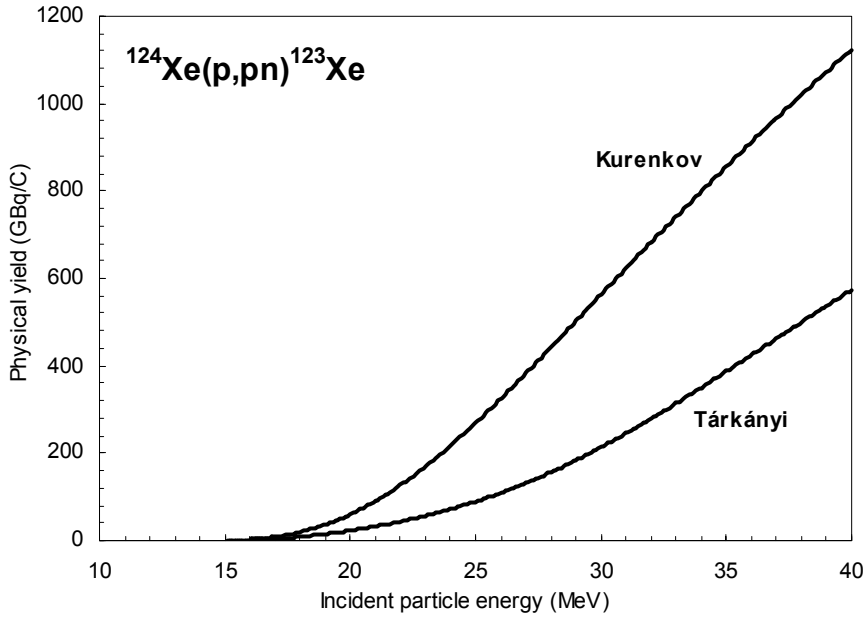

Figure 5.1.13d. Yield of ^{123}Xe calculated from the fitted cross-sections.

TABLE 5.1.13a. FITTED CROSS-SECTIONS FOR THE $^{124}Xe(p,pn)^{123}Xe$ REACTION DATA

Kurenkov et al. data

Energy MeV	Cross-section mb	Energy MeV	Cross-section mb	Energy MeV	Cross-section mb	Energy MeV	Cross-section mb
15.5	9.4	22.0	171	28.5	216.7	35.0	173.9
16.0	20.0	22.5	181	29.0	214.6	35.5	170.3
16.5	31.4	23.0	190	29.5	212.1	36.0	166.8
17.0	43	23.5	198	30.0	209.2	36.5	163.3
17.5	56	24.0	204	30.5	206.2	37.0	160.0
18.0	69	24.5	209	31.0	202.9	37.5	156.7
18.5	83	25.0	213	31.5	199.4	38.0	153.4
19.0	96	25.5	216	32.0	195.8	38.5	150.3
19.5	110	26.0	219	32.5	192.2	39.0	147.2
20.0	123	26.5	220	33.0	188.5	39.5	144.3
20.5	136	27.0	220	33.5	184.9	40.0	141.4
21.0	149	27.5	219	34.0	181.2		
21.5	160	28.0	218	34.5	177.5		

Tárkányi et al. data

Energy MeV	Cross-section mb	Energy MeV	Cross-section mb	Energy MeV	Cross-section mb	Energy MeV	Cross-section mb
16.5	23.0	22.5	55	28.5	98.2	34.5	115.3
17.0	25.0	23.0	59	29.0	101.2	35.0	114.8
17.5	27.2	23.5	62	29.5	103.9	35.5	114.1
18.0	29	24.0	66	30.0	106.4	36.0	113.1
18.5	32	24.5	70	30.5	108.6	36.5	112.0
19.0	34	25.0	73	31.0	110.6	37.0	110.6
19.5	37	25.5	77	31.5	112.2	37.5	109.2
20.0	40	26.0	81	32.0	113.5	38.0	107.5
20.5	43	26.5	85	32.5	114.4	38.5	105.8
21.0	46	27.0	88	33.0	115.1	39.0	104.0
21.5	49	27.5	92	33.5	115.5	39.5	102.1
22.0	52	28.0	95	34.0	115.5	40.0	100.2

TABLE 5.1.13b. YIELDS CALCULATED FROM THE RECOMMENDED CROSS-SECTION DATA FOR THE $^{124}Xe(p,pn)^{123}Xe$ REACTION. Y: PHYSICAL YIELD, A_1: ACTIVITY AFTER 1 HOUR AND 1 μA IRRADIATION, A_2: SATURATION ACTIVITY FOR 1 μA IRRADIATION

Kurenkov et al.

Energy	Physical yield	Activity		Energy	Physical yield	Activity	
MeV	GBq/C	GBq	GBq	MeV	GBq/C	GBq	GBq
	Y	A_1	A_2		Y	A_1	A_2
15.5	0.480	0.0015	0.00518	28.0	442	1.35	4.78
16.0	1.91	0.006	0.021	28.5	472	1.45	5.10
16.5	4.4	0.013	0.05	29.0	502	1.54	5.43
17.0	8.1	0.02	0.09	29.5	533	1.63	5.75
17.5	13.0	0.04	0.14	30.0	563	1.72	6.08
18.0	19.3	0.06	0.21	30.5	593	1.82	6.41
18.5	27.1	0.08	0.29	31.0	623	1.91	6.73
19.0	36.4	0.11	0.39	31.5	653	2.00	7.05
19.5	47.3	0.14	0.51	32.0	683	2.09	7.37
20.0	59.9	0.18	0.65	32.5	712	2.18	7.69
20.5	74.1	0.23	0.80	33.0	741	2.27	8.01
21.0	90.0	0.28	0.97	33.5	771	2.36	8.32
21.5	108	0.33	1.16	34.0	799	2.45	8.64
22.0	127	0.39	1.37	34.5	828	2.53	8.94
22.5	147	0.45	1.59	35.0	856	2.62	9.25
23.0	169	0.52	1.83	35.5	884	2.71	9.55
23.5	193	0.59	2.08	36.0	912	2.79	9.85
24.0	217	0.66	2.35	36.5	940	2.88	10.1
24.5	243	0.74	2.62	37.0	967	2.96	10.4
25.0	269	0.82	2.91	37.5	994	3.04	10.7
25.5	297	0.91	3.21	38.0	1020	3.12	11.0
26.0	325	0.99	3.51	38.5	1047	3.20	11.3
26.5	354	1.08	3.82	39.0	1073	3.28	11.6
27.0	383	1.17	4.14	39.5	1099	3.36	11.9
27.5	412	1.26	4.46	40.0	1124	3.44	12.1

TABLE 5.1.13b. (cont.)

Tárkányi et al.

Energy MeV	Physical yield GBq/C Y	Activity GBq A_1	Activity GBq A_2	Energy MeV	Physical yield GBq/C Y	Activity GBq A_1	Activity GBq A_2
16.5	0.853	0.0026	0.00921	28.5	170	0.52	1.84
17.0	3.15	0.010	0.034	29.0	184	0.56	1.99
17.5	5.70	0.017	0.06	29.5	198	0.61	2.14
18.0	8.52	0.03	0.09	30.0	214	0.65	2.31
18.5	11.6	0.04	0.13	30.5	229	0.70	2.48
19.0	15.0	0.05	0.16	31.0	245	0.75	2.65
19.5	18.8	0.06	0.20	31.5	262	0.80	2.83
20.0	22.9	0.07	0.25	32.0	279	0.85	3.01
20.5	27.4	0.08	0.30	32.5	296	0.91	3.20
21.0	32.3	0.10	0.35	33.0	314	0.96	3.39
21.5	37.7	0.12	0.41	33.5	332	1.02	3.59
22.0	43.5	0.13	0.47	34.0	350	1.07	3.78
22.5	49.7	0.15	0.54	34.5	369	1.13	3.98
23.0	56.5	0.17	0.61	35.0	387	1.19	4.18
23.5	63.9	0.20	0.69	35.5	406	1.24	4.39
24.0	71.7	0.22	0.77	36.0	425	1.30	4.59
24.5	80.2	0.25	0.87	36.5	444	1.36	4.79
25.0	89.2	0.27	0.96	37.0	462	1.42	4.99
25.5	98.9	0.30	1.07	37.5	481	1.47	5.20
26.0	109	0.33	1.18	38.0	500	1.53	5.40
26.5	120	0.37	1.30	38.5	518	1.59	5.60
27.0	132	0.40	1.42	39.0	537	1.64	5.80
27.5	144	0.44	1.55	39.5	555	1.70	5.99
28.0	156	0.48	1.69	40.0	573	1.75	6.19

5.1.14. ^{203}Tl(p,3n)^{201}Pb→^{201}Tl

A total of 8 cross-section data sets (in 7 works) were found in the literature. From these, 4 data sets were excluded while the other 4 were selected for further evaluation. Only in Bonardi (83)b data for partially (87%) enriched ^{203}Tl targets were published. All the other data were converted from measurements on natural targets, adopting 29.5% isotopic abundance of ^{203}Tl. The list of related references given below is accompanied with additional information. We mention availability of data in the computerized database EXFOR (if available, unique EXFOR reference number is given). Furthermore, we indicate a reason why a data set was excluded (reference denoted by an asterisk *).

*** Blue, J.W., Liu, D.C., Smathers, J.B.:**
Thallium 201 production with the idle beam from neutron therapy.
Medical Physics **5** (1978) 532
— Exfor: none
— Data excluded: cross-section values too low.

Bonardi, M., Birattari, C., Salomone, A.:
^{201}Tl production for medical use by (p,xn) nuclear reactions on Tl and Hg natural and enriched targets.
Proc. Int. Conf. Nuclear Data for Science and Technology, September 1982, Antwerp, Belgium (ed. Böckhoff, K.H.), D. Riedel, The Netherlands (1983) 916
Additional information in: F. Girardi, L. Goetz, E. Sabbioni, E. Marafante, M. Merlini, E. Acerbi, C. Birattari, M. Castiglioni, F. Resmini
Preparation of ^{203}Pb compounds for studies on pathways and effects of lead pollution
Int. J. Applied Radiation Isotopes **26** (1975) 267
— Exfor: none
— Data on natural targets excluded: cross-section values too low.

Hermanne, A., Walravens, N., Cichelli, C.:
Optimisation of isotope production by cross-section determination.
Proc. Int. Conf. Nuclear Data for Science and Technology, May 1991, Jülich, FRG
(ed. Qaim, S.M.) Springer Verlag, Berlin (1992) 616
also private communication by authors
— Exfor: A0494

Lagunas-Solar, M.C., Jungerman, J.A., Peek, N.F., Theus, R.M.:
Thallium-201 yields and excitation functions for the lead activities produced by irradiation of natural thallium with 15-60 MeV protons.
Int. J. Applied Radiation Isotopes **29** (1978) 159
— Exfor: B0168

*** Lebowitz, G., Greene, M.W., Fairchild, R., Bradley-Moore, P.R., Atkins, H.L., Ansari, A.N., Richards, P., Belgrave, E.:**
Thallium-201 for medical use.
J. Nuclear Medicine **16** (1975) 151
— Exfor: none
— Data excluded: cross-section values too low.

*** Sakai, M., Ikegama, H., Yamazaki, T., Saito, K.:**
Nuclear Physics **65** (1965) 177
Data file in Physics Data Nr. 15-5, 1982
— Exfor: P013
— Data excluded: discrepant.

Qaim, S.M., Weinreich, R., Ollig, H.:
Production of ^{201}Tl and ^{203}Pb via proton induced nuclear reactions on natural thallium.
Int. J. Applied Radiation Isotopes **30** (1979) 85
— Exfor: none

The data from papers where experimental numerical values were available (8 data sets in 7 papers) are collected in Fig. 5.1.14a. From these, 4 works were excluded while the remaining 4 were selected for further evaluation.

Cross-sections were calculated by two different versions of the nuclear reaction model code ALICE (denoted as HMS(FG) and IPPE), by the model code PREMOD-HFMOD (denoted as HF) and by spline fit method. The results are compared with the selected experimental data in Fig. 5.1.14b. The model calculations do not predict well enough the experimental cross-sections. The best approximation was judged to be the spline fit. Recommended cross-sections are compared with selected experimental data, including their error bars, in Fig. 5.1.14c. Yields calculated from the recommended cross-sections are presented in Fig. 5.1.14d. The corresponding numerical values for recommended cross-sections and yields are tabulated in Table 5.1.14a and Table 5.1.14b, respectively.

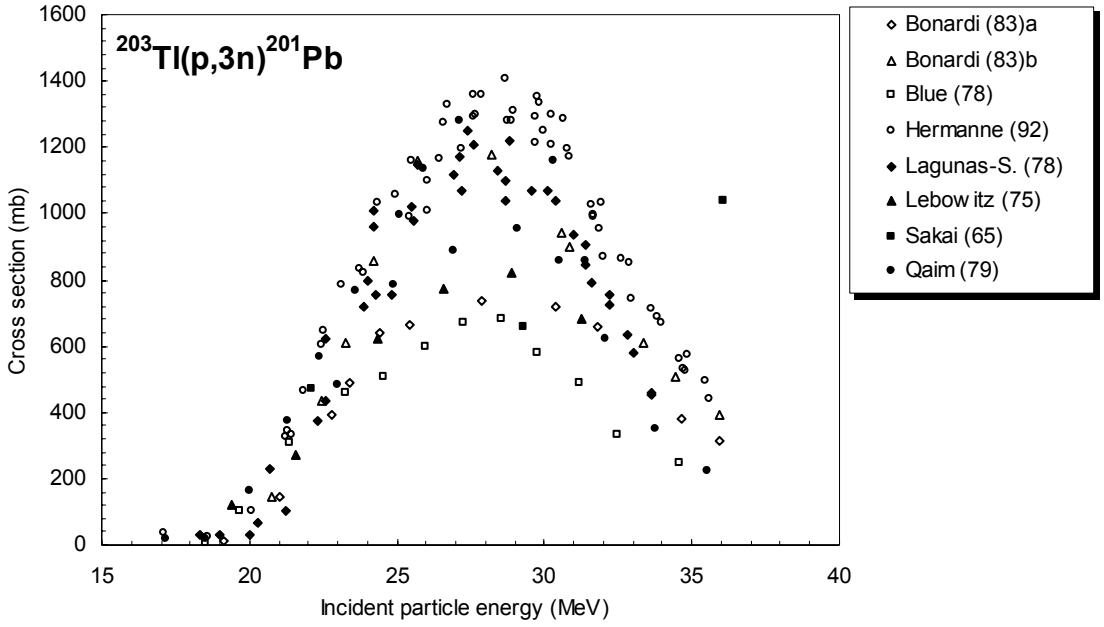

Figure 5.1.14a. All experimental data.

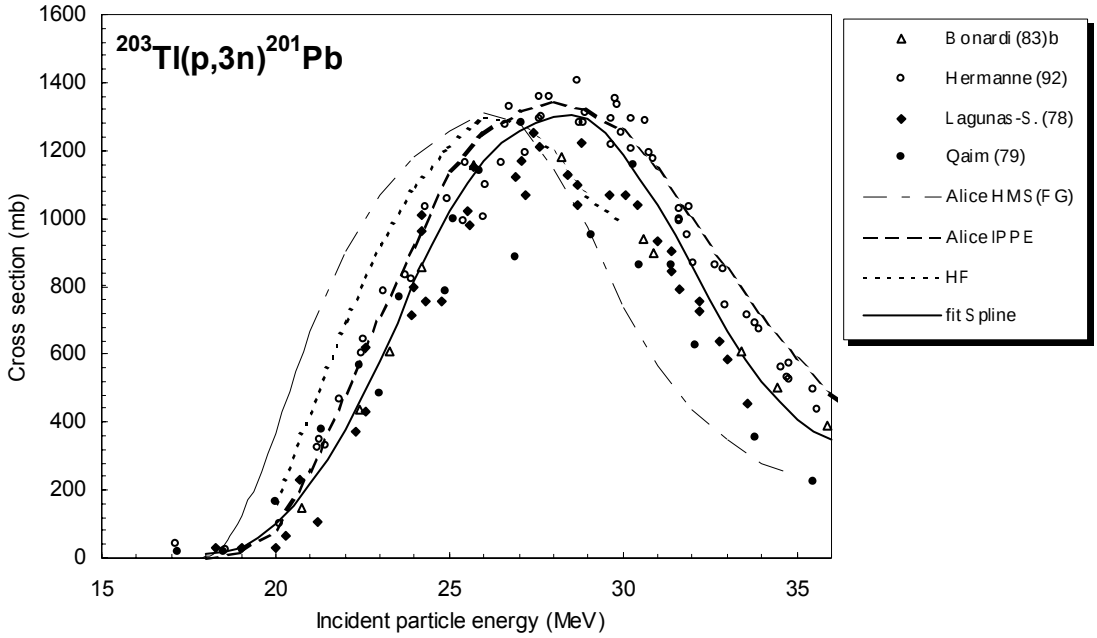

Figure 5.1.14b. Selected experimental data in comparison with theoretical calculations and fits

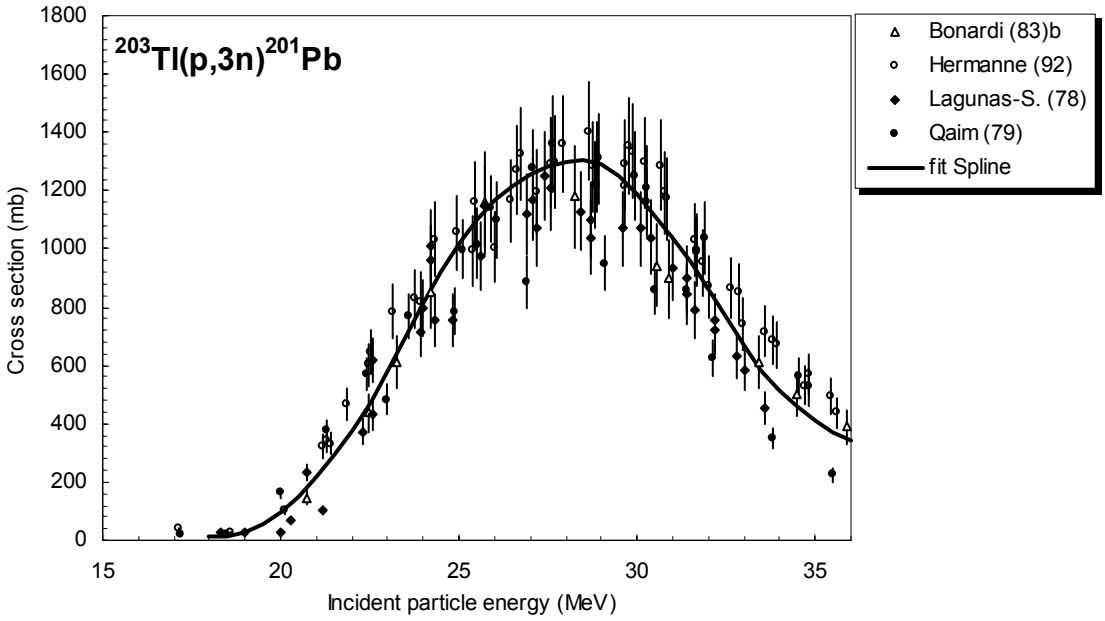

Figure 5.1.14c. Selected experimental data and recommended cross-section curve.

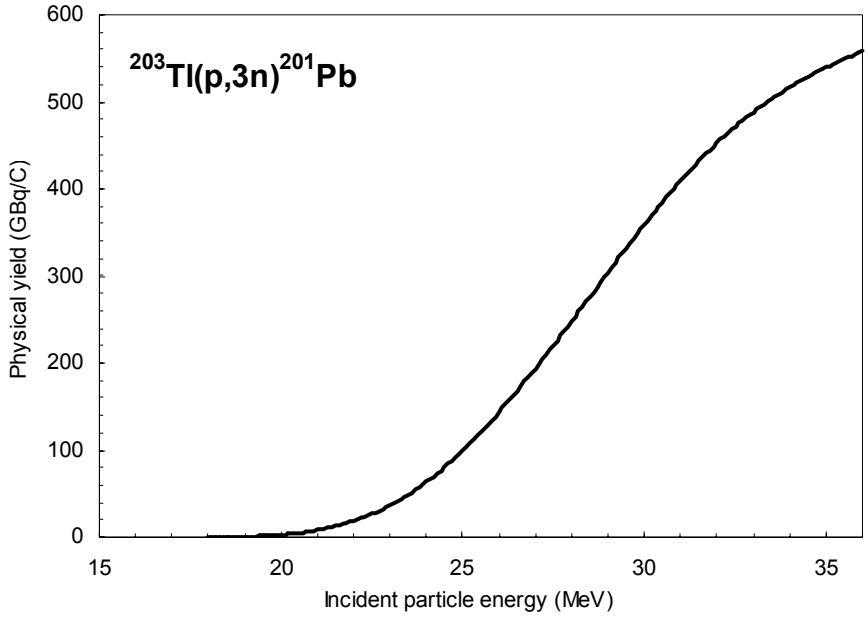

Figure 5.1.14d. Yield of ^{201}Pb calculated from the recommended cross-sections.

TABLE 5.1.14a. RECOMMENDED CROSS-SECTIONS FOR THE $^{203}Tl(p,3n)^{201}Pb$ REACTION

Energy MeV	Cross-section mb	Energy MeV	Cross-section mb	Energy MeV	Cross-section mb	Energy MeV	Cross-section mb
18.0	12.9	23.0	579	28.0	1299	33.0	668
18.5	15.3	23.5	693	28.5	1304	33.5	587
19.0	30.4	24.0	812	29.0	1289	34.0	517
19.5	58.2	24.5	923	29.5	1249	34.5	458
20.0	98.6	25.0	1020	30.0	1187	35.0	410
20.5	152	25.5	1102	30.5	1115	35.5	373
21.0	217	26.0	1168	31.0	1037	36.0	347
21.5	292	26.5	1219	31.5	953		
22.0	378	27.0	1255	32.0	859		
22.5	473	27.5	1282	32.5	760		

TABLE 5.1.14b. YIELDS CALCULATED FROM THE RECOMMENDED CROSS-SECTION DATA FOR THE $^{203}Tl(p,3n)^{201}Pb$ REACTION. Y: PHYSICAL YIELD, A_1: ACTIVITY AFTER 1 HOUR AND 1 μA IRRADIATION, A_2: SATURATION ACTIVITY FOR 1 μA IRRADIATION (*)

Energy MeV	Physical yield GBq/C Y	Activity GBq A_1	Activity GBq A_2	Energy MeV	Physical yield GBq/C Y	Activity GBq A_1	Activity GBq A_2
18.0	0.04	0.00014	0.00196	27.5	220	0.76	10.7
18.5	0.26	0.001	0.012	28.0	248	0.86	12.0
19.0	0.63	0.002	0.03	28.5	276	0.96	13.4
19.5	1.4	0.00	0.07	29.0	304	1.05	14.7
20.0	2.8	0.01	0.13	29.5	332	1.15	16.1
20.5	5.0	0.02	0.24	30.0	359	1.25	17.4
21.0	8.2	0.03	0.40	30.5	385	1.33	18.6
21.5	12.8	0.04	0.62	31.0	409	1.42	19.8
22.0	19.0	0.07	0.92	31.5	432	1.50	20.9
22.5	26.8	0.09	1.30	32.0	453	1.57	21.9
23.0	36.7	0.13	1.78	32.5	472	1.64	22.9
23.5	48.8	0.17	2.37	33.0	488	1.69	23.7
24.0	63.4	0.22	3.07	33.5	503	1.75	24.4
24.5	80.3	0.28	3.89	34.0	517	1.79	25.0
25.0	100	0.35	4.82	34.5	528	1.83	25.6
25.5	121	0.42	5.85	35.0	539	1.87	26.1
26.0	144	0.50	6.97	35.5	549	1.90	26.6
26.5	168	0.58	8.15	36.0	558	1.94	27.0
27.0	194	0.67	9.39				

* Regarding the yield values see ‘Remark’ in the appendix.

5.1.15 ^{203}Tl(p,2n)^{202m}Pb→^{202}Tl

This reaction is the major contributor to the radionuclidic impurities in the production of ^{201}Pb→^{201}Tl.

A total of 4 cross-section data sets were found in the literature in the energy range considered. All of them were selected for further evaluation. Data measured on natural targets were transformed to represent the ^{203}Tl(p,2n)^{202m}Pb reaction only up to 27 MeV (below threshold of ^{205}Tl (p,4n) reaction). Only data sets that where already selected for the ^{203}Tl(p,3n)^{201}Pb reaction were considered.

The list of related references given below is accompanied with additional information. We mention availability of data in the computerized database EXFOR (if available, unique EXFOR reference number is given). Furthermore, we indicate a reason why a data set was excluded (reference denoted by an asterisk *).

Bonardi, M., Birattari, C., Salomone, A.:
^{201}Tl production for medical use by (p,xn) nuclear reactions on Tl and Hg natural and enriched targets.
Proc. Int. Conf. Nuclear Data for Science and Technology, September 1982, Antwerp, Belgium (ed. Böckhoff, K.H.), D. Reidel, The Netherlands (1983) 916
Additional information in: F. Girardi, L. Goetz, E. Sabbioni, E. Marafante, M. Merlini, E Acerbi, C. Birattari, M. Castiglioni, F. Resmini
Preparation of ^{203}Pb compounds for studies on pathways and effects of lead pollution
Int. J. Applied Radiation Isotopes **26** (1975) 267
— Exfor: none

Hermanne, A., Walravens, N., Cichelli, C.:
Optimisation of isotope production by cross-section determination.
Proc. Int. Conf. Nuclear Data for Science and Technology, May 1991, Jülich, FRG
(ed. Qaim, S.M.) Springer Verlag, Berlin (1992) 616
also private communication by authors
— Exfor: A0494

Lagunas-Solar, M.C., Jungerman, J.A., Peek, N.F., Theus, R.M.:
Thallium-201 yields and excitation functions for the lead activities produced by irradiation of natural thallium with 15-60 MeV protons.
Int. J. Applied Radiation Isotopes **29** (1978) 159
— Exfor: B0168

Qaim, S.M., Weinreich, R., Ollig, H.:
Production of ^{201}Tl and ^{203}Pb via proton induced nuclear reactions on natural thallium.
Int. J. Applied Radiation Isotopes **30** (1979) 85
— Exfor: none

The data from papers where experimental numerical values were available (4 papers) are collected in Fig. 5.1.15a. All the 4 works were selected for further evaluation.

No calculations were performed as the codes only give access to total cross-sections and not to separate isomers.

Cross-sections were calculated by Padé fit with 20 parameters. The results are compared with the selected experimental data in Fig. 5.1.15b. The best approximation was judged to be the Padé fit. Recommended cross-sections are compared with selected experimental data, including their error bars, in Fig. 5.1.15c. Yields calculated from the recommended cross-sections are presented in Fig. 5.1.15d. The corresponding numerical values for recommended cross-sections and yields are tabulated in Table 5.1.15a and Table 5.1.15b, respectively.

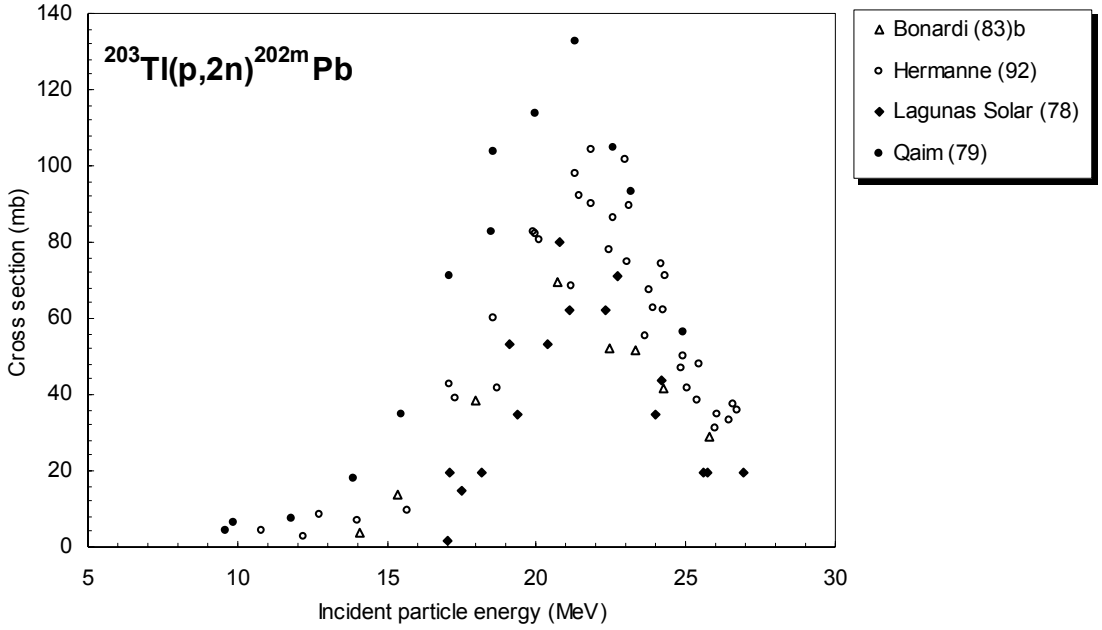

Figure 5.1.15a. All experimental data.

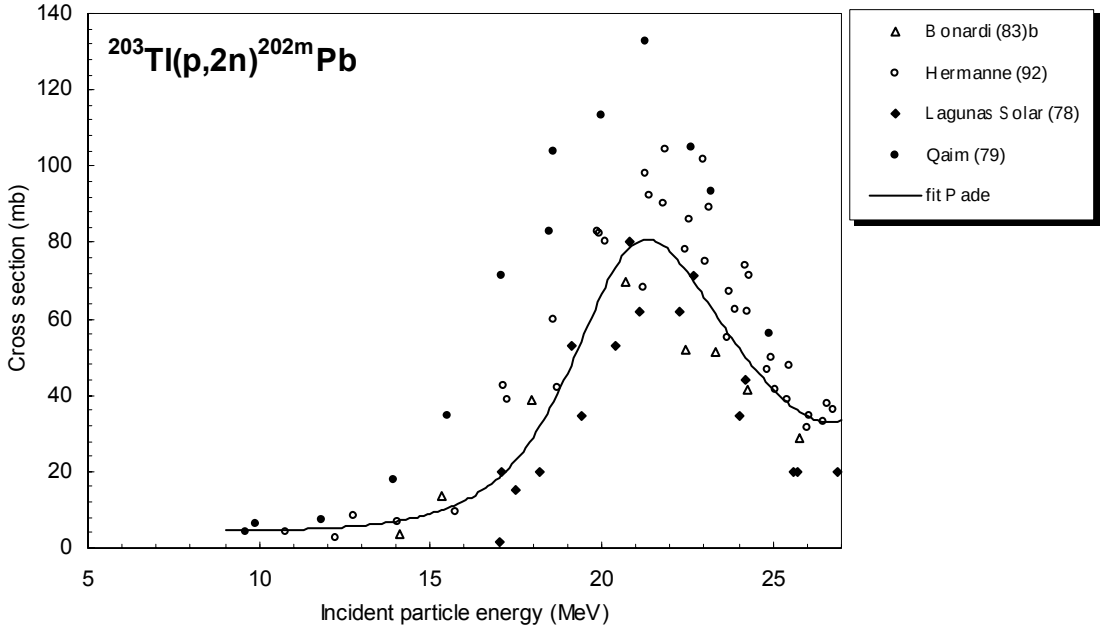

Figure 5.1.15b. Selected experimental data in comparison with fits.

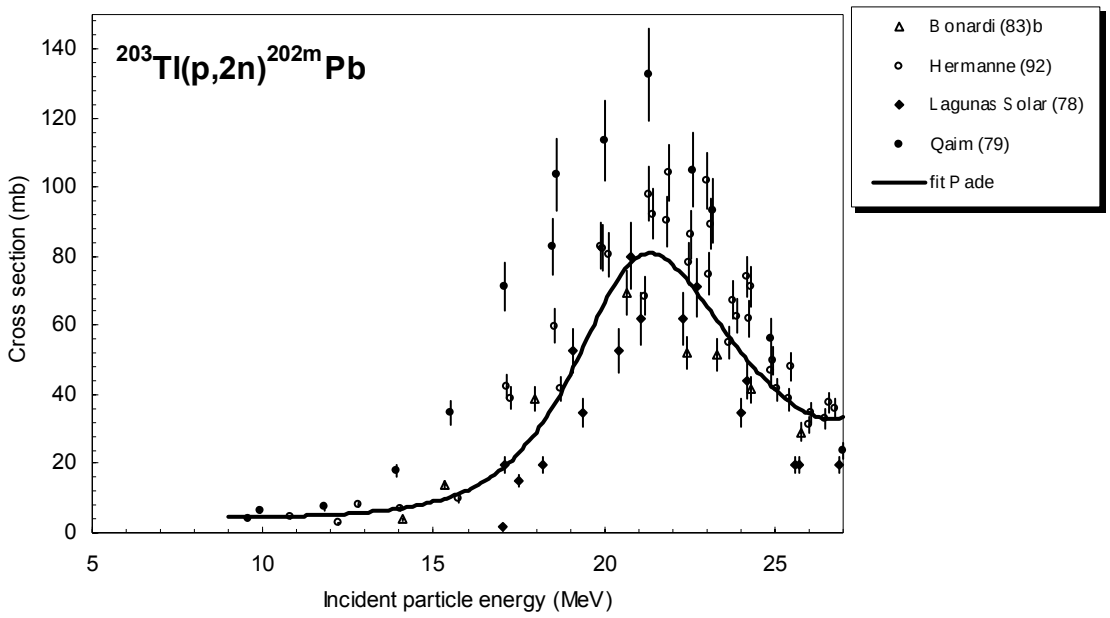

Figure 5.1.15c. Selected experimental data and recommended cross-section curve.

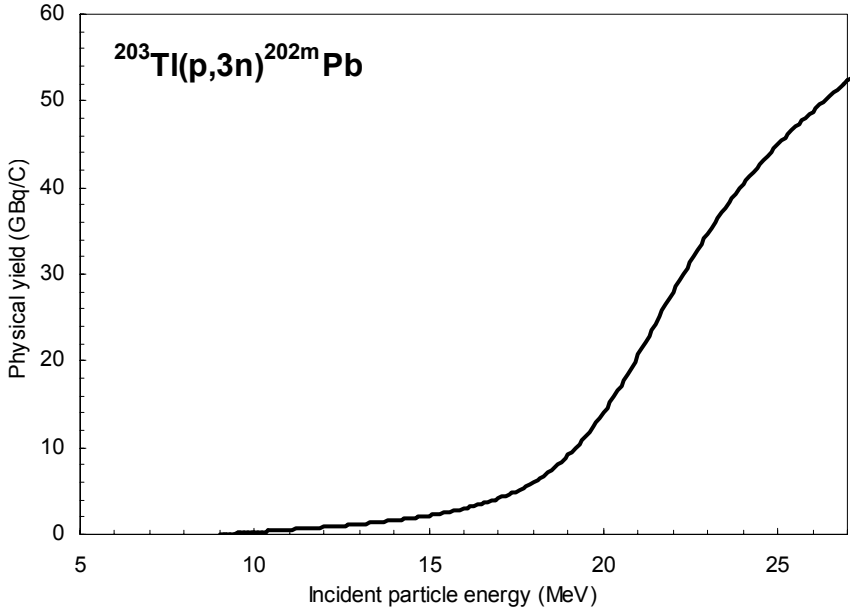

Figure 5.1.15d. Yield of ^{202m}Pb calculated from the recommended cross-sections.

TABLE 5.1.15b. RECOMMENDED CROSS-SECTIONS FOR THE $^{203}Tl(p,2n)^{202m}Pb$ REACTION

Energy MeV	Cross-section mb	Energy MeV	Cross-section mb	Energy MeV	Cross-section mb	Energy MeV	Cross-section mb
9.0	4.46	14.0	7.03	19.0	45.8	24.0	52.4
9.5	4.53	14.5	7.87	19.5	56.2	24.5	46.6
10.0	4.61	15.0	9.0	20.0	66.5	25.0	41.5
10.5	4.72	15.5	10.4	20.5	75.0	25.5	37.4
11.0	4.85	16.0	12.4	21.0	79.9	26.0	34.5
11.5	5.02	16.5	15.0	21.5	80.6	26.5	33.0
12.0	5.25	17.0	18.5	22.0	77.7	27.0	33.5
12.5	5.53	17.5	23.0	22.5	72.2		
13.0	5.91	18.0	29.0	23.0	65.7		
13.5	6.39	18.5	36.6	23.5	58.9		

TABLE 5.1.15b. YIELDS CALCULATED FROM THE RECOMMENDED CROSS-SECTION DATA FOR THE $^{203}Tl(p,2n)^{202m}Pb$ REACTION. Y: PHYSICAL YIELD, A_1: ACTIVITY AFTER 1 HOUR AND 1 μA IRRADIATION, A_2: SATURATION ACTIVITY FOR 1 μA IRRADIATION

Energy	Physical yield	Activity		Energy	Physical yield	Activity	
MeV	GBq/C	MBq	MBq	MeV	GBq/C	MBq	MBq
	Y	A_1	A_2		Y	A_1	A_2
9.0	0.02	0.074	0.425	18.5	7.4	24.2	139
9.5	0.14	0.46	2.61	19.0	9.1	29.9	172
10.0	0.26	0.86	4.92	19.5	11.3	37.1	213
10.5	0.39	1.28	7.35	20.0	14.0	45.9	264
11.0	0.53	1.73	9.92	20.5	17.2	56.2	323
11.5	0.67	2.21	12.7	21.0	20.7	67.7	388
12.0	0.83	2.72	15.6	21.5	24.3	79.7	457
12.5	1.00	3.27	18.8	22.0	28.0	91.6	526
13.0	1.18	3.87	22.2	22.5	31.4	103	591
13.5	1.38	4.54	26.0	23.0	34.7	114	652
14.0	1.61	5.28	30.3	23.5	37.7	123	708
14.5	1.87	6.13	35.2	24.0	40.4	132	759
15.0	2.17	7.11	40.8	24.5	42.8	140	804
15.5	2.52	8.27	47.5	25.0	45.0	147	846
16.0	2.95	9.67	55.5	25.5	47.0	154	883
16.5	3.48	11.4	65.4	26.0	48.8	160	918
17.0	4.13	13.5	77.7	26.5	50.6	166	951
17.5	4.96	16.2	93.2	27.0	52.3	171	984
18.0	6.02	19.7	113				

5.1.16. ^{203}Tl(p,4n)^{200}Pb→^{200}Tl

This reaction is responsible for one of the major radionuclidic impurities in the production of ^{201}Pb→^{201}Tl.

A total of 6 cross-section data sets (in 5 publications) were found in the literature in the energy range considered. From these, 2 sets were excluded while the other 4 were selected for further evaluation. Data measured on natural targets were transformed to represent the ^{203}Tl(p,4n)^{200}Pb reaction. The list of related references given below is accompanied with additional information. We mention availability of data in the computerized database EXFOR (if available, unique EXFOR reference number is given). Furthermore, we indicate a reason why a data set was excluded (reference denoted by an asterisk *).

*** Blue, J.W., Liu, D.C., Smathers, J.B.:**
Thallium 201 production with the idle beam from neutron therapy.
Medical Physics **5** (1978) 532
— Exfor: none
— Data excluded: only data sets that were selected for the ^{203}Tl(p,3n)^{201}Pb reaction were considered.

Bonardi, M., Birattari, C., Salomone, A.:
^{201}Tl production for medical use by (p,xn) nuclear reactions on Tl and Hg natural and enriched targets.
Proc. Int. Conf. Nuclear Data for Science and Technology, September 1982, Antwerp, Belgium (ed. Böckhoff, K.H.), D. Reidel, The Netherlands (1983) 916
Additional information in: F. Girardi, L. Goetz, E. Sabbioni, E. Marafante, M. Merlini, E Acerbi, C. Birattari, M. Castiglioni and F. Resmini
Preparation of ^{203}Pb compounds for studies on pathways and effects of lead pollution
Int. J. Applied Radiation Isotopes **26** (1975) 267
— Exfor: none
— Data on natural targets excluded: only data sets that were selected for the ^{203}Tl(p,3n)^{201}Pb reaction were considered.

Hermanne, A., Walravens, N., Cichelli, C.:
Optimisation of isotope production by cross-section determination.
Proc. Int. Conf. Nuclear Data for Science and Technology, May 1991, Jülich, FRG
(ed. Qaim, S.M.) Springer Verlag, Berlin (1992) 616
also private communication by authors
— Exfor: A0494

Lagunas-Solar, M.C., Jungerman, J.A., Peek, N.F., Theus, R.M.:
Thallium-201 yields and excitation functions for the lead activities produced by irradiation of natural thallium with 15-60 MeV protons.
Int. J. Applied Radiation Isotopes **29** (1978) 159
— Exfor: B0168

Qaim, S.M., Weinreich, R., Ollig, H.:
Production of ^{201}Tl and ^{203}Pb via proton induced nuclear reactions on natural thallium.
Int. J. Applied Radiation Isotopes **30** (1979) 85
— Exfor: none

The data from papers where experimental numerical values were available (6 data set in 5 papers) are collected in Fig. 5.1.16a. From these 4 sets were selected for further evaluation.

Cross-sections were calculated by two different versions of the nuclear reaction model code ALICE (denoted as HMS(KR) and IPPE), by the model code PREMOD-HFMOD (denoted as HF) and by two fitting procedures (Padé with 9 parameters and Spline). The results are compared with the selected experimental data in Fig. 5.1.16b. It is seen that the HF code overestimates the cross-sections while the others give better predictions. The best approximation was judged to be the spline fit. Recommended cross-sections are compared with selected experimental data, including their error bars, in Fig. 5.1.16c. Yields calculated from the recommended cross-sections are presented in Fig. 5.1.16d. The corresponding numerical values for recommended cross-sections and yields are tabulated in Table 5.1.16a and Table 5.1.16b, respectively.

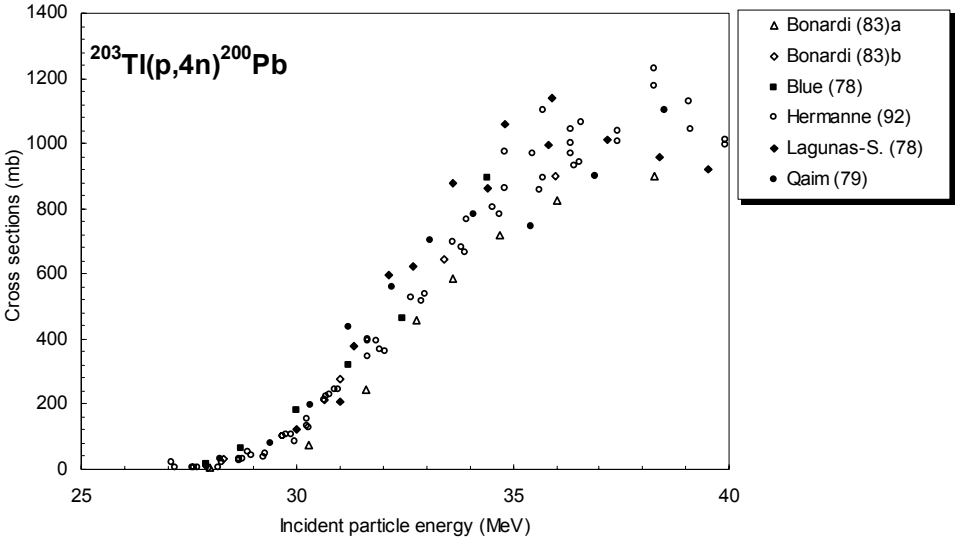

Figure 5.1.16a. All experimental data.

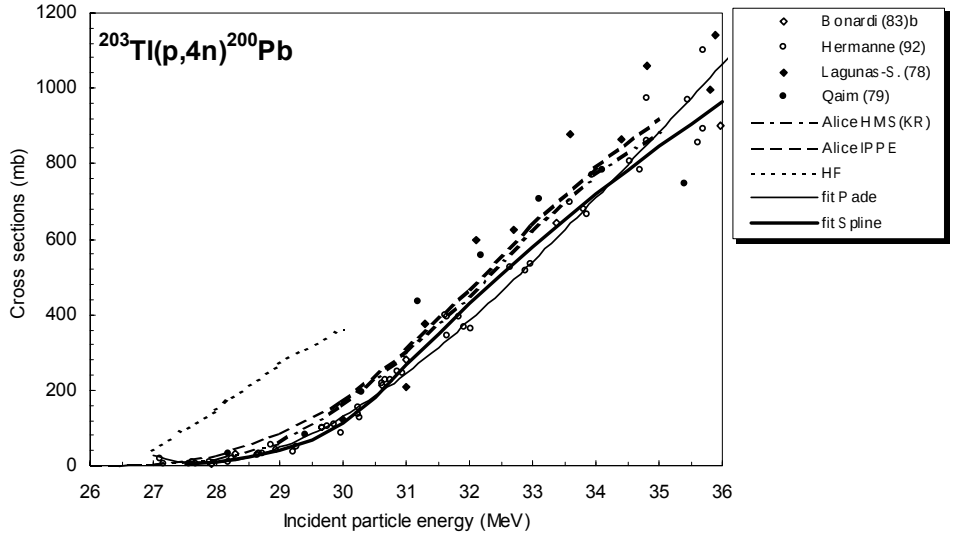

Figure 5.1.16b. Selected experimental data in comparison with theoretical calculations and fits

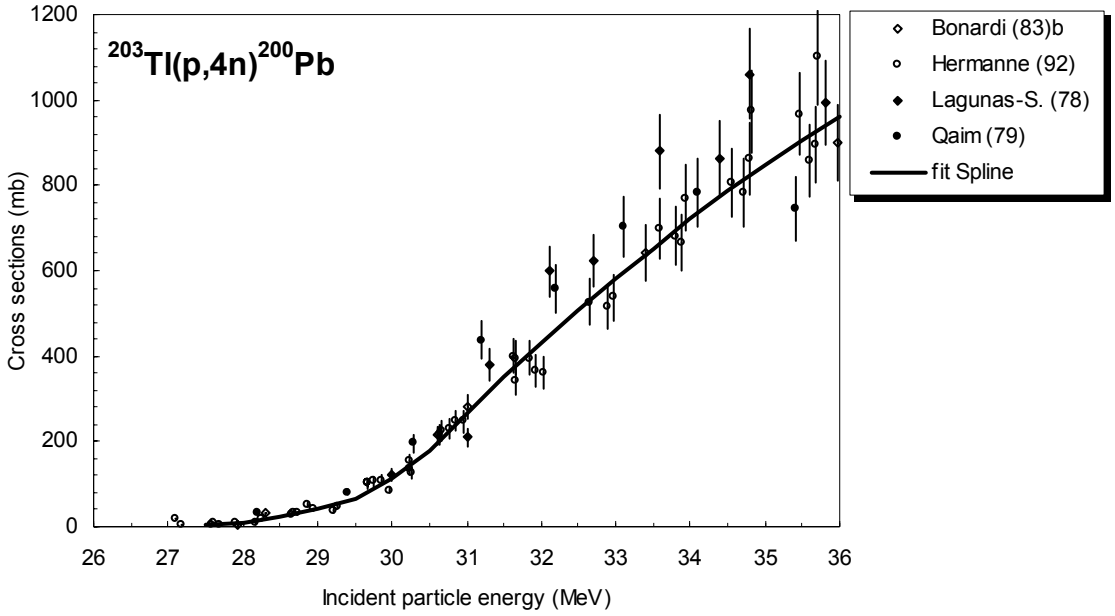

Figure 5.1.16c. Selected experimental data and recommended cross-section curve.

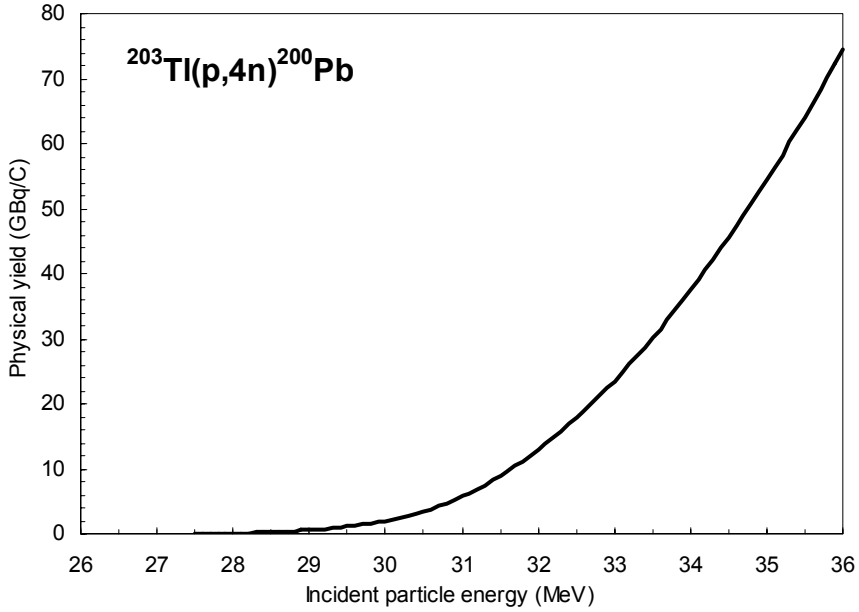

Figure 5.1.16d. Yield of ^{200}Pb calculated from the recommended cross-sections.

TABLE 5.1.16a. RECOMMENDED CROSS-SECTIONS FOR THE $^{203}Tl(p,4n)^{200}Pb$ REACTION

Energy MeV	Cross-section mb	Energy MeV	Cross-section mb	Energy MeV	Cross-section mb	Energy MeV	Cross-section mb
27.5	6.30	30.0	111	32.5	507	35.0	848
28.0	10.8	30.5	181	33.0	581	35.5	907
28.5	22.2	31.0	266	33.5	652	36.0	963
29.0	40.8	31.5	349	34.0	720		
29.5	67.2	32.0	430	34.5	785		

TABLE 5.1.16b. YIELDS CALCULATED FROM THE RECOMMENDED CROSS-SECTION DATA FOR THE $^{203}Tl(p,4n)^{200}Pb$ REACTION. Y: PHYSICAL YIELD, A_1: ACTIVITY AFTER 1 HOUR AND 1 μA IRRADIATION, A_2: SATURATION ACTIVITY FOR 1 μA IRRADIATION.

Energy	Physical yield	Activity		Energy	Physical yield	Activity	
MeV	GBq/C	MBq	MBq	MeV	GBq/C	MBq	MBq
	Y	A_1	A_2		Y	A_1	A_2
27.5	0.012	0.041	1.28	32.0	12.9	45.8	1444
28.0	0.091	0.32	10.2	32.5	17.8	63.1	1989
28.5	0.25	0.88	27.9	33.0	23.5	83.4	2627
29.0	0.56	1.98	62.5	33.5	30.1	107	3358
29.5	1.09	3.87	122	34.0	37.4	133	4178
30.0	1.98	7.01	221	34.5	45.6	161	5087
30.5	3.46	12.2	386	35.0	54.5	193	6082
31.0	5.74	20.3	641	35.5	64.1	227	7163
31.5	8.91	31.6	995	36.0	74.6	264	8325

5.2. POSITRON EMITTERS

(Prepared by, S.M. Qaim, F. Tárkányi, S. Takács, A. Hermanne, M. Nortier, P. Obložinský, B. Scholten, Yu.N. Shubin, Zhuang Youxiang)

The list of positron emitters is long and for each commonly used positron emitter several production routes have been reported (cf. Qaim et al., in Positron Emission Tomography-Methodology Aspects, G. Stöcklin and, V. Pike, Editors, Kluwer, Dordrecht, 1993). In this project attention was focused on common routes of production. The list of production reactions evaluated in the present project includes altogether 10 reactions, see Table 5.2. Among them are 6 reactions for production of short-lived "organic" positron emitters and 4 reactions to produce longer-lived isotopes for supply of PET radioisotopes via generators. Energies of incident particles cover the range from a few MeV up to100 MeV.

The adopted evaluation procedure consisted of three steps, explained in more detail in Chapters 2 and 3. First, experimental data were collected and subjected to critical analysis, resulting in the creation of a reduced set of selected experimental data to be used for further evaluation. The second step consisted of performing theoretical calculations with nuclear reaction model codes and comparison with the selected experimental data as well as of fitting those selected data. The third step represented final judgment as regards the agreement between selected experimental data, theoretical calculations and fits. Based on the consensus of all participants and evaluators involved in this project, recommended cross-sections were deduced, most often the preferred choice being a fit. Finally, as the fourth step, based on the recommended cross-sections, the production yield was calculated in different representations.

Excitation functions of most of the reactions relevant to the production of "organic" short-lived positron emitters have a resonance character at low energies. For successful fitting it was necessary to consider those resonances. Therefore some corrections were made by the compilers in the energy scale of the activation data. Those corrections were based on resonance data obtained with higher precision via direct particle counting (e.g. neutrons).

In the following, production reactions for positron emitters are presented. For each reaction, the above four evaluation steps are described, each step being accompanied by a figure. Then, recommended cross-sections and the calculated yields are presented in a tabular form.

TABLE 5.2. PRODUCTION REACTIONS FOR POSITRON EMITTERS

Reaction	$T_{1/2}$ of product nucleus	β^+ branching (%)	Projectile energy range (MeV)
$^{14}N(p,\alpha)^{11}C$	20.39 min	99.8	4–25
$^{16}O(p,\alpha)^{13}N$	9.96 min	99.8	6–20
$^{14}N(d,n)^{15}O$	2.04 min	99.9	1–15
$^{15}N(p,n)^{15}O$	2.04 min	99.9	4–20
$^{18}O(p,n)^{18}F$	109.8 min	97.0	2.5–20
$^{nat}Ne(d,\alpha)^{18}F$	109.8 min	97.0	1.5–21
$^{69}Ga(p,2n)^{68}Ge$*	270.8 d		13–40
$^{nat}Ga(p,xn)^{68}Ge$*	270.8 d		11.5–60
$^{85}Rb(p,4n)^{82}Sr$*	25.55 d		36.5–70
$^{nat}Rb(p,xn)^{82}Sr$*	25.55 d		33–100

* The long-lived ^{68}Ge and ^{82}Sr are produced more commonly via the spallation process. The spallation yields are generally well known. Here only the low energy processes are given. The positron emitting products ^{68}Ga(68.3 min) and ^{82}Rb(1.3 min) have β^+ branching of 89.0 and 95.0%, respectively.

5.2.1. $^{14}N(p,\alpha)^{11}C$

There were 13 experimental data sets available in 11 published papers. Four works were excluded from the selection process. The remaining 7 papers were selected for further evaluation. The list of related references given below is accompanied with additional information. We mention availability of data in the computerized database EXFOR (if available, unique EXFOR reference number is given). Furthermore, we indicate a reason why a data set was excluded (reference denoted by an asterisk *).

Bida, G.T., Ruth, T.J., Wolf, A.P.:
Experimentally determined thick target yields for the $^{14}N(p,\alpha)^{11}C$ reaction.
Radiochimica Acta **27** (1980) 181
— Exfor: A0286

Blaser, J.-P., Marmier, P., Sempert, M.:
Anregungsfunktion der Kernreaktion $^{14}N(p,\alpha)^{11}C$.
Helvetia Physica Acta **25** (1952) 442
— Exfor: none
Remarks: The cross-section data were multiplied by a factor of 1.3; to get resonances at comparable positions with other authors the energy scale was shifted to lower energy by 0.07 MeV.

Casella, V.R., Christman, D.R., Ido, T., Wolf, A.P.:
Excitation functions for the $^{14}N(p,\alpha)^{11}C$ reaction up to 15 MeV.
Radiochimica Acta **25** (1978) 17
— Exfor: C0177/R0010

*** Epherre, M., Seide, C.:**
Excitation functions of ^{7}Be and ^{11}C produced in nitrogen by low-energy protons.
Physical Review **C3** (1971) 2167
— Exfor: R0018
— Data excluded: only averaged cross-sections over relatively wide energy ranges available, because thick pellets were used as targets.

Ingalls, P.D., Schweitzer, J.S., Anderson, B.D.:
$^{14}N(p,\alpha)^{11}C$ cross-sections from 3.8 to 6.4 MeV.
Physical Review **C13** (1976) 524
— Exfor: C0178

Jacobs, W.W., Bodansky, D., Chamberlein, D., Oberg, D.L.:
Production of Li and B in proton and alpha particle reactions on ^{14}N at low energies.
Physical Review **C9** (1974) 2134
— Exfor: R0025

Köhl, F., Krauskopf, J., Misaelides, P., Michelmann, R., Wolf, G., Bethge, K.:
Determination of nitrogen in semiconductor materials using the $^{14}N(p,\alpha)^{11}C$ and $^{14}N(d,n)^{15}O$ nuclear reactions.
Nuclear Instruments Methods **B50** (1990) 19
— Exfor: none
Remark: Cross-section data were downscaled by a factor of 1.4 to get lower values, the energy scale remained unchanged.

*** Laumer, H., Austin, S.M., Panggabean, L.M., Davis, C.N.:**
Production of light elements lithium, beryllium and boron by proton-induced spallation of ^{14}N.
Physical Review **C8** (1973) 483
— Exfor: none
— Data excluded: detection of charged particle was done in a counter telescope; we concentrated on activation studies.

*** MacLeod, A.M., Reid, J.M.:**
Proton nuclear reaction cross-sections in nitrogen at 13 MeV.
Proceedings of Physical Society **87** (1966) 437
— Exfor: none
— Data excluded: data were obtained using a cloud chamber; we concentrated on activation studies.

Nozaki, T., Okuo, T., Akutsu, H., Furukawa, M.:
The radioactivation analysis of semiconductor graphite for nitrogen by the $^{14}N(p,\alpha)^{11}C$ reaction.
Bulletin Chemical Society Japan **39** (1966) 2685
— Exfor: R0026
Remark: In this work three data sets were reported.

*** Valentin, L., Alboy, G., Cohen, J.P., Gusakow, M.:**
Fonctions d'excitation des reactions (p,pn) et (p,2p2n) dans les novyaux legers entre 15 et 155 MeV.
Journal de Physique (Paris) **25** (1964) 704
— Exfor: none
— Data excluded: emphasis on high energy region

The 13 data sets are collected in Fig. 5.2.1a. The selected 9 sets were used for further evaluation.

Cross-sections were calculated by the nuclear reaction model code SPEC and by two fitting procedures (Padé in two fitting interval with 40 and 28 parameters, and Spline). These results are compared with the selected experimental data in Fig. 5.2.1b. It is seen that the SPEC model calculation cannot reproduce the resonances. The fits are better. It should, however, be pointed out that in the fitting process the available knowledge on the experimentally observed resonances was fed in. The well defined resonances at 6.15, 6.80, 7.20, 9.6, 10.7 and 13.2 MeV are understandable in terms of the level structure of the product nucleus ^{11}C.

The best approximation was judged to be the Padé fit. Recommended cross-sections are compared with the selected experimental data, including their error bars, in Fig. 5.2.1c. The yields calculated from the recommended cross-sections are presented in Fig. 5.2.1d. The corresponding numerical values for recommended cross-sections and yields are tabulated in Table 5.2.1a and Table 5.2.1b, respectively.

It is worth empahsizing that the $^{14}N(p,\alpha)^{11}C$ reaction is a very important process since ^{11}C plays a significant role in PET studies. There has been considerable controversy about the data. The situation now, however, is good and the recommended curve could be adopted with confidence.

Worth mentioning is the fact that the reaction $^{14}N(p,\alpha)^{11}C$ is interesting in the nuclear astrophysics too. It is listed in the most recent compilation (cf. Introduction, page 1) on this topic. The present evaluation may therefore be of some use to astrophysicists as well.

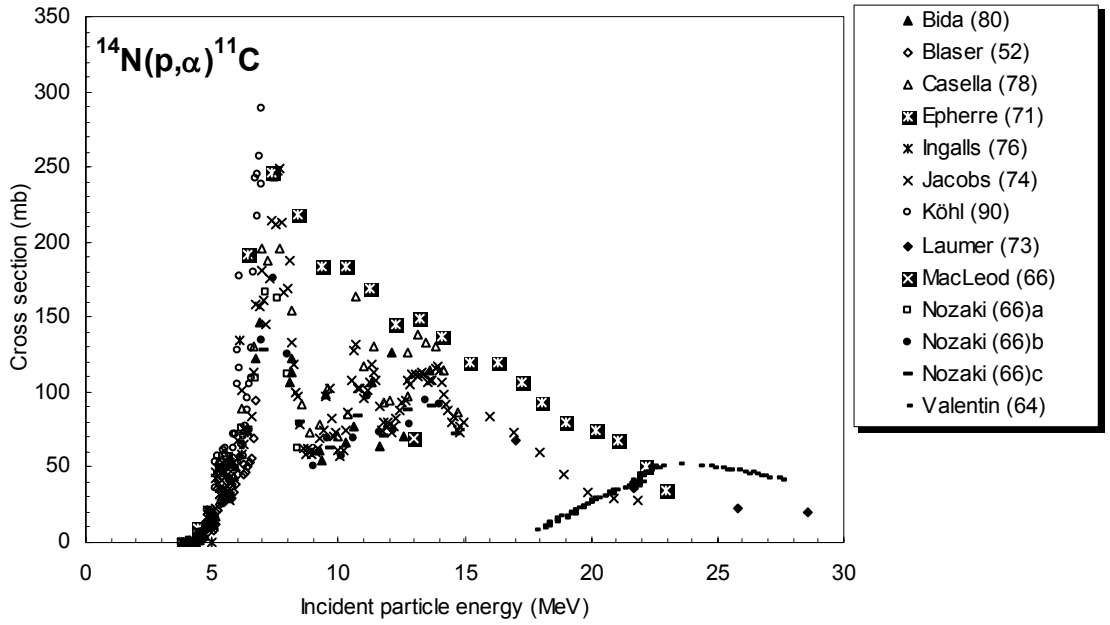

Figure 5.2.1a. All experimental data.

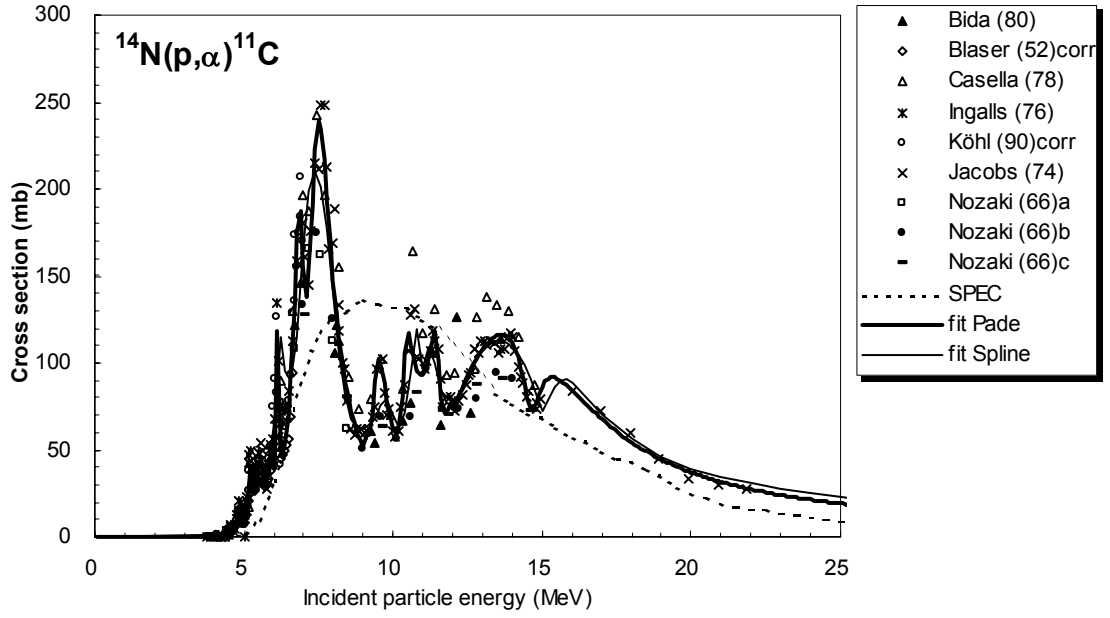

Figure 5.2.1b. Selected experimental data in comparison with theoretical calculations and fit

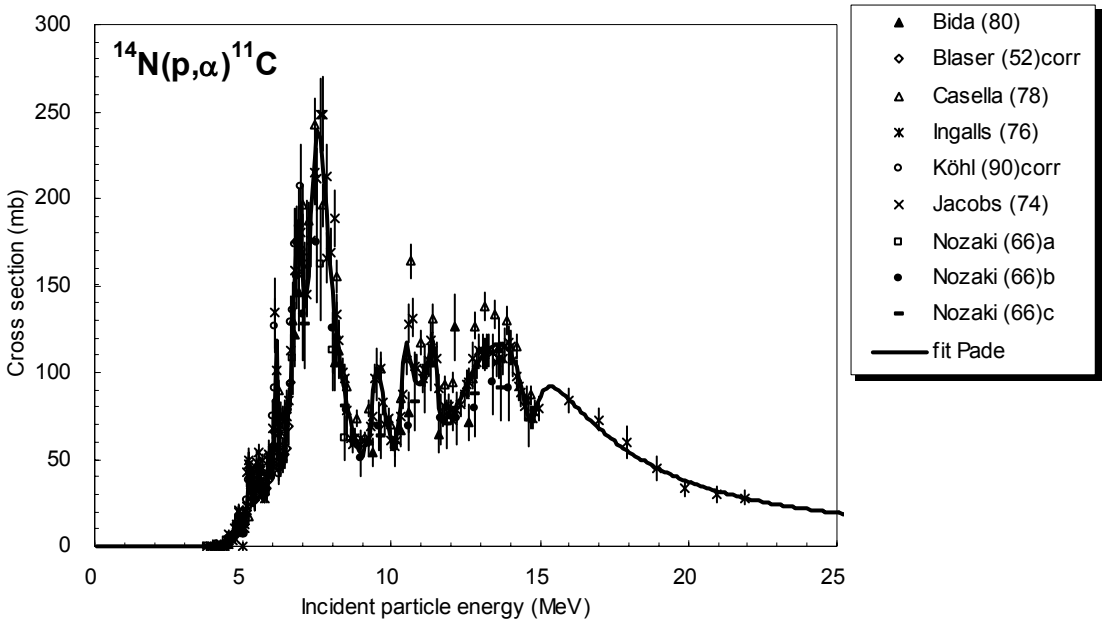

Figure 5.2.1c. Selected experimental data and recommended cross-section curve.

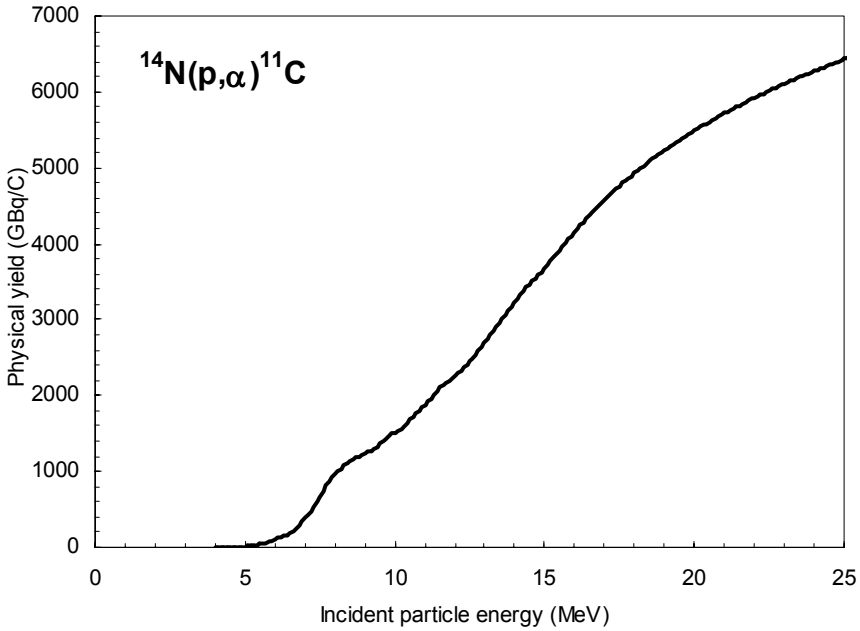

Figure 5.2.1d. Yield of ^{11}C calculated from the recommended cross-sections.

TABLE 5.2.1a. RECOMMENDED CROSS-SECTIONS FOR THE $^{14}N(p,\alpha)^{11}C$ REACTION

Energy MeV	Cross-section mb	Energy MeV	Cross-section mb	Energy MeV	Cross-section mb	Energy MeV	Cross-section mb
4.0	0.1	9.3	69.8	14.6	74.0	19.9	37.7
4.1	0.2	9.4	89.2	14.7	73.0	20.0	37.1
4.2	0.3	9.5	102.2	14.8	76.6	20.1	36.5
4.3	0.4	9.6	99.2	14.9	81.9	20.2	35.9
4.4	0.8	9.7	88.2	15.0	86.3	20.3	35.3
4.5	1.4	9.8	77.1	15.1	89.4	20.4	34.7
4.6	2.7	9.9	68.3	15.2	91.0	20.5	34.2
4.7	5.8	10.0	62.2	15.3	91.6	20.6	33.6
4.8	13.4	10.1	59.8	15.4	91.5	20.7	33.1
4.9	14.5	10.2	63.9	15.5	90.9	20.8	32.6
5.0	7.6	10.3	80.3	15.6	89.9	20.9	32.1
5.1	19.1	10.4	106.1	15.7	88.6	21.0	31.6
5.2	39.2	10.5	116.7	15.8	87.2	21.1	31.1
5.3	31.8	10.6	110.2	15.9	85.7	21.2	30.7
5.4	30.0	10.7	101.5	16.0	84.0	21.3	30.2
5.5	40.9	10.8	95.5	16.1	82.4	21.4	29.8
5.6	38.9	10.9	92.7	16.2	80.7	21.5	29.4
5.7	29.3	11.0	92.8	16.3	79.0	21.6	28.9
5.8	36.3	11.1	96.1	16.4	77.3	21.7	28.5
5.9	48.3	11.2	103.1	16.5	75.6	21.8	28.1
6.0	39.6	11.3	113.6	16.6	73.9	21.9	27.7
6.1	118.3	11.4	118.9	16.7	72.3	22.0	27.4
6.2	53.4	11.5	101.4	16.8	70.7	22.1	27.0
6.3	46.8	11.6	79.2	16.9	69.1	22.2	26.6
6.4	54.1	11.7	71.0	17.0	67.6	22.3	26.3
6.5	70.0	11.8	71.8	17.1	66.1	22.4	25.9
6.6	95.7	11.9	76.9	17.2	64.6	22.5	25.6
6.7	132.9	12.0	73.7	17.3	63.2	22.6	25.3
6.8	174.8	12.1	77.4	17.4	61.8	22.7	25.0
6.9	187.0	12.2	81.2	17.5	60.4	22.8	24.7
7.0	155.3	12.3	84.9	17.6	59.1	22.9	24.3
7.1	137.8	12.4	88.5	17.7	57.8	23.0	24.0
7.2	155.2	12.5	92.1	17.8	56.6	23.1	23.8
7.3	190.6	12.6	95.6	17.9	55.4	23.2	23.5
7.4	223.5	12.7	98.9	18.0	54.2	23.3	23.2
7.5	239.3	12.8	102.0	18.1	53.1	23.4	22.9
7.6	235.0	12.9	105.0	18.2	52.0	23.5	22.6
7.7	216.9	13.0	107.6	18.3	51.0	23.6	22.4
7.8	193.1	13.1	110.0	18.4	49.9	23.7	22.1
7.9	169.1	13.2	112.0	18.5	48.9	23.8	21.9
8.0	147.5	13.3	113.7	18.6	48.0	23.9	21.6
8.1	128.9	13.4	115.0	18.7	47.0	24.0	21.4
8.2	113.3	13.5	115.9	18.8	46.1	24.1	21.1
8.3	100.2	13.6	116.2	18.9	45.2	24.2	20.9
8.4	89.3	13.7	116.1	19.0	44.4	24.3	20.7
8.5	80.2	13.8	115.3	19.1	43.6	24.4	20.5
8.6	72.5	13.9	113.8	19.2	42.8	24.5	20.2
8.7	65.9	14.0	111.5	19.3	42.0	24.6	20.0
8.8	60.3	14.1	108.1	19.4	41.2	24.7	19.8
8.9	55.4	14.2	103.3	19.5	40.5	24.8	19.6
9.0	51.2	14.3	96.8	19.6	39.8	24.9	19.4
9.1	59.0	14.4	88.7	19.7	39.1	25.0	19.2
9.2	59.0	14.5	80.1	19.8	38.4		

TABLE 5.2.1b. YIELDS CALCULATED FROM THE RECOMMENDED CROSS-SECTION DATA FOR THE $^{14}N(p,\alpha)^{11}C$ REACTION Y: PHYSICAL YIELD, A_1: ACTIVITY AFTER 1 HOUR AND 1 μA IRRADIATION, A_2: SATURATION ACTIVITY FOR 1 μA IRRADIATION

Energy	Physical yield	Activity		Energy	Physical yield	Activity	
MeV	GBq/C	GBq	GBq	MeV	GBq/C	GBq	GBq
	Y	A_1	A_2		Y	A_1	A_2
4.0	0.023	0.00003	0.00004	15.0	3675	5.64	6.49
4.5	0.63	0.001	0.001	15.5	3916	6.01	6.91
5.0	10.0	0.02	0.02	16.0	4153	6.38	7.33
5.5	46.9	0.07	0.08	16.5	4373	6.72	7.72
6.0	94.1	0.14	0.17	17.0	4576	7.03	8.08
6.5	183	0.28	0.32	17.5	4761	7.31	8.40
7.0	391	0.60	0.69	18.0	4931	7.57	8.70
7.5	670	1.03	1.18	18.5	5087	7.81	8.98
8.0	966	1.48	1.71	19.0	5231	8.03	9.23
8.5	1132	1.74	2.00	19.5	5366	8.24	9.47
9.0	1236	1.90	2.18	20.0	5491	8.43	9.69
9.5	1371	2.10	2.42	20.5	5609	8.61	9.90
10.0	1517	2.33	2.68	21.0	5720	8.78	10.1
10.5	1682	2.58	2.97	21.5	5824	8.94	10.3
11.0	1880	2.89	3.32	22.0	5924	9.10	10.5
11.5	2102	3.23	3.71	22.5	6018	9.24	10.6
12.0	2262	3.47	3.99	23.0	6108	9.38	10.8
12.5	2451	3.76	4.33	23.5	6195	9.51	10.9
13.0	2685	4.12	4.74	24.0	6278	9.64	11.1
13.5	2953	4.53	5.21	24.5	6358	9.76	11.2
14.0	3233	4.96	5.71	25.0	6434	9.88	11.4
14.5	3472	5.33	6.13				

5.2.2. $^{16}O(p,\alpha)^{13}N$

A total of 11 published experimental papers were available. One work was excluded from the selection process. We selected the remaining 10 papers for further evaluation. The data originally presented in graphical format were digitized by different compilers with somewhat different results, both in number of points and their values. We redigitized all of these data in one laboratory. For the critical selection we did not find any serious argument which could explain the observed disagreements, especially near the region of the sharp resonances. The observed energy shifts are small compared to the energy shifts observed in other excitation functions. In our opinion, the status of the experimental database is acceptable. The cross-section data of Furukawa et al. were multiplied by a factor of 0.7. The energy scale of Whitehead et al. was shifted to lower energy by 0.3 MeV. For several works we made the necessary transformation of the projectile energy to the laboratory system. The list of related references given below is accompanied with additional information. We mention availability of data in the computerized database EXFOR (if available, unique EXFOR reference number is given). Furthermore, we indicate a reason why a data set was excluded (reference denoted by an asterisk *).

*** Albouy, M.G., Cohen, J.-P., Gusakow, M., Poffe, N., Sergolle, H., Valentin, L.V.:**
Spallation de l'oxygene par des protons de 20 a 150 MeV.
Physics Letters **2** (1962) 306
— Exfor: none
— Data excluded: scarce data in energy region of interest, the data up to 20 MeV are too low.

Dangle, R.L., Oppliger, L.D., Hardie, G.:
$^{16}O(p,\alpha)^{13}N$ and $^{16}O(p,p')^{16}O$ differential cross-sections.
Physical Review **3B** (1964) 647
Numerical data from: Clayton, D.D., Woosley, E.:
Thermonuclear astrophysics. Reviews Modern Physics **46** (1964) 755
— Exfor: none

Furukawa, M., Ishizaki, Y., Nakano, Y., Nozaki, T., Saji, Y., Tanaka, S.:
Excitation function for the reaction $^{11}B(p,n)^{11}C$ up to E_p=15 MeV and energy levels of ^{12}C.
J. Physical Society Japan **15** (1960) 2167
— Exfor: P0045
Remark: Cross-sections multiplied by a factor of 0.7.

Gruhle, W., Kober, B.:
The reactions $^{16}O(p,\alpha)$, $^{20}Ne(p,\alpha)$ and $^{24}Mg(p,\alpha)$.
Nuclear Physics **A286** (1977) 523
— Exfor: B0157

Hille, H.A., Haase, E.L., Knudsen, D.B.:
High-resolution measurements of the $^{16}O(p,\alpha)^{13}N$ excitation function.
Physical Review **123** (1961) 1301
— Exfor: none

Kitwanga, S.W., Leleux, P., Pipnik, P., Vanhorenbeeck, J.:
Production of ^{13}N radioactive nuclei from $^{13}C(p,n)$ or $^{16}O(p,\alpha)$ reactions.
Physical Review **C40** (1989) 35
— Exfor: P0051

Maxson, D.R.:
$^{16}O(p,\alpha)^{13}N$ angular distributions at 13.5–18.1 MeV.
Physical Review **123** (1961) 1304
— Exfor: C0246

McCamis, R.H., Moss, G.A., Casmeron, J.M.:
Total cross-section of $^{16}O(p,\alpha)^{13}N$ from threshold to 7.7 MeV.
Canadian, J. Physics **51** (1973) 1689
— Exfor: R0043

Nero, A.V., Howard, A.J.:
$^{16}O(p,\alpha_0)^{13}N$ cross-section measurements.
Nuclear Physics **A219** (1973) 60
— Exfor: none

Sajjad, M., Lambrecht, R.M., Wolf, A.P.:
Cyclotron isotopes and radiopharmaceuticals XXXVII. Excitation functions for the $^{16}O(p,\alpha)^{13}N$ and $^{14}N(p,pn)^{13}N$ reactions.
Radiochimica Acta **39** (1986) 165
— Exfor: C0202

Whitehead, A.B., Foster, J.S.:
Activation cross-sections for $^{12}C(p,pn)^{11}C$, $^{16}O(p,\alpha)^{13}N$ and $^{19}F(p,pn)^{18}F$.
Canadian, J. Physics **36** (1958) 1276
— Exfor: P0051
Remark: small energy shift to higher energies compared to others

The 11 data sets are collected in Fig. 5.2.2a. Ten works were selected for further evaluation.

Cross-sections were calculated by the fitting procedure Padé (with 24 parameters). The result is compared with the selected experimental data in Fig. 5.2.2b. Similar to ^{11}C, in the fitting proecess for ^{13}N the available knowledge on the experimentally observed resonances was fed in. The curve reproduces fairly well the resonances at 7.9, 8.4, 11.0, 12.7, 14.4 and 17.4 MeV observed in spectral studies. Fig. 5.2.2c reproduces the same data with error bars. The fit was adopted as the recommended curve.

The yields calculated from the recommended cross-sections are presented in Fig. 5.2.2d. The corresponding numerical values for recommended cross-sections and yields are tabulated in Table 5.2.2a and Table 5.2.2b, respectively.

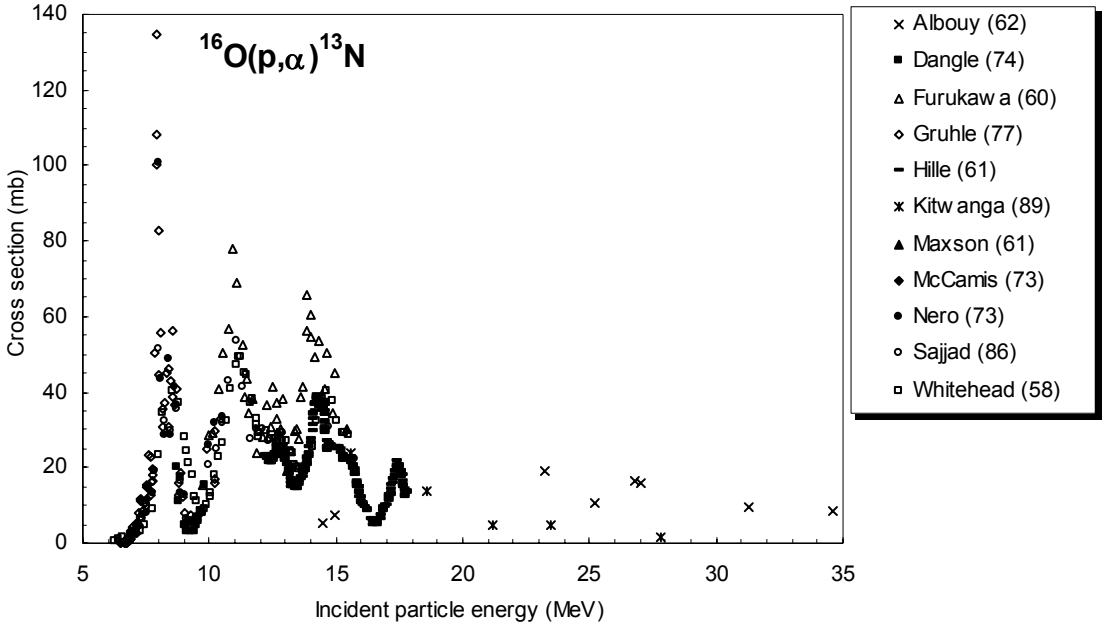

Figure 5.2.2a. All experimental data.

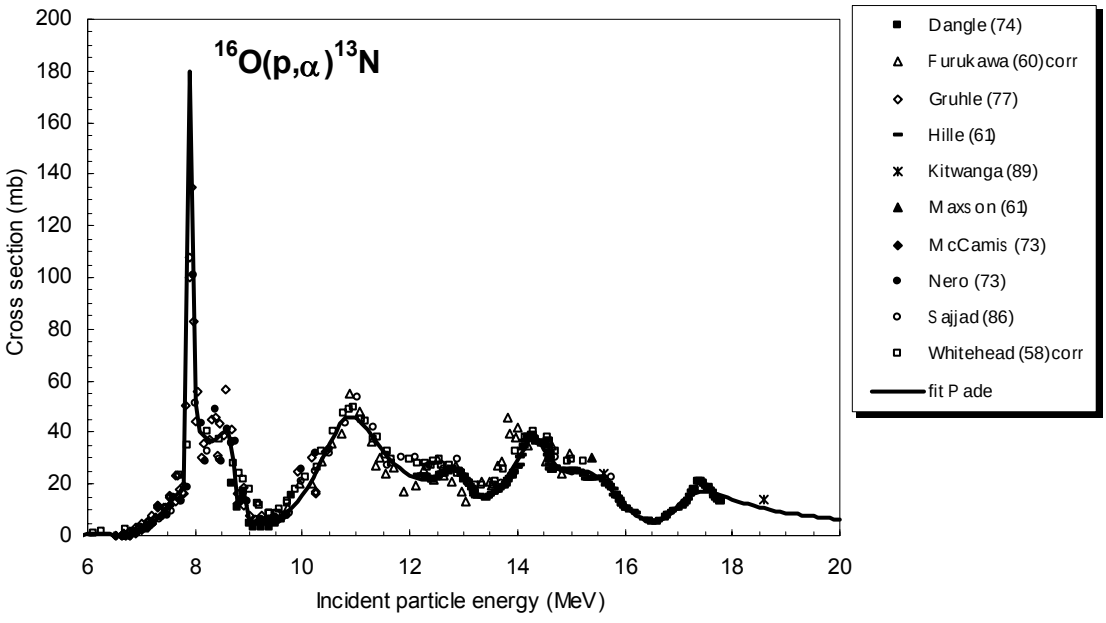

Figure 5.2.2b. Selected experimental data in comparison with a fit.

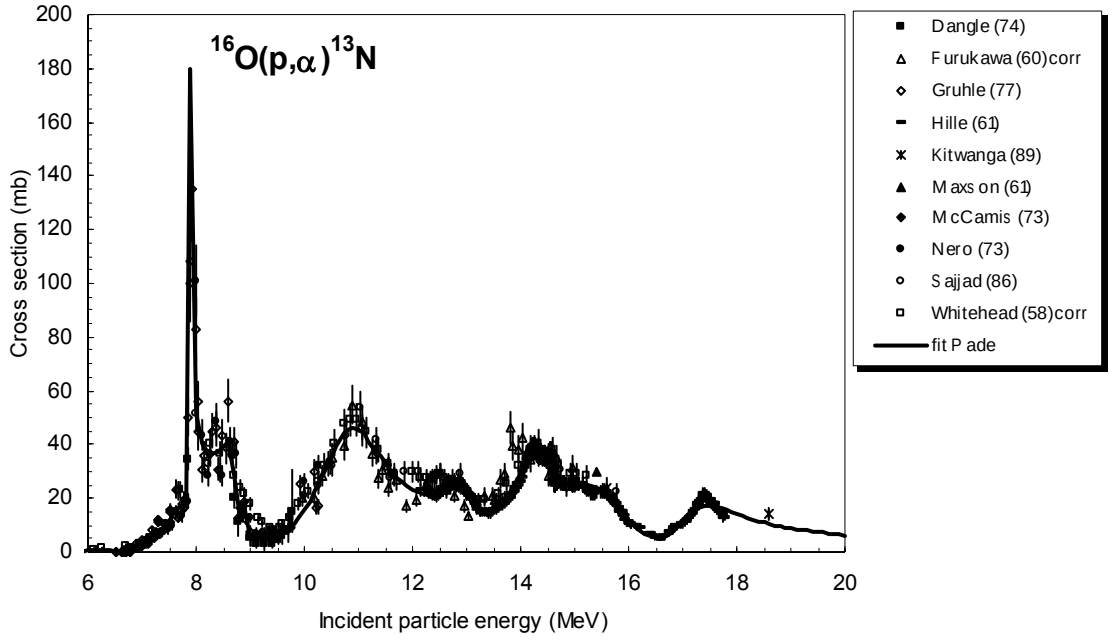

Figure 5.2.2c. Selected experimental data and recommended cross-section curve.

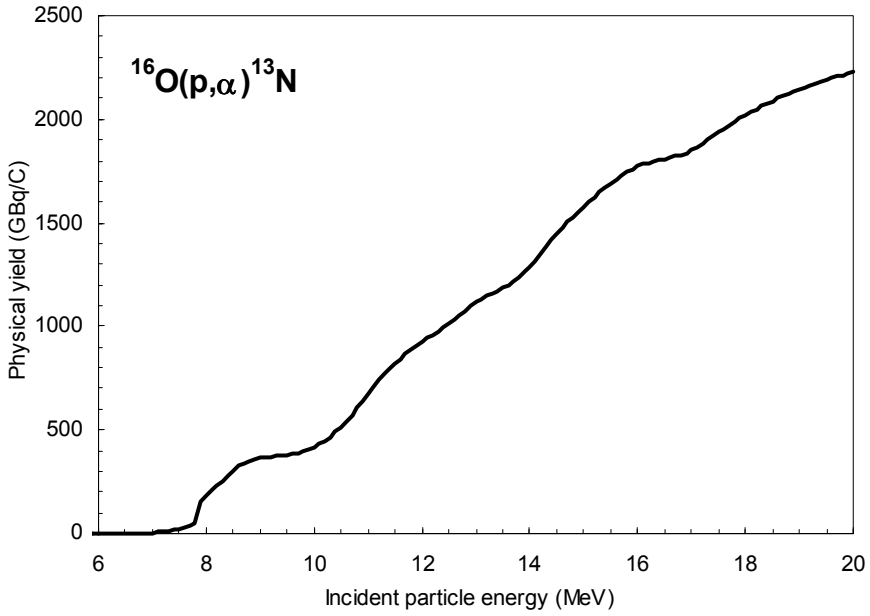

Figure 5.2.2d. Yield of ^{13}N calculated from the recommended cross-sections.

TABLE 5.2.2a. RECOMMENDED CROSS-SECTIONS FOR THE $^{16}O(p,\alpha)^{13}N$ REACTION

Energy MeV	Cross-section mb	Energy MeV	Cross-section mb	Energy MeV	Cross-section mb	Energy MeV	Cross-section mb
6.0	0.6	9.6	6.5	13.2	16.4	16.8	7.4
6.1	1.0	9.7	8.8	13.3	15.3	16.9	9.5
6.2	1.1	9.8	10.7	13.4	15.1	17.0	11.7
6.3	0.9	9.9	13.0	13.5	15.7	17.1	13.9
6.4	0.4	10.0	15.7	13.6	17.0	17.2	15.6
6.5	0.1	10.1	18.9	13.7	19.0	17.3	16.6
6.6	0.0	10.2	22.6	13.8	21.7	17.4	17.1
6.7	0.2	10.3	26.7	13.9	25.3	17.5	17.0
6.8	0.7	10.4	31.2	14.0	29.4	17.6	16.7
6.9	1.3	10.5	35.7	14.1	33.7	17.7	16.1
7.0	2.2	10.6	39.9	14.2	37.0	17.8	15.4
7.1	3.4	10.7	43.2	14.3	38.1	17.9	14.7
7.2	4.9	10.8	45.4	14.4	36.6	18.0	14.0
7.3	6.8	10.9	46.1	14.5	33.5	18.1	13.3
7.4	9.1	11.0	45.5	14.6	30.0	18.2	12.7
7.5	11.8	11.1	43.7	14.7	27.2	18.3	12.1
7.6	14.6	11.2	41.3	14.8	25.4	18.4	11.5
7.7	17.2	11.3	38.4	14.9	24.5	18.5	11.0
7.8	19.0	11.4	35.5	15.0	24.3	18.6	10.5
7.9	180.1	11.5	32.7	15.1	24.5	18.7	10.0
8.0	51.3	11.6	30.2	15.2	24.8	18.8	9.6
8.1	40.4	11.7	27.9	15.3	24.7	18.9	9.2
8.2	37.7	11.8	26.0	15.4	24.0	19.0	8.9
8.3	36.8	11.9	24.4	15.5	22.8	19.1	8.5
8.4	37.2	12.0	23.2	15.6	20.9	19.2	8.2
8.5	39.3	12.1	22.2	15.7	18.7	19.3	7.9
8.6	41.3	12.2	21.6	15.8	16.3	19.4	7.7
8.7	28.6	12.3	21.5	15.9	14.0	19.5	7.4
8.8	11.7	12.4	21.7	16.0	11.7	19.6	7.2
8.9	17.3	12.5	22.4	16.1	9.7	19.7	6.9
9.0	5.3	12.6	23.7	16.2	8.0	19.8	6.7
9.1	5.2	12.7	25.1	16.3	6.6	19.9	6.5
9.2	5.2	12.8	26.0	16.4	5.6	20.0	6.3
9.3	5.1	12.9	25.0	16.5	5.1		
9.4	5.0	13.0	22.0	16.6	5.2		
9.5	4.8	13.1	18.7	16.7	6.0		

TABLE 5.2.2b. YIELDS CALCULATED FROM THE RECOMMENDED CROSS-SECTION DATA FOR THE $^{16}O(p,\alpha)^{13}N$ REACTION Y: PHYSICAL YIELD, A_1: ACTIVITY AFTER 1 HOUR AND 1 μA IRRADIATION, A_2: SATURATION ACTIVITY FOR 1 μA IRRADIATION

Energy	Physical yield	Activity		Energy	Physical yield	Activity	
MeV	GBq/C	GBq	GBq	MeV	GBq/C	GBq	GBq
	Y	A_1	A_2		Y	A_1	A_2
6.0	0.4210	0.0004	0.0004	13.5	1186	1.01	1.02
6.5	2.08	0.0018	0.002	14.0	1286	1.09	1.11
7.0	4.40	0.0037	0.004	14.5	1451	1.23	1.25
7.5	23.9	0.020	0.021	15.0	1574	1.34	1.36
8.0	185.2	0.157	0.160	15.5	1691	1.44	1.46
8.5	300	0.254	0.26	16.0	1773	1.51	1.53
9.0	364	0.309	0.31	16.5	1808	1.54	1.56
9.5	380	0.323	0.33	17.0	1850	1.57	1.60
10.0	418	0.355	0.36	17.5	1936	1.64	1.67
10.5	513	0.44	0.44	18.0	2020	1.72	1.74
11.0	675	0.57	0.58	18.5	2088	1.77	1.80
11.5	820	0.70	0.71	19.0	2143	1.82	1.85
12.0	924	0.78	0.80	19.5	2189	1.86	1.89
12.5	1013	0.86	0.87	20.0	2229	1.89	1.92
13.0	1115	0.95	0.96				

5.2.3. $^{14}N(d,n)^{15}O$

There were 9 experimental papers available which measured the activation product. The reaction has been additionally investigated through characterisation of emitted neutron spectra. Four works were excluded from the selection process. The remaining 5 papers were selected for further evaluation. The list of related references given below is accompanied with additional information. We mention availability of data in the computerized database EXFOR (if available, unique EXFOR reference number is given). Furthermore, we indicate a reason why a data set was excluded (reference denoted by an asterisk *).

Köhl, E., Krauskopf, J., Misaelides, P., Michelmann, R., Wolf, G., Bethge, K.:
Determination of nitrogen in semiconductor materials using the $^{14}N(p,\alpha)^{11}C$ and $^{14}N(d,n)^{15}O$ nuclear reactions.
Nuclear Instruments Methods **B50** (1990) 19
— Exfor: none

*** Morita, S., Kawai, N., Goto, Y., Maki, T., Mukae, M.:**
The $^{14}N(d,n)^{15}O$ reaction in the energy range from 1.5 to 2.9 MeV.
J. Physical Society Japan **15** (1960) 2170
— Exfor: none
— Data excluded: differential cross-sections measured were integrated to get total cross-sections. The shapes of the yield curves usually agree with the other authors, but the absolute cross-sections obtained are different. On the basis of the published experimental conditions there is no possibility to find errors in the method used to obtain absolute values and to explain why they are lower by an order of magnitude.

Nonaka, I., Morita, S., Kawai, N., Ishimatsu, T., Takeshita, K., Nakajima, Y., Takano, N.:
On the neutrons from the $^{14}N(d,n)^{15}O$ reaction-II.
J. Physical Society Japan **12** (1957) 841
— Exfor: none

*** Newson, H.:**
Transmutation functions at high bombarding energies.
Physical Review **51** (1937) 620
— Exfor: none
— Data excluded: differential cross-sections measured were integrated to get total cross-sections. The shapes of the yield curves usually agree with the other authors, but the absolute cross-sections obtained are different. On the basis of the published experimental conditions there is no possibility to find errors in the method used to obtain absolute values and to explain why they are lower by an order of magnitude.

***, T. Retz-Schmidt and, J., L. Weil:**
Excitation curves and angular distributions for $^{14}N(d,n)^{15}O$
Physical Review **119** (1960) 1079
— Exfor: none
— Data excluded: Differential cross-sections measured were integrated to get total cross-sections. The shapes of the yield curves usually agree with the other authors, but the absolute cross-sections obtained are different. On the basis of the published experimental conditions there is no possibility to find errors in the method used to obtain absolute values and to explain why they are lower by an order of magnitude.

Sajjad, M., Lambrecht, R.M., Wolf, A.P.:
Cyclotron isotopes and radiopharmaceuticals XXXVI. Investigation of some excitation functions for the preparation of ^{15}O, ^{13}N and ^{11}C.
Radiochimica Acta **38** (1985) 57
— Exfor: A0316

Szücs, Z., Hamkens, W., Takács, S., Tárkányi, F., Coenen, H.H., Qaim, S.M.:
Excitation functions of $^{14}N(d,t)^{13}N$ and $^{14}N(d,\alpha n)^{11}C$ reactions from threshold to 12.3 MeV: Radionuclidic purity of ^{15}O produced via the $^{14}N(d,n)^{15}O$ reaction.
Radiochimica Acta **80** (1998) 59
— Exfor: none
Remark: error up to of 20%.

Vera Ruiz, H., Wolf, A.P.:
Excitation functions for ^{15}O production via the $^{14}N(d,n)^{15}O$ reaction.
Radiochimica Acta **24** (1977) 65
— Exfor: B0125/D0025

*** Wohlleben, K., Schuster, E.:**
Aktivierungsanalyse mit Deuteronen. Der totale Wirkungsquerschnitt der Reaktionen $^{10}B(d,n)^{11}C$, $^{14}N(d,n)^{15}O$ und $^{16}O(d,n)^{17}F$ bis 3,2 MeV.
Radiochimica Acta **12** (1969) 75
— Exfor: D0026/F0289
— Data excluded: they are systematically high and have errors of 20%.

The 9 data sets are collected in Fig. 5.2.3a. The selected 5 were used for further evaluation.

Cross-sections were calculated using the nuclear reaction model codes ALICE IPPE and SPEC and by two fitting procedures (Padé with 9 parameters and Spline). These results are compared with the selected experimental data in Fig. 5.2.3b. Evidently, the ALICE calculation cannot make a good prediction while SPEC model calculations and the fits reproduce the experimental cross-sections relatively well. The best approximation was judged to be the Padé fit. Recommended cross-sections are compared with the selected experimental data, including their error bars, in Fig. 5.2.3c. The yields calculated from the recommended cross-sections are presented in Fig. 5.2.3d. The corresponding numerical values for the recommended cross-sections and yields are tabulated in Table 5.2.3a and Table 5.2.3b, respectively.

The $^{14}N(d,n)^{15}O$ reaction is a very important reaction for ^{15}O production which is extensively used in brain studies with PET. In this reaction as well, some resonances may be present. However, in the present fitting procedure they could not be resolved.

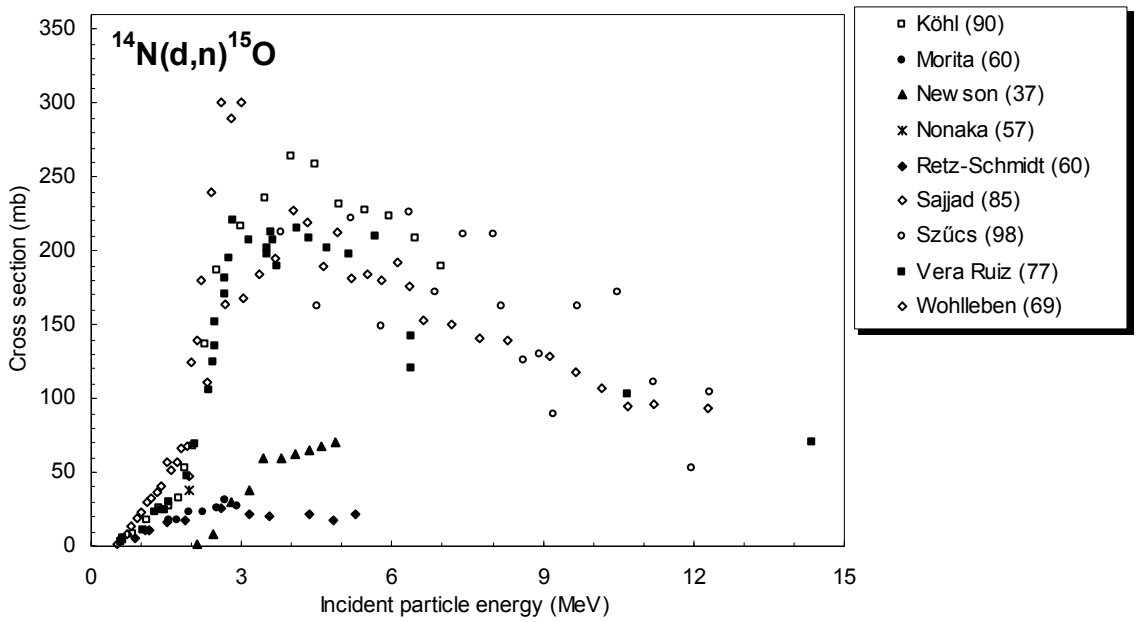

Figure 5.2.3a. All experimental data.

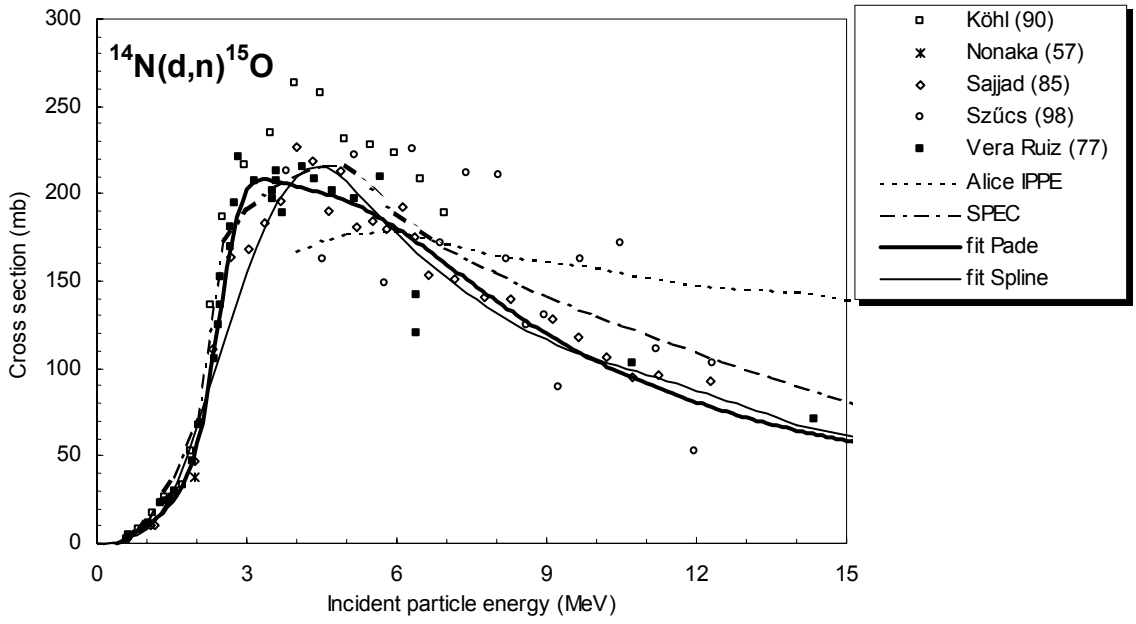

Figure 5.2.3b. Selected experimental data in comparison with theoretical calculations and fits.

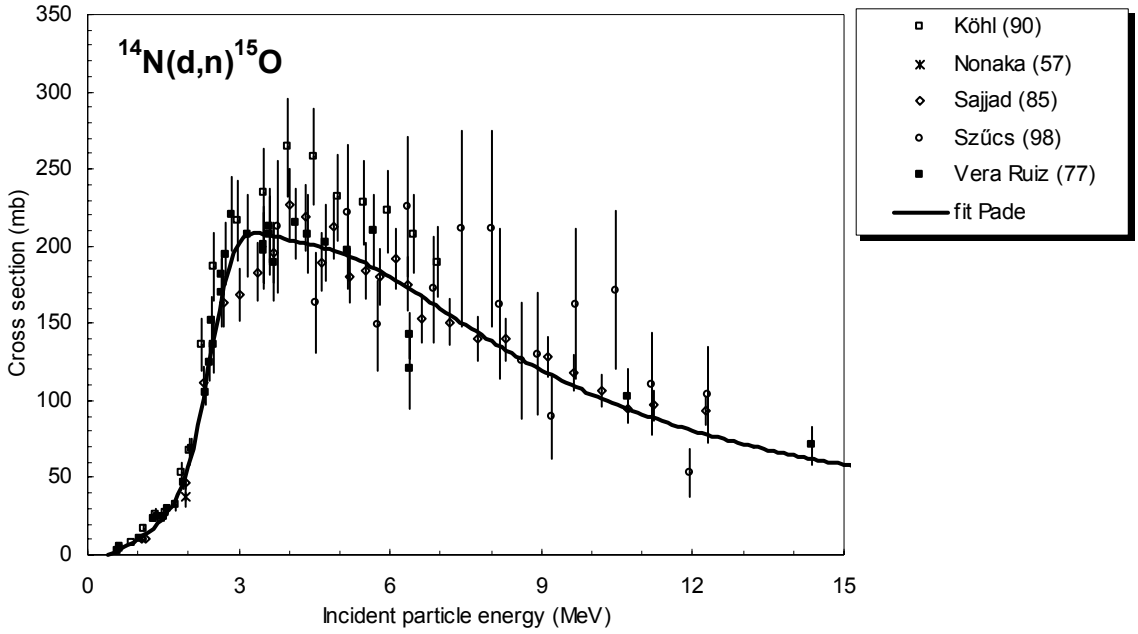

Figure 5.2.3c. Selected experimental data and recommended cross-section curve.

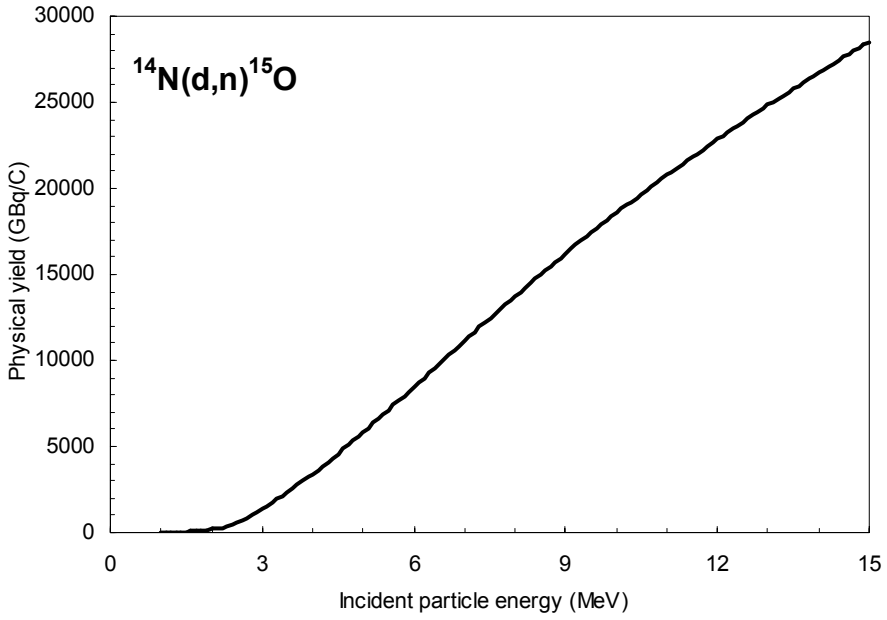

Figure 5.2.3d. Yield of ^{15}O calculated from the recommended cross-sections.

TABLE 5.2.3a. RECOMMENDED CROSS-SECTIONS FOR THE $^{14}N(d,n)^{15}O$ REACTION

Energy MeV	Cross-section mb	Energy MeV	Cross-section mb	Energy MeV	Cross-section mb	Energy MeV	Cross-section mb
1.0	10.3	4.6	199.6	8.2	134.5	11.8	82.5
1.1	12.4	4.7	198.7	8.3	132.6	11.9	81.5
1.2	14.7	4.8	197.8	8.4	130.6	12.0	80.5
1.3	17.3	4.9	196.8	8.5	128.8	12.1	79.6
1.4	20.3	5.0	195.6	8.6	126.9	12.2	78.7
1.5	23.8	5.1	194.5	8.7	125.1	12.3	77.7
1.6	27.9	5.2	193.2	8.8	123.3	12.4	76.8
1.7	32.9	5.3	191.8	8.9	121.5	12.5	76.0
1.8	39.2	5.4	190.4	9.0	119.8	12.6	75.1
1.9	47.0	5.5	188.8	9.1	118.1	12.7	74.3
2.0	56.8	5.6	187.2	9.2	116.4	12.8	73.4
2.1	69.0	5.7	185.5	9.3	114.7	12.9	72.6
2.2	83.7	5.8	183.8	9.4	113.1	13.0	71.8
2.3	101.0	5.9	182.0	9.5	111.5	13.1	71.0
2.4	120.1	6.0	180.1	9.6	110.0	13.2	70.3
2.5	139.7	6.1	178.2	9.7	108.5	13.3	69.5
2.6	158.3	6.2	176.2	9.8	107.0	13.4	68.8
2.7	174.3	6.3	174.2	9.9	105.5	13.5	68.0
2.8	187.0	6.4	172.1	10.0	104.1	13.6	67.3
2.9	196.2	6.5	170.1	10.1	102.6	13.7	66.6
3.0	202.2	6.6	168.0	10.2	101.3	13.8	65.9
3.1	205.7	6.7	165.8	10.3	99.9	13.9	65.3
3.2	207.5	6.8	163.7	10.4	98.6	14.0	64.6
3.3	208.2	6.9	161.6	10.5	97.3	14.1	63.9
3.4	208.1	7.0	159.4	10.6	96.0	14.2	63.3
3.5	207.7	7.1	157.3	10.7	94.7	14.3	62.7
3.6	207.0	7.2	155.1	10.8	93.5	14.4	62.1
3.7	206.3	7.3	153.0	10.9	92.3	14.5	61.4
3.8	205.6	7.4	150.9	11.0	91.1	14.6	60.8
3.9	204.8	7.5	148.8	11.1	90.0	14.7	60.3
4.0	204.1	7.6	146.7	11.2	88.8	14.8	59.7
4.1	203.4	7.7	144.6	11.3	87.7	14.9	59.1
4.2	202.7	7.8	142.5	11.4	86.6	15.0	58.6
4.3	202.0	7.9	140.5	11.5	85.6		
4.4	201.2	8.0	138.5	11.6	84.5		
4.5	200.5	8.1	136.5	11.7	83.5		

TABLE 5.2.3b. YIELDS CALCULATED FROM THE RECOMMENDED CROSS-SECTION DATA FOR THE $^{14}N(d,n)^{15}O$ REACTION Y: PHYSICAL YIELD, A_1: ACTIVITY AFTER 1 HOUR AND 1 μA IRRADIATION, A_2: SATURATION ACTIVITY FOR 1 μA IRRADIATION.

Energy	Physical yield	Activity		Energy	Physical yield	Activity	
MeV	GBq/C	GBq	GBq	MeV	GBq/C	GBq	GBq
	Y	A_1	A_2		Y	A_1	A_2
1.0	4.3	0.0008	0.0008	8.5	14993	2.64	2.64
1.5	48.9	0.009	0.009	9.0	16216	2.86	2.86
2.0	176	0.031	0.031	9.5	17405	3.07	3.07
2.5	561	0.10	0.10	10.0	18561	3.27	3.27
3.0	1345	0.24	0.24	10.5	19682	3.47	3.47
3.5	2336	0.41	0.41	11.0	20768	3.66	3.66
4.0	3424	0.60	0.60	11.5	21822	3.85	3.85
4.5	4593	0.81	0.81	12.0	22856	4.03	4.03
5.0	5835	1.03	1.03	12.5	23858	4.21	4.21
5.5	7130	1.26	1.26	13.0	24832	4.38	4.38
6.0	8458	1.49	1.49	13.5	25782	4.55	4.55
6.5	9797	1.73	1.73	14.0	26711	4.71	4.71
7.0	11131	1.96	1.96	14.5	27620	4.87	4.87
7.5	12447	2.19	2.19	15.0	28509	5.03	5.03
8.0	13735	2.42	2.42				

5.2.4. $^{15}N(p,n)^{15}O$

There were 4 experimental papers available dealing with the measurement of the activation product. The reaction has been additionally investigated through characterisation of emitted neutron spectra but those works were not considered here. All papers were selected for further evaluation. The list of related references given below is accompanied with additional information. We mention availability of data in the computerized database EXFOR (if available, unique EXFOR reference number is given). Furthermore, we indicate a reason why a data set was excluded (reference denoted by an asterisk *).

Barnett, A.R.:
16 Analogue states in the $^{15}N(p,n)^{15}O$ reaction.
Nuclear Physics **A120** (1968) 342
— Exfor: none
Remark: A large number of relative measurements using β^+ counting were performed. All data points were considered after renormalising by a factor 0.5.

Chew, S.H., Lowe, J., Nelson, J.M., Barnett, A.R.:
Resonance structure in $^{15}N(p,n)^{15}O$ in the region E_p = 8.5–19.0 MeV.
Nuclear Physics **A298** (1978) 19
— Exfor: none

Kitwanga, S.W., Leleux, P., Lipnik, P., Vanhorenbeeck, J.:
Production of $^{14,15}O$, ^{18}F and ^{19}Ne radioactive nuclei from (p,n) reactions up to 30 MeV.
Physical Review **C42** (1990) 748
— Exfor: none

Sajjad, M., Lambrecht, R.M., Wolf, A.P.:
Excitation function for the $^{15}N(p,n)^{15}O$ reaction.
Radiochimica Acta **36** (1984) 159
— Exfor: A0313

In all 5 data sets were published (in the 4 papers cited above) and they are collected in Fig. 5.2.4a. All the data were selected for further evaluation.

Cross-sections were calculated by two fitting procedures (Padé with 28 parameters and Spline). These results are compared with the selected experimental data in Fig. 5.2.4b. It is seen that fits cannot exactly describe the experimental cross-sections. The better approximation was judged to be the Padé fit. The major resonances at 4.4, 5.4, 6.2, 7.6 and 12.0 MeV are described well, but the weak resonances at about 6.6, 6.9, 8.8 and 10.8 MeV are not reproduced. The recommended curve is compared with the selected experimental data, including their error bars, in Fig. 5.2.4c. The yields calculated from the recommended cross-sections are presented in Fig. 5.2.4d. The corresponding numerical values for recommended cross-sections and yields are tabulated in Table 5.2.4a and Table 5.2.4b, respectively.

The $^{15}N(p,n)^{15}O$ reaction is used for ^{15}O production at small-sized cyclotrons with only proton beam (i.e. without deuteron beam). The procedure utilizes highly enriched $^{15}N_2$ gas as target material.

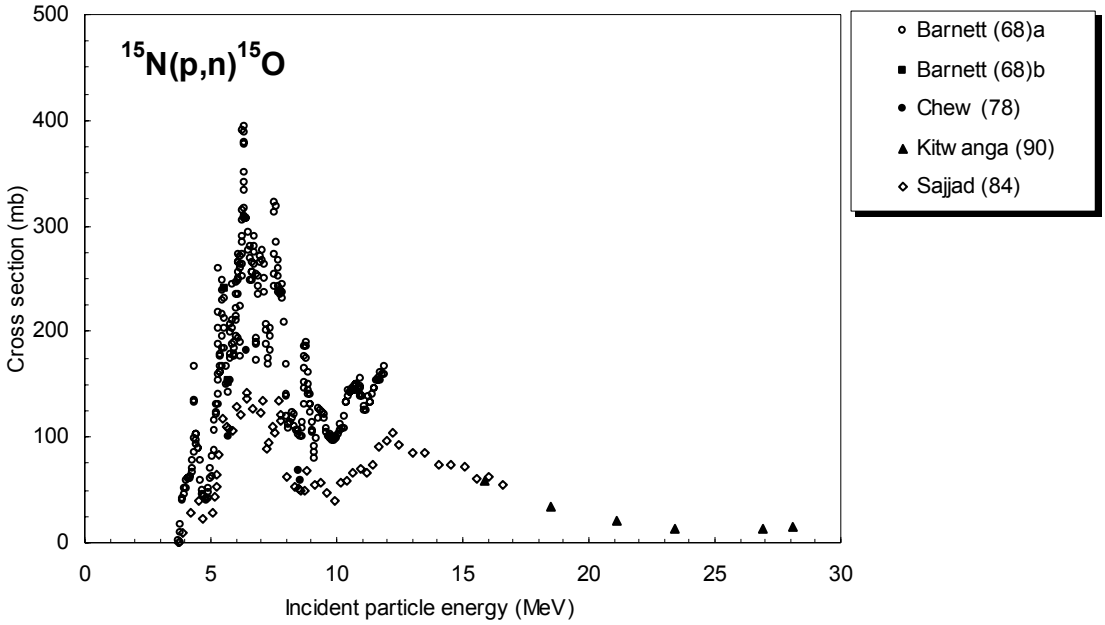

Figure 5.2.4a. All experimental data.

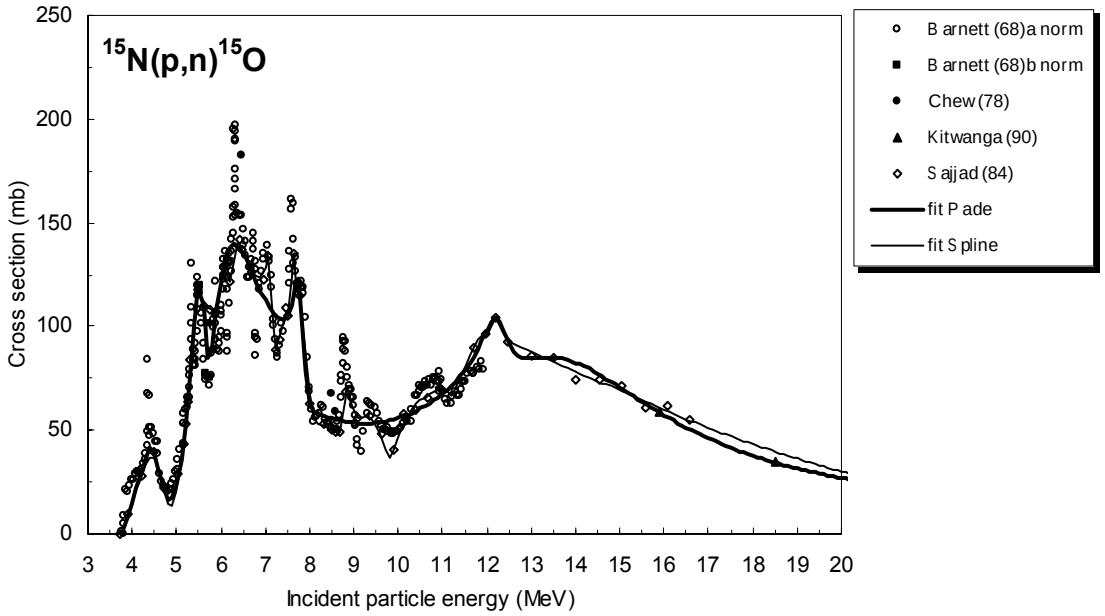

Figure 5.2.4b. Selected experimental data in comparison with fits.

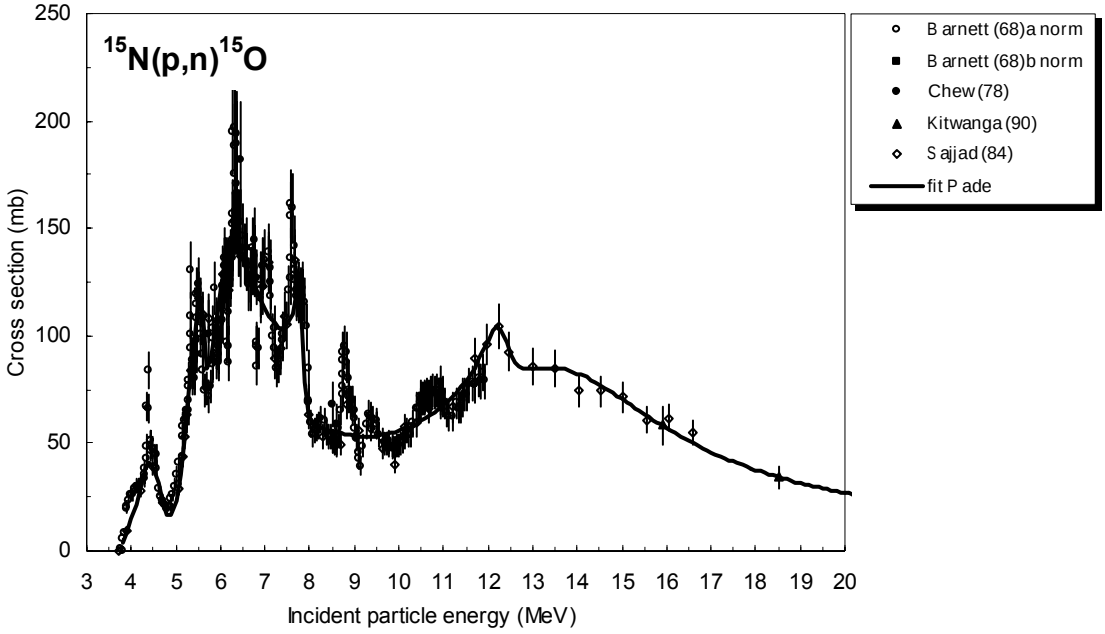

Figure 5.2.4c. Selected experimental data and recommended cross-section curve.

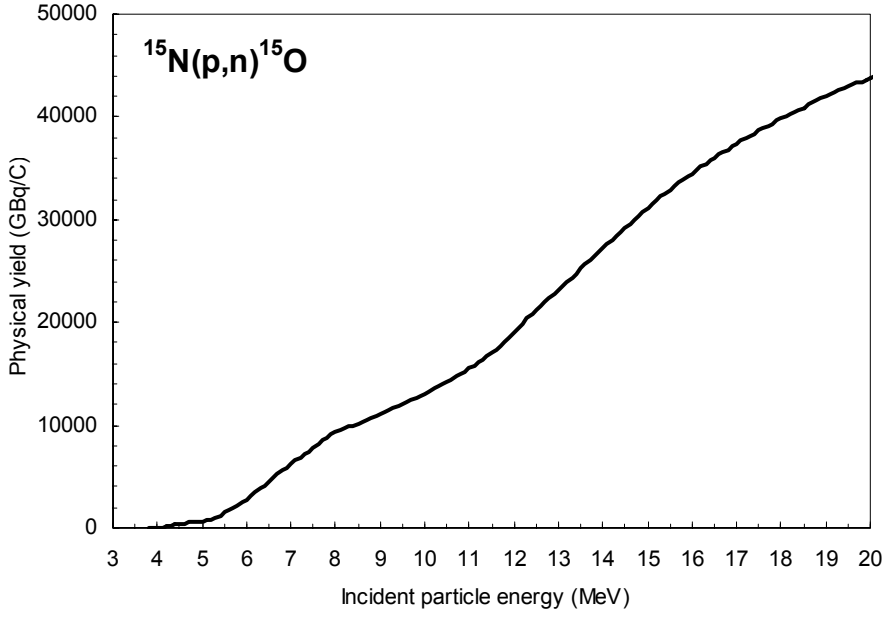

Figure 5.2.4d. Yield of ^{15}O calculated from the recommended cross-sections.

TABLE 5.2.4a. RECOMMENDED CROSS-SECTIONS FOR THE $^{15}N(p,n)^{15}O$ REACTION

Energy MeV	Cross-section mb	Energy MeV	Cross-section mb	Energy MeV	Cross-section mb	Energy MeV	Cross-section mb
4.0	14.6	8.1	58.9	12.2	104.6	16.3	53.5
4.1	21.9	8.2	57.5	12.3	102.7	16.4	52.4
4.2	29.9	8.3	56.8	12.4	97.4	16.5	51.2
4.3	37.1	8.4	56.2	12.5	91.8	16.6	50.1
4.4	41.1	8.5	55.6	12.6	88.0	16.7	49.1
4.5	39.1	8.6	55.1	12.7	85.9	16.8	48.0
4.6	31.4	8.7	54.6	12.8	85.0	16.9	47.0
4.7	22.3	8.8	54.2	12.9	84.8	17.0	46.1
4.8	16.8	8.9	53.9	13.0	84.8	17.1	45.1
4.9	17.1	9.0	53.6	13.1	85.0	17.2	44.2
5.0	23.4	9.1	53.4	13.2	85.2	17.3	43.3
5.1	35.4	9.2	53.4	13.3	85.3	17.4	42.4
5.2	52.7	9.3	53.3	13.4	85.3	17.5	41.6
5.3	74.8	9.4	53.4	13.5	85.1	17.6	40.8
5.4	99.7	9.5	53.6	13.6	84.9	17.7	40.0
5.5	118.7	9.6	53.8	13.7	84.5	17.8	39.2
5.6	109.7	9.7	54.2	13.8	84.0	17.9	38.5
5.7	84.8	9.8	54.6	13.9	83.3	18.0	37.7
5.8	89.1	9.9	55.1	14.0	82.5	18.1	37.0
5.9	106.9	10.0	55.8	14.1	81.7	18.2	36.3
6.0	122.6	10.1	56.5	14.2	80.7	18.3	35.7
6.1	132.9	10.2	57.3	14.3	79.6	18.4	35.0
6.2	138.1	10.3	58.2	14.4	78.5	18.5	34.4
6.3	139.5	10.4	59.2	14.5	77.3	18.6	33.8
6.4	138.1	10.5	60.4	14.6	76.0	18.7	33.2
6.5	135.0	10.6	61.6	14.7	74.7	18.8	32.7
6.6	130.9	10.7	63.0	14.8	73.4	18.9	32.1
6.7	126.2	10.8	64.4	14.9	72.0	19.0	31.6
6.8	121.5	10.9	66.0	15.0	70.7	19.1	31.1
6.9	116.9	11.0	67.7	15.1	69.3	19.2	30.5
7.0	112.7	11.1	69.6	15.2	67.9	19.3	30.1
7.1	109.0	11.2	71.6	15.3	66.5	19.4	29.6
7.2	106.0	11.3	73.8	15.4	65.1	19.5	29.1
7.3	104.0	11.4	76.3	15.5	63.7	19.6	28.7
7.4	103.4	11.5	78.9	15.6	62.4	19.7	28.2
7.5	105.0	11.6	81.9	15.7	61.0	19.8	27.8
7.6	110.4	11.7	85.3	15.8	59.7	19.9	27.4
7.7	120.4	11.8	89.1	15.9	58.4	20.0	27.0
7.8	114.6	11.9	93.5	16.0	57.2		
7.9	78.5	12.0	98.1	16.1	55.9		
8.0	62.9	12.1	102.4	16.2	54.7		

TABLE 5.2.4b. YIELDS CALCULATED FROM THE RECOMMENDED CROSS-SECTION DATA FOR THE $^{15}N(p,n)^{15}O$ REACTION Y_1: PHYSICAL YIELD, A_1: ACTIVITY AFTER 1 HOUR AND 1 μA IRRADIATION, A_2: SATURATION ACTIVITY FOR 1 μA IRRADIATION

Energy	Physical yield	Activity		Energy	Physical yield	Activity	
MeV	GBq/C	GBq	GBq	MeV	GBq/C	GBq	GBq
	Y	A_1	A_2		Y	A_1	A_2
4.0	48	0.0084	0.0084	12.5	21206	3.74	3.74
4.5	378	0.0666	0.067	13.0	23173	4.09	4.09
5.0	612	0.1079	0.108	13.5	25195	4.44	4.44
5.5	1490	0.263	0.263	14.0	27243	4.80	4.80
6.0	2751	0.49	0.485	14.5	29242	5.16	5.16
6.5	4540	0.80	0.80	15.0	31136	5.49	5.49
7.0	6226	1.10	1.10	15.5	32899	5.80	5.80
7.5	7776	1.37	1.37	16.0	34526	6.09	6.09
8.0	9277	1.64	1.64	16.5	36022	6.35	6.35
8.5	10203	1.80	1.80	17.0	37397	6.59	6.59
9.0	11128	1.96	1.96	17.5	38667	6.82	6.82
9.5	12078	2.13	2.13	18.0	39844	7.03	7.03
10.0	13094	2.31	2.31	18.5	40938	7.22	7.22
10.5	14221	2.51	2.51	19.0	41962	7.40	7.40
11.0	15514	2.74	2.74	19.5	42924	7.57	7.57
11.5	17056	3.01	3.01	20.0	43834	7.73	7.73
12.0	18986	3.35	3.35				

5.2.5. $^{18}O(p,n)^{18}F$

A total of 7 experimental papers deal with this reaction. The reaction has been investigated both through characterisation of emitted neutron spectra and measurement of the activation product ^{18}F. All papers were selected for further evaluation. The list of references given below is accompanied with additional information. We mention availability of data in the computerized database EXFOR (if available, unique EXFOR reference number is given). Furthermore, we indicate a reason why a data set was excluded (reference denoted by an asterisk *).

Anderson, J.D., Bloom, S.D., Wong, C., Hornyak, W.F., Madsen,V.A.:
Effective two-body force inferred from the (p,n) reaction on ^{17}O, ^{18}O, ^{27}Al and other light nuclei.
Physical Review **177** (1969) 1416
— Exfor: none
Remarks: The cross-section data were deduced from absolute neutron yield measurements. The energy region below 6 MeV was not investigated. Cross-sections for the population of different low levels were deduced from angular distribution measurements, but the data are not complete. The data are not available over the whole energy range for all levels. We summarized the available (scanty) values to obtain an idea about the magnitude and tendency of the total cross-section. They are in acceptable agreement with other literature data.

Bair, J.K.:
Total neutron yields from the proton bombardment of $^{17,18}O$.
Physical Review **C8** (1973) 120
— Exfor: none
Remark: Extremely low values in the investigated energy regions.

Bair, J.K., Miller, P.D., Wieland, B.W.:
Neutron yields from the 4-12 MeV proton bombardment of ^{11}B, ^{13}C and ^{18}O as related to the production of ^{11}C, ^{13}N and ^{18}F.
Int. J. Applied Radiation Isotopes **32** (1981) 389
— Exfor: none
Remarks: A series of investigations were made by these authors in the period 1956–81. They observed neutron yield in forward direction and measured activation cross-sections using a recoil technique. They also measured total neutron yields in different energy ranges.

Blaser, J.-P., Boehm, F.M., Marmier, P., Preiswerk, P., Scherrer, P.:
Function d'excitation de la reaction ^{18}O (p,n) ^{18}F.
Helvetia Physica Acta **22** (1949) 598
— Exfor: none
Remarks: The residual ^{18}F activity was measured by a stacked-foil technique with rather poor resolution up to 7 MeV.
The values are extremely low in the investigated energy region.

Blaser, J.-P., Boehm, F.M., Marmier, P., Scherrer, P.:
Function d'excitation de la reaction (p,n) (III) elements legers.
Helvetia Physica Acta **24** (1952) 465
— Exfor: none
Remarks: Some disagreement in the energy scale was noticed with the earlier publication of the same authors. This publication is probably a corrected version of the earlier one

Kitwanga, S.W., Leleux, P., Lipnik, P., Vanhorenbeeck, J.:
Production of $^{14,15}O$, ^{18}F and ^{19}Ne radioactive nuclei from (p,n) reactions up to 30 MeV.
Physical Review **C42** (1990) 748
— Exfor: none
Remark: Data points only above 10 MeV.

Ruth, T.J., Wolf, A.P.:
Absolute cross-sections for the production of ^{18}F via $^{18}O(p,n)^{18}F$ reaction.
Radiochimica Acta **26** (1979) 21
— Exfor: A0235
Remark: If we do not consider the old data of Blaser et al (1949 and 1951), this is the only work based on the measurement of ^{18}F up to 10 MeV. Above 10 MeV some data of Kitwanga et al (1990) are also available. The results seem to be reliable. This work is considered now as a reference experimental work.

The 6 data sets including those deduced from emitted neutrons (corrected values) are collected in Fig. 5.2.5a.

Cross-sections were calculated by the fitting procedure Padé (with 14 and 20 parameters in two connecting energy regions). The result is compared with the selected experimental data in Fig. 5.2.5b. It is seen that the fit does not follow well all the resonances. However, the major resonances at 3.5, 4.2, 5.2, 6.1 and 6.7 MeV are reproduced. This fit was chosen as the recommended curve. The yields calculated from the recommended cross-sections are presented in Fig. 5.2.5c. The corresponding numerical values for recommended cross-sections and yields are tabulated in Table 5.2.5a and Table 5.2.5b, respectively.

The radionuclide ^{18}F is the most commonly used radioisotope in PET studies and the method of choice for its production is the $^{18}O(p,n)^{18}F$ reaction. In view of the extreme importance of this reaction and considering the discrepancies in the data, especially in the energy regions of the resonances, new measurements are recommended.

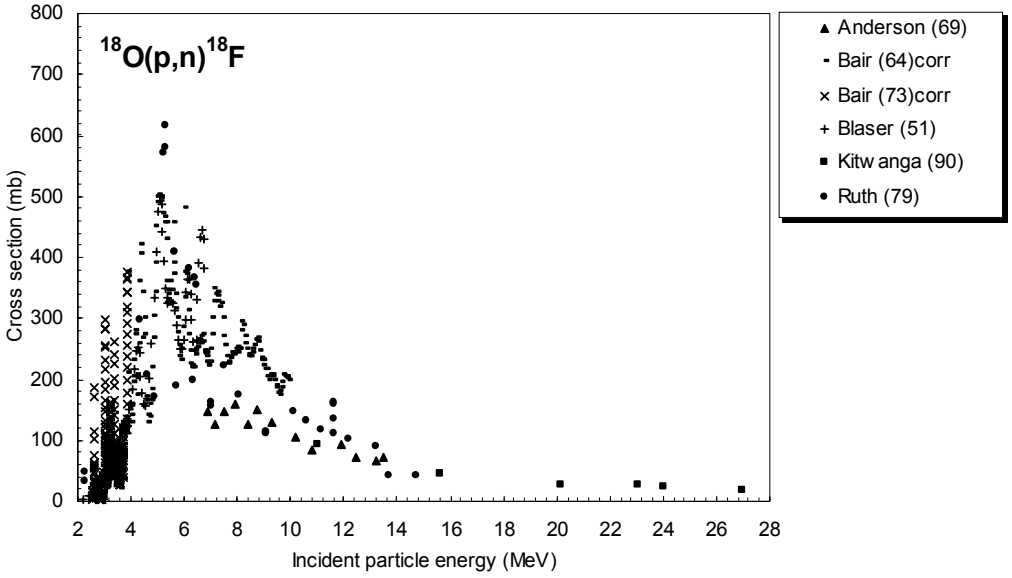

Figure 5.2.5a. All experimental data.

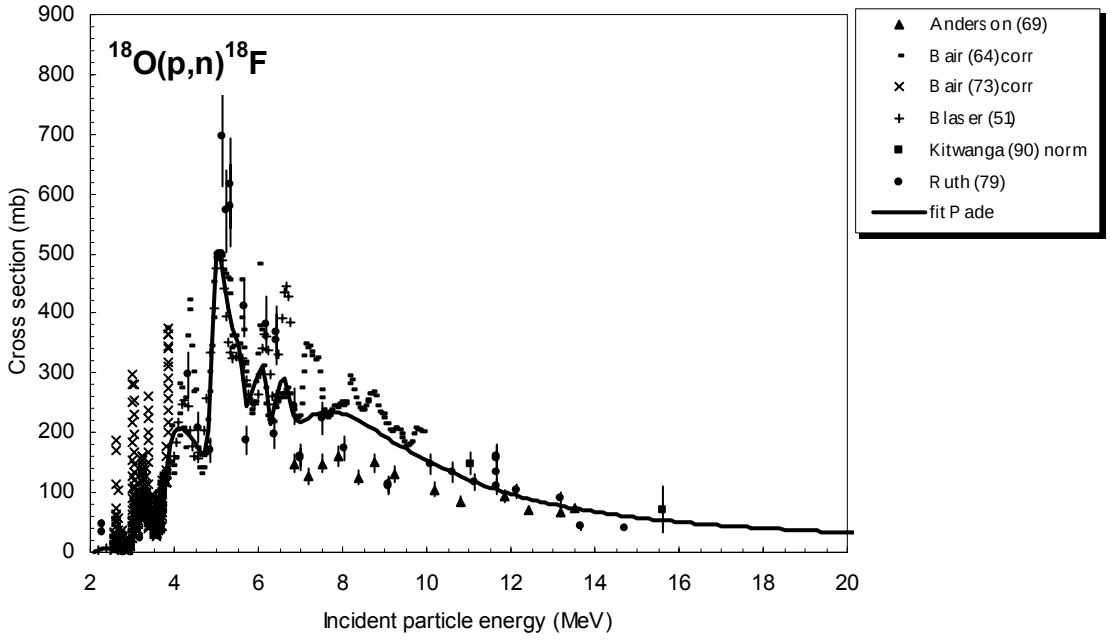

Figure 5.2.5b. Selected experimental data and recommended cross-section curve.

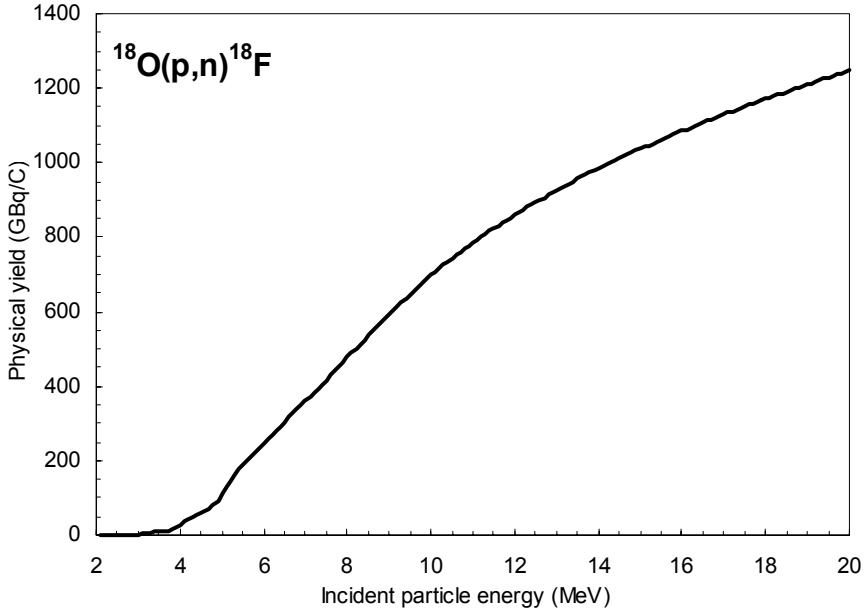

Figure 5.2.5c. Yield of ^{18}F calculated from the recommended cross-sections.

TABLE 5.2.5a. RECOMMENDED CROSS-SECTIONS FOR THE $^{18}O(p,n)^{18}F$ REACTION

Energy MeV	Cross-section mb	Energy MeV	Cross-section mb	Energy MeV	Cross-section mb	Energy MeV	Cross-section mb
2.5	8.3	6.9	220	11.3	113	15.7	52.9
2.6	17.1	7.0	218	11.4	110	15.8	52.2
2.7	8.7	7.1	221	11.5	108	15.9	51.5
2.8	4.2	7.2	225	11.6	106	16.0	50.9
2.9	6.4	7.3	229	11.7	104	16.1	50.2
3.0	33.4	7.4	232	11.8	101	16.2	49.6
3.1	61.1	7.5	234	11.9	99	16.3	49.0
3.2	69.8	7.6	235	12.0	97	16.4	48.4
3.3	67.8	7.7	236	12.1	95	16.5	47.8
3.4	58.9	7.8	235	12.2	94	16.6	47.2
3.5	44.4	7.9	234	12.3	92	16.7	46.6
3.6	36.1	8.0	232	12.4	90	16.8	46.1
3.7	67.8	8.1	229	12.5	88	16.9	45.5
3.8	134	8.2	226	12.6	87	17.0	45.0
3.9	180	8.3	223	12.7	85	17.1	44.5
4.0	199	8.4	220	12.8	83	17.2	44.0
4.1	206	8.5	216	12.9	82	17.3	43.5
4.2	206	8.6	212	13.0	80	17.4	43.0
4.3	202	8.7	207	13.1	79	17.5	42.5
4.4	194	8.8	203	13.2	78	17.6	42.0
4.5	182	8.9	199	13.3	76	17.7	41.6
4.6	169	9.0	194	13.4	75	17.8	41.1
4.7	163	9.1	190	13.5	74	17.9	40.7
4.8	203	9.2	186	13.6	72	18.0	40.3
4.9	358	9.3	181	13.7	71	18.1	39.8
5.0	501	9.4	177	13.8	70	18.2	39.4
5.1	496	9.5	173	13.9	69	18.3	39.0
5.2	449	9.6	169	14.0	68	18.4	38.6
5.3	407	9.7	165	14.1	67	18.5	38.2
5.4	374	9.8	161	14.2	66	18.6	37.8
5.5	349	9.9	157	14.3	65	18.7	37.5
5.6	300	10.0	153	14.4	64	18.8	37.1
5.7	244	10.1	149	14.5	63	18.9	36.7
5.8	262	10.2	146	14.6	62	19.0	36.4
5.9	280	10.3	142	14.7	61	19.1	36.0
6.0	299	10.4	139	14.8	60	19.2	35.7
6.1	311	10.5	136	14.9	59	19.3	35.3
6.2	279	10.6	132	15.0	58	19.4	35.0
6.3	214	10.7	129	15.1	58	19.5	34.7
6.4	243	10.8	126	15.2	57	19.6	34.3
6.5	284	10.9	124	15.3	56	19.7	34.0
6.6	291	11.0	121	15.4	55	19.8	33.7
6.7	263	11.1	118	15.5	54	19.9	33.4
6.8	233	11.2	115	15.6	54	20.0	33.1

TABLE 5.2.5b. YIELDS CALCULATED FROM THE RECOMMENDED CROSS-SECTION DATA FOR THE $^{18}O(p,n)^{18}F$ REACTION Y_1: PHYSICAL YIELD, A_1: ACTIVITY AFTER 1 HOUR AND 1 μA IRRADIATION, A_2: SATURATION ACTIVITY FOR 1 μA IRRADIATION

Energy	Physical yield	Activity		Energy	Physical yield	Activity	
MeV	GBq/C	GBq	GBq	MeV	GBq/C	GBq	GBq
	Y	A_1	A_2		Y	A_1	A_2
2.5	0.543	0.0016	0.0052	11.5	824	2.47	7.83
3.0	2	0.01	0.02	12.0	860	2.58	8.18
3.5	10	0.03	0.10	12.5	894	2.68	8.50
4.0	29	0.09	0.27	13.0	926	2.78	8.80
4.5	61	0.18	0.58	13.5	956	2.87	9.09
5.0	110	0.33	1.05	14.0	984	2.95	9.36
5.5	189	0.57	1.80	14.5	1011	3.03	9.61
6.0	246	0.74	2.34	15.0	1037	3.11	9.86
6.5	304	0.91	2.89	15.5	1062	3.18	10.09
7.0	360	1.08	3.43	16.0	1085	3.25	10.31
7.5	416	1.247	3.96	16.5	1108	3.32	10.53
8.0	477	1.428	4.53	17.0	1130	3.39	10.74
8.5	537	1.609	5.10	17.5	1151	3.45	10.94
9.0	594	1.781	5.65	18.0	1171	3.51	11.13
9.5	647.9	1.942	6.158	18.5	1191	3.57	11.32
10.0	697.5	2.090	6.630	19.0	1210	3.63	11.50
10.5	743.2	2.2270	7.063	19.5	1229	3.68	11.68
11.0	785.22	2.3531	7.463	20.0	1247	3.74	11.85

5.2.6. $^{nat}Ne(d,x)^{18}F$

There were 6 experimental published papers dealing with the measurement of the activation product ^{18}F. From the papers considered here 3 works were excluded and the remaining 3 were selected for further evaluation. The list of related references given below is accompanied with additional information. We mention availability of data in the computerized database EXFOR (if available, unique EXFOR reference number is given). Furthermore, we indicate a reason why a data set was excluded (reference denoted by an asterisk *).

It should be pointed out that at low energies the $^{20}Ne(d,\alpha)^{18}F$ reaction is the only contributing process to the formation of ^{18}F. Above 30 MeV the $^{20}Ne(d,2p2n)^{18}F$ reaction also contributes. The contributions from reactions induced on ^{21}Ne and ^{22}Ne are expected to be significant only at high energies.

Backhausen, H., Stöcklin, G., Weinreich, R.:
Formation of ^{18}F via its ^{18}Ne precursor: excitation functions of reactions $^{20}Ne(d,x)^{18}Ne$ and $^{20}Ne(^{3}He,\alpha n)^{18}Ne$.
Radiochimica Acta **29** (1981) 1
— Exfor: none

Fenyvesi, A., Takács, S., Merchel, S., Pető, G., Szelecsényi, F., Molnár, T., Tárkányi, F., Qaim, S., M.:
Excitation functions of charged particle induced reactions on neon: relevance to the production of $^{22,24}Na$ and ^{18}F.
"Nuclear Data for Science and Technology" Conference Proceedings Vol. 59
(eds. Reffo, G., Ventura, A., Grandi, C.)
SIF, Bologna (1997) 1707
— Exfor: none

*** Guillaume, M.:**
Production en routine par cyclotron de fluor-18 et potassium-43 a usage medical au moyen d'une cible gazeuse télécommandée.
Nuclear Instruments Methods **136** (1976) 185
— Exfor:
— Data excluded: shift in energy by 2.1 MeV

Nozaki, T., Iwamoto, M., Ido, T.:
Yield of ^{18}F for various reactions from oxygen and neon.
Int. J. Applied Radiation Isotopes **25** (1974) 393
— Exfor: none

*** Morand, C., Beaumvieille, H., Dauchy, A., Dumazet, G., Lambert, M., Meynadier, C.:**
Journal de Physique C2 31 (1970) 205
Data taken from de Lassus St-Genies, C.-H., Tobailem, J.
Sections efficaces des reactions nucleaires induites par protons, deuterons, particules alpha.
II. Fluor, Neon, Sodium, Magnesium.
Raport CEA-N-1466(2), CEA, France, 1972
— Exfor:
— Data excluded: only a single energy point reported; too low value.

*** Takamatsu, K.:**
J. Physical Society Japan **17** (1962) 896
Data taken from de Lassus St-Genies, C.-H., Tobailem, J.
Sections efficaces des reactions nucleaires induites par protons, deuterons, particules alpha.
II. Fluor, Neon, Sodium, Magnesium.
Report CEA-N-1466(2), CEA, France, 1972
— Exfor: none
— Data excluded: only one rather low value.

The data from papers where experimental numerical values were available (6 papers) are collected in Fig. 5.2.6a. From these, 3 works were excluded while the remaining 3 were selected for further evaluation.

Cross-sections were calculated by two fitting procedures (Padé with 9 parameters and Spline). The results are compared with the selected experimental data in Fig. 5.2.6b. The best approximation was judged to be the spline fit. The recommended cross-section curve is compared with selected experimental data, including their error bars, in Fig. 5.2.6c. The yields calculated from the recommended cross-sections are presented in Fig. 5.2.6d. The corresponding numerical values for recommended cross-sections and yields are tabulated in Table 5.2.6a and Table 5.2.6b, respectively.

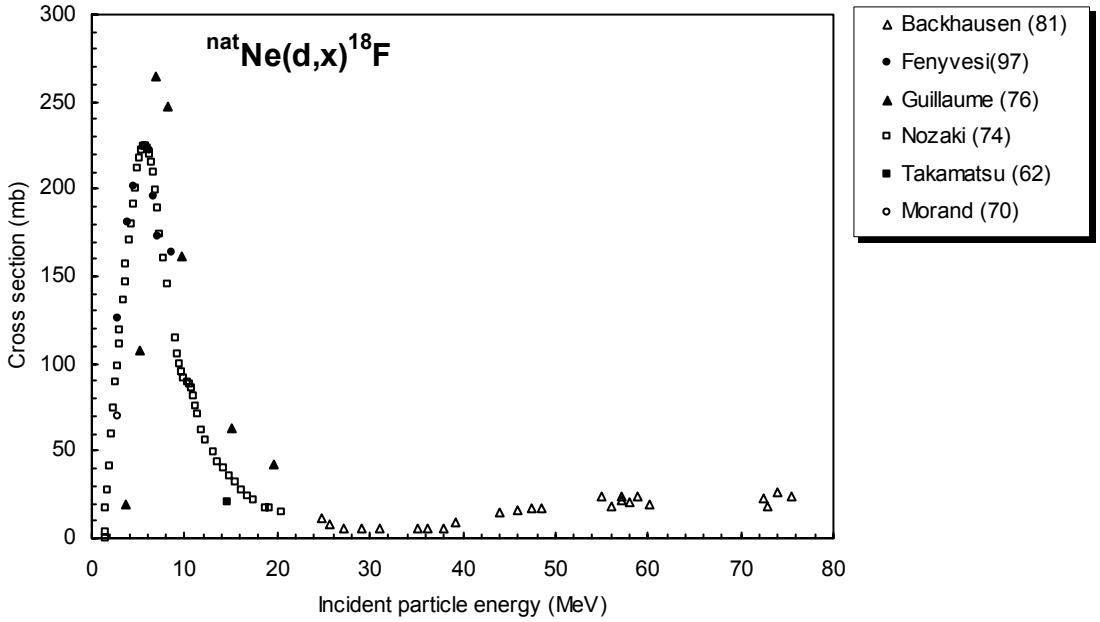

Figure 5.2.6a. All experimental data.

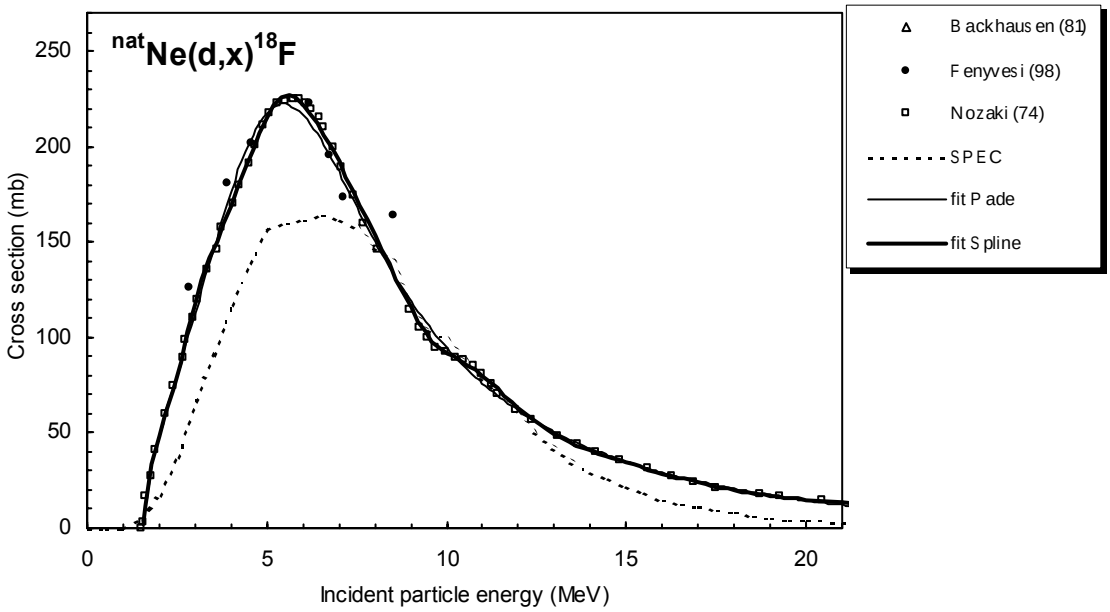

Figure 5.2.6b. Selected experimental data in comparison with fits.

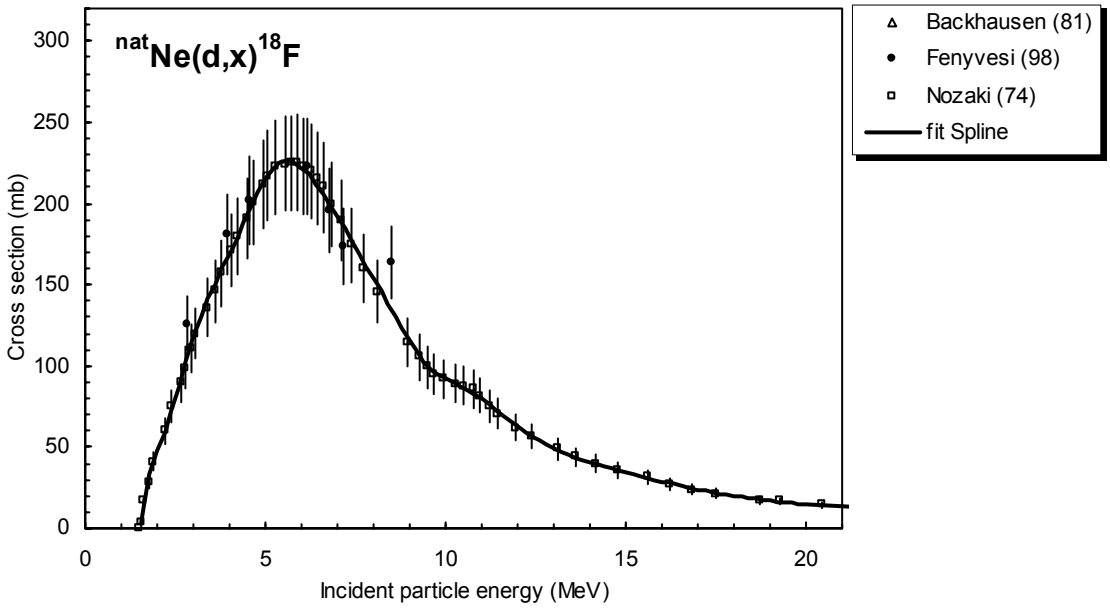

Figure 5.2.6c. Selected experimental data and recommended cross-section curve.

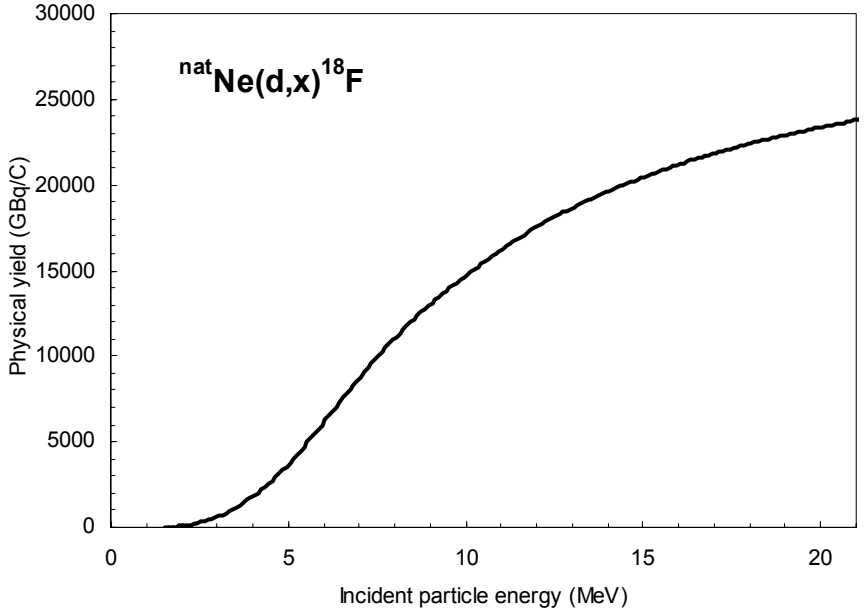

Figure 5.2.6d. Yield of ^{18}F calculated from the recommended cross-sections.

TABLE 5.2.6a. RECOMMENDED CROSS-SECTIONS FOR THE $^{NAT}Ne(d,x)^{18}F$ PROCESS

Energy MeV	Cross-section mb	Energy MeV	Cross-section mb	Energy MeV	Cross-section mb	Energy MeV	Cross-section mb
1.5	3.4	6.5	208.0	11.5	70.5	16.5	26.1
2.0	50.3	7.0	190.6	12.0	62.1	17.0	23.8
2.5	82.6	7.5	171.3	12.5	54.9	17.5	21.7
3.0	120.1	8.0	152.1	13.0	48.9	18.0	19.9
3.5	148.1	8.5	132.9	13.5	44.0	18.5	18.3
4.0	171.2	9.0	114.0	14.0	40.3	19.0	16.9
4.5	195.5	9.5	99.2	14.5	37.1	19.5	15.8
5.0	216.6	10.0	91.4	15.0	34.2	20.0	14.8
5.5	226.3	10.5	85.9	15.5	31.3	20.5	14.0
6.0	221.4	11.0	78.9	16.0	28.6	21.0	13.3

TABLE 5.2.5b. YIELDS CALCULATED FROM THE RECOMMENDED CROSS-SECTION DATA FOR THE $^{NAT}Ne(d,x)^{18}F$ PROCESS Y_1: PHYSICAL YIELD, A_1: ACTIVITY AFTER 1 HOUR AND 1 μA IRRADIATION, A_2: SATURATION ACTIVITY FOR 1 μA IRRADIATION

Energy MeV	Physical yield GBq/C Y	Activity GBq A_1	Activity GBq A_2	Energy MeV	Physical yield GBq/C Y	Activity GBq A_1	Activity GBq A_2
1.5	1.6	0.0003	0.0003	11.5	16966	2.99	2.99
2.0	95	0.017	0.017	12.0	17600	3.10	3.10
2.5	304	0.054	0.054	12.5	18177	3.21	3.21
3.0	666	0.117	0.117	13.0	18703	3.30	3.30
3.5	1194	0.21	0.21	13.5	19188	3.38	3.38
4.0	1879	0.33	0.33	14.0	19643	3.46	3.46
4.5	2734	0.48	0.48	14.5	20073	3.54	3.54
5.0	3774	0.67	0.67	15.0	20480	3.61	3.61
5.5	4969	0.88	0.88	15.5	20863	3.68	3.68
6.0	6247	1.10	1.10	16.0	21221	3.74	3.74
6.5	7541	1.33	1.33	16.5	21556	3.80	3.80
7.0	8807	1.55	1.55	17.0	21870	3.86	3.86
7.5	10014	1.77	1.77	17.5	22162	3.91	3.91
8.0	11145	1.97	1.97	18.0	22435	3.96	3.96
8.5	12188	2.15	2.15	18.5	22691	4.00	4.00
9.0	13130	2.32	2.32	19.0	22932	4.04	4.04
9.5	13974	2.46	2.46	19.5	23162	4.08	4.08
10.0	14766	2.60	2.60	20.0	23381	4.12	4.12
10.5	15536	2.74	2.74	20.5	23592	4.16	4.16
11.0	16276	2.87	2.87	21.0	23796	4.20	4.20

5.2.7. ^{69}Ga(p,2n)^{68}Ge

As mentioned above, ^{68}Ge($T_{1/2}$ = 270.8d) is the long-lived parent of the short-lived positron emitter ^{68}Ga($T_{1/2}$ = 68.3min). The common route of production is spallation. Over the energy range under consideration in this project, only the (p,xn) processes are of interest.

There were 3 published experimental papers available. One work was excluded and the remaining 2 were selected for further evaluation. The list of related references given below is accompanied with additional information. We mention availability of data in the computerized database EXFOR (if available, unique EXFOR reference number is given). Furthermore, we indicate a reason why a data set was excluded (reference denoted by an asterisk *).

*** Cohen, B.L., Newman, E.:**
(p,pn) and (p,p2n) cross-sections in medium weight elements.
Physical Review **99** (1955) 718
— Exfor: B0050
— Data excluded: only one data point available, does not confirm other data

Levkovski, V.N.:
Activation cross-sections for the nuclides of medium mass region (A = 40-100) with protons and α particles at medium (E = 10–50 MeV) energies. (Experiment and systematics)
Inter-Vesi, Moscow (1991)
— Exfor: A0510

Porile, N.T., Tanaka, H., Amano, H.:
Nuclear reactions of ^{69}Ga and ^{71}Ga with 13–56 MeV protons.
Nuclear Physics **43** (1963) 500
— Exfor: P0014

The data from papers where experimental numerical values were available (3 papers) are collected in Fig. 5.2.7a. From these, 1 work was excluded while the remaining 2 were selected for further evaluation.

Cross-sections were calculated by the nuclear reaction model code ALICE IPPE and by two fitting procedures Padé and Spline. These results are compared with the selected experimental data in Fig. 5.2.7b. Evidently, the ALICE model calculation gives too high cross-sections. The best approximation was judged to be the Padé fit. The recommended cross-section curve is compared with selected experimental data, including their error bars, in Fig. 5.2.7c. The yields calculated from the recommended cross-sections are presented in Fig. 5.2.7d. The corresponding numerical values for recommended cross-sections and yields are tabulated in Table 5.2.7a and Table 5.2.7b, respectively.

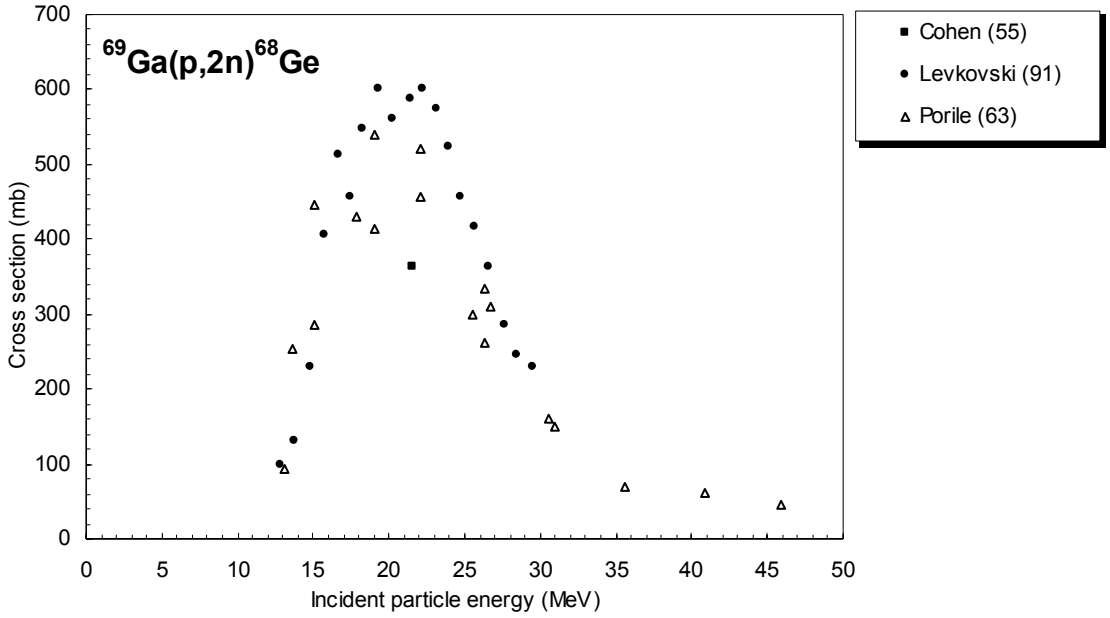

Figure 5.2.7a. All experimental data.

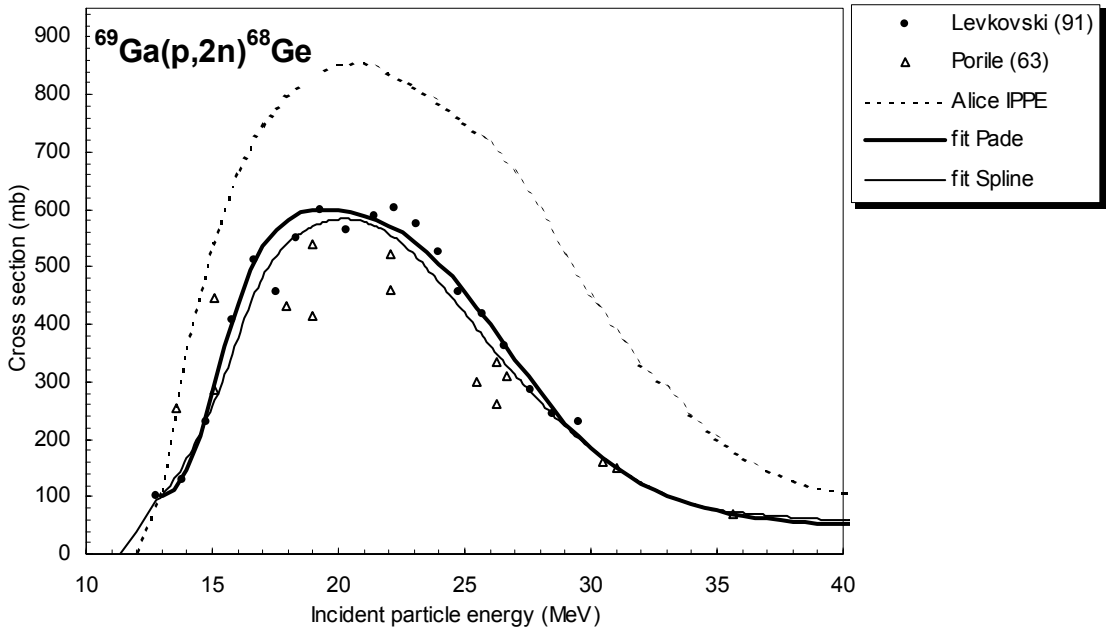

Figure 5.2.7b. Selected experimental data in comparison with a theoretical calculation and fits

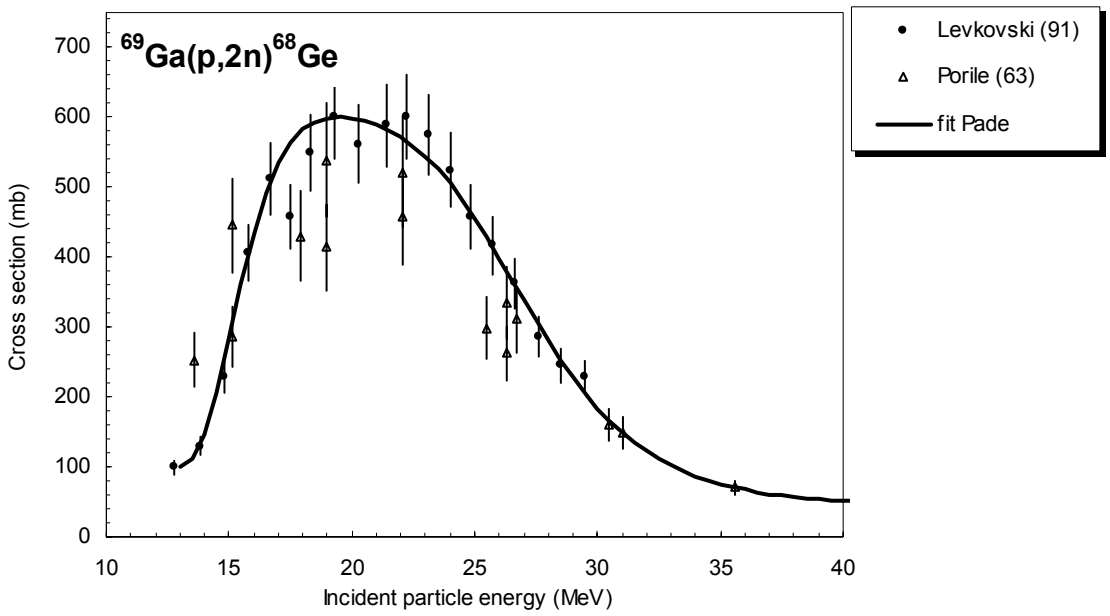

Figure 5.2.7c. Selected experimental data and recommended cross-section curve.

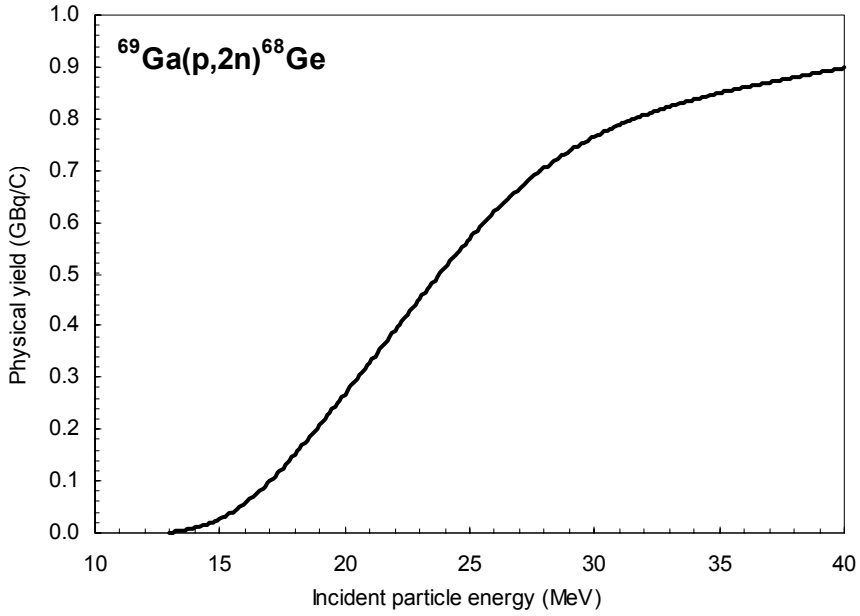

Figure 5.2.7d. Yield of ^{68}Ge calculated from the recommended cross-sections.

TABLE 5.2.7a. RECOMMENDED CROSS-SECTIONS FOR THE $^{69}Ga(p,2n)^{68}Ge$ REACTION

Energy MeV	Cross-section mb	Energy MeV	Cross-section mb	Energy MeV	Cross-section mb	Energy MeV	Cross-section mb
13.0	97.7	20.0	600	27.0	339	34.0	86.6
13.5	114	20.5	596	27.5	309	34.5	80.6
14.0	149	21.0	590	28.0	280	35.0	75.5
14.5	207	21.5	582	28.5	253	35.5	71.1
15.0	279	22.0	571	29.0	228	36.0	67.3
15.5	356	22.5	559	29.5	205	36.5	64.1
16.0	427	23.0	544	30.0	184	37.0	61.4
16.5	486	23.5	526	30.5	165	37.5	59.0
17.0	531	24.0	505	31.0	149	38.0	57.0
17.5	563	24.5	482	31.5	135	38.5	55.3
18.0	584	25.0	456	32.0	122	39.0	53.8
18.5	595	25.5	428	32.5	111	39.5	52.5
19.0	601	26.0	399	33.0	102	40.0	51.4
19.5	602	26.5	369	33.5	93.6		

TABLE 5.2.7b. YIELDS CALCULATED FROM THE RECOMMENDED CROSS-SECTION DATA FOR THE $^{69}Ga(p,2n)^{68}Ge$ REACTION Y: PHYSICAL YIELD, A_1: ACTIVITY AFTER 1 HOUR AND 1 μA IRRADIATION, A_2: SATURATION ACTIVITY FOR 1 μA IRRADIATION

Energy	Physical yield	Activity		Energy	Physical yield	Activity	
MeV	MBq/C	MBq	GBq	MeV	MBq/C	MBq	GBq
	Y	A_1	A_2		Y	A_1	A_2
13.0	0.71	0.003	0.024	27.0	665	2.40	22.5
13.5	4.68	0.02	0.16	27.5	686	2.47	23.1
14.0	9.78	0.04	0.33	28.0	705	2.54	23.8
14.5	16.9	0.06	0.57	28.5	722	2.60	24.4
15.0	27.0	0.10	0.91	29.0	738	2.66	24.9
15.5	40.4	0.15	1.36	29.5	752	2.71	25.4
16.0	57.2	0.21	1.93	30.0	765	2.75	25.8
16.5	77.4	0.28	2.61	30.5	777	2.80	26.2
17.0	100	0.36	3.38	31.0	788	2.84	26.6
17.5	125	0.45	4.22	31.5	798	2.87	26.9
18.0	152	0.55	5.12	32.0	807	2.90	27.2
18.5	180	0.65	6.06	32.5	815	2.93	27.5
19.0	208	0.75	7.03	33.0	823	2.96	27.8
19.5	238	0.86	8.03	33.5	830	2.99	28.0
20.0	268	0.96	9.04	34.0	837	3.01	28.2
20.5	298	1.07	10.1	34.5	843	3.04	28.5
21.0	329	1.18	11.1	35.0	849	3.06	28.7
21.5	360	1.30	12.1	35.5	855	3.08	28.9
22.0	391	1.41	13.2	36.0	860	3.10	29.0
22.5	422	1.52	14.2	36.5	865	3.12	29.2
23.0	452	1.63	15.3	37.0	870	3.13	29.4
23.5	482	1.74	16.3	37.5	875	3.15	29.5
24.0	512	1.84	17.3	38.0	880	3.17	29.7
24.5	541	1.95	18.2	38.5	885	3.18	29.9
25.0	568	2.05	19.2	39.0	889	3.20	30.0
25.5	595	2.14	20.1	39.5	894	3.22	30.2
26.0	620	2.23	20.9	40.0	898	3.23	30.3
26.5	643	2.32	21.7				

5.2.8. ^{nat}Ga(p,xn)^{68}Ge

No experimental work on proton induced reactions on ^{nat}Ga was available. Only one publication mentions measurements on both the Ga isotopes separately. The results of this work were combined to yield information on the cross-section above the threshold of the ^{71}Ga(p,4n)^{68}Ge reaction. The results of other two available works were converted into cross-sections on natural Ga target. The list of related references given below is accompanied with additional information. We mention availability of data in the computerised database EXFOR (if available, unique EXFOR reference number is given). Furthermore, we indicate a reason why a data set was excluded (reference denoted by an asterisk *).

*** Cohen, B.L., Newman, E.:**
(p,pn) and (p,p2n) cross-sections in medium weight elements.
Physics Review **99** (1955) 718
— Exfor: B0050
— Data excluded: only one data point available, does not confirm other data

Levkovski, V.N.:
Activation cross-sections for the nuclides of medium mass region (A = 40-100) with protons and α particles at medium (E = 10-50 MeV) energies. (Experiment and systematics)
Inter-Vesi, Moscow (1991)
— Exfor: A0510

Porile, N.T., Tanaka, H., Amano, H.:
Nuclear reactions of ^{69}Ga and ^{71}Ga with 13-56 MeV protons.
Nuclear Physics **43** (1963) 500
— Exfor: P0014

The deduced data from all papers are collected in Fig. 5.2.8a. From these, 1 work was excluded while the remaining 2 works were selected for further evaluation.

Cross-sections were calculated by the nuclear reaction model code SPEC and by the fitting procedure Spline. These results are compared with the selected experimental data in Fig. 5.2.8b. The SPEC model calculation overpredicts the cross-sections, especially at energies above 30 MeV. The best approximation was judged to be the spline fit. The fitted cross-section curve is compared with the selected experimental data, including their error bars, in Fig. 5.2.8c. The yields calculated from the recommended cross-sections are presented in Fig. 5.2.8d. The corresponding numerical values for recommended cross-sections and yields are tabulated in Table 5.2.8a and Table 5.2.8b, respectively.

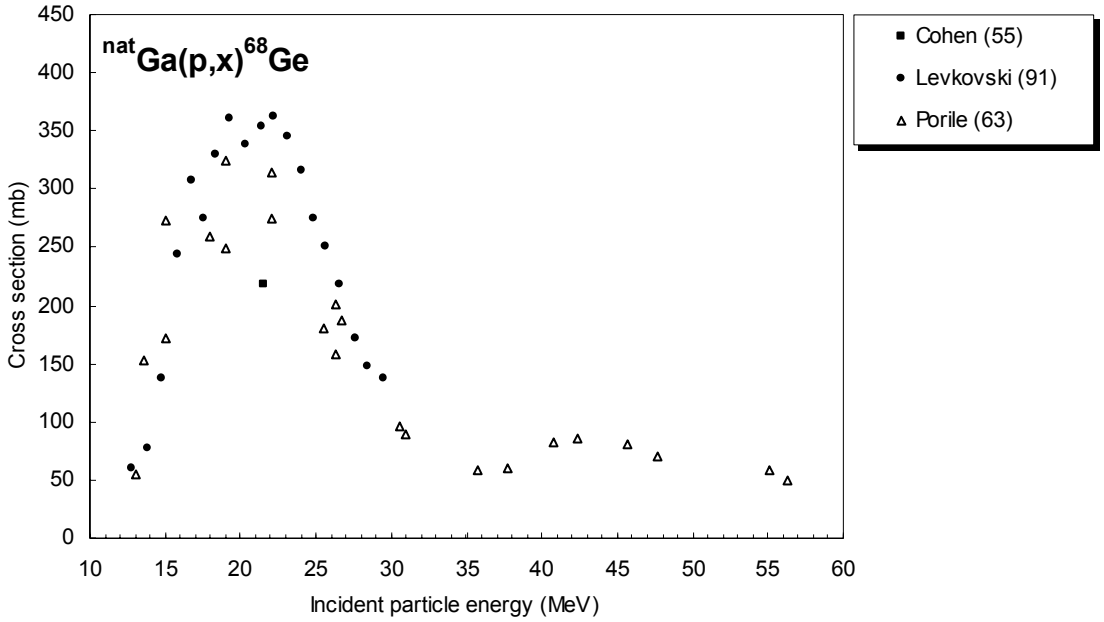

Figure 5.2.8a. All experimental data.

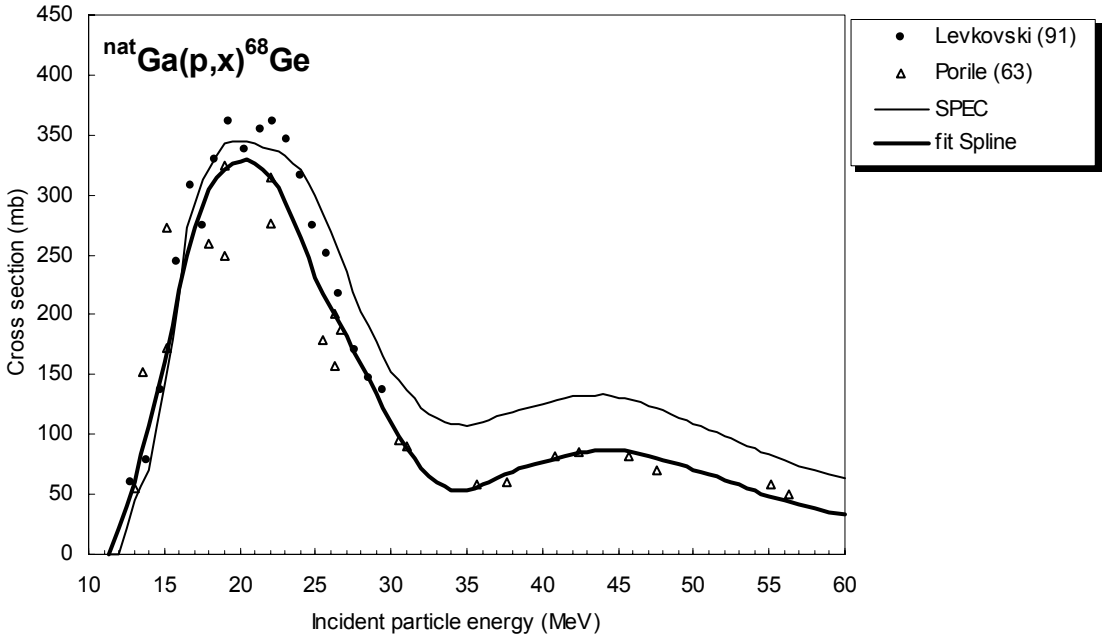

Figure 5.2.8b. Selected experimental data in comparison with a theoretical calculation and a fit.

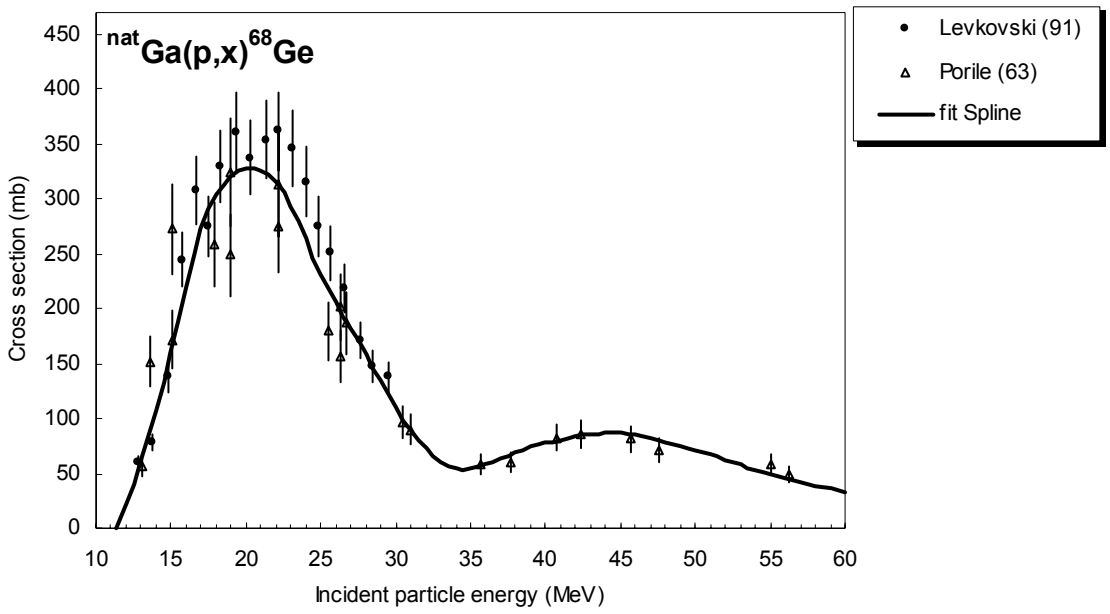

Figure 5.2.8c. Selected experimental data and recommended cross-section curve.

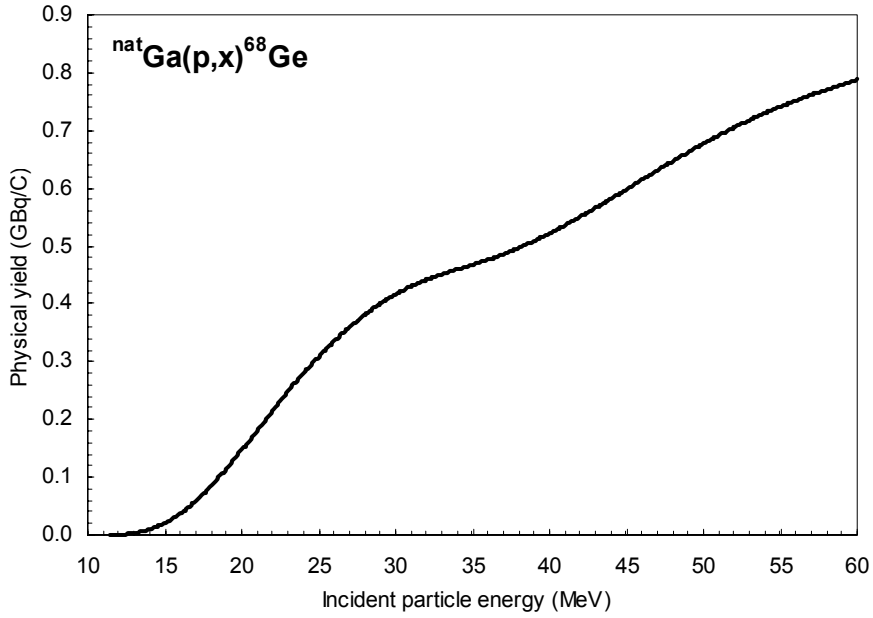

Figure 5.2.8d. Yield of ^{68}Ge calculated from the recommended cross-sections.

TABLE 5.2.8a. RECOMMENDED CROSS-SECTIONS FOR THE $^{nat}Ga(p,x)^{68}Ge$ PROCESS

Energy MeV	Cross-section mb	Energy MeV	Cross-section mb	Energy MeV	Cross-section mb	Energy MeV	Cross-section mb
11.5	5.2	24.0	264	36.5	60.5	49.0	75.1
12.0	21.7	24.5	249	37.0	63.3	49.5	73.0
12.5	40.0	25.0	234	37.5	66.2	50.0	71.0
13.0	60.6	25.5	220.1	38.0	69.0	50.5	69.0
13.5	83.3	26.0	206.7	38.5	71.6	51.0	66.9
14.0	108	26.5	194.1	39.0	73.9	51.5	64.7
14.5	135	27.0	181.9	39.5	75.9	52.0	62.5
15.0	163	27.5	169.9	40.0	77.7	52.5	60.2
15.5	191	28.0	157.9	40.5	79.4	53.0	57.8
16.0	219	28.5	145.9	41.0	80.9	53.5	55.4
16.5	244	29.0	133.8	41.5	82.4	54.0	53.0
17.0	267	29.5	121.7	42.0	83.8	54.5	50.8
17.5	286	30.0	110.1	42.5	84.9	55.0	48.6
18.0	302	30.5	99.1	43.0	85.7	55.5	46.6
18.5	314	31.0	89.1	43.5	86.3	56.0	44.8
19.0	322	31.5	80.1	44.0	86.7	56.5	43.0
19.5	327	32.0	72.3	44.5	86.9	57.0	41.4
20.0	330	32.5	65.7	45.0	86.8	57.5	39.7
20.5	329	33.0	60.4	45.5	86.3	58.0	38.2
21.0	326	33.5	56.6	46.0	85.4	58.5	36.9
21.5	321	34.0	54.3	46.5	84.1	59.0	35.6
22.0	313	34.5	53.6	47.0	82.6	59.5	34.4
22.5	303	35.0	54.2	47.5	80.9	60.0	33.2
23.0	292	35.5	55.8	48.0	79.0		
23.5	278	36.0	58.0	48.5	77.1		

TABLE 5.2.8b. YIELDS CALCULATED FROM THE RECOMMENDED CROSS-SECTION DATA FOR THE $^{nat}Ga(p,x)^{68}Ge$ REACTION Y: PHYSICAL YIELD, A_1: ACTIVITY AFTER 1 HOUR AND 1 μA IRRADIATION, A_2: SATURATION ACTIVITY FOR 1 μA IRRADIATION

Energy	Physical yield	Activity		Energy	Physical yield	Activity	
MeV	MBq/C	MBq	GBq	MeV	MBq/C	MBq	GBq
	Y	A_1	A_2		Y	A_1	A_2
11.5	0.048	0.00017	0.0016	36.0	477	1.72	16.1
12.0	0.56	0.0020	0.019	36.5	481	1.73	16.2
12.5	1.70	0.0061	0.057	37.0	486	1.75	16.4
13.0	3.58	0.013	0.12	37.5	492	1.77	16.6
13.5	6.33	0.023	0.21	38.0	497	1.79	16.8
14.0	10.1	0.036	0.34	38.5	503	1.81	17.0
14.5	14.9	0.054	0.50	39.0	509	1.83	17.2
15.0	21.0	0.076	0.71	39.5	516	1.86	17.4
15.5	28.4	0.10	0.96	40.0	522	1.88	17.6
16.0	37.2	0.13	1.26	40.5	529	1.90	17.9
16.5	47.4	0.17	1.60	41.0	536	1.93	18.1
17.0	58.7	0.21	1.98	41.5	543	1.96	18.3
17.5	71.3	0.26	2.41	42.0	551	1.98	18.6
18.0	85.0	0.31	2.87	42.5	558	2.01	18.8
18.5	99.6	0.36	3.36	43.0	566	2.04	19.1
19.0	115	0.41	3.88	43.5	574	2.07	19.4
19.5	131	0.47	4.42	44.0	582	2.09	19.6
20.0	147	0.53	4.97	44.5	590	2.12	19.9
20.5	164	0.59	5.54	45.0	598	2.15	20.2
21.0	181	0.65	6.11	45.5	606	2.18	20.5
21.5	198	0.71	6.69	46.0	615	2.21	20.7
22.0	215	0.77	7.26	46.5	623	2.24	21.0
22.5	232	0.84	7.83	47.0	631	2.27	21.3
23.0	249	0.89	8.39	47.5	639	2.30	21.6
23.5	265	0.95	8.93	48.0	647	2.33	21.8
24.0	280	1.01	9.45	48.5	655	2.36	22.1
24.5	295	1.06	10.0	49.0	662	2.38	22.4
25.0	309	1.11	10.4	49.5	670	2.41	22.6
25.5	323	1.16	10.9	50.0	677	2.44	22.9
26.0	336	1.21	11.3	50.5	685	2.46	23.1
26.5	348	1.25	11.7	51.0	692	2.49	23.3
27.0	360	1.29	12.1	51.5	699	2.51	23.6
27.5	371	1.33	12.5	52.0	705	2.54	23.8
28.0	381	1.37	12.9	52.5	712	2.56	24.0
28.5	391	1.41	13.2	53.0	718	2.59	24.2
29.0	400	1.44	13.5	53.5	724	2.61	24.4
29.5	409	1.47	13.8	54.0	730	2.63	24.6
30.0	417	1.50	14.1	54.5	736	2.65	24.8
30.5	424	1.53	14.3	55.0	741	2.67	25.0
31.0	430	1.55	14.5	55.5	747	2.69	25.2
31.5	436	1.57	14.7	56.0	752	2.71	25.4
32.0	442	1.59	14.9	56.5	757	2.72	25.5
32.5	447	1.61	15.1	57.0	762	2.74	25.7
33.0	451	1.62	15.2	57.5	766	2.76	25.9
33.5	455	1.64	15.4	58.0	771	2.77	26.0
34.0	460	1.65	15.5	58.5	775	2.79	26.2
34.5	464	1.67	15.7	59.0	779	2.81	26.3
35.0	468	1.68	15.8	59.5	784	2.82	26.4
35.5	472	1.70	15.9	60.0	788	2.83	26.6

5.2.9. ^{85}Rb(p,4n)^{82}Sr

As mentioned above, ^{82}Sr($T_{1/2}$ = 25.55d) is the long-lived parent of the short-lived positron emitter ^{82}Rb($T_{1/2}$ = 1.3min). It finds wide application as a generator system. The common route of production of ^{82}Sr is spallation. Over the energy range under consideration in this project, only the (p,xn) processes are of interest.

Only one experimental work on the reaction under consideration was found in the literature. We mention availability of data in the computerized database EXFOR (if available, unique EXFOR reference number is given).

Horiguchi, T., Noma, H., Yoshizawa, Y., Takemi, H., Hasai, H., Kiso, Y.:
Excitation functions of proton induced nuclear reactions on ^{85}Rb.
Int. J. Applied Radiation Isotopes **31** (1980) 141
— Exfor: B0111

The data are reproduced in Fig. 5.2.9a. Cross-sections were calculated by the nuclear reaction model codes ALICE IPPE and SPEC and by two fitting procedures (Padé with 8 parameters and Spline). These results are compared with the experimental data in Fig. 5.2.9a. The ALICE calculation underestimates while SPEC calculation overpredicts the experimental cross-sections. The best approximation was judged to be the spline fit. In view of limited experimental information no attempt was made to provide recommended cross-sections and yields.

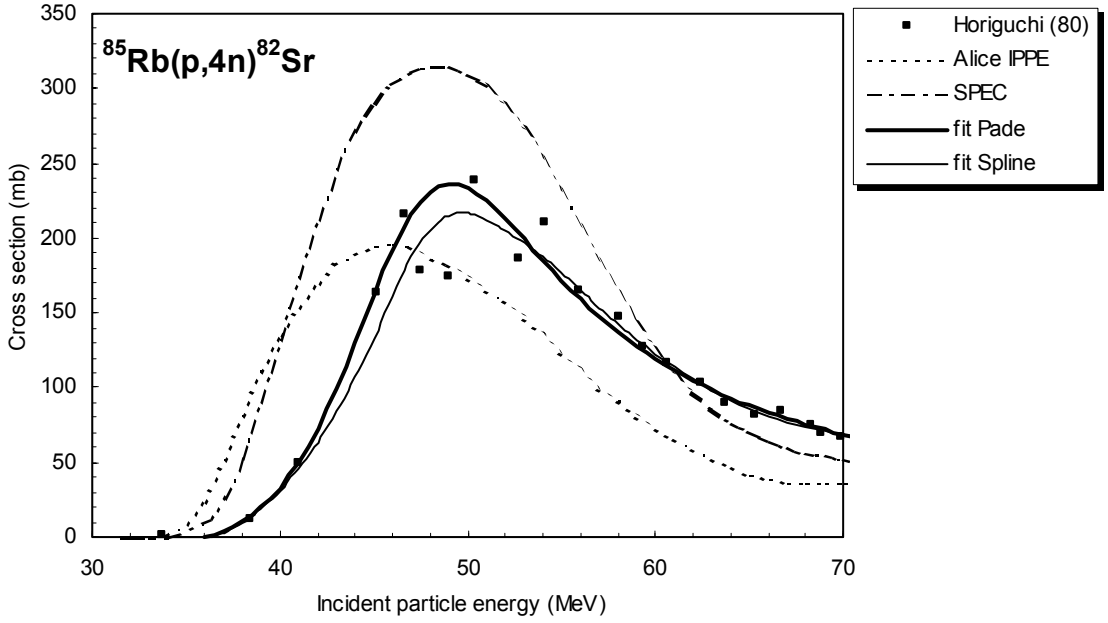

Figure 5.2.9a. Experimental data in comparison with theoretical calculations and fits.

5.2.10. ^{nat}Rb(p,xn)^{82}Sr

Only two works were found in the literature which used natural Rb target and one measurement used enriched target. Two papers were selected for further evaluation. The list of related references given below is accompanied with additional information. We mention availability of data in the computerised database EXFOR (if available, unique EXFOR reference number is given). Furthermore, we indicate a reason why a data set was excluded (reference denoted by an asterisk *).

Deptula, C., Khalkin, V.A., Han, K.S., Knotek, O., Konov, V.A., Mikecz, P., Popenkova, L.M., Rurarz, E., Zaitseva, N.G.:
Excitation function and yields for medically important generators ^{82}Sr→^{82}Rb, ^{123}Xe→^{123}I and ^{201}Bi→^{201}Pb→^{201}TI obtained with 100 MeV protons.
Nucleonika **35** (1990) 3
— Exfor: O0306

Horiguchi, T., Noma, H., Yoshizawa, Y., Takemi, H., Hasai, H., Kiso, Y.:
Excitation functions of proton induced nuclear reactions on ^{85}Rb.
Int. J. Applied Radiation Isotopes **31** (1980) 141
— Exfor: B0111

***Lagunas-Solar:**
Radionuclide production with >70-MeV proton accelerators: current and future prospects
Nuclear Instruments Methods **B69** (1992) 452
— Exfor: none
— Excluded: unusual shape of excitation function.

All the data are collected in Fig. 5.2.10a. Two works were used for further evaluation.

Cross-sections were calculated by the nuclear reaction model codes ALICE IPPE and SPEC. These results are compared with the selected experimental data in Fig. 5.2.10b. It is seen that the ALICE calculation underestimates while SPEC calculation overpredicts the experimental cross-sections. Because of scarcity of data no recommendation is given.

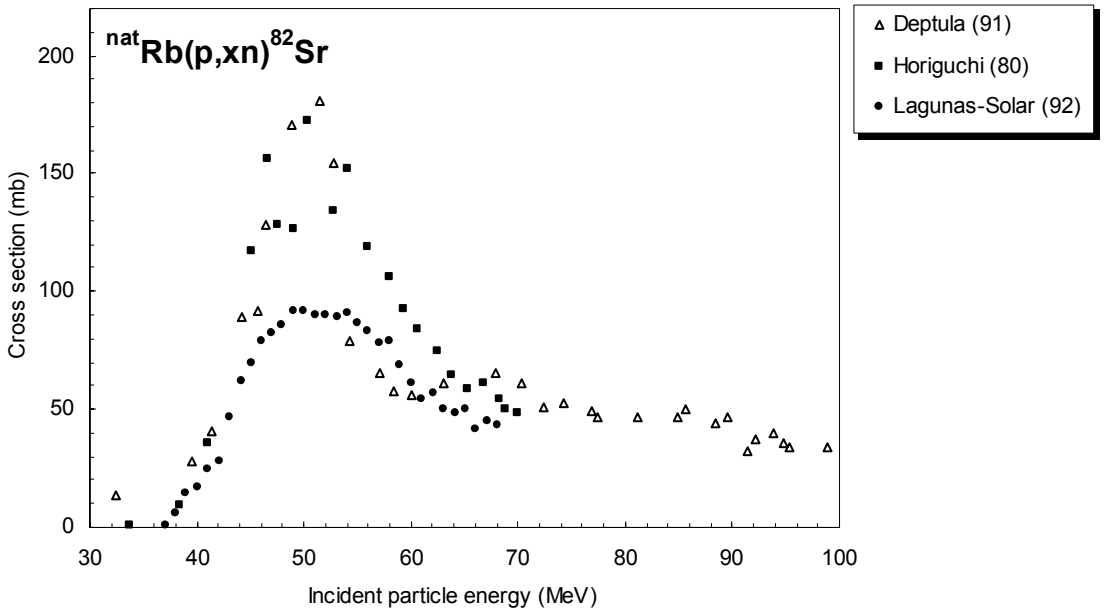

Figure 5.2.10a. All experimental data.

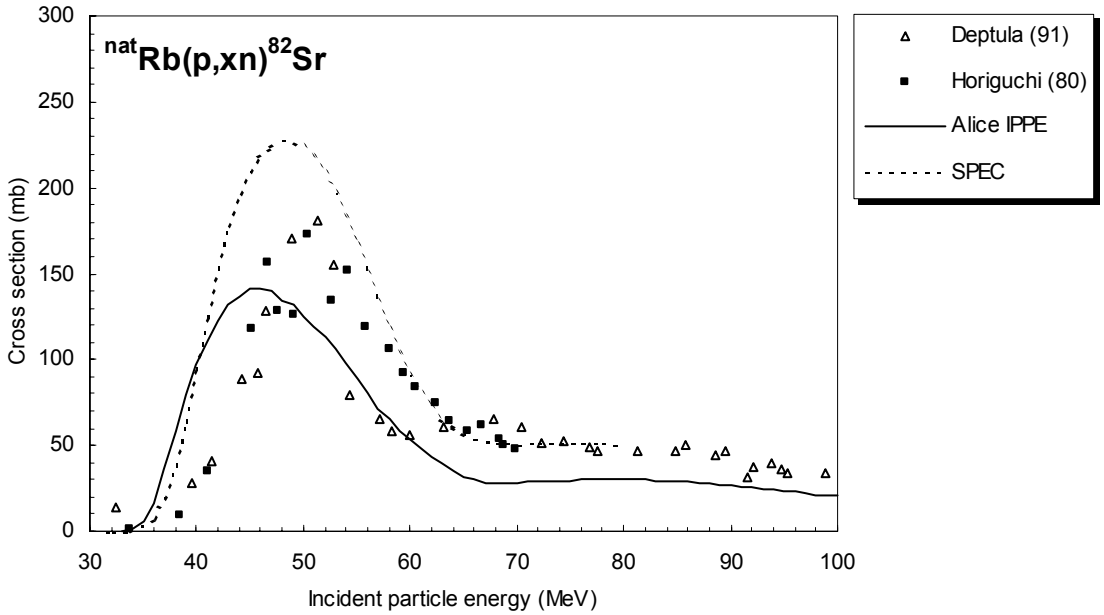

Figure 5.2.10b. Selected experimental data in comparison with theoretical calculations.

Appendix

CROSS-SECTIONS AND YIELDS: DEFINITIONS

The terms cross-section and yield, widely used in practical radioisotope production, often differ from basic definitions used in nuclear reactions theory. Different application oriented groups use these terms in a non-standard way. In order to avoid misinterpretation of the data in the present TECDOC we briefly summarize definitions of the most important quantities describing nuclear reactions in the field of practical radioisotope production and activation technology.

Production cross-section

When an accelerated charged particle interacts with a target nucleus a nuclear reaction takes place, ultimately leading to a stable or radioactive product nucleus. A nuclear reaction is characterized by a cross-section, a geometrical quantity given in barn (10^{-24}cm^2), describing a probability that a particle, with a beam intensity of 1 particle per 1 cm^2, incident on 1 target nucleus will lead to a specific physical process, where the incident particle, target nucleus, reaction channel and the final nucleus are exactly specified.

In isotope production and application of monitor reactions, usually the activity of the product radioisotope is measured. The related quantity of interest is then the integral cross-section or the production cross-section. It refers to a sum of cross-sections of all reaction channels on a well-defined target nucleus, which lead to direct production of the final nuclide. The same final nuclide can also be produced indirectly via the decay of progenitors produced simultaneously on the target nucleus. In many cases the separation of direct and indirect routes becomes unimportant and one uses the cumulative production cross-section to describe these two routes together. This becomes even more complicated when one uses a natural multi-isotopic target element where different reaction channels on different target nuclei can contribute to the production of the same final radioisotope. In this case one uses the elemental production cross-section to describe all production routes together. It should be noted that in doing so one must properly calculate the number of target nuclei, by summing nuclei of all contributing target isotopes. If one considers also indirect production routes, the elemental cumulative production cross-section should be used. Similarly, the notation isotopic production cross-section is used to describe reactions with mono-isotopic target elements.

The present document aims to address the needs of every day practice, where one uses elemental targets that are generally multi-isotopic and sometimes mono-isotopic. Throughout this document we consistently use the term cross-section. In Chapter 4, devoted to beam monitor reactions, this term means cumulative elemental production or cumulative isotopic production cross-section of the final nuclide. In Chapter 5, devoted to medical radioisotope production, this term means elemental production or isotopic production cross-section of the final nuclide.

Production yield

A thin target has a thickness so small that the reaction cross-section can be considered as constant through the whole target. This is equivalent to the energy loss being negligible when compared to the energy range needed to see significant changes in the reaction cross-section. A thick target has its thickness comparable or larger than the range of the incident particle in the target material.

The yield for a target having any thickness can be defined as the ratio of the number of nuclei formed in the nuclear reaction to the number of particles incident on the target. It is termed as the physical yield, Y. It is customary to express the number of radioactive nuclei in terms of the activity, and the number of incident particles in terms of the charge. Thus, Y can be given as activity per Coulomb, in units of GBq/C. The analytical meaning of the physical yield is the slope (at the beginning of the irradiation) of the curve of the growing activity of the produced radionuclide versus irradiation time.

Radioisotopes disintegrate during the bombardment, therefore for practical applications other yield definitions are used taking into account this effect. The activity at the end of a bombardment performed at a constant 1μA beam current on a target during 1 hour is closely related to the measured activity in every day isotope production by accelerators, the so called 1h–1μA yield, A_1. In practice, this latter quantity can be used when the bombardment time is significantly shorter than or comparable with the half-life of the produced isotope.

When the irradiation time is much longer than the half-life of the produced isotope, a saturation of the number of the radioactive nuclei present in the target is reached, and their activity becomes practically independent of the bombardment time (at a constant beam current). This activity produced by a unit number of incident beam particles is the so-called saturation yield, A_2.

There are close relationships between the above-mentioned yields. Using the decay constant of the radionuclide λ and the irradiation time t one gets

$$Y = A_1 \frac{\lambda}{1 - e^{-\lambda t}} = A_2 \lambda .$$

Several other definitions are often used. Differential or thin target yield is defined for negligibly small (unit) energy loss of the incident beam in the thin target material. Thick target yield is defined for a fixed macroscopic energy loss, E_{in}-E_{out}, in a thick target. Integral yield is defined for a finite energy loss down to the threshold of the reaction, E_{in}-E_{th}. The thin target yield is easily related to the reaction cross-section and the stopping power of the target material for the beam considered, see Bonardi [1].

In Chapter 5, the three above-mentioned yield quantities were calculated, namely the physical yield Y, activity in 1 hour activation with 1 μA intensity beam A_1, and saturation activity in 1 μA irradiation A_2. To this end, recommended cross-sections discussed in the present document were used. In addition, the target stopping powers of Ziegler [2, 3] and Andersen and Ziegler [4] and nuclear decay data of Browne and Firestone [5] were used. In the tables and figures we give physical yields Y in 0.5 MeV or 1 MeV energy steps, except for cases where only cumulative cross-sections are known. In those cases only saturation yields are given.

The yield for any target thickness, Y_{thick} can be obtained from the simple formula

$$Y_{thick}(E_{in}\text{-}E_{out}) = Y(E_{in})\text{-}Y(E_{out}),$$

where E_{in} is the incident particle energy and E_{out} is its outgoing energy. For a more detailed discussion and for practical calculations we refer to the extensive list of references in the literature (cf. Bonardi [1] and Dmitriev [6]).

Remark:

For radioisotopes formed via contributions from various nuclear decay processes, the yield and activities were calculated from the total production cross-sections (i.e. cross-sections measured after total decay of possible isomeric states and/or parent nuclei). Actual production yields can be deduced from the data given in the tables in Chapter 5 only after the complete decay of isomeric states and/or parent nuclei (cf. ^{81}Rb, ^{111}In, ^{123}Cs, ^{201}Pb).

REFERENCES

[1] BONARDI, M., "The contribution to nuclear data for biomedical radioisotope production from the Milan Cyclotron Laboratory", Data Requirements for Medical Radioisotope Production, Proc. Consultants Mtg Tokyo, Japan, 1987 (Okamoto K., ed.), Rep. INDC(NDS)-193, IAEA, Vienna (1988).

[2] ZIEGLER, J.F., Handbook of Stopping Cross-Sections for Energetic Ions in all Elements, Vol.5, Pergamon Press, Oxford (1980).

[3] ZIEGLER, J.F., Stopping and Ranges Elements, Vol. 4: Helium, Pergamon Press, Oxford (1977).

[4] ANDERSEN, H.H., ZIEGLER, J.F., Hydrogen Stopping Powers and Ranges in all Elements, Vol. 3, Pergamon Press, Oxford (1977).

[5] BROWNE, E., FIRESTONE, R.B., Table of Radioactive Isotopes (Shirley V.S., ed.), Wiley, New York (1986).

[6] DMITRIEV, P.P., Radionuclide Yield in Reactions with Protons, Deuterons, Alpha Particles and Helium-3 (Handbook), Moscow, Energoatomizdat, 1986; Rep. INDC(CCP)-263, IAEA, Vienna (1986).

CONTRIBUTORS TO DRAFTING AND REVIEW

Gul, K.	Pakistan Institute of Nuclear Science and Technology, Pakistan
Hermanne, A.	Vrije Universiteit Brussel, Belgium
Mustafa, M.G.	Lawrence Livermore National Laboratory, United States of America
Nortier, F.M.	National Accelerator Centre. South Africa
Obložinský, P.	International Atomic Energy Agency
Qaim, S.M.	Forschungszentrum Jülich GmbH, Germany
Scholten, B.	Forschungszentrum Jülich GmbH, Germany
Shubin, Y.	Fiziko-Energeticheskij Institut, Russian Federation
Takács, S.	Hungarian Academy of Sciences, Hungary
Tárkányi, F.T.	Hungarian Academy of Sciences, Hungary
Zhuang, Y.	China Institute of Atomic Energy, China